frontiers | Research Topics

Heavy metal(loid) stress-alleviating and phytostimulating microorganisms: Dual-performing warhorses in soil-bioremediation

Edited by
Krishnendu Pramanik, Pablo Cornejo and Narayan Chandra Mandal

Published in
Frontiers in Microbiology
Frontiers in Sustainable Food Systems

ISSN 1664-8714
ISBN 978-2-8325-2923-2
DOI 10.3389/978-2-8325-2923-2

About Frontiers

Frontiers is more than just an open access publisher of scholarly articles: it is a pioneering approach to the world of academia, radically improving the way scholarly research is managed. The grand vision of Frontiers is a world where all people have an equal opportunity to seek, share and generate knowledge. Frontiers provides immediate and permanent online open access to all its publications, but this alone is not enough to realize our grand goals.

Frontiers journal series

The Frontiers journal series is a multi-tier and interdisciplinary set of open-access, online journals, promising a paradigm shift from the current review, selection and dissemination processes in academic publishing. All Frontiers journals are driven by researchers for researchers; therefore, they constitute a service to the scholarly community. At the same time, the *Frontiers journal series* operates on a revolutionary invention, the tiered publishing system, initially addressing specific communities of scholars, and gradually climbing up to broader public understanding, thus serving the interests of the lay society, too.

Dedication to quality

Each Frontiers article is a landmark of the highest quality, thanks to genuinely collaborative interactions between authors and review editors, who include some of the world's best academicians. Research must be certified by peers before entering a stream of knowledge that may eventually reach the public - and shape society; therefore, Frontiers only applies the most rigorous and unbiased reviews. Frontiers revolutionizes research publishing by freely delivering the most outstanding research, evaluated with no bias from both the academic and social point of view. By applying the most advanced information technologies, Frontiers is catapulting scholarly publishing into a new generation.

What are Frontiers Research Topics?

Frontiers Research Topics are very popular trademarks of the *Frontiers journals series*: they are collections of at least ten articles, all centered on a particular subject. With their unique mix of varied contributions from Original Research to Review Articles, Frontiers Research Topics unify the most influential researchers, the latest key findings and historical advances in a hot research area.

Find out more on how to host your own Frontiers Research Topic or contribute to one as an author by contacting the Frontiers editorial office: frontiersin.org/about/contact

Heavy metal(loid) stress-alleviating and phytostimulating microorganisms: Dual-performing warhorses in soil-bioremediation

Topic editors

Krishnendu Pramanik — Cooch Behar Panchanan Barma University, India
Pablo Cornejo — University of La Frontera, Chile
Narayan Chandra Mandal — Visva-Bharati University, India

Citation

Pramanik, K., Cornejo, P., Mandal, N. C., eds. (2023). *Heavy metal(loid) stress-alleviating and phytostimulating microorganisms: Dual-performing warhorses in soil-bioremediation*. Lausanne: Frontiers Media SA.
doi: 10.3389/978-2-8325-2923-2

Table of contents

frontiers in Microbiology

ORIGINAL RESEARCH
published: 24 January 2022
doi: 10.3389/fmicb.2021.758144

Deciphering Cadmium (Cd) Tolerance in Newly Isolated Bacterial Strain, *Ochrobactrum intermedium* BB12, and Its Role in Alleviation of Cd Stress in Spinach Plant (*Spinacia oleracea* L.)

S. Renu[1]†, Khan Mohd. Sarim[1†], Dhananjaya Pratap Singh[1,2], Upasana Sahu[1], Manish S. Bhoyar[3], Asha Sahu[4], Baljeet Kaur[5], Amrita Gupta[1], Asit Mandal[4], Jyoti Kumar Thakur[4], Madhab C. Manna[4] and Anil Kumar Saxena[1]*

[1] ICAR-National Bureau of Agriculturally Important Microorganisms, Maunath Bhanjan, India, [2] ICAR-Indian Institute of Vegetable Research, Varanasi, India, [3] Intellectual Property Management Unit, National Innovation Foundation, Gandhinagar, India, [4] ICAR-Indian Institute of Soil Sciences, Bhopal, India, [5] ICAR-Indian Agricultural Research Institute, New Delhi, India

A cadmium (Cd)–tolerant bacterium *Ochrobactrum intermedium* BB12 was isolated from sewage waste collected from the municipal sewage dumping site of Bhopal, India. The bacterium showed multiple heavy metal tolerance ability and had the highest minimum inhibitory concentration of 150 mg L^{-1} of Cd. Growth kinetics, biosorption, scanning electron microscopy (SEM), transmission electron microscopy (TEM), and Fourier transform infrared (FTIR) spectroscopy studies on BB12 in the presence of Cd suggested biosorption as primary mode of interaction. SEM and TEM studies revealed surface deposition of Cd. FTIR spectra indicated nitrogen atom in exopolysaccharides secreted by BB12 to be the main site for Cd attachment. The potential of BB12 to alleviate the impact of Cd toxicity in spinach plants (*Spinacia oleracea* L.) var. F1-MULAYAM grown in the soil containing Cd at 25, 50, and 75 mg kg^{-1} was evaluated. Without bacterial inoculation, plants showed delayed germination, decrease in the chlorophyll content, and stunted growth at 50 and 75 mg kg^{-1} Cd content. Bacterial inoculation, however, resulted in the early germination, increased chlorophyll, and increase in shoot (28.33%) and root fresh weight (72.60%) at 50 mg kg^{-1} of Cd concentration after 75 days of sowing. Due to bacterial inoculation, elevated proline accumulation and lowered down superoxide dismutase (SOD) enzyme activity was observed in the Cd-stressed plants. The isolate BB12 was capable of alleviating Cd from the soil by biosorption as evident from significant reduction in the uptake/translocation and bioaccumulation of Cd in bacteria itself and in the plant parts of treated spinach. Potential PGP prospects and heavy metal bioremediation capability of BB12 can make the environmental application of the organism a promising approach to reduce Cd toxicity in the crops grown in metal-contaminated soils.

Keywords: cadmium, toxicity, bioremediation, *Ochrobactrum intermedium* BB12, spinach

OPEN ACCESS

Edited by:
Krishnendu Pramanik, Visva-Bharati University, India

Reviewed by:
Ahmed Idris Hassen, Agricultural Research Council of South Africa (ARC-SA), South Africa
Ravindra Soni, Indira Gandhi Krishi Vishwavidyalaya, India
Nadia Massa, University of Eastern Piedmont, Italy
Elisa Bona, University of Eastern Piedmont, Italy

***Correspondence:**
S. Renu
renuiari@rediffmail.com

† These authors have contributed equally to this work

Specialty section:
This article was submitted to Microbe and Virus Interactions with Plants, a section of the journal Frontiers in Microbiology

Received: *24 August 2021*
Accepted: *13 December 2021*
Published: *24 January 2022*

Citation:
Renu S, Sarim KM, Singh DP, Sahu U, Bhoyar MS, Sahu A, Kaur B, Gupta A, Mandal A, Thakur JK, Manna MC and Saxena AK (2022) Deciphering Cadmium (Cd) Tolerance in Newly Isolated Bacterial Strain, Ochrobactrum intermedium BB12, and Its Role in Alleviation of Cd Stress in Spinach Plant (Spinacia oleracea L.). Front. Microbiol. 12:758144. doi: 10.3389/fmicb.2021.758144

INTRODUCTION

Cadmium (Cd) is a transitional metal being excessively used in alloy plating, pigment production, and manufacturing of rechargeable batteries and phosphatic fertilizers (Muehe et al., 2013). Increased anthropogenic activities and geochemical processes in the last few decades have pounded the Cd level many folds in the aquatic and agricultural environment (Juan et al., 2018). In addition, the other most common route of Cd exposure for the human being is the consumption of contaminated food and deadly cigarette smoke (Rahimzadeh et al., 2017). Cd pollution has increased in various geographical regions at a steady rate over the last few decades, causing deadly threat to human health (Godt et al., 2006). The World Health Organization (WHO) has set the maximum permissible limit of Cd in drinking water (0.05 mg L^{-1}) and in the plants (0.02 mg kg^{-1}) (World Health Organization [WHO], 2008). Shi et al. (2019) comprehensively reported increased level of Cd in agricultural soils in China from 1981 to 2016. Average Cd content in rice plants grown at different locations was recorded to be 0.45 mg kg^{-1}, a level exceeding the permissible limit of Cd in the food grains (Mu et al., 2019). Cd content in the food commodities and drinking water in many parts of world has been reported to be above the permissible limit as indicated in the reports from western Uttar Pradesh, India (Idrees et al., 2018); Bangladesh (Shaheen et al., 2016; Islam et al., 2018); Pakistan (Rehman et al., 2017); South Korea (Zhai et al., 2008); and China (Mu et al., 2019). High Cd content can inhibit the nutrient uptake from soil, restrict soil microbial population indirectly (Sanità Di Toppi and Gabbrielli, 1999), and affect the uptake of various growth-promoting elements, i.e., Ca, P, Mn, and K (Das et al., 1997). Cd in plants induces oxidative stress, destroys photosynthetic pigments, reduces stomata opening, and can severely damage the DNA (Wang et al., 2004). In animals and humans, evidence of Cd accumulation was found in the vital organs like kidney (Clemens et al., 2013). Hence, there is a dire need for the removal of such a life-threatening contaminant from the soil system, food chain, and human environment.

Physical and chemical methods, *viz.*, chemical precipitation, flocculation, membrane filtration, ultrafiltration, ion exchange, reverse osmosis, and electro-dialysis of Cd removal from the contaminated sites, are expensive, time consuming, and labor intensive (Yadav et al., 2021). Biological methods, on the other hand, are eco-friendly, safer for the soil and water systems, cost-effective, and are sustainable solutions. Microorganisms from different habitats, as biological systems, have been a premium choice for the heavy metal bioremediation (Renu et al., 2020; Shukla et al., 2020). The use of plant growth-promoting (PGP) bacteria for eco-friendly plant growth promotion in various crops has intensified in present time (Oleńska et al., 2020). Several mechanisms such as phosphate solubilization, nitrogen fixation, siderophore synthesis, and phytohormone production have already been documented (Kloepper et al., 1989; Glick, 1995; Patten and Glick, 1996; Glick et al., 1999). These microorganisms also possess multiple traits of bioremediation, biotransformation, biodecomposition, and biodegradation that may help to relieve the environment, soils, water, and plants from the toxicity of heavy metals and other contaminants (Hrynkiewicz and Baum, 2014; Ma et al., 2016). Metal-resistant PGP bacteria are reported to stimulate shoot and root growth of plants at enhanced levels of heavy metals and help plants to overcome metal stress (Igiri et al., 2018). To combat metal stress, microorganisms employ variety of mechanisms including biosorption on cell surface, immobilization/mobilization, extra/intracellular sequestration, complex formation with thiol-containing molecules, active efflux system, and conversion of highly toxic forms of compounds into less toxic (Gibbons et al., 2011). Biosorption has been considered as the environmentally and economically efficient process used by many researchers to revive environmental niches from heavy metal contamination (Kobya, 2004; Sarin and Pant, 2006; Saha and Orvig, 2010; Ayangbenro and Babalola, 2017).

Direct remediation of Cd by microbial system is less studied. This is because of the fact that Cd exists in the environment in only one state, i.e., +2. Thus, the direct transformation of Cd (like arsenic and chromium) is not possible. Biosorption has been reported as the primary and effective way of heavy metal removal by the microorganisms (Kanamarlapudi et al., 2018). Bioaccumulation of Cd in different pockets of cells has been demonstrated in *Burkholderia cepacia* (Zhang et al., 2019). Synergistic association of heavy metal–tolerant PGP bacteria with plants provides great opportunities for remediation potential of metal-contaminated habitats (Gururani et al., 2013; Babu et al., 2015; Gupta et al., 2018). In the present study, we have reported a Cd-tolerant bacterium isolated from the metal-contaminated site for its bioremediation potential and evaluated PGP ability on spinach. The study focuses on the ability of spinach plants to withstand Cd stress in the presence of the bacterium with PGP traits. We also reported in-depth mechanism of Cd tolerance in the bacterium and possible role of the isolate in alleviation of Cd toxicity in the spinach plants.

MATERIALS AND METHODS

Sample Collection and Heavy Metal Analysis

Survey of various heavy metal–polluted sites and collection of metal-polluted bulk soils, rhizosphere soils of plants growing on metal-contaminated sites, and polluted water body samples was performed in Nagpur and Bhopal, India, as per the procedures mentioned by Leung et al. (2021) following the United State Environmental Protection Agency (USEPA) methods (**Supplementary Table 1**). Samples were collected in sterilized tight screw cap tubes and polyethylene bags, transported in an icebox, and stored in the laboratory at 4°C to avoid further oxidation/contamination. Collected samples were analyzed for heavy metal content using inductively coupled plasma (ICP) spectrometry as per the standard method (Krishna et al., 2009).

Test Chemicals and Media

The stock solution of Cd (1,000 mg L^{-1}) was prepared by dissolving Cd chloride ($CdCl_2$) in Milli-Q water and filter sterilized through 22-μm filter (Axiva). Working test metal solution (20 mg L^{-1}) was prepared by diluting the concentrated

stock solution. All the glasswares were acid washed before use to avoid binding of metals. All the chemicals and culture media were of analytical grade and obtained from Sigma, Merck, and HiMedia.

Isolation and Morphological Characterization of Bacteria

Various heavy metal–tolerant bacteria were isolated by serial dilution technique on Nutrient Agar (NA) media plates incubated at 37 ± 1°C for 24–48 h (Lima e Silva et al., 2012). Pure bacterial cultures were observed for characters like growth type and growth rate, and the bacterial colonies were subjected to microscopic observation using a light microscope (Olympus, Inc.). The observation on colony characteristics (color, texture, size, shape, margins, elevation, etc.) was recorded. Stereomicroscopic photographs of all the bacterial cultures were documented. Collection site, sample source, and Cd content in the samples are reported in **Supplementary Table 1**.

Determination of Minimum Inhibitory Concentration

Minimum inhibitory concentration (MIC) of Cd for the bacterial isolates was determined following the method of Dey et al. (2016). Comparative MIC value of eight bacterial isolates for other heavy metals was also determined. Spot inoculation of 10 μl of 10^8 cells ml^{-1} bacterial suspension was performed on NA plates amended with Cd salt concentrations from 30 to 150 mg L^{-1}. For other heavy metals, varied tested concentrations are mentioned in **Supplementary Table 2**. The results were recorded after 48 h of incubation at 28°C. The concentration of the metal that permitted growth and beyond which there was no growth was considered as the MIC of the metal against the tested isolate. Appropriate positive controls were kept without heavy metal content for the observation of growth of bacterial isolate. Out of all these isolates, the isolate BB12 was found most appropriate on trait basis to extend the study further.

Mechanism of Cadmium Tolerance in Potential Bacterial Isolates

In vitro Growth Pattern and Biosorption Potential of Cadmium-Tolerant Bacterium

On the basis of MIC results, eight potential Cd-tolerant bacterial isolates, namely, BA3, BA4, BB4, BB12, BB13, BB14, BB15, and NR5, were selected for a batch culture study over the period of 10 days and were grown in the presence of 90 mg L^{-1} Cd in nutrient broth (NB) medium except BB15, which was grown in 40-mg Cd-amended NB medium. All the flasks were incubated on a rotary shaker (150 rpm), and optical density (OD) was measured at 600 nm every 2 h in spectrophotometer (Shimadzu, Japan). Growth was recorded against a reference. At 12, 24, 120, 168, and 240 h, 100-ml aliquot from each flask was withdrawn and pelleted by centrifugation at 6,000*g* for 10 min. Both pellet and supernatant were stored at 4°C and were analyzed for the presence of Cd through inductively coupled plasma atomic emission spectroscopy (ICP-AES).

Identification of Potential Cadmium-Tolerant Isolate BB12

Total genomic DNA was extracted using the CTAB method (Wilson, 2001). Primers pA (5′AGAGTTTGA TC CTGGCTCAG3′) and pH (5′AAGGAGGTGATCCAGCCG CA3′) were used for the amplification of 16S rDNA (Edwards et al., 1989). A 25-μl reaction mixture was prepared using 1.0 μl of 100-pM forward and reverse primers, deoxynucleoside triphosphate (DNTP) (200 nM), and 2 μl of 100-ng template. The amplification conditions were as follows: initial denaturation of 5 min at 94°C followed by 40 cycles of 40 s at 94°C, 40 s at 53°C, and 1 min and 30 s at 72°C, and a final extension period of 7 min at 72°C. The nucleotide sequences were dideoxy cycle sequenced with fluorescent terminators (Big Dye, Applied Biosystems) and run in 3130xl Applied Biosystems ABI prism automated DNA sequencer. Sequence alignment and comparison were performed using the multiple sequence alignment program CLUSTAL W (Thompson et al., 1994). The phylogenetic tree was reconstructed on the aligned datasets using neighbor joining (NJ) by Saitou and Nei's (1987) method in MEGA 6 program (Tamura et al., 2013). Bootstrap analysis was performed as described by Felsenstein (1985) on 1,000 random samples taken from the multiple alignments. Partial 16S rRNA gene sequence of the bacterium was submitted to NCBI GenBank, and well-characterized strain was submitted to ICAR-National Agriculturally Important Microorganisms Culture Collection (NAIMCC), Mau, India.

Scanning Electron Microscopy and Fourier Transform Infrared Analysis of the Isolate BB12

The changes in cell surface morphology of the bacterial isolate were observed under scanning electron microscopy (SEM) and Fourier transform infrared (FTIR) as described by Sodhi et al. (2020). The isolate BB12 was raised in NB amended with 25 mg L^{-1} of Cd concentration. Cells were visualized under scanning electron microscope as described by Hou et al. (2015). Bacterial cells were harvested and fixed in 2.5% glutaraldehyde solution for 4 h at 4°C following washing thrice in 0.1 M phosphate buffer (pH 7.4). Post-fixation was done by treating samples with 1% osmium tetraoxide for 2 h at 4°C and washing thrice again for 15 min. Specimens were dehydrated using increasing concentrations (30, 50, 70, 90, and 100%) of ethanol for 30 min each time to evacuate water. Specimens were air-dried, mounted on aluminum stubs with carbon tape, and observed under scanning electron microscope. The infrared (IR) spectrum was obtained from FTIR spectrometer (Thermo Scientific) using potassium bromide (KBr) pellets (Gola et al., 2018). Bacterial cells (100 mg) were washed and freeze-dried, and 1-mg grounded biomass was mixed with 99 parts of KBr. This mixture was mounted on KBr to make it in to pellet form. FTIR analysis of freshly prepared bacteria-KBr pellet was performed in between wavelength of 400 to 4,000 cm^{-1}.

Transmission Electron Microscopy Analysis of the Isolate BB12

For transmission electron microscopy (TEM) analysis, the isolate BB12 was grown (as in SEM analysis), and one drop of bacterial

cells was placed on carbon-coated grid, stained with 2% urinyl acetate, and was drained with Whatman filter paper and viewed under TEM (TEM Jeol 1011, Japan) 80 KVA (Jain and Bhatt, 2014). Each treatment was prepared in triplicate.

Antibiotic Resistance and Plant Growth-Promoting Traits in the Isolate BB12

Antibiotic resistance/susceptibility of the isolate BB12 was ascertained against 20 antibiotics, *viz*., Amikacin (30 μg), amipicillin (10 μg), amoxicillin (10 μg), cefoperazone (75 μg), cefadroxil (30 μg), ceftazidime (30 μg), ceftriaxone (30 μg), chloramphenial (30 μg), ciprofloxacin (5 μg), cloxacillin (1 μg), co-trimoxazale (25 μg), erythromycin (15 μg), gentamicin (10 μg), nalidixic acid (10 μg), netillin (10 μg), nitrofurantain (300 μg), norfloxacin (10 μg), penicillin (10 units), tobramycin (10 μg), and (30 μg). The culture of BB12 was plated onto a nutrient agar plate, and an antibiotic disc (Icosa 002, HiMedia Pvt., Ltd.) was placed over it. Subsequently, the plates were incubated at 30°C for 24 h to observe the bacterial tolerance against different antibiotics by measuring zone diameter.

The isolate BB12 was also screened *in vitro* for various PGP traits such as siderophore production by the CAS agar method and Universal Chemical Assay (CAS) by Schwyn and Neilands (1987) and Milagres et al. (1999); ammonia production by Cappuccino and Sherman (2014); phosphate solubilization (Nautiyal, 1999); IAA production by Gordon and Weber (1951) and Loper and Schroth (1986); and K solubilization on modified Aleksandrov medium plates by the spot test method (Sindhu et al., 1999). The impact of 0, 25, 50, and 75 mg L^{-1} Cd was tested on PGP activity of the isolate BB12.

Evaluation of Cadmium Toxicity Alleviation Ability of BB12 in Spinach

The effect of varying concentrations of Cd on spinach plants was studied in a pot trial in complete randomized design (CRD). Sandy loam textured soil was collected from non-contaminated fields, air-dried, sieved through a 2-mm mesh, and homogenized. A total of 5.0 kg of air-dried sterilized soil was placed in each pot. Three concentrations (25, 50, and 75 mg kg^{-1}) of Cd supplied in the form of $CdCl_2$ were mixed with soil and kept for a week to stabilize the mixture. The soil without metal treatments served as a control. Seeds were placed on a paper towel and were allowed to germinate, and further seed biopriming was done by treating seeds with 0.1% carboxymethylcellulose and freshly grown culture of BB12 having cfu > 10^8 ml^{-1}. Seeds were allowed to dry and sown in the pots containing soil having various concentrations of Cd. There were a total of four treatments, each having three replications. Pots were kept in the glasshouse and watered at regular intervals. In each pot, eight seeds were sown at a depth of 5 cm. After germination, five seedlings were maintained in each pot. Samples were withdrawn at different time intervals [i.e., 45 and 75 days after sowing (DAS)] and tested for physiological and biochemical attributes like chlorophyll (Chl) (Arnon, 1949), proline (Bates et al., 1973), and SOD (Beauchamp and Fridovich, 1971). To assess the impact of Cd content and Cd-tolerant bacteria on spinach, data on shoot length, shoot fresh and dry weight and root length, and root fresh and dry weight were recorded and were subjected to principal component analysis (PCA) and clustering analysis.

For estimation of Cd concentration, plants were harvested and roots and shoots were oven dried at 70°C for 48 h, powdered, and sieved through 2-mm mesh size. Residual Cd in dried shoot, root, and soil was estimated through ICP-OES. Translocation factor (TF) is the ability of plants to translocate heavy metal from root to shoot. Bioaccumulation factor (BAF) is expressed in terms of the ratio of Cd accumulated in shoot versus the content remained in the soil. TF and BAF were calculated using formulas given in Eqs 1, 2:

$$\text{Translocation factor(TF)} = \text{Cd concentration in shoot} / \text{Cd concentration in root} \quad (1)$$

$$\text{Bioaccumulation factor(BAF)} = \text{Cd concentration in shoot} / \text{Cd concentration in soil} \quad (2)$$

Statistical Analysis

Unless otherwise stated, all the experiments were performed in triplicate. The data from the experiments were subjected to the Analysis of Variance (ANOVA) using SPSS Statistics V 20.0 with Duncan's multiple range test (DMRT) at $p < 0.05$. Variation in the experimental data was expressed in terms of standard deviation (SD) and $p < 0.05$. PCA and cluster analysis was performed in PAST 4.03.

RESULTS

Heavy Metals Content in Soil and Water Samples

Upon estimation, the content of majority of heavy metals was found above their permissible limit set by WHO and Central Pollution Control Board (CPCB), India. An alarming contamination level of Cd, i.e., 11.48 and 11.19 mg kg^{-1}, was estimated in the sample collected from the Municipal Sewage Waste dumping site, Bhanpura, Bhopal (sample BB) and agricultural soil irrigated with Nag river water (sample MF1), respectively. Beside Cd contamination, the content of other heavy metals including Pb (1,716 mg kg^{-1}), Cr (156.92 mg kg^{-1}), and Co (58.98 mg kg^{-1}) was also recorded in the bulk soil of heavy metal–contaminated site of Bhanpura, Bhopal (BB). Although the river of water of Nag contained low quantity of heavy metals except for Pb, the samples collected from the river irrigated soils of Nagpur, Maharashtra, India, showed high heavy metal content (**Supplementary Table 1**).

Morphological Features of the Bacterial Isolates

For all the 45 bacteria isolated from the contaminated sites, the optimum growth temperature was found to be 37°C, and the optimum time ranged from 12 to 48 h. The colony color ranged

from white to yellow to brown; the shape of the colony was mostly round with pointed at end; irregular and colony thread-like size ranged from 0.01 to 1 cm; surface smooth or rough and elevation was either flat or convex or raised.

Heavy Metal Tolerance Using Minimum Inhibitory Concentration Test

Eight bacterial isolates exhibiting MIC for Cd in the range of 50–150 mg L^{-1} were selected for further studies (**Supplementary Table 2**). MIC of the isolates against eight other heavy metals, *viz*., Pb^{+2}, Ni^{+2}, Cr^{+3}, Hg^{+2}, Cu^{+2}, Zn^{+2}, Co^{+2}, and As^{+2}, was found to be in the range of 250–1,100 mg L^{-1} for As; 200–1,000 mg L^{-1} for Pb; 70–150 mg L^{-1} for Co; 200 mg L^{-1} for Cu; 100–500 mg L^{-1} of Cr; 100 mg L^{-1} for Hg; 100–150 mg L^{-1} for Ni; and 100–400 mg L^{-1} for Zn (**Supplementary Table 2**). Among all the isolates, BB12 was found to have highest MIC value (150 mg L^{-1}) against Cd, and therefore, it was selected for further studies with this heavy metal.

Identification of BB12 Isolate

On the basis of 16S rRNA gene sequence analysis, potential Cd-tolerating bacterium BB12 was identified as *Ochrobactrum intermedium* BB12 (**Figure 1**). The sequence was deposited in GenBank with accession number KY454689. The culture was submitted to National Depository ICAR-NAIMCC, Mau, India, with the accession number NAIMCC-B-02114.

Bioremediation Character of Cadmium-Tolerant *Ochrobactrum intermedium* BB12

A biosorption study with the BB12 bacterial isolate was conducted by growing the bacterium in the Cd-containing media. With the help of ICP-AES analysis, it was possible to trace the pellet and supernatant for the Cd concentration at different time intervals of growth. Decreased Cd concentration in the supernatant but increased content in the corresponding cell pellet clearly indicated a possible mechanism of biosorption or bioaccumulation for Cd tolerance in the bacterium BB12. The highest level of Cd was observed in the pellets of BB12 (435.0 ± 1.00 mg kg^{-1}) after 240 h of inoculation showing the biosorption potentials of these isolates (**Supplementary Table 3**). This prompted us to further evaluate the mechanism of biosorption in the bacterium.

Scanning Electron Microscopy and Fourier Transform Infrared Analysis of *Ochrobactrum intermedium* BB12

Scanning electron microscopy results indicated that the cells of *O. intermedium* BB12 without Cd were healthy with an average diameter of 1.48 ± 0.11 μm × 0.433 ± 0.01 μm. When grown with Cd-stressed condition, cell size was approximately 1.40 ± 0.11 μm × 0.414 ± 0.01 μm as observed under SEM. Cell surface deposition of Cd could be observed by the presence of a thick layer and distorted cell wall in the presence of Cd (**Figures 2A,B**).

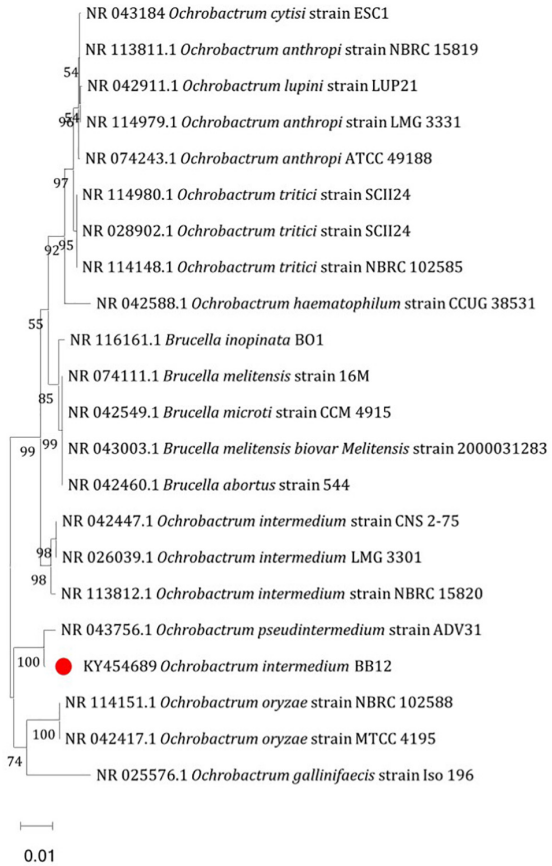

FIGURE 1 | Neighbor-joining tree based on 16S rRNA sequence of heavy metal–tolerant bacteria *Ochrobactrum intermedium* BB12 by MEGA 6. The bars that corresponded to 0.01 substitutions per nucleotide position were indicative of scales of genetic distances. The numbers at branching nodes indicated the levels of bootstrap support (% of 1,000 replications); only those values above 50% are given.

The interaction between bacterial cell wall and Cd was assessed by FTIR analysis. The FTIR spectrum was recorded from 400 to 4000 cm^{-1}, which indicated that the Cd-treated *O. intermedium* BB12 revealed peaks at 1,662.3 and 1,537.3 cm^{-1}, which were mainly attributed to the amide (I and II). The bands in non-treated cells had shifted to 1,654.9 and 1,539.8 cm^{-1}, respectively. In Cd-treated cells, there was appearance of a peak at 3,548.7 cm^{-1} and shifting of 3,272.5, 3,078.2, and 2,924.9 to 3,280.4, 3,074.3, and 2,925.5 cm^{-1} that generally correspond to interaction with hydroxy and amino moieties of cell surface. Shifting of peaks at 1,450.6, 1,389.0, and 1,066.9 to 1,452.5, 1,394.9, and 1,076.0 cm^{-1}, respectively, on exposure to Cd was also observed (**Figures 3A,B**).

Transmission Electron Microscopy Analysis of *Ochrobactrum intermedium* BB12

Ochrobactrum intermedium colonies raised in the absence and presence of Cd (25 mg L^{-1}) were subjected to the examination under TEM for the possible accumulation of Cd.

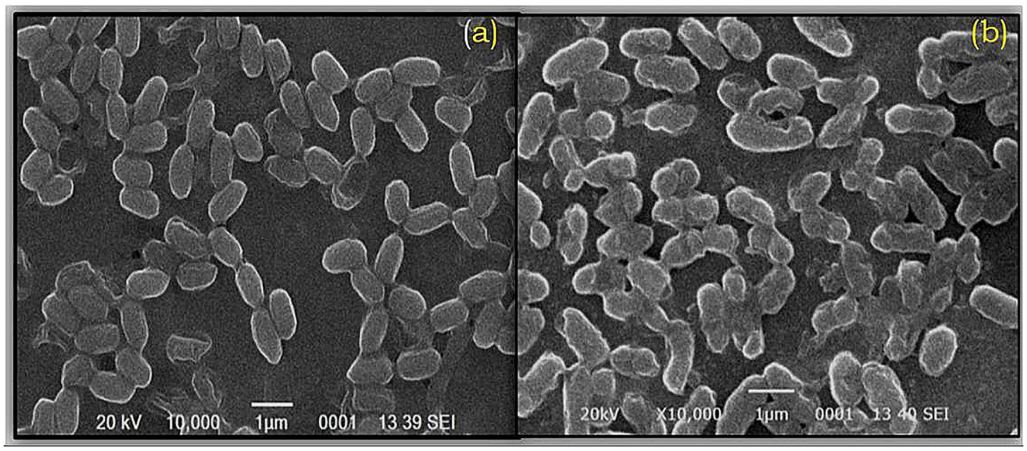

FIGURE 2 | Scanning electron microscopy (SEM) of *Ochrobactrum intermedium* BB12 grown in **(a)** nutrient broth (control condition) and **(b)** nutrient broth amended with 25 mg L^{-1} Cd concentration (magnification × 10,000; 20 kV).

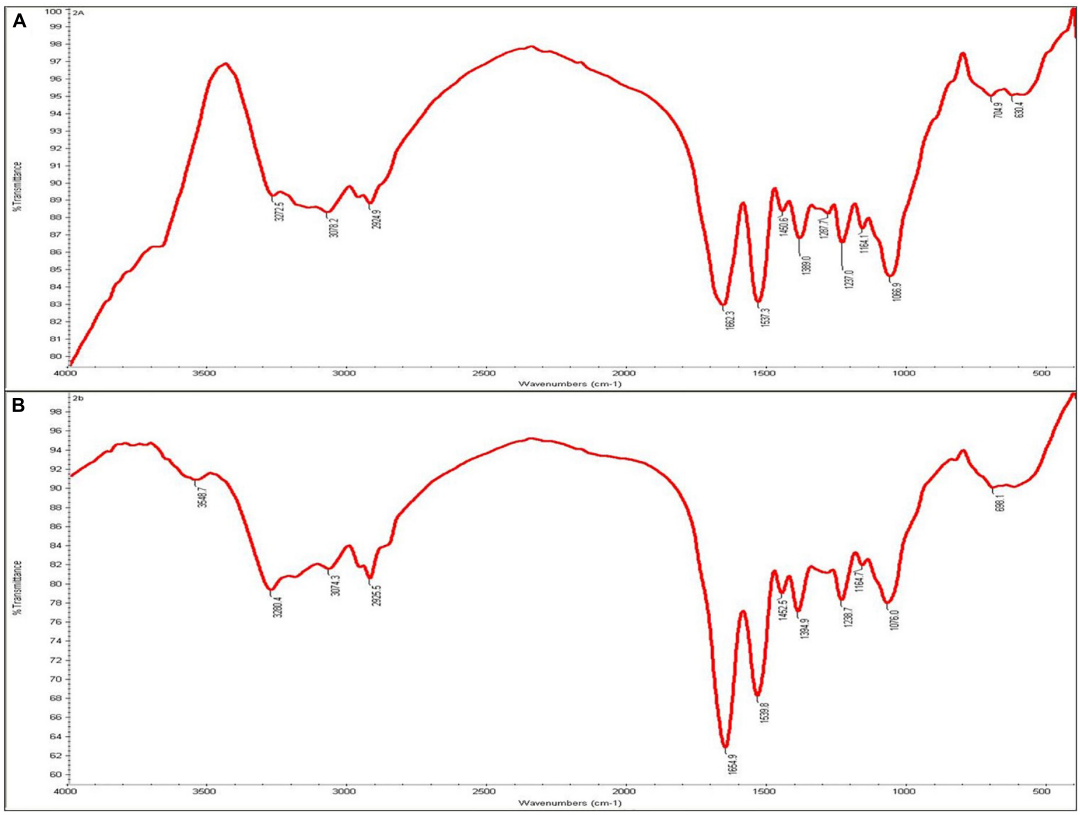

FIGURE 3 | Infrared spectra of **(A)** *Ochrobactrum intermedium* BB12 grown in nutrient broth (control) and **(B)** media amended with 25 mg L^{-1} Cd concentration.

Unstained bacterial preparation of in Cd control showed a clear homogenous cell cytoplasm with only a few tiny electron dense structures around the cell (**Figures 4A,B**). In contrast, the transmission electron micrograph of Cd-stressed bacterial cells exhibited opaque, electron dense area near the periphery of cells, clearly indicating the accumulation of Cd.

Evaluation of Antibiotic Resistance and Plant Growth-Promoting Traits in *Ochrobactrum intermedium* BB12

Ochrobactrum intermedium BB12 was found to be resistant to amipicillin, amoxicillin, cefadroxil, ceftazidime, ceftriaxone, cloxacillin, nitrofurantoin, penicillin, and vancomycin and

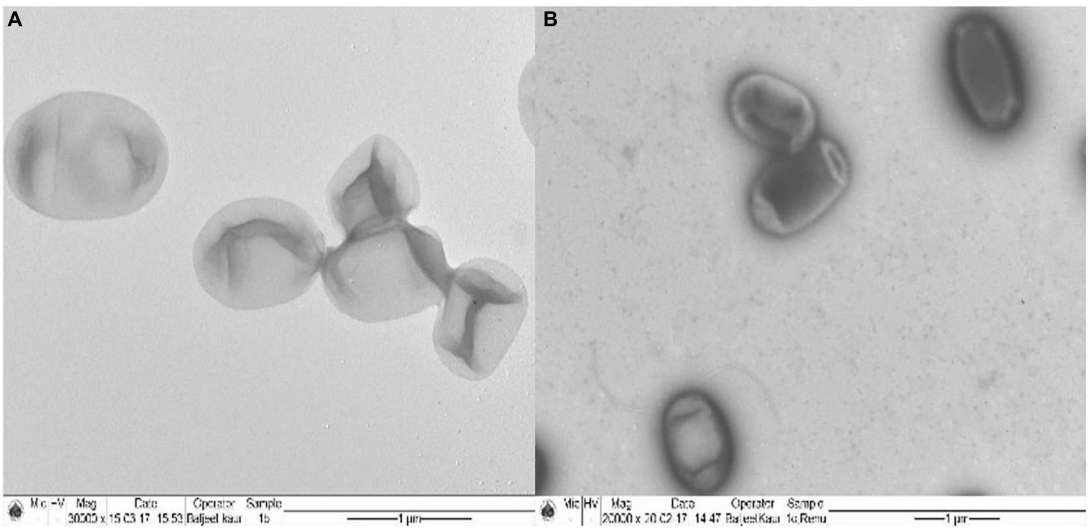

FIGURE 4 | Transmission electron micrograph of **(A)** *Ochrobactrum intermedium* BB12 grown in **(A)** nutrient broth (control) (magnification, ×30,000) and **(B)** in media containing 25 mg L^{-1} Cd concentration (magnification, ×20,000).

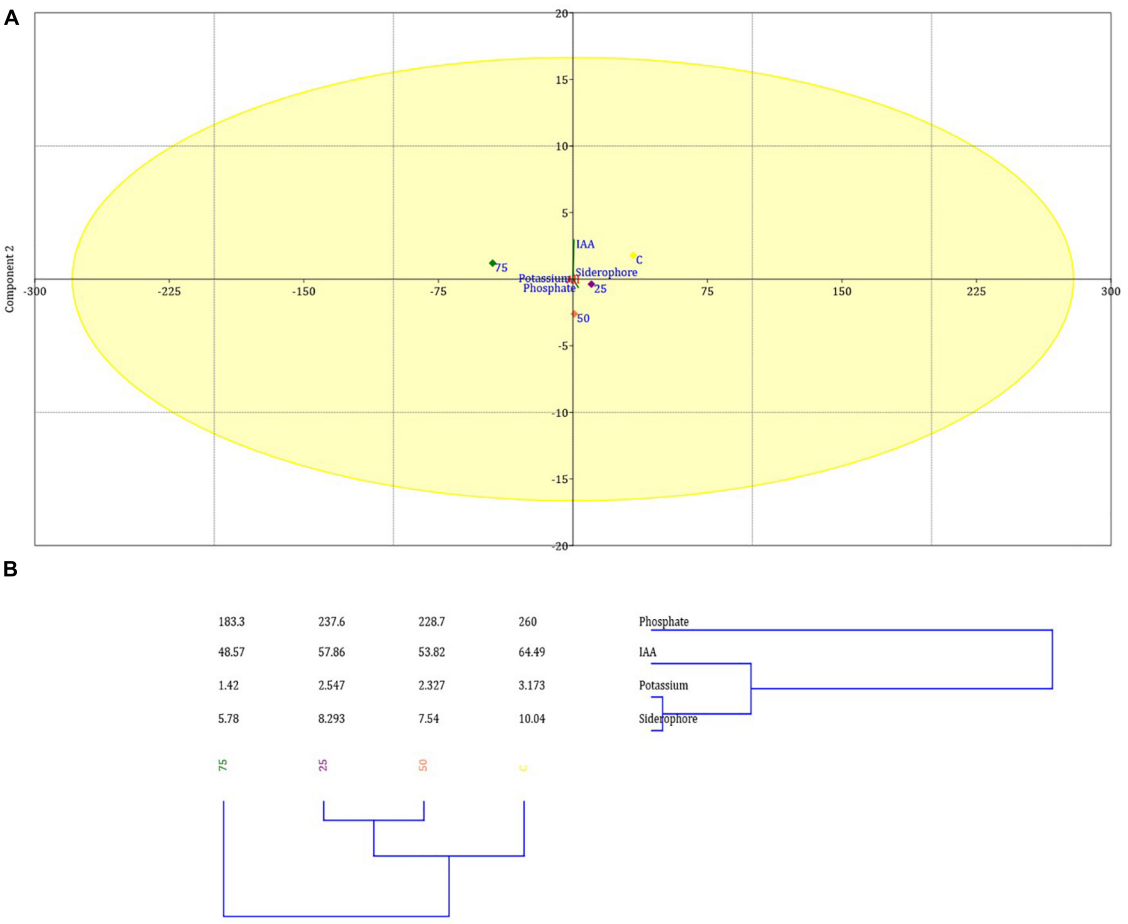

FIGURE 5 | Principal component analysis **(A)** and clustering analysis **(B)** showing the impact of 25, 50, and 75 mg L^{-1} Cd concentration on various PGP traits of *O. intermedium* BB12 in the culture media. Mean of PCA-axis values ± SD ($n = 3$, $p < 0.05$).

TABLE 1 | Effect of *Ochrobactrum intermedium* BB12 on growth parameters of spinach plants under 25, 50, and 75 mg kg^{-1} Cd content at 45 and 75 days after sowing (DAS).

Growth parameters	DAS	T1	T2	T3	T4	T5	T6	T7
Number of leaves	45	3.67 ± 0.2^{a}	3.67 ± 0.2^{a}	4.00 ± 0.2^{a}	3.33 ± 0.2^{a}	4.00 ± 0.0^{a}	3.33 ± 0.2^{a}	3.67 ± 0.23^{a}
	75	8.00 ± 1.00^{ab}	6.67 ± 0.33^{b}	9.67 ± 0.88^{a}	8.00 ± 1.00^{ab}	10.00 ± 0.58^{a}	7.00 ± 0.33^{b}	10.00 ± 0.67^{a}
Root length (cm)	45	5.33 ± 0.88^{d}	6.33 ± 0.88^{d}	7.33 ± 0.33^{c}	8.33 ± 0.33^{bc}	11.33 ± 0.33^{a}	9.67 ± 0.88^{ab}	10.33 ± 0.88^{ab}
	75	6.67 ± 0.67^{ab}	10.33 ± 0.33^{c}	12.00 ± 1.15^{a}	10.67 ± 1.67^{bc}	10.00 ± 0.58^{ab}	11.00 ± 1.00^{bc}	8.83 ± 0.93^{ab}
Shoot length (cm)	45	14.33 ± 1.18^{abc}	15.67 ± 1.16^{c}	18.33 ± 1.19^{a}	15.67 ± 1.19^{b}	19.00 ± 1.28^{a}	15.00 ± 1.20^{b}	18.00 ± 1.29^{a}
	75	47.33 ± 0.67^{a}	36.33 ± 0.88^{c}	43.33 ± 0.88^{b}	32.67 ± 0.33^{d}	47.00 ± 1.00^{a}	35.33 ± 0.88^{c}	36.67 ± 0.88^{c}
Root fresh weight (g)	45	0.30 ± 0.06^{c}	$0.36 \pm 0.06b^{c}$	0.41 ± 0.01^{bc}	0.38 ± 0.04^{bc}	0.51 ± 0.08^{ab}	0.53 ± 0.03^{ab}	0.62 ± 0.07^{a}
	75	0.31 ± 0.4^{c}	0.72 ± 0.16^{ab}	1.01 ± 0.24^{a}	0.73 ± 0.09^{ab}	1.26 ± 0.23^{a}	0.86 ± 0.08^{ab}	1.13 ± 0.15^{a}
Shoot fresh weight (g)	45	$6.17 \pm 0.50a^{3}$	6.27 ± 1.63^{a2}	6.37 ± 0.79^{a1}	4.60 ± 0.06^{a6}	4.60 ± 0.52^{a5}	4.20 ± 1.00^{a7}	5.70 ± 0.21^{a4}
	75	10.70 ± 0.90^{a}	9.03 ± 1.07^{bc}	9.47 ± 0.77^{ab}	7.27 ± 0.79^{bc}	9.33 ± 0.33^{abc}	8.10 ± 1.15abc	6.67 ± 0.13^{c}
Root dry weight (g)	45	0.23 ± 0.05^{b}	0.25 ± 0.04^{b}	0.32 ± 0.03^{ab}	0.30 ± 0.09^{ab}	0.38 ± 0.09^{ab}	0.31 ± 0.03^{ab}	0.46 ± 0.17^{a}
	75	0.20 ± 0.02^{d}	0.31 ± 0.12^{cd}	0.52 ± 0.23^{bcd}	0.50 ± 0.18cd	0.86 ± 0.27^{d}	0.61 ± 0.16^{abc}	0.84 ± 0.17^{ab}
Shoot dry weight (g)	45	2.13 ± 0.58^{c}	3.67 ± 0.25^{ab}	4.07 ± 0.30^{a}	3.60 ± 0.20^{ab}	4.10 ± 0.10^{a}	3.37 ± 0.20^{b}	4.00 ± 0.20^{a}
	75	2.67 ± 0.31^{bc}	3.37 ± 0.84^{ab}	3.63 ± 0.76^{ab}	2.73 ± 0.23^{abc}	3.13 ± 0.50^{ab}	2.00 ± 0.66^{c}	3.77 ± 0.31^{a}

Values are the means (±SD) of three replicates; within the same row with different letters, values are significantly different at $p \leq 0.05$ in DMRT.
SD, standard deviation.
"a" stands for highest variation, followed by "b" and lowest by "d" from the experimental control; T1, control without Cd and Ochrobactrum intermedium BB12; T2, T4, and T6, Cd control at 25, 50, and 75 mg kg^{-1} Cd, respectively, without O. intermedium BB12 inoculation; T3, T5, and T7, O. intermedium BB12-treated plants under 25, 50, and 75 mg kg^{-1} Cd stress, respectively.

susceptible to amikacin, cefaperazone, chloramphenial, ciprofloxacin, co-trimoxazole, erythromycin, gentamicin, nalidixic acid, netillin, norfloxacin, and tobramycin (**Supplementary Table 4**).

Ochrobactrum intermedium BB12 was also screened *in vitro* for various PGP traits and was found positive for siderophore and IAA production and P and K solubilization (**Supplementary Table 5**). The relationship between test variables, *viz.*, indole acetic acid (IAA), siderophore, phosphate, and potassium against 0, 25, 50, and 75 mg kg^{-1} Cd content, was shown to be Cd concentration dependent as reflected in the PCA and clustering analysis of PGP traits (**Figures 5A,B**). Higher Cd concentration diminished the PGP attribute. The first two PCs have explained >80% variance of the data (**Supplementary Table 6**). It was observed that the first component contributed most in IAA, potassium, and siderophore production, whereas the second one contributed mostly in the P solubilization. The percent of PC1 was 99.645 followed by PC2 0.35422.

Evaluation of *Ochrobactrum intermedium* BB12 on Alleviation of Cadmium Toxicity in Spinach

The exposure of various levels of Cd resulted in the growth retardation. Delay in the growth and development of Cd-stressed spinach plants was observed as compared to the control. All the seeds irrespective of various levels of Cd treatment germinated after 18 DAS, whereas in the control without *O. intermedium* BB12 treatment and without Cd stress, seeds germinated after 10 DAS. In bacteria-amended soil, the seed germination was recorded after 10–14 DAS. It was, therefore, speculated that *O. intermedium* helped in reducing the time of seed germination in the Cd-treated soil.

The treatment of 25 mg kg^{-1} of Cd in the soil significantly reduced the shoot length and shoot fresh weight but root length and root fresh weight were increased. On the other hand, root length and fresh weight in Cd-treated and bacterium-augmented plants were also higher than the control plants but less than only Cd-treated plants. There was decrease in shoot fresh weight, *viz.*, 9.03 ± 1.07, 7.27 ± 0.79, and 8.10 ± 1.15 gm in plants under 25, 50, and 75 mg kg^{-1} Cd content, respectively, in comparison to control (10.70 ± 0.90 gm). The application of bacteria increased the growth parameters like the number of leaves, root and shoot length, and fresh and dry weight of root and shoot observed at different days of sowing at different concentrations of Cd as compared to plants growing in Cd stress without bacterial treatment (**Table 1**). The presence of bulgy roots exhibits the ability of plants to counter heavy metal stress in bacteria-augmented plants under heavy metal stressed plants (**Figure 6**). In comparison to the plants grown in normal soil (control) (**Figure 6A**), those exposed to 50 mg kg^{-1} Cd concentration were reduced drastically in growth, but when the soil containing the same Cd concentration was inoculated with the bacteria, plant growth showed significant revival (**Figure 6C**). The PCA analysis suggested that Cd treatment (25, 50, and 75 mg kg^{-1}) severely affected the growth parameters of plants (**Figure 7A**). For the observed impact of BB12 on the reduction of Cd uptake and physiological growth of spinach at 0, 25, 50, and 75 mg kg^{-1} of Cd, PC1 showed the % variance of 90.97% followed by PC2 8.8299 (**Supplementary Table 7**). It was observed that soil treatment with the bacteria BB12 exhibited improved plant growth against respective Cd concentrations. Cd25 + BB12 and Cd50 + BB12 treatments performed well although not much significant growth was observed in Cd75 + BB12 treatment, possibly because high concentration of metal restricted the growth. Further cluster analysis (**Figure 7B**) also strengthened these observations and

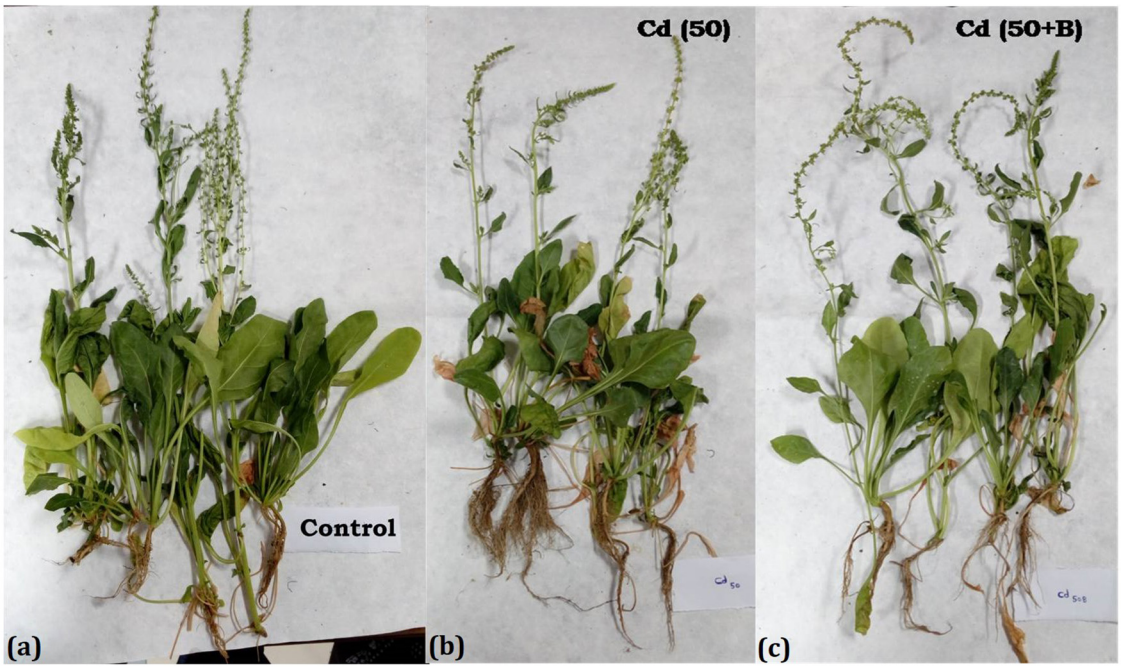

FIGURE 6 | Growth of spinach in the soil treated with Cd and amended with the *Ochrobactrum intermedium* BB12 at 75 DAI. **(a)** Control: plants grown in the soil without any treatment; **(b)** Cd50: plants grown in soil containing 50 mg kg^{-1} Cd; and **(c)** Cd50 + B: plants grown in the soil containing 50 mg kg^{-1} Cd and inoculated with *O. intermedium* BB12.

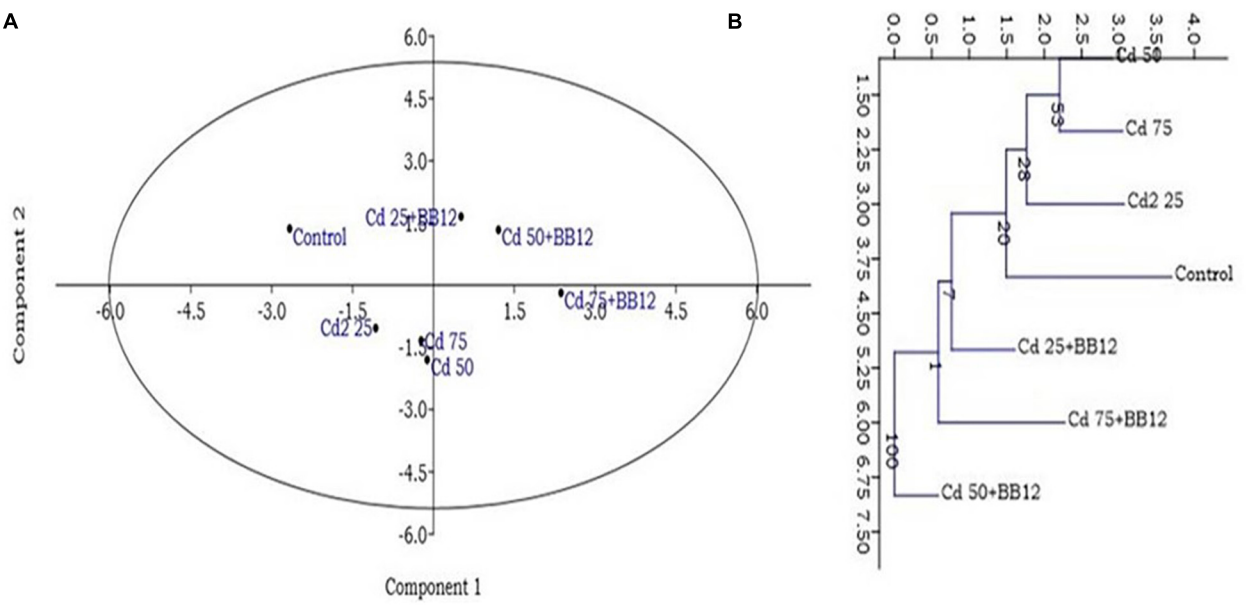

FIGURE 7 | Principal component analysis (PCA) **(A)** and clustering analysis **(B)** showing the impact of 25, 50, and 75 mg kg^{-1} Cd concentration on the spinach plants grown in the soil containing Cd as compared to normal soils with no Cd concentration. Mean of PCA-axis values ± SD ($n = 3$, $p < 0.05$).

suggested that reduced growth parameters are proportional to Cd concentration in the soil.

The physiology of spinach plant was also altered under Cd stress condition. Chl content revealed the changes in the amount of pigment in expanding leaves at different concentrations of Cd. Chl-a concentration was significantly lower than that of Chl-b in plants. The pigment content in plants showed almost linear decrease in response to increase in Cd concentration in the soil. At 75 DAS, total Chl content (74.36 ± 3.16, 89.91 ± 3.55, and 70.54 ± 2.91 μg g^{-1}) of plants under various levels of Cd stress

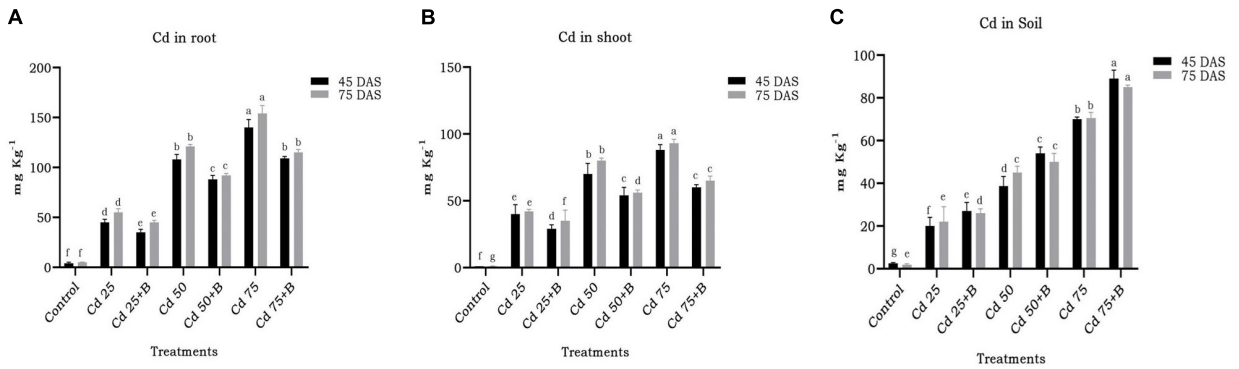

FIGURE 8 | Effect of the application of *Ochrobactrum intermedium* BB12 on the uptake of Cd by the root **(A)** and shoot **(B)** of spinach plants grown in the soil containing 25 (Cd25), 50 (Cd50), and 75 (Cd75) mg kg^{-1} metal concentration at 45 and 75 days of sowing (DAS). Cd content in the soil measured at the same time interval is shown in panel **(C)**. B denotes the treatment containing bacteria *O. intermedium*. Values are the means (±SD) of three replicates; within the same column with different letters, values are significantly different at $p \leq 0.05$ in DMRT. SD, standard deviation. "a" stands for highest variation, followed by "b" and lowest by "f" from the experimental control.

(25, 50, and 75 mg kg^{-1}, respectively) was found to be lower and in decreasing order of Cd content in comparison to control (88.31 ± 4.57 μg g^{-1}). On the other hand, the total Chl content of 77.17 ± 4.43, 93.23 ± 4.97, and 78.97 ± 3.53 μg g^{-1} in the plants grown in the soil containing 25, 50, and 75 mg kg^{-1} Cd content, respectively, with bacterial inoculation indicated reduced impact of the Cd stress (**Supplementary Table 8**). Proline content was found to increase with increase in the level of Cd content, whereas bacteria treatment in the soil lowered down the proline content in Cd-stressed plants. At 45 DAS, proline content in the control plants (without Cd) was recorded as 0.63 ± 0.04 μmole g^{-1}, which increased with the increase in Cd content (1.44 ± 0.27, 1.80 ± 0.05, and 1.89 ± 0.27 μmole g^{-1}). In bacteria-amended plants, proline content was lowered down to 0.76 ± 0.02, 0.92 ± 0.04, and 1.09 ± 0.23 μmole g^{-1} at 45 DAS at 25, 50, and 75 mg kg^{-1}, respectively (**Supplementary Table 8**). Soil inoculation with the bacteria lowered down the proline content in the plants as compared to those growing in the soil with Cd only. A similar trend was observed in the case of SOD enzyme production also.

Biopriming of spinach seeds with *O. intermedium* BB12 led to statistically significant reduction in the uptake of Cd in different plant parts (**Figure 7**). In general, there was more accumulation of Cd in roots than shoots (**Figure 8**). In BB12-treated plant at 45 DAS, there was 22.22, 18.51, and 22.14% reduction, and, at 75 DAS, there was 18.18, 23.96, and 25.32% reduction of Cd uptake in roots in plants grown in soil amended with 25, 50, and 75 mg kg^{-1} Cd, respectively, as compared to without BB12-treated plants. Similarly, at 45 DAS, there was 27.5, 22.85, and 31.81% reduction, and, at 75 DAS, there was 16.66, 30, and 30.10% reduction of Cd uptake in shoots in the plants grown in soil amended with 25, 50, and 75 mg kg^{-1} Cd, respectively. Cd accumulation was 35, 39.53, and 27.14% more at 45 DAS and 18.18, 11.11, and 13.21% more at 75 DAS in 25, 50, and 75 mg kg^{-1} Cd-amended soil, indicating direct support of bacterial biopriming for the plants.

Translocation of Cd from root to shoot decreased due to bacterial inoculation but only at limited level. The effect of inoculation of BB12 was significant at 50 and 75 mg kg^{-1} Cd in reducing the translocation in comparison to the plants with Cd treatment only. The observed effect at 45 and 75 DAS was almost the same, thus indicating no impact of the time interval in translocation (**Figure 9A**). Bacterial inoculation resulted in bioaccumulation of Cd in the soil in which bacteria had significant effect at 50 and 75 mg kg^{-1} Cd in the soil at 45 and 75 DAS. Even at the higher dose of 75 mg kg^{-1} Cd, BB12 influenced Cd bioaccumulation in the soil to a greater extent (**Figure 9B**).

Ochrobactrum intermedium BB12 Population in the Rhizospheres

Bacterial population in the rhizosphere of spinach was tested as CFU count at 35, 45, and 75 days of inoculation. At 75 days, the CFU count of BB12 was 4.3×10^5, 4.0×10^5, and 3.4×10^5 cfu g^{-1} rhizosphere soil, respectively, in 25, 50, and 75 mg kg^{-1} Cd-amended soil, indicating relatively lesser effect at different levels of Cd content in the soil on bacterial population.

DISCUSSION

Presence of heavy metals in the soils and high accumulation in plant parts resulted in retarded growth of several crop plants (Yadav, 2010; Chibuike and Obiora, 2014). Microorganisms tolerant to stress due to heavy metals can bioremediate soils with metal contamination (Ojuederie and Babalola, 2017). Similarly, their inoculation in the rhizosphere not only can help in alleviating the effect of metal stress in plants but also can support growth and development to a greater extent (Rajkumar et al., 2010). We have identified a bacterium having various PGP traits like siderophore and phytohormone production and P solubilization to hold Cd tolerance potential. The bacterial isolate BB12 obtained from a heavy metal–contaminated site in

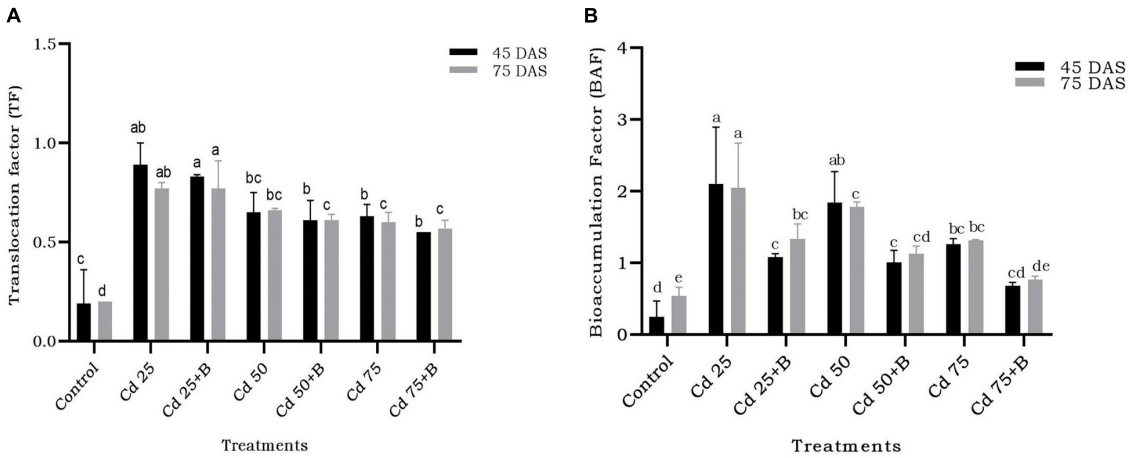

FIGURE 9 | Effect of the application of *Ochrobactrum intermedium* BB12 on **(A)** translocation factor and **(B)** bioaccumulation factor of Cd by spinach plants grown in the soil containing 25 (Cd25), 50 (Cd50), and 75 (Cd75) mg kg^{-1} Cd content at 45 and 75 DAS. Values are the means (±SD) of three replicates; within the same column with different letters, values are significantly different at $p \leq 0.05$ in DMRT. SD, standard deviation. "a" stands for highest variation, followed by "b" and lowest by "e" from the experimental control.

India was identified as *O. intermedium*. Although the species of the genus *Ochrobactrum* in general has been reported as opportunistic human pathogens of low virulence in humans (Ryan and Pembroke, 2020) and the species *O. intermedium* was implicated in a single case of liver infection (Wisplinghoff, 2017), these soil organisms possess multiple traits too. Several species have been investigated for their potential as biodegrader of xenobiotic compounds and detoxifier of heavy metals in a variety of environmental conditions (El-Sayed et al., 2003; Sultan and Hasnain, 2007). The bacterium has also been characterized to possess plant growth promotional traits and biofertilizer potential (Sharma et al., 2016). We have examined multiple traits of agricultural importance of the isolate BB12, which showed promise not only in plant growth promotion but also in the bioremediation of the soils contaminated with the heavy metals. All these multiple traits along with the ability to withstand high concentrations of Cd metal in the soils owe ecological stability to the organism to stand in the unfavorable conditions as well, thereby offering plants better protection against metal stresses. Besides Cd, the identified isolate has also shown tolerance against arsenic, chromium, cobalt, lead, and nickel, thereby indicating multi-metal tolerance and that also up to different limits of high concentration. Such organisms could be a better choice in the search of microbial inoculants as bioremediaters of metal-contaminated environmental sites.

Batch culture studies with tolerant strains inoculated in Cd-amended broth over a period of 10 days revealed the differential accumulation of Cd in the cell pellet and the supernatant. In general, the higher Cd concentration in the bacterial cell pellets as compared to that in the culture supernatant suggested that the mechanism of tolerance may either be the adsorption of Cd on cell surface or the bioaccumulation. Several studies have reported biosorption and intracellular accumulation as the two primary mechanisms of heavy metal tolerance in bacteria (Lu et al., 2006; Rajesh et al., 2014; Hou et al., 2015). The co-existence of heavy metal and antibiotic resistance in bacteria has been explained (Chen et al., 2019). Kaur et al. (2018) described that increased Cd concentration altered the susceptibility of bacterium against ampicillin, cefizoxime, chloramphenicol, and ciprofloxacin in *Salmonella enterica* and caused simultaneous morphological, biochemical, and physiological changes. Similar observation was also reported by Nath et al. (2019) who isolated heavy metal–tolerant bacteria from the industrial region with resistance to penicillin, ampicillin, vancomycin, co-trimoxazole, etc. Therefore, our observation on the simultaneous tolerance against Cd and resistance against several antibiotics in BB12 is in accordance with the earlier reports.

Scanning electron microscopy studies on *O. intermedium* revealed the distortions and changes in the cell morphology with bulging of the cell surface. The bulging could be due to high exopolysaccharide production under Cd stress as compared to control. Sultan et al. (2008) reported that the cell surfaces of cultures treated with Cd chloride tended to be rough, suggesting that the cell increased its surface to improve the interaction of toxic substances with the cell surface. El-Helow et al. (2000) and Sinha and Mukherjee (2009) demonstrated that *Bacillus* sp. contains cell wall components such as epoxypolysaccharides (EPS), teichoic and teichuronic acids or phospholipid layers, and functional groups can be responsible for the heavy metal bioremediation through the secretion of extracellular substances. Zhang et al. (2019) reported that, in *B. cepacia* GYP1, although there was distortion in the cell structure due to heavy metal toxicity, the integrity of cells remained intact. Similar to our observation, the authors have also emphasized that the accumulation of Cd was mainly on the outer membrane surface at the beginning, whereas the intracellular Cd intake increased and held stable after 2 days. Afterward, the increased amount of Cd was mainly located extracellular and was related to the secreted EPS. Our results on TEM of *O. intermedium* could reveal the

intracellular sites of Cd accumulation. High density of electron was observed in periplasmic space of the cells, whereas some deposition was also seen in the cytosol and toward cell envelop. This has indicated that the Cd was also deposited within the bacterial cells. Intracellular deposition of Cd by TEM in various bacterial strains has already been reported (Vicentin et al., 2018; Zhang et al., 2019). Therefore, both the SEM and the TEM results strongly suggested that the bacteria possess the capability to withhold the Cd metal as extracellular deposition on its cell surface, and it can also deposit the metal in intracellular parts in the cytosolic region.

Fourier transform infrared analysis of cell surface provides a deep insight of functional groups on bacterial cell surface involved in the metal bacteria interaction. Negatively charged groups tend to bind positively charged heavy metal ion and *vice versa*. FTIR results showed that -COOH is the most active functional group involved in the cell–metal interaction. This was also previously reported by Pradhan and Sandle (1999) and Rajandas et al. (2012). The region from 3,700 to 3,300 cm^{-1} in IR spectra is characteristic of O-H and N-H stretching vibrations and 3,300–3,000 cm^{-1} of C-H stretching vibrations of C≡C, C=C, and Ar-H. The region from 3,000 to 2,700 cm^{-1} is dominated by the C-H stretching vibrations of $-CH_3$, $>CH_2$, CH, and CHO functional groups, respectively (Dumas and Miller, 2003; Guo and Zhang, 2004). In FTIR spectra of *O. intermedium* BB12, there was appearance of peak at 3,548.7 cm^{-1} and shifting of 3,272.5, 3,078.2, and 2,924.9 to 3,280.4, 3,074.3, and 2,925 in Cd-treated bacterial cells. Such shiftings could be attributed to O-H, N-H, and C-H stretching and thus indicated participation of hydroxyl and amino group in Cd interaction. It is interesting to note that –OH being negatively charged ion can have electrostatic interaction with the Cd ion easily. Shifting of peaks at 1,662.3 and 1,537.3 cm^{-1} to 1,654.9 and 1,539.8^{-1} cm, respectively, in Cd-stressed bacterial cells suggested the involvement of amino group in Cd^{2+} attachment. The region from 1,600 to 1,500 cm^{-1} is specific for amide-II bands, which is due to N-H bending vibrations (Fischer et al., 2006). The region between 1,700 and 1,600 cm^{-1} is specific for amide-I bands (Dumas and Miller, 2003), which is mainly due to C=O stretching vibrations of the peptide bond (Backmann et al., 1996). Similar results were also obtained with Cd-resistant *S. enterica* 43C, in which chemical interaction with Cd due to amide group of the bacterium was inferred due to the shift in peaks at 1,635 and 1,552 cm^{-1} (Khan et al., 2016).

The intensity and stretching of the peak clearly demonstrated the alteration in the functional groups associated with the cell surface and strongly indicated molecular bonding of the metal ion at the surface. This could be one of the strong possible mechanisms of Cd removal from the culture media, in which the bacterium was grown and caused less concentration of Cd in the supernatant and high concentration in the cell pellets. On the other hand, shifting of any peak in IR spectra also informs about the change in hybridization state of molecular bonding. There was also shifting of peaks at 1,450.6, 1,389.0, and 1,066.9 to 1,452.5, 1,394.9, and 1,076.0, respectively. The bands in the 1,500–1,200 cm^{-1} region arise mainly from the C-H bending vibrations of CH_3, CH_2, and CH functional groups. The region from 1200 to 900 cm^{-1} is mainly dominated by a sequence of bands due to C-O, C-C, C-O-C, and C-O-P stretching vibrations of polysaccharides (Wolkers et al., 2004; Yee et al., 2004) as well as CH_3 and CH_2 rocking modes by Wolpert and Hellwig (2006). In our study, shifting of peaks in the above regions can also be attributed to the binding of Cd to polysaccharides, either associated with the outer membrane or excreted EPS on the surface, as has been suggested by Alessi et al. (2014). Zhang et al. (2019) have reported organic functional groups, such as carboxyl, amino, and phosphoryl groups on cell wall or extracellular polymeric substances to be involved in the removal of Cd by complexation with *B. cepacia* GYP1. It was also observed that, in case of both strains, the percentage transmittance was lesser in Cd-treated bacteria than in control. According to Chakravarty and Banerjee (2012) due to the presence of Cd, stretching of bonds occurred to a lesser degree, resulting in reduction in their percentage transmittance. Similar observations were also recorded in the interaction of *S. enterica* 43C with Cd (Khan et al., 2016). Therefore, our observations are very well in accordance with those reported earlier.

The above findings of the laboratory suggested that Cd-tolerant PGP bacterium *O. intermedium* BB12 may influence the mobilization of Cd in the soil and could be a suitable choice for bioremediation purposes. To validate the effects of BB12 inoculation in spinach under varying concentrations of Cd, pot experiments were designed with the soils containing different content of Cd. Spinach is a well-known hyperaccumulator of various heavy metals including Cd (Alia et al., 2015). The Cd stress affected all studied plant growth attributes, which were improved due to the inoculation with BB12. These observations were parallel to the existing report on the PGP attributes of the genus *Ochrobactrum* (Sharma et al., 2016). Even under Cd treatment conditions, the observed improvement in the growth and development of plants may cumulatively be attributed to the PGP traits like siderophore and phytohormone production and P solubilization of the bacteria. Alternatively, the observed effect on plant growth may be linked with the ability of the bacteria to remove Cd from the plant rhizosphere, thereby minimizing the exposure of roots with the heavy metal. This may also be resulted due to the ability of bacterial association to induce intrinsic defense mechanisms in the plants against the metal to tolerate toxicity effects of the Cd. Several workers have studied the heavy metal toxicity alleviation using PGP bacteria possessing traits like P solubilization, nitrogen fixation, siderophore, and phytohormone production (Tiwari and Lata, 2018; Caracciolo and Terenzi, 2021). These attributes have stimulated shoot and root growth of plants in the presence of enhanced levels of heavy metal and thus helped them in overcoming metal stress. The identified isolate BB12, besides having Cd tolerance, was also found to be a phosphate solubilizer and siderophore and phytohormone producer, and these are the agriculturally important traits for any microorganism to support plant growth and development in the field conditions. It has been reported that contamination of soil with heavy metal results in iron deficiency in different plant species (Mishra and Kar, 1974; Römheld and Marschner, 1986; Wallace et al., 1992;

Ma and Nomoto, 1993; Burd et al., 2000; Gupta et al., 2018; El-Meihy et al., 2019) and causes inhibition of both chloroplast development and Chl biosynthesis, resulting in chlorosis in plants (Imsande, 1998). Microbial siderophore complexes with iron that can be taken up by plants help in iron acquisition (Reid et al., 1986; Bar-Ness et al., 1991; Wang et al., 1993). Hence, siderophore-producing bacteria could be a good choice for growing crops in the metal-contaminated soils to prevent plants from becoming chlorotic due to heavy metal impact. We also reported reduction in the Chl production in plants under Cd stress, but again, it was improved due to the application of bacterial inoculation.

Physiological parameters based on defense-related biomolecules and antioxidant enzymes were also found to affect plant growth and development during metal stress (Hasanuzzaman et al., 2020). In plants, stress induces production of reactive oxygen species (ROS), which are even more toxic to plant cells, and, for such reasons, bacteria accumulate stress-induced compounds like proline and antioxidant enzymes in the cells to rapidly reduce the load due to stresses (Sun et al., 2018). Proline serves as a plant-friendly metabolic osmolyte and does not sequester the contaminants but performs major functions to lower down the ROS production and restrict the role of GSH (Sharma et al., 2012). Similarly, during environmental stresses, ROS production increases causing high oxidative damage, which is controlled by these antioxidant enzymes like superoxide dismutase (SOD), which converts superoxide into H_2O_2. Altered activities of SOD have been reported as indicators of Cd stress in different plants (Foroozesh et al., 2012; Li et al., 2013). Increasing concentrations of Cd increased the proline production and SOD activity in spinach. However, in the presence of BB12, both proline production and SOD activity were decreased. This may be speculated due to the ability of BB12 to reduce the exposure of Cd stress to the plants. Reduced uptake of Cd was observed due to the inoculation of BB12. TF of bacteria-amended plant was found <1, thus indicating the low translocation. BAF is also greatly reduced in plants amended with Cd-tolerant bacteria. With the results, we realize that, owing to the Cd biosorption by the BB12 as indicated in *in vitro* tests, the minimized exposure of plant rhizosphere for the uptake of Cd up to such a level that could become toxic for plants has been restricted. In this way, the bacterium *O. intermedium* performed the role of microbial bioremediation to help spinach withstand with the metal stress. The study presents possibility of utilizing multi-trait microbial species like *O. intermedium* as inoculants for ensuring plant growth promotion in soils contaminated with heavy metals. Although, the occasional pathogenicity of *O. intermedium* may restrict its wide-scale direct application in the field conditions as bioremediator-cum-biofertilizer agent, as can be recommended for the bacteria with similar level agriculturally important traits, its high biosorption capability can be utilized for contained environmental applications to remediate highly heavy metal–contaminated sites. Alternatively, the immobilized cells of the bacteria BB12 on various low cost biosorbents can be applied for Cd remediation of contaminated sites and/or seed biopriming for supporting physiological growth of the plants as the ways of applications in industrial and agricultural fields.

DATA AVAILABILITY STATEMENT

The datasets presented in this study can be found in online repositories. The names of the repository/repositories and accession number(s) can be found in the article/ **Supplementary Material**.

AUTHOR CONTRIBUTIONS

SR and ASx conceived and designed the study. KS, MB, US, AG, and SR performed laboratory and pot experiments, SEM, and FTIR. BK performed TEM. ASh, AM, JT, and MM conducted Cd analysis of *in vitro* and pot experiment samples. DS and KS analyzed the data. SR, KS, DS, and ASx drafted the manuscript. All authors commented on the manuscript and made suggestions.

FUNDING

We were grateful to Indian Council of Agricultural Research (ICAR), Ministry of Agriculture and Farmers Welfare, Government of India, for financial support.

ACKNOWLEDGMENTS

Present research is a part of institutional project "Isolation and characterization of heavy metal–resistant bacteria and evaluation for their use in agriculture" funded by Indian Council of Agricultural Research (ICAR), Ministry of Agriculture and Farmers Welfare, Government of India. We are thankful to Head, USIC, BBAU Lucknow, for providing facility of SEM and FTIR analysis and the Head, Division of Plant Pathology, ICAR-Indian Agricultural Research Institute, New Delhi, for TEM analysis.

SUPPLEMENTARY MATERIAL

The Supplementary Material for this article can be found online at: https://www.frontiersin.org/articles/10.3389/fmicb.2021.758144/full#supplementary-material

REFERENCES

Alessi, D. S., Lezama-Pacheco, J. S., Stubbs, J. E., Janousch, M., Bargar, J. R., Persson, P., et al. (2014). The product of microbial uranium reduction includes multiple species with U (IV)-phosphate coordination. *Geochimi. Cosmochim. Acta* 131, 115–127. doi: 10.1016/j.gca.2014.01.005

Alia, N., Sardar, K., Said, M., Salma, K., Sadia, A., Sadaf, S., et al. (2015). Toxicity and bioaccumulation of heavy metals in spinach (*Spinacia oleracea*) grown in

a controlled environment. *Int. J. Environ. Res. Public Health* 12, 7400–7416. doi: 10.3390/ijerph120707400

Arnon, D. I. (1949). Copper enzymes in isolated chloroplasts, polyphenoloxidase in *Beta vulgaris*. *Plant. Physiol.* 24, 1–5. doi: 10.1104/pp.24.1.1

Ayangbenro, S. A., and Babalola, O. O. (2017). A new strategy for heavy metal polluted environments: a review of microbial biosorbents. *Int. J. Environ. Res. Public Health* 14:94. doi: 10.3390/ijerph14010094

Babu, A. G., Shea, P. J., Sudhakar, D., Jung, I. B., and Oh, B. T. (2015). Potential use of *Pseudomonas koreensis* AGB-1 in association with *Miscanthus sinensis* to remediate heavy metal(loid)-contaminated mining site soil. *J. Environ. Manage.* 151, 160–166. doi: 10.1016/j.jenvman.2014.12.045

Backmann, J., Schultz, C., Fabian, H., Hahn, U., Saenger, W., and Naumann, D. (1996). Thermally induced hydrogen exchange processes in small proteins as seen by FTIR spectroscopy. *Proteins Struct. Funct. Genet.* 24, 379–387. doi: 10.1002/(SICI)1097-0134(199603)24:3<379::AID-PROT11>3.0.CO;2-J

Bar-Ness, E., Chen, Y., Hadar, Y., Marschner, H., and Romheld, V. (1991). Siderophores of *Pseudomonas putida* as an iron source for dicot and monocot plants. *Plant Soil* 130, 231–281. doi: 10.1007/BF00011878

Bates, L. S., Waldren, R. P., and Teare, I. D. (1973). Rapid determination of free proline for water-stress studies. *Plant Soil* 39, 205–207. doi: 10.1007/BF00018060

Beauchamp, C., and Fridovich, I. (1971). Superoxide dismutase: improved assays and an assay applicable to acrylamide gels. *Anal. Biochem.* 44, 276–287. doi: 10.1016/0003-2697(71)90370-8

Burd, G. I., Dixon, D. G., and Glick, B. R. (2000). Plant growth-promoting bacteria that decrease heavy metal toxicity in plants. *Can. J. Microbiol.* 46, 237–245. doi: 10.1139/w99-143

Cappuccino, J. G., and Sherman, N. (2014). *Microbiology: A Laboratory Manual*, 10th Edn. London: Pearson.

Caracciolo, A. B., and Terenzi, V. (2021). Rhizosphere microbial communities and heavy metals. *Microorganisms* 9:1462. doi: 10.3390/microorganisms9071462

Chakravarty, R., and Banerjee, P. C. (2012). Mechanism of cadmium binding on the cell wall of an acidophilic bacterium. *Bioresource. Technol.* 1, 176–183. doi: 10.1016/j.biortech.2011.12.100

Chen, J., Li, J., Zhang, H., Shi, W., and Liu, Y. (2019). Bacterial heavy-metal and antibiotic resistance genes in a copper tailing dam area in northern China. *Front. Microbiol.* 20:1916. doi: 10.3389/fmicb.2019.01916

Chibuike, G. U., and Obiora, S. C. (2014). Heavy metal polluted soils: effect on plants and bioremediation methods. *Appl. Environ. Soil Sci.* 2014:752708. doi: 10.1155/2014/752708

Clemens, S., Aarts, M. G. M., Thomine, S., and Verbruggen, N. (2013). Plant science: the key to preventing slow cadmium poisoning. *Trends Plant Sci.* 18, 92–99. doi: 10.1016/j.tplants.2012.08.003

Das, P., Samantaray, S., and Rout, G. R. (1997). Studies on cadmium toxicity in plants: a review. *Environ. Pollut.* 98, 29–36. doi: 10.1016/S0269-7491(97)00110-3

Dey, U., Chatterjee, S., and Mondal, N. K. (2016). Isolation and characterization of arsenic-resistant bacteria and possible application in bioremediation. *Biotechnol. Rep.* 1, 1–7. doi: 10.1016/j.btre.2016.02.002

Dumas, P., and Miller, L. (2003). The use of synchrotron infrared microspectroscopy in biological and biomedical investigations. *Vib. Spec.* 32, 3–21. doi: 10.1016/S0924-2031(03)00043-2

Edwards, U., Rogall, T., Blöcker, H., Emde, M., and Böttger, E. C. (1989). Isolation and direct complete nucleotide determination of entire genes. Characterization of a gene coding for 16S ribosomal RNA. *Nucleic Acids Res.* 17, 7843–7853. doi: 10.1093/nar/17.19.7843

El-Helow, E. R., Sabry, S. A., and Amer, R. M. (2000). Cadmium biosorption by a cadmium resistant strain of *Bacillus thuringiensis*: regulation and optimization of cell surface affinity for metal cations. *Biometals* 13, 273–280. doi: 10.1023/A:1009291931258

El-Meihy, R. M., Abou-Aly, H. E., Youssef, A. M., Tewfike, T. A., and El-Alkshar, E. A. (2019). Efficiency of heavy metals-tolerant plant growth promoting bacteria for alleviating heavy metals toxicity on sorghum. *Environ. Exp. Bot.* 162, 295–301. doi: 10.1016/j.envexpbot.2019.03.005

El-Sayed, W. S., Ibrahim, M. K., Abu-Shady, M., El-Beih, F., Ohmura, N., Saiki, H., et al. (2003). Isolation and identification of a novel strain of the genus *Ochrobactrum* with phenol-degrading activity. *J. Biosci. Bioeng.* 96, 310–312. doi: 10.1016/S1389-1723(03)80200-1

Felsenstein, J. (1985). Confidence limits on phylogenies: an approach using the bootstrap. *Evolution* 39, 783–791. doi: 10.1111/j.1558-5646.1985.tb00420.x

Fischer, G., Braun, S., Thissen, R., and Dott, W. (2006). FT-IR spectroscopy as a tool for rapid identification and intra-species characterization of airborne filamentous fungi. *J. Microbiol. Methods* 64, 63–77. doi: 10.1016/j.mimet.2005.04.005

Foroozesh, P., Bahmani, R., Pazouki, A., Asgharzadeh, A., Rahimdabbagh, S., and Ahmad, A. (2012). Effect of Cadmium stress on antioxidant enzymes activity in different bean genotypes. *J. Agric. Biol. Sci.* 7, 351–356.

Gibbons, S. M., Feris, K., McGuirl, M. A., Morales, S. E., Hynninen, A., Ramsey, P. W., et al. (2011). Use of microcalorimetry to determine the costs and benefits to *Pseudomonas putida* strain KT2440 of harboring cadmium efflux genes. *Appl. Environ. Microbiol.* 77, 108–113. doi: 10.1128/AEM.01187-10

Glick, B. R. (1995). The enhancement of plant growth by free-living bacteria. *Can. J. Microbiol.* 41, 109–117. doi: 10.1139/m95-015

Glick, B. R., Patten, C. L., Holguin, G., and Penrose, D. M. (1999). *Biochemical and Genetic Mechanisms Used by Plant Growth Promoting Bacteria*. Canada: University of Waterloo. doi: 10.1142/p130

Godt, J., Scheidig, F., Grosse-Siestrup, C., Esche, V., Brandenburg, P., Reich, A., et al. (2006). The toxicity of cadmium and resulting hazards for human health. *J. Occup. Med. Toxicol.* 1:22. doi: 10.1186/1745-6673-1-22

Gola, D., Malik, A., Namburath, M., and Ahammad, S. Z. (2018). Removal of industrial dyes and heavy metals by *Beauveriabassiana*: FTIR, SEM, TEM and AFM investigations with Pb(II). *Environ. Sci. Pollut. Res.* 25, 20486–20496. doi: 10.1007/s11356-017-0246-1

Gordon, S. A., and Weber, R. P. (1951). Colorimetric estimation of indole acetic acid. *Plant. Physiol.* 26, 192–195. doi: 10.1104/pp.26.1.192

Guo, J., and Zhang, X. (2004). Metal-ion interactions with sugar. The crystal structure and FTIR study of an SrCl2-fructose complex. *Carbohydr. Res.* 339, 1421–1426. doi: 10.1016/j.carres.2004.03.004

Gupta, P., Rani, R., Chandra, A., and Kumar, V. (2018). Potential applications of *Pseudomonas* sp. (strain CPSB21) to ameliorate Cr6+ stress and phytoremediation of tannery effluent contaminated agricultural soils. *Sci. Rep.* 8:4860. doi: 10.1038/s41598-018-23322-5

Gururani, M. A., Upadhyaya, C. P., Baskar, V., Venkatesh, J., Nookaraju, A., and Park, S. W. (2013). Plant growth-promoting rhizobacteriaenhance abiotic stress tolerance in *Solanum* tuberosumthroughinducing changes in the expression of ROS-scavenging enzymes and improved pohotosyntheticperformance. *J. Plant. Growth Regul.* 32, 245–258. doi: 10.1007/s00344-012-9292-6

Hasanuzzaman, M., Bhuyan, M. H. M. B., Zulfiqar, F., Raza, A., Mohsin, S. M., Al Mahmud, J., et al. (2020). Reactive oxygen species and antioxidant defense in plants under abiotic stress: revisiting the crucial role of a universal defense regulator. *Antioxidants* 9:681. doi: 10.3390/antiox9080681

Hou, Y., Cheng, K., Li, Z., Ma, X., Wei, Y., Zhang, L., et al. (2015). Biosorption of cadmium and manganese using free cells of *Klebsiella* sp. isolated from waste water. *PLoS One* 10:e0140962. doi: 10.1371/journal.pone.0140962

Hrynkiewicz, K., and Baum, C. (2014). "Application of microorganisms in bioremediation of environment from heavy metals," in *Environmental Deterioration and Human Health: Natural and Anthropogenic Determinants*, eds A. Malik, E. Grohmann, and R. Akhtar (Berlin: Springer), 215–227. doi: 10.1007/978-94-007-7890-0_9

Idrees, N., Tabassum, B., Abd Allah, E. F., Hashem, A., Sarah, R., and Hashim, M. (2018). Groundwater contamination with cadmium concentrations in some West U.P. Regions, India. *Saudi J. Biol. Sci.* 25, 1365–1368. doi: 10.1016/j.sjbs.2018.07.005

Igiri, B. E., Okoduwa, S. I. R., Idoko, G. O., Akabuogu, E. P., Adeyi, A. O., and Ejiogu, I. K. (2018). Toxicity and bioremediation of heavy metals contaminated ecosystem from tannery wastewater: a review. *J. Toxicol.* 2018:2568038. doi: 10.1155/2018/2568038

Imsande, J. (1998). Iron, sulfur, and chlorophyll deficiencies: a need for an integrative approach in plant physiology. *Physiol. Plant.* 103, 139–144. doi: 10.1034/j.1399-3054.1998.1030117.x

Islam, M. M., Karim, M. R., Zheng, X., and Li, X. (2018). Heavy metal and metalloid pollution of soil, water and foods in Bangladesh: a critical review. *Int. J. Environ. Res. Public Health* 15:2825. doi: 10.3390/ijerph15122825

Jain, S., and Bhatt, A. (2014). Molecular and in situ characterization of cadmium-resistant diversified extremophilic strains of *Pseudomonas* for their bioremediation potential. *3Biotech* 4, 297–304. doi: 10.1007/s13205-013-0155-z

Juan, C. C., María, C. C., and Manuel, C. B. (2018). Biosorption of Cd by non-toxic extracellular polymeric substances (EPS) synthesized by bacteria from marine intertidal biofilms. *Int. J. Environ. Res. Public Health* 15:314. doi: 10.3390/ijerph15020314

Kanamarlapudi, S. L. R. K., Chintalpudi, K. V., and Muddada, S. (2018). *Application of Biosorption for Removal of Heavy Metals From Waste Water, Biosorption, Jan Derco and Branislav Vrana*. London: IntechOpen. doi: 10.5772/intechopen.77315

Kaur, U. J., Preet, S., and Rishi, P. (2018). Augmented antibiotic resistance associated with cadmium induced alterations in *Salmonella enterica* serovar Typhi. *Sci. Rep.* 8:12818. doi: 10.1038/s41598-018-31143-9

Khan, Z., Rehman, A., Hussain, S. Z., Nisar, M. A., Zulfiqar, S., and Shakoori, A. R. (2016). Cadmium resistance and uptake by bacterium, *Salmonella enterica* 43C, isolated from industrial effluent. *AMB Express.* 6, 1–6. doi: 10.1186/s13568-016-0225-9

Kloepper, J. W., Lifshitz, R., and Zablotowicz, R. M. (1989). Free-living bacterial inocula for enhancing crop productivity. *Trends Biotechnol.* 7, 39–44. doi: 10.1016/0167-7799(89)90057-7

Kobya, M. (2004). Removal of Cr(VI) from aqueous solutions by adsorption onto hazelnut shell activated carbon: kinetic and equilibrium studies. *Bioresour. Technol.* 91, 317–321. doi: 10.1016/j.biortech.2003.07.001

Krishna, A. K., Mohan, K. R., and Murthy, N. N. (2009). Determination of heavy metals in soil, sediment, and rock by inductively coupled plasma optical emission spectrometry: microwave-assisted acid digestion versus open acid digestion technique. *Atom. Spectrosc.* 1, 75–81.

Leung, H. M., Cheung, K. C., Au, C. K., Yung, K. K. L., and Li, W. C. (2021). An assessment of heavy metal contamination in the marine soil/sediment of Coles Bay Area, Svalbard, and Greater Bay Area, China: a baseline survey from a rapidly developing bay. *Environ. Sci. Pollut. Res.* 28, 22170–22178. doi: 10.1007/s11356-021-13489-2

Li, F. T., Qi, J. M., Zhang, G. Y., Lin, L. H., Fang, P., Tao, A. F., et al. (2013). Effect of cadmium stress on the growth, antioxidative enzymes and lipid peroxidation in two kenaf (*Hibiscus cannabinus* L.) plant seedlings. *J. Integr. Agric.* 12, 610–620. doi: 10.1016/S2095-3119(13)60279-8

Lima e Silva, A. A., Carvalho, M. A., de Souza, S. A., Dias, P. M., Silva Filho, R. G., Saramago, C. S., et al. (2012). Heavy metal tolerance (Cr, Ag and Hg) in bacteria isolated from sewage. *Braz. J. Microbiol.* 43, 1620–1631. doi: 10.1590/S1517-83822012000400047

Loper, J. E., and Schroth, M. N. (1986). Influence of bacterial sources of indole-3-acetic acid on root elongation of sugar beet. *Phytopathology* 76, 386–389. Available online at: https://www.apsnet.org/publications/phytopathology/backissues/Documents/1986Articles/Phyto76n04_386.PDF

Lu, W. B., Shi, J. J., Wang, C. H., and Chang, J. S. (2006). Biosorption of lead, copper and cadmium by an indigenous isolate *Enterobacter* sp. J1 possessing high heavy-metal resistance. *J. Hazard. Mater.* 134, 80–86. doi: 10.1016/j.jhazmat.2005.10.036

Ma, J. F., and Nomoto, K. (1993). Two related biosynthetic pathways for mugineic acids in gramineous plants. *Plant Physiol.* 102, 373–378. doi: 10.1104/pp.102.2.373

Ma, Y., Rajkumar, M., Zhang, C., and Freitas, H. (2016). Beneficial role of bacterial endophytes in heavy metal phytoremediation. *J. Environ. Manag.* 174, 14–25. doi: 10.1016/j.jenvman.2016.02.047

Milagres, A. M. F., Machuca, A., and Napoleão, D. (1999). Detection of siderophore production from several fungi and bacteria by a modification of chrome azurol S (CAS) agar plate assay. *J. Microbiol. Methods* 37, 1–6. doi: 10.1016/S0167-7012(99)00028-7

Mishra, D., and Kar, M. (1974). Nickel in plant growth and metabolism. *Bot. Rev.* 40, 395–452. doi: 10.1007/BF02860020

Mu, T., Wu, T., Zhou, T., Li, Z., Ouyang, Y., Jiang, J., et al. (2019). Geographical variation in arsenic, cadmium, and lead of soils and rice in the major rice producing regions of China. *Sci. Total Environ.* 677, 373–381. doi: 10.1016/j.scitotenv.2019.04.337

Muehe, E. M., Obst, M., Hitchcock, A., Tyliszczak, T., Behrens, S., Schröder, C., et al. (2013). Fate of Cd during microbial Fe(III) mineral reduction by a novel and Cd-tolerant *Geobacter* sp. *Environ. Sci. Technol.* 47, 14099–14109. doi: 10.1021/es403365w

Nath, S., Paul, P., Roy, R., Bhattacharjee, S., and Deb, B. (2019). Isolation and identification of metal-tolerant and antibiotic-resistant bacteria from soil samples of Cachar district of Assam, India. *SN Appl. Sci.* 1, 1–9. doi: 10.1007/s42452-019-0762-3

Nautiyal, C. S. (1999). An efficient microbiological growth medium for screening phosphate solubilizing microorganisms. *FEMS Microbiol. Lett.* 170, 265–270. doi: 10.1111/j.1574-6968.1999.tb13383.x

Ojuederie, O. B., and Babalola, O. O. (2017). Microbial and plant-assisted bioremediation of heavy metal polluted environments: areview. *Int. J. Environ. Res. Public Health* 14:1504. doi: 10.3390/ijerph14121504

Oleńska, E., Małek, W., Wójcik, M., Swiecicka, I., Thijs, S., and Vangronsveld, J. (2020). Beneficial features of plant growth-promoting rhizobacteria for improving plant growth and health in challenging conditions: a methodical review. *Sci. Total. Environ.* 743:140682. doi: 10.1016/j.scitotenv.2020.140682

Patten, C. L., and Glick, B. R. (1996). Bacterial biosynthesis of indole-3-acetic acid. *Can. J. Microbiol.* 42, 207–220. doi: 10.1139/m96-032

Pradhan, B. K., and Sandle, N. K. (1999). Effect of different oxidizing agent treatments on the surface properties of activated carbons. *Carbon* 1, 1323–1332. doi: 10.1016/S0008-6223(98)00328-5

Rahimzadeh, M. R., Rahimzadeh, M. R., Kazemi, S., and Moghadamnia, A.-A. (2017). Cadmium toxicity and treatment: an update. *Caspian. J. Intern. Med.* 8, 135–145.

Rajandas, H., Parimannan, S., Sathasivam, K., Ravichandran, M., and Su Yin, L. (2012). A novel FTIR-ATR spectroscopy based technique for the estimation of low-density polyethylene biodegradation. *Polym. Test.* 31, 1094–1099. doi: 10.1016/j.polymertesting.2012.07.015

Rajesh, V., Kumar, A. S., and Rajesh, N. (2014). Biosorption of Cd using a novel bacterium isolated from an electronic industry effluent. *Chem. Eng. J.* 235, 176–185. doi: 10.1016/j.cej.2013.09.016

Rajkumar, M., Ae, N., Prasad, M. N. V., and Freitas, H. (2010). Potential of siderophore-producing bacteria for improving heavy metal phytoextraction. *Trends Biotechnol.* 28, 142–149. doi: 10.1016/j.tibtech.2009.12.002

Rehman, Z. U., Khan, S., Brusseau, M. L., and Shah, M. T. (2017). Lead and cadmium contamination and exposure risk assessment via consumption of vegetables grown in agricultural soils of five-selected regions of Pakistan. *Chemosphere* 168, 1589–1596. doi: 10.1016/j.chemosphere.2016.11.152

Reid, C. P., Szaniszlo, P. J., and Crowley, D. E. (1986). *Siderophore Involvement in Plant Iron Nutrition. Iron, Siderophores, and Plant Diseases*. Boston, MA: Springer, 29–42. doi: 10.1007/978-1-4615-9480-2_5

Renu, K. M., Sahu, U., Bhoyar, M. S., Singh, D. P., Singh, U. B., et al. (2020). Augmentation of metal-tolerant bacteria elevates growth and reduces metal toxicity in spinach. *Bioremediation* 1, 1–20.

Römheld, V., and Marschner, H. (1986). Evidence for a specific uptake system for iron phytosiderophores in roots of grasses. *Plant Physiol.* 80, 175–180. doi: 10.1104/pp.80.1.175

Ryan, M. P., and Pembroke, J. T. (2020). The genus *Ochrobactrum* as major opportunistic pathogens. *Microorganisms* 8:1797. doi: 10.3390/microorganisms8111797

Saha, B., and Orvig, C. (2010). Biosorbents for hexavalent chromium elimination from industrial and municipal effluents. *Coord. Chem. Rev.* 254, 2959–2972. doi: 10.1016/j.ccr.2010.06.005

Saitou, N., and Nei, M. (1987). The neighbor joining method: a new method for reconstructing phylogenetic trees. *Mol. Biol. Evol.* 14, 406–425. doi: 10.1093/oxfordjournals.molbev.a040454

Sanità Di Toppi, L., and Gabbrielli, R. (1999). Response to cadmium in higher plants. *Environ. Exp. Bot.* 41, 105–130. doi: 10.1016/S0098-8472(98)00058-6

Sarin, V., and Pant, K. K. (2006). Removal of chromium from industrial waste by using eucalyptus bark. *Bioresour. Technol.* 97, 15–20. doi: 10.1016/j.biortech.2005.02.010

Schwyn, B., and Neilands, J. B. (1987). Universal chemical assay for the detection and determination of siderophores. *Anal. Biochem.* 160, 47–56. doi: 10.1016/0003-2697(87)90612-9

Shaheen, N., Irfan, N. M., Khan, I. N., Islam, S., Islam, M. S., and Ahmed, M. K. (2016). Presence of heavy metals in fruits and vegetables: health risk implications in Bangladesh. *Chemosphere* 152, 431–438. doi: 10.1016/j.chemosphere.2016.02.060

Sharma, P., Jha, A. B., Dubey, R. S., and Pessarakli, M. (2012). Reactive oxygen species, oxidative damage, and antioxidative defense mechanism in plants under stressful conditions. *Antioxidants* 2012:217037. doi: 10.1155/2012/217037

Sharma, S., Kulkarni, J., and Jha, B. (2016). Halotolerant rhizobacteriapromote growth and enhance salinity tolerance in peanut. *Front. Microbiol.* 7:1600. doi: 10.3389/fmicb.2016.01600

Shi, T., Zhang, Y., Gong, Y., Ma, J., Wei, H., Wu, X., et al. (2019). Status of Cd accumulation in agricultural soils across China (1975–2016): from temporal and spatial variations to risk assessment. *Chemosphere* 230, 136–143. doi: 10.1016/j.chemosphere.2019.04.208

Shukla, R., Sarim, K. M., and Singh, D. P. (2020). Microbe-mediated management of arsenic contamination: current status and future prospects. *Environ. Sustain.* 3, 83–90. doi: 10.1007/s42398-019-00090-0

Sindhu, S. S., Gupta, S. K., and Dadarwal, K. R. (1999). Antagonistic effect of *Pseudomonas* spp. on pathogenic fungi and enhancement of growth of green gram (*Vigna radiata*). *Biol. Fertil. Soils* 29, 62–68. doi: 10.1007/s003740050525

Sinha, S., and Mukherjee, S. K. (2009). *Pseudomonas aeruginosa* KUCd1, a possible candidate for cadmium bioremediation. *Braz. J. Microbiol.* 40, 655–662. doi: 10.1590/S1517-83822009000300030

Sodhi, K. K., Kumar, M., and Singh, D. K. (2020). Multi-metal resistance and potential of *Alcaligenes* sp. MMA for the removal of heavy metals. *SN Appl. Sci.* 2:1885. doi: 10.1007/s42452-020-03583-4

Sultan, M., Schulz, M. H., Richard, H., Magen, A., Klingenhoff, A., Scherf, M., et al. (2008). A global view of gene activity and alternative splicing by deep sequencing of the human transcriptome. *Science* 321, 956–960. doi: 10.1126/science.1160342

Sultan, S., and Hasnain, S. (2007). Reduction of toxic hexavalent chromium by *Ochrobactrum* intermedium strain SDCr-5 stimulated by heavy metals. *Bioresour. Technol.* 98, 340–344. doi: 10.1016/j.biortech.2005.12.025

Sun, W., Xiao, E., Krumins, V., Häggblom, M. M., Dong, Y., Pu, Z., et al. (2018). Rhizosphere microbial response to multiple metal(loid)s in different contaminated arable soils indicates crop-specific metal-microbe interactions. *Appl. Environ. Microbiol.* 84, e701–e718. doi: 10.1128/AEM.00701-18

Tamura, K., Stecher, G., Peterson, D., Filipski, A., and Kumar, S. (2013). MEGA6: molecular evolutionary genetics analysis version 6.0. *Mol. Biol. Evol.* 30, 2725–2729. doi: 10.1093/molbev/mst197

Thompson, J. D., Higgins, D. G., and Gibson, T. J. (1994). CLUSTAL W: improving the sensitivity of progressive multiple sequence alignment through sequence weighting, position-specific gap penalties and weight matrix choice. *Nucleic Acids Res.* 22, 4673–4680. doi: 10.1093/nar/22.22.4673

Tiwari, S., and Lata, C. (2018). Heavy metal stress, signaling, and tolerance due to plant-associated microbes: an overview. *Front. Plant. Sci.* 9:452. doi: 10.3389/fpls.2018.00452

Vicentin, R. P., Dos-Santos, J. V., Labory, C. R. G., Da Costa, A. M., Moreira, F. M., de, S., et al. (2018). Tolerance to and accumulation of cadmium, copper, and zinc by *Cupriavidusnecator*. *Rev. Bras. Cienc. do Solo* 42:80. doi: 10.1590/18069657rbcs20170080

Wallace, A., Wallace, G. A., and Cha, J. W. (1992). Some modifications in trace metal toxicities and deficiencies in plants resulting from interactions with other elements and chelating agents-The special case of iron. *J. Plant Nutr.* 15, 1589–1598. doi: 10.1080/01904169209364424

Wang, Y., Brown, H. N., Crowley, D. E., and Szaniszlo, P. J. (1993). Evidence for direct utilization of a siderophore, ferrioxamine B, in axenically grown cucumber. *Plant Cell Environ.* 16, 579–585. doi: 10.1111/j.1365-3040.1993.tb00906.x

Wang, Y., Fang, J., Leonard, S. S., and Rao, K. M. K. (2004). Cadmium inhibits the electron transfer chain and induces reactive oxygen species. *Free Radic. Biol. Med.* 36, 1434–1443. doi: 10.1016/j.freeradbiomed.2004.03.010

Wilson, K. (2001). Preparation of genomic DNA from bacteria. *Curr.Protoc. Mol. Biol.* 56, 2–4. doi: 10.1002/0471142727.mb0204s56

Wisplinghoff, H. (2017). "*Pseudomonas* spp., *Acenetobacter* spp. and miscellaneous gram-negative bacilli," in *Infectious Diseases (Fourth Edn.)*, eds J. Cohen, W. G. Powderly, and S. M. Opal (Amsterdam: Elsevier). doi: 10.1016/B978-0-7020-6285-8.00181-7

Wolkers, W. F., Oliver, A. E., Tablin, F., and Crowe, J. H. (2004). A Fourier transform infrared spectroscopy study of sugar glasses. *Carbohydr. Res.* 339, 1077–1085. doi: 10.1016/j.carres.2004.01.016

Wolpert, M., and Hellwig, P. (2006). Infrared spectra and molar absorption coefficients of the 20 alpha amino acids in aqueous solutions in the spectral range from 1800 to 500 cm-1. *Spectrochim. Acta A Mol. Biomol. Spectrosc.* 64, 987–1001. doi: 10.1016/j.saa.2005.08.025

World Health Organization [WHO] (2008). *Guidelines for Drinking-Water Quality [Electronic Resource]: Incorporating 1st and 2nd Addenda, Vol.1, Recommendations*, 3rd Edn. Geneva: World Health Organization [WHO].

Yadav, M. M., Singh, G., and Jadeja, R. N. (2021). *Physical and Chemical Methods for Heavy Metal Removal*. Hoboken, NJ: Wiley Online. doi: 10.1002/9781119693635.ch15

Yadav, S. K. (2010). Heavy metals toxicity in plants: an overview on the role of glutathione and phytochelatins in heavy metal stress tolerance of plants. *S. Afr. J. Bot.* 76, 167–179. doi: 10.1016/j.sajb.2009.10.007

Yee, N., Benning, L. G., Phoenix, V. R., and Ferris, F. G. (2004). Characterization of metal cyanobacteria sorption reactions: a combined macroscopic and infrared spectroscopic investigation. *Environ. Sci. Technol.* 38, 775–782. doi: 10.1021/es0346680

Zhai, L., Liao, X., Chen, T., Yan, X., Xie, H., Wu, B., et al. (2008). Regional assessment of cadmium pollution in agricultural lands and the potential health risk related to intensive mining activities: a case study in Chenzhou City, China. *J. Environ. Sci.* 20, 696–703. doi: 10.1016/S1001-0742(08)62115-4

Zhang, J., Li, Q., Zeng, Y., Zhang, Jian, Lu, G., et al. (2019). Bioaccumulation and distribution of cadmium by *Burkholderia cepacia* GYP1 under oligotrophic condition and mechanism analysis at proteome level. *Ecotoxicol. Environ. Saf.* 176, 162–169. doi: 10.1016/j.ecoenv.2019.03.091

Conflict of Interest: The authors declare that the research was conducted in the absence of any commercial or financial relationships that could be construed as a potential conflict of interest.

Publisher's Note: All claims expressed in this article are solely those of the authors and do not necessarily represent those of their affiliated organizations, or those of the publisher, the editors and the reviewers. Any product that may be evaluated in this article, or claim that may be made by its manufacturer, is not guaranteed or endorsed by the publisher.

frontiers in Sustainable Food Systems

REVIEW
published: 31 January 2022
doi: 10.3389/fsufs.2021.817932

Heavy Metal Stress Alleviation Through Omics Analysis of Soil and Plant Microbiome

*Laccy Phurailatpam, Vijay Kumar Dalal, Namrata Singh and Sushma Mishra**

Plant Biotechnology Laboratory, Dayalbagh Educational Institute, Deemed-to-be-University, Agra, India

Heavy metal (HM) contamination of soil and water resources is a global concern, which not only limits crop yield and quality, but also has serious environmental effects. Due to the non-biodegradable nature and toxicity, high concentration of HMs in food and environment is a serious threat to the entire ecosystem. Moreover, the target of supplying safe and quality food to the rising human population (expected to reach ∼9–10 bn by the year 2050), necessitates effective treatment of the HM-contaminated soil. Various microbe-mediated bioremediation strategies such as biosorption, bioprecipiation, biostimulation, etc., have been found to be effective in uptake and conversion of HMs to less toxic forms. Further, in the past few years, the use of soil and plant-associated microbiome for HM stress alleviation is gaining attention among the scientific community. In general, microbes are spectacular in being dynamic and more responsive to environmental conditions in comparison to their host plants. Moreover, with the advancements in high throughput sequencing technologies, the focus is eventually shifting from just structural characterization to functional insights into the microbiome. The microbes inhabiting the HM-contaminated environments or associated with HM-tolerant plants are a source for exploring HM-tolerant microbial communities, which could be used for enhancing bioremediation efficiency and conferring HM tolerance in plants. This review discusses the application of omics techniques including metagenomics, metatranscriptomics, metaproteomics, and metabolomics, for rapid and robust identification of HM-tolerant microbial communities, mining novel HM resistance genes, and fabricating the HM resistome.

Keywords: heavy metal, abiotic stress, bioremediation, omics, microbiome

OPEN ACCESS

Edited by:
Krishnendu Pramanik, Visva-Bharati University, India

Reviewed by:
Anirudha R. Dixit, Kennedy Space Center, United States
Tapan Kumar Adhya, KIIT University, India

****Correspondence:***
Sushma Mishra
sushmamishra87@gmail.com
orcid.org/0000-0001-8012-3382

Specialty section:
This article was submitted to Crop Biology and Sustainability, a section of the journal Frontiers in Sustainable Food Systems

Received: *18 November 2021*
Accepted: *30 December 2021*
Published: *31 January 2022*

Citation:
Phurailatpam L, Dalal VK, Singh N and Mishra S (2022) Heavy Metal Stress Alleviation Through Omics Analysis of Soil and Plant Microbiome. Front. Sustain. Food Syst. 5:817932. doi: 10.3389/fsufs.2021.817932

INTRODUCTION

Heavy metals (HMs) constitute a class of non-biodegradable environmental pollutants, which have detrimental effects on both terrestrial and aquatic ecosystems (Banach et al., 2020). Heavy metals refer to the d-block elements with density >5 g/cm^3 (Singh et al., 2016). Some HMs such as zinc (Zn), manganese (Mn), copper (Cu), iron (Fe), and nickel (Ni) act as enzyme cofactors (hence, are essential for physiological functions); most of them, however, disrupt normal cellular metabolism (Goyal et al., 2020). On the basis of their physiochemical characteristics, HMs could be divided into redox metals and non-redox metals. Redox active metals such as Mn, chromium (Cr), Cu, and Fe are responsible for causing oxidative damage to plant cells through production

of reactive oxygen species (ROS) by Haber-Weiss and Fenton reactions (Valko and Cronin, 2005; Jozefczak et al., 2012). Such severe oxidative injury leads to disruption in cell homeostasis, degradation of DNA, proteins, and cell membrane components, and destruction of photosynthetic pigments, which may finally result in cell death (Schutzendubel and Polle, 2002; Flora, 2009). On the other hand, non-redox active metals such as aluminum (Al), cadmium (Cd), Zn, Ni, and mercury (Hg) generate oxidative stress indirectly by inhibiting the activity of antioxidants (through glutathione consumption or binding to sulfhydryl groups of proteins) or inducing the activity of ROS-producing enzymes (Emamverdian et al., 2015). Irrespective of the mode of action, consumption of HM-contaminated food and water leads to severe health complications such as kidney damage, cardiovascular diseases, neurological disorders, lung damage, and gastro-intestinal problems (Järup, 2003; Johri et al., 2010). HM-contamination of soil results in loss of fertility, primarily by altering the structure and composition of microbial communities and soil physicochemistry. For example, high concentration of Cd alters the soil microbial population and modifies the soil physiochemistry, thereby resulting in loss of some indigenous microbial species (that are unable to adapt Cd stress) (Salam et al., 2020). Therefore, considering the growing rate of organ-disorders in humans and environmental degradation, there is a need to employ effective measures to reduce HM contamination in environment, as well as to devise novel strategies for HM stress alleviation. This review article focuses on the application of omics technologies for identification of HM-tolerant microbiota, their genes/operons and mechanism of HM stress alleviation, for bioremediation and for imparting HM tolerance to crop plants.

CONTRIBUTION OF MICROBIOME IN HM STRESS TOLERANCE

The toxic concentrations of HMs in soil find its way through the vascular system and interfere with the function of biomolecules (such as protein, DNA, etc.) present in plant cells. However, as an adaptation to prolonged HM stress, some plant species have evolved morphological (formation of hairy roots, trichomes, thick wall, cuticle, etc.), and physiological (secretion of root exudates rich in organic acids, proline accumulation, and phytohormone production) adaptations (Rajkumar et al., 2012; Hauser, 2014; Boiteau et al., 2018; Tiwari and Lata, 2018). At the cellular level, tolerant plants use mechanisms including HM uptake and efflux, transport, sequestration, and chelation (Viehweger, 2014). Examples of some metal-tolerant plant species include *Arabidopsis arenosa, Arabidopsis halleri, Deschampsia caespitosa*, and *Silene vulgaris* (Borymski et al., 2018). The HM-tolerant plants could be divided into two groups, based on the tolerance mechanism: (i) species that avoid HM-uptake and hence, prevent accumulation in shoot system (ii) species that (hyper)accumulate and tolerate high concentrations of HMs. The hyperaccumulators include plant species such as *Azolla filiculoides, Combretum erythrophyllum, A. halleri*, etc., which employ measures such as over-expression of transport systems, high concentration of metal chelators, and greater ability to detoxify and accumulate HMs in their aerial organs (Viehweger, 2014).

In nature, plants do not exist as isolated entities; they are associated with microbial communities in the rhizosphere (soil around plant roots), phyllosphere (aerial parts of plant), and endosphere (inside the plant tissues), to form the *holobiont*. Research carried out in the past few decades have highlighted the role of microbiome in affecting overall plant health and responses, especially under abiotic and biotic stress conditions (Phurailatpam and Mishra, 2020; Mishra et al., 2021a,b). Moreover, since microbes are highly sensitive as well as adaptable to environmental factors (including HM contaminants), they act as powerful model systems to decipher mechanisms for alleviating HM stress in crop plants (**Figure 1**). Therefore, researchers have focused on analyzing the microbiota associated with metal tolerant plant species, to understand the contribution of microbiome in HM tolerance of the holobiont (**Table 1**). Omics techniques (such as metagenomics, metatranscriptomics, metaproteomics, and metabolomics) have provided important leads on the microbial structure and composition (species abundance and diversity), metabolic potential (HM-tolerant/detoxification genes and proteins), and plant-microbe crosstalk, in response to HM stress.

OMICS APPROACHES FOR UNDERSTANDING THE ROLE OF MICROBIOME IN HM STRESS RESPONSE

Until the past few decades, most of our knowledge on HM stress tolerance of plant-associated microbiota was based on culture-dependent approaches. For example, a culture-dependent study of two HM-contaminated sites in Portugal reported altered abundance and composition of bacterial communities, with most species belonging to *Actinobacteria, Firmicutes,* and *Proteobacteria*, and predominant genera belonging to *Pseudomonas, Arthrobacter,* and *Bacillus* (Pires et al., 2017). The HM-tolerant strains native to the contaminated sites, are promising candidates for their application in bioremediation. Though this approach enables isolation of microbial strains in tangible form; majority of the microbial communities being unculturable (under standard laboratory conditions) remains unnoticed and hence, unexplored (Staley and Konopka, 1985). Another approach involving PCR amplification of HM stress tolerance genes enables rapid screening of microbial strains; it however, suffers from the limitation of not being able to reveal novel candidates. Therefore, in order to circumvent such limitations, techniques based on functional analysis of metagenome have helped in identification and isolation of novel candidates (Handelsman et al., 1998; Majernik et al., 2001). The procedure involves extraction of total DNA from microbial communities of a particular environment, followed by screening for the desired "activity," for example, screening for $Na^+(Li^+)/H^+$ antiporter activity in *Escherichia coli* (Majernik

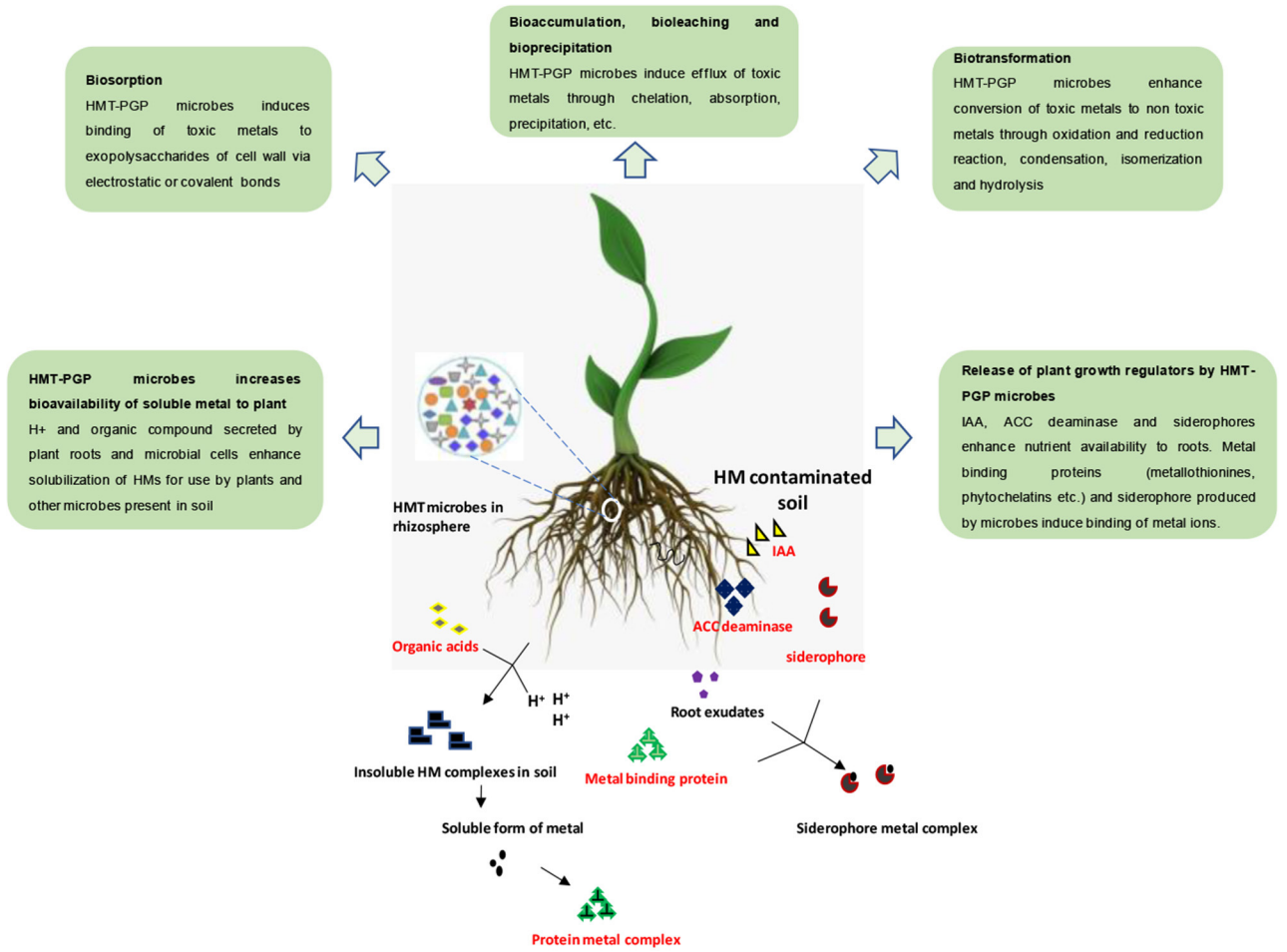

FIGURE 1 | Mechanism of action of HM-tolerant (HMT) microbiome in bioremediation of HM-contaminated soil. The HMT microbiota present in the rhizosphere may exhibit plant growth promoting traits including secretion of phytohormones, siderophores, etc. (Adapted from Mishra et al., 2017).

et al., 2001). This promising approach has been successfully used in detection and identification of genes inducing lithium-resistant phenotypes in *E. coli.*

The next generation sequencing (NGS) technologies have contributed toward increasing our understanding of various fields including plant microbiome. This is mainly attributed to the fact that majority of the microorganisms are unculturable under laboratory conditions, a phenomenon commonly known as "the great plate count anomaly" (Staley and Konopka, 1985). However, with recent technological advancements such as culturomics and FACS metagenomics, the percentage of 99% unculturability (Staley and Konopka, 1985) has been brought down to ∼80% or even lesser (Bellali et al., 2021). Next generation sequencing offers an economical and rapid method for unraveling microbial diversity, which is otherwise inaccessible by conventional methods. The omics approaches have identified several genes from plants (Singh et al., 2016) and plant-associated microbiota, which could be utilized for imparting HM stress tolerance to the holobiont (**Figure 2**). For example, whole genome sequencing of *Methylobacterium radiotolerans* MAMP 4754, an endophytic strain associated with the hyperaccumulator plant *Combretum erythrophyllum,* has identified HM tolerance genes against Zn, Ni, and Cu (Photolo et al., 2021). Further, the knowledge of HM-tolerant microbiota (and their genes) could be incorporated in plant breeding programs aimed at generating HM-tolerant crops, in an approach known as *holobiont breeding* (Sahu and Mishra, 2021). The contribution of various omics approaches, namely metagenomics, metatranscriptomics, metaproteomics, and metabolomics in microbe-mediated HM tolerance, have been discussed below.

Metagenomics

In metagenomics, microbial DNA sequencing is performed directly from the environmental sample, without involving the isolation of microbial communities (Akinsanya et al., 2015). Used for analyzing the structure and function of microbial communities, metagenomics could be divided into two types: high-throughput targeted amplicon sequencing and whole-genome shotgun metagenomics

TABLE 1 | Some recent studies involving omics technologies for unraveling the role of microbiota in HM-tolerance.

S. No.	Plant species	Heavy metal	Omics technique	Associated microbe(s)	Major findings of the study	References
1.	*Oryza sativa*	Cadmium	Proteomics	*Piriformospora indica*	Fungi helped plants to endure Cd toxicity by relieving oxidative stress.	Sagonda et al., 2021
2.	*Acacia farnesiana*	Arsenic	Proteomics	*Methylobacterium* sp.	As-tolerance of the plant is enhanced by bacteria.	Alcántara-Martínez et al., 2018
3.	*Triticum aestivum*	Cd and lead	Metabolomics and proteomics	*Enterobacter bugandensis* TJ6	Secretion of Indole-3-acetic acid (IAA), arginine and betaine under Cd and Pb stress; phytohormones, DNA repair, and antioxidant activity of the plant increased under stress.	Han et al., 2021
4.	*Zea mays*	Copper	Metabolomics and proteomics	*Pseudomonas* sp. TLC 6-6	Metabolomic analysis of maize revealed that PGPB inoculation upregulated photosynthesis, hormone biosynthesis, and tricarboxylic acid cycle metabolites. Proteomic analysis identified upregulation of proteins related to plant development and stress response.	Li et al., 2014
5.	*Sedum alfredii*	Cadmium	Transcriptomics and metabolomics	*Pseudomonas fluorescens*	Inoculation with *P. fluorescens* promoted lateral root formation in host plants, leading to a higher Cd phytoremediation efficiency.	Wu et al., 2020
6.	*Phragmites australis*	Copper	Proteomics	*Phragmites australis*	*P. australis* accumulated large amounts of Cu in its roots; increased ascorbic acid and proline levels enhanced Cu tolerance and protected photosynthesis.	Wu et al., 2021
7.	Soil	Cadmium	Metagenomics	*Proteobacteria, Sulfuricella,* and *Thiobacillus*	KEGG pathway analysis revealed genes encoding for ABC transporter, detoxification systems.	Feng et al., 2018
8.	*Hydrilla verticillata*	Arsenic	Metagenomics	*Epiphytic bacteria*	As-reducing bacteria induced As uptake and increased As(III) efflux from plant cells.	Zhen et al., 2020
9.	Alfalfa	Cadmium	Transcriptomics	Rhizobia, arbuscular mycorrhiza fungi (AMF)	Co-inoculation of alfalfa with Rhizobia or AMF improved tolerance to Cd stress.	Wang et al., 2021
10.	*Triticum aestivum*	Cadmium	Proteomics	*Bacillus megaterium* N3	Strain N3 reduced the Cd content in wheat roots.	Qin et al., 2021
11.	*Combretum erythrophyllum*	Zinc, copper, and nickel	Genomics	*Methylobacterium radiotolerans*	Identification of proteins that confer heavy metal resistance, the *in vitro* characterization of heavy metal resistance, and the production of plant growth-promoting (PGP) volatiles.	Photolo et al., 2021

(Continued)

TABLE 1 | Continued

S. No.	Plant species	Heavy metal	Omics technique	Associated microbe(s)	Major findings of the study	References
12.	*Vigna unguiculata*	Mercury	Genomics	*Photobacterium* spp. strain MELD1	Presence of *mer* operon in the genome of MELD1 strain; Enhanced growth of plant in Hg contaminated soil; increased Hg uptake in roots; significantly decreased Hg concentration in pods.	Mathew et al., 2015
13.	*Eucalyptus tereticornis*	Copper and cadmium	Metatranscriptomics	*Pisolithus albus* PaMT1	Plants colonized with *P. albus* exposed to Cu and Cd stress showed better growth.	Reddy et al., 2016
14.	*Triticum aestivum*	Zinc	Targeted metagenomics	*Bacillus halotolerant* J143, *Enterobacter hormaechei* J146, and *Pseudomonas frederiksbergensis* J158	Improved seed germination, plant growth in wheat, and Zn absorption.	Fahsi et al., 2021
15.	Alfalfa	Cadmium	Non-targeted metabolomics	*Bacillus subtilis*	*B. subtilis* inoculation to alfa alfa improved growth and Cd uptake ability; Metabolite levels of amino acids, fatty acids, carbohydrates, and flavonoids were regulated.	Li et al., 2021

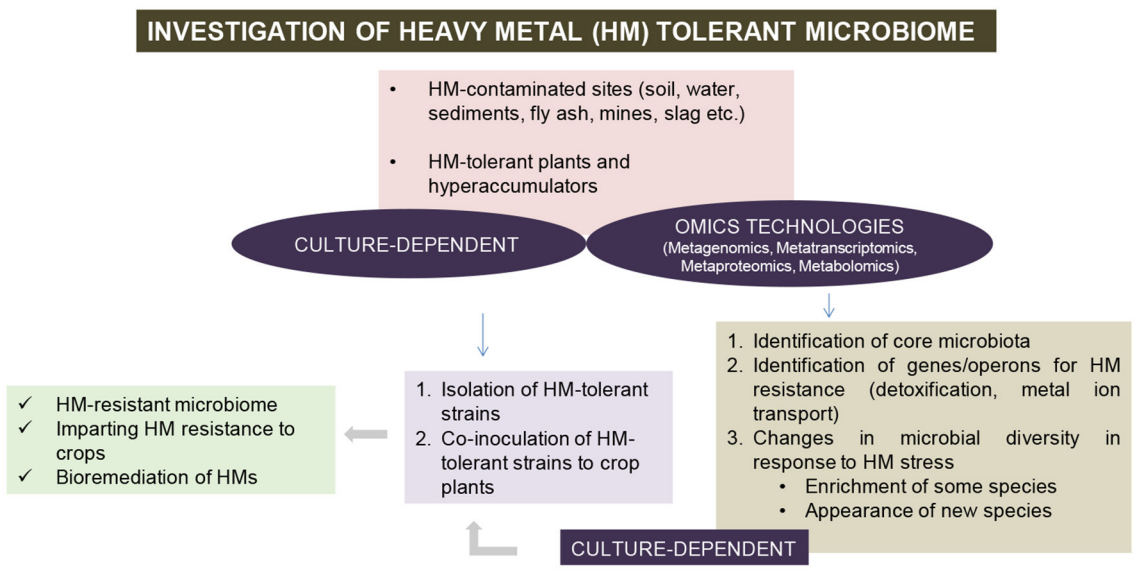

FIGURE 2 | Strategies for investigation of HM-tolerant (HMT) microbiome.

(Meena et al., 2017; Mishra et al., 2021b). The targeted amplicon sequencing involves specific amplification of ribosomal RNA genes (16S rRNA for bacteria and archaea and 18S rRNA or ITS for fungi) for determining the composition and diversity of microbial communities present in the samples. Being a cost-effective technique, 16S rRNA gene sequencing has been widely used for taxonomic profiling of microbial communities associated with HM-contaminated soil samples. For example, a study involving 16S rRNA gene sequencing of two nickel contaminated sites in southwest Slovakia revealed that phyla

Euryarcheota followed by *Crenarchaeota* (both belonging to domain Archaea) were present in both regions, with same species richness at the genus level (Remenár et al., 2017). Likewise, a recent study involving targeted sequencing of V3–V4 region of 16S rRNA gene investigated the bacteriome composition of *A. filiculoides* (a metal hyperaccumulator) exposed to HM stress (Banach et al., 2020). It was found that Cyanobacteria and Proteobacteria comprised >97% of the sequencing reads. Apart from confirming the occurrence of known metal-tolerant genera, some (previously unidentified) potential metal tolerant genera were reported, which include *Acinetobacter*, *Asticcacaulis*, *Anabaena*, *Bacillus*, *Brevundimonas*, *Burkholderia*, *Dyella*, *Methyloversatilis*, *Rhizobium,* and *Staphylococcus* (Banach et al., 2020). It needs to be noted that although targeted amplicon sequencing does not directly provide information on the functional contribution of the associated microbial communities, some predictive metagenomics software such as PICRUSt and Tax4Fun predict the metabolic potential of bacterial communities (Douglas et al., 2020; Mishra et al., 2021b).

Shotgun metagenomics, on the other hand, provides information about both structural and functional attributes of the microbial communities. A recently conducted shotgun metagenomics study determined the HM resistome (collection of all the heavy metal resistance genes) of agricultural soil in Nigeria with (250 mg/kg) or without Cd contamination (Salam et al., 2020). The authors reported functional annotation of genes encoding for HM-translocating P-type ATPases, which are responsible for efflux and detoxification of Cd such as *czcA*, *czcD*, *czrA*, etc. In addition, resistance genes against other classes of HMs such as Co, Ni, Cu, Fe, Hg, etc. were also reported (Salam et al., 2020). Using multiple techniques namely comparative metagenomics, 16S rRNA gene sequencing and qPCR analysis, the diversity of bacterial microbiome in sediments of three HM-contaminated rivers of China were investigated (Chen et al., 2018). The core microbiota of contaminated sediments were represented by bacterial species belonging to the phyla *Proteobacteria, Bacteroidetes,* and *Firmicutes,* which were present in higher abundance at all the three sites. Besides, the functional annotation in shotgun metagenomics revealed genes mainly involved in DNA recombination and repair, and HM-resistance genes in the contaminated rivers (Chen et al., 2018). In a recent study, shotgun metagenomics approach was used to unravel the HM (and antibiotic) resistome of hydrocarbon-polluted soil samples collected from an automobile workshop at Taiwo, Nigeria (Salam, 2020). The functional annotation of the ORFs revealed several antibiotic (majority representing β-lactamase encoding genes) and HM tolerant genes, which constitute the resistome of the polluted area (Salam, 2020). The resistance genes against a wide range of HMs such as Cu, Ag, Ga, Zn, Fe, Cu, Cd, Ni, etc., were represented in the soil sample. Interestingly, most of the tolerant genes were found to reside on the mobile genetic elements, to promote their spread in the polluted soil (Salam, 2020).

Apart from identifying the HM-tolerant genera and HM-resistance genes in the environmental samples, metagenomic analyses have also provided insights into the role of microbial inoculation in enhancing the remediation capacity of some plant species. In one such study, the inoculation of a rhizobial bacterial species, *Mesorhizobium loti* HZ76, improved the phytoremediation ability of *Robinia pseudoacacia* (a deciduous tree, also known as black locust) growing in HM-contaminated soil (Fan et al., 2018). The 16S rRNA gene sequencing and shotgun metagenome sequencing of the rhizospheric microbes of *R. pseudoacacia* revealed that upon rhizobial inoculation, the genes encoding ATP-binding cassette transporters were upregulated, thereby highlighting the role of plant-microbiota interactions in enhancing the phytoremediation efficiency of the holobiont (Fan et al., 2018).

Metatranscriptomics

Metatranscriptomics is a high throughput method for detection of *active* microbial species and genes (that are actively transcribed in the sample) under the particular set of environmental conditions (Simon and Daniel, 2011; White et al., 2017). This technique has enabled researchers to explore changes in microbial mRNA pool of environmental samples, and to study the response mechanism of microbial communities to HM stress (Yu et al., 2021). Further, functional metatranscriptomics approach allows identification of genes from microbial communities responsible for adapting to extreme environmental conditions. A protocol for functional metatranscriptomics study would involve isolation of total RNA from an environmental sample, construction of cDNA library, screening for HM tolerance transcripts through bacterial or yeast complementation system, and finally sequencing for identification of transcripts of interest (Thakur et al., 2018; Mukherjee and Reddy, 2020). Thakur et al. (2018) used this approach to screen cDNA library prepared from Cd contaminated site. The study revealed a yeast transformant that exhibited significant tolerance against multiple stresses (2–4 mM Co, 150–300 μM Cu, and 10–12 mM Zn; Thakur et al., 2018).

Lehembre et al. (2013) used the functional metatranscriptomics approach to decipher the functional contribution of microbiota toward HM resistance. The researchers performed functional screening of the soil eukaryotic metatranscriptome library (constituting total RNA from all the soil inhabiting microbes) for the ability to rescue (complement) the Cd or Zn sensitive phenotype of yeast mutants. The study identified some novel proteins which were previously uncharacterized with respect to HM resistance, such as BolA proteins and saccaropine dehydrogenase (for Zn tolerance), and C-terminal of aldehyde dehydrogenase (ADH) for Cd tolerance (Lehembre et al., 2013). In another study involving screening of eukaryotic cDNA library (prepared from HM contaminated soil), a clone (PLCc38) homologous to ADH, was found to be tolerant to Cu, Cd, Zn, and Co (Mukherjee et al., 2019). Aldehyde dehydrogenase enzymes eliminate the toxic aldehydes generated during various abiotic stresses (including HM stress).

In a recent published report, Yu et al. (2021) studied the response of soil microbiota to short term Cr^{6+} stress (1 mM Cr^{6+} for 30 min), using metatranscriptomics (and metagenomics) approach. The metagenomics study showed that 99% of the microbial communities (at genera level) were common between the control and stress groups. In contrast, the

metatranscriptomics approach revealed that 83% of the microbes showed change in relative abundance (at RNA level) in response to stress. Among the upregulated genes were those involved in oxidative stress, and transport, resistance, and reduction of Cr^{6+}. Further, ectopic expression of two unknown (upregulated) genes in *Escherichia coli* demonstrated their role in Cr^{6+} remediation. In a previous study, comparative metagenomic and metatranscriptomic study on Cr^{6+}-contaminated (long term) riparian soil have been used to screen for genes involved in Cr^{6+} remediation (Pei et al., 2020). The omics analysis enabled the identification of six novel genes with Cr^{6+} tolerance property. Protein expression studies in *E. coli* with two genes, *mcr* and *gsr,* demonstrated reduction of ∼50% Cr^{6+} in industrial wastewater contaminated with 200–600 μM of Cr^{6+} within 17 days (Pei et al., 2020).

Metaproteomics

Metaproteomics, also known as community proteomics or environmental proteomics, involves high-throughput study of all the proteins from microbial communities, extracted directly from the environment (Bastida et al., 2009; Gutleben et al., 2018; Li et al., 2019). A typical metaproteomics approach involves extraction of proteins from the environmental sample (soil, water, sediments, etc.), digestion of protein into peptides, followed by fractionation using 2D gel electrophoresis or liquid chromatography, and protein identification by mass spectrometry (against comparison to protein sequence database). It is a rapid method to identify and quantify the protein complement as well as protein–protein interactions in the community. Further, it provides a more authentic picture of the functional contribution of microbiota as often the DNA or RNA abundance does not co-relate well with protein abundance. Mattarozzi et al. (2017) investigated the rhizosphere of *Biscutella laevigata* (HM-tolerant) and *Noccaea caerulescens* (Ni hyperaccumulator) plants growing on serpentine soils by 16S rRNA gene sequencing and an LC-HRMS-based metaproteomics approach (Mattarozzi et al., 2017). Serpentine soils are characterized by high pH and HM concentration, and are low in nutrients and water holding capacity (Brady et al., 2005). The structural and functional characterization of microbial communities residing in soils contaminated with Ni, Co, and Cr revealed proteins involved in response to stimulus and metal transport. In addition, the taxonomic characterization revealed higher abundance of bacterial species namely *Microbacterium oxidans*, *Pseudomonas oryzihabitans*, *Stenotrophomonas rhizophila,* and *Bacillus methylotrophicus*, in the rhizosphere of these tolerant plants, in comparison to bulk soil (Mattarozzi et al., 2017). This study also highlighted the key interactions between bacterial communities and metal tolerant and hyperaccumulator plants in tackling HM stress. Moreover, another previous study examining the microbial diversity of Ni-contaminated serpentine soil has demonstrated that bacterial genera such as *Pseudomonas* and *Streptomyces* had over the years, become resistant to nickel ions by developing a highly potent nickel-resistant niche within the soil atmosphere (Mengoni et al., 2001).

The microbial transformation of Hg to MeHg, a potent neurotoxin that can bioaccumulate and biomagnify in food webs, is carried out by a group of bacteria known as mercury methylating bacteria. It is known that this transformation is an anaerobic process and depends upon the presence of *hgcAB* gene pair. Christensen et al. (2019) used a combination of shotgun metagenomics, 16S rRNA pyrosequencing, and metaproteomics approaches to determine the presence, distribution and diversity of mercury methylating bacteria in eight different sites in the USA. The metaproteomic (and metagenomic) analysis revealed that members belonging to Deltaproteobacteria phylum constituted the majority (∼40–70%) of mercury methylators at all the sites. Further, there was poor co-relation between the Hg concentration in soil samples and abundance of mercury methylating bacteria (Christensen et al., 2019).

The shoot proteome analysis of *A. halleri* (a hyperaccumulator) grown under Cd and Zn stress, either in the presence or absence of Cd- and Zn-resistant bacterial strains, was investigated by Farinati et al. (2011). The proteomic analysis revealed that in the presence of Cd- and Zn-resistant microbes, there was an enhanced uptake of Cd and Zn in the shoots, upregulation of photosynthesis and stress-related proteins (for example, rubisco, malate dehydrogenase, and superoxide dismutase) and decreased abundance of plant defense-related proteins (Farinati et al., 2011).

Metabolomics

Metabolomics is the large-scale study of total low-molecular weight compounds (<2 kDa) present at a particular developmental stage or environmental conditions (Grim et al., 2019). Metabolites are closer to the final phenotype of the organism, in comparison to transcripts and proteins. Besides, metabolomics studies are instrumental in bridging the gap between genotype and phenotype. Some plants known as metallophytes, have evolved mechanisms to tolerate high concentrations of HMs. Heavy Metal-tolerant plants could be obligate metallophytes that can survive only in high HM areas, or facultative metallophytes that are found in both normal and high HM-contaminated soils. Further, the recruitment of specific microbial communities in the rhizosphere could enhance the overall HM tolerance, and hence, remediation ability of plants. Plants produce a cocktail of small and large molecular weight, organic and inorganic compounds within their rhizosphere, to provide a nutrient rich environment for the microbial communities. The rhizosphere of metallophytes has been investigated to understand the exudates which could aid in the recruitment of specific metal-resistant microbial communities (Zhang et al., 2012; Borymski et al., 2018). Often the metal-resistant microbiota exhibit plant growth promoting properties such as nutrient solubilization, secretion of phytohormones, and enzymes such as 1-aminocyclopropane-1-carboxylate deaminase (Sessitsch et al., 2013; Sasse et al., 2018), which enable plants to survive in metalliferous soils that are nutrient poor.

Metabolomics of HM-contaminated soils and tolerant plants inhabiting HM-rich areas have been instrumental in identification of metal-resistant microbiota. Toyama et al. (2011) reported the production of plant metabolites such as

sugar, short-chained organic acids, amino acids, and phenols, which act as source of nutrients for rhizospheric microbes, and accelerated the phytoremediation of pyrene and benzopyrene. The role of rhizospheric bacteria in biodegradation of these contaminants was indicated by their persistence in the control set (with autoclaved rhizosphere sediments of sterilized plants) (Toyama et al., 2011). For example, *Phragmites australis*, also known as common reed, is a tall wetland grass used for wetland phytoremediation. Further, a recent study used metabolomics approach to analyze 73 metabolomes associated with *P. australis* growing in different acid mine drainage sites. The researchers observed that the distinct parts of roots (endosphere vs. rhizosphere) secreted spatially defined metabolites, depending upon total dissolved solutes, pH, and the presence of different metals such as Fe, Cr, Cu, and Zn (Kalu et al., 2021). It also needs to be emphasized that the secreted metabolites did not significantly vary between the different acid mine drainage sites, indicating a conserved response to these contaminants.

Metabolomic studies of plants with or without microbial inoculation have been used to decipher the mechanism of HM tolerance. For instance, the Pb accumulation ability of *Salix integra* upon inoculation with some indigenous rhizospheric microbes was investigated by targeted metabolomics approach (Niu et al., 2021). Inoculation with Pb-resistant *Bacillus* sp. and *Aspergillus niger*, showed enhanced proline levels as well as increased superoxide dismutase and catalase (antioxidants) activity (Niu et al., 2021). This study also identified 410 metabolites, which mainly constituted organic acids, amino acids and carbohydrates, in response to microbial inoculation. Further, around half of the identified metabolites were associated with HM bioavailability (Niu et al., 2021), thereby corroborating the role of microbes in increasing the phytoremediation efficiency. In another recent report, metabolomics and proteomics approach was used to study the mechanism of enhanced tolerance of wheat to Cd and Pd stress on inoculation with *Enterobacter bugandensis* TJ6 strain, a HM-immobilizing bacterium (Han et al., 2021). The TJ6 bacterial strain employed multiple strategies, including ∼50% reduced accumulation of Cd and Pd uptake, enhanced bioprecipitation and extracellular absorption, and secretion of arginine, betaine, and IAA. Further, the better tolerance of host plants was evident through improved DNA repair ability and antioxidant enzyme activity, and increased level of phytohormones in wheat roots (Han et al., 2021).

PLANT-MICROBE ASSOCIATION FOR HM STRESS ALLEVIATION

Phytoremediation is a cost-effective and environmental friendly approach. However, its large-scale application is limited by its lower efficiency. This issue could be addressed by inoculation of plants with microbes, in an approach known as *plant-microbial remediation* (Niu et al., 2021). For instance, the legume-Rhizobia interaction has been exploited to increase the phytoremediation ability of plants. The dual co-cultivation of *Agrobacterium tumefaciens* CCNWGS0286 (an IAA producing bacteria) and *Sinorhizobium meliloti* (nitrogen fixation) in alfa-alfa increases the zinc and copper accumulation ability, apart from promoting plant growth (Jian et al., 2019). The synergistic action of *A. tumefaciens* and *S. meliloti* enhanced the root nodulation (48% higher nodule number) and plant biomass (by >30% dry weight) under Cu and Zn stress, by promoting the antioxidant activity of plants (Jian et al., 2019). Similar mode of action of microbe-mediated HM stress alleviation was reported in a recently published study involving Cd stress in alfa alfa by Li et al. (2021). The growth and Cd uptake ability of alfa alfa was promoted upon inoculation with *Bacillus subtilis* due to enhanced antioxidant enzyme activity and reduced malondialdehyde (an indicator of oxidative lipid damage) levels in plants. In addition, the microbial inoculation increased Cd removal ability by >130%, and facilitated nutrient recycling as well (Li et al., 2021).

CONCLUSIONS AND FUTURE PERSPECTIVES

Natural environments, including HM-contaminated areas, contain many important microbial species that are unculturable (under standard lab conditions), and hence, inaccessible for further characterization. Omics approaches have been a boon in microbiome research, enabling identification and characterization of uncultured microbes, that constitute a major fraction (>90%) of the environmental samples. Further, metratranscriptomics and metaproteomics provide an insight into the "expressed" component of the community. Often two or more omics approaches are combined to corroborate the results and obtain an authentic picture of the microbiome. For instance, combining metaproteomics with metagenomics enables a co-relation between potential genetic diversity and actual "activity" occurring in the microbial communities.

However, the omics techniques are limited by technological challenges associated with extraction and fractionation procedures (high amounts of humic substances in soil), requirement of robust bioinformatic tools (huge computational load resulting from omics, normally from megabytes to terabytes of data) and sophisticated equipment and procedures. A major challenge associated with metabolomics study is the diverse chemical nature of metabolites, due to which no one protocol could be used to estimate all metabolites produced in a cell. Likewise, the metaproteome extracted from environmental samples are contaminated by proteins from other organisms such as protozoa, nematodes, etc. Therefore, a prior separation of microbial cells from the sample, followed by protein extraction and fractionation would be a better representation of protein fingerprint.

Investigation of HM-tolerant microbial communities from rhizospheric and endophytic microbiota associated with hyperaccumulator and facultative metallophytes (grown in high HM concentrations), is a powerful strategy of bioprospecting for bioremediation (Photolo et al., 2021). The higher abundance of some bacterial and fungal species in HM-contaminated sites represents the indigenous/native resistant population, which could be exploited for remediation of HMs. However, the isolation of microbial strains (in tangible/physical form) is

a pre-requisite to explore the functional and ecological roles of potential microbial communities. Subsequently, carefully optimized media and culture conditions (mimicking the natural environmental conditions) could be used to isolate "unculturable" and novel species. Several such prokaryotic uncultivated but well-characterized species have been placed under the nomenclature *Candidatus*.

Another major challenge for plant-microbial remediation of HMs is the inability of inoculated microbes to maintain their number and sustain the remediation activity under field conditions. Therefore, it is important to consider the interaction between the added inoculants and microbial communities in nature (bulk soil, rhizosphere, and endosphere). Further, advancements in the field of protein and metabolite extraction, fractionation, and characterization methods as well as advances in instrumentation would boost the research on functional microbial ecology (focusing on the microbiome component of the plant holobiont), and open avenues for solving environmental issues, including HM contamination of environment. Further, the knowledge of HM-tolerant microbiota could be incorporated to assist the plant breeding programs aimed at generating HM-tolerant crops, in an approach known as holobiont breeding.

AUTHOR CONTRIBUTIONS

SM conceived the idea of the manuscript. LP, VD, NS, and SM prepared the manuscript and figures. All authors have read and approved the final version of the manuscript.

FUNDING

SM and VD would like to acknowledge the financial support provided by the Dayalbagh Educational Institute (Deemed-to-be-University), Agra, India, in the form of minor research project [Grant No. DEI/GBMF (1732020)/43].

REFERENCES

Akinsanya, M. A., Goh, J. K., Lim, S. P., and Ting, A. S. Y. (2015). Metagenomics study of endophytic bacteria in *Aloe vera* using next-generation technology. *Genom. Data* 6, 159–163. doi: 10.1016/j.gdata.2015.09.004

Alcántara-Martínez, N., Figueroa-Martínez, F., Rivera-Cabrera, F., Gutiérrez-Sánchez, G., and Volke-Sepúlveda, T. (2018). An endophytic strain of *Methylobacterium* sp. increases arsenate tolerance in *Acacia farnesiana* (L.) Willd: a proteomic approach. *Sci. Total Environ.* 625, 762–774. doi: 10.1016/j.scitotenv.2017.12.314

Banach, A. M., Kuzniar, A., Grzadziel, J., and Wolińska, A. (2020). *Azolla filiculoides* L. as a source of metal-tolerant microorganisms. *PLoS ONE* 15, e0232699. doi: 10.1371/journal.pone.0232699

Bastida, F., Moreno, J. L., Nicolas, C., Hernandez, T., and Garcia, C. (2009). Soil metaproteomics: a review of an emerging environmental science. Significance, methodology and perspectives. *Eur. J. Soil Sci.* 60, 845–859. doi: 10.1111/j.1365-2389.2009.01184.x

Bellali, S., Lagier, J.-C., Million, M., Anani, H., Haddad, G., Francis, R., et al. (2021). Running after ghosts: are dead bacteria the dark matter of the human gut microbiota? *Gut Microbes* 13, 1–12. doi: 10.1080/19490976.2021.1897208

Boiteau, R. M., Shaw, J. B., Pasa-Tolic, L., Koppenaal, D. W., and Jansson, J. K. (2018). Micronutrient metal speciation is controlled by competitive organic chelation in grassland soils. *Soil Biol. Biochem.* 120, 283–291. doi: 10.1016/j.soilbio.2018.02.018

Borymski, S., Cycoń, M., Beckmann, M., Mur, L. A., and Piotrowska-Seget, Z. (2018). Plant species and heavy metals affect biodiversity of microbial communities associated with metal-tolerant plants in metalliferous soils. *Front. Microbiol.* 9, 1425. doi: 10.3389/fmicb.2018.01425

Brady, K. U., Kruckeberg, A. R., and Bradshaw Jr, H. D. (2005). Evolutionary ecology of plant adaptation to serpentine soils. *Annu. Rev. Ecol. Evol. Syst.* 36, 243–266. doi: 10.1146/annurev.ecolsys.35.021103.105730

Chen, Y., Jiang, Y., Huang, H., Mou, L., Ru, J., Zhao, J., et al. (2018). Long-term and high-concentration heavy-metal contamination strongly influences the microbiome and functional genes in Yellow River sediments. *Sci. Total Environ.* 637, 1400–1412. doi: 10.1016/j.scitotenv.2018.05.109

Christensen, G. A., Gionfriddo, C. M., King, A. J., Moberly, J. G., Miller, C. L., Somenahally, A. C., et al. (2019). Determining the reliability of measuring mercury cycling gene abundance with correlations with mercury and methylmercury concentrations. *Environ. Sci. Technol.* 53, 8649–8663. doi: 10.1021/acs.est.8b06389

Douglas, G. M., Maffei, V. J., Zaneveld, J. R., Yurgel, S. N., Brown, J. R., Taylor, C. M., et al. (2020). PICRUSt2 for prediction of metagenome functions. *Nat. Biotechnol.* 38, 685–688. doi: 10.1038/s41587-020-0548-6

Emamverdian, A., Ding, Y., Mokhberdoran, F., and Xie, Y. (2015). Heavy metal stress and some mechanisms of plant defense response. *ScientificWorldJournal.* (2015) 2015, 756120. doi: 10.1155/2015/756120

Fahsi, N., Mahdi, I., Mesfioui, A., Biskri, L., and Allaoui, A. (2021). Plant growth-promoting Rhizobacteria isolated from the Jujube (*Ziziphus lotus*) plant enhance wheat growth, Zn uptake, and heavy metal tolerance. *Agriculture* 11, 316. doi: 10.3390/agriculture11040316

Fan, M., Xiao, X., Guo, Y., Zhang, J., Wang, E., Chen, W., et al. (2018). Enhanced phytoremdiation of *Robinia pseudoacacia* in heavy metal-contaminated soils with rhizobia and the associated bacterial community structure and function. *Chemosphere* 197, 729–740. doi: 10.1016/j.chemosphere.2018.01.102

Farinati, S., DalCorso, G., Panigati, M., and Furini, A. (2011). Interaction between selected bacterial strains and *Arabidopsis halleri* modulates shoot proteome and cadmium and zinc accumulation. *J. Exp. Bot.* 62, 3433–3447. doi: 10.1093/jxb/err015

Feng, G., Xie, T., Wang, X., Bai, J., Tang, L., Zhao, H., et al. (2018). Metagenomic analysis of microbial community and function involved in cd-contaminated soil. *BMC Microbial.* 18, 11. doi: 10.1186/s12866-018-1152-5

Flora, S. J. (2009). Structural, chemical and biological aspects of antioxidants for strategies against metal and metalloid exposure. *Oxid. Med. Cell. Longev.* 2, 191–206. doi: 10.4161/oxim.2.4.9112

Goyal, D., Yadav, A., Prasad, M., Singh, T. B., Shrivastav, P., Ali, A., et al. (2020). "Effect of heavy metals on plant growth: an overview," in *Contaminants in Agriculture*, eds G. S. Naeem and A. Ansari (Cham: Springer), 79–101. doi: 10.1007/978-3-030-41552-5_4

Grim, C. M., Luu, G. T., and Sanchez, L. M. (2019). Staring into the void: demystifying microbial metabolomics. *FEMS Microbiol. Lett.* 366, fnz135. doi: 10.1093/femsle/fnz135

Gutleben, J., Chaib De Mares, M., Van Elsas, J. D., Smidt, H., Overmann, J., and Sipkema, D. (2018). The multi-omics promise in context: from sequence to microbial isolate. *Crit. Rev. Microbiol.* 44, 212–229. doi: 10.1080/1040841X.2017.1332003

Han, H., Zhang, H., Qin, S., Zhang, J., Yao, L., Chen, Z., et al. (2021). Mechanisms of *Enterobacter bugandensis* TJ6 immobilization of heavy metals and inhibition of Cd and Pb uptake by wheat based on metabolomics and proteomics. *Chemosphere* 276, 130157. doi: 10.1016/j.chemosphere.2021.130157

Handelsman, J., Rondon, M. R., Brady, S. F., Clardy, J., and Goodman, R. M. (1998). Molecular biological access to the chemistry of unknown soil

microbes: a new frontier for natural products. *Chem. Biol*. 5, R245–R249. doi: 10.1016/S1074-5521(98)90108-9

Hauser, M. T. (2014). Molecular basis of natural variation and environmental control of trichome patterning. *Front. Plant Sci.* 5, 320. doi: 10.3389/fpls.2014.00320

Järup, L. (2003). Hazards of heavy metal contamination. *Br. Med. Bull*. 68, 167–182. doi: 10.1093/bmb/ldg032

Jian, L., Bai, X., Zhang, H., Song, X., and Li, Z. (2019). Promotion of growth and metal accumulation of alfalfa by coinoculation with *Sinorhizobium* and *Agrobacterium* under copper and zinc stress. *PeerJ* 7, e6875. doi: 10.7717/peerj.6875

Johri, N., Jacquillet, G., and Unwin, R. (2010). Heavy metal poisoning: the effects of cadmium on the kidney. *Biometals* 23, 783–792. doi: 10.1007/s10534-010-9328-y

Jozefczak, M., Remans, T., Vangronsveld, J., and Cuypers, A. (2012). Glutathione is a key player in metal-induced oxidative stress defenses. *Int. J. Mol. Sci*. 13, 3145–3175. doi: 10.3390/ijms13033145

Kalu, C. M., Ogola, H. J. O., Selvarajan, R., Tekere, M., and Ntushelo, K. (2021). Fungal and metabolome diversity of the rhizosphere and endosphere of *Phragmites australis* in an AMD-polluted environment. *Heliyon* 7, e06399. doi: 10.1016/j.heliyon.2021.e06399

Lehembre, F., Doillon, D., David, E., Perrotto, S., Baude, J., Foulon, J., et al. (2013). Soil metatranscriptomics for mining eukaryotic heavy metal resistance genes. *Environ. Microbiol*. 15, 2829–2840. doi: 10.1111/1462-2920.12143

Li, K., Pidatala, V. R., Shaik, R., Datta, R., and Ramakrishna, W. (2014). Integrated metabolomic and proteomic approaches dissect the effect of metal-resistant bacteria on maize biomass and copper uptake. *Environ. Sci. Technol*. 48, 1184–1193. doi: 10.1021/es4047395

Li, Q., Xing, Y., Fu, X., Ji, L., Li, T., Wang, J., et al. (2021). Biochemical mechanisms of rhizospheric *Bacillus subtilis*-facilitated phytoextraction by alfalfa under cadmium stress–Microbial diversity and metabolomics analyses. *Ecotoxicol. Environ. Saf*. 212, 112016. doi: 10.1016/j.ecoenv.2021.112016

Li, S., Hu, S., Shi, S., Ren, L., Yan, W., and Zhao, H. (2019). Microbial diversity and metaproteomic analysis of activated sludge responses to naphthalene and anthracene exposure. *RSC Adv*. 9, 22841–22852. doi: 10.1039/C9RA04674G

Majernik, A., Gottschalk, G., and Daniel, R. (2001). Screening of environmental DNA libraries for the presence of genes conferring Na+ (Li+)/H+ antiporter activity on *Escherichia coli*: characterization of the recovered genes and the corresponding gene products. *J. Bacteriol. Res*. 183, 6645–6653. doi: 10.1128/JB.183.22.6645-6653.2001

Mathew, D. C., Ho, Y. N., Gicana, R. G., Mathew, G. M., Chien, M. C., and Huang, C. C. (2015). A rhizosphere-associated symbiont, *Photobacterium* spp. strain MELD1, and its targeted synergistic activity for phytoprotection against mercury. *PLoS ONE*. 10, e0121178. doi: 10.1371/journal.pone.0121178

Mattarozzi, M., Manfredi, M., Montanini, B., Gosetti, F., Sanangelantoni, A. M., Marengo, E., et al. (2017). A metaproteomic approach dissecting major bacterial functions in the rhizosphere of plants living in serpentine soil. *Anal. Bioanal. Chem*. 409, 2327–2339. doi: 10.1007/s00216-016-0175-8

Meena, K. K., Sorty, A. M., Bitla, U. M., Choudhary, K., Gupta, P., Pareek, A., et al. (2017). Abiotic stress responses and microbe-mediated mitigation in plants: the omics strategies. *Front. Plant Sci*. 8, 172. doi: 10.3389/fpls.2017.00172

Mengoni, A., Barzanti, R., Gonnelli, C., Gabbrielli, R., and Bazzicalupo, M. (2001). Characterization of nickel-resistant bacteria isolated from serpentine soil. *Environ. Microbiol*. 3, 691–698. doi: 10.1046/j.1462-2920.2001.00243.x

Mishra, J., Singh, R., and Arora, N. K. (2017). Alleviation of heavy metal stress in plants and remediation of soil by rhizosphere microorganisms. *Front. Microbiol*. 8, 1706. doi: 10.3389/fmicb.2017.01706

Mishra, S., Bhattacharjee, A., and Sharma, S. (2021a). An ecological insight into the multifaceted world of plant-endophyte association. *Crit. Rev. Plant Sci*. 40, 127–146. doi: 10.1080/07352689.2021.1901044

Mishra, S., Goyal, D., and Phurailatpam, L. (2021b). Targeted 16S rRNA gene and ITS2 amplicon sequencing of leaf and spike tissues of *Piper longum* identifies new candidates for bioprospecting of bioactive compounds. *Arch. Microbiol*. 203, 3851–3867. doi: 10.1007/s00203-021-02356-w

Mukherjee, A., and Reddy, M. S. (2020). Metatranscriptomics: an approach for retrieving novel eukaryotic genes from polluted and related environments. *3 Biotech* 10, 1–19. doi: 10.1007/s13205-020-2057-1

Mukherjee, A., Yadav, R., Marmeisse, R., Fraissinet-Tachet, L., and Reddy, M. S. (2019). Heavy metal hypertolerant eukaryotic aldehyde dehydrogenase isolated from metal contaminated soil by metatranscriptomics approach. *Biochimie* 160, 183–192. doi: 10.1016/j.biochi.2019.03.010

Niu, X. Y., Wang, S. K., Zhou, J., Di, D. L., Sun, P., and Huang, D. Z. (2021). Inoculation with indigenous rhizosphere microbes enhances aboveground accumulation of lead in *Salix integra* Thunb. by improving transport coefficients. *Front. Microbiol*. 12, 686812. doi: 10.3389/fmicb.2021.686812

Pei, Y., Tao, C., Ling, Z., Yu, Z., Ji, J., Khan, A., et al. (2020). Exploring novel Cr (VI) remediation genes for Cr (VI)-contaminated industrial wastewater treatment by comparative metatranscriptomics and metagenomics. *Sci. Total Environ*. 742, 140435. doi: 10.1016/j.scitotenv.2020.140435

Photolo, M. M., Sitole, L., Mavumengwana, V., and Tlou, M. G. (2021). Genomic and physiological investigation of heavy metal resistance from plant endophytic *Methylobacterium radiotolerans* MAMP 4754, Isolated from *Combretum erythrophyllum*. *Int. J. Environ. Res. Public Health* 18, 997. doi: 10.3390/ijerph18030997

Phurailatpam, L., and Mishra, S. (2020). "Role of plant endophytes in conferring abiotic stress tolerance," in Plant Ecophysiology and Adaptation under Climate Change: Mechanisms and Perspectives II, ed M. Hasanuzzaman (Springer, Singapore), 603–628. doi: 10.1007/978-981-15-2172-0_22

Pires, C., Franco, A. R., Pereira, S. I., Henriques, I., Correia, A., Magan, N., et al. (2017). Metal (loid)-contaminated soils as a source of culturable heterotrophic aerobic bacteria for remediation applications. *Geomicrobiol. J*. 34, 760–768. doi: 10.1080/01490451.2016.1261968

Qin, S., Wu, X., Han, H., Pang, F., Zhang, J., and Chen, Z. (2021). Polyamine-producing bacterium *Bacillus megaterium* N3 reduced Cd accumulation in wheat and increased the expression of DNA repair-and plant hormone-related proteins in wheat roots. *Environ. Exp. Bot*. 189, 104563. doi: 10.1016/j.envexpbot.2021.104563

Rajkumar, M., Sandhya, S., Prasad, M. N. V., and Freitas, H. (2012). Perspectives of plant-associated microbes in heavy metal phytoremediation. *Biotechnol. Adv*. 30, 1562–1574. doi: 10.1016/j.biotechadv.2012.04.011

Reddy, M. S., Kour, M., Aggarwal, S., Ahuja, S., Marmeisse, R., and Fraissinet-Tachet, L. (2016). Metal induction of a *Pisolithus albus* metallothionein and its potential involvement in heavy metal tolerance during mycorrhizal symbiosis. *Environ. Microbiol*. 18, 2446–2454. doi: 10.1111/1462-2920.13149

Remenár, M., Harichová, J., Zámocký, M., Pangallo, D., Szemes, T., Budiš, J., et al. (2017). Metagenomics of a nickel-resistant bacterial community in an anthropogenic nickel-contaminated soil in southwest Slovakia. *Biol. Plant*. 72, 971–981. doi: 10.1515/biolog-2017-0117

Sagonda, T., Adil, M. F., Sehar, S., Rasheed, A., Joan, H. I., Ouyang, Y., et al. (2021). Physio-ultrastructural footprints and iTRAQ-based proteomic approach unravel the role of *Piriformospora indica*-colonization in counteracting cadmium toxicity in rice. *Ecotoxicol. Environ. Saf*. 220, 112390. doi: 10.1016/j.ecoenv.2021.112390

Sahu, P. K., and Mishra, S. (2021). Effect of hybridization on endophytes: the endo-microbiome dynamics. *Symbiosis* 84, 369–377. doi: 10.1007/s13199-021-00760-w

Salam, L. B. (2020). Unravelling the antibiotic and heavy metal resistome of a chronically polluted soil. *3 Biotech* 10, 1–23. doi: 10.1007/s13205-020-02219-z

Salam, L. B., Obayori, O. S., Ilori, M. O., and Amund, O. O. (2020). Effects of cadmium perturbation on the microbial community structure and heavy metal resistome of a tropical agricultural soil. *Bioresour. Bioprocess*. 7, 1–19. doi: 10.1186/s40643-020-00314-w

Sasse, J., Martinoia, E., and Northen, T. (2018). Feed your friends: do plant exudates shape the root microbiome? *Trends Plant Sci*. 23, 25–41. doi: 10.1016/j.tplants.2017.09.003

Schutzendubel, A., and Polle, A. (2002). Plant responses to abiotic stresses: heavy metal-induced oxidative stress and protection by mycorrhization. *J. Exp. Bot*. 53, 1351–1365. doi: 10.1093/jexbot/53.372.1351

Sessitsch, A., Kuffner, M., Kidd, P., Vangronsveld, J., Wenzel, W. W., Fallmann, K., et al. (2013). The role of plant-associated bacteria in the mobilization and phytoextraction of trace elements in contaminated soils. *Soil Biol. Biochem*. 60, 182–194. doi: 10.1016/j.soilbio.2013.01.012

Simon, C., and Daniel, R. (2011). Metagenomic analyses: past and future trends. *Appl. Environ. Microbiol.* 77, 1153–1161. doi: 10.1128/AEM.02345-10

Singh, S., Parihar, P., Singh, R., Singh, V. P., and Prasad, S. M. (2016). Heavy metal tolerance in plants: role of transcriptomics, proteomics, metabolomics, and ionomics. *Front. Plant Sci.* 6, 1143. doi: 10.3389/fpls.2015.01143

Staley, J. T., and Konopka, A. (1985). Measurement of *in situ* activities of nonphotosynthetic microorganisms in aquatic and terrestrial habitats. *Annu. Rev. Microbiol.* 39, 321–346. doi: 10.1146/annurev.mi.39.100185.001541

Thakur, B., Yadav, R., Fraissinet-Tachet, L., Marmeisse, R., and Reddy, M. S. (2018). Isolation of multi-metal tolerant ubiquitin fusion protein from metal polluted soil by metatranscriptomic approach. *J. Microbiol. Methods* 152, 119–125. doi: 10.1016/j.mimet.2018.08.001

Tiwari, S., and Lata, C. (2018). Heavy metal stress, signaling, and tolerance due to plant-associated microbes: an overview. *Front. Plant Sci.* 9, 452. doi: 10.3389/fpls.2018.00452

Toyama, T., Furukawa, T., Maeda, N., Inoue, D., Sei, K., Mori, K., et al. (2011). Accelerated biodegradation of pyrene and benzo [a] pyrene in the *Phragmites australis* rhizosphere by bacteria–root exudate interactions. *Water Res.* 45, 1629–1638. doi: 10.1016/j.watres.2010.11.044

Valko, M. Morris, H., and Cronin, M. T. D. (2005). Metals, toxicity and oxidative stress. *Curr. Med. Chem.* 12, 1161–1208. doi: 10.2174/0929867053764635

Viehweger, K. (2014). How plants cope with heavy metals. *Bot. Stud.* 55, 1–12. doi: 10.1186/1999-3110-55-35

Wang, X., Fang, L., Beiyuan, J., Cui, Y., Peng, Q., Zhu, S., et al. (2021). Improvement of alfalfa resistance against Cd stress through rhizobia and arbuscular mycorrhiza fungi co-inoculation in Cd-contaminated soil. *Environ. Pollut.* 277, 116758. doi: 10.1016/j.envpol.2021.116758

White, R. A., Borkum, M. I., Rivas-Ubach, A., Bilbao, A., Wendler, J. P., Colby, S. M., et al. (2017). From data to knowledge: the future of multi-omics data analysis for the rhizosphere. *Rhizosphere* 3, 222–229. doi: 10.1016/j.rhisph.2017.05.001

Wu, J., Hu, J., Wang, L., Zhao, L., and Ma, F. (2021). Responses of Phragmites australis to copper stress: a combined analysis of plant morphology, physiology and proteomics. *Plant Biol.* 23, 351–362. doi: 10.1111/plb.13175

Wu, Y., Ma, L., Liu, Q., Vestergård, M., Topalovic, O., Wang, Q., et al. (2020). The plant-growth promoting bacteria promote cadmium uptake by inducing a hormonal crosstalk and lateral root formation in a hyperaccumulator plant *Sedum alfredii*. *J. Hazard. Mater.* 395, 122661. doi: 10.1016/j.jhazmat.2020.122661

Yu, Z., Pei, Y., and Zhao, S. (2021). Metatranscriptomic analysis reveals active microbes and genes responded to short-term Cr(VI) stress. *Ecotoxicology* 30, 1527–1537. doi: 10.1007/s10646-020-02290-5

Zhang, W. H., Huang, Z., He, L. Y., and Sheng, X. F. (2012). Assessment of bacterial communities and characterization of lead-resistant bacteria in the rhizosphere soils of metal-tolerant *Chenopodium ambrosioides* grown on lead–zinc mine tailings. *Chemosphere* 87, 1171–1178. doi: 10.1016/j.chemosphere.2012.02.036

Zhen, Z., Yan, C., and Zhao, Y. (2020). Influence of epiphytic bacteria on arsenic metabolism in *Hydrilla verticillata*. *Environ. Pollut.* 261, 114232. doi: 10.1016/j.envpol.2020.114232

Conflict of Interest: The authors declare that the research was conducted in the absence of any commercial or financial relationships that could be construed as a potential conflict of interest.

Publisher's Note: All claims expressed in this article are solely those of the authors and do not necessarily represent those of their affiliated organizations, or those of the publisher, the editors and the reviewers. Any product that may be evaluated in this article, or claim that may be made by its manufacturer, is not guaranteed or endorsed by the publisher.

frontiers | Frontiers in Sustainable Food Systems

ORIGINAL RESEARCH
published: 04 April 2022
doi: 10.3389/fsufs.2022.845512

Biohardening of Banana cv. Karpooravalli (ABB; Pisang Awak) With *Bacillus velezensis* YEBBR6 Promotes Plant Growth and Reprograms the Innate Immune Response Against *Fusarium oxysporum* f.sp. *cubense*

R. Saravanan[1], *S. Nakkeeran*[1]*, *N. Saranya*[2], *M. Kavino*[3], *V. Ragapriya*[2], *S. Varanavasiappan*[4], *M. Raveendran*[4], *A. S. Krishnamoorthy*[1], *V. G. Malathy*[1] and *S. Haripriya*[5]

[1] Department of Plant Pathology, Tamil Nadu Agricultural University, Coimbatore, India, [2] Department of Plant Molecular Biology and Bioinformatics, Tamil Nadu Agricultural University, Coimbatore, India, [3] Department of Fruit Science, Tamil Nadu Agricultural University, Coimbatore, India, [4] Department of Plant Biotechnology, Tamil Nadu Agricultural University, Coimbatore, India, [5] Department of Nano Science and Technology, Tamil Nadu Agricultural University, Coimbatore, India

OPEN ACCESS

Edited by:
Narayan Chandra Mandal, Visva-Bharati University, India

Reviewed by:
Sudisha Jogaiah, Karnatak University, India
Veerubommu Shanmugam, Indian Agricultural Research Institute (ICAR), India

***Correspondence:**
S. Nakkeeran
nakkeeranayya@tnau.ac.in

Specialty section:
This article was submitted to Crop Biology and Sustainability, a section of the journal Frontiers in Sustainable Food Systems

Received: 29 December 2021
Accepted: 18 February 2022
Published: 04 April 2022

Citation:
Saravanan R, Nakkeeran S, Saranya N, Kavino M, Ragapriya V, Varanavasiappan S, Raveendran M, Krishnamoorthy AS, Malathy VG and Haripriya S (2022) Biohardening of Banana cv. Karpooravalli (ABB; Pisang Awak) With Bacillus velezensis YEBBR6 Promotes Plant Growth and Reprograms the Innate Immune Response Against Fusarium oxysporum f.sp. cubense. Front. Sustain. Food Syst. 6:845512. doi: 10.3389/fsufs.2022.845512

Fungicides play an immense role in quenching the infection of Panama wilt in banana. However, the use of fungicides and the monoculture of banana cultivars have resulted in the development of new races like race 4 which challenges scientists across the globe to identify new candidates for biological suppression of *Fusarium oxysporum* f.sp. *cubense* (*Foc*). Hence, attempts were made to dissect the endophytes from resistant banana cultivar YKM5 (Yengambi–AAA) to suppress *Foc* KP (race 4) infecting cv. Karpooravalli (ABB; Pisang Awak). Among the various endophytes, *Bacillus velezensis* YEBBR6 inhibited the mycelial growth up to 63% over control and hyper-parasitized the mycelium of *Foc* KP. Scanning electron microscope analysis revealed the ramification by *B. velezensis* over the hyphae of *Foc* KP leading to lysis. Analysis of VOCs/NVOCs compounds from the zone of inhibition, confirmed the presence of unique biomolecules including linoelaedic acid, nonanol, acetylvaleryl, 5–hydroxyl methyl furfural, clindamycin, allobarbital, 3-thiazolidine carboxamide, azulene, aminomorpholine, procyclidine, campholic acid, 3 amino-4 hydroxy phenyl sulfone, 3–deoxy mannoic lactone, hexadecanoic acid, oleic acid, and dihydroacridine of an antifungal and antimicrobial nature. Considering the diverse antimicrobial property, biohardening of micropropagated banana cv. Karpooravalli (ABB) with a liquid formulation of *B. velezensis* YEBBR6 (8×10^8 cfu/ml) and challenge inoculation with *Foc* KP promoted plant growth compared to uninoculated control. Besides, incidence of *Fusarium* wilt was reduced by 100% over inoculated control in greenhouse conditions. Furthermore, the expression of transcription factors and defense genes WRKY, MAPK, CERK 1, LOX, and PAL increased by several folds compared to inoculated and healthy control and thus suppressed *Fusarium* wilt of banana cv. Karpooravalli (ABB). Also, cytoscape analysis of defense

genes indicated the coordinated expression of various other genes associated with it. Hence, our study confirmed the scope for exploring *B. velezensis* on a commercial scale for the management of *Fusarium* wilt race 4 causing wilt across genomes of banana.

Keywords: banana, *Fusarium* wilt, *Bacillus velezensis*, biohardening, VOCs/NVOCs compounds, defense genes expression

INTRODUCTION

Globally, banana is commercially cultivated in several tropical and subtropical regions. Monoculture of banana has resulted in the outbreak of *Fusarium* wilt. Panama wilt of banana caused by *Fusarium oxysporum* f.sp. *cubense* (*Foc)* is a dreadful disease affecting the livelihood of the farming community and the sustainability of banana-based industries. Pathogens survive as chlamydospores in soil for decades. Furthermore, owing to the proliferation of pathogens, outbreak of race 4 has emerged as a most destructive pathogen worldwide (Butler, 2013). Race 4 was observed in 90% of banana plantations in South China (Cheng et al., 2012). Recently in India, *Foc* TR4 has been reported in Gujarat and Bihar, indicating the potential spread and threat in the near future (Nakkeeran et al., 2021). Hence, to date there are no effective fungicides to curb the spread and infection of banana by race 4. This lacuna warrants the development of a novel management strategy to quench *Fusarium* wilt of banana. Besides, one school of thought also emphasizes that continuous application of chemical fertilizers acidifies the soil and accentuates the multiplication of *Foc* resulting in severe outbreaks of *Fusarium* wilt (Zhao et al., 2018). Considering the serious threat imposed by *Foc*, an effective alternate method has to be developed for the management of *Fusarium* wilt of banana. To reach sustainability and profitability in food production, plant growth-promoting rhizobacteria (PGPR) play a key role and also aid in increasing the productivity of plants both under biotic and abiotic stress. Furthermore, PGPR suppress plant pathogens through competition, antibiosis, lysis, and through induction of systemic resistance (Anupama et al., 2014; Narasimha Murthy et al., 2021). In this juncture, biological control will pave the way for the sustainable management of wilt caused by different races of *Foc*. Amidst the various biocontrol agents, bacterial endophytes can be well explored for the same, rather than fungicides (Nel et al., 2006). Several endophytic *Bacillus* spp. have been explored for the management of *Fusarium* wilt of banana as they are bestowed with beneficial attributes including plant growth promotion, induction of immune response, and suppression of *Foc* (Nakkeeran et al., 2021; Saravanan et al., 2021a). In the recent past, *Bacillus* spp. have been well explored for the management of soil-borne and foliar diseases. The antagonistic *Bacillus* spp. quench plant pathogens through the

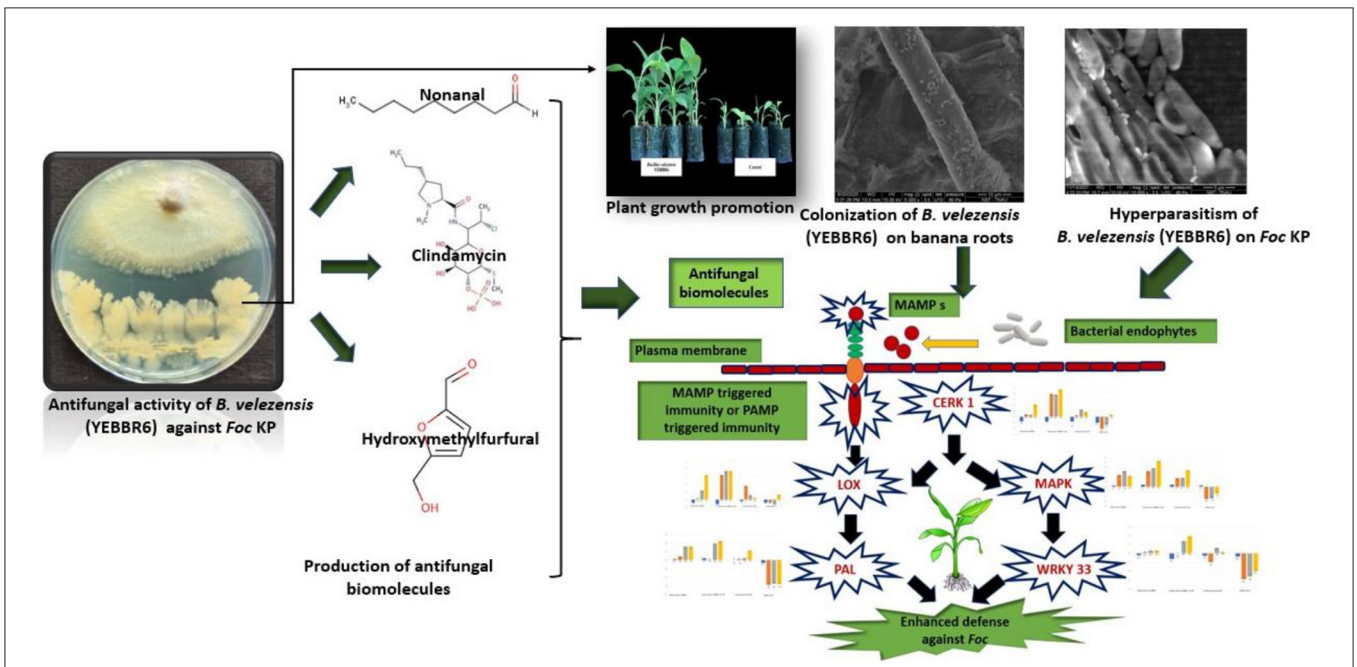

GRAPHICAL ABSTRACT | Induction of innate immune response and growth promotion in banana by *B. velezensis* against Foc.

production of antifungal biomolecules, antimicrobial peptides, and through the induction of an immune response (Nakkeeran et al., 2019). However, the versatile *Bacillus* spp. genome of *B. velezensis* comprises genes coding for different antimicrobial peptides, hydrolytic enzymes, growth hormones, and induction of immune response contributing to antiviral and antifungal action (Saravanan et al., 2021b). Moreover, *B. velezensis* has broad-spectrum action against several fungal pathogens (Meng and Hao, 2017). However, based on the perusal of literature there are no reports describing the exploration of immune response mediated by *B. velezensis* to manage *Foc* infection in banana. In the current investigation, *B. velezensis* YEBBR6 isolated from the bract of resistant genotype YKM 5 was evaluated for antifungal activity, growth promotion, secondary metabolite production, and reprogramming of immune response for the management of *Fusarium* wilt of banana through biohardening of micropropagated cv. Karpooravalli (Pisang Awak–ABB) plantlets.

MATERIALS AND METHODS

Isolation and Molecular Confirmation of *Fusarium oxysporum* f. sp. *cubense*

The wilt affected banana corms from different banana-cultivating provinces of Tamil Nadu, India pertaining to Lakshmipuram village of Theni province (10° 11′ 16.62″ N77° 47′ 34.4112″E/ latitude 10.187950/ longitude 77.792892), Chinnamanur village of Theni province (9° 50′ 22.776″N77° 22′ 58.0692″E/ latitude 9.839660/ longitude 77.382797), Thondamuthur village of Coimbatore province (11°00′35″N 76°49′41″E/ latitude 10.9905/ longitude 10.9905), Sirumugai village of Coimbatore province (11° 19′ 16.9″N, 77° 0′ 18.8″E/ latitude 11.3183/ longitude 77.0066), Ammapalayam village of Salem province (11° 40.7123′ N 78° 7.4319′ E/ latitude 11.678539/ longitude 78.123865), Athani village of Erode province (11.5232° N, 77.5120° E/ latitude 11.515219/ longitude 77.452367), Andhiyur village of Erode province (11° 34′ 37.4628″N 77° 35′ 15.8280″E/ latitude 11.577073/ longitude 77.587730), and Gobichettipalayam village of Erode province (11.4548° N, 77.4365° E/ latitude 11.450410/ longitude 77.430036) were collected. Pathogenic *Fusarium* spp. associated with banana cultivars susceptible to Panama wilt of banana were isolated as per the protocol described by Nelson et al. (1983). Genomic DNA of *Fusarium* was extracted from the mycelium of pure culture through the CTAB method (Griffith and Shaw, 1998). Genomic DNA was used as a template for PCR amplification of *Foc* isolates using ITS1 (5′-TCCGTAGGTGAACCTGCGG-3′) and ITS4 (5′-TCCTCCGCTTATTGATATGC-3′) primers (White et al., 1990). Further to confirm the *Foc* races, secreted in Xylem (SIX) Six13c 343 F (5′CAGCCTCCTAGCGTCGAAAA 3′) and Six13c R (5′CCGTGATGGGGTACGTTGTA 3′) were used (Czislowski et al., 2018). The program cycle comprised of initial denaturation (95°C) for 2 min, followed by 40 cycles of denaturation (95°C) for 1 min, annealing at 58°C for 1 min, extension for 1 min at 72°C, and with a final extension at 72°C. Gel electrophoresis and staining was done by loading 10 μl of PCR product on 1% agarose gel in TAE buffer at 80 V for 50 min at 25°C. A 1 kb DNA ladder was used to determine the size of amplified genomic products. PCR products were photographed using a gel documentation system. The amplified genomic product was sequenced by Eurofins Genomics Biotech Pvt. Ltd., Bangalore, India. Gene homology searches were performed using NCBI BLAST. Sequences were compared with different *Foc* isolates retrieved from the GenBank database. Newly obtained sequences were submitted to the GenBank database (New York, USA) and accession numbers were obtained. Phylogenetic analysis was performed with MEGA7 software (Tamura et al., 2007).

Isolation and Characterization of Bacterial Endophytes From Banana cv. Yengambi KM5 (AAA)

An antagonistic bacterial endophyte was isolated from 11-month-old *Foc*-resistant banana cv. Yengambi KM5 (AAA) maintained at the Banana Field Gene Bank, Tamil Nadu Agricultural University, Coimbatore (latitude: 11° 07′ 3.36" N, longitude: 76° 59′ 39.91" E), Tamil Nadu, India. The identity of antagonistic bacterial endophytes against *Foc* KP was confirmed using a 1.5 kb full-length 16S rRNA gene: 8 F (5′AGAGTT TGATCCTGGCTCAG-3′), 1492 R (5′GGGTTACCTTG TTACGACTT-3′). Antagonistic isolates YEBBR6, YEBN2, YEBRH5, YEBRT4, YEBFR1, and YEBFL6 that inhibited *Foc* KP were confirmed as *Bacillus velezensis* (MT372157), *Bacillus albus* (MT120179), *Achromobacter xylosoxidans* (MK258170), *Beijerinckia fluminensis* (MK263670), *Acinetobacter refrigeratoris* (MT326234), and *Bacillus endophyticus* (MT326238), respectively (Saravanan et al., 2021a).

GC/MS Analysis of Volatile Organic Compounds and Non-volatile Organic Compounds Extracted From the Zone of Inhibition of *Foc* KP and *B. velezensis* YEBBR6

The efficacy of bacterial endophyte *B. velezensis* YEBBR6, isolated from resistant banana cv. Yengambi KM5 (AAA) was tested *in vitro* against *F. oxysporum* f. sp. *cubense Foc* KP (NCBI accession no. MW 436477). The ability of the antagonist *B. velezensis* to suppress *Foc* KP was assessed through a dual culture technique. A 9 mm mycelial disc was excised using a sterile cork borer from a 7-day-old culture of *Foc* KP. It was placed on one side of a Petri plate containing PDA medium, 10 mm away from the periphery. The bacterial endophyte (24 h old) was streaked on the medium 10 mm away from the periphery, exactly opposite the mycelial disc of *Foc* KP. The plates were incubated at 28 ± 2°C for 7 days. The VOCs/NVOCs produced by *B. velezensis* YEBBR6 in PDA medium from the zone of inhibition were extracted by excising the agar from the zone of inhibition using a sterile scalpel. Excised agar with VOCs/NVOCs was blended with HPLC-grade acetonitrile in 1:4 ratios (5 g agar in 20 ml of HPLC grade acetonitrile). The mixture was sonicated twice for 30 s at 30% of the power of the sonicator for homogenization. After homogenization, samples were centrifuged and filtered to remove solid particles. The samples were dried in a vacuum

flash evaporator (Rotrva Equitron Make). After removing the eluent, the final product was dissolved in 1 ml of HPLC-grade methanol (Cawoy et al., 2015). The difference in VOCs/NVOCs profile produced during the interaction of *B. velezensis* YEBBR6 with *Foc* KP was characterized with PDA control, pathogen-inoculated control and bacterial antagonist-inoculated control through GC/MS (GC Clarus 500 Perkin Elmer Analysis) using the NIST version 2005 MS data library.

Development of Liquid Formulation of Antagonistic Bacterial Endophytes

Liquid formulation was developed by inoculating single colonies of *B. velezensis* YEBBR6, *B. albus* YEBN2, *Achromobacter xylosoxidans* YEBRH5, *Beijerinckia fluminensis* YEBRT4, *Acinetobacter refrigeratoris* YEBFR1, and *Bacillus endophyticus* YEBFL6 in Luria Bertani (LB) broth. Inoculated LB broth was incubated at 28 ± 2°C for 72 h in an orbital shaker at 150 rpm. The concentration of bacterial cells in the culture broth was assessed by measuring the absorbance at 600 nm in a bio-spectrophotometer (Eppendorf Make) at an optical density (OD) of 1.0 ABS. Later, bacterial suspension in LB broth pertaining to six different bacterial antagonists was blended with 10 ml of glycerol (1%), 10 ml of tween 20 (1%), and 1% poly vinylpyrrolidone (PVP) supplied from Sigma–Aldrich. The resultant mixture of individual bacterial antagonists was mixed by incubation in an orbital shaker at 150 rpm for 10 min. The formulation of individual bacterial antagonists was adjusted to 8×10^8 cfu/ml (Vinodkumar et al., 2017).

Biohardening of Micropropagated Banana cv. Karpooravalli (ABB) Plantlets With a Liquid Formulation of Antagonistic Bacterial Endophytes

Micropropagated banana cv. Karpooravalli (ABB) plantlets were biohardened with a liquid formulation of antagonistic bacterial endophytes (8×10^8 cfu/ml). Micropropagated plantlets maintained in the protrays were biohardened on days 15 and 30 by drenching the root zone with 1% bacterial formulation. Biohardened plantlets were planted in polybags filled with EC (< 0.6 mS / cm) and pH (7)-stabilized sterile Cocopeat and incubated in the mist chamber. After 1 month of primary hardening, the micropropagated plantlets were subjected to secondary hardening. During secondary hardening, banana plantlets were transplanted in polybags (10 cm x 15 cm) containing one part of sterile red soil, one part of sterile sand, and one part of sterile farmyard manure mixture. The plantlets were hardened twice at 15-day intervals with 1% liquid formulation of antagonistic bacterial endophytes (8×10^8 cfu/ml) in the root zone until saturation and maintained in a greenhouse for further studies. Micropropagated banana cv. Karpooravalli (ABB) plantlets drenched with water served as untreated control.

The photosynthetic rate (μmol CO_2 m^{-2} s^{-1}), transpiration rate (mmol H_2O m^{-2} s^{-1}), stomatal conductance (m mol $m^{-2}s$), chlorophyll stability index, and relative water content (%) were recorded on the fully expanded leaves of banana plantlets using the LI-COR (LI-6400XT) Portable Photosynthesis System (PPS). The leaf chamber was the open type and measurements were taken at 10:00 h (IST). While taking measurements, photosynthetically active radiation of 1,500 μmol m^{-2} s^{-1} was maintained with an inbuilt light source. A temperature of 25 ± 5°C, relative humidity of 65 ± 5%, and reference carbon dioxide at a concentration of 380 mol CO_2 mol air^{-1} were also maintained. Observations were recorded after the plant reached steady-state photosynthesis (15 days after transferring to the greenhouse).

Evaluation of Micropropagated Banana cv. Karpooravalli (ABB) Plantlets Biohardened With Antagonistic Bacterial Endophytes Against *Foc* KP in a Greenhouse

The experiment consisted of six treatments, *viz., B. velezensis* YEBBR6, *B. albus* YEBN2, *Achromobacter xylosoxidans* YEBRH5, *Beijerinckia fluminensis* YEBRT4, *Acinetobacter refrigeratoris* YEBFR1, and *Bacillus endophyticus* YEBFL6, replicated three times with 10 plantlets per replication. Inoculum of *Foc* KP was multiplied in quarter-strength Potato Dextrose Broth (PDB) incubated for 7 days at 28 ± 2°C. Conidial load in the culture broth was assessed using a hemocytometer. Concentration of conidia was adjusted to 1×10^6 spores per ml (Catambacan and Cumagun, 2021). Biohardened micropropagated banana cv. Karpooravalli (ABB; Pisang Awak) plantlets with different bacterial endophytes were challenged with conidial suspension of *Foc* KP. Simultaneously, untreated control was also maintained. Banana plantlets biohardened with different bacterial endophytes challenged with *Foc* KP were watered regularly until saturation of soil moisture. Eight weeks after inoculation of *Foc* KP, the degree of disease severity was assessed. It was assessed based on leaf yellowing using a modified disease rating scale (Dita et al., 2014). The intensity of rhizome discoloration was scored by examining the longitudinal section of the pseudostem to the rhizome using a modified rating scale (Carlier et al., 2003).

Scoring for External Symptoms

S. No	Symptom description	Scale
1.	No symptoms	0
2.	Yellowing of lower leaves at initial stage	1
3.	Yellowing of all the lower leaves with discoloration of younger leaves	2
4.	All leaves with intense yellowing or plant dead	3

Scoring for Internal Rhizome Symptoms

S. No	Symptom description	Scale
1.	No symptoms	0
2.	Initial rhizome discoloration (1–20%)	1
3.	Slight rhizome discoloration along with the discoloration of the whole vascular system (21–40%)	2
4.	Rhizome with most of the internal tissues expressing necrosis (> 40%)	3

Percent disease severity was calculated as:

$$\text{Percent disease severity} = \sum \frac{\text{Number of plants in a specific scale category} \times \text{specific scale category}}{\text{Total number of samples} \times \text{maximum scale category}} \times \boxed{100}$$

Colonization of Rhizoplane by *B. velezensis* YEBBR6 and *Foc* KP in Biohardened Micropropagated Banana cv. Karpooravalli (ABB) Documented Through Scanning Electron Microscopy

One centimeter of banana root bits were fixed in 2.5% glutaraldehyde and 2.5% formaldehyde prepared in 0.1 M phosphate buffer of pH 7.2 (Liu et al., 2014) for 24 h at 4°C. Samples were exposed to a mild vacuum so as to ensure rapid infiltration of the fixative into the specimens. The fixed specimens were washed three times with 0.1 M phosphate buffer (pH 7.2) by incubation at 23°C for 30 min each time. The specimens were infiltrated overnight with 30% glycerol in water as a cryoprotectant. Later, specimens were frozen in liquid nitrogen, then cross-sectioned with a sterile scalpel. Later, specimens were post-fixed in 1% OsO4 in 0.1 M phosphate buffer (pH 7.2) for 1 h. Subsequently, samples were washed three times in deionized water and incubated for 30 min for each wash. Next, specimens were dehydrated in 100% ethanol and air-dried to remove the ethanol residues. The dried specimens were mounted on aluminum stubs and sputter-coated with gold. SEM photographs pertaining to colonization of the rhizoplane by *B. velezensis* YEBBR6 and *Foc* KP and hyperparasitic interaction of *B. velezensis* YEBBR6 on *Foc* KP were documented with Hitachi S-3500N 143 SEM at 15 kV.

Assessment of Defense Gene Expression in Micropropagated Banana cv. Karpooravalli (ABB) Plantlets During the Interaction of *B. velezensis* YEBBR6 and *Foc* KP Through qRT-PCR

Total RNA was extracted from the roots of banana biohardened with *B. velezensis* YEBBR6 challenged with *Foc* KP using Trizol (Sigma Aldrich) at 0 h, 24 h, 48 h, and 72 h after *Foc* KP inoculation (Chomczynski and Sacchi, 1987). Similarly, RNA was extracted from untreated healthy control, *B. velezensis* YEBBR6 alone, and *Foc* KP-inoculated control. RNA extracted from different treatments was made up to 3,000 ng/l using Nanodrop (Eppendorf Make, Germany). According to the manufacturer's protocol, respective RNA from different treatments was digested using DNase I (Sigma Aldrich, USA). Further, the quality of RNA was determined by measuring the absorbance value at an A260/A280 ratio. RNA was converted to cDNA with the ThermoFischer Scientific-RevertAid First Strand cDNA Synthesis Kit (cat. # K1622). A ratio of 1.8 + 0.2 indicated the best quality of nucleic acid. The cDNA was diluted 10-fold and used for qRT-PCR analysis. It was performed in a BIO-RAD CFX manager system. The reaction mixture for qRT-PCR comprised 3 μl of cDNA template, 10 μl of SYBR Green master mix (KAPA SYBR@FAST for LightCycler 480, Cat-KK4610), 0.8 μl of 10 μM forward primer, and 0.8 μl of 10 μM reverse primer. The final volume was made up to 20 μl using nuclease free water. The PCR program included denaturation at 95°C for 10 min, amplification for 40 cycles at 95°C for 30 s, 60°C for 30 s, and 72°C for 30 s. It was followed by standard melting temperature analysis. The major defense gene transcripts assessed for the induction of resistance response against *Foc* KP infection were WRKY33, mitogen-activated protein kinase (MAPK), chitin elicitor receptor kinase (CERK 1), lipoxygenase (LOX), and phenylalanine ammonia lyase (PAL). For each defense gene expression study, three biological replicates and two technical replicates were maintained throughout the study. The fold changes in gene expression were calculated using the formula $\Delta\Delta Ct = \Delta$ Ct sample– Δ Ct reference. The relative fold changes in the transcript level were represented graphically by converting the $\Delta\Delta$CT value to $2^{-\Delta\Delta Ct}$ (Livak and Schmittgen, 2001). Statistical analysis for relative fold change was performed using TIBCO Spotfire Analyst version 7.11.1.

Protein-Protein Interaction Analysis

Defense-related proteins in banana cv. Karpooravalli (ABB) plantlets that had a predominant role against *Foc* KP infection were further investigated for their interacting partners using the STRING database (Szklarczyk et al., 2021). Protein sequences of WRKY33, MAPK, CERK1, PAL, and LOX were used as a query against the double haploid Pahang (*Musa acuminata*) banana genome to understand the interacting protein partners. Information regarding interacting partners was obtained based on text mining, experiments, databases, co-expression, neighborhood, gene fusion, and co-occurrence results. Query protein and their interacting protein domain information in addition to the number of interacting partners belonging to a particular domain in the network were analyzed. A degree-sorted network was constructed using transcription factor, defense related genes, and their interacting proteins. Protein domains of all the interacting partners were analyzed to understand the functional relevance and their association with query protein. A medium confidence level of 0.40 and minimum of 10 interactors were used as parameters for the construction of the network.

Analysis of protein-protein interaction network between WRKY33, MAPK, CERK1, PAL, and LOX proteins was obtained using the STRING database. It was exported to Cytoscape 3.9 version for analysis. Using STRING and enrichment

map applications in Cytoscape, STRING enrichment was performed and a map was constructed. Functional enrichment was performed by merging all the five proteins with their interacting partners.

RESULTS

Molecular Confirmation of *Foc* Isolates

Amplification of internal transcribed spacers of eight different isolates of *Foc* for ITS 1 and ITS 4 regions with specific primers yielded an expected amplicon size of 560 bp. Nucleotide sequences of amplicons pertaining to eight different isolates confirmed the identity of *Foc*. The sequences subjected to multiple alignments were submitted to GenBank and were provided with accession numbers, *viz.,* *Foc* KP MW436477, *Foc* KP MW 436476, *Foc* NP1 MW436482, *Foc* NP2 MW436483, *Foc* KP2 MW436485, *Foc* RS2 MW436581, *Foc* RS3 MW436484, and *Foc* RS1 MW43658. Phylogenetic analysis of *Foc* isolates revealed the presence of three major clusters. Cluster 1 comprised *Foc* KP MW 436476, *Foc* KP MW436477, and *Foc* NP1 MW436482. Cluster 2 had five isolates including *Foc* NP2 MW436483, *Foc* KP2 MW436485, *Foc* RS2 MW436581, *Foc* RS3 MW436484, and *Foc* RS1 MW43658. Cluster 3 comprised *Fusarium oxysporum* f.sp. *lycopersici* (*Fol*) as an out group (**Supplementary Figure S1**). Based on the pathogenicity study, *Foc* KP was most virulent compared to other isolates. Sequencing of *Six*13c for the isolate *Foc* KP confirmed the presence of race 4 bearing the accession number MW323435. It had similarity with *Foc* isolate BRIP62892 bearing the accession number KX435021 and also matched with VCG group 0122 pertaining to the Cavendish group (AAA) of Philippines origin. Hence, *Foc* KP was used throughout the study.

Antifungal Activity of *B. velezensis* YEBBR6

Bacillus velezensis YEBBR6 inhibited the mycelial growth of *Foc* KP up to 63% compared to untreated control (**Supplementary Figure S2**). Other bacterial endophytes, *B. albus* YEBN2, *A. xylosoxidans* YEBRH2, *Beijerinckia fluminensis* YEBRT4, *Acinetobacter refrigeratoris* YEBFR1, and *B. endophyticus* YEBFL6 were not equally effective as *B. velezensis* YEBBR6 in the suppression of mycelial growth of *Foc* KP *in vitro*.

GC/MS Analysis of VOCs/NVOCs Bioactive Metabolites Extracted From the Zone of Inhibition Produced During the Interaction of *B. velezensis* YEBBR6 With *Foc* KP

Fifteen bioactive metabolites were characterized through GC/MS from the zone of inhibition during the ditrophic interaction between *B. velezenzis* YEBBR6 and *Foc* KP. They included dihydro acridine, nonanol, hexadecanoic acid, oleic acid, clindamycin, 5-hydroxymethylfurfural, azulene, 3 amino-4 hydroxy phenyl sulfone, campholic acid, procyclidine, linoelaedic acid, acetylvaleryl, allobarbital, aminomorpholine, and 3-thiazolidine carboxamide (**Supplementary Figure S3** and **Supplementary Table S1**). Six bioactive metabolites were produced by *B. velezensis* YEBBR6 in the absence of *Foc* KP. They were identified as 1,3-propanediol, clindamycin, 4H-pyran, pentanoic acid, acetaldehyde, and hexadecanoic acid (**Supplementary Figure S4** and **Supplementary Table S2**). Bioactive metabolites produced by *Foc* KP were identified as 2-propen-1-ol, 3H-pyrazol-3-one, hexanoic acid, cyclohexan, 1H-azonine, trioxsalen, and butanamide (**Supplementary Figure S5** and **Supplementary Table S3**). The Venn diagram of differentially expressed bioactive metabolites during the interaction of bacterial endophyte *B. velezensis* YEBBR6, either with *Foc* KP or without *Foc* KP, and *Foc* KP alone revealed that *B. velezensis* YEBBR6 produced six bioactive metabolites. But, during the interaction of *B. velezensis* YEBBR6 with *Foc* KP, 15 bioactive metabolites were produced. Comparison of bioactive metabolites between *B. velezensis* YEBBR6 alone and *B. velezensis* YEBBR6 with *Foc* KP revealed the production of two bioactive metabolites in common, *viz*., hexadecanoic acid and clindamycin (**Figure 1**).

Plant Growth Promotion and Physiology of Micropropagated Banana cv. Karpooravalli (ABB) Plantlets Biohardened With Bacterial Endophytes

Micropropagated banana plantlets treated with *B. velezensis* YEBBR6, *B. albus* YEBN2, *A. xylosoxidans* YEBRH2, *Beijerinckia fluminensis* YEBRT4, *Acinetobacter refrigeratoris YEBFR*1, and *B. endophyticus* YEBFL6 increased plant growth parameters (**Figure 2**). Among the bacterial endophytes, *B. velezensis* YEBBR6 significantly increased pseudostem height (38.63 cm), pseudostem width (5.9 cm), leaf area (1.290 m^2), root length (54.75 cm), and leaf emergence rate (Phyllochron) (6.0), compared to 11.21 cm, 3.2 cm, 0.09 m^2, 36.1 cm, and 12.0 in control plants, respectively (**Figure 3A** and **Supplementary Figures S6–S10**). *B. velezensis* YEBBR6-treated banana plants also enhanced the photosynthetic rate to 24.61 mol m^{-2} s^{-1} against 13.09 mol m^{-2} s^{-1} in non-bacterized control plants. Further, transpiration rate and stomatal conductance in *B. velezensis*-treated banana plants was 3.95 mol.cm^{-2} s^{-1}, 1.01 mmol m^{-2} s, while it was 2.64 mol.cm^{-2} s^{-1}, 0.06 mmol m^{-2} s in non-bacterized control plants. Biohardened banana plants had higher levels of total chlorophyll (1.29 mg/g^1), chlorophyll stability index (88.6%), and relative water content (83.3%) than non-bacterized control plants (**Supplementary Table S4**).

Effect of Bacterial Endophytes on the Suppression of *Fusarium* Wilt of Banana Plantlets

Banana plantlets biohardened with *B. velezensis* YEBBR6, *B. albus* YEBN2, *Achromobacter xylosoxidans* YEBRH2, *Beijerinckia fluminensis* YEBRT4, *Acinetobacter refrigeratoris* YEBFR1, and *B. endophyticus* YEBFL6 against *Foc* KP indicated that banana plantlets biohardened with *B. velezensis* at 10 ml/plant had zero incidence of wilt. But, the banana plantlets biohardened with *B. albus* and *Acinetobacter refrigeratoris* had 10 % wilt against 30 % in banana plants biohardened with *B. endophyticus*. However, 100 % wilt incidence was observed in inoculated control (**Figure 3B** and **Supplementary Table S5**). As *B. velezensis* YEBBR6 was

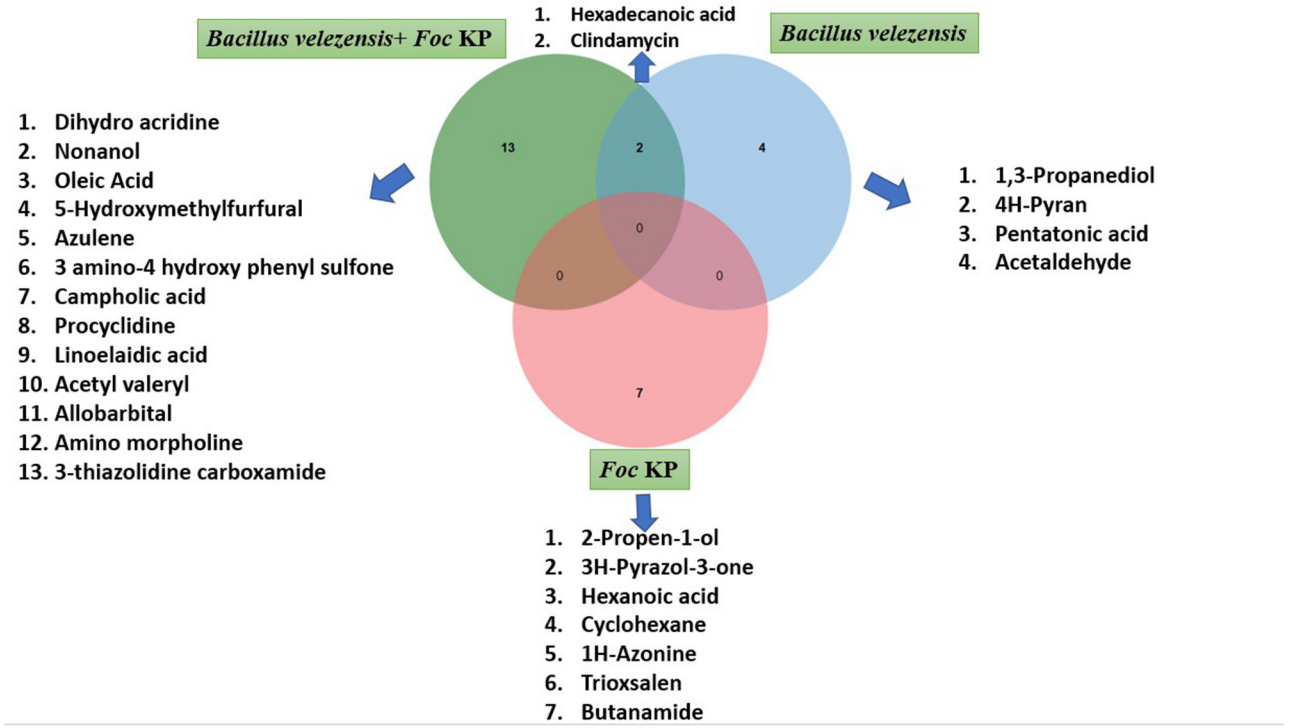

FIGURE 1 | Comparative distribution of VOCs/NVOCs produced by *B. velezensis* YEBBR6, *B. velezensis* YEBBR6 + *Foc* KP, and + *Foc* KP alone.

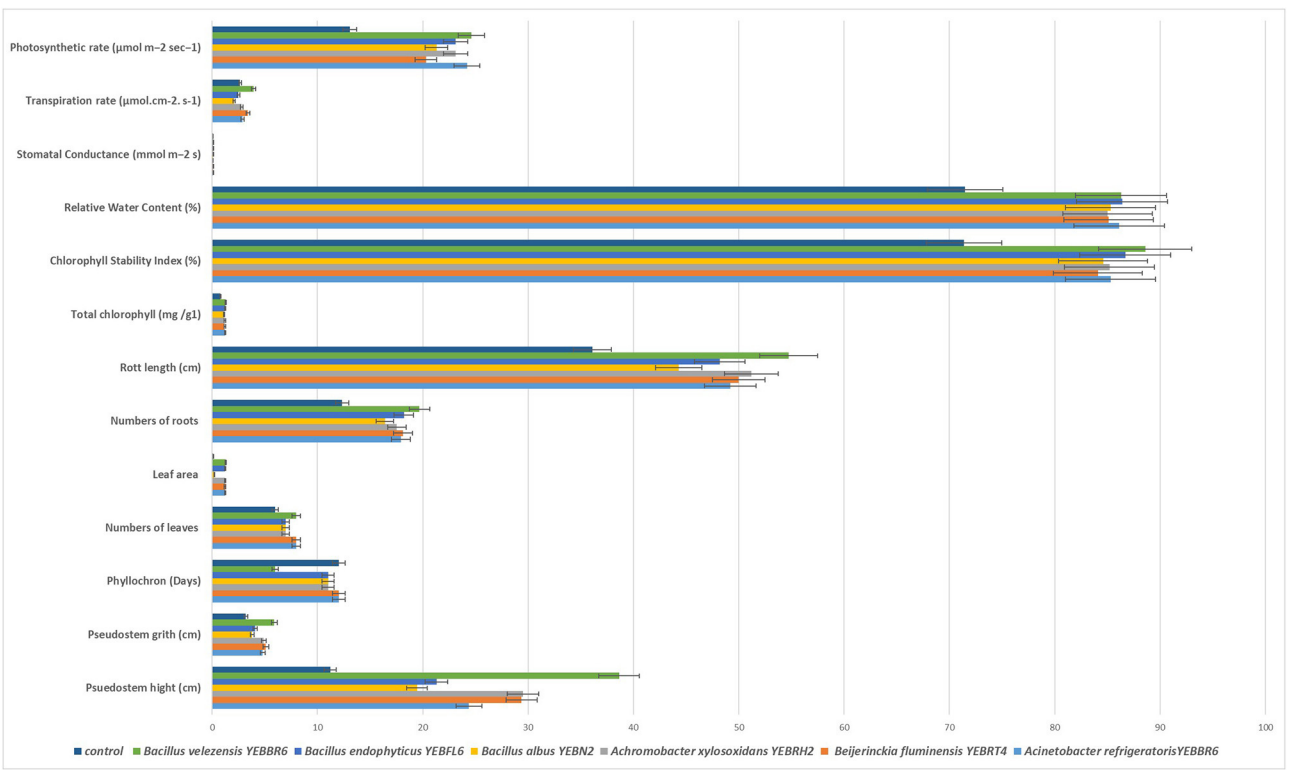

FIGURE 2 | Phenotypic response and plant growth promotion of micropropagated banana plantlets biohardened with bacterial endophytes.

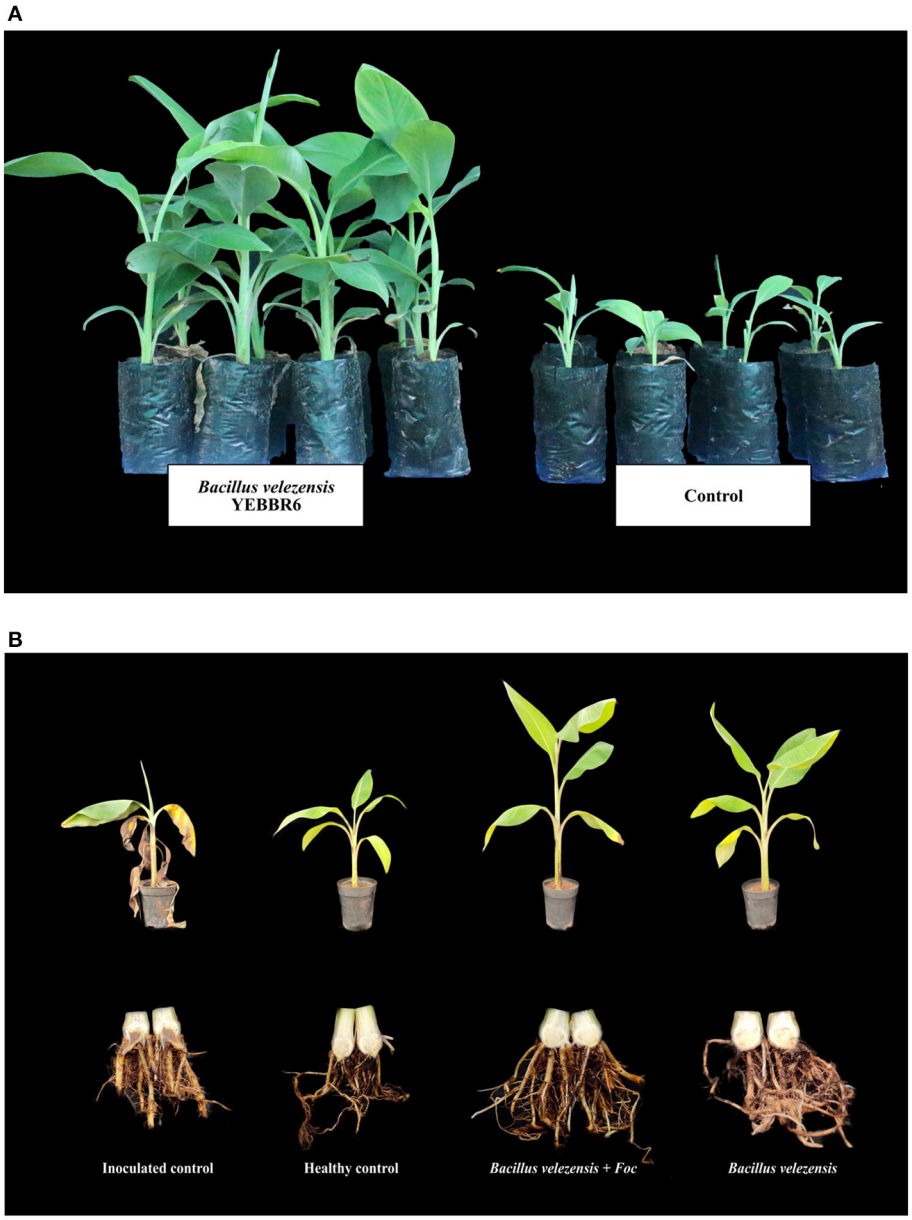

FIGURE 3 | (A) Plant growth promotion of micropropagated banana plantlets biohardened with *Bacillus velezensis* YEBBR6. **(B)** Effect of *Fusarium* wilt on biohardened micropropagated Karpooravalli banana plantlets with *Bacillus velezensis* YEBBR6 against *Foc* in pot culture.

effective in the suppression of *Fusarium* wilt, it was subsequently used for further studies.

Effect of *B. velezensis* YEBBR6 on Root Colonization of Banana Plantlets

Analysis of the roots of banana plantlets biohardened with *B. velezensis* YEBBR6 using scanning electron microscopy confirmed the colonization of bacterial cells on the root surface. Agglomerates of bacterial cells resulted in the formation of biofilm on the root surface (**Figure 4A**). Besides, the roots of banana plantlets biohardened with *B. velezensis* YEBBR6 followed by challenge inoculation with *Foc* KP witnessed hyperparasitism of *Foc* KP mycelium and microconidia by the bacterial cells of *B. velezensis* (**Figures 4B,C**). However, in pathogen-inoculated control, proliferation of microconidia was noticed along the root zone of banana plantlets (**Figure 4D**).

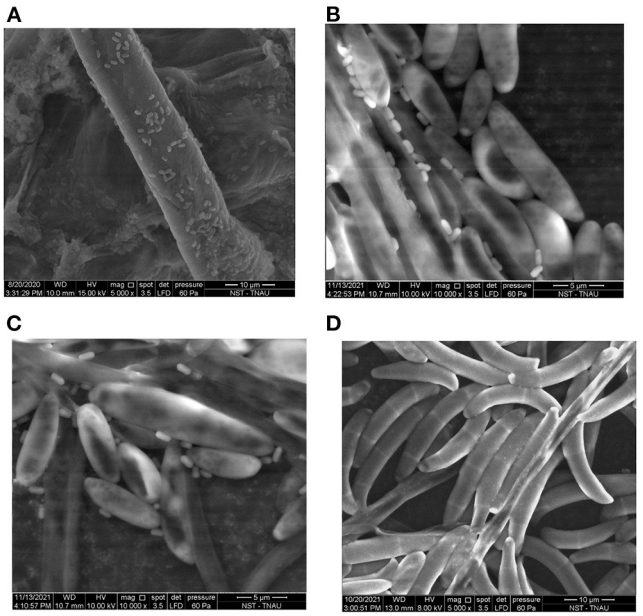

FIGURE 4 | (A) Colonization of *Bacillus velezensis* YEBBR6 in the root zone of biohardened banana plantlets. **(B,C)** Colonization of *Bacillus velezensis* YEBBR6 in the mycelium and microconidia of *Foc* KP on biohardened banana plantlets after challenge inoculation with *Foc* KP. **(D)** Colonization of micro and macroconidia in infected plantlets after challenge inoculation with *Foc* KP.

Induction of Defense Gene Transcripts in Banana Plantlets Biohardened With *B. velezensis* YEBBR6 Challenged With *Foc* KP

Biohardening of banana plantlets with *B. velezensis* YEBBR6 challenged with or without *Foc* KP altered the expression of the WRKY transcription factor, MAPK, chitin elicitor receptor kinase, lipoxygense, and PAL genes responsible for plant defense. Irrespective of different treatments, the WRKY 33 transcript was downregulated in all the treatments at 0 h. The transcription rate of the WRKY 33 gene was affected immediately after inoculation with *Foc* KP and in biohardened plants. The level of the transcript in *Foc* KP-inoculated control increased after 24 h and declined after 48 and 72 h. However, the transcript of WRKY 33 was upregulated in banana plantlets biohardened with *B. velezensis* at 24, 48, and 72 h after treatment. Interestingly, a 1.87-fold increase of the WRKY 33 gene transcript was observed in banana plantlets biohardened with *B. velezensis* YEBBR6 challenged with *Foc* KP. But, in untreated healthy control, upregulation of WRKY 33 (0.33-fold) was noticed only at 72 h (**Figure 5A**).

The expression level of MAPK transcripts varied between different treatments. Banana plantlets biohardened with *B. velezensis* YEBBR6 challenged with *Foc* KP increased the expression of MAPK transcripts up to 2.32-fold after 72 h in comparison with biohardened plants that were not challenged with *Foc* KP. Besides, only a 0.69-fold change of the WRKY 33 transcript was noticed in pathogen-inoculated control after 48 h and it decreased further after 72 h of inoculation (**Figure 5B**).

Induction of the chitin elicitor receptor kinase (CERK 1) transcript associated with innate immune response was initiated after 24 h of inoculation with pathogen *Foc* KP. However, upregulation was more pronounced after 72 h in plantlets biohardened with *B. velezensis* YEBBR6 coupled with challenge inoculation of *Foc* KP. The expression of the CERK1 transcript was 2.2-fold higher than in biohardened plants that had not been inoculated with *Foc* KP. Furthermore, the expression level of CERK1 transcripts was reduced in untreated healthy control compared to pathogen-inoculated and biohardened plantlets challenged with *Foc* KP (**Figure 5C**).

Lipoxygenase (LOX) is a key enzyme involved in the induction of the immune response in plants, therefore attempts were made to understand the ability of *B. velezensis* YEBBR6 to modulate immune response against *Foc* KP. Biohardened plants challenged with *Foc* KP increased the transcript level of fatty acid dioxygenase LOX up to 2.6-fold after 72 h of inoculation. The expression of the LOX transcript was 1.6-fold greater in *B. velezensis* YEBBR6 and was downregulated after 72 h. Comparison on the expression of the LOX transcript in inoculated control reflected a 1.7-fold change after 72 h, while in healthy control, there was no increase in the LOX gene transcripts (**Figure 5D**).

Assessing the expression of phenylalanine ammonia lyase (PAL) revealed a significant increase of PAL transcripts in *B. velezensis* YEBBR6 biohardened banana plantlets challenged with *Foc* KP. After 48 h of challenge inoculation with *Foc* KP, the level of induction of the PAL transcript was 1.9 times higher than other treatments. After 48 h, the PAL transcript in *Foc* KP-inoculated control was observed only up to 0.6-fold, and decreased after 72 h. However, the activity of PAL was downregulated in healthy control (**Figure 5E**).

Analysis of Protein-Protein Interaction Between Defense Genes in *B. velezensis* YEBBR6 Biohardened Banana Plantlets Challenged With *Foc* KP

STRING analysis was performed to understand the functional association of defense-related genes with other proteins and their conserved domains. From our analysis, most of the interacting proteins for each query protein had similar conserved domains and were clustered together in the network. Protein sequences of defense-related genes were used as input to retrieve the interacting partners based on the double haploid Pahang (*Musa acuminata*) banana genome. Details on the query protein and their interacting protein domain and number of interacting partners in the network are listed in **Supplementary Table S6**. The degree-sorted network constructed using transcription factor and defense-related genes and their interacting proteins are illustrated in **Figure 6**.

Protein-protein interaction of WRKY transcription factor indicated the involvement of a large protein family with diverse functions. They were expressed in response to pathogens, elicitors, and defense-related phytohormones such as salicylic

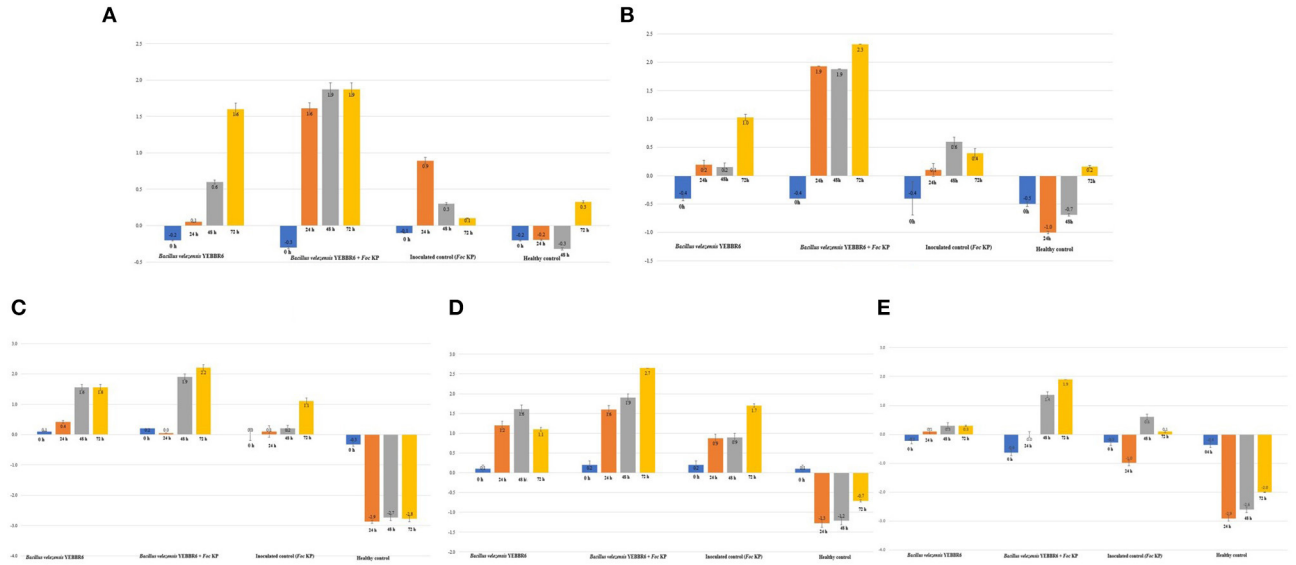

FIGURE 5 | (A) Expression pattern of WRKY 33 transcription factor in biohardened banana cv. Karpooravalli (ABB) under mono, di, and tritrophic interactions at different time periods. **(B)** Expression pattern of MAPK in biohardened banana cv. Karpooravalli (ABB) under mono, di, and tritrophic interactions at different time periods. **(C)** Expression pattern of CERK 1 in biohardened banana cv. Karpooravalli (ABB) under mono, di, and tritrophic interactions at different time periods. **(D)** Expression pattern of LOX in biohardened banana cv. Karpooravalli (ABB) under mono, di, and tritrophic interactions at different time periods. **(E)** Expression pattern of PAL in biohardened banana cv. Karpooravalli (ABB) banana under mono, di, and tritrophic interactions at different time periods.

acid (SA) or jasmonic acid (JA). Protein-protein interaction of MAPK revealed that it belongs to the kinase family and interacted with G protein domains and protein tyrosine phosphatase domains similar to chitin elicitor receptor kinase 1-like protein. Besides, functional domains of five out of ten interacting proteins were uncharacterized in the given network. CERK 1 protein pertaining to the protein kinase family protected plants at multiple layers against invading pathogens by conferring PAMP-triggered immunity (PTI) or effector-triggered immunity (ETI). Regardless, CERK proteins interacted with the LysM domain and guanine nucleotide-binding domain (**Supplementary Table S6**). Protein interaction of LOX indicated that it interacted with proteins containing LOX, phospholipase, and PLAT/LH2 conserved domains. These proteins were associated with membrane or lipid-associated proteins. Similarly, protein-protein interaction of PAL reflected that chalcone synthase (CHS) was essential for the formation of 4,2′, 4′,6′-tetrahydroxychalcone, responsible for the biosynthesis of anthocyanin pigments, anti-microbial phytoalexins, and flavonoid inducers of *Rhizobium* nodulation genes. Nonetheless, stilbene synthases (STSs) occurred in a limited number of unrelated plants and synthesized the backbone of stilbene phytoalexins that have antifungal properties and contribute to pathogen defense. Despite the other genes, PAL also induced defense against pathogens by triggering other enzymes linked with different pathways.

Merging of WRKY33, MAPK, CERK1, PAL, and LOX resulted in the formation of an enlarged network comprising of 52 nodes. Three isoforms of guanine nucleotide-binding proteins interacted commonly with CERK and MAPK protein targets. Apart from this, there was no common interacting proteins between the five protein targets. Functional enrichment analysis resulted in the formation of more than five clusters. A heat cluster map was generated based on the functional relevance of each of the proteins. In the enrichment figure, each cluster was linked with the query protein to indicate the commonality and the difference observed with the five query proteins and their interaction partners. Based on the enrichment map, domain, and pathway information of five proteins, CERK1 was linked with the LysM domain and guanine nucleotide-binding protein domain. LOX was linked with linoleic acid, alpha-linolenic acid, arachidonic acid metabolism, ether lipid metabolism, glycerophospholipid metabolism, lipoxygenase, phospholipase, and PLAT/LH2 conserved domains. The MAPK gene was associated with G protein domains and protein tyrosine phosphatase domains. While, PAL was coordinated with AMP binding, chalcone synthase, polyketide synthase, and thiolase-like domains. The WRKY transcription factor was associated with the VQ5 domain and WD40 repeat containing domain (**Figure 7**).

DISCUSSION

Fusarium wilt of banana, caused by *Fusarium oxysporum* f. sp. *cubense* (*Foc*), is one of the most devastating diseases hindering the banana industry. A recent outbreak of *Foc* tropical race 4 (*Foc* TR4) can infect and destroy almost all banana cultivars. Hence, the present study, using molecular approaches to understand the versatile nature and distribution of *Foc* races infecting banana in Tamil Nadu province of South India through ITS 1 and 4 and Six 13c, revealed the presence of race 4 (*Foc* KP–MW323435).

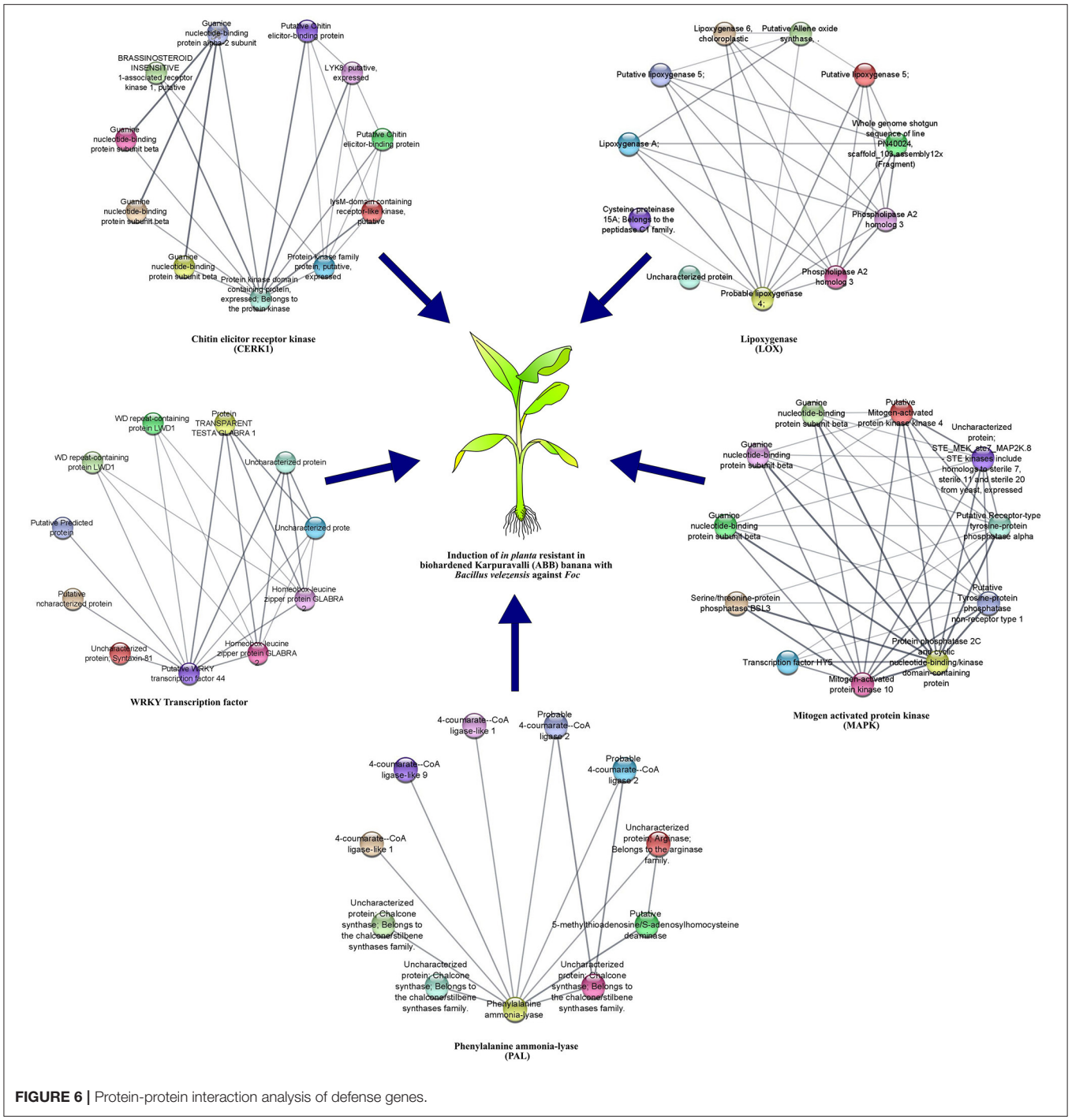

FIGURE 6 | Protein-protein interaction analysis of defense genes.

Likewise, ITS region has been used as a molecular marker to confirm the identity of *Foc*-infecting *Musa* spp. (ABB) in Southern Mexico (Leong et al., 2009; Maldonado-Bonilla et al., 2019). Further, in the present study, sequencing of Six 13c-343 for the isolate *Foc* KP confirmed the presence of race 4 bearing the accession number MW323435. Sequences of the isolate *Foc* KP had the similarity with *Foc* isolate BRIP62892 bearing the accession number KX435021. Further, it also matched with VCG group 0122 pertaining to the Cavendish (*Musa* AAA) group of banana with Philippines origin (Czislowski et al., 2018; Carvalhais et al., 2019). Similarly, Wong et al. (2019) confirmed the presence of *Foc* TR4 in Peninsular Malaysia based on transcription elongation factor (TEF-1) and reported the shift in genetic variability among *Foc* isolates. Despite the existence of different races, management of race 4 remains a challenging task. Though fungicides are effective, usages of

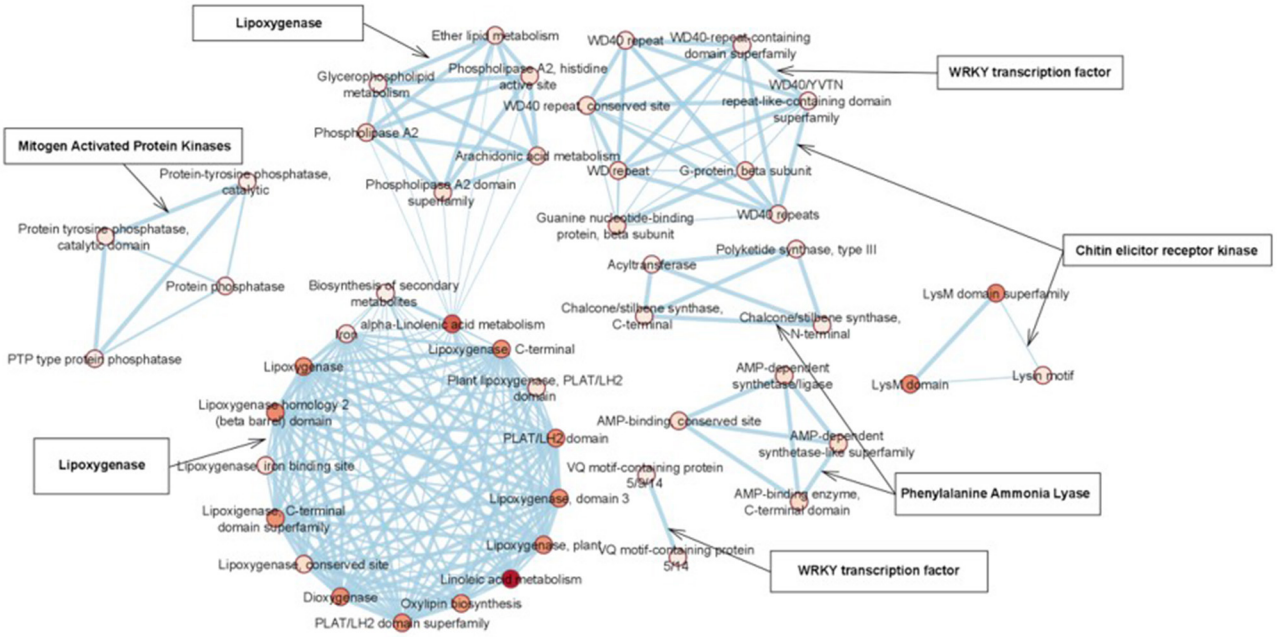

FIGURE 7 | Functional enrichment analysis of defense genes in biohardened Karpooravalli (ABB) banana plantlets.

fungicides are discouraged due to environmental concern and resistance development among plant pathogens (Raza et al., 2017). Moreover, none of the fungicides confer 100 % protection against *Foc*. Due to the detrimental effect of chemical fungicides on the environment, human health, and other living organisms, researchers have focused on discovering potential biocontrol candidates as a viable alternative for plant disease management (Syed Ab Rahman et al., 2018).

Considering this critical situation, structuring the rhizosphere and endosphere with potential bacterial antagonists in the susceptible banana cultivars will pave the way for the management of *Foc*. Among all bacterial endophytes, the *Bacillus* species were exploited largely for suppression of soil-borne pathogens around the globe due to rapid growth and the ability to synthesize a large number of secondary metabolites which play a key role in antibiosis against deleterious microorganisms (Radhakrishnan et al., 2017; Fira et al., 2018; Aloo et al., 2019). Besides, in the recent past, biological control of plant diseases has gained popularity as an eco-friendly disease management strategy.

Based on the significance in the management of *Fusarium* wilt of banana, our finding has furthered the introduction of a potential endophyte *B. velezensis* YEBBR6 with multifaceted attributes contributing to the suppression of *Foc* KP. Similarly, the versatile nature of antifungal secondary metabolites from endophytic *Brachybacterium paraconglomeratum* isolated from the resistant cultivar YKM5 was also responsible for the suppression of *Foc* under *in vitro* conditions (Saravanan et al., 2021a). The VOCs and NVOCs are also referred to as small signaling molecules (SSMs), which are involved in cellular crosstalk. They play a significant role in competition, synergistic interaction, and communication (Adnani et al., 2017). SSMs from the antagonistic microflora also promote the growth of symbionts and inhibit plant pathogens (Khalid and Keller, 2021). Like the cellular crosstalk mediated by small signaling molecules between the beneficial microbiome and inimical microbes dwelling in the rhizosphere, small signaling molecules were also induced during the interaction between the fungal pathogen and bacterial antagonist *in vitro*. Likewise, co-culturing of *B. velezensis* YRBBR6 along with *Foc* KP also induced the secretion of secondary metabolites, *viz*., dihydroacridine, nonanol, hexadecanoic acid, oleic acid, clindamycin, 5-hydroxymethylfurfural, azulene, 3 amino-4 hydroxy phenyl sulfone, campholic acid, procyclidine, linoelaedic acid, acetylvaleryl, allobarbital, aminomorpholine, and 3-thiazolidine carboxamide. Gatasheh et al. (2017) reported that dihydroacridine disrupted DNA synthesis and served as a DNA intercalating agent in several microorganisms leading to broad-spectrum antimicrobial activity. Mohamad et al. (2018) explained that *B. atrophaeus* strain XEGI50 inhibited the mycelial growth of *V. dahliae* by producing 13 putative compounds, including 1,2-benzenedicarboxylic acid, bis (2-methylpropyl) ester 9,12-octadecadienoic acid (Z, Z)-, methyl ester 9-octadecenoic acid, methyl ester decanedioic acid, bis(2-ethylhexyl) ester, and hexadecanoic acid. Walters et al. (2004) reported that fatty acids, *viz.,* linolenic acid, linoleic acid, erucic acid, and oleic acid promoted plant growth and possessed antifungal action against *Rhizoctonia solani, Pythium ultimum,* and *Pyrenophora avenae*. The antifungal activity of nonanol produced by endophytic *B. velezensis* ZSY-1

was also reported by Gao et al. (2017) against *A. solani* and *B. cinerea*. Zhang et al. (2017) reported the broad spectrum antimicrobial activity of a-phellandrene and nonanal against Penicillium cyclopium. Further, Guay (2007) reported the antimicrobial action of clindamycin against different microbes. Abd Alhameed et al. (2020) reported the antimicrobial activity of thiazolidine-2,4-dione carboxamide against bacteria and fungus. To our surprise, *B. velezensis* YRBBR6 also produced dihydroacridine, clindamycin, and nonanol bestowed with antifungal action against *Foc* KP. Thus, the bacterial endophyte *B. velezensis* YRBBR6 is unique in the sense that it produced novel biomolecules responsible for the suppression of mycelial growth of *Foc* KP, which has not been reported earlier by other researchers for the management of *Foc*. Hence, it is hypothesized that an array of secondary metabolites produced by *B. velezensis* YRBBR6 might be responsible for the suppression of *Foc* KP.

Endophytic *B. velezensis* YRBBR6 not only possessed antifungal property but also promoted plant growth. This was also endorsed by the research findings of Compant et al. (2016) who reported that the bacterial endophytes improved plant health and growth through a variety of mechanisms, including phytohormone synthesis, nitrogen fixation, phosphate solubilization, stimulation of defense responses, and reduction of abiotic stress by lowering ethylene levels. Yuan et al. (2013) reported that *B. amyloliquefaciens* strain NJN-6 served as a biofertilizer and promoted the growth of micropropagated banana plants treated with *B. amyloliquefaciens* NJN-6. Biohardening of banana cv. Karpooravalli (ABB) plants with *B. velezensis* (YEBR6) promoted plant growth through the increase in pseudostem height, width, leaf area, root length, and emergence of new leaves. The research finding of Gamez and his associates emphasized that the banana plants inoculated with rhizobacteria increased plant height, leaf number, leaf area, pseudostem thickness, root and shoot fresh weight, and root and shoot dry weight (Gamez et al., 2019). Micropropagated banana plantlets treated with *Bacillus* and *Pseudomonas* promoted plant growth by increasing pseudostem height, width, number of leaves, leaf area, and yield parameters (Kavino et al., 2011). Kavino et al. (2014) also observed a significant difference in phyllochrons in biohardened banana plants compared to untreated control. Further, Ajit kumar et al. (2020) also reported that bacterial endophytes improved pseudostem height, pseudostem width (diameter), number of roots, and total number of leaves in banana plants. Rajamanickam et al. (2018) recorded increased growth parameters in biohardened banana plants compared to untreated control. Thus, the phytobiome plays a key role in improving plant health. Colonization of the endosphere and rhizosphere by bacterial endophytes enhanced plant growth by mobilizing nitrogen, production of phytohormones, acquisition of nutrients, and also conferred resistance to biotic and abiotic stresses (Kandel et al., 2017). Thus, to harness the potential benefits mediated through endophytes, colonization of the rhizosphere and endosphere is very crucial. Successful colonization of the rhizoplane by bacterial antagonists is a prerequisite for biocontrol and plant growth promotion (Gao et al., 2016; Kang et al., 2019). Considering the significance of colonization by endophytes, the present investigation confirmed the colonization of endophytic *B. velezensis* YEBBR6 on the rhizosphere. Similarly, scanning electron microscopy analysis of a cucumber root surface applied with *B. amyloliquefaciens* UCMB5113 revealed the colonization of bacterial cells and formation of biofilm leading to plant growth promotion (Palmqvist et al., 2015). In corroboration with our findings, micropropagated banana plantlets inoculated with *B. velezensis* RFP-N67 colonized roots xylem cells in a successful manner. On the other hand, it also entered inside the root at a higher population density of bacterial cells. Likewise, we could observe the colonization of the banana pseudostem by endophytic isolate YEBBR6 through SEM. It was also speculated that *B. velezensis* RFP-N67 proliferated normally in banana to impose their biocontrol functions, and in particular during the presence of *Foc*, antagonistic bacterial isolate RFP-N67 can quickly inhibit the growth of the pathogen (He et al., 2021). Similar responses were also induced by the antagonistic bacterial endophyte in the presence of *Foc* KP responsible for quenching the infection of the wilt pathogen. It was also witnessed through the hyperparasitic behavior of the antagonistic bacteria *B. velezensis* YEBBR6 in the micropropagated banana cv. Karpooravalli (ABB) plantlets through scanning electron micrographs.

As *B. velezensis* YEBBR6 promoted plant growth, we further focused our studies to assess the impact of the bacterial antagonist on physiological attributes of banana plantlets. Physiological attributes contribute toward plant defense and serve as the medium of interaction with the environment and climatic conditions. These attributes are linked with the physiological development associated with cellular processes including transpiration, photosynthesis, stomatal conductance, relative water content, and regulation of plant hormones (Shah et al., 2020). In our study, micropropagated banana plants treated with *B. velezensis* YEBBR6 increased major physiological parameters including photosynthetic rate, stomatal conductance, relative water content, and chlorophyll stability index compared to untreated control. Similarly, Shamsuddin et al. (2000) reported that inoculation of banana plantlets with PGPR had the highest photosynthetic rate and stomatal conductance. Besides, it also increased stomatal conductance and lowered proline concentration in leaves of banana seedling grown under abiotic stress (Shamsuddin et al., 1999). Similarly, biohardened banana plants with *B. velezensis* YEBBR6 also increased stomatal conductance.

Soil application of *B. amyloliquefaciens* NJN6 to banana plantlets increased the population density of beneficial rhizomicrobiome and thus aided in the management of *Fusarium* wilt by decreasing colonization of *Foc* in the banana rhizosphere (Xue et al., 2015). *In vitro* bacterization of tissue-cultured banana plantlets with endophytic *B. subtilis* EPB56 and EPB10 reduced *Fusarium* wilt by 78 % compared to pathogen-inoculated control (Kavino and Manoranjitham, 2018). *B. velezensis* isolates (Y6 and F7) enhanced the antagonistic activity against banana *Fusarium* wilt (Cao et al., 2018). Combined application of *B. velezensis* H-6 with acid soil ameliorant (ASA) suppressed the incidence of *Foc* race 4 up to 63.3% to 66.7%. Besides, it also enhanced growth promotion in banana plants (Huang et al., 2019). Furthermore, Wang et al. (2013) reported

that *B. amyloliquefaciens* W19 acted in synergy with organic fertilizer to reduce the incidence of *Fusarium* wilt other than plant growth promotion. Hitherto, biohardening of banana cv. Karpooravalli (ABB) with endophytic *B. velezensis* YEBBR6 completely protected the plantlets from the establishment of the host pathogen relationship of *Foc* KP compared to the other bacterial endophytes investigated in the present study. Bacterial endophyte *B. velezensis* YEBBR6 not only suppressed the host pathogen relationship of *Foc* KP, but also reduced mycelial proliferation *in vitro* and promoted plant growth. Hence, attempts were also made to understand the regulation of transcription factors and defense genes expressed during mono, di, and tritrophic interactions with *B. velezensis* YEBBR6 and *Foc* KP in biohardened banana plantlets. Bacterial endophytes can induce immune response in plants by its macromolecules and MAMP molecules via host signals (Wei et al., 1991). Profiling the expression in biohardened micropropagated banana cv. Karpooravalli (ABB) with *B. velezensis* YEBBR6 had a clear upregulation pattern of WRKY 33 transcription factor, PAL, LOX, MAPK, and CERK 1 in biohardened plants challenged with *Foc* KP compared to inoculated control and untreated control plants. Transcription parameters regulate a broad range of signal transduction pathways with various tasks, and thus play a key role in the induction of plant defense. WRKY, being a group of transcription regulators in plants, can bind to box in promoters of target genes to regulate transcription (Eulgem et al., 2000). WRKY transcription factors also coordinate a variety of signaling pathways and have a crucial regulatory role in plant defense responses (Zhang et al., 2019). They also regulate pathogen-associated molecular pattern-triggered immunity (PTI) and effector-triggered immunity (Chen et al., 2019).

WRKYs also interact with mitogen-activated protein kinase (Rushton et al., 2010; Mao et al., 2011), MAP kinase kinase kinase (MEKK) (Guan et al., 2014), calmodulin (Rushton et al., 2010), and histone deacetylases (HDAs). Zhang et al. (2019) recorded the expression of seven different WRKY genes, including WRKY4 (Ma10_g03630), WRKY22 (Ma10_g06870), WRKY25 (Ma06_g34370), and WRKY26 (Ma03_g09270, Ma06_g01150, Ma08_g01650, and Ma11_g18140) during *Foc* infection and suggested that expression of these WRKY genes might be responsible for the constitutive defense mechanism. Thus, the multiple fold increase of WRKY 33 transcription factor in bacterized banana cv. Karpooravalli (ABB) plants by *B. velezensis* YEBBR6 might have triggered the constitutive defense response against *Foc* KP. In agreement with our finding, Vanthana et al. (2019) reported that MAMP molecules of *B. velezensis* VB7 increased the expression of the WRKY gene in tomato plants compared to control against GBNV. Next to the WRKY transcription factor, phosphorylation of appropriate protein substrates is highly essential to catalyze the expression of defense genes and regulation of cell functions in the midst of biotic and abiotic stress through the association of MAPKs, one of the largest group of transferases (Onyilo et al., 2017; Xu et al., 2017; Jagodzik et al., 2018; Vanthana et al., 2019). In addition, MAPK cascades play an important role in signal transduction and regulate crosstalk between important hormonal pathways including auxin (AUX), abscisic acid (ABA), jasmonic acid (JA), salicylic acid (SA), ethylene (ET), brassinosteroids (BR), and gibberellins (GA) (Mishra et al., 2006; Rodriguez et al., 2010; Lu et al., 2015). Furthermore, cascades of MAPK are also involved in regulation of signaling related to multiple defense responses, defense hormones, reactive oxygen species (ROS) generation, stomatal closure, defense gene activation, phytoalexin biosynthesis, cell wall strengthening, and hypersensitive response (HR) cell death (Meng and Zhang, 2013). Considering the significant impact of MAPK, our focus on understanding the regulation of MAPK in *B. velezensis* YEBBR6-treated banana plants challenged with *Foc* KP confirmed a 2.42-fold increased expression of the MAPK gene. McNeece et al. (2019) also reported the co-expression of five different types of defense genes related to MAPK influencing PTI and ETI against plant pathogenic *Fusarium* species.

Despite the induction of WRKY 33 and MAPK defense genes, PAL, LOX, and CERK 1 transcripts were also increased in *B. velezensis*-treated banana cv. Karpooravalli (ABB) plantlets compared to in untreated control. PAL, being the first enzyme involved in the phenylpropanoid pathway during biotic and abiotic stress, catalyzes the first step in the phenylpropanoid pathway and regulates defense signaling (Lyne et al., 1976). It is also involved in the conversion of phenylalanine to trans-cinnamic acid which is the entry step for channeling carbon from primary metabolism into phenylpropanoid secondary metabolism in plants (Campbell and Ellis, 1992; Ritter and Schulz, 2004). All these pathways bestowed the metabolites with antifungal activity. Apart from the induction of metabolites with antifungal activity, PAL interacts with chalcone synthase, polyketide synthase, and stilbene synthases which are responsible for antifungal action (Schanz et al., 1992; Okada et al., 2004; Zhu et al., 2004). Induction of PAL in banana plants suppressed *Foc* infection (Wang et al., 2016). Application of bacterial endophytes against *Foc* accumulated defense-related enzymes such as PO, PPO, and PAL (Ajit kumar et al., 2020). Thus, based on protein-protein interaction, increase in the expression of PAL transcripts in banana plantlets biohardened with *B. velezensis* YEBBR6 against *Foc* KP might have simultaneously induced various pathways and proteins responsible for the suppression of *Fusarium* wilt via the induction of SAR. Interestingly, banana plantlets of banana cv. Karpooravalli (ABB) biohardened with *B. velezensis* YEBBR6 against *Foc* KP also increased the transcript levels of CERK 1 and LOX genes. CERK 1, being a cell surface receptor, plays a pivotal role in the induction of innate immunity against biotic and abiotic stresses (Shinya et al., 2014). Expression of CERK 1 also can co-express LysM domain-based defense genes contributing to the immune response against *Foc* KP. Besides, CERK 1 protein and its interacting partners recognize pathogen entry and mediate signaling events leading to suppression of the pathogen. Induction of LOX in biohardened banana cv. Karpooravalli (ABB) plantlets by *B. velezensis* and *Foc* KP might have promoted plant growth and plant defense. Hydroperoxidation products of the LOX pathway are responsible for seed germination, plant growth, development, plant senescence, and plant defense against insect and disease attacks.

Ultimately, the present investigation emphasized that biohardening of micropropagated banana cv. Karpooravalli (ABB) with *B. velezensis* YEBBR6 promoted plant growth and suppressed the infection of *Fusarium* wilt through the induction of WRKY 33 transcription factor, MAPK, and defense genes including PAL, LOX, and CERK 1. Further protein-protein interaction also confirmed the co-expression of different domains involved in innate immunity and growth promotion. Subsequently, *B. velezensis* YEBBR6 also produced antifungal metabolites clindamycin and nonanol which are responsible for inhibiting the mycelial growth of *Foc* KP. Thus, biohardening with multifaceted *B. velezensis* YRBBR6 can be explored for the management of *Fusarium* wilt of banana.

CONCLUSION

Investigation on biohardening of the micropropagated susceptible cultivar cv. Karpooravalli (Pisang Awak ABB) with bacterial endophyte *B. velezensis* YEBBR6 derived from the resistant genotype YKM5 on reprogramming of innate immunity against *Foc* KP revealed the versatile production of metabolically active biomolecules contributing to the suppression of *Foc* KP. On the other hand, biohardening enhanced the growth promotion of banana plantlets by increasing the plant height and production of number of leaves in comparison with untreated control. Scanning electron micrographs also confirmed the colonization of the rhizoplane by *B. velezensis* YEBBR6, followed by hyperparasitism of *Foc* KP in the rhizosphere. Challenge inoculation of biohardened cv. Karpooravalli (Pisang Awak ABB) with *Foc* KP enhanced the transcript level of WRKY transcription factor, MAPK, and other defense genes including CERK 1, LOX, and PAL. Functional enrichment of different defense genes and transcription factors was linked with different domains responsible for growth promotion, induction of systemic resistance, and systemic-acquired resistance. As a result, the current study has opened up the scope for exploring the immense potential of *B. velezensis* YEBBR6 to bioharden micropropagated banana plantlets on a commercial scale to create preimmunized seedlings for the management of *Foc* KP (race 4).

DATA AVAILABILITY STATEMENT

The original contributions presented in the study are included in the article/**Supplementary Material**, further inquiries can be directed to the corresponding author.

AUTHOR CONTRIBUTIONS

SN conceptualized the research and was associated with technically guiding and executing the research. RS performed lab experiments. NS and VR carried out the bioinformatics analysis. MK and SV coordinated the experiments associated with defense gene expression. MR, AK, SH, and VM edited the manuscript. All authors read and approved the final manuscript.

ACKNOWLEDGMENTS

The authors extend their sincere appreciation to the Department of Plant Pathology, Department of Plant Biotechnology, DBT-BTIS facility at Department of Plant Molecular Biology and Bioinformatics, Department of Fruit science, Department of Nanoscience and Technology, Tamil Nadu Agricultural University, Coimbatore, Tamil Nadu, India for providing facilities.

SUPPLEMENTARY MATERIAL

The Supplementary Material for this article can be found online at: https://www.frontiersin.org/articles/10.3389/fsufs.2022.845512/full#supplementary-material

REFERENCES

Abd Alhameed, R., Almarhoon, Z., Bukhari, S. I., El-Faham, A., de la Torre, B. G., and Albericio, F. (2020). Synthesis and antimicrobial activity of a new series of thiazolidine-2, 4-diones carboxamide and amino acid derivatives. *Molecules* 25, 105. doi: 10.3390/molecules25010105

Adnani, N., Chevrette, M. G., Adibhatla, S. N., Zhang, F., Yu, Q., Braun, D. R., et al. (2017). Coculture of marine invertebrate-associated bacteria and interdisciplinary technologies enable biosynthesis and discovery of a new antibiotic, keyicin. *ACS Chem. Biol.* 12, 3093–3102. doi: 10.1021/acschembio.7b00688

Ajit kumar, S., Bhattacharyya, A., and Baruah, A. (2020). Endophyte mediated activation of defense enzymes in banana plants pre-immunized with covert endophytes. *Indian Phytopathol.* 73, 433–441. doi: 10.1007/s42360-020-00245-8

Aloo, B. N., Makumba, B. A., and Mbega, E. R. (2019). The potential of *Bacilli* rhizobacteria for sustainable crop production and environmental sustainability. *Microbiol. Res.* 219, 26–39. doi: 10.1016/j.micres.2018.10.011

Anupama, N., Murali, M., Jogaiah,S., and Amruthesh, K. N. (2014). Crude oligosacchraides from *Alternaria solani* with *Bacillus subtilis* enhance defense activity and induce resistance against early blight disease of tomato. *Asian J. Sci. Technol.* 5, 412–416. Available online at: https://www.fao.org/fileadmin/templates/banana/documents/Docs_Resources_2015/TR4/13ManualFusarium.pdf

Butler, D. (2013). Fungus threatens top banana. *Nature News* 504, 195. doi: 10.1038/504195a

Campbell, M. M., and Ellis, B. E. (1992). Fungal elicitor-mediated responses in pine cell cultures: III. Purification and characterization of phenylalanine ammonia-lyase. *Plant Physiol.* 98, 62–70. doi: 10.1104/pp.98.1.62

Cao, Y., Pi, H., Chandrangsu, P., Li, Y., Wang, Y., Zhou, H., et al. (2018). Antagonism of two plant-growth promoting *Bacillus velezensis* isolates against *Ralstonia solanacearum* and *Fusarium oxysporum*. *Sci. Rep.* 8, 1–14. doi: 10.1038/s41598-018-22782-z

Carlier, J., De Waele, D., and Escalant, J. V. (2003). "Global evaluation of musa germplasm for resistance to fusarium wilt, Mycosphaerella leaf spot diseases and nematodes: in-dept evaluation," in *INIBAP Technical Guidelines 7*, eds A. V'ezina and C. Picq (Montpellier: The International Network for the Improvement of Banana and Plantain Arceaux 49 Press), 12.

Carvalhais, L. C., Henderson, J., Rincon-Florez, V. A., O'Dwyer, C., Czislowski, E., Aitken, E. A., et al. (2019). Molecular diagnostics of banana *Fusarium* Wilt targeting secreted-in-xylem genes. *Front. Plant Sci.* 10, 547. doi: 10.3389/fpls.2019.00547

Catambacan, D. G., and Cumagun, C. J. R. (2021). Weed-associated fungal endophytes as biocontrol agents of *Fusarium oxysporum* f. sp. *cubense* TR4 in cavendish banana. *J. Fungi*. 7, 224. doi: 10.3390/jof7030224

Cawoy, H., Debois, D., Franzil, L., De Pauw, E., Thonart, P., and Ongena, M. (2015). Lipopeptides as main ingredients for inhibition of fungal phytopathogens by *Bacillus subtilis*/*amyloliquefaciens*. *Microb. Biotechnol*. 8, 281–295. doi: 10.1111/1751-7915.12238

Chen, X., Li, C., Wang, H., and Guo, Z. (2019). WRKY transcription factors: evolution, binding, and action. *Phytopathol Res*. 1, 1–15. doi: 10.1186/s42483-019-0022-x

Cheng, Y., Zhou, Y., Yang, Y., Chi, Y. J., Zhou, J., Chen, J. Y., et al. (2012). Structural and functional analysis of VQ motif-containing proteins in *Arabidopsis* as interacting proteins of WRKY transcription factors. *Plant Physiol*. 159, 810–825. doi: 10.1104/pp.112.196816

Chomczynski, P., and Sacchi, N. (1987). Single-step method of RNA isolation by acid guanidinium thiocyanate-phenol-chloroform extraction. *Anal. Biochem*. 16, 156–159. doi: 10.1016/0003-2697(87)90021-2

Compant, S., Saikkonen, K., Mitter, B., Campisano, A., and Mercado-Blanco, J. (2016). Editorial special issue: soil, plants and endophytes. *Plant Soil*. 405, 1–11. doi: 10.1007/s11104-016-2927-9

Czislowski, E., Fraser-Smith, S., Zander, M., O'Neill, W. T., Meldrum, R. A., Tran-Nguyen, L. T., et al. (2018). Investigation of the diversity of effector genes in the banana pathogen, *Fusarium oxysporum* f. sp. cubense, reveals evidence of horizontal gene transfer. *Mol. Plant Pathol*. 19, 1155–1171. doi: 10.1111/mpp.12594

Dita, M. A., Pérez-Vicente, L., and Martínez, E. (2014). Inoculation of *Fusarium oxysporum* f. sp. *cubense* causal agent of fusarium wilt in banana. *Technical manual prevention and diagnostic of Fusarium wilt (Panama disease) of banana caused by Fusarium oxysporum f. sp. cubense. Tropical Race*. 4, 55–58.

Eulgem, T., Rushton, P. J., Robatzek, S., and Somssich, I. E. (2000). The WRKY superfamily of plant transcription factors. *Trends Plant Sci*. 5, 199–206. doi: 10.1016/S1360-1385(00)01600-9

Fira, D., Dimki,ć, I., Beri,ć, T., Lozo, J., and Stankovi,ć, S. (2018). Biological control of plant pathogens by *Bacillus* species. *J. Biotechnol*. 285, 44–55. doi: 10.1016/j.jbiotec.2018.07.044

Gamez, R., Cardinale, M., Montes, M., Ramirez, S., Schnell, S., and Rodriguez, F. (2019). Screening, plant growth promotion and root colonization pattern of two rhizobacteria (*Pseudomonas fluorescens* Ps006 and *Bacillus amyloliquefaciens* Bs006) on banana cv. Williams (Musa acuminata Colla). *Microbiol. Res*. 220, 12–20. doi: 10.1016/j.micres.2018.11.006

Gao, S., Wu, H., Yu, X., Qian, L., and Gao, X. (2016). Swarming motility plays the major role in migration during tomato root colonization by *Bacillus subtilis* SWR01. *Biol. Control*. 98, 11–17. doi: 10.1016/j.biocontrol.2016.03.011

Gao, Z., Zhang, B., Liu, H., Han, J., and Zhang, Y. (2017). Identification of endophytic *Bacillus velezensis* ZSY-1 strain and antifungal activity of its volatile compounds against *Alternaria solani* and *Botrytis cinerea*. *Biol.Control* 105, 27–39. doi: 10.1016/j.biocontrol.2016.11.007

Gatasheh, M. K., Kannan, S., Hemalatha, K., and Imrana, N. (2017). Proflavine an acridine DNA intercalating agent and strong antimicrobial possessing potential properties of carcinogen. *Karbala Int. J. Mod. Sci.* 3, 272–278. doi: 10.1016/j.kijoms.2017.07.003

Griffith, G. W., and Shaw, D. S. (1998), Polymorphisms in *Phytophthora infestans*: four mitochondrial haplotypes are detected after PCR amplification of DNA from pure cultures or from host lesions. *Appl.Environ. Microbiol*. 64, 4007–4014. doi: 10.1128/AEM.64.10.4007-4014.1998

Guan, Y., Lu, J., Xu, J., McClure, B., and Zhang, S. (2014). Two mitogen-activated protein kinases, MPK3 and MPK6, are required for funicular guidance of pollen tubes in Arabidopsis. *Plant Physiol*. 165, 528–533. doi: 10.1104/pp.113.231274

Guay, D. (2007). Update on clindamycin in the management of bacterial, fungal and protozoal infections. *Expert Opin. Pharmacother*. 8, 2401–2444. doi: 10.1517/14656566.8.14.2401

He, P., Li, S., Xu, S., Fan, H., Wang, Y., Zhou, W., et al. (2021). Monitoring Tritrophic Biocontrol Interactions Between *Bacillus* spp., *Fusarium oxysporum* f. sp. *cubense*, tropical race 4, and banana plants *in vivo* based on fluorescent transformation system. *Front. Microbiol*. 3089. doi: 10.3389/fmicb.2021.754918

Huang, J., Pang, Y., Zhang, F., Huang, Q., Zhang, M., Tang, S., et al. (2019). Suppression of Fusarium wilt of banana by combining acid soil ameliorant with biofertilizer made from *Bacillus velezensis* H-6. *Eur. J. Plant Pathol*. 154, 585–596. doi: 10.1007/s10658-019-01683-5

Jagodzik, P., Tajdel-Zielinska, M., Ciesla, A., Marczak, M., and Ludwikow, A. (2018). Mitogen-activated protein kinase cascades in plant hormone signaling. *Front. Plant Sci*. 9, 1387. doi: 10.3389/fpls.2018.01387

Kandel, S. L., Joubert, P. M., and Doty, S. L. (2017). Bacterial endophyte colonization and distribution within plants. *Microorganisms* 5, 77. doi: 10.3390/microorganisms5040077

Kang, X., Guo, Y., Leng, S., Xiao, L., Wang, L., Xue, Y., et al. (2019). Comparative Transcriptome Profiling of *Gaeumannomyces graminis* var. *tritici* in Wheat Roots in the Absence and Presence of Biocontrol *Bacillus velezensis* CC09. *Front. Microbiol*. 10, 1474. doi: 10.3389/fmicb.2019.01474

Kavino, M., and Manoranjitham, S. K. (2018). In vitro bacterization of banana (*Musa* spp.) with native endophytic and rhizospheric bacterial isolates: novel ways to combat *Fusarium* wilt. *Eur. J. Plant Pathol*. 151, 371–387. doi: 10.1007/s10658-017-1379-2

Kavino, M., Manoranjitham, S. K., Balamohan, T. N., Kumar, N., Karthiba, L., and Samiyappan, R. (2011), December. Enhancement of growth and Panama wilt resistance in banana by in vitro co-culturing of banana plantlets with PGPR and endophytes. *Int. Symp. Trop. Subtrop. Fruits* 1024, 277–282.

Kavino, M., Manoranjitham, S. K., Balamohan, T. N., Kumar, N., Karthiba, L., and Samiyappan, R. (2014). Enhancement of growth and panama wilt resistance in banana by in vitro co-culturing of banana plantlets with pgpr and endophytes. *Acta Hortic*. 1024, 277–282. doi: 10.17660/ActaHortic.2014.1024.37

Khalid, S., and Keller, N. P. (2021). Chemical signals driving bacterial–fungal interactions. *Environ. Microbiol*. 23, 1334–1347. doi: 10.1111/1462-2920.15410

Leong, S. K., Latiffah, Z., and Baharuddin, S. (2009). Molecular characterization of *Fusarium oxysporum* f. sp. cubense of banana. *Am. J. Appl. Sci*. 6, 1301–1307. doi: 10.3844/ajassp.2009.1301.1307

Liu, Y., Zhang, N., Qiu, M., Feng, H., Vivanco, J. M., Shen, Q., et al. (2014). Enhanced rhizosphere colonization of beneficial *Bacillus amyloliquefaciens* SQR9 by pathogen infection. *FEMS Microbiol. Lett*. 353, 49–56. doi: 10.1111/1574-6968.12406

Livak, K. J., and Schmittgen, T. D. (2001). Analysis of relative gene expression data using real-time quantitative PCR and the 2(-Delta Delta C(T)) Method. *Methods* 25, 402–408. doi: 10.1006/meth.2001.1262

Lu, K., Guo, W., Lu, J., Yu, H., Qu, C., Tang, Z., et al. (2015). Genome-wide survey and expression profile analysis of the mitogen-activated protein kinase (MAPK) gene family in *Brassica rapa*. *PLoS ONE* 10, 0132051. doi: 10.1371/journal.pone.0132051

Lyne, R. L., Mulheirn, L. J., and Leworthy, D. P. (1976). New pterocarpinoid phytoalexins of soybean. *J. Chem. Soc. Chem. Comm*. 13, 497–498. doi: 10.1039/c39760000497

Maldonado-Bonilla, L. D., Calderón-Oropeza, M. A., Villarruel-Ordaz, J. L., and Sánchez-Espinosa, A. C. (2019). Identification of novel potential causal agents of Fusarium wilt of *Musa* sp. AAB in southern Mexico. *Plant Pathol. Microbiol*. 10, 10–24105. doi: 10.35248/2157-7471.10.479

Mao, G., Meng, X., Liu, Y., Zheng, Z., Chen, Z., and Zhang, S. (2011). Phosphorylation of a WRKY transcription factor by two pathogen-responsive MAPKs drives phytoalexin biosynthesis in *Arabidopsis*. *Plant Cell*. 23, 1639–1653. doi: 10.1105/tpc.111.084996

McNeece, B. T., Sharma, K., Lawrence, G. W., Lawrence, K. S., and Klink, V. P. (2019). The mitogen activated protein kinase (MAPK) gene family functions as a cohort during the *Glycine max* defense response to *Heterodera glycines*. *Plant Physiol. Biochem*. 137, 25–41. doi: 10.1016/j.plaphy.2019.01.018

Meng, Q., and Hao, J. J. (2017). Optimizing the application of Bacillus velezensis BAC03 in controlling the disease caused by *Streptomyces scabies*. *Biol. Control*. 62, 535–544. doi: 10.1007/s10526-017-9799-7

Meng, X., and Zhang, S. (2013). MAPK cascades in plant disease resistance signaling. *Annu. Rev. Phytopathol*. 51, 245–266. doi: 10.1146/annurev-phyto-082712-102314

Mishra, N. S., Tuteja, R., and Tuteja, N. (2006). Signaling through MAP kinase networks in plants. *Arch. Biochem. Biophys*. 452, 55–68. doi: 10.1016/j.abb.2006.05.001

Mohamad, O. A., Li, L., Ma, J. B., Hatab, S., Xu, L., Guo, J. W., et al. (2018). Evaluation of the antimicrobial activity of endophytic bacterial populations from Chinese traditional medicinal plant licorice and characterization of

the bioactive secondary metabolites produced by *Bacillus atrophaeus* against *Verticillium dahliae*. *Front. Microbiol.* 9, 924. doi: 10.3389/fmicb.2018.00924

Nakkeeran, S., Rajamanickam, S., Saravanan, R., Vanthana, M., and Soorianathasundaram, K. (2021). Bacterial endophytome-mediated resistance in banana for the management of *Fusarium* wilt. *3 Biotech.* 11, 1–13. doi: 10.1007/s13205-021-02833-5

Nakkeeran,S., Vinodkumar,S., Renukadevi, P., Rajamanicam, S., and Jogaiah,S. (2019). "Bioactive molecule from *Bacillus* spp., an effective tool for plant stress management," in *Bioactive Molecules in Plant Defense*. 1–23. Available online at: https://www.springerprofessional.de/bioactive-molecules-from-bacillus-spp-an-effective-tool-for-plan/17190160.

Narasimha Murthy, K., Soumya, K., Udayashankar, A. C., Srinivas, C., and Jogaiah, (2021). "Biocontrol potential of plant growth promoting rhizobacteria (PGPR) against Ralstonia solanacearum: Current and future prospects," in *Biocontrol Agents and Secondary Metabolites. Karnatak University, Dharwad, Karnataka, India*, 153–180.

Nel, B., Steinberg, C., Labuschagne, N., and Viljoen, A. (2006). The potential of nonpathogenic *Fusarium oxysporum* and other biological control organisms for suppressing *Fusarium* wilt of banana. *Plant Pathol.* 55, 217–223. doi: 10.1111/j.1365-3059.2006.01344.x

Nelson, P. E., Toussoun, T. A., and Marasas, W. F. (1983). *Fusarium species: An Illustrated Manual for Identification*. University Park, PA: Pennsylvania State University Press.

Okada, Y., Sano, Y., Kaneko, T., Abe, I., Noguchi, H., and Ito, K. (2004). Enzymatic reactions by five chalcone synthase homologs from hop (*Humulus lupulus* L.). *Biosci. Biotechnol. Biochem.* 68, 1142–1145. doi: 10.1271/bbb.68.1142

Onyilo, F., Tusiime, G., Chen, L. H., Falk, B., Stergiopoulos, I., Tripathi, J. N., et al. (2017). Agrobacterium tumefaciens-mediated transformation of *Pseudocercospora fijiensis* to determine the role of PfHog1 in osmotic stress regulation and virulence modulation. *Front. Microbiol.* 8, 830. doi: 10.3389/fmicb.2017.00830

Palmqvist, N. G. M., Bejai, S., Meijer, J., Seisenbaeva, G. A., and Kessler, V. G. (2015). Nano titania aided clustering and adhesion of beneficial bacteria to plant roots to enhance crop growth and stress management. *Sci. Rep.* 5, 1–12. doi: 10.1038/srep10146

Radhakrishnan, R., Hashem, A., and Abd_Allah, E. F. (2017). *Bacillus*: a biological tool for crop improvement through bio-molecular changes in adverse environments. *Front. Physiol.* 8, 667. doi: 10.3389/fphys.2017.00667

Rajamanickam, S., Karthikeyan, G., Kavino, M., and Manoranjitham, S. K. (2018). Biohardening of micropropagated banana using endophytic bacteria to induce plant growth promotion and restrain rhizome rot disease caused by *Pectobacterium carotovorum* subsp. carotovorum. *Sci. Hortic.* 231, 179–187. doi: 10.1016/j.scienta.2017.12.037

Raza, W., Ling, N., Zhang, R., Huang, Q., Xu, Y., and Shen, Q. (2017). Success evaluation of the biological control of *Fusarium* wilts of cucumber, banana, and tomato since 2000 and future research strategies. *Crit. Rev. Biotechnol.* 37, 202–212. doi: 10.3109/07388551.2015.1130683

Ritter, H., and Schulz, G. E. (2004). Structural basis for the entrance into the phenylpropanoid metabolism catalyzed by phenylalanine ammonia-lyase. *Plant Cell.* 16, 3426–3436. doi: 10.1105/tpc.104.025288

Rodriguez, M. C., Petersen, M., and Mundy, J. (2010). Mitogen-activated protein kinase signaling in plants. *Annu. Rev. Plant Biol.* 61, 621–649. doi: 10.1146/annurev-arplant-042809-112252

Rushton, P. J., Somssich, I. E., Ringler, P., and Shen, Q. J. (2010). WRKY transcription factors. *Trends Plant Sci.* 15, 247–258. doi: 10.1016/j.tplants.2010.02.006

Saravanan, R., Nakkeeran, S., Saranya, N., Haripriya, S., Kavino, M., Anandham, R., et al. (2021a). Differential bacterial endophytome in Foc-resistant banana cultivar displays enhanced antagonistic activity against *Fusarium oxysporum f.* sp. cubense (Foc). *Environ. Microbiol.*

Saravanan, R., Nakkeeran, S., Saranya, N., Senthilraja, C., Renukadevi, P., Krishnamoorthy, A. S., et al. (2021b). Mining the Genome of *Bacillus velezensis* VB7 (CP047587) for MAMP genes and non-ribosomal peptide synthetase gene clusters conferring antiviral and antifungal activity. *Microorganisms* 9, 2511. doi: 10.3390/microorganisms9122511

Schanz, S., Schröder, G., and Schröder, J. (1992). Stilbene synthase from Scots pine (*Pinus sylvestris*). *FEBS Lett.* 313, 71–74. doi: 10.1016/0014-5793(92)81187-Q

Shah, A. A., Khan, W. U., Yasin, N. A., Akram, W., Ahmad, A., Abbas, M., et al. (2020). Butanolide alleviated cadmium stress by improving plant growth, photosynthetic parameters and antioxidant defense system of *Brassica oleracea*. *Chemosphere* 261, 127728. doi: 10.1016/j.chemosphere.2020.127728

Shamsuddin, Z.H., Mia, M.A.B., Wahab, and Marziah, M. (2000). "Growth and physiological attributes of hydroponically grown bananas inoculated with plant growth promoting rhizobacteria," in *Tropical Plant Biology Research in Malaysia: Fruit and Vegetables: Joint Proceedings of the 11th Malaysian Society of Plant Physiology Conference and 2nd National Banana Seminar* (Malaysian Society of Plant Physiology), 324–327.

Shamsuddin, Z. H., Amr, H. G., Mia, M. A. B., Halimi, M. S., Zakaria, W., and Marziah, M. (1999). Symbiotic and associative N2 fixation with vegetable soybean, oil palm and bananas. *Biotechnol. Sustain. Utilizat. Biol. Resour. Trop.* 14. 102–118.

Shinya, T., Yamaguchi, K., Desaki, Y., Yamada, K., Narisawa, T., Kobayashi, Y., et al. (2014). Selective regulation of the chitin-induced defense response by the Arabidopsis receptor-like cytoplasmic kinase PBL 27. *Plant J.* 79, 56–66. doi: 10.1111/tpj.12535

Syed Ab Rahman, S. F., Singh, E., Pieterse, C. M. J., and Schenk, P. M. (2018). Emerging microbial biocontrol strategies for plant pathogens. *Plant Sci.* 267, 102–111. doi: 10.1016/j.plantsci.2017.11.012

Szklarczyk, D., Gable, A. L., Nastou, K. C., Lyon, D., Kirsch, R., Pyysalo, S., et al. (2021). The STRING database in 2021: customizable protein–protein networks, and functional characterization of user-uploaded gene/measurement sets. *Nucleic Acids Res.* 49, D605–D612. doi: 10.1093/nar/gkab835

Tamura, K., Dudley, J., Nei, M., and Kumar, S. (2007). MEGA4: molecular evolutionary genetics analysis (MEGA) software version 4.0. *Mol. Biol. Evol.* 24, 1596–1599. doi: 10.1093/molbev/msm092

Vanthana, M., Nakkeeran, S., Malathi, V. G., Renukadevi, P., and Vinodkumar, S. (2019). Induction of in planta resistance by flagellin (Flg) and elongation factor-TU (EF-Tu) of *Bacillus amyloliquefaciens* (VB7) against groundnut bud necrosis virus in tomato. *Microb. Pathog.* 137, 103757. doi: 10.1016/j.micpath.2019.103757

Vinodkumar, S., Nakkeeran, S., Renukadevi, P., and Malathi, V. G. (2017). Biocontrol potentials of antimicrobial peptide producing *Bacillus* species: multifaceted antagonists for the management of stem rot of carnation caused by *Sclerotinia sclerotiorum*. *Front. Microbiol.* 8, 446. doi: 10.3389/fmicb.2017.00446

Walters, D., Raynor, L., Mitchell, A., Walker, R., and Walker, K. (2004). Antifungal activities of four fatty acids against plant pathogenic fungi. *Mycopathologia* 157, 87–90. doi: 10.1023/B:MYCO.0000012222.68156.2c

Wang, B., Yuan, J., Zhang, J., Shen, Z., Zhang, M., Li, R., et al. (2013). Effects of novel bioorganic fertilizer produced by *Bacillus amyloliquefaciens* W19 on antagonism of Fusarium wilt of banana. *Biol. Fertil. Soils.* 49, 435–446. doi: 10.1007/s00374-012-0739-5

Wang, Z., Li, J. Y., Jia, C. H., Li, J. P., Xu, B. Y., and Jin, Z. Q. (2016). Molecular cloning and expression of four phenylalanine ammonia lyase genes from banana interacting with *Fusarium oxysporum*. *Biol. Plant.* 60, 459–468. doi: 10.1007/s10535-016-0619-1

Wei, G., Kloepper, J. W., and Tuzun, S. (1991). Induction of systemic resistance of cucumber to *Colletotrichum orbiculare* by select strains of plant growth-promoting rhizobacteria. *Phytopathology* 81, 1508–1512. doi: 10.1094/Phyto-81-1508

White, T. J., Bruns, T., Lee, S. J., and Taylor, J. (1990). Amplification and direct sequencing of fungal ribosomal RNA genes for phylogenetics. *PCR Protocols* 18, 315–322. doi: 10.1016/B978-0-12-372180-8.50042-1

Wong, C. K. F., Zulperi, D., Vadamalai, G., Saidi, N. B., and Teh, C. Y. (2019). Phylogenetic Analysis of *Fusarium oxysporum* f. *sp.* cubense Associated with Fusarium Wilt of Bananas from Peninsular Malaysia. *Sains Malaysiana* 48, 1593–1600. doi: 10.17576/jsm-2019-4808-04

Xu, C., Liu, R., Zhang, Q., Chen, X., Qian, Y., and Fang, W. (2017). The diversification of evolutionarily conserved MAPK cascades correlates with the evolution of fungal species and development of lifestyles. *Genome Biol. Evol.* 9, 311–322. doi: 10.1093/gbe/evw051

Xue, C., Penton, C. R., Shen, Z., Zhang, R., Huang, Q., Li, R., et al. (2015). Manipulating the banana rhizosphere microbiome for biological control of Panama disease. *Sci. Rep.* 5, 1–11. doi: 10.1038/srep11124

Yuan, J., Ruan, Y., Wang, B., Zhang, J., Waseem, R., Huang, Q., et al. (2013). Plant growth-promoting rhizobacteria strain *Bacillus amyloliquefaciens* NJN-6-enriched bio-organic fertilizer suppressed Fusarium wilt and promoted the growth of banana plants. *J. Agric. Food Chem*. 61, 3774–3780. doi: 10.1021/jf400038z

Zhang, J. H., Sun, H. L., Chen, S. Y., Zeng, L., and Wang, T. T. (2017). Anti-fungal activity, mechanism studies on α-Phellandrene and Nonanal against *Penicillium cyclopium*. *Bot. Stud*. 58, 1–9. doi: 10.1186/s40529-017-0168-8

Zhang, L., Cenci, A., Rouard, M., Zhang, D., Wang, Y., Tang, W., et al. (2019). Transcriptomic analysis of resistant and susceptible banana corms in response to infection by *Fusarium oxysporum* f. sp. *cubense* tropical race 4. *Sci. Rep*. 9, 1-14. doi: 10.1038/s41598-019-44637-x

Zhao, M., Yuan, J., Zhang, R., Dong, M., Deng, X., Zhu, C., et al. (2018). Microflora that harbor the NRPS gene are responsible for Fusarium wilt disease-suppressive soil. *Agric,. Ecosyst. Environ., Appl. Soil Ecol.* 132, 83–90. doi: 10.1016/j.apsoil.2018.08.022

Zhu, Y. J., Agbayani, R., Jackson, M. C., Tang, C. S., and Moore, P. H. (2004). Expression of the grapevine stilbene synthase gene VST 1 in papaya provides increased resistance against diseases caused by *Phytophthora palmivora*. *Planta* 220, 241–250. doi: 10.1007/s00425-004-1343-1

Conflict of Interest: The authors declare that the research was conducted in the absence of any commercial or financial relationships that could be construed as a potential conflict of interest.

Publisher's Note: All claims expressed in this article are solely those of the authors and do not necessarily represent those of their affiliated organizations, or those of the publisher, the editors and the reviewers. Any product that may be evaluated in this article, or claim that may be made by its manufacturer, is not guaranteed or endorsed by the publisher.

frontiers | Frontiers in Microbiology

ORIGINAL RESEARCH
published: 06 April 2022
doi: 10.3389/fmicb.2022.802512

Amelioration of Chromium-Induced Oxidative Stress by Combined Treatment of Selected Plant-Growth-Promoting Rhizobacteria and Earthworms *via* Modulating the Expression of Genes Related to Reactive Oxygen Species Metabolism in *Brassica juncea*

Pooja Sharma[1,2], Rekha Chouhan[3], Palak Bakshi[2], Sumit G. Gandhi[3]*, Rupinder Kaur[4], Ashutosh Sharma[5]* and Renu Bhardwaj[2]*

[1] Department of Microbiology, DAV University, Jalandhar, India, [2] Department of Botanical and Environmental Sciences, Guru Nanak Dev University, Amritsar, India, [3] Indian Institute of Integrative Medicine (CSIR), Jammu, India, [4] Department of Biotechnology, DAV College, Amritsar, India, [5] Faculty of Agricultural Sciences, DAV University, Jalandhar, India

OPEN ACCESS

Edited by:
Krishnendu Pramanik, Visva-Bharati University, India

Reviewed by:
Hayssam M. Ali, King Saud University, Saudi Arabia
Muhammad Arslan Ashraf, Government College University, Faisalabad, Pakistan

***Correspondence:**
Sumit G. Gandhi
sumit@iiim.res.in
Ashutosh Sharma
sharma_tosh_ashu@yahoo.co.in
Renu Bhardwaj
renubhardwaj82@gmail.com

Specialty section:
This article was submitted to Terrestrial Microbiology, a section of the journal Frontiers in Microbiology

Received: *26 October 2021*
Accepted: *25 January 2022*
Published: *06 April 2022*

Citation:
Sharma P, Chouhan R, Bakshi P, Gandhi SG, Kaur R, Sharma A and Bhardwaj R (2022) Amelioration of Chromium-Induced Oxidative Stress by Combined Treatment of Selected Plant-Growth-Promoting Rhizobacteria and Earthworms via Modulating the Expression of Genes Related to Reactive Oxygen Species Metabolism in Brassica juncea. Front. Microbiol. 13:802512. doi: 10.3389/fmicb.2022.802512

Chromium (Cr) toxicity leads to the enhanced production of reactive oxygen species (ROS), which are extremely toxic to the plant and must be minimized to protect the plant from oxidative stress. The potential of plant-growth-promoting rhizobacteria (PGPR) and earthworms in plant growth and development has been extensively studied. The present study was aimed at investigating the effect of two PGPR (*Pseudomonas aeruginosa* and *Burkholderia gladioli*) along with earthworms (*Eisenia fetida*) on the antioxidant defense system in *Brassica juncea* seedlings under Cr stress. The Cr toxicity reduced the fresh and dry weights of seedlings, enhanced the levels of superoxide anion ($O_2\bullet^-$), hydrogen peroxide (H_2O_2), malondialdehyde (MDA), and electrolyte leakage (EL), which lead to membrane as well as the nuclear damage and reduced cellular viability in *B. juncea* seedlings. The activities of the antioxidant enzymes, *viz*., superoxide dismutase (SOD), guaiacol peroxidase (POD), ascorbate peroxidase (APOX), glutathione peroxidase (GPOX), dehydroascorbate reductase (DHAR), and glutathione reductase (GR) were increased; however, a reduction was observed in the activity of catalase (CAT) in the seedlings under Cr stress. Inoculation of the PGPR and the addition of earthworms enhanced the activities of all other antioxidant enzymes except GPOX, in which a reduction of the activity was observed. For total lipid- and water-soluble antioxidants and the non-enzymatic antioxidants, *viz*., ascorbic acid and glutathione, an enhance accumulation was observed upon the inoculation with PGPR and earthworms. The supplementation of PGPR with earthworms (combined treatment) reduced both the reactive oxygen species (ROS) and the MDA content by modulating the defense system

of the plant. The histochemical studies also corroborated that the combined application of PGPR and earthworms reduced $O_2\bullet^-$, H_2O_2, lipid peroxidation, and membrane and nuclear damage and improved cell viability. The expression of key antioxidant enzyme genes, *viz.*, *SOD, CAT, POD, APOX, GR, DHAR,* and *GST* showed the upregulation of these genes at post-transcriptional level upon the combined treatment of the PGPR and earthworms, thereby corresponding to the improved plant biomass. However, a reduced expression of *RBOH1* gene was noticed in seedlings supplemented under the effect of PGPR and earthworms grown under Cr stress. The results provided sufficient evidence regarding the role of PGPR and earthworms in the amelioration of Cr-induced oxidative stress in *B. juncea*.

Keywords: *Burkholderia gladioli*, *Eisenia fetida*, reactive oxygen species, *Pseudomonas aeruginosa*, oxidative stress, glutathione, ascorbate, antioxidant enzyme

INTRODUCTION

In the recent past, rapid industrialization and increased urbanization led to an enhanced level of heavy metal contamination in the environment, which has emerged as a global concern (Saleem et al., 2018). Soil contamination with heavy metals is a major concern due to their non-biodegradable nature, bio-accumulation, and persistence in the environment (Din et al., 2020). Chromium (Cr) contamination has increased in the soil and into the water because of the release of Cr containing effluents from various industries such as electroplating, alloying, metallurgy, tannery, textile dyes, paints, and timber processing (Ganesh et al., 2009; Gill et al., 2016). Cr exists in six oxidation states, but Cr (III) and Cr (VI) are the most stable forms in the aquatic and terrestrial environments (Santos et al., 2009; Augustynowicz et al., 2010). Cr (VI) is considered extremely toxic, as it is a strong oxidizing agent having high redox potential, which is responsible for the prompt production of reactive oxygen species (ROS) (Shanker et al., 2005). Due to its highly soluble nature and capacity to pass through the plasma membrane, it enters the cytoplasm and reacts with intracellular structures (Ma et al., 2016). Increased deposition of Cr in soil results in its accumulation in plants, which affects various physiological and biochemical activities (Gangwar et al., 2011; Wang et al., 2013; Askari et al., 2021). Cr is a biologically non-essential element and shows toxicity beyond certain limits. Soil is known to accumulate as high as 2.6% (25,900 mg/kg) chromium (Palmer and Wittbrodt, 1991). The Cr plants exposed to Cr contamination have a marked reduction in growth and biomass (Qureshi et al., 2020). It is not required for the plant metabolism and impairs the growth and development of the plant at the cellular, organ, and at genetic level (Dixit et al., 2002; Wakeel et al., 2018). Cr exposure affects the plant metabolism, seed germination, photosynthesis, nutrient balance, water status, and antioxidant enzymes (Tripathi et al., 2015; Mahmud et al., 2017). Cr phytotoxicity is attributed to the enhanced production of ROS comprising superoxide anion ($O_2\bullet^-$), hydrogen peroxide (H_2O_2), hydroxyl radical ($OH\bullet$), and singlet oxygen (O_1) species as a remedial strategy adapted by plants to alter the cellular redox status of plant, which results in severe oxidative damage (Ali et al., 2015; Ma et al., 2017). Since ROS are quite reactive, therefore, they may oxidize the cellular macromolecules like lipids, proteins, nucleic acids leading to oxidative burst, causing cellular damage, electrolyte leakage, and cell death (Apel and Hirt, 2004; Huang et al., 2014; Demidchik, 2015; Sharma et al., 2019; Gupta et al., 2020). Plasma-membrane-bound reduced nicotinamide adenine dinucleotide phosphate (NADPH) oxidase, also called as respiratory burst oxidase homolog (RBOH), is one the major enzymes responsible for the ROS generation under plant stress (Sharma et al., 2021). Accretion of malondialdehyde (MDA) level, a product of lipid peroxidation, is a potential indicator of oxidative damage under Cr stress (Anjum et al., 2017; Sallah-Ud-Din et al., 2017; Habiba et al., 2019).

Plants have complex and coordinated antioxidant defense system to maintain a steady-state level of ROS by scavenging the ROS generated to cope up the oxidative stress (Gill and Tuteja, 2010; Ma et al., 2017; Ashraf et al., 2021). The defense system comprising enzymes such as superoxide dismutase (SOD), catalase (CAT), ascorbate peroxidase (APOX), guaicol peroxidase (POD), dehydroascorbate reductase (DHAR), monodehydroascorbate reductase (MDHAR), glutathione reductase (GR), and glutathione peroxidase (GPOX) plays an imperative role in scavenging ROS produced due to metal toxicity (Gill and Tuteja, 2010). Numerous studies have reported altered activities of various antioxidant enzymes in different plant species under Cr stress (Gill et al., 2015; Kanwar et al., 2015; Handa et al., 2018). Non-enzymatic antioxidants (ascorbic acid, tocopherols, glutathione) also work in a coordinated manner with enzymatic antioxidants to neutralize Cr-induced ROS. For instance, the level of glutathione and ascorbic acid are increased under Cr stress (Ashger et al., 2018; Ulhassan et al., 2019). These antioxidants minimize the ROS- induced oxidative damage by acting as quenchers of ROS and lipid radicals (Noctor and Foyer, 1998; Smirnoff, 2000; Holländer-Czytko et al., 2005). *Brassica juncea* L. is an oil-yielding crop having medicinal properties. It is fast growing, produces a large amount of biomass, and possesses a sturdy and well-studied antioxidant defense system. Heavy metal stress results in a significant loss of its yield (Bhuiyan et al., 2011; Shekhawat et al., 2012).

Plant-growth-promoting rhizobacteria (PGPR) colonizing the rhizosphere of the plant have auspicious role in promoting plant growth and endurance and alleviating toxicity or injury to plants

under heavy metal stress (Etesami and Maheshwari, 2018). The rhizospheric zone of the growing plants, rich in nutrients due to accretion of plant exudates, is a hotspot for microbial activity in the soil (Gray and Smith, 2005; De la Fuente Cantó et al., 2020). Plant-associated microorganisms such as rhizobacteria secrete various metabolites in the vicinity of plant roots that endorse the plant growth and development under stressed conditions (Kumar and Verma, 2018; Khoshru et al., 2020). These beneficial bacteria have the potential to mitigate the heavy metal toxicity by improved plant growth, reduced oxidative stress through altered activities of enzymatic antioxidants, and enhanced synthesis of non-enzymatic antioxidants (Islam et al., 2014). Implication of PGPR in improving plant health and alleviating heavy metal toxicity in plants unveils their potential for safe food production (Etesami and Beattie, 2017). Recently, augmentation of *Bacillus cereus* has been found to lower the MDA level and maintain membrane integrity in *Brassica nigra* under Cr stress (Akhtar et al., 2021). Supplementation of PGPR enhanced the tolerance of tomato plant to oxidative damage from Cr stress by the enhanced levels of enzymatic and non-enzymatic antioxidants (Gupta et al., 2020).

Soil microorganisms (like PGPR) have a positive interaction with macroorganisms (like earthworms), which plays an important role in organic matter decomposition and nutrient cycling (Brown et al., 2000; Lavelle, 2002). Earthworms have a positive impact on the growth of the plants (Kaur et al., 2017; Mahohi and Raiesi, 2021), which is owed to signal molecules released in the soil possibly due to the activation of PGPR (Elmer, 2009; Puga-Freitas et al., 2012). Humic acid and vermi-wash secreted by the earthworms are rich in nutrients, hormones, vitamins, and enzymes, which promote plant growth and development (Varghese and Prabha, 2014; Sharma et al., 2020). Plant growth is improved indirectly by the earthworms through the stimulation of the defense system of the plant (Blouin et al., 2005; Kaur et al., 2019).

PGPR and earthworms naturally coinhabit the soil and have an imperative role in nutrient acquisition and improving plant growth (Abd El and Bashandy, 2019; Mahohi and Raiesi, 2019). Numerous authors have reported the potential of combined inoculation of earthworms and PGPR in plant growth and development and nutrient acquisition (Edith Castellanos Wu et al., 2012; Suarez et al., 2014; Abd El and Bashandy, 2019). Although it is evident from the existing literature that the PGPR alleviates the harmful effects of heavy metals by strengthening the antioxidant defense system and endorsing plant growth; however, to the best of our knowledge, there is no information available on the potential of the combined treatment by PGPR and earthworms in ameliorating heavy metal stress, especially Cr. Therefore, the present study was conducted to investigate the role of PGPR (*Pseudomonas aeruginosa*, *Burkholderia gladioli*) and earthworms (*Eisenia fetida*), alone and in combination, on the mitigation of Cr stress in *Brassica juncea* to study their effect on plant biomass, stress-related biochemical changes, ROS generation, and the modulation of the antioxidant defense system. The results of biochemical assays are further supported by the histochemical staining methods for visualization of stress bio-markers *in situ*. Therefore, to the best of our knowledge, it is the first attempt to study the Cr stress ameliorative potential of the combined treatment of PGPR and Earthworms using three different approaches, *viz*., changes in cellular stress biochemistry, *in situ* visualization of stress biomarkers, and the changes in the expression of genes involved in ROS metabolism, to get a holistic insight into the amelioration process.

MATERIALS AND METHODS

Microbial Culture

Pseudomonas aeruginosa MTCC7195 and *B. gladioli* MTCC10242 (obtained from Microbial Type Culture Collection, IMTECH Chandigarh, India) were revived in Nutrient Broth Medium (HiMedia Laboratories, Mumbai, India). Bacterial strains were incubated at 28°C for 24–48 h. The bacterial suspension was centrifuged at 4,000 rpm for 10 min at 4°C to obtain the pellet. The pellet was washed twice and resuspended in sterile distilled water to get uniform density of 10^9 cells/ml.

Plant Material and Experimental Design

Brassica juncea L., variety RLC-3, were obtained from Punjab Agriculture University, Ludhiana. Seeds were surface sterilized using sodium hypochlorite (0.5% v/v) followed by repeated washing with sterilized DW. The experiments were conducted under controlled conditions in plastic pots. Soil was mixed with organic manure in the ratio of 2:1. The soil mixture was autoclaved at 121°C for 30 min. The autoclaved soil (300 g) was poured into each plastic pot and amended with 0.5 mM Chromium solution in the form of potassium chromate (K_2CrO_4) obtained from Qualigens, Mumbai, India. Pots were inoculated with earthworms (three earthworms per pot) and bacterial suspension at the concentration of 109 cells/ml. The following experimental combinations were made: Control (Cn), Cr, CrE, CrM1, CrM2, CrM1M2, CrEM1, CrEM2, and CrEM1M2. Once the seeds were sown, the pots were maintained for 10 days in a seed germinator at 25 ± 2°C with a light intensity of 175 μmol m^{-2} s^{-1} and photoperiod of 16 h. The seedlings were harvested after 10 days, washed thoroughly with distilled water for various the morphological, biochemical, histochemical, and gene expression analysis. All the analysis for each treatment was conducted in triplicates.

Determination of Bio-Mass

Bio-mass was measured in terms of fresh and dry weight of 10-day-old *B. juncea* seedlings. Weight of freshly harvested seedlings was recorded and considered as fresh weight. Dry weight of seedlings was determined by drying them in an oven at 60°C for 48 h.

Assessment of Electrolyte Leakage

Electrolyte leakage (EL) was measured by following the method of Ahmad et al. (2016). Seedlings were placed in test tubes comprising 15 ml deionized water. The test tubes were placed in a shaking incubator at 30°C for 4 h, and then, the electrical conductivity (EC1) of the initial medium was measured. Afterward, all the test tubes were placed in an autoclave at

121°C for 20 min followed by cooling up to 25°C, and electrical conductivity (EC2) was measured and calculated by using the following formula:

$$EL = \frac{EC1}{EC2} \times 100 \quad (1)$$

Estimation of Oxidative Stress Markers

Superoxide Anion Content

Superoxide content (O_2.-) was determined by the method of Wu et al. (2010). One gram of fresh seedlings was homogenized with 3 ml of phosphate buffer 65 mM, pH 7.8, and then centrifuged at 12,000 rpm for 10 min. A supernatant (0.5 ml) was collected, and 0.1 ml of 10 mM hydroxylamine hydrochloride was added, followed by incubation at 25°C for 30 min. Afterward, 1 ml of 3-aminobenzenesulphonic acid and 1 ml of 1-naphthylamine were added to the reaction mixture. This mixture was again incubated at 25°C for 20 min, and the absorbance was read at 530 nm. The concentration of superoxide anion was determined using sodium nitrite as a standard and expressed as μmol g^{-1} FW.

Hydrogen Peroxide Content

Estimation of H_2O_2 content was done by the protocol of Velikova et al. (2000). Fresh seedlings were macerated in 2 ml of 0.1% trichloroacetic acid (TCA) followed by centrifugation at 12,000 rpm for 15 min. Of the supernatant, 0.4 ml was mixed with an equal volume of 10 mM potassium phosphate buffer, pH 7.0. Potassium iodide (0.8 ml) was added to the mixture. The absorbance of the reaction mixture was read at 390 nm. The concentration of H_2O_2 was determined the standard curve of H_2O_2 and expressed as μmol g^{-1} FW.

Malondialdehyde Content

MDA content was quantified following the protocol of Heath and Packer (1968). One gram of fresh seedlings was extracted in 3 ml of 0.1% TCA and then centrifuged at 12,000 rpm for 15 min in chilled conditions. Following centrifugation, 4 ml 0.5% thiobarbituric in 20% TCA acid was added to the collected supernatant. The mixture was heated at 95°C for 30 min and immediately cooled for termination of reaction by keeping it on ice bath. The absorbance of the colored complex was taken at 532 and 600 nm. MDA content was calculated by taking the difference in absorbance using an extinction coefficient of 155 mM^{-1} cm^{-1} and expressed as μM g^{-1} FW.

In situ Visualization of Superoxide Anion, Hydrogen Peroxide, Lipid Peroxidation, Cell Viability, and Membrane and Nuclear Damage

Histochemical Detection of Superoxide Anion and Hydrogen Peroxide

Histochemical detection of $O_2\bullet^-$ and H_2O_2 was accomplished using nitroblue tetrazolium (NBT) and 3,3′-diaminobenzidine (DAB) following the methods of Thordal-Christensen et al. (1997) and Frahry and Schopfer (2001), respectively. Cotyledons of the seedlings were immersed in NBT and DAB followed by boiling in ethanol to clearly visualize blue and brown spots, respectively. In *B. juncea* roots, H_2O_2 was tagged with 2′,7′-dichlorofluorescin diacetate (DCF-DA) following the method given by Rodríguez-Serrano et al. (2009). Root tips were stained by immersing in 25 μM DCF-DA for 30 min in dark. Following staining, the roots were washed with distilled water and mounted on glass slides and observed under a fluorescent microscope at an excitation wavelength of 488 nm and an emission wavelength of 530 nm.

Lipid Peroxidation and Cell Viability

In situ visualization of lipid peroxidation and cell viability was done using Schiff's reagent and Evans's blue following the method given by Pompella et al. (1987) and Yamamoto et al. (2001), respectively. Cotyledons of the seedlings were engrossed in Schiff's reagent and Evans's blue for 20 min. Afterward, the cotyledons were bleached by immersing them in boiling ethanol. Cotyledons were placed on glass slides and photographed.

Fluorescent Imaging of Membrane and Nuclear Damage

The membrane and nuclear damages were visualized using fluorescent dyes propidium iodide (PI) and 4,6-diamino-2-phenylindole (DAPI) according to the method of Callard et al. (1996) and Gutiérrez-Alcalá et al. (2000), respectively. For *in situ* visualization of membrane damage, the roots of *B. juncea* seedlings were soaked in PI (50 μM, Sigma-Aldrich, Mumbai, India) for 15 min followed by washing with distilled water. Roots were mounted on glass slides and visualized under a Ti2 fluorescent microscope at an excitation wavelength of 543 nm and emission wavelength of 617 nm. For visualization of nuclear damage, the roots were stained using DAPI and incubated in dark for 30 min followed by rinsing with PBS and finally mounted on slides and observed under fluorescent microscope at an excitation wavelength of 358 nm and emission wave length of 461 nm.

Determination of the Activities of Antioxidant Enzymes

To assess the activities of various antioxidant enzymes and determine protein content, 1 g of fresh plant sample was homogenized in 3 ml of 50 mM potassium phosphate buffer (PPB) having pH 7.0 in a pre-chilled pestle mortar. To assess the SOD activity, 50 mM sodium carbonate buffer having pH 10.2 was used for crushing the plant sample. The homogenate was centrifuged at 12,000 rpm at 4°C for 20 min. The supernatant was used to assess the activities of antioxidant enzymes and protein content. Determination of protein content was done following the method given by Bradford (1976). Protein content was calculated using the standard curve of bovine serum albumin.

Superoxide Dismutase (SOD EC. 1.15.1.1)

The activity of SOD was assessed by the protocol given by Kono (1978). The reaction mixture comprised of 50 mM sodium carbonate (Na_2CO_3) buffer, 0.03% Triton X-100, 1 mM hydroxylamine hydrochloride (pH 6), 24 μM nitroblue tetrazolium (NBT), and 0.1 M ethylenediaminetetraacetic acid (EDTA) and plant extract. Reaction mixture was incubated for

2 min, and the absorbance was taken at 540 nm for 1 min. Activity of SOD was determined by computing the inhibition of NBT. SOD unit activity is defined as the quantity of enzyme required for 50% inhibition. Specific activity was expressed as units per minute per milligram of the protein.

Guaiacol Peroxidase (POD EC 1.11.1.7)

Activity of POD was assessed by the method of Pütter (1974). The reaction mixture included the plant extract, 50 mM of potassium phosphate buffer (pH 7.0), 20.1 mM guaiacol solution, and 123 mM H_2O_2. The increase in absorbance due to the formation of guaiacol dehydrogenation product was read at 436 nm for 1 min using $\varepsilon = 26.6\ mM^{-1}\ cm^{-1}$.

Catalase (CAT EC 1.11.1.6)

The activity of CAT was determined by the procedure described by Aebi (1984). The reaction mixture contained plant extract, 50 mM phosphate buffer pH 7.0), and15 mM H_2O_2. The decrease in absorbance due to decomposition of H_2O_2 was measured at 240 nm for 1 min using $\varepsilon = 39.4\ mM^{-1}\ cm^{-1}$.

Ascorbate Peroxidase (APOX EC 1.11.1.11)

The activity of APOX was assessed by following the protocol mentioned by Nakano and Asada (1981). The reaction mixture comprised of 50 mM phosphate buffer (pH 7.0), 0.5 mM ascorbate, 1 mM H_2O_2, and enzyme extract. Decline in absorbance was read at 290 nm for 1 min by using extinction coefficient of $2.8\ mM^{-1}\ cm^{-1}$.

Dehydroascorbate Reductase (DHAR EC 1.8.5.1)

Activity of DHAR was assessed by protocol presented by Dalton et al. (1986). The reaction mixture comprised of 50 mM phosphate buffer (pH 7.0), enzyme extract, 0.1 mM EDTA, 0.2 mM dehydroascorbate, and 1.5 mM reduced glutathione (GSH). The change in absorbance was read at 265 nm for 1 min by using an extinction coefficient of $14\ mM^{-1}\ cm^{-1}$.

Glutathione Reductase (GR EC 1.6.4.2)

Activity of GR was determined by the method described by Carlberg and Mannervik (1975). The reaction mixture comprised of 50 mM phosphate buffer (pH 7.0), enzyme extract, 0.1 mM nicotinamide adenine dinucleotide phosphate reductase (NADPH), 1 mM glutathione disulfide (GSSG), 1 mM EDTA, and the plant extract. The decrease in absorbance was measured at 340 nm for 1 min by using an extinction coefficient of $6.22\ mM^{-1}\ cm^{-1}$.

Glutathione Peroxidase (GPOX EC 1.11.1.9)

Activity of GPOX was determined by the method given by Flohé and Günzler (1984). The reaction mixture comprised of the plant extract, 50 mM phosphate buffer pH (7.0), 1 mM sodium azide, 0.5 mM EDTA, 1 mM reduced glutathione, 0.15 mM NADPH, and 0.15 mM H_2O_2. The decline in absorbance was measured at 340 nm for 1 min by using an extinction coefficient of $6.22\ mM^{-1}\ cm^{-1}$.

Glutathione-S-Transferase (GST EC 2.5.1.18)

The activity of GST was assessed by the procedure described by Habig et al. (1974). The reaction mixture comprised of 0.1 M phosphate buffer (pH 7.4), 1 mM 2,4 dinitrochlorobenzene (cDNB), 20 mM GSH, and the plant extract. The absorbance was read at 340 nm by using an extinction coefficient of $9.6\ mM^{-1}\ cm^{-1}$.

Estimation of Non-enzymatic Antioxidants

For the estimation of non-enzymatic antioxidants, 1 g of fresh plant sample was homogenized in 50 mM Tris buffer (pH 10) and centrifuged at 13,000 rpm for 20 min at 4°C. The supernatant was used for measurement of non-enzymatic antioxidants.

Ascorbic Acid

Ascorbic acid content was estimated by following the protocol of Roe and Kuether (1943). Plant extract (0.5 ml) was mixed with 0.5 ml of 50% trichloroacetic acid (TCA). Activated charcoal (100 mg) and 4 ml of double-distilled water was added to the mixture. The mixture was thoroughly mixed and filtered using Whatman filter paper No. 1. The filtrate was collected, and 0.4 ml of 2,4- dinitrophenyl hydrazine (DNPH) was added. The reaction mixture was incubated at 37°C for 3 h. Chilled sulfuric acid (65%) (1.6 ml) was added, and the mixture was cooled at room temperature for 30 min, and the absorbance was measured at 520 nm. Ascorbic acid (1 mg/100 ml) was used as the standard.

Glutathione

The glutathione content was estimated following the method proposed by Sedalk and Lindsay (1968). The reaction mixture containing 100 μl of plant extract, 50 μl of Ellman's reagent, 1 ml of Tris buffer, and 4 ml of absolute ethanol was incubated at room temperature for 15 min. The reaction mixture was centrifuged at 3,000 rpm for 15 min. The absorbance of the supernatant was recorded at 412 nm. GSH (1 mg/100 ml) was used as standard.

Fluorescent Tagging of Glutathione

Glutathione tagging was done in roots following the method of Fricker and Mayer (2001). The roots were stained with 25 μM monochlorobimane (MCB) containing 5 μM sodium azide for 15–20 min. After incubation, roots were washed with distilled water, and images were obtained with a fluorescent microscope at excitation wavelength of 351–364 nm and emission wavelength of 477 nm.

Determination of Total Antioxidant Capacity

Total lipid- and water-soluble antioxidant capacity was determined by an antioxidant analyzer (PHOTOCHEM BU, Analytik Jena, Germany). One gram of fresh plant sample was extracted in 5 ml 50 mM Tris (pH 10.0) for water-soluble antioxidants and 1.5 ml methanol for lipid-soluble antioxidants under chilled environment, followed by centrifugation at 13,000 rpm at 4°C for 20 min. The antioxidant capacity was determined using standard kits and instructions provided in the manual available with the antioxidant analyzer. Total lipid- and water-soluble antioxidants were expressed in micromoles per gram.

Analysis of Gene Expression

RNA Isolation and Preparation of cDNA

RNA isolation from *B. juncea* seedlings was done using Trizol (Invitrogen, Waltham, MA, United States). It was quantified using a Nanodrop spectrophotometer (Thermo Fisher Scientific, Waltham, MA, United States). Qualitative analysis of RNA was done on 2% agarose gel electrophoresis. The isolated RNA was incubated with DNase (Ambion TURBO DNA free, Life Technologies, Carlsbad, CA, United States) to eliminate any potential DNA impurity. The first-strand of the cDNA was prepared from 1 μg of DNAse-treated RNA using reverse transcriptase (Promega, Madison, WI, United States) with oligo (dt) primer.

Expression Analysis

The qRT-PCR-based quantification was done in triplicates and conducted on ROTOR-GENE Q RT-PCR system (Qiagen, United States) following the manufacturer's instructions. Reaction mixture consisted of SYBER Green Master mix, diluted cDNA, and specific primer for the genes designed with Primer 3 software (**Table 1**) and cDNA. The conditions for qRT-PCR were 95°C for 10–12 min for initial denaturation, followed by 40 cycles of three steps of amplification 95°C (10 s), 66°C (10 s), and 72°C (15 s). All reactions were performed in triplicates using gene-specific primers and selecting actin gene as reference gene to normalize the data, and threshold cycle (Ct) values were used for calculation. Quantification of the relative gene expression of a gene was done by using $2^{-\Delta\Delta ct}$ method (Livak and Schmittgen, 2001; Awasthi et al., 2015).

Statistical Analysis

The experiments were performed in triplicates, and the results presented are in means ± SE in figures. Statistical analysis was performed using one-way analysis of variance (ANOVA) using SPSS 16.0 followed by Tukey's honestly significant difference (HSD) test to determine significant differences among means of the treatments at 5% level of significance.

RESULTS

Effect of Earthworms and Plant-Growth-Promoting Rhizobacteria on Biomass of *Brassica juncea* Seedlings Under Chromium Stress

To assess the effect of earthworms and PGPR inoculation on biomass of *B. juncea* under Cr stress, fresh and dry weights were determined in terms of fresh weight and dry weight (**Figures 1A,B**). Cr exposure to the seedlings significantly reduced the fresh weight of the seedlings by 32.91% and dry weight by 54.86% in comparison to untreated control. However, supplementation of earthworms and PGPR (M1 and M2) alone and in combinations significantly improved the seedlings biomass. Supplementation of earthworms enhanced the fresh and dry weights by 13.42 and 39.85% when compared with Cr only. Simultaneously, inoculation of M1, M2, and M1M2 under Cr stress also significantly enhanced the biomass of the seedlings when compared with Cr treatment only. Dual inoculation of both PGPR along with earthworms under Cr contamination resulted in highest significant increase in fresh weight by 58.82% and dry weight by 129.69 as compared with sole Cr-treated seedlings. The results depict that Cr had a negative impact on the seedling biomass, which was improved by supplementation with earthworms and PGPR showing that earthworms and PGPR promote the biomass.

Effect of Earthworms and Plant-Growth-Promoting Rhizobacteria on Oxidative Stress in *Brassica juncea* Seedlings Under Chromium Stress

Brassica juncea seedlings exposed to Cr unveiled high levels of oxidative stress due to enhanced production of ROS, *viz.*, $O_2\bullet^-$ and H_2O_2. A severe rise in the level of $O_2\bullet^-$ by 84.32% and H_2O_2 by 58.41% in Cr-treated seedlings was revealed in comparison to control seedlings. Diminution in oxidative stress in Cr-treated seedlings was revealed with sole earthworms and

TABLE 1 | Sequences of the gene specific primers for used for qRT-PCR.

Gene	Primer sequence
Actin	Forward Primer 5′ ACTGGTATTGTGCTTGACTCTG3′ Reverse Primer 5′ AGCTTCTCTTTAATGTCACGGAC3′
SOD	Forward Primer 5′ CACATTTCAACCCTGATGGTAA3′ Reverse Primer 5′ACAGCCCTTCCGACAATA3′
POD	Forward Primer 5′TTCGAACGGAAAAAGATGCT3′ Reverse Primer 5′AACCCTCCATGAAGGACCTC3′
CAT	Forward Primer 5′GTTCGACTTTGACCCACT3′ Reverse Primer 5′ATCCCAGGAACAATGATAGC3′
APOX	Forward Primer 5′CCACTTGAGACAGGTGTTACTA3′ Reverse Primer 5′TCCTTGAAGTAAGAGTTGTCGAAA3′
DHAR	Forward Primer 5′CTGGATGAGCTTAGTACATTCAAC3′ Reverse Primer 5′GGAAAGAAAGTGAATCTGGAACA3′
GR	Forward Primer 5′GATGCAGCGCTTGATTTAC3′ Reverse Primer 5′TCCCTAACGTCTTCATCAAACC3′
GST	Forward Primer 5′GAGCACAAGAAAGAGCCC3′ Reverse Primer 5′TGTTCTTGGAGTCGGCTG 3′
RBOH	Forward Primer 5′ACGGGGTGTGATAGAGATGC3′ Reverse Primer 5′TTTTTCCAGTTGGGTCTTGC3′

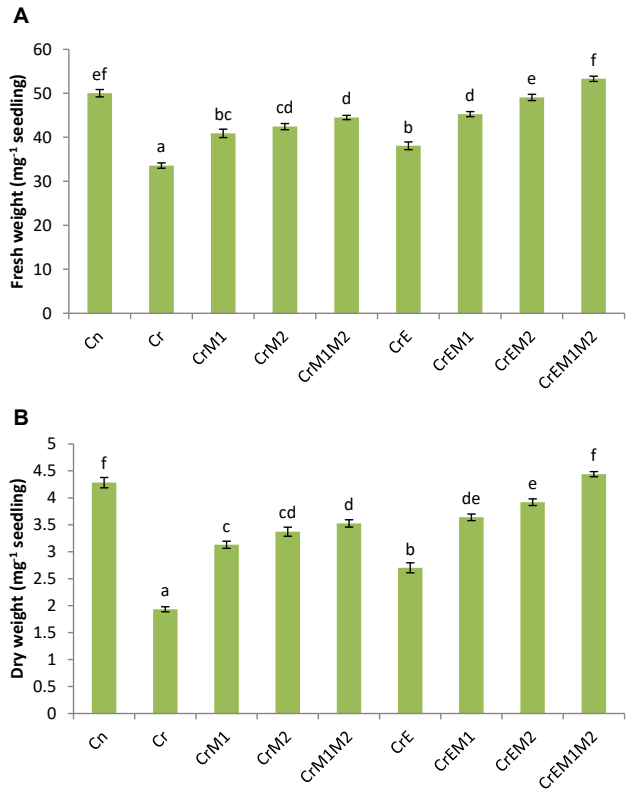

FIGURE 1 | Effect of PGPR [*Pseudomonas aeruginosa* (M1) & *Burkholderia gladioli* (M2)] and the earthworms [*Eisenia fetida* (E)] on **(A)** fresh weight and **(B)** dryweight of 10-day-old *B. juncea* seedlings under chromium (Cr) toxicity. Data are presented as means of three independent replicates ± S.E. (standard error). Different letterson the bar graphs indicate that mean values of the treatments are significantly different at $p \leq 0.05$ (Tukey's test).

PGPR inoculation and their combined applications as compared to only Cr-treated seedlings. However, a steep decline in $O_2\bullet^-$ content by 50.59% (**Figure 2A**) and H_2O_2 content by 49.27% (**Figure 2B**) was observed in seedlings raised with the combined inoculation of earthworms along with both PGPR (M1M2).

The spectroscopic observations obtained for $O_2\bullet^-$ and H_2O_2 content are in conformity with their histochemical detection in cotyledons with NBT and DAB, respectively. Blue spots and dark brown patches portray the accumulation of $O_2\bullet^-$ and H_2O_2 (**Figures 3A,B**), respectively, in *B. juncea* cotyledons under Cr treatment. However, supplementation of earthworms and PGPR alone and in combinations reduced the spots on the cotyledons produced by $O_2\bullet^-$ and H_2O_2 signifying reduction in ROS accumulation compared to Cr stress. In addition, the annotations obtained from fluorescent tagging of H_2O_2 with 2,7-dichloroflourcein diacetate (DCF-DA) in roots of *B. juncea* seedlings showed bright fluorescent green color under Cr stress (**Figure 4A**). However, roots of seedlings grown in control and in combinations with earthworms and PGPR exhibited the faint green appearance of DCF suggesting the ameliorative role of earthworms and PGPR in busting ROS.

Effect of Earthworms and Plant-Growth-Promoting Rhizobacteria on Lipid Peroxidation, Electrolyte Leakage, and Cell Viability of *Brassica juncea* Seedlings Under Chromium Stress

Lipid peroxidation in seedlings was measured as MDA content. *Brassica juncea* seedlings raised in Cr-contaminated soils showed a sharp increase in the MDA content (122.34%) and electrolyte leakage (50.19%) as compared to treatment without Cr. However, inoculation of earthworms to Cr-treated seedlings reduced the MDA content and electrolyte leakage by 15.41 and 10.22%, respectively, as compared with the Cr-stressed seedlings. MDA and electrolyte leakage showed maximum reduction by 52.77 and 36.48%, respectively, when inoculated with earthworms and M1M2 (**Figures 2C,D**). The results of *in situ* histochemical visualization of lipid peroxidation reagent and cell viability using Schiff's reagent and Evan's blue, respectively, in cotyledons of *B. juncea* are depicted in **Figures 3C,D**. Seedlings grown in Cr only showed a dark pink hue indicator of lipid peroxidation (**Figure 3C**), and a deep blue color signifies loss of cell viability (**Figure 3D**), which, on inoculation with earthworms and PGPR, showed a light staining pattern, indicating improved lipid peroxidation and cell viability. Membrane damage and damages were visualized *in situ* through a fluorescent microscope using PI and DAPI showing accumulation of red and blue color, as a measure of membrane and nuclear damage, respectively, in a concentration-dependent manner. The inoculation of earthworms alone or in the presence of PGPR led to appreciable lowering of red and blue color, which showed reduced membrane and nuclear damages. Earthworms and PGPR play an imperative role in mitigating Cr toxicity by lowering the MDA content and electrolyte leakage, which improved lipid peroxidation, prevented membrane and nuclear damages, and reinstated cell viability.

Effect of Earthworms and Plant-Growth-Promoting Rhizobacteria on Antioxidant Enzyme Activity of *Brassica juncea* Seedlings Under Chromium Stress

To assess the effect of earthworms and PGPR on various antioxidant enzymes, activities of various antioxidant enzymes were evaluated. **Table 2** shows that Cr treatment modulated the activities of these enzymes. The activities of SOD, POD, APOX, GPOX, DHAR, GR, and GST were enhanced by 70.16, 32.99, 41.49, 116.76, 88.99, 60.01, and 51.51% in *B. juncea* in response to Cr treatment, while the activity of CAT was found to be declined by 26.69% as compared to control. Inoculation of earthworms along with PGPR further enhanced the activities of SOD, POD, CAT, APOX, DHAR, GR, and GST in seedlings under Cr stress. However, a decline in GPOX activity was observed upon inoculation with PGPR and earthworms. The maximum increase in activities of SOD, POD, CAT, APOX, DHAR, GR, and GST was noticed in seedlings grown in Cr

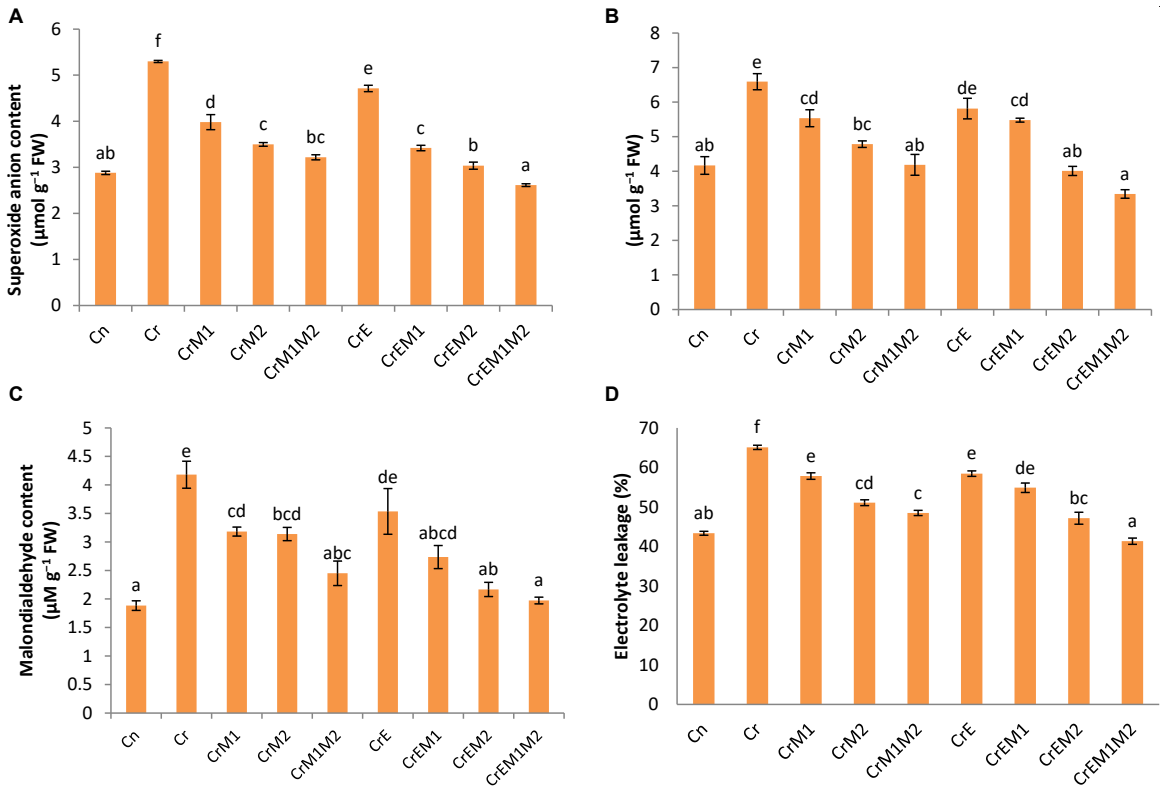

FIGURE 2 | Effect of PGPR [*Pseudomonas aeruginosa* (M1) & *Burkholderia gladioli* (M2)] and earthworms [*Eisenia fetida* (E)] on **(A)** superoxide anion, **(B)** hydrogenperoxide, **(C)** MDA content, and **(D)** electrolyte leakage in 10-day-old *B. juncea* seedlings, under chromium (Cr) stress. Data are presented as means of three independent replicates ± S.E (standard error). Different letters on the bar graphs indicate that mean values of the treatments are significantly different at $p \leq 0.05$ (Tukey's test).

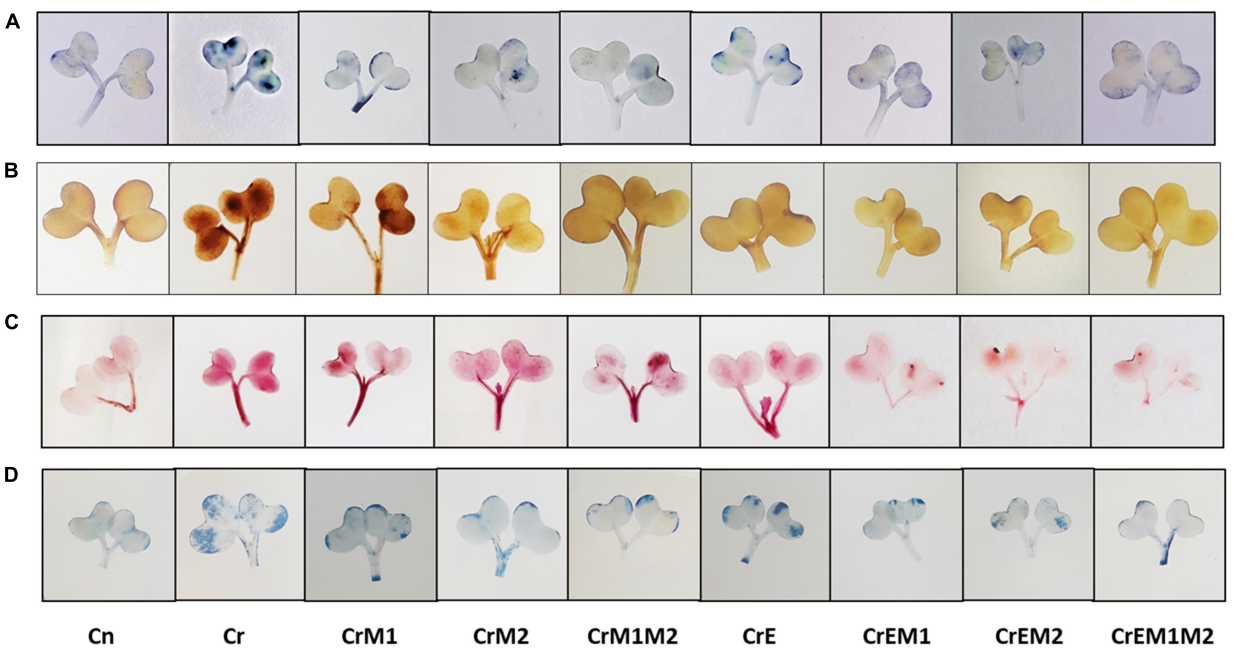

FIGURE 3 | *In vivo* imaging of **(A)** superoxide anion ($O_2\bullet^-$) stained with NBT, **(B)** hydrogen peroxide (H_2O_2) detected using DAB, **(C)** lipid peroxidation, asMDA content stained using Schiff's reagent, and **(D)** cell viability visualized using Evan's blue in *B. juncea* seedlings, under Cr stress.

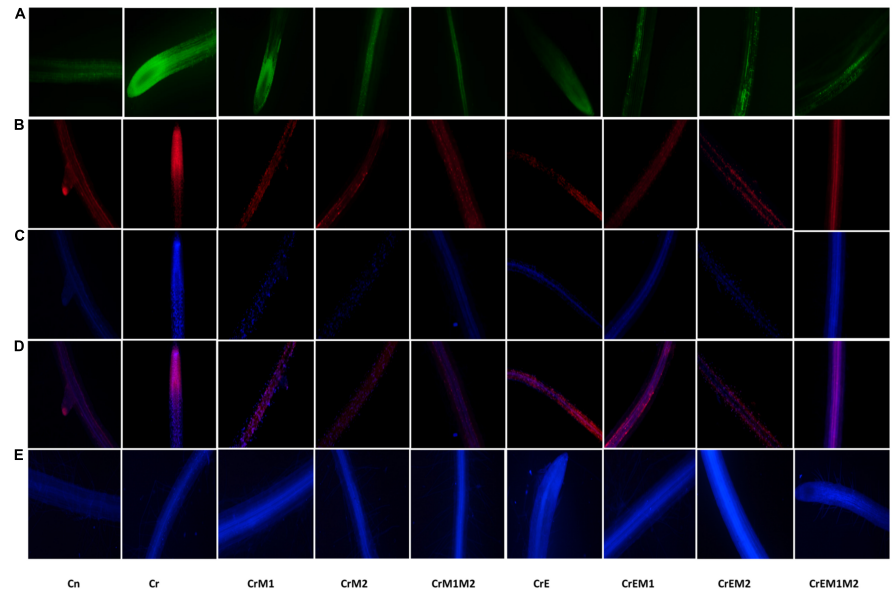

FIGURE 4 | *In vivo* fluorescence visualization of **(A)** hydrogen peroxide (H_2O_2) stained with DCF-DA, **(B)** membrane damage detected using PI, **(C)** nuclear damagemarked with DAPI, **(D)** composite of PI and DAPI, and **(E)** glutathione tagged with MCB.

TABLE 2 | Effect of PGPR [*Pseudomonas aeruginosa* (M1) & *Burkholderia gladioli* (M2)] and the earthworms [*Eisenia fetida* (E)] on the activity of SOD, POD, CAT, APOX, DHAR, GR,GPOX, GST in 10 day old *B. juncea* seedlings under chromium (Cr) toxicity.

Treatments	SOD	POD	CAT	APOX	DHAR	GR	GPOX	GST
Cn	11.17 ± 1.55^{a}	23.79 ± 1.02^{a}	24.94 ± 0.97^{a}	8.41 ± 0.95^{a}	6.14 ± 0.77^{a}	7.03 ± 0.11^{a}	12.04 ± 0.15^{a}	10.13 ± 0.43^{a}
Cr	19.01 ± 1.92^{b}	31.65 ± 1.11^{b}	18.28 ± 0.47^{ab}	11.90 ± 1.54^{a}	11.61 ± 0.84^{ab}	11.24 ± 0.39^{b}	26.10 ± 0.67^{e}	15.36 ± 1.04^{b}
CrM1	27.74 ± 1.77^{cd}	43.94 ± 1.06^{d}	25.88 ± 1.39^{cd}	19.99 ± 1.00^{b}	21.12 ± 1.11^{cd}	13.93 ± 0.54^{cd}	17.82 ± 0.52^{cd}	20.25 ± 0.98^{cd}
CrM2	29.69 ± 0.88^{cd}	45.27 ± 1.40^{de}	29.84 ± 1.36^{cd}	22.80 ± 1.11^{bc}	$23.49 \pm 1.08d^{e}$	16.31 ± 0.29^{e}	17.73 ± 0.57^{cd}	21.17 ± 0.62^{cd}
CrM1M2	33.62 ± 1.25^{e}	49.54 ± 1.98^{def}	32.46 ± 1.52^{ef}	26.04 ± 0.56^{c}	27.34 ± 1.42^{de}	15.95 ± 0.77^{de}	14.59 ± 0.62^{ab}	24.17 ± 0.39^{def}
CrE	26.15 ± 1.94^{bc}	39.28 ± 0.66^{c}	23.86 ± 0.98^{bc}	20.06 ± 0.92^{b}	15.34 ± 1.36^{bc}	12.73 ± 0.69^{bc}	20.26 ± 0.75^{d}	18.38 ± 0.52^{bc}
CrM1E	$3\,4.05 \pm 1.26^{de}$	46.20 ± 1.25^{def}	29.24 ± 0.93^{cde}	33.07 ± 1.24^{d}	24.87 ± 0.89^{ef}	16.24 ± 0.45^{e}	15.67 ± 0.3^{bc}	23.43 ± 0.65^{de}
CrM2E	38.93 ± 1.02^{ef}	49.89 ± 0.70^{ef}	34.12 ± 0.78^{ef}	35.46 ± 1.11^{de}	30.97 ± 1.69^{fg}	19.09 ± 0.25^{f}	12.13 ± 0.4^{a}	26.08 ± 1.30^{ef}
CrM1M2E	41.61 ± 1.29^{f}	51.74 ± 0.46^{f}	37.37 ± 0.65^{f}	38.35 ± 0.82^{e}	36.82 ± 1.30^{g}	16.53 ± 0.18^{e}	12.09 ± 0.20^{a}	28.02 ± 1.56^{f}

Data is presented as means of 3 replicates ± S.E (standard error). Different letters in the table indicate that mean values of the treatments are significantly different at ($p \leq 0.05$, Tukey's test).

stress supplemented with earthworms along with combined inoculation of M1M2 by 118.79, 63.48, 104.43, 222.23, 217.12, 69.80, and 82.45%, respectively, in comparison to the seedlings treated with Cr only. The activity of GPOX declined extremely by 82.46% with the supplementation of earthworms along with dual inoculation of M1M2.

Effect of Earthworms and Plant-Growth-Promoting Rhizobacteria on Total Antioxidant Capacity and Non-enzymatic Antioxidants of *Brassica juncea* Seedlings Under Chromium Stress

Total antioxidant content was enhanced under Cr stress. Concentration of water-soluble antioxidants was enhanced by 35.69% and that of lipid-soluble antioxidants got increased by 47.56% under Cr stress in comparison to control. The addition of earthworms to Cr-treated seedlings further enhanced the levels of water- and lipid-soluble antioxidants by 24.60 and 47.56%, respectively. M1 and M2 treatment along with earthworms further enhanced water- and lipid-soluble antioxidants by 128.11 and 143.03%, respectively, as compared to the seedlings grown in Cr only (**Figures 5A,B**). Non-enzymatic antioxidants like ascorbic acid and glutathione content were observed to be increased in Cr-stressed seedlings, and inoculation of earthworms and PGPR further boosted their activity. A tremendous increase of 21.4% in ascorbic acid content was observed in Cr stressed seedlings as compared to control, which was further promoted by 56.07% with earthworms and M2 treatment (**Figure 5C**). Glutathione content was increased by 24.09% under Cr stress relative to control seedlings. Amendment of Cr-stressed seedlings with earthworms and M2 enhanced the glutathione content

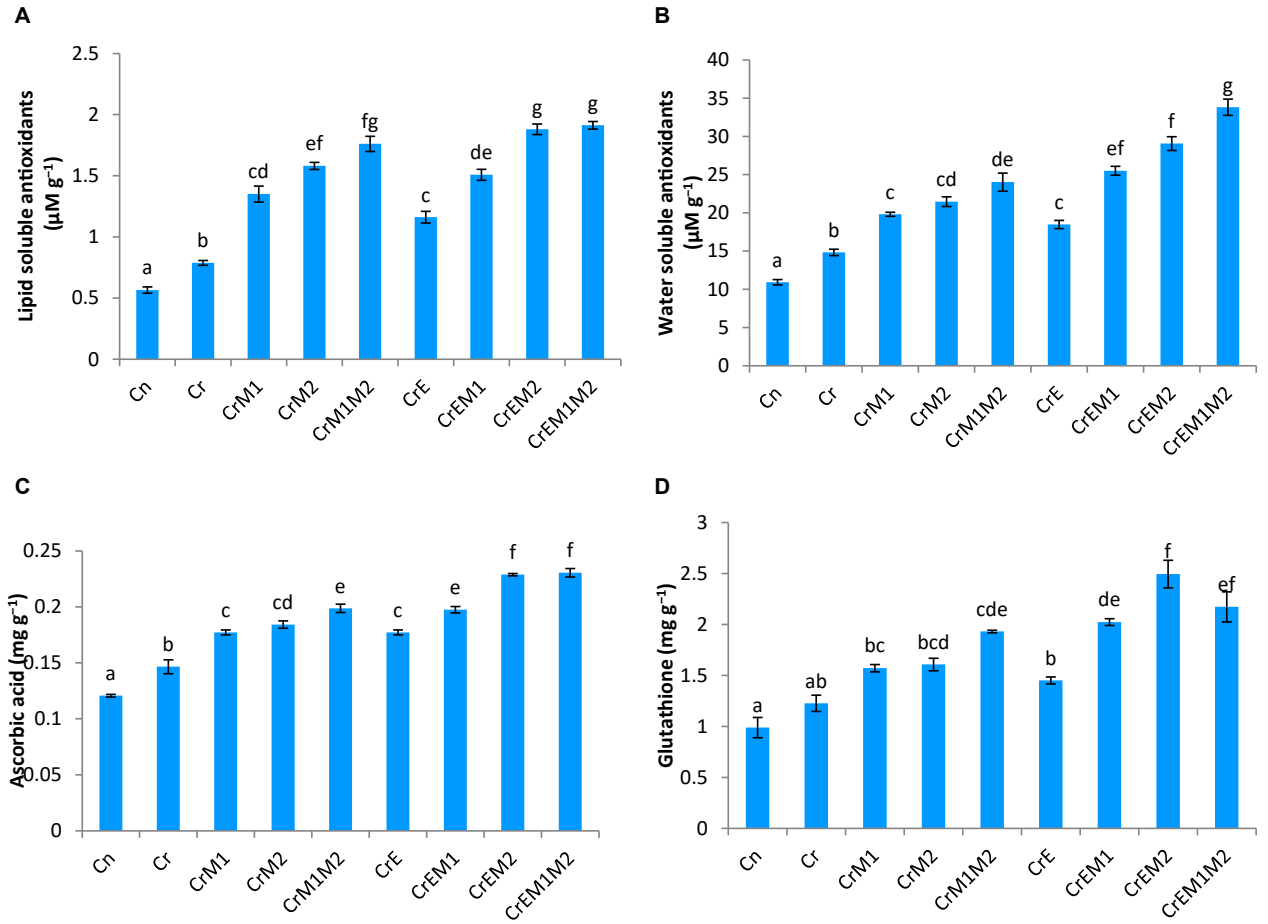

FIGURE 5 | Effect of PGPR [*Pseudomonas aeruginosa* (M1) & *Burkholderia gladioli* (M2)] and earthworms [*Eisenia fetida* (E)] on **(A)** lipid soluble antioxidants, **(B)** watersoluble antioxidants, **(C)** ascorbic acid, and **(D)** glutathione content in 10-day-old *B. juncea* seedlings, under chromium (Cr) toxicity. Data are presented as means of 3 independent replicates ± S.E (standard error). Different letters on the bar graphs indicate that mean values of the treatments are significantly different at $p \leq 0.05$ (Tukey's test).

by 103.28% (**Figure 5D**). Intracellular glutathione in root sections were tagged using non-fluorescent probe MCB. MCB binds with glutathione and other low molecular weight thiols to form a fluorescent blue conjugate, glutathione-S-bimane (GSB). Fluorescent microscopy suggested that roots of Cr-stressed seedlings showed an intensive blue color, which shows enhanced levels of glutathione as compared to the control (**Figure 4D**). The intensity of blue color was further enhanced in Cr-stressed seedlings inoculated with earthworms along with PGPR.

Effect of Earthworms and Plant-Growth-Promoting Rhizobacteria on Expression of Key Genes of Antioxidant Enzymes of *Brassica juncea* Seedlings Under Chromium Stress

The expression analysis of key genes of antioxidant enzymes, *viz.*, SOD, POD, CAT, APOX, DHAR, GR, and GST, at the transcript level was carried out in Cr-stressed *B. juncea* seedlings, which revealed the upregulation of these genes under Cr stress as compared to control. The reduction in CAT activity was noticed under Cr stress as compared to control. Supplementation of earthworms alone and along with PGPR (M1, M2 alone, and their binary combination, i.e., M1M2) enhanced the expression of the aforementioned enzymes in *B. juncea* seedlings grown under Cr stress as compared to Cr treatment only. The maximum augmentation in the expression of *SOD* (4.44– fold), *POD* (2.30-fold), *CAT* (3.79-fold), *APOX* (1.70-fold), *DHAR* (2.48-fold), *GR* (2.50-fold), and *GST* (3.67-fold) (**Figures 6A–G**) was observed in Cr-stressed seedlings treated with earthworms along with binary combination of M1 and M2, i.e., EM1M2 when compared to Cr-stressed seedlings only. Furthermore, upregulation of the RBOH1 (respiratory burst oxidase 1) gene in Cr-stressed *B. juncea* seedlings was noticed in comparison to control. Maximum reduction of 0.185-fold in the expression of RBOH1 was noticed with the addition of earthworms along with M1M2, i.e., EM1M2 in Cr-stressed *B. juncea* seedlings in comparison to Cr stress only (**Figure 6H**).

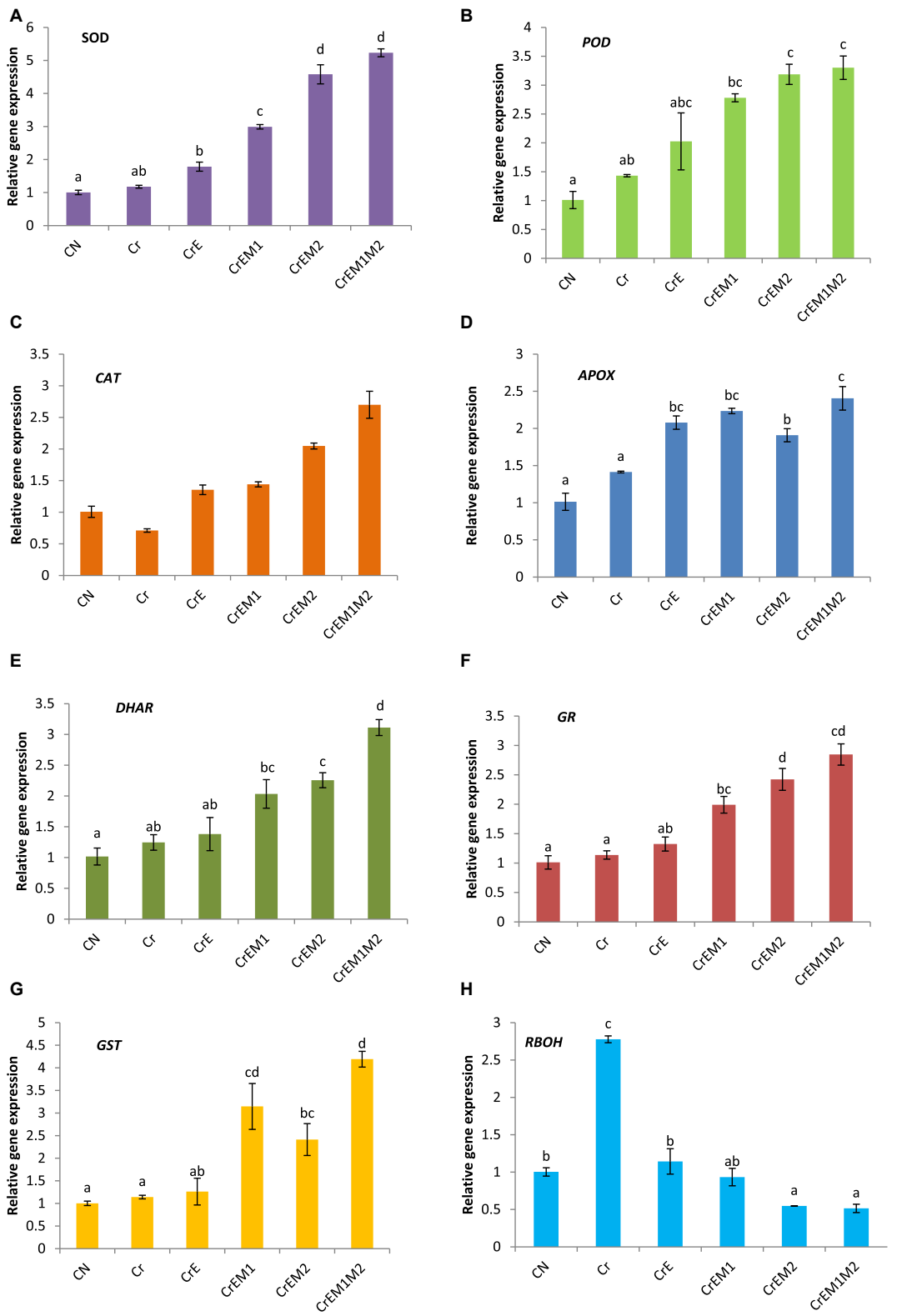

FIGURE 6 | Effect of PGPR [*Pseudomonas aeruginosa* (M1) & *Burkholderia gladioli* (M2)] and earthworms [*Eisenia fetida* (E)] on the gene expression of **(A)** SOD, **(B)** POD, **(C)** CAT, **(D)** APOX, **(E)** DHAR, **(F)** GR, **(G)** GST, and **(H)** RBOH in 10-day-old *B. juncea* seedlings, under chromium (Cr) stress. Data are presented as means of 3 independent replicates ± S.E (standard error). Different letters on the bar graphs indicate that mean values of the treatments are significantly different at $p \leq 0.05$ (Tukey's test).

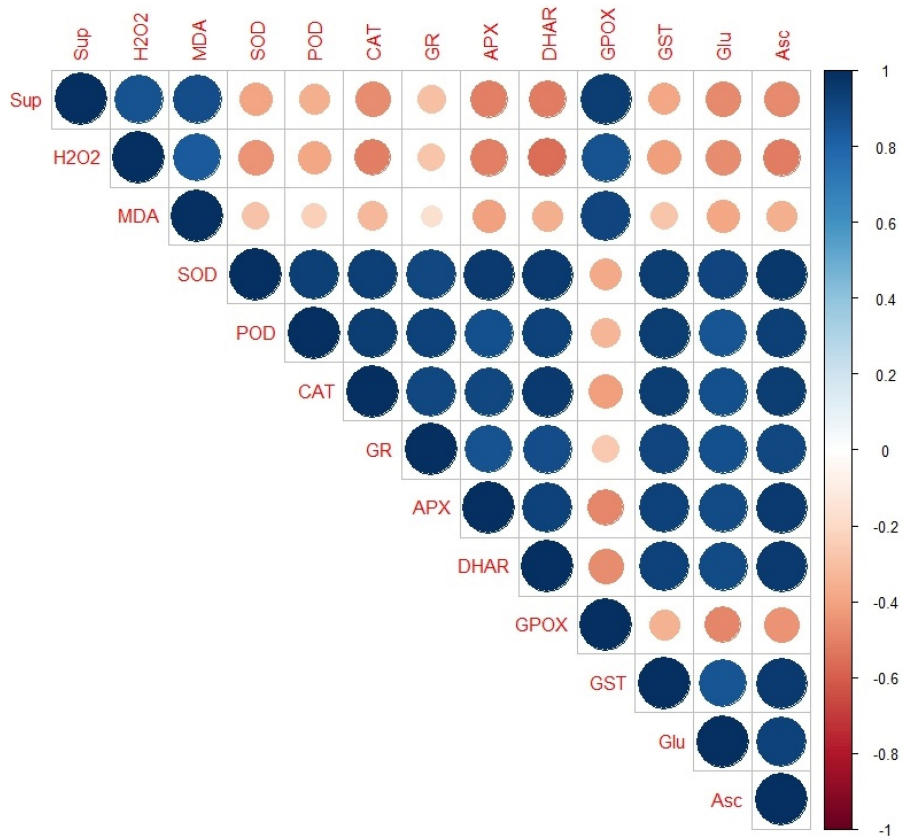

FIGURE 7 | Corr-plot representing the Pearson's correlation analysis between the oxidative stress markers and oxidative defence molecules (enzymatic andnon-enzymatic). Here, the size of the circles is proportional to the absolute value of correlation coefficients, whereas their colour represents the value in positive or negative correlation region as represented in the right bar of varying colour intensities from intense blue to intense red, ranging from +1 to −1, respectively. Sup, superoxide anion; H_2O_2,hydrogen peroxide; MDA, malondialdehyde; SOD, superoxide dismutase; POD, guaiacol peroxidase; CAT, catalase; GR, glutathione reductase; APX/APOX, ascorbate peroxidase; DHAR, dehydroascorbate reductase; GPOX, glutathione peroxidase; GST, glutathione-S-transferase; Glu, glutathione; and Asc, ascorbic acid.

Correlation Analysis

The Corr plot was made (**Figure 7**) using based on Pearson's correlation analysis between the oxidative stress markers and oxidative defense molecules (both enzymatic and non-enzymatic). It was found that except GPOX, all the antioxidant enzymes (SOD, POD, CAT, GR, APX/APOX, DHAR, GPOX, and GST) and the non-enzymatic antioxidants (Glu and Asc) had a strong positive correlation among themselves but a week negative correlation with the two ROS species, i.e., superoxide anion and H_2O_2 and the MDA content.

DISCUSSION

Plants imperiled to heavy metal stress have harmful effects on various metabolic processes due to generation of ROS resulting in reduced plant biomass, production, and yield. Disproportionate generation of ROS has deleterious effects on various cellular components, which affect the cellular integrity, leading to cell death (Askari et al., 2021). Cr stress has damaging effect on plant biomass and augments the production of ROS that hinders the function of the plant (Qureshi et al., 2020). Soil micro- and macroorganisms can be reconnoitered as plant growth promoters to diminish the adverse effect of Cr stress *via* the modulation of enzymatic and non-enzymatic antioxidants. The present study demonstrated the efficacy of PGPR and earthworms in ameliorating Cr-induced oxidative damage in *B. juncea* seedlings *via* production of enzymatic and non-enzymatic antioxidant molecules. In the present investigation, Cr stress significantly affected the bio-mass of *B. juncea* seedlings as indicated by reduction in fresh and dry weights of seedlings (**Figures 1A,B**). Cr toxicity has also been shown to reduce biomass in *B. juncea* (Mahmud et al., 2017), *S. seban* (Din et al., 2020), tomato, and brinjal (Singh and Prasad, 2019). The reduction in biomass in Cr-stressed seedlings could be attributed to the excessive production of ROS (**Figures 2A,B**) and reduced water and nutrient uptake. According to several studies, PGPR enhances the nutrient uptake and secrete various plant-growth-promoting metabolites in the rhizosphere, which aid in iron and phosphate solubilization. Furthermore, they may also release phytohormones, which restore plant growth and biomass in stressed conditions

(Cai et al., 2019; Shreya et al., 2020). Earthworms promote plant growth by improving soil structure and enhancing the nutrient availability and microbial activity in rhizosphere (Kaur et al., 2017). The growth-promoting role of earthworms has been reported by Jusselme et al. (2012). Concomitantly, Gupta et al. (2020) documented that *Enterobacter* sp. and *Klebsiella* sp. improved the biomass of tomato plant under Cr stress. Our results indicated that inoculation of PGPR and earthworms to the stressed seedlings considerably improved the fresh and dry weights of the seedlings.

Implication of Cr causes the excessive generation of ROS due to altered redox status and antioxidant defense system leading to the cellular condition considered as oxidative stress. Overgeneration of ROS damages the cellular macromolecules, which results in lipid peroxidation destroying membrane integrity and causing cell death (Sharma et al., 2019; Singh and Prasad, 2019). In the present study, the Cr-induced oxidative stress was revealed as the overproduction of $O_2\bullet^-$ and H_2O_2 in *B. juncea* seedlings, which is evident from their concentration at cellular levels (**Figures 2A,B**) and results from histochemical studies (**Figures 3A,B**, **4A**), which is also in agreement with the biochemical data. The present study also revealed the upregulation of respiratory burst oxidase homolog gene in Cr-stressed plants as compared to control (**Figure 6H**). In plants, ROS bursts take place through NADPH oxidase/respiratory burst oxidase homolog (RBOH 1) proteins [responsible for superoxide generation) under various abiotic stress conditions (Kaur et al., 2014; Chapman et al., 2019)]. A sudden increase in ROS accumulation was also observed previously by Handa et al. (2018) in *B. juncea* seedlings grown under Cr stress. The results of the present study revealed the synergistic interactions of earthworms with both PGPR in successfully ameliorating oxidative stress in *B. juncea* seedlings under Cr stress. However, supplementation of both M1 and M2 along with earthworms significantly abridged ROS accumulation by downregulating the expression of gene for ROS production (*RBOH1* for $O_2\bullet^-$ production). Our results are in alliance with Wang et al. (2020) who showed that *Sphingomonas* SaMR12 inoculation to *B. juncea* under Cd stress lowered $O_2\bullet^-$ and H_2O_2 content. Cr application to *B. juncea* seedlings also escalated the accumulation MDA (**Figure 2C**), which is produced as a result of peroxidation of membrane lipids and prominent indicator of membrane damage due to oxidative stress. MDA damages cell by reacting with free amino groups and disrupting inter- and intramolecular cross-linkages of proteins (Islam et al., 2016). The elevated levels of MDA have also been reported in *Arabidopsis thaliana*, *Zea mays*, and *Brassica napus* under Cr stress (Afshan et al., 2015; Anjum et al., 2017; Ding et al., 2019). Histochemical data of ROS and their concomitant damage to lipids and membranes depicted that Cr toxicity elevated their content in seedlings (**Figure 3C**). The magnitude of membrane and nuclear damages caused due to Cr toxicity in *B. juncea* roots was also corroborated using fluorescence microscopy (**Figures 4B,C**). Decreased lipid peroxidation was documented upon the inoculation of *Klebsiella* sp. and *Enterobacter* sp. to *Helianthus annuus* exposed to Cr stress (Gupta et al., 2020). The reduced level of MDA observed upon inoculation with PGPR might owe to altered antioxidant defense system of the plants (Janmohammadi et al., 2013). Concurrently, supplementation of *E. fetida* to Cd-stressed *B. juncea* seedlings lowered the $O_2\bullet^-$, H_2O_2, and MDA level (Kaur et al., 2019). Lipid peroxidation also aggravates electrolyte leakage in Cr-stressed *B. juncea* seedlings (**Figure 2D**) leading to reduced cell viability (**Figure 3D**) and enhanced membrane and nuclear damage (**Figures 4B,C**). Our findings are in line with several researchers who reported increase in electrolyte leakage in *O. sativa* (Sing and Shah, 2014), sunflower (Farid et al., 2017), and *S. sesban* (Din et al., 2020). However, the application of PGPR and earthworms reduced ROS accumulation, MDA content, and electrolyte leakage supporting the seedlings under Cr-stressed conditions. Therefore, the co-inoculation with PGPR and earthworms signifies their role in regulating cellular homeostasis and improving the membrane integrity under Cr stress.

In order to accomplish vital metabolic functions of cells, plants possessing a natural well-developed defense system known as ascorbate-glutathione (AsA-GSH) pathway, which takes place in various subcellular organelles, comprising of enzymatic and non-enzymatic antioxidants, is of prime importance that plays crucial role in combating the oxidative stress. The modulation in activities of enzymatic antioxidants might be concomitant to overcome the wrong doings of ROS and persuade tolerance to stressed plants (Hasanuzzaman et al., 2019). Our results revealed Cr stress altered the activities of antioxidant enzymes of *B. juncea* seedlings. Cr exposure enhanced the activities of SOD, POD, APX, GPOX, GR, DHAR, and GST but inhibited the activity of CAT (**Table 2**). The reduction in CAT activity might be due to excessive ROS accumulation, intrusion with the subunits, or altered synthesis (Bakshi et al., 2021). A similar decrease in CAT activity was observed in *Oryza sativa* (Ma et al., 2016), *B. juncea* (Mahmud et al., 2017), and *Zea mays* (Islam et al., 2016). Supplementation of earthworms and M1 and M2, alone and in amalgamation with earthworms to Cr-stressed seedlings, upregulated the activities of SOD, CAT, POD, APX, GR, DHAR, and GST except GPOX. Enhanced activity of SOD was concomitant with reduced $O_2\bullet^-$ content as the conversion of $O_2\bullet^-$ to H_2O_2 is controlled by SOD (Kaur et al., 2019). Elevated activity of POD was observed in Cr stress seedlings augmented with earthworms and PGPR, a result similar to that reported by Kaur et al. (2019) and Khanna et al. (2019). In addition, reduction in H_2O_2 content following the rhizospheric amendments of *B. juncea* seedlings with earthworms and PGPR alone and in combination under Cr stress was probably due to detoxification of H_2O_2 by CAT, POD, and APOX. Enhancement in the activities of CAT, POD, and APOX in the present study is because of the fact that these enzymes convert H_2O_2 to H_2O and O_2 and play an important role in the management of oxidative stress. Decline in GPOX activity observed upon inoculation of earthworms, M1, and M2 can be due to the involvement of CAT and APOX in scavenging H_2O_2, as APOX has higher affinity for H_2O_2 as compared to CAT and POD (Gill and Tuteja, 2010). Enhanced activities of GR and DHAR were also observed in inoculated Cr-treated

seedlings. It is a potential enzyme of the ASH-GSH cycle and plays an essential role in the defense system against ROS by sustaining the reduced status of GSH. GR is also involved in the ascorbate–glutathione pathway. GR maintains the GSH/GSSH ratios by converting GSSH into GSH *via* NADPH (Noctor and Foyer, 1998). GST plays an imperative role in detoxification of heavy metals (Ghelfi et al., 2011) and catalyzes the conjugation of toxic substrates with the tripeptide glutathione (Gill et al., 2013). Similar findings were reported by Saleem et al. (2018) who found that the *Pseudomonas fluorescens* enhanced the activities of APX, SOD, CAT, and GR in sunflower grown in soils contaminated with lead. Enhanced activities of SOD, POD, and CAT were noticed in *Sesbania sesban* plant inoculated with *Bacillus xiamenensis* grown in Cr-contaminated soils (Din et al., 2020). Similarly, augmented activities of APX, CAT, POD, and SOD were observed in *Capsicum annum* seedlings inoculated with *Bradyrhizobium japonicum* under Cr^{6+} stress (Nemat et al., 2020). The expression studies of the genes for SOD, POD, CAT, APOX, GR, and DHAR in the inoculated Cr-treated seedlings are concomitant to upregulated expression of these genes at transcript levels as depicted by gene expression analysis using qRT-PCR. Inoculation of earthworms and PGPR leads to the increase in the activities of antioxidant enzymes, suggesting the affirmative attribute toward ROS detoxification and improving the ability of plants to cope up with metal stress situations.

The non-enzymatic antioxidants of AsA-GSH pathway, i.e., ascorbic acid and glutathione, are important redox buffering mediators of cell, which regularize oxidative stress by quenching ROS and conserve the redox status of the cell (Noctor et al., 2018). Moreover, ascorbic acid and glutathione are also involved in governing several developmental functions like pollen growth, cell division and differentiation, phytohormones homeostasis, etc. (Noctor et al., 2012; Potter et al., 2012). The findings of the present study showed the elevated level of ascorbic acid glutathione in Cr-treated seedlings, which is similar to the results observed in *O. sativa* (Chen et al., 2017), *B. napus* (Ulhassan et al., 2019), *Z. mays* (Adhikari et al., 2020) under Cr stress. Moreover, addition of earthworms and PGPR alone or in combination significantly upregulated the ascorbic acid and glutathione content. The results of the present study are in alliance with the findings of Gomes et al. (2013) and Islam et al. (2014), which also reported the enhancement of ascorbic acid upon strain inoculation under metal stress conditions. Fluorescent tagging of glutathione in *B. juncea* roots (**Figure 4E**) also depicted an increase in glutathione content upon treatment with earthworms and PGPR. Furthermore, upon addition of earthworms and M2, the most significant rise was observed. Significant augmentation in ascorbic acid and glutathione content upon inoculation of earthworms and PGPR in Cr-treated seedlings induces reduced environment in the cell, which is necessary for the survival of cell and thus assists in scavenging of ROS (Singh and Prasad, 2019). Hence, the upregulation of AsA-GSH pathway upon inoculation of earthworms and PGPR can be considered a key strategy for mitigating Cr toxicity.

CONCLUSION AND FUTURE PROSPECTS

It was concluded from the present investigation that *B. juncea* seedlings manifest reduction in biomass under Cr stress. Cr stress causes oxidative damage due to enhanced accumulation of ROS, leading to lipid peroxidation, membrane damage, and cell injury. However, the positive association of earthworms and PGPR is helpful in mitigation of Cr-induced oxidative stress in *B. juncea* seedlings. PGPR and earthworms alleviate the Cr-induced oxidative stress by modulating the activities of antioxidant enzymes and the non-enzymatic antioxidants accompanied by the decreased ROS accumulation and lipid peroxidation and improved cellular viability, thereby facilitating the seedlings to survive better under Cr stress. The present investigation provided insights into the understanding of the stress-ameliorative properties of the combined treatments of selected PGPR and earthworms by studies at three different levels. The data obtained from the bio-chemical studies, histochemical studies, and the studies of the expression of key antioxidant enzyme genes provided a holistic picture of the stress amelioration process mediated by the combined treatment of PGPR and earthworms. It will help the researchers to design-suitable strategies to enhance plant growth and productivity in the heavy-metal-affected soils. Therefore, the adoption of such techniques after optimization with the type of crop plants and the level of heavy metal stress may help in improving productivity on farm scale under the heavy-metal-affected environments. Furthermore, the identification of key players in the stress amelioration process may help in designing genetically engineered plant better suited for the high productivity under Cr stress or in designing micro- and macroorganism assisted phytoremediation of Cr polluted soils by *B. juncea*.

DATA AVAILABILITY STATEMENT

The original contributions presented in the study are included in the article/supplementary material, further inquiries can be directed to the corresponding author/s.

AUTHOR CONTRIBUTIONS

RB, SG, and AS designed the experiments. PS, PB, and RC performed the experiments and analyzed the data. PS and RK wrote the manuscript. RK and AS reviewed and edited the manuscript. All authors contributed to the article and approved the submitted version.

ACKNOWLEDGMENTS

We express sincere thanks to the Department of Science and Technology (DST), New Delhi, for financial support under Scheme of Young Scientist and Technologist (SYST; SP/YO/099/2017).

REFERENCES

Abd El, F. E., and Bashandy, S. R. (2019). Dose-dependent effects of *Pseudomonas* trivialis rhizobacteria and synergistic growth stimulation effect with earthworms on the common radish. *Rhizosphere* 10:100156.

Adhikari, A., Adhikari, S., Ghosh, S., Azahar, I., Shaw, A. K., Roy, D., et al. (2020). Imbalance of redox homeostasis and antioxidant defense status in maize under chromium (VI) stress. *Environ. Exp. Bot.* 169:103873. doi: 10.1016/j.envexpbot.2019.103873

Aebi, H. (1984). Catalase in vitro. *Methods Enzymol.* 105, 121–126. doi: 10.1016/s0076-6879(84)05016-3

Afshan, S., Ali, S., Bharwana, S. A., Rizwan, M., Farid, M., Abbas, F., et al. (2015). Citric acid enhances the phytoextraction of chromium, plant growth, and photosynthesis by alleviating the oxidative damages in *Brassica napus* L. *Environ. Sci. Pollut. Res.* 22, 11679–11689. doi: 10.1007/s11356-015-4396-8

Ahmad, I., Akhtar, M. J., Asghar, H. N., Ghafoor, U., and Shahid, M. (2016). Differential effects of plant growth-promoting rhizobacteria on maize growth and cadmium uptake. *J. Plant Growth Regulat.* 35, 303–315.

Akhtar, N., Ilyas, N., Yasmin, H., Sayyed, R. Z., Hasnain, Z., Elsayed, E., et al. (2021). Role of *Bacillus cereus* in improving the growth and phytoextractability of *Brassica nigra* (L.) K. koch in chromium contaminated soil. *Molecules* 26:1569. doi: 10.3390/molecules26061569

Ali, S., Chaudhary, A., Rizwan, M., Anwar, H. T., Adrees, M., Farid, M., et al. (2015). Alleviation of chromium toxicity by glycinebetaine is related to elevated antioxidant enzymes and suppressed chromium uptake and oxidative stress in wheat (*Triticum aestivum* L.). *Environ. Sci. Pollut. Res.* 22, 10669–10678. doi: 10.1007/s11356-015-4193-4

Anjum, S. A., Ashraf, U., Imran, K. H. A. N., Tanveer, M., Shahid, M., Shakoor, A., et al. (2017). Phyto-toxicity of chromium in maize: oxidative damage, osmolyte accumulation, anti-oxidative defense and chromium uptake. *Pedosphere* 27, 262–273. doi: 10.1016/s1002-0160(17)60315-1

Apel, K., and Hirt, H. (2004). Reactive oxygen species: metabolism, oxidative stress, and signal transduction. *Annu. Rev. Plant Biol.* 55, 373–399. doi: 10.1146/annurev.arplant.55.031903.141701

Ashger, M., Per, T. S., Verma, S., Pandith, S. A., Masood, A., and Khan, N. A. (2018). Ethylene supplementation increases PSII efficiency and alleviates chromium-inhibited photosynthesis through increased nitrogen and sulfur assimilation in mustard. *J. Plant Growth Regulat.* 37, 1300–1317.

Ashraf, M. A., Rasheed, R., Zafar, S., Iqbal, M., and Saqib, Z. A. (2021). Menadione sodium bisulfite neutralizes chromium phytotoxic effects in okra by regulating cytosolutes, lipid peroxidation, antioxidant system and metal uptake. *Int. J. Phytoremed.* 23, 736–746. doi: 10.1080/15226514.2020.1854171

Askari, S. H., Ashraf, M. A., Ali, S., Rizwan, M., and Rasheed, R. (2021). Menadione sodium bisulfite alleviated chromium effects on wheat by regulating oxidative defense, chromium speciation, and ion homeostasis. *Environ. Sci. Pollut. Res.* 28, 1–21. doi: 10.1007/s11356-021-13221-0

Augustynowicz, J., Grosicki, M., Hanus-Fajerska, E., Lekka, M., Waloszek, A., and Kołoczek, H. (2010). Chromium (VI) bioremediation by aquatic macrophyte callitriche cophocarpa sendtn. *Chemosphere* 79, 1077–1083. doi: 10.1016/j.chemosphere.2010.03.019

Awasthi, P., Mahajan, V., Rather, I. A., Gupta, A. P., Rasool, S., Bedi, Y. S., et al. (2015). Plant omics: isolation, identification, and expression analysis of cytochrome P450 gene sequences from coleus forskohlii. *OMICS J. Integrat. Biol.* 19, 782–792. doi: 10.1089/omi.2015.0148

Bakshi, P., Chouhan, R., Sharma, P., Mir, B. A., Gandhi, S. G., Landi, M., et al. (2021). Amelioration of chlorpyrifos-induced toxicity in *Brassica juncea* L. by combination of 24-epibrassinolide and plant-growth-promoting rhizobacteria. *Biomolecules* 11:877. doi: 10.3390/biom11060877

Bhuiyan, M. S. U., Min, S. R., Jeong, W. J., Sultana, S., Choi, K. S., Song, W. Y., et al. (2011). Overexpression of a yeast cadmium factor 1 (YCF1) enhances heavy metal tolerance and accumulation in *Brassica juncea*. *Plant Cell Tissue Organ Culture* 105, 85–91.

Blouin, M., Zuily-Fodil, Y., Pham-Thi, A. T., Laffray, D., Reversat, G., Pando, A., et al. (2005). Belowground organism activities affect plant aboveground phenotype, inducing plant tolerance to parasites. *Ecol. Lett.* 8, 202–208.

Bradford, M. M. (1976). A rapid and sensitive method for the quantitation of microgram quantities of protein utilizing the principle of protein-dye binding. *Analy. Biochem.* 72, 248–254. doi: 10.1006/abio.1976.9999

Brown, G. G., Barois, I., and Lavelle, P. (2000). Regulation of soil organic matter dynamics and microbial activity in the drilosphere and the role of interactions with other edaphic functional domains. *Eur. J. Soil Biol.* 36, 177–198.

Cai, M., Hu, C., Wang, X., Zhao, Y., Jia, W., Sun, X., et al. (2019). Selenium induces changes of rhizosphere bacterial characteristics and enzyme activities affecting chromium/selenium uptake by pak choi (*Brassica campestris* l. ssp. chinensis makino) in chromium contaminated soil. *Environ. Pollut.* 249, 716–727. doi: 10.1016/j.envpol.2019.03.079

Callard, D., Axelos, M., and Mazzolini, L. (1996). Novel molecular markers for late phases of the growth cycle of *Arabidopsis thaliana* cell-suspension cultures are expressed during organ senescence. *Plant Physiol.* 112, 705–715. doi: 10.1104/pp.112.2.705

Carlberg, I. N., and Mannervik, B. E. (1975). Purification and characterization of the flavoenzyme glutathione reductase from rat liver. *J. Biol. Chem.* 250, 5475–5480.

Chapman, J. M., Muhlemann, J. K., Gayomba, S. R., and Muday, G. K. (2019). RBOH-dependent ROS synthesis and ROS scavenging by plant specialized metabolites to modulate plant development and stress responses. *Chem. Res. Toxicol.* 32, 370–396. doi: 10.1021/acs.chemrestox.9b00028

Chen, Q., Zhang, X., Liu, Y., Wei, J., Shen, W., Shen, Z., et al. (2017). Hemin-mediated alleviation of zinc, lead and chromium toxicity is associated with elevated photosynthesis, antioxidative capacity; suppressed metal uptake and oxidative stress in rice seedlings. *Plant Growth Regul.* 81, 253–264.

Dalton, D. A., Russell, S. A., Hanus, F. J., Pascoe, G. A., and Evans, H. J. (1986). Enzymatic reactions of ascorbate and glutathione that prevent peroxide damage in soybean root nodules. *Proc. Natl. Acad. Sci. U.S.A.* 83, 3811–3815. doi: 10.1073/pnas.83.11.3811

De la Fuente Cantó, C., Simonin, M., King, E., Moulin, L., Bennett, M. J., Castrillo, G., et al. (2020). An extended root phenotype: the rhizosphere, its formation and impacts on plant fitness. *Plant J.* 103, 951–964. doi: 10.1111/tpj.14781

Demidchik, V. (2015). Mechanisms of oxidative stress in plants: from classical chemistry to cell biology. *Environ. Exp. Bot.* 109, 212–228.

Din, B. U., Rafique, M., Javed, M. T., Kamran, M. A., Mehmood, S., Khan, M., et al. (2020). Assisted phytoremediation of chromium spiked soils by sesbania sesban in association with *Bacillus xiamenensis* PM14: a biochemical analysis. *Plant Physiol. Biochem.* 146, 249–258. doi: 10.1016/j.plaphy.2019.11.010

Ding, G., Jin, Z., Han, Y., Sun, P., Li, G., and Li, W. (2019). Mitigation of chromium toxicity in *Arabidopsis thaliana* by sulfur supplementation. *Ecotoxicol. Environ. Safety* 182:109379. doi: 10.1016/j.ecoenv.2019.109379

Dixit, V., Pandey, V., and Shyam, R. (2002). Chromium ions inactivate electron transport and enhance superoxide generation in vivo in pea (*Pisum sativum* L. cv. azad) root mitochondria. *Plant Cell Environ.* 25, 687–693.

Elmer, W. H. (2009). Influence of earthworm activity on soil microbes and soilborne diseases of vegetables. *Plant Dis.* 93, 175–179. doi: 10.1094/PDIS-93-2-0175

Etesami, H., and Beattie, G. A. (2017). Mining halophytes for plant growth-promoting halotolerant bacteria to enhance the salinity tolerance of non-halophytic crops. *Front. Microbiol.* 9:148. doi: 10.3389/fmicb.2018.00148

Etesami, H., and Maheshwari, D. K. (2018). Use of plant growth promoting rhizobacteria (PGPRs) with multiple plant growth promoting traits in stress agriculture: action mechanisms and future prospects. *Ecotoxicol. Environ. Safety* 156, 225–246. doi: 10.1016/j.ecoenv.2018.03.013

Farid, M., Ali, S., Rizwan, M., Ali, Q., Abbas, F., Bukhari, S. A. H., et al. (2017). Citric acid assisted phytoextraction of chromium by sunflower; morpho-physiological and biochemical alterations in plants. *Ecotoxicol. Environ. Safety* 145, 90–102. doi: 10.1016/j.ecoenv.2017.07.016

Flohé, L., and Günzler, W. A. (1984). [12] assays of glutathione peroxidase. *Methods Enzymol.* 105, 114–120.

Frahry, G., and Schopfer, P. (2001). NADH-stimulated, cyanide-resistant superoxide production in maize coleoptiles analyzed with a tetrazolium-based assay. *Planta* 212, 175–183. doi: 10.1007/s004250000376

Fricker, M. D., and Mayer, A. J. (2001). Confocal imaging of metabolism in vivo: pitfalls and possibilities. *J. Exp. Bot.* 52, 631–640.

Ganesh, K. S., Baskaran, L., Chidambaram, A., and Sundaramoorthy, P. (2009). Influence of chromium stress on proline accumulation in soybean (*Glycine max* L. merr.) genotypes. *Global J. Environ. Res.* 3, 106–108.

Gangwar, S., Singh, V. P., Srivastava, P. K., and Maurya, J. N. (2011). Modification of chromium (VI) phytotoxicity by exogenous gibberellic acid application in *Pisum sativum* (L.) seedlings. *Acta Physiol. Plantarum* 33, 1385–1397.

Ghelfi, A., Gaziola, S. A., Cia, M. C., Chabregas, S. M., Falco, M. C., Kuser-Falcão, P. R., et al. (2011). Cloning, expression, molecular modelling and docking analysis of glutathione transferase from Saccharum officinarum. *Ann. Appl. Biol.* 159, 267–280.

Gill, R. A., Zang, L., Ali, B., Farooq, M. A., Cui, P., Yang, S., et al. (2015). Chromium-induced physio-chemical and ultrastructural changes in four cultivars of *Brassica napus* L. *Chemosphere* 120, 154–164. doi: 10.1016/j.chemosphere.2014.06.029

Gill, R. A., Zhang, N., Ali, B., Farooq, M. A., Xu, J., Gill, M. B., et al. (2016). Role of exogenous salicylic acid in regulating physio-morphic and molecular changes under chromium toxicity in black-and yellow-seeded *Brassica napus* L. *Environ. Sci. Pollut. Res.* 23, 20483–20496. doi: 10.1007/s11356-016-7167-2

Gill, S. S., Anjum, N. A., Hasanuzzaman, M., Gill, R., Trivedi, D. K., Ahmad, I., et al. (2013). Glutathione and glutathione reductase: a boon in disguise for plant abiotic stress defense operations. *Plant Physiol. Biochem.* 70, 204–212. doi: 10.1016/j.plaphy.2013.05.032

Gill, S. S., and Tuteja, N. (2010). Reactive oxygen species and antioxidant machinery in abiotic stress tolerance in crop plants. *Plant Physiol. Biochem.* 48, 909–930. doi: 10.1016/j.plaphy.2010.08.016

Gomes, M. P., Duarte, D. M., Carneiro, M., Barreto, L. C., Carvalho, M., Soares, A. M., et al. (2013). Zinc tolerance modulation in *Myracrodruon urundeuva* plants. *Plant Physiol. Biochem.* 67, 1–6. doi: 10.1016/j.plaphy.2013.02.018

Gray, E. J., and Smith, D. L. (2005). Intracellular and extracellular PGPR: commonalities and distinctions in the plant-bacterium signaling processes. *Soil Biol. Biochem.* 37, 395–412.

Gupta, P., Kumar, V., Usmani, Z., Rani, R., Chandra, A., and Gupta, V. K. (2020). Implications of plant growth promoting klebsiella sp. CPSB4 and *Enterobacter* sp. CPSB49 in luxuriant growth of tomato plants under chromium stress. *Chemosphere* 240:124944. doi: 10.1016/j.chemosphere.2019.124944

Gutiérrez-Alcalá, G., Gotor, C., Meyer, A. J., Fricker, M., Vega, J. M., and Romero, L. C. (2000). Glutathione biosynthesis in *Arabidopsis trichome* cells. *Proc. Natl. Acad. Sci. U.S.A.* 97, 11108–11113.

Habiba, U., Ali, S., Rizwan, M., Ibrahim, M., Hussain, A., Shahid, M. R., et al. (2019). Alleviative role of exogenously applied mannitol in maize cultivars differing in chromium stress tolerance. *Environ. Sci. Pollut. Res.* 26, 5111–5121. doi: 10.1007/s11356-018-3970-2

Habig, W. H., Pabst, M. J., and Jakoby, W. B. (1974). Glutathione S-transferases: the first enzymatic step in mercapturic acid formation. *J. Biol. Chem.* 249, 7130–7139.

Handa, N., Kohli, S. K., Sharma, A., Thukral, A. K., Bhardwaj, R., Alyemeni, M. N., et al. (2018). Selenium ameliorates chromium toxicity through modifications in pigment system, antioxidative capacity, osmotic system, and metal chelators in *Brassica juncea* seedlings. *South Afr. J. Bot.* 119, 1–10.

Hasanuzzaman, M., Bhuyan, M. H. M., Anee, T. I., Parvin, K., Nahar, K., Mahmud, J. A., et al. (2019). Regulation of ascorbate-glutathione pathway in mitigating oxidative damage in plants under abiotic stress. *Antioxidants* 8:384. doi: 10.3390/antiox8090384

Heath, R. L., and Packer, L. (1968). Photoperoxidation in isolated chloroplasts: I. kinetics and stoichiometry of fatty acid peroxidation. *Arch. Biochem. Biophys.* 125, 189–198. doi: 10.1016/0003-9861(68)90654-1

Holländer-Czytko, H., Grabowski, J., Sandorf, I., Weckermann, K., and Weiler, E. W. (2005). Tocopherol content and activities of tyrosine aminotransferase and cystine lyase in *Arabidopsis* under stress conditions. *J. Plant Physiol.* 162, 767–770. doi: 10.1016/j.jplph.2005.04.019

Huang, B., DaCosta, M., and Jiang, Y. (2014). Research advances in mechanisms of turfgrass tolerance to abiotic stresses: from physiology to molecular biology. *Crit. Rev. Plant Sci.* 33, 141–189.

Islam, F., Yasmeen, T., Ali, Q., Ali, S., Arif, M. S., Hussain, S., et al. (2014). Influence of *Pseudomonas aeruginosa* as PGPR on oxidative stress tolerance in wheat under Zn stress. *Ecotoxicol. Environ. Safety* 104, 285–293. doi: 10.1016/j.ecoenv.2014.03.008

Islam, F., Yasmeen, T., Arif, M. S., Riaz, M., Shahzad, S. M., Imran, Q., et al. (2016). Combined ability of chromium (Cr) tolerant plant growth promoting bacteria (PGPB) and salicylic acid (SA) in attenuation of chromium stress in maize plants. *Plant Physiol. Biochem.* 108, 456–467. doi: 10.1016/j.plaphy.2016.08.014

Janmohammadi, M., Bihamta, M. R., and Ghasemzadeh, F. (2013). Influence of rhizobacteria inoculation and lead stress on the physiological and biochemical attributes of wheat genotypes. *Cercet. Agron. Mol.* 46, 49–67. doi: 10.2478/v10298-012-0074-x

Jusselme, M. D., Poly, F., Miambi, E., Mora, P., Blouin, M., Pando, A., et al. (2012). Effect of earthworms on plant Lantana camara Pb-uptake and on bacterial communities in root-adhering soil. *Sci. Total Environ.* 416, 200–207. doi: 10.1016/j.scitotenv.2011.10.070

Kanwar, M. K., Poonam, P. S., and Bhardwaj, R. (2015). Involvement of asada-halliwell pathway during phytoremediation of chromium (VI) in *Brassica juncea* L. plants. *Int. J. Phytoremed.* 17, 1237–1243. doi: 10.1080/15226514.2015.1058326

Kaur, G., Sharma, A., Guruprasad, K., and Pati, P. K. (2014). Versatile roles of plant NADPH oxidases and emerging concepts. *Biotechnol. Adv.* 32, 551–563. doi: 10.1016/j.biotechadv.2014.02.002

Kaur, P., Bali, S., Sharma, A., Kohli, S. K., Vig, A. P., Bhardwaj, R., et al. (2019). Cd induced generation of free radical species in *Brassica juncea* is regulated by supplementation of earthworms in the drilosphere. *Sci. Total Environ.* 655, 663–675. doi: 10.1016/j.scitotenv.2018.11.096

Kaur, P., Bali, S., Sharma, A., Vig, A. P., and Bhardwaj, R. (2017). Effect of earthworms on growth, photosynthetic efficiency and metal uptake in *Brassica juncea* L. plants grown in cadmium- polluted soils. *Environ. Sci. Pollut. Res.* 24, 13452–13465. doi: 10.1007/s11356-017-8947-z

Khanna, K., Jamwal, V. L., Kohli, S. K., Gandhi, S. G., Ohri, P., Bhardwaj, R., et al. (2019). Plant growth promoting rhizobacteria induced Cd tolerance in *Lycopersicon esculentum* through altered antioxidative defense expression. *Chemosphere* 217, 463–474. doi: 10.1016/j.chemosphere.2018.11.005

Khoshru, B., Mitra, D., Khoshmanzar, E., Myo, E. M., Uniyal, N., Mahakur, B., et al. (2020). Current scenario and future prospects of plant growth-promoting rhizobacteria: an economic valuable resource for the agriculture revival under stressful conditions. *J. Plant Nutr.* 43, 3062–3092. doi: 10.1080/01904167.2020.1799004

Kono, Y. (1978). Generation of superoxide radical during autoxidation of hydroxylamine and an assay for superoxide dismutase. *Arch. Biochem. Biophys.* 186, 189–195. doi: 10.1016/0003-9861(78)90479-4

Kumar, A., and Verma, J. P. (2018). Does plant-microbe interaction confer stress tolerance in plants: a review? *Microbiol. Res.* 207, 41–52. doi: 10.1016/j.micres.2017.11.004

Lavelle, P. (2002). Functional domains in soils. *Ecol. Res.* 17, 441–450. doi: 10.1046/j.1440-1703.2002.00509.x

Livak, K. J., and Schmittgen, T. D. (2001). Analysis of relative gene expression data using real-time quantitative PCR and the 2- ΔΔCT method. *Methods* 25, 402–408.

Ma, J., Lv, C., Xu, M., Chen, G., Lv, C., and Gao, Z. (2016). Photosynthesis performance, antioxidant enzymes, and ultrastructural analyses of rice seedlings under chromium stress. *Environ. Sci. Pollut. Res.* 23, 1768–1778. doi: 10.1007/s11356-015-5439-x

Ma, Q., Cao, X., Ma, J., Tan, X., Xie, Y., Xiao, H., et al. (2017). Hexavalent chromium stress enhances the uptake of nitrate but reduces the uptake of ammonium and glycine in pak choi (*Brassica chinensis* L.). *Ecotoxicol. Environ. Safety* 139, 384–393. doi: 10.1016/j.ecoenv.2017.02.009

Mahmud, J. A., Hasanuzzaman, M., Nahar, K., Rahman, A., Hossain, M. S., and Fujita, M. (2017). γ-aminobutyric acid (GABA) confers chromium stress tolerance in *Brassica juncea* L. by modulating the antioxidant defense and glyoxalase systems. *Ecotoxicology* 26, 675–690. doi: 10.1007/s10646-017-1800-9

Mahohi, A., and Raiesi, F. (2019). Functionally dissimilar soil organisms improve growth and Pb/Zn uptake by *Stachys inflata* grown in a calcareous soil highly polluted with mining activities. *J. Environ. Manage.* 247, 780–789. doi: 10.1016/j.jenvman.2019.06.130

Mahohi, A., and Raiesi, F. (2021). The performance of mycorrhizae, rhizobacteria, and earthworms to improve *Bermuda grass* (*Cynodon dactylon*) growth and Pb uptake in a Pb-contaminated soil. *Environ. Sci. Pollut. Res.* 28, 3019–3034. doi: 10.1007/s11356-020-10636-z

Nakano, Y., and Asada, K. (1981). Hydrogen peroxide is scavenged by ascorbate-specific peroxidase in spinach chloroplasts. *Plant Cell Physiol.* 22, 867–880.

Nemat, H., Shah, A. A., Akram, W., Ramzan, M., and Yasin, N. A. (2020). Ameliorative effect of co-application of *Bradyrhizobium japonicum* EI09 and se to mitigate chromium stress in *Capsicum annum* L. *Int. J. Phytoremed.* 22, 1396–1407. doi: 10.1080/15226514.2020.1780412

Noctor, G., and Foyer, C. H. (1998). Ascorbate and glutathione: keeping active oxygen under control. *Ann. Rev. Plant Biol.* 49, 249–279. doi: 10.1146/annurev.arplant.49.1.249

Noctor, G., Mhamdi, A., Chaouch, S., Han, Y. I., Neukermans, J., Marquez-Garcia, B., et al. (2012). Glutathione in plants: an integrated overview. *Plant Cell Environ.* 35, 454–484. doi: 10.1111/j.1365-3040.2011.02400.x

Noctor, G., Reichheld, J. P., and Foyer, C. H. (2018). ROS-related redox regulation and signaling in plants. *Seminars Cell Dev. Biol.* 80, 3–12. doi: 10.1016/j.semcdb.2017.07.013

Palmer, C. D., and Wittbrodt, P. R. (1991). Processes affecting the remediation of chromium-contaminated sites. *Environ. Health Perspect.* 92, 25–40. doi: 10.1289/ehp.919225

Pompella, A., Maellaro, E., Casini, A. F., and Comporti, M. (1987). Histochemical detection of lipid peroxidation in the liver of bromobenzene-poisoned mice. *Am. J. Pathol.* 129:295.

Potter, A. J., Trappetti, C., and Paton, J. C. (2012). *Streptococcus pneumoniae* uses glutathione to defend against oxidative stress and metal ion toxicity. *J. Bacteriol.* 194, 6248–6254. doi: 10.1128/JB.01393-12

Puga-Freitas, R., Barot, S., Taconnat, L., Renou, J. P., and Blouin, M. (2012). Signal molecules mediate the impact of the earthworm *Aporrectodea caliginosa* on growth, development and defence of the plant *Arabidopsis thaliana*. *PLoS One* 7:e49504. doi: 10.1371/journal.pone.0049504

Pütter, J. (1974). "Peroxidases," in *Methods of Enzymatic Analysis*, ed. H. U. Bergmeyer (Academic Press), 685–690.

Qureshi, F. F., Ashraf, M. A., Rasheed, R., Ali, S., Hussain, I., Ahmed, A., et al. (2020). Organic chelates decrease phytotoxic effects and enhance chromium uptake by regulating chromium-speciation in castor bean (*Ricinus communis* L.). *Sci. Total Environ.* 716:137061. doi: 10.1016/j.scitotenv.2020.137061

Rodríguez-Serrano, M., Romero-Puertas, M. C., Pazmino, D. M., Testillano, P. S., Risueño, M. C., Del Río, L. A., et al. (2009). Cellular response of pea plants to cadmium toxicity: cross talk between reactive oxygen species, nitric oxide, and calcium. *Plant Physiol.* 150, 229–243. doi: 10.1104/pp.108.131524

Roe, J. H., and Kuether, C. A. (1943). The determination of ascorbic acid in whole blood and urine through the 2, 4-dinitrophenylhydrazine derivative of dehydroascorbic acid. *J. Biol. Chem.* 147, 399–407. doi: 10.1016/s0021-9258(18)72395-8

Saleem, M., Asghar, H. N., Zahir, Z. A., and Shahid, M. (2018). Impact of lead tolerant plant growth promoting rhizobacteria on growth, physiology, antioxidant activities, yield and lead content in sunflower in lead contaminated soil. *Chemosphere* 195, 606–614. doi: 10.1016/j.chemosphere.2017.12.117

Sallah-Ud-Din, R., Farid, M., Saeed, R., Ali, S., Rizwan, M., Tauqeer, H. M., et al. (2017). Citric acid enhanced the antioxidant defense system and chromium uptake by *Lemna minor* L. grown in hydroponics under Cr stress. *Environ. Sci. Pollut. Res.* 24, 17669–17678. doi: 10.1007/s11356-017-9290-0

Santos, A. D., Oliveira, L. C. D., Botero, W. G., Mendonça, A. G. R., Santos, F. A. D., Rocha, J. C., et al. (2009). Distribution and bioavailability of chromium in contaminated soils by tannery residues. *Química Nova* 32, 1693–1697.

Sedalk, J., and Lindsay, R. H. (1968). Estimation of total, protein-bound, and nonprotein sulfhydryl groups in tissue with Ellman's reagent. *Analy. Biochem.* 25, 192–205. doi: 10.1016/0003-2697(68)90092-4

Shanker, A. K., Cervantes, C., Loza-Tavera, H., and Avudainayagam, S. (2005). Chromium toxicity in plants. *Environ. Int.* 31, 739–753. doi: 10.1016/j.envint.2005.02.003

Sharma, A., Sharma, P., Kumar, R., Sharma, V., Bhardwaj, R., and Sharma, I. (2021). "Role of reactive oxygen species in the regulation of abiotic stress tolerance in legumes" in *Abiotic Stress and Legumeseds Singh*, eds V. P. Singh, S. Singh, D. K. Tripathi, S. M. Prasad, R. Bhardwaj and D. K. Chauhan (Cambridge, MA: Academic Press, Elsevier), 217–243.

Sharma, P., Bakshi, P., Kour, J., Singh, A. D., Dhiman, S., Kumar, P., et al. (2020). "PGPR and earthworm-assisted phytoremediation of heavy metals," in *Earthworm Assisted Remediation of Effluents and Wastes*, eds S. Bhat, A. Vig, F. Li, and B. Ravindran (Springer), 227–245.

Sharma, P., Sharma, P., Arora, P., Verma, V., Khanna, K., Saini, P., et al. (2019). Role and regulation of ROS and antioxidants as signaling molecules in response to abiotic stresses. *Plant Sign. Mol.* 2019, 141–156.

Shekhawat, K., Rathore, S. S., Premi, O. P., Kandpal, B. K., and Chauhan, J. S. (2012). Advances in agronomic management of Indian mustard (*Brassica juncea* (L.) czernj. cosson): an overview. *Int. J. Agron.* 2012, 1–14.

Shreya, D., Jinal, H. N., Kartik, V. P., and Amaresan, N. (2020). Amelioration effect of chromium- tolerant bacteria on growth, physiological properties and chromium mobilization in chickpea (*Cicer arietinum*) under chromium stress. *Arch. Microbiol.* 202, 887–894. doi: 10.1007/s00203-019-01801-1

Sing, P., and Shah, K. (2014). Evidences for reduced metal-uptake and membrane injury upon application of nitric oxide donor in cadmium stressed rice seedlings. *Plant Physiol. Biochem.* 83, 180–184. doi: 10.1016/j.plaphy.2014.07.018

Singh, S., and Prasad, S. M. (2019). Management of chromium (VI) toxicity by calcium and sulfur in tomato and brinjal: implication of nitric oxide. *J. Hazardous Mater.* 373, 212–223. doi: 10.1016/j.jhazmat.2019.01.044

Smirnoff, N. (2000). Ascorbic acid: metabolism and functions of a multi-facetted molecule. *Curr. Opin. Plant Biol.* 3, 229–235.

Suarez, D. E. C., Gigon, A., Puga-Freitas, R., Lavelle, P., Velasquez, E., and Blouin, M. (2014). Combined effects of earthworms and IAA-producing rhizobacteria on plant growth and development. *Appl. Soil Ecol.* 80, 100–107.

Thordal-Christensen, H., Zhang, Z., Wei, Y., and Collinge, D. B. (1997). Subcellular localization of H_2O_2 in plants. H_2O_2 accumulation in papillae and hypersensitive response during the barley- powdery mildew interaction. *Plant Journal* 11, 1187–1194.

Tripathi, D. K., Singh, V. P., Prasad, S. M., Chauhan, D. K., and Dubey, N. K. (2015). Silicon nanoparticles (SiNp) alleviate chromium (VI) phytotoxicity in *Pisum sativum* (L.) seedlings. *Plant Physiol. Biochem.* 96, 189–198. doi: 10.1016/j.plaphy.2015.07.026

Ulhassan, Z., Gill, R. A., Huang, H., Ali, S., Mwamba, T. M., Ali, B., et al. (2019). Selenium mitigates the chromium toxicity in *Brassicca napus* L. by ameliorating nutrients uptake, amino acids metabolism and antioxidant defense system. *Plant Physiol. Biochem.* 145, 142–152. doi: 10.1016/j.plaphy.2019.10.035

Varghese, S. M., and Prabha, M. L. (2014). Biochemical characterization of vermiwash and its effect on growth of capsicum frutescens. *Malaya J. Biosci.* 1, 86–91.

Velikova, V., Yordanov, I., and Edreva, A. (2000). Oxidative stress and some antioxidant systems in acid rain-treated bean plants: protective role of exogenous polyamines. *Plant Sci.* 151, 59–66.

Wakeel, A., Ali, I., Upreti, S., Azizullah, A., Liu, B., Khan, A. R., et al. (2018). Ethylene mediates dichromate-induced inhibition of primary root growth by altering AUX1 expression and auxin accumulation in *Arabidopsis thaliana*. *Plant Cell Environ.* 41, 1453–1467. doi: 10.1111/pce.13174

Wang, Q., Ge, C., Xu, S. A., Wu, Y., Sahito, Z. A., Ma, L., et al. (2020). The endophytic bacterium *Sphingomonas* SaMR12 alleviates Cd stress in oilseed rape through regulation of the GSH-AsA cycle and antioxidative enzymes. *BMC Plant Biol.* 20:1–14. doi: 10.1186/s12870-020-2273-1

Wang, R., Gao, F., Guo, B. Q., Huang, J. C., Wang, L., and Zhou, Y. J. (2013). Short-term chromium-stress-induced alterations in the maize leaf proteome. *Int. J. Mol. Sci.* 14, 11125–11144. doi: 10.3390/ijms140611125

Wu, F., Wan, J. H. C., Wu, S., and Wong, M. (2012). Effects of earthworms and plant growth– promoting rhizobacteria (PGPR) on availability of nitrogen, phosphorus, and potassium in soil. *J. Plant Nutr. Soil Sci.* 175, 423–433.

Wu, Q. S., Zou, Y. N., Liu, W., Ye, X. F., Zai, H. F., and Zhao, L. J. (2010). Alleviation of salt stress in citrus seedlings inoculated with mycorrhiza: changes in leaf antioxidant defense systems. *Plant Soil Environ.* 56, 470–475.

Yamamoto, Y., Kobayashi, Y., and Matsumoto, H. (2001). Lipid peroxidation is an early symptom triggered by aluminum, but not the primary cause of elongation inhibition in pea roots. *Plant Physiol.* 125, 199–208. doi: 10.1104/pp.125.1.199

Conflict of Interest: The authors declare that the research was conducted in the absence of any commercial or financial relationships that could be construed as a potential conflict of interest.

frontiers | Frontiers in Microbiology

ORIGINAL RESEARCH
published: 15 April 2022
doi: 10.3389/fmicb.2022.853407

An Alliance of *Trifolium repens*—*Rhizobium leguminosarum* bv. *trifolii*—Mycorrhizal Fungi From an Old Zn-Pb-Cd Rich Waste Heap as a Promising Tripartite System for Phytostabilization of Metal Polluted Soils

Ewa Oleńska[1], Wanda Małek[2], Marzena Sujkowska-Rybkowska[3], Sebastian Szopa[4], Tadeusz Włostowski[1], Olgierd Aleksandrowicz[1], Izabela Swiecicka[1,5], Małgorzata Wójcik[2], Sofie Thijs[6] and Jaco Vangronsveld[2,6]*

[1] Faculty of Biology, University of Bialystok, Bialystok, Poland, [2] Faculty of Biology and Biotechnology, Institute of Biological Sciences, Maria Curie-Skłodowska University, Lublin, Poland, [3] Institute of Biology, Warsaw University of Life Sciences-SGGW, Warsaw, Poland, [4] SHIM-POL A.M. Borzymowski, Izabelin, Poland, [5] Laboratory of Applied Microbiology, University of Bialystok, Bialystok, Poland, [6] Environmental Biology, Centre for Environmental Sciences, Hasselt University, Diepenbeek, Belgium

The Bolesław waste heap in South Poland, with total soil Zn concentrations higher than 50,000 mg kg^{-1}, 5,000 mg Pb kg^{-1}, and 500 mg Cd kg^{-1}, is a unique habitat for metallicolous plants, such as *Trifolium repens* L. The purpose of this study was to characterize the association between *T. repens* and its microbial symbionts, i.e., *Rhizobium leguminosarum* bv. *trifolii* and mycorrhizal fungi and to evaluate its applicability for phytostabilization of metal-polluted soils. Rhizobia originating from the nutrient-poor waste heap area showed to be efficient in plant nodulation and nitrogen fixation. They demonstrated not only potential plant growth promotion traits *in vitro*, but they also improved the growth of *T. repens* plants to a similar extent as strains from a non-polluted reference area. Our results revealed that the adaptations of *T. repens* to high Zn-Pb-Cd concentrations are related to the storage of metals predominantly in the roots (excluder strategy) due to nodule apoplast modifications (i.e., thickening and suberization of cell walls, vacuolar storage), and symbiosis with arbuscular mycorrhizal fungi of a substantial genetic diversity. As a result, the rhizobia-mycorrhizal fungi-*T. repens* association appears to be a promising tool for phytostabilization of Zn-Pb-Cd-polluted soils.

Keywords: white clover, plant growth-promoting bacteria (PGPB), nitrogenase, nodule anatomy, metal tolerance, ICP-OES, gas chromatography, transmission electron microscopy

OPEN ACCESS

Edited by:
Krishnendu Pramanik, Visva-Bharati University, India

Reviewed by:
Kamila Jadwiga Rachwał, University of Life Sciences in Lublin, Poland
Jean-Jacques Drevon, Domaine Experimental du Val d'Ainan (DEVA), France
Nakkeeran S, Tamil Nadu Agricultural University, India

****Correspondence:***
Ewa Oleńska
chwelat@uwb.edu.pl

Specialty section:
This article was submitted to Terrestrial Microbiology, a section of the journal Frontiers in Microbiology

Received: *12 January 2022*
Accepted: *15 March 2022*
Published: *15 April 2022*

Citation:
Oleńska E, Małek W, Sujkowska-Rybkowska M, Szopa S, Włostowski T, Aleksandrowicz O, Swiecicka I, Wójcik M, Thijs S and Vangronsveld J (2022) An Alliance of Trifolium repens—Rhizobium leguminosarum bv. trifolii—Mycorrhizal Fungi From an Old Zn-Pb-Cd Rich Waste Heap as a Promising Tripartite System for Phytostabilization of Metal Polluted Soils. Front. Microbiol. 13:853407. doi: 10.3389/fmicb.2022.853407

INTRODUCTION

Metal pollution of soils is a significant problem worldwide; it undermines the quality and fertility of soils and is an obstacle to sustainable development (Tchounwou et al., 2012). Soils can be natural as well as anthropogenically enriched with trace metals, which can be taken up by plants, and thereafter spread through the food chains (Walker et al., 2012). Metal ions, even at low concentrations, can hamper living organisms by disturbing cell metabolism, damaging the anatomical structure of tissues, leading to growth reduction, accelerated senescence, and necrosis, which may result in a reduction of population size, density, and genetic variability (Jaishankar et al., 2014). Consequently, metal pollution acts as a natural selection power on non-fit organisms and favors the survival and reproduction of individuals that carry adaptive traits (Macnair, 1997).

Certain plants have evolved ways to deal with high metal pollution (Viehweger, 2014; Wójcik et al., 2017; Nikalje and Suprasanna, 2018), and are associated with specific microbial communities that can be valuable in the remediation of polluted areas (Weyens et al., 2009a,b; Thijs and Vangronsveld, 2015; Yan et al., 2020). Metal accumulators possess the ability to store metal ions in aerial tissues (Lange et al., 2017), while excluders retain metals in their roots, thereby preventing metal translocation into the shoots (Shackira and Puthur, 2019; Zgorelec et al., 2020). Microorganisms inhabiting the rhizosphere of such plants can be of significant importance for their application in phytostabilization (Thijs and Vangronsveld, 2015; Wang et al., 2020). The beneficial effects of plant growth-promoting (PGP) bacteria on the metal tolerance of their hosts can be attributed to a lowered external or internal availability of metals due to incorporation of metals in the bacterial cell walls, metal sequestration inside bacterial cells, efflux and precipitation of metal ions on bacterial cell walls, or exopolysaccharide production. PGP bacteria can also indirectly improve plant growth due to traits like enhancing nutrient availability, synthesis of growth hormones, increasing the antioxidative status of plants, and/or protecting the plants from diseases and pathogens (Hayat et al., 2010; Abhilash et al., 2012; Oleńska et al., 2020a). Hence, identification of the most effective plant-microbe association is of significant importance for phytostabilization.

Legumes (*Fabaceae*) are commonly found as pioneer plants on metal-polluted sites, also on waste deposits of metal ore mining and processing in southern Poland (Nowak et al., 2011). They are well suited for site stabilization since they possess extensive root systems to protect soil from erosion, improve aeration for microbial activity, increase soil humus content, synthesize substantial amounts of biomass rich in proteins, and co-exist in symbiosis with rhizobia providing ammonium in the process of atmospheric nitrogen reduction (Padilla and Pugnaire, 2006; Li et al., 2007; Fterich et al., 2014; Roa-Fuentes et al., 2015). In southern Poland, some sites are extremely polluted with metals from the anthropogenic origin, including postindustrial waste deposits, where the soils are additionally highly deficient in water and nutrients (Wójcik et al., 2014). White clover (*Trifolium repens*), a member of the legume family, is found frequently on the more than 100-year-old Zn-Pb waste heap Bolesław in southern Poland (Nowak et al., 2011; Oleńska and Małek, 2013b). *Rhizobium leguminosarum* bv. *trifolii* bacteria were identified as inhabitants of plant root nodules (Oleńska and Małek, 2015), and this partnership might be a promising plant-microbe association for site stabilization. Earlier results (Oleńska and Małek, 2013b) revealed that *R. leguminosarum* bv. *trifolii* of the Bolesław waste heap carries genes whose products are involved in metal ion exclusion, metal tolerance as well as the production of exopolysaccharides with specific sugar composition (Oleńska et al., 2021). Moreover, Oleńska and Małek (2015, 2019) found that *R. leguminosarum* bv. *trifolii* populations inhabiting root nodules of white clover established on the Bolesław Zn-Pb waste heap show a moderate level of genetic diversity, while studies of other European *R. leguminosarum* bv. *trifolii* populations from metal-polluted sites show a drastic reduction of genetic diversity of these populations, which were not able to fix nitrogen (e.g., in Woburn, United Kingdom), and even lack any rhizobial symbionts (e.g., in Braunschweig, Germany) (Chaudri et al., 1993; Giller et al., 1998; Lakzian et al., 2002).

Since the level of genetic polymorphism of bacterial populations stands for adaptability and tolerance of bacteria to changing environmental conditions, *T. repens* nodule microsymbionts from the Bolesław waste heap might be interesting partners for symbiosis. It is worth noting that a symbiosis may also be established between *T. repens* and mycorrhizal fungi (Li et al., 2005). Indeed, endo- or ectomycorrhizal fungi were found to improve the growth of many plant species under metal stress conditions (Luo et al., 2014; Ważny et al., 2021). For example, symbiotic mycorrhizal fungi can sequester metal ions in their hyphae, acting as a barrier toward metals, and thus indirectly protect plant roots. Hence, white clover fitness in metal-polluted areas, such as the Bolesław waste heap, might be increased due to the joint action of rhizobia and mycorrhizal fungi.

In this study, we characterized the *R. leguminosarum* bv. *trifolii*—arbuscular mycorrhizal fungi (AMF)—white clover association as a potential tool in phytostabilization of metal-polluted soils. To investigate the activities of the *T. repens* nodule microsymbionts, *R. leguminosarum* bv. *trifolii* strains were isolated from root nodules of white clover growing on the Bolesław waste heap as well as on the reference grasslands of Bolestraszyce (Przemyskie Fothills). The rhizobial strains were studied for their Zn, Pb, and Cd tolerance, nodulation ability, the polymorphism of *nodA* genes encoding proteins involved in the nodulation process, nitrogenase enzyme activity, as well as for their PGP traits. To determine the effects of *R. leguminosarum* bv. *trifolii* on white clover growth, morphological parameters of plants, as well as biochemical ones of *T. repens* inoculated with the waste heap and reference site rhizobia, were studied. To define the strategy of the plants to deal with metals (accumulator vs. excluder), metal concentrations in leaves and roots were determined. Both light and transmission electron microscopy (TEM) analysis of root nodules were used to evaluate the adaptation of *T. repens* to metals. Soil nutrients (total N and nitrate, ammonia) and micro/macro-element concentrations were determined. The presence of mycorrhiza in white clover roots was investigated using TEM, and the genetic diversity of

mycorrhizal populations was estimated using ARISA (automated ribosomal intergenic spacer analysis) fingerprinting.

MATERIALS AND METHODS

Five *T. repens* root and leaf samples, soil samples, as well as forty-two *R. leguminosarum* bv. *trifolii* strains that were previously isolated (Oleńska and Małek, 2015) from nodules of *T. repens* that originated from the more than 100-year-old Zn-Pb waste heap in Bolesław (50°17′N 19°29′E, Silesia-Krakow Upland, Poland) and a grassland in the Bolestraszyce (49°48′N 22°50′E, Przemyskie Foothills, Poland) reference area, were used in this study (**Supplementary Table 1**).

Rhizobium leguminosarum bv. *trifolii* Analysis

Rhizobium leguminosarum bv. *trifolii* Tolerance to Metals

The studied rhizobial strains were tested for their Zn, Pb, and Cd tolerance on plates with solid a 79CA medium (Oleńska and Małek, 2015) enriched with metal salts, i.e., 0.1, 0.5, and 2.5-mM $ZnSO_4 \times 7\ H_2O$; 0.1, 0.5, and 1-mM $CdCl_2 \times 2.5\ H_2O$; 0.1, 0.5, 0.5, 1, and 2.5-mM $Pb(NO_3)_2$ in three replicates (Lakzian et al., 2002, 2007). After 4 days of incubation, positive or negative rhizobial growth results were presented as a binary system (0—no growth, 1—growth).

Rhizobium leguminosarum bv. *trifolii* Nodulation Ability

The nodulation abilities of the waste heap as well as reference origin *R. leguminosarum* bv. *trifolii* strains were investigated in a laboratory plant test. Commercially certified seeds of *T. repens* cultivar Tasman were sterilized and germinated according to the conditions described by Oleńska and Małek (2015). Two-day-old white clover seedlings were placed in a nitrogen-deficient Hoagland medium in tubes (Oleńska and Małek, 2015), inoculated with the rhizobial strains, and cultivated in a greenhouse for 6 weeks at 19–23°C with a 12/12-h light/darkness cycle. To determine the ability of *R. leguminosarum* bv. *trifolii* to establish a symbiosis with *T. repens*, the presence and the color of root nodules as well as the size and color of plants were estimated in comparison to plants non-inoculated.

Rhizobium leguminosarum bv. *trifolii* Genetic Diversity of the *nodA* Gene

Genomic DNA was isolated from *R. leguminosarum* bv. *trifolii* strains according to the procedure described by Oleńska and Małek (2015). To amplify the *R. leguminosarum* bv. *trifolii* strains *nodA* gene fragment, the following primers were used: nodA-1 (5′-TGCRGTGGAARNTRNNCTGGGAAA-3′), and nodA-2 (5′-GGNCCGTCRTCRAAWGTCARGTA-3′) (Haukka et al., 1998) under optimized PCR cycling conditions: initial denaturation at 95°C for 15 min, 35 cycles of denaturation at 94°C for 45 s, annealing at 55°C for 45 s, extension at 68°C for 2 min, and final extension at 72°C for 5 min (Ardley et al., 2013). The *nodA* gene sequences of the studied strains, as well as reference ones obtained from the GenBank database (National Center for Biotechnology Information, NCBI), were aligned and inspected using the BioEdit program (Hall, 1999). Phylogenetic analysis of the *nodA* gene, as well as a determination of *R. leguminosarum* bv. *trifolii* strains NodA protein amino acid sequences, were performed using MEGA version 7.0 software (Kumar et al., 2016). Phylogenetic Neighbor Joining tree construction involved an analysis of 1,000 resampled data sets according to the Maximum Composite Likelihood model.

Rhizobium leguminosarum bv. *trifolii* Nitrogenase Activity

Nitrogenase activity of rhizobia was evaluated using the acetylene reduction assay (ARA) that relies on a gas chromatography monitoring the reduction of acetylene (C_2H_2) to ethylene (C_2H_4) (Seefeldt et al., 2013; Haskett et al., 2021). For this purpose, from tubes that were tightly closed with rubber caps and containing the inoculated 6-week-old *T. repens* plants growing in a nitrogen-deficient Hoagland medium, 10% (v/v) of the gas phase was replaced with acetylene. After 1-h incubation at room temperature, 1 mL of gas sample was taken from the tubes, injected into the Hewlett Packard GC system (HP 5890 series II, Hewlett Packard, Inc., United States) to determine the ethylene concentration. A 274.3-cm long stainless-steel column packed with Porapak^{TM} Q (80–100 mesh) was used. The temperatures of the injector, column oven, and detector were 150, 230, and 230°C, respectively. Nitrogen of ultrahigh purity was used as a carrier gas. Nitrogenase activity was displayed as ethylene concentration (nMe) $nmol \cdot h^{-1}$ calculated on the basis of the percentage of acetylene conversion (% Ac) and the ethylene volume (Ve) using formulas described in Staal et al. (2001).

In vitro Plant Growth-Promoting Properties of the *Rhizobium leguminosarum* bv. *trifolii* Strains

Beneficial traits of the rhizobia for plants were estimated as: (i) nutrient availability enhancers (production of siderophores and organic acids and solubilization of phosphate), (ii) production of plant growth regulators (IAA and ACCD), and (iii) production of compounds involved in plant disease prevention (acetoin synthesis). Most of the tests were qualitatively, colorimetrically assessed. A phosphate solubilization index (SI) was estimated by plating on a selective NBRIP medium, and IAA production, as well as ACCD activity, was quantitatively assessed. The ability to synthesize organic acids was assessed using Alizarine Red S according to Cunningham and Kuiack (1992). Siderophore production was tested using chrome-azurol S according to Schwyn and Neilands (1987), and a 284 medium (Schlegel et al., 1961). Bacterial acetoin production was examined using the α-naphthol method (Romick and Fleming, 1998). The capacity to solubilize phosphate was tested according to Pikovskaya (1948) with the modifications of Nautiyal (1999), and the phosphate solubilization index (SI) was calculated using an equation described in Pande et al. (2017). The capability of bacteria to synthesize IAA was investigated according to Patten and Glick (2002). Quantification of the synthesized IAA by the rhizobial strains was performed according to Penrose and Glick (2004) using the calibration curve equation

(**Supplementary Table 1**) obtained as a result of the optical density measurements of 0-, 1-, 5-, 10-, 25-, and 45-μg mL^{-1} IAA solutions at a wavelength of 535 nm. Bacterial ACCD activity was studied according to Belimov et al. (2005) and was expressed as α-ketobutyrate concentration and converted into protein concentration. The α-ketobutyrate concentration was estimated using a calibration curve equation (**Supplementary Table 1**) based on the correlation of the optical density: 0. 1-, 0. 2-, 0. 5-, 0. 8-, 1-μM α-ketobutyrate mL^{-1} measured at wavelength of 540 nm. Finally, the ACCD activity was expressed as nM α-ketobutyrate mg^{-1} protein. Protein concentrations were determined according to the method described by Bradford (1976) and calculated on the basis of a calibration curve equation (**Supplementary Table 1**), where 0. 125-, 0. 25-, 0. 5-, 0. 75-, 1.-, 1. 5-, 2.-mg protein mL^{-1} of bovine serum albumin (BSA), used as a standard, were measured at a wavelength of 595 nm.

Effects of *Rhizobium leguminosarum bv. trifolii* on Growth of White Clover

In order to evaluate the effects of *R. leguminosarum* bv. *trifolii* on *T. repens* growth, the morphological and biochemical parameters of plants were determined after 6 weeks of growth. Plants were inoculated with *R. leguminosarum* bv. *trifolii* strains from the metal-polluted waste heap (WH group) or from the non-polluted reference area rhizobia (R group) (100-μL of an 18-h old liquid bacterial culture adjusted to 0.6 at OD_{590}); control plants were not inoculated (NI group). The following morphological parameters were determined: dry and fresh weight of shoots and fresh weight of roots, length of main root, number and length of side roots, total length of the root system, number of nodules and leaves, and ash content.

As biochemical parameters, concentrations of photosynthetic pigments (chlorophyll *a*, *b*, total chlorophyll, and chlorophyll *a* to *b* ratio), and protein concentrations in leaves of *T. repens* were used. Two leaflets (first and third) of a trifoliate leaf of white clover were washed in distilled water, weighted, homogenized in TissueLyser LT (Qiagen), and examined for the photosynthetic pigments according to Wellburn and Lichtenthaler (1984) with modifications described in Wellburn (1994). Photosynthetic pigments concentrations were expressed as μg of a photosynthetic pigment per g of fresh weight of plant tissue. Quantitative estimation of proteins was done using the Lowry et al. (1951) method in one leaflet (central) of a trifoliate leaf, and its concentration was expressed as *mg* of proteins g^{-1} fresh weight.

Trifolium repens Analysis

Root Nodule Anatomy and Arbuscular Mycorrhizal Fungi in Roots

Nodules of different size and stages of development were collected from *T. repens* plants grown on the waste heap in Bolesław and the reference area in Bolestraszyce. The nodules were fixed according to Karnovsky (1965) and Łotocka et al. (1997) for 24-h at 21°C ± 0.5 and air pressure of –0.4-$kGcm^{-2}$. Subsequently, nodules were post-fixated in 1% OsO_4 for 4-h at 4°C, dehydrated in increasing concentrations of ethanol, and embedded in glycid ether 100 epoxy resin (SERVA) according to Sujkowska-Rybkowska et al. (2012). Blocks were sectioned using microtomes (Jung RM 2065 and Ultracut UCT, Leica). Semithin sections of epoxy resin-embedded nodule tissue blocks were stained with methylene blue and azur A, and examined under a light microscope (Olympus-Provis, Japan). Next, thin sections were collected on copper grids, contrasted with uranyl acetate followed by lead citrate for 1 min, and examined under a TEM Morgagni 268D (Philips, Netherlands).

Metal Concentrations in *Trifolium repens* Leaves and Roots

Dry samples of roots and leaves were digested as described earlier (Oleńska et al., 2020b). After digestion, the samples were diluted (Karaś et al., 2021), and an ICPE-9820 (Shimadzu, Kyoto, Japan) with a mini-torch was used for the qualitative and quantitative detection of elements (Zn, Pb, Cd). Prior to analysis, the Sigma-Aldrich (St. Louis, MO, United States) periodic table mix 1 for ICP containing 10-mg L^{-1} of Zn, Pb, and Cd in 10% nitric acid (comprising HF traces) was used for calibration of the ICP-OES (inductively coupled plasma optical emission spectrometry). Simultaneously, analysis was performed for standards. Standard curve equations are given in **Supplementary Table 1**. Both a negative control (a blanc sample) and a positive control (tomato leaves, NIST® 1573a, Sigma-Aldrich) were included. To preserve the standard/sample conditions, the matrix match method was used.

Nutrient Concentrations in Soils and Soil Dry Weight

Mg, Ca, K, and Na Concentration in Soil

Macroelements were determined by ICP-OES after mineralization of five samples, representative to the Bolesław waste heap and the non-polluted reference grassland, according to the protocol described earlier (Oleńska et al., 2020b). Simultaneously, nutrient contents were determined in a blanc sample, and a standard reference material Montana II soil (NIST® 2711a, Sigma-Aldrich). Soil dry weight was determined according to PN-ISO-11465:1999.

Total Kjeldahl Nitrogen

Air-dry soil samples (5-g) were digested with 15-mL concentrated sulfuric acid (H_2SO_4) in the presence of 15-g catalyst (96% K_2SO_4 and 4% $CuSO_4 \times 5\ H_2O$) using an automated digestion block Digestor™ 2520 (FOSS) at 420°C for 3-h [Association of Official Analytical Chemist (AOAC), 1990]. In result, nitrogen present in the soil was transformed to ammonium sulfate (NH_4HSO_4) (PN-EN 13342:2002, PN-ISO 5664:2002). After cooling, the acid digestion mixtures were distilled by alkalization with 50% NaOH using the auto distillation unit Kjeltec™ 2200 (FOSS) to convert NH_4^+ and obtain ammonia NH_3 gas in solution. To quantify the amount of ammonia in solution, ammonium trapped as ammonium borate in 4% boric acid solution was titrated with 0.01-M HCl in the presence of a Tashiro indicator (0.1-g 100-mL^{-1} bromocresol green and 0.1-g 100-mL^{-1} methyl red in 1-L 95% ethanol). Simultaneously, the digestion, distillation, and titration of the blank sample (sucrose, 1-g) were performed.

Quantity of ammonia (TKN determination) was expressed as percentage and calculated according to the formula

$$\%N = \frac{(Vx - Vo) \times 0.014 \times N}{G\ (100 - w)}\ 100\%$$

where:

Vx – volume of 0.01-M HCl solution used for sample titration, mL

Vo – volume of 0.01-M HCl solution used for blind sample titration, mL

0.014 – nitrogen amount corresponding to 1-mL 1-M HCl solution, g

N – molarity of used HCl solution, $M \times L^{-1}$

G – aerial dry soil weight, g

w – water percentage content in an analyzed sample.

Determination of Mineral Forms of Nitrogen (Ammonium and Nitrate)

Soil samples (10-g) extracted with 1% K_2SO_4 for 24-h were centrifuged at 2,000 rpm for 10 min, and absorbance of the supernatant [ammonium (NH_4^+) and nitrate (NO_3^-) concentrations] were measured automatically in a colorimetric nutrient flow analyzer AA100 (SEAL Analytical). In order to evaluate the NH_4^+ concentration, the supernatant was treated with salicylic acid, and dichloroisocyanuric acid with nitroprusside as a catalyst giving a blue solution and absorbance was determined at 660 nm (WBJ-2/IB/159). To determine the nitrate (NO_3^-) concentration, the supernatant was administered on a cadmium ion column. Nitrate (NO_3^-) in the supernatant in a phosphate buffer pH = 8.5 is reduced to nitrite (NO_2^-) by Cd in the ion column, and nitrite is detected by the Griess reaction method based on the conversion of sulfanilic acid (1%) to diazonium salt by reaction with NO_2^- in an acid solution. The diazonium salt is then coupled to 0.1% NED (N-1-naphthylethylenediamine dihydrochloride), forming a pink azo dye that was spectrophotometrically quantified based on absorbance measurement at 540 nm.

Genetic Fingerprint of Fungi Associated With *Trifolium repens* Rhizosphere, Roots, and Nodules

Total DNA was extracted from roots and nodules of six *T. repens* plants collected from the metal-polluted waste heap and the reference area according to Valledor et al. (2014), and from white clover rhizosphere using the MO BIO PowerSoil protocol (Qiagen). A determination of fungal genetic diversity was performed using ARISA (automated rRNA intergenic spacer analysis) fingerprinting based on an analysis of variable size of the 18S-28S rRNA internal transcribed spacer (ITS) region that, in eukaryotes, is divided into two subregions ITS1, involving 18S-5.8S rRNA genes and ITS2 comprised of 5.8S-28S rRNA genes (Ranjard et al., 2001; Johnston-Monje and Lopez Mejia, 2020). ITS1-5.8S-ITS2 region amplification was performed in a final volume of 25-μL, consisting of a 2.5-μL Fast-Start HF Reactive Buffer (0.9-mM $MgCl_2$) (FastStart High Fidelity PCR System, Roche, Sigma Aldrich), 0.5-μL PCR grade nucleotide mix (100-μM of each dNTP), 0.25-μL a Fast-Start HF Enzyme Blend (1.25 U), 20.25-μL nuclease-free water, 0.5-μL DNA as a template, and 0.5-μL each of the fluorescence-labeled primers (0.04-μM), representing consensus sequences found at the 3′ end of the 18S gene for 2234C (5′-GTTTCCGTAGGTGAACCTGC-3′) and with the 5′ end of the 28S gene for 3126T (5′-ATATGCTTAAGTTCAGCGGGT-3′) (Biolegio, Netherlands). Amplification was performed in conditions as follows: initial denaturation at 94°C for 3 min, 34 cycles of denaturation at 94°C for 1 min, annealing at 55°C for 45 s, and elongation at 72°C for 1 min, and a final elongation at 72°C for 7 min. Automated electrophoresis of amplified intergenic spacer region products was performed according to the Agilent DNA 1000 assay protocol. Post-PCR products were added to the Agilent DNAchip (On-Chip Electrophoresis, Agilent Technologies, United States) for a subsequent analysis in the Agilent 2100 Bioanalyzer, equipped with DNA 2100 Expert software. The genetic diversity of fungi was determined with the R × 64 version 3.6.2 program and the StatFingerprints package (Michelland et al., 2009).

Statistical Analysis

Results were presented as means ± SD, analyzed with one-way ANOVA, and significant differences between means were estimated with the multiple range Duncan's test using Statistica version 13 (TIBCO).

RESULTS

Trifolium repens Root Nodule Microsymbionts Activity

R. leguminosarum bv. *trifolii* strains originating from the metal-polluted waste heap demonstrated a significantly higher percentage (52%) of tolerance to toxic metals in comparison to strains from the reference area (11%) (**Supplementary Table 2**). Plant tests showed that all studied rhizobia entered a symbiotic interaction with white clover, and as nodule inhabitants effectively transformed atmospheric nitrogen into ammonia (**Table 1**). Rhizobial strains of waste heap origin were similar in nitrogenase activity to rhizobia isolated from the nodules of *T. repens* growing on the reference site (**Table 1**). Examination of the *nodA* gene sequences, which product N-acyltransferase participates in the Nod factor formation, allowed to identify five rhizobial genotypes (A-E) (NCBI accession numbers MZ231019-23), including some specific to rhizobia, originating from the non-polluted reference area (genotypes A, D, and E), one characteristic to rhizobia from the waste heap area (genotype C), and one common to the rhizobia of waste heap and the reference area (genotype B) (**Table 2**). *R. leguminosarum* bv. *trifolii* reference strains (NCBI, GenBank) of *nodA* genotypes formed an independent branch in the phylogram compared to other rhizobia species (**Figure 1**). The *R. leguminosarum* bv. *trifolii* genotype B appeared to be the most frequent one ($f = 0.38$) among all determined genotypes; bacteria of the genotypes A, C, and D revealed frequencies of 0.17, whereas rhizobia of the

TABLE 1 | Morphological and biochemical parameters of growth of *T. repens* inoculated with *R. leguminosarum* bv. *trifolii* from the reference area (R group), the metal-polluted waste heap (WH group), and non-inoculated with rhizobia strains (NI group).

Parameter	R group	WH group	NI group
Morphological parameters			
Leaf fresh weight	0.0051 ± 0.0011^{a}	0.0045 ± 0.0010^{a}	0.0018 ± 0.0005^{b}
Leaf dry wet	0.0012 ± 0.0005^{a}	0.0012 ± 0.0004^{a}	0.0005 ± 0.0000^{b}
Ash content [% f. w.]	4^{a}	4^{a}	2^{b}
Lateral roots length [mm]	9 ± 0.56^{a}	9 ± 1.12^{a}	6 ± 0.95^{b}
Main root length [mm]	39.22 ± 10.24^{a}	40.81 ± 13.61^{a}	39.48 ± 10.47^{a}
Lateral roots number	2.1 ± 1.33^{a}	1.75 ± 1.20^{a}	1.85 ± 0.56^{a}
Leaves number	3.10 ± 0.95^{a}	2.95 ± 0.94^{a}	2.95 ± 0.69^{a}
Nodules number	4.25 ± 1.85^{a}	5.8 ± 2.20^{a}	0^{b}
Biochemical parameters			
Chla [$\mu g \times g^{-1}$]	46.97 ± 4.81^{a}	51.50 ± 16.15^{a}	10.91 ± 3.79^{b}
Chlb [$\mu g \times g^{-1}$]	0.045 ± 0.004^{a}	0.046 ± 0.004^{a}	0.08 ± 0.006^{b}
Chl_{a+b}[$\mu g \times g^{-1}$]	66.03 ± 14.69^{a}	71.17 ± 12.83^{a}	30.95 ± 8.88^{b}
$Chl_{a/b}$ [$\mu g \times g^{-1}$]	1.01 ± 0.39^{a}	1.12 ± 0.32^{a}	0.14 ± 0.05^{b}
Proteins [$mg \times g^{-1}$]	32.89 ± 2.28^{a}	67.17 ± 11.96^{b}	20.25 ± 6.24^{c}
Nitrogenase activity	169.65 ± 63.37^{a}	163.35 ± 71.22^{a}	0^{b}

Values are represented as means ± SD (n = 20). Significant differences between groups were marked with different letters.

TABLE 2 | Variable sites in 416-bp long fragments of the *nodA* gene (A) and corresponding amino acid sequences of NodA protein (B) of *R. leguminosarum* bv. *trifolii* strains from the metal-polluted waste heap and the reference area.

(A).

Genotype	Number of variable site														
	16	**97**	**166**	**178**	**202**	**217**	**247**	**253**	**272**	**283**	**340**	**394**	**402**	**Frequency**	**Strains**
A	T	C	T	T	T	T	C	C	G	C	G	G	C	0.17	1.6 K, 1.7 K, 4.3 K, 4.4 K, 4.8 K, 4.10 K, 5.5 K
B	C	.	.	C	.	.	A	G	.	.	A	T	A	0.38	2.9 K, 9.9 K, 4.51 H, 5.1 H, 5.2 H, 5.5 H, 6.3 H, 6.5 H, 6.12 H, 6.13 H, 7.1 H, 7.2 H, 7.3 H, 7.4 H, 7.6 H, 7.7 H
C	.	A	C	T	C	C	C	C	A	T	G	.	.	0.17	3.3 H, 3.5 H, 4.1 H, 4.2 H, 4.3 H, 4.4 H, 4.5 H
D	T	.	.	.	.	.	.	.	.	.	.	.	.	0.17	3.2 K, 5.3 K, 5.7 K, 5.10 K, 6.5 K, 6.6 K, 8.8 K
E	.	.	T	.	.	.	.	.	.	.	.	.	.	0.11	3.3 K, 3.5 K, 3.9 K, 9.2 K, 9.3 K

(B).

Genotype	Number of variable site										
	6	**33**	**56**	**60**	**73**	**83**	**85**	**91**	**95**	**114**	**131**
A	F	H	C	Y	F	L	P	R	H	V	A
B	L	.	.	H	.	I	A	.	.	M	S
C	.	N	R	Y	L	L	P	Q	Y	.	.
D	F	.	.	.	.	.	.	.	.	.	.
E	.	.	C	.	.	.	.	.	.	.	.

A, alanine; C, cysteine; F, phenylalanine; H, histidine; I, isoleucine; L, leucine; M, methionine; N, aspartic acid; P, proline; Q, glutamic acid; R, arginine; S, serine; Y, tyrosine; V, valine.

genotype E showed the lowest frequency ($f = 0.11$). The 416 bp *nodA* gene sequence analysis revealed 13 variable sites involving substitutions, including nine transitions and four transversions, which influenced 138 amino acid protein sequences with 11 variable sites representing missense mutations (**Table 2**).

The *in vitro* tests indicated that all studied *R. leguminosarum* bv. *trifolii* strains showed potential to promote plant growth (**Supplementary Table 3**); 32% of the strains appeared positive for all six traits tested, 16% were positive for five traits, 37% of the tested strains were positive for four traits, and 21% for three traits.

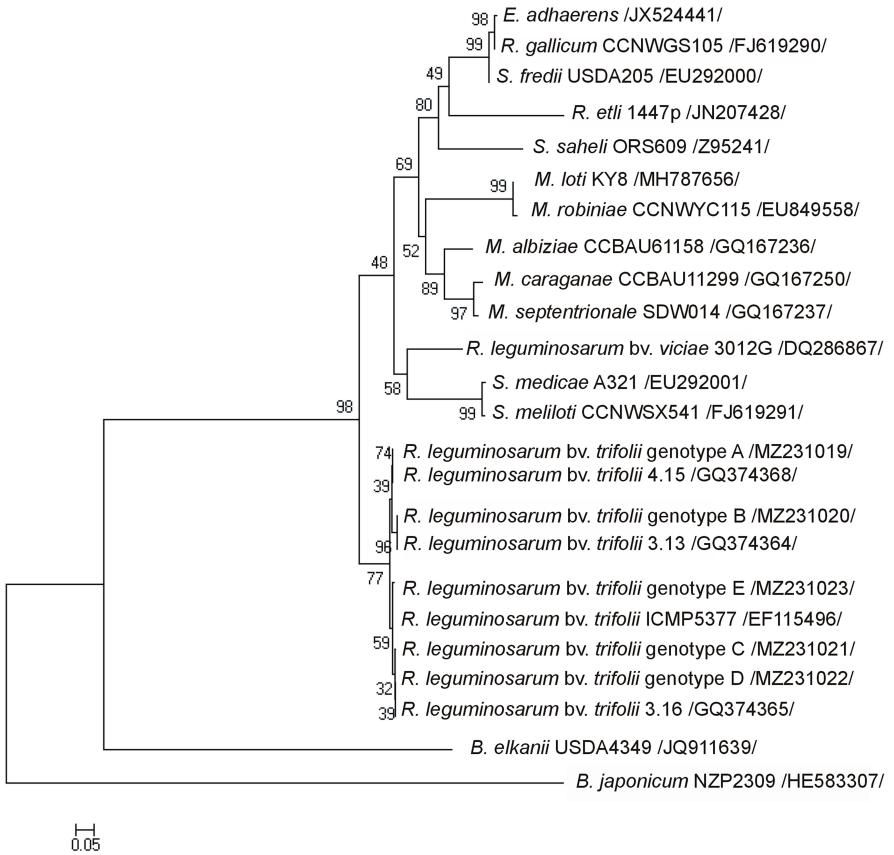

FIGURE 1 | The phylogenetic Neighbor Joining tree based on 416-bp *nodA* gene sequences showing the relationship of *R. leguminosarum* bv. *trifolii* genotypes (A–E) and reference strains (the GenBank database). Numbers at nods indicate levels of bootstrap support based on an analysis of 1,000 resampled data sets. Accession numbers of reference strains representative of the studied strains are shown in parentheses. The scale bar indicates the number of substitutions per site.

About 95% of the studied rhizobial strains showed the ability to synthesize indole-3-acetic acid, 90% produced ACCD, 84% were able to solubilize phosphates, 63% were active producers of organic acids and siderophores, while 47% synthesized acetoin (**Supplementary Table 3**). The *in vitro* tests revealed significant differences in potential PGP traits between rhizobial strains of waste heap and the reference area origin. The rhizobial strains from the metal-polluted area were significantly more effective (80%) in acetoin production than strains from the reference area (11%), whereas more strains from the reference area (100%) could synthesize IAA than rhizobial strains from the Bolesław waste heap (80%) (**Table 3**). Quantitative analysis revealed similar concentrations of IAA and ACCD for *R. leguminosarum* bv. *trifolii* strains originating from the metal-polluted waste heap and the non-polluted reference area (**Table 3**). There were significant differences in the numbers of strains with regard to positive or negative reactions in the *in vitro* tests. Almost 50% of the *R. leguminosarum* bv. *trifolii* strains originating from the metal-polluted area appeared positive for all six tested traits, 30% were positive for four tested characteristics, and 10% were positive for five and three tested traits, while, among the rhizobia from the reference area, 11% were positive for all six as well five studied traits, 44 and 34% of the strains appeared positive, respectively, for four and three evaluated characteristics (**Supplementary Table 3**).

TABLE 3 | Potential plant-growth-promoting traits of *R. leguminosarum* bv. *trifolii* strains isolated from nodules of *T. repens* from the metal-polluted waste heap (WH) and non-polluted reference grassland (R).

Plant growth promotion trait	WH	R
Acetoin [%]	80	11*
ACCD [%]	90	89
Mean ACCD activity [μM α-ketobutyrate×mg protein^{-1}]	0.064 ± 0.09	0.062 ± 0.16
IAA [%]	80	100
Mean IAA concentration [μg×mL^{-1}]	50.17 ± 14.26	35.79 ± 18.71
Organic acids [%]	70	56
Siderophores [%]	70	56
P solubilization [%]	90	78

Significant differences between groups were marked with an asterisk.

TABLE 4 | Zinc, lead, and cadmium concentrations (mg×kg^{-1} dry soil) as well in roots and leaves of *T. repens* originating from the metal-polluted waste heap (WH) and the non-polluted reference (R) area.

	Soil			Root			Leaves		
Study area	**Zn**	**Pb**	**Cd**	**Zn**	**Pb**	**Cd**	**Zn**	**Pb**	**Cd**
WH	50,008 ± 9,356^{a}	5,008 ± 998^{a}	490 ± 26.89^{a}	2,390 ± 553$^{a\#}$	2,310 ± 118$^{a\#}$	156 ± 12.14$^{a\#}$	289 ± 56.47$^{a\#\#}$	90.18 ± 15.89$^{a\#\#}$	2.46 ± 0.45$^{a\#\#}$
R	83.41 ± 11.39^{b}	9.86 ± 0.87^{b}	2.51 ± 0.21^{b}	52.46 ± 10.59$^{b\#}$	2.88 ± 0.27$^{b\#}$	0.26 ± 0.09$^{b\#}$	39.36 ± 9.25$^{b\#\#}$	0.52 ± 0.13$^{b\#\#}$	0.01 ± 0.004$^{b\#\#}$

Values were presented as means ± SD. Significant differences between values derived from the waste heap and reference areas were marked with different letters in a superscript. Significant differences between values received from the plant organs were marked with a number sign.

Effects of *Rhizobium leguminosarum* bv. *trifolii* on Growth of White Clover

Morphological and Biochemical Parameters

The fresh and dry weight, ash content, total root length, and mean length of lateral roots as well as mean numbers of nodules of *T. repens* inoculated with *R. leguminosarum* bv. *trifolii* strains from both metal-polluted and non-polluted origin were significantly higher in comparison to non-inoculated plants (**Table 1**). No significant differences were observed for these plant-growth parameters between *T. repens* inoculated with rhizobia from the metal-polluted waste heap and from the reference area (**Figure 2**). The concentrations of photosynthetic pigments in leaves of white clover plants inoculated with rhizobial strains from the metal-polluted area and the reference area were similar, whereas the protein concentration was significantly higher in *T. repens* inoculated with rhizobia from the metal-polluted waste heap than in plants inoculated with rhizobia from the non-polluted reference area (**Table 1**).

Anatomical Analysis of *Trifolium repens* Root Nodule

Light Microscopy Examination

The root nodules of *T. repens* growing on the metal-polluted waste heap in Bolesław and the non-polluted reference area are of the indeterminate type and, by consequence, characterized by typical zonation (**Figures 3A,D**), i.e., zone of: meristem, infection thread penetration, early symbiosis, nitrogen fixation, and the senescence one. Nodules of waste heap and non-polluted reference origin plants were surrounded by peripheral tissues, which consisted of a nodule cortex, nodule endodermis, and nodule parenchyma (**Figures 3A,D**). The outer cortex and parenchyma of the nodules from the waste heap plants consisted of large, thick-walled cells, with vacuoles filled with dark precipitates (**Figure 3C**). In nodule tissues of plants from the reference area, such precipitates were not detected (**Figure 3F**). The outer cortex of both, waste heap and reference origin plant nodules, was separated from the parenchyma by a dark-stained layer of endodermis (**Figures 3C,F**). The nodules were composed of an apical persistent meristem, vascular system, nodule cortex, and the central tissue, containing nitrogen-fixing forms of rhizobia (bacteroids) (**Figures 3A,D**). The apically situated meristem consisted of small dividing cells, and, unlike the reference plant nodules, in the waste heap origin ones both, meristematic cells and adjacent cortex cells, contain large dark precipitates in vacuoles (**Figures 3B,E**). Below the meristem of waste heap origin nodules, the infection thread penetration zone (or the early symbiosis zone, zone I) was penetrated by a few, small infection threads (**Figure 3B**) in contrast to the reference origin nodules (**Figure 3E**), in which the infection thread penetration zone comprised of many large, long infection threads. Beneath, the infection thread penetration zone, infected cells containing large amyloplasts characteristic for an inter-zone II/III (**Figures 3A,D**), were observed. Next, the nitrogen-fixing zone (III) of bacteroidal tissue, infected cells with dense cytoplasm, numerous symbiosomes, and small amyloplasts situated close to the intercellular spaces were detected. In the waste heap origin plant nodules, the zone III cells were separated by non-infected cells with vacuoles filled with dark precipitates, whereas, in corresponding cells of the reference area origin nodules, such dark material in vacuoles was not detected (**Figures 3A,D**).

FIGURE 2 | The growth habit of *Trifolium repens* inoculated with *R. leguminosarum* bv. *trifolii* from the non-polluted reference Bolestraszyce area (R), the Bolesław metal-polluted waste heap area (WH), and not inoculated with rhizobia (NI).

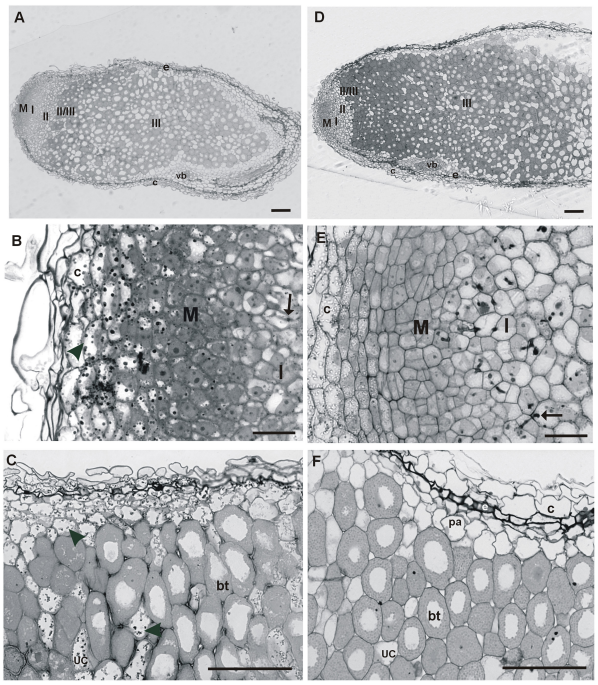

FIGURE 3 | Longitudinal sections of fully developed *T. repens* root nodules from the metal-polluted waste heap **(A–C)** and non-polluted reference **(D–F)** area. M—meristem, I—infection thread penetration zone, II—early symbiosis zone, II/III—inter-zone with large amyloplasts, III—nitrogen fixation zone; arrow—infection thread, arrowhead—precipitates in vacuoles, bt—bacteroidal tissue, c—nodule cortex, e—nodule endodermis, pa—nodule parenchyma, uc—uninfected cell, vb—vascular bundle. Scale bars on images **(A,B)** correspond to 100 μm, while scale bars on images **(C–F)** correspond to 50 μm.

Transmission Electron Microscopy Nodule Investigation

TEM analysis revealed that the three-layer cortex cells of white clover nodules were strongly vacuolated, possessed few organelles, and these originating from nodules of the Bolesław waste heap area contained vacuolar dark precipitates (**Figures 4A,G**). The nodule endodermis of reference origin plant nodules was single-layered and consisted of flat cells devoid of precipitates (**Figure 4G**), whereas the endodermis of waste heap origin plant nodules was double layered with vacuolar dark precipitates (**Figure 4A**). The waste heap origin nodule parenchyma, as well as endodermis cell walls, were substantially thicker than in the reference area origin nodules. Moreover, the endodermis of waste heap origin nodules consisted of characteristically striated suberized layers (**Figures 4A,G**).

The apically situated meristem of the white clover nodules from both, waste heap as well as reference area origin, consisted of poorly vacuolated small dividing cells surrounded by thick walls. Vacuoles of waste heap origin plant nodules contained numerous dark precipitates (**Figure 4B**). In contrast, the reference origin nodules did not contain such vacuolar inclusions (**Figure 4H**). Only in *T. repens* nodules originating from the waste heap, some vacuoles of infected cells were also filled with granular material that sometimes replaced the central vacuole.

In the nodules of waste heap clover plants, the walls of cells of the infection threads penetration zone were substantially thicker (**Figure 4C**) than these of reference origin ones (**Figure 4I**), and consisted of many layers of fibrous material with numerous membrane invaginations that were not observed in nodules of plants from the non-polluted reference area. Thick walls of infection threads can cause disturbances in the bacteria release and endocytosis that was found in fully developed infected cells of waste heap origin nodules (**Figure 4E**) but not in non-polluted reference origin ones (**Figure 4I**). However, no abnormalities in the formation of bacteroids were observed in *T. repens* nodules regardless of their waste heap or reference area origin. In nodules of both origins, the process of bacteroid degradation began early in the zone of young symbiosis, where deformations of peribacteroidal membranes and widening of peribacteroidal spaces of young bacteroids were observed (**Figure 4**).

The microscopic analysis also showed the occurrence of AMF in the roots of waste heap plants (**Figure 5**), in contrast to plants originating from the reference area where no mycorrhiza was found. Hyphae, arbuscules, and vesicles of the AMF were found in the parenchyma cells of the root cortex (**Figure 5**).

Plant Types of Toxic Metals Adaptation (Accumulator vs. Excluder) and Nutrient Soil Resources

Significantly higher concentrations of Zn, Pb, and Cd were found in the soil of the Bolesław waste heap in comparison to the non-polluted reference one. Moreover, metal concentrations in leaves and roots of *T. repens* from the metal-polluted area were significantly higher compared to those in leaves and roots of plants from the non-polluted area. Leaves of *T. repens* contained substantial concentrations of metals, but these were significantly lower than in the roots showing thus clearly an excluder strategy (**Table 4**). The concentrations of Zn were higher than those of Pb and Cd.

The soil originating from the waste heap area had a lower dry weight as well as lower concentrations of ammonium and nitrate compared with the reference area (**Table 5**). No significant differences in total Kjeldahl nitrogen were found between the two soils (**Table 5**). The soil from the waste heap contained higher concentrations of calcium and magnesium and lower concentrations of potassium and sodium than the reference grassland (**Table 5**).

Mycorrhizal Fungi Associated With *Trifolium repens* Roots

The ITS1-5.8S-ITS2 rRNA gene region length analysis revealed a low genetic diversity of mycorrhizal fungi in the rhizosphere of *T. repens* growing on the non-polluted reference area, and a richer genetic diversity (more bands, amplicons) of fungal symbionts in the rhizosphere of white clover from the metal-polluted waste heap (**Figure 6**). The roots of *T. repens* from the metal-polluted soil showed also more diverse fingerprint patterns of fungal symbionts than the root of plants from the non-polluted area. Clear dominance of one fungus fingerprint amplicon in

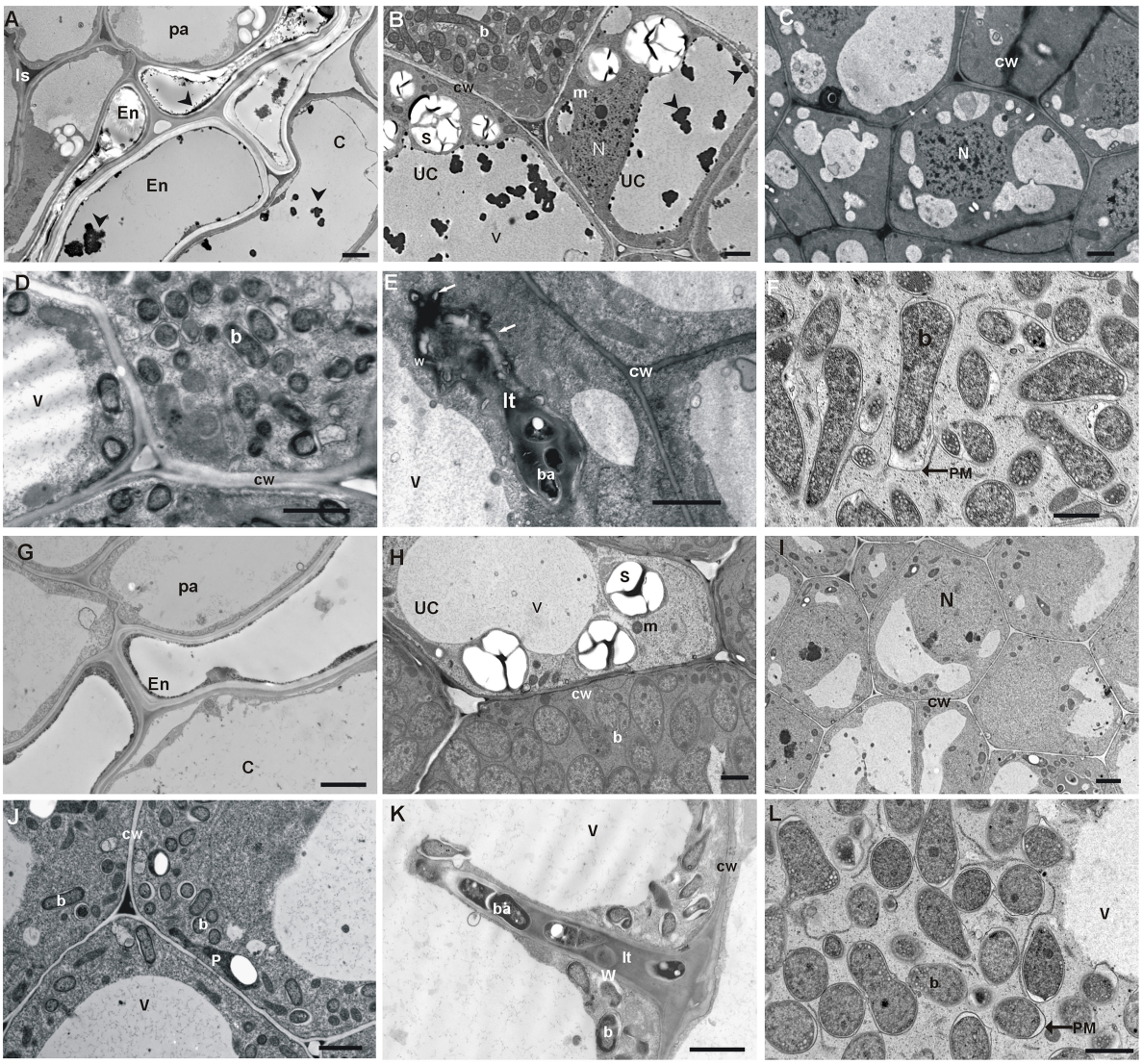

FIGURE 4 | TEM micrographs of waste heap origin *T. repens* nodules **(A–F)** and non-polluted reference ones **(G–L)**. **(A)** Nodule cortex tissues: thick-walled parenchyma (pa) cells with dark inclusion in intercellular spaces (ls), and double-layer nodule endodermis (En), and cortex cells with dark precipitates (an arrowhead) in their vacuoles. **(B)** Visible dark inclusions (an arrowhead) in central and small vacuoles of uninfected cells (uc). **(C,D)** Abnormal thick-walled cells in the thread penetration zone and the early symbiosis zone. **(E)** Abnormal thick-walled infection thread with lateral bulges (arrows) containing electron-dense depositions of matrix material. **(F)** Infected cells from the early symbiosis zone and symptoms of early bacteroids degradation (peribacteroidal membrane—PM outgrowths and widening of the peribacteroidal space (an asterisk). **(G–L)** Control nodules and typical nodule cortex tissues with thin-walled parenchyma (pa) cells; one layer of endodermis and cortex cells without inclusion in vacuoles **(G)**. **(H)** Typical vacuoles of bacteroidal tissue devoid of precipitates. **(I,J)** Typical thin-walled cells of bacteroidal tissues. **(K)** Thin-walled infection threads and bacteria endocytosis from an un-walled thread tip. **(L)** Typical bacteroid differentiation and early symptoms of bacteroids degradation. b, bacteroid; ba, bacterium; cw, cell wall; lt, infection thread; m, mitochondrion; N, nucleus; p, plastid; s, starch granule; v, vacuole; w, infection thread wall. Scale bars on images correspond to 2 μm.

the nodules of both polluted and non-polluted areas, clustering together in the dendrogram, was found (**Figure 6**).

DISCUSSION

The results of this study demonstrate that *R. leguminosarum* bv. *trifolii* bacteria isolated from nodules of *T. repens* growing on the polluted Bolesław waste heap harbor traits that can be beneficial to plant growth and health. Rhizobia, together with their host plant, which is a metal excluder, enter into a symbiosis with AMF, which have (AMF means arbuscular mycorrhizal fungi, fungi is a plural form) the potential to be adopted in phytostabilization. Chaudri et al. (1993) and Giller et al. (1998) reported that, on metal-polluted areas (Woburn, United Kingdom) *R. leguminosarum* bv. *trifolii* bacteria formed an ineffective symbiosis with clover, and were classified into only a few genotypes. In this study, we show that rhizobia from

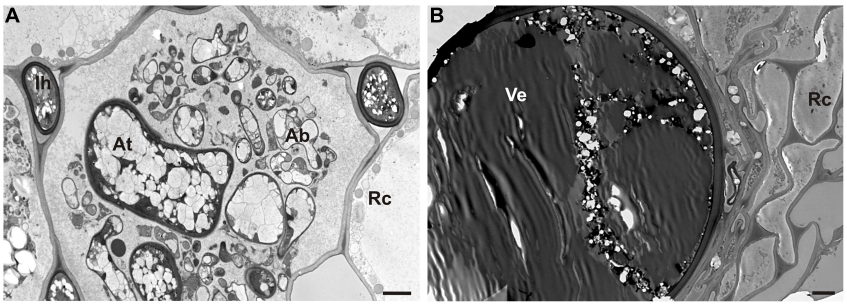

FIGURE 5 | TEM micrographs of symbiotic mycorrhizal fungi in roots of nodulated *T. repens* from the metal-polluted waste heap area. **(A)** Arbuscule (Ab) and intercellular hyphae (Ih) of arbuscular mycorrhiza fungi in root cortex cells (Rc). At, arbuscule trunk. **(B)** Visible large vesicle (Ve) inside root cortex cells (Rc). Scale bars correspond to 2 μm.

an old metal-polluted waste heap are tolerant to metals, enter into symbiosis with white clover, exhibit substantial nitrogenase activity, and are equipped with nodulation genes (i.e., *nodA*). The *nodA* gene is a member of the canonical core *nodABC* genes and encodes an enzyme that is involved in the transfer of an N-acyl residue into a lipochitooligosaccharide Nod factor, which plays a crucial role in nodule development. The Nod molecule is a host-specificity determinant that triggers, *i.a.*, the plant cell developmental program resulting in the formation of a nodule, the entry of rhizobia into plant cells, and the progress in nodule formation (Franche et al., 2009). Moreover, we found that rhizobia from the waste heap area do not differ in nodulation ability as well as nitrogenase activity from rhizobia from the non-polluted area (**Table 1** and **Supplementary Table 1**). Consequently, metal-tolerant rhizobia from the metal-polluted area can be considered as effective microsymbionts of leguminous plants on the extremely high-metal-polluted Bolesław waste heap.

Bacteria-induced improvement of plant fitness on metal-polluted soils may be achieved by direct interactions of microorganisms with metals, i.e., modifications of the cellular barrier permeability, preventing the transfer of metal ions into the cytoplasm, efflux of metal ions out of the cell, enzymatic reduction of metal ions, extracellular sequestration of metal ions by bacterial metabolites, and intracellular sequestration of ions (Ji and Silver, 1995; Silver and Phung, 1996; Bruins et al., 2000; Oleńska and Małek, 2013a) or/and by indirect beneficial effects on plant growth on metal-polluted sites (Oleńska et al., 2020a). It was demonstrated that *R. leguminosarum* bv. *trifolii* bacteria from the metal-polluted waste heap are equipped with some adaptation mechanisms to metals. For instance, they possess a gene, whose product may be potentially involved in chemiosmotic removal of Cd (Oleńska and Małek, 2013b). Moreover, it has also been shown recently that the *R. leguminosarum* bv. *trifolii* bacteria from the waste heap produce exopolysaccharides that differ substantially from the exopolysaccharides of rhizobia from the reference soil in both qualitative and quantitative compositions, suggesting a significant role of these compounds in direct interactions of rhizobia with metals (Oleńska et al., 2021). In biofilm studies, rhizobia from the waste heap show a significantly higher survival rate in non-exposed as well as metal-exposed conditions in comparison with strains from the non-polluted area, implying the adaptation of the waste heap strains to metals (Oleńska et al., 2021).

The present study shows that *R. leguminosarum* bv. *trifolii* bacteria from the metal-polluted waste heap possess traits that have the potential to indirectly improve the tolerance of their host to toxic metals through a beneficial influence on plant growth (**Table 3**). The percentage of rhizobia isolated from nodules of plants growing on the metal-polluted waste heap showing acetoin production is higher than for those from the non-polluted area. Acetoin (3-hydroxy-2-butanone) is considered as a significant inducer of induced systemic resistance (ISR) (Wang et al., 2009) and as a volatile organic compound (VOC), playing a role in the bacterial life cycle (e.g., regulation of bacterial motility, antibiotic resistance, biofilm formation) and as a compound participating in bacterial association with host plants (e.g., increases of plant biomass, fruit yield, seed production, lateral root and root hair formation, nutrient uptake, and photosynthetic activity) (Sharifi and Ryu, 2018a,b; Morcillo et al., 2020a,b). Oleńska et al. (2020b) reported that in *in vitro* studies also other bacterial taxa exhibit traits that can promote plant growth in conditions of toxic metal concentrations. For example, *Bacillus thuringiensis*, *Chryseobacterium lathyri*, *Pseudomonas putida*, *Bacillus cereus*, *Stenotrophomonas maltophilia*, which are also inhabitants of nodules of *T. repens* growing on the

TABLE 5 | Macroelements concentration in the metal-polluted waste heap (WH) and non-polluted reference (R) soils.

Concentration (in soil d.w.)	WH	R
Ca [mg×kg^{-1}]	14,250 ± 8,586	3,179 ± 596*
K [mg×kg^{-1}]	7,312 ± 2,059	22,489 ± 1,064*
Na [mg×kg^{-1}]	570 ± 117	6,327 ± 741*
Mg [mg×kg^{-1}]	7,739 ± 561	2,403 ± 465*
N_{og} [%]	0.23 ± 0.10	0.12 ± 0.05
N-NH_4^+ [mg×kg^{-1}]	3.36 ± 0.57	5.04 ± 2.25*
N-NO_3^- [mg×kg^{-1}]	0.38 ± 0.13	3.11 ± 0.53*
d.w. [%]	77.70 ± 2.77	88.93 ± 3.49*

d.w., *dry weight. Significant differences between groups were marked with an asterisk.*

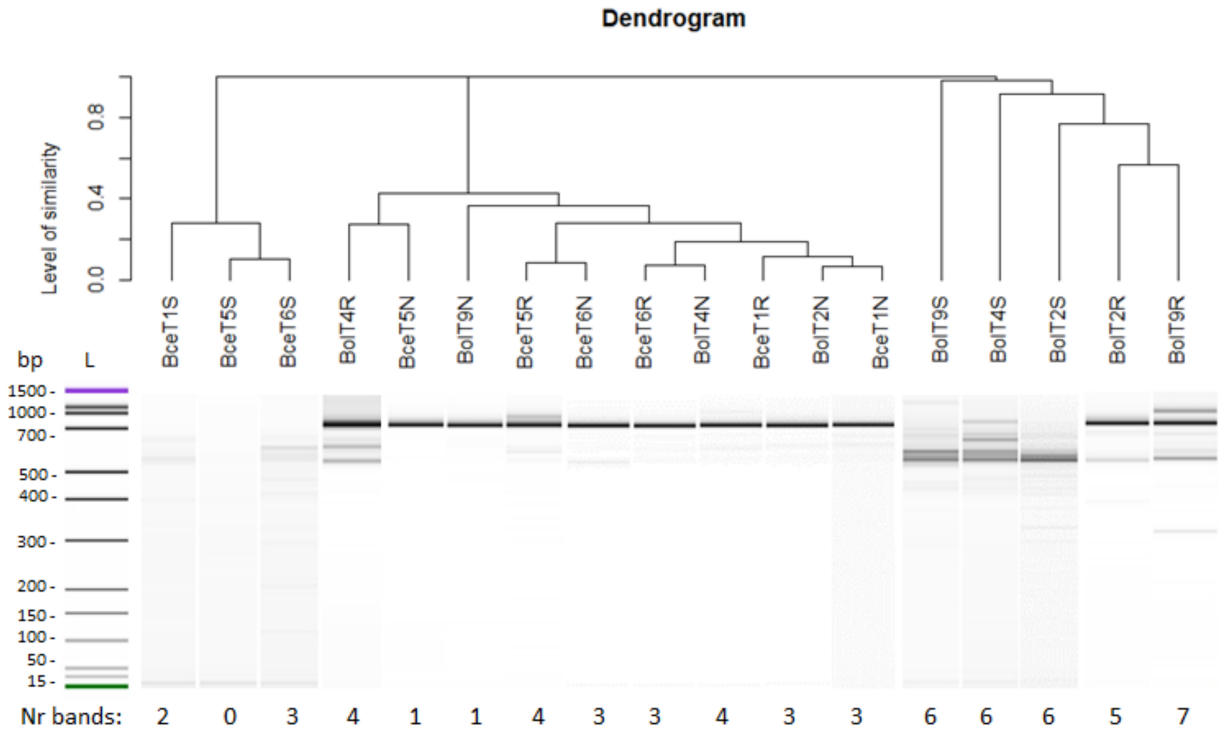

FIGURE 6 | Genetic diversity of arbuscular mycorrhizal fungi (AMF) isolated from samples of soil (S), roots (R), and nodules (N) of *T. repens* from the metal-polluted waste heap (Bol) and the non-polluted reference area (Bce).

Bolesław waste heap, showed able to, e.g., synthesize acetoin, siderophores, IAA, ACCD, fix N_2, solubilize phosphates, as well as to tolerate exposure to increased metal concentrations. Furthermore, Sánchez-López et al. (2018) revealed that, in case of high concentrations of Zn/Pb/Cd in soil, the *Methylobacterium* sp. strain Cp3 possesses potentially beneficial traits, i.e., plant growth promotion and metal tolerance. It is also known that bacteria producing siderophores, which are low molecular (400–1,500 Da) weight chelators, with a high affinity for unavailable Fe(III) and transforming it into Fe(II), supply plants with iron that is crucial for chlorophyll synthesis, maintenance of chloroplast structure and function, DNA synthesis, respiration, and is a constituent of many enzyme prosthetic groups (Rout and Sahoo, 2015; Jian et al., 2019). Shi et al. (2017) reported enhanced siderophore synthesis in *Pseudomonas aeruginosa* under Cd(II) and Zn(II) stress, while Złoch et al. (2016) showed synthesis of hydroxamate-, catecholate-, and phenolate-type siderophores production by *Streptomyces* sp. from *Betula pendula* and *Alnus glutinosa* growing in the presence of Cd(II). The *Bacillus* spp. strain PZ-1 synthesized hydroxamate-type siderophores when exposed to toxic Pb(II) concentrations and enhanced the storage of this metal in the underground tissues of *Brassica juncea* (Yu et al., 2017; Jinal et al., 2019). Auxins are key regulators of plant development, e.g., cell division, expansion, and differentiation (Paque and Weijers, 2016). Increased expression of IAA was reported, for instance, for *Pseudomonas grimontii* strain Bc09, *Pantoea vagans* strain So23, *Pseudomonas veronii* strain E03, and *Pseudomonas fluorescens* strain Oj24 that positively influenced biomass production of switchgrass under Cd(II) stress (Begum et al., 2019). Similarly, *Leifsonia xyli* strain SE134 under Cu exposure showed an enhanced IAA synthesis (Kang et al., 2017). In plants inoculated with ACCD-producing bacteria, longer roots and higher resistance to pathogens were reported (Ravanbakhsh et al., 2017; Ghosh et al., 2018; Saikia et al., 2018; Gupta and Pandey, 2019). Han et al. (2015) showed a positive effect of ACCD-producing *Pseudomonas stutzeri* A1501 strain on rice biomass. Solubilization of inorganic phosphates by bacteria is predominantly performed as the result of production of organic acids (Zhao and Zhang, 2015; Naraian and Kumari, 2017). Oves et al. (2017) revealed that, under metal stress, *Ensifer adhaerens* strain OS3 is a phosphate solubilizer and a chromium reducer. Taking into consideration that the rhizobia from the metal-polluted waste heap exhibit positive traits *in vitro*, we may assume that these bacteria may accomplish a substantial role in improving plant growth, including these able to accumulate toxic metals and being useful for remediation purposes.

Rhizobia from both, the waste heap and the reference area, influence positively the growth of *T. repens* (**Table 1** and **Figure 2**). No significant differences in chlorophyll *a* and *b*, the sum of chlorophylls, the chlorophyll *a* to *b* ratio, except protein concentration, were found between white clover inoculated with rhizobia from the waste heap and the reference area. Therefore, it can be assumed that *R. leguminosarum* bv. *trifolii* bacteria originating from the waste heap can be proposed as endophytes efficient to improve the growth of *T. repens* in conditions of high metal pollution, where

phytostabilization is required. Bidar et al. (2007) suggested that *T. repens* can be used as a phytostabilizing plant species in metal-polluted areas; Oleńska et al. (2020b) suggested that white clover has the potential to be used for phytostabilization on the Bolesław waste heap. The results of the present study demonstrate that *T. repens* accumulates metals in roots and leaves, and that the root is the predominant location of metal accumulation (**Table 4**). Light and transmission electron microscopy investigation of nodules of *T. repens* growing on the waste heap revealed morphological adaptations of plants to toxic metals that are manifested predominantly as apoplast modifications (**Figures 3**, **4**). Suberinization of the cortex cell walls, as well as the presence of granules in their vacuoles, suggest redirection of stored material (conceivably polyphenols and metals connected with organic acids) into the apoplast, what was found exclusively in plants from the waste heap and can be considered as adaptations to metal stress. Redirection of ions in extracellular (i.e., cell walls) and intracellular (i.e., vacuole) spaces is the first line of plant defense against toxic metals (Hasan et al., 2017). After entering into root cells, metal ions can form complexes with different ligands, e.g., organic acids and as carbonate, sulfate, or phosphate precipitates, which are accumulated among others in vacuoles, preventing the accumulation of free metal ions in a cytosol (Ali et al., 2013; Yan et al., 2020).

Ważny et al. (2021) claimed that mycorrhiza may serve as a significant, sufficient constituent of plant adaptations to metal-polluted areas. Mycorrhizal fungi can enhance the metal tolerance of their host plants by increasing the uptake of water, nutrients, as well as plant growth-promoting traits, e.g., by binding metals in the mycelium (Luo et al., 2014). In mycorrhized plants under metal stress, Turnau (1998) reported preferential accumulation of metals in intraradical fungal structures rather than in root tissues. Yang et al. (2016) reported a higher Pb uptake in *Robinia pseudoacacia* roots mycorrhized with *Rhizophagus intraradices* compared to non-mycorrhizal plants. Also, biomass as well as nutrients (i.e., N, P, S, and Mg) uptake were reported to increase in case of AMF presence in roots. In addition, these authors found that the presence of other mycorrhized legume herbs, i.e., *Trifolium pratense* and *Medicago sativa* increased the mycorrhization of *R. pseudoacacia*, possibly due to a common signaling pathway turned on by mycorrhiza and rhizobia. Leguminous plants also lowered soil pH, resulting in higher availability of Pb ions. Dhalaria et al. (2020) reported a substantial role of mycorrhizal fungi vesicles in the accumulation of metals as well as the synthesis of glycoprotein chelators (e.g., glomalin) by mycorrhizal fungi and enhancing the antioxidative responses in metal stress conditions. Our microscopic analyses of *T. repens* roots revealed the presence of AMF only in plants from the metal-polluted waste heap (**Figure 5**). This may suggest that these AMF fulfill an important role in the adaptation of the plants to the extreme conditions on the waste heap. Martínez-Hildago and Hirsch (2017) reported a substantial role for AMF in the selection of bacterial nodule residents, and Rodríguez-Caballero et al. (2017) showed changes in the plant bacterial communities under influence of AMF. It was also demonstrated that AMF may trigger plant metabolism, e.g., induce a systemic response through leaf protein expression (Lingua et al., 2012). Moreover, Scheublin et al. (2004) reported arbuscular mycorrhizal fungi invasion of legume nodules, and that AMF communities vary depending on plant species as well as parts of a root system.

CONCLUDING REMARKS AND FUTURE PROSPECTS

The present study shows that the Bolesław waste heap, besides the occurrence of very high metal concentrations, is also deficient in nutrients, including bioavailable forms of nitrogen, i.e., ammonium and nitrate ions (**Table 5**). It is obvious that the presence of rhizobia, effectively fixing nitrogen and reducing it into ammonia that is available to leguminous plants, is of significant importance for their hosts, inhabiting such challenging metal-polluted and nutrient-poor areas. Also, the presence of genetically diverse AMF communities in roots and nodules of *T. repens*, originating from the metal-polluted waste heap area, is promising in the function of protection of leguminous plants against toxic metals. However, the taxonomy and characteristics of these AMF still must be studied more in detail. Taking into consideration that leguminous plants, entering in symbiotic interaction with rhizobia fixing N_2, are pioneers on nutrient-poor soils (Padilla and Pugnaire, 2006; Li et al., 2007; Fterich et al., 2014; Roa-Fuentes et al., 2015), we may conclude that *R. leguminosarum* bv. *trifolii*, mycorrhizal fungi, and *T. repens*, together constituting a metaorganism (Thijs et al., 2016), can be a promising tool for phytostabilization of Zn-, Pb-, and Cd-polluted soils.

DATA AVAILABILITY STATEMENT

The data presented in the study are deposited in the NCBI GenBank repository, accession numbers MZ231019-23.

AUTHOR CONTRIBUTIONS

EO contributed to conceptualization, data curation, project administration, resources, and writing the original draft. EO, MS-R, ST, SS, and OA contributed to formal analysis. EO and JV contributed to funding acquisition. EO and ST investigated the study and contributed to software. TW, ST, SS, EO, and MS-R contributed to methodology. JV and WM contributed to supervision. MW, IS, and WM contributed to validation. EO, ST, and MS-R contributed to visualization. JV, MW, WM, and MS-R contributed to writing, reviewing, and editing. All authors contributed to the article and approved the submitted version.

FUNDING

This research was funded by the Ministry of Education and Science Republic of Poland bailout for the University of Bialystok

(EO), and was also supported by BOF Special Research Fund to EO from Hasselt University as well as by support from the UHasselt Methusalem Project 08M03VGRJ to JV. The Article Processing Charge was funded by University of Bialystok.

ACKNOWLEDGMENTS

We would like to express gratitude to Carine Put, Ann Wijgaerts, Monika Rybakowska, Renata Dudzińska, Karolina Wasilewska, Magdalena Sieśkiewicz, Marta Stępniak, Diana Stankiewicz, Anna Mroczko, Edyta Żuk-Kempa, Katarzyna A. Jadwiszczak, Agata N. Banaszek, and Barbara Łaszkiewicz-Tiszczenko.

SUPPLEMENTARY MATERIAL

The Supplementary Material for this article can be found online at: https://www.frontiersin.org/articles/10.3389/fmicb.2022.853407/full#supplementary-material

REFERENCES

Abhilash, P. C., Powell, J. R., Singh, H. B., and Singh, B. K. (2012). Plant–microbe interactions: novel applications for exploitation in multipurpose remediation technologies. *Trends Biotechnol.* 30, 416–420. doi: 10.1016/j.tibtech.2012.04.004

Ali, H., Khan, E., and Sajad, M. A. (2013). Phytoremediation of heavy metals-concepts and applications. *Chemosphere* 91, 869–881.

Ardley, J. K., Reeve, W. G., O'Hara, G. W., Yates, R. J., Dilworth, M. J., and Howieson, J. G. (2013). Nodule morphology, symbiotic specificity and association with unusual rhizobia are distinguishing features of the genus Listia within the southern African crotalarioid clade Lotononiss.l. *Ann. Bot.* 112, 1–15. doi: 10.1093/aob/mct095

Association of Official Analytical Chemist (AOAC) (1990). *Official Methods of Analysis*, 15th Edn. Washington D.C: Association of Official Analytical Chemist.

Begum, N., Hu, Z., Cai, Q., and Lou, L. (2019). Influence of PGPB inoculation on HSP70 and HMA3 gene expression in switchgrass under cadmium stress. *Plants* 8:504. doi: 10.3390/plants8110504

Belimov, A. A., Hontzeas, N., Safronova, V. I, Demchinskaya, S. V., Piluzza, G., Bullitta, S., et al. (2005). Cadmium-tolerant plant growth-promoting bacteria associated with the roots of Indian mustard (*Brassica juncea* L. Czern.). *Soil Biol. Biochem.* 37, 241–250.

Bidar, G., Garçon, G., Pruvot, C., Dewaele, D., Cazier, F., Douay, F., et al. (2007). Behavior of *Trifolium repens* and *Lolium perenne* growing in a heavy metal contaminated field: plant metal concentration and phytotoxicity. *Environ. Pollut.* 147, 546–553. doi: 10.1016/j.envpol.2006.10.013

Bradford, M. M. (1976). A rapid and sensitive method for the quantitation of microgram quantities of protein utilizing the principle of protein-dye binding. *Anal. Biochem.* 7, 248–254. doi: 10.1006/abio.1976.9999

Bruins, M. R., Kapil, S., and Oehme, F. W. (2000). Microbial resistance to metals in the environment. *Ecotoxicol. Environ. Saf.* 45, 198–207.

Chaudri, A. M., McGrath, S. P., Giller, K. E., Rietz, E., and Sauerbeck, D. (1993). Enumeration of indigenous *Rhizobium leguminosarum* bv. trifolii in soils previously treated with metal-contaminated sewage sludge. *Soil Biol. Biochem.* 25, 301–309.

Cunningham, J. E., and Kuiack, C. (1992). Production of citric and oxalic acids and solubilization of calcium phosphate by *Penicillium bilaii*. *Appl. Environ. Microbiol.* 58, 1451–1458.

Dhalaria, R., Kumar, D., Kumar, H., Nepovimova, E., Kuča, K., Islam, M. T., et al. (2020). Arbuscular mycorrhizal fungi as potential agents in ameliorating heavy metal stress in plants. *Agronomy* 10:815. doi: 10.3390/agronomy10060815

Franche, C., Lindström, K., and Elmerich, C. (2009). Nitrogen-fixing bacteria associated with leguminous and non-leguminous plants. *Plant Soil* 321, 35–59. doi: 10.1007/s11104-008-9833-8

Fterich, A., Mahdhi, M., and Mars, M. (2014). The effects of *Acacia tortilis* subsp. raddiana, soil texture and soil depth on soil microbial and biochemical characteristics in arid zones of Tunisia. *Land Degrad. Dev.* 25, 143–152. doi: 10.1002/ldr.1154

Ghosh, P. K., De, T. K., and Maiti, T. K. (2018). "Role of ACC deaminase as a stress ameliorating enzyme of plant growth-promoting rhizobacteria useful in stress agriculture: a review," in *Role of Rhizospheric Microbes in Soil: Stress Management and Agricultural Sustainability*, ed. V. S. Meena (Singapore: Springer), 57–106. doi: 10.1007/978-981-10-8402-7_3

Giller, K. E., Witter, E., and McGrath, S. P. (1998). Toxicity of heavy metals to microorganisms and microbial processes in agricultural soils: a review. *Soil Biol. Biochem.* 30, 1389–1414. doi: 10.1016/S0038-0717(97)00270-8

Gupta, S., and Pandey, S. (2019). ACC deaminase producing bacteria with multifarious plant growth promoting traits alleviates salinity stress in french bean (*Phaseolus vulgaris*) plants. *Front. Microbiol.* 10:1506. doi: 10.3389/fmicb.2019.01506

Hall, T. A. (1999). BioEdit: a user-friendly biological sequence alignment editor and analysis program for Windows 95/98/NT. *Nucleic Acid Symposium Series* 41, 95–98.

Han, Y., Wang, R., Yang, Z., Zhan, Y., Ma, Y., Ping, S., et al. (2015). 1-Aminocyclopropane-1-carboxylate deaminase from *Pseudomonas stutzeri* A1501 facilitates the growth of rice in the presence of salt or heavy metals. *J. Microbiol. Biotechnol.* 25, 1119–1128. doi: 10.4014/jmb.1412.12053

Hasan, M. K., Cheng, Y., Kanwar, M. K., Chu, X.-Y., Ahammed, G. J., and Qi, Z.-Y. (2017). Responses of plant proteins to heavy metal stress – a review. *Front. Plant Sci.* 8:1492. doi: 10.3389/fpls.2017.01492

Haskett, T. L., Knights, H. E., Jorrin, B., Mendes, M. D., and Poole, P. S. (2021). A simple *in situ* assay to assess plant-associative bacterial nitrogenase activity. *Front. Microbiol.* 12:690439. doi: 10.3389/fmicb.2021.690439

Haukka, K., Lindström, K., and Young, J. P. W. (1998). Three phylogenetic groups of nodA and nifH genes in *Sinorhizobium* and *Mesorhizobium* isolates from leguminous trees growing in Africa and Latin America. *Appl. Environ. Microbiol.* 64, 419–426.

Hayat, R., Ali, S., Amara, U., Khalid, R., and Ahmed, I. (2010). Soil beneficial bacteria and their role in plant growth promotion: a review. *Ann. Microbiol.* 60, 579–598. doi: 10.1007/s13213-010-0117-1

Jaishankar, M., Tseten, T., Anbalagan, N., Mathew, B. B., and Beeregowda, K. N. (2014). Toxicity, mechanism and health effects of some heavy metals. *Interdiscip. Toxicol.* 7, 60–72. doi: 10.2478/intox-2014-0009

Ji, G., and Silver, S. (1995). Bacterial resistance mechanisms for heavy metals of environmental concern. *J. Ind. Microbiol.* 14, 61–75.

Jian, L., Bai, X., Zhang, H., Song, X., and Li, Z. (2019). Promotion of growth and metal accumulation of alfalfa by coinoculation with *Sinorhizobium* and *Agrobacterium* under copper and zinc stress. *PeerJ* 7:e6875. doi: 10.7717/peerj.6875

Jinal, H. N., Gopi, K., Prittesh, P., Kartik, V. P., and Amaresan, N. (2019). Phytoextraction of iron from contaminated soils by inoculation of iron-tolerant plant growth-promoting bacteria in *Brassica juncea* L. Czern. *Environ. Sci. Pollut. Res.* 26, 32815–32823. doi: 10.1007/s11356-019-06394-2

Johnston-Monje, D., and Lopez Mejia, J. (2020). Botanical microbiomes on the cheap: inexpensive molecular fingerprinting methods to study plant-associated communities of bacteria and fungi. *Appl. Plant Sci.* 8:e11334. doi: 10.1002/aps3.11334

Kang, S.-M., Waqas, M., Hamayun, M., Asaf, S., Khan, A. L., Kim, A.-Y., et al. (2017). Gibberellins and indole-3-acetic acid producing rhizospheric bacterium *Leifsonia xyli* SE134 mitigates the adverse effects of copper-mediated stress on tomato. *J. Plant Int.* 12, 373–380. doi: 10.1080/17429145.2017.1370142

Karaś, K., Zioła-Frankowska, A., Bartoszewicz, M., Krzyśko, G., and Frankowski, M. (2021). Investigation of chocolate types on the content of selected metals and non-metals determined by ICP-OES analytical technique. *Food Addit. Contam. Part A* 38, 293–303. doi: 10.1080/19440049.2020.1853821

Karnovsky, M. J. (1965). A formaldehyde-glutaraldehyde fixative of high osmolality for use in electron microscopy. *J. Cell Biol.* 27, 137A–138A.

Kumar, S., Stecher, G., and Tamura, K. (2016). MEGA7: molecular evolutionary genetics analysis version 7.0 for bigger datasets. *Mol. Biol. Evol.* 33, 1870–1874. doi: 10.1093/molbev/msw054

Lakzian, A., Murphy, P., and Giller, K. E. (2007). Transfer and loss of naturally occurring plasmids among isolates of *Rhizobium leguminosarum* bv. *viciae* in heavy metal contaminated soils. *Soil Biol. Biochem.* 39, 1066–1077. doi: 10.1016/j.soilbio.2006.12.018

Lakzian, A., Murphy, P., Turner, A., Beynon, J. L., and Giller, K. E. (2002). *Rhizobium leguminosarum* bv. *viciae* populations in soils with increasing heavy metal contamination: abundance, plasmid profiles, diversity and metal tolerance. *Soil Biol. Biochem.* 34, 519–529. doi: 10.1016/S0038-0717(01)00210-3

Lange, B., van der Ent, A., Baker, A. J. M., Echevarria, G., Mahy, G., and Malaise, F. (2017). Copper and cobalt accumulation in plants: a critical assessment of the current state of knowledge. *New Phytol.* 213, 537–551. doi: 10.1111/nph.14175

Li, J., Fang, X., Jia, J., and Wang, G. (2007). Effect of legume species introduction to early abandoned field on vegetation development. *Plant Ecol.* 191, 1–9. doi: 10.1007/s11258-006-9209-1

Li, L., Yang, A., and Zhao, Z. (2005). Seasonality of arbuscular mycorrhizal symbiosis and dark septate endophytes in a grassland site in southwest China. *FEMS Microbiol. Ecol.* 54, 367–373. doi: 10.1016/j.femsec.2005.04.011

Lingua, G., Bona, E., Todeschini, V., Cattaneo, C., Marsano, F., Berta, G., et al. (2012). Effects of heavy metals and arbuscular mycorrhiza on the leaf proteome of a selected poplar clone: a time course analysis. *PLoS One* 7:e38662. doi: 10.1371/journal.pone.0038662

Łotocka, B., Kopcińska, J., and Golinowski, W. (1997). Morphogenesis of root nodules in white clover. I. effective root nodules induced by the wild type *Rhizobium leguminosarum* biovar. *trifolii*. *Acta Soc. Bot. Polon.* 66, 273–292.

Lowry, O. H., Rosebrough, N. J., Farr, A. L., and Randall, R. J. (1951). Protein measurement with the Folin phenol reagent. *J. Biol. Chem.* 193, 265–275. doi: 10.1016/S0021-9258(19)52451-6

Luo, Z.-B., Wu, C. H., Zhang, C. H., Li, H., Lipka, U., and Polle, A. (2014). The role of ectomycorrhizas in heavy metal stress tolerance of host plants. *Environ. Experim. Bot.* 108, 47–62. doi: 10.1016/j.envexpbot.2013.10.018

Macnair, M. R. (1997). "The evolution of plants in metal-contaminated environments," in *Environmental Stress, Adaptation and Evolution*, eds R. Bijlsma and V. Loeschcke (Basel: Experientia, Birkhäuser).

Martínez-Hildago, P., and Hirsch, A. M. (2017). The nodule microbiome: N2 – fixing rhizobia do not live alone. *Phytobiomes* 1, 70–82. doi: 10.1094/PBIOMES-12-16-0019-RVW

Michelland, R. J., Dejean, S., Combes, S., Fortun-Lamothe, L., and Cauquil, L. (2009). StatFingerprints: a friendly graphical interface program for processing and analysis of microbial fingerprint profiles. *Mol. Ecol. Resour.* 9, 1359–1363. doi: 10.1111/j.1755-0998.2009.02609.x

Morcillo, R. J. L., Singh, S. K., He, D., An, G., Vílchez, J. I., Tang, K., et al. (2020a). Rhizobacterium-derived diacetyl modulates plant immunity in a phosphate-dependent manner. *EMBO J.* 39:e102602. doi: 10.15252/embj.2019102602

Morcillo, R. J. L., Singh, S. K., He, D., Vílchez, J. I., Kaushal, R., Wang, W., et al. (2020b). Bacteria-derived diacetyl enhances *Arabidopsis* phosphate starvation responses partially through the DELLA-dependent gibberellin signaling pathway. *Plant Signal. Behav.* 15:1740872. doi: 10.1080/15592324.2020.1740872

Naraian, R., and Kumari, S. (2017). "Microbial production of organic acids," in *Microbial Functional Foods and Nutraceuticals*, eds V. K. Gupta, H. Treichel, V. Shapaval, L. A. de Oliveira, and M. G. Tuohy (Hoboken, NJ: Wiley Online Library), 93–121. doi: 10.1002/9781119048961.ch5

Nautiyal, C. S. (1999). An efficient microbiological growth medium for screening phosphate solubilizing microorganisms. *FEMS Microbiol. Lett.* 170, 265–270.

Nikalje, G. C., and Suprasanna, P. (2018). Coping with metal toxicity – cues from halophytes. *Front. Plant Sci.* 9:777. doi: 10.3389/fpls.2018.00777

Nowak, T., Kapusta, P., Jędrzejczyk-Korycińska, M., Szarek-Łukaszewska, G., and Godzik, B. (2011). *The Vascular Plants of the Olkusz Ore-bearing Region*. Krakow: Szafer Institute of Botany Polish Academy of Sciences.

Oleńska, E., and Małek, W. (2013a). Mechanisms of heavy metal resistance in bacteria. *Adv. Microbiol.* 52, 363–371.

Oleńska, E., and Małek, W. (2013b). Sequence analysis of hypothetical lysine exporter genes of *Rhizobium leguminosarum* bv. *trifolii* from calamine old waste heaps and their evolutionary history. *Curr. Microbiol.* 66, 493–498. doi: 10.1007/s00284-013-0303-z

Oleńska, E., and Małek, W. (2015). Genetic differentiation of *Trifolium repens* microsymbionts deriving from Zn–Pb waste-heap and control area in Poland. *J. Basic Microbiol.* 55, 462–470. doi: 10.1002/jobm.201400604

Oleńska, E., and Małek, W. (2019). Genomic polymorphism of *Trifolium repens* root nodule symbionts from heavy metal-abundant 100-year-old waste heap in southern Poland. *Arch. Microbiol.* 201, 1405–1414. doi: 10.1007/s00203-019-01708-x

Oleńska, E., Małek, W., Wójcik, M., Swiecicka, I., Thijs, S., and Vangronsveld, J. (2020a). Beneficial features of plant growth-promoting rhizobacteria for improving plant growth and health in challenging conditions: a methodological review. *Sci. Tot. Environ.* 743:140682. doi: 10.1016/j.scitotenv.2020.140682

Oleńska, E., Imperato, V., Małek, W., Włostowski, T., Wójcik, M., Swiecicka, I., et al. (2020b). Trifolium repens-associated bacteria as a potential tool to facilitate phytostabilization of zinc and lead polluted waste heaps. *Plants* 9:1002. doi: 10.3390/plants9081002

Oleńska, E., Małek, W., Kotowska, U., Wydrych, J., Polińska, W., Swiecicka, I., et al. (2021). Exopolysaccharide carbohydrate structure and biofilm formation by *Rhizobium leguminosarum* bv. *trifolii* strains inhabiting nodules of *Trifolium repens* growing on an old Zn–Pb–Cd-polluted waste heap area. *Int. J. Mol. Sci.* 22:2808. doi: 10.3390/ijms22062808

Oves, M., Khan, M. S., and Qari, H. A. (2017). *Ensifer adhaerens* for heavy metal bioaccumulation, biosorption, and phosphate solubilization under metal stress condition. *J. Taiwan Instit. Chem. Eng.* 80, 540–552. doi: 10.1016/j.jtice.2017.08.026

Padilla, F. M., and Pugnaire, F. I. (2006). The role of nurse plants in the restoration of degraded environments. *Front. Ecol. Environ.* 4:196–202. doi: 10.1890/1540-92952006004

Pande, A., Pandey, P., Mehra, S., Singh, M., and Kaushik, S. (2017). Phenotypic and genotypic characterization of phosphate solubilizing bacteria and their efficiency on the growth of maize. *J. Genet. Eng. Biotechnol.* 15, 379–391. doi: 10.1016/j.jgeb.2017.06.005

Paque, S., and Weijers, D. (2016). Auxin: the plant molecule that influences almost anything. *BMC Biol.* 14:67. doi: 10.1186/s12915-016-0291-0

Patten, C. L., and Glick, B. R. (2002). Role of *Pseudomonas putida* indoleacetic acid in development of host plant root system. *Appl. Environ. Microbiol.* 68, 3795–3801. doi: 10.1128/AEM.68.8.3795-3801.2002

Penrose, D. M., and Glick, B. R. (2004). "Quantifying the impact of ACC deaminase-containing bacteria on plants," in *Plant Surface Microbiology*, eds A. Varma, L. Abbott, D. Werner, and R. Hampp (Berlin: Springer-Verlag).

Pikovskaya, R. I. (1948). Mobilization of phosphorus in soil connection with the vital activity of some microbial species. *Microbiology* 17, 362–370.

Ranjard, L., Poly, F., Lata, J.-C., Mougel, C., Thioulouse, J., and Nazaret, S. (2001). Characterization of bacterial and fungal soil communities by automated ribosomal intergenic spacer analysis fingerprints: biological and methodological variability. *Appl. Environ. Microbiol.* 67, 4479–4487.

Ravanbakhsh, M., Sasidharan, R., Voesenek, L. A., Kowalchuk, G. A., and Jousset, A. (2017). ACC deaminase-producing rhizosphere bacteria modulate plant responses to flooding. *J. Ecol.* 105, 979–986. doi: 10.1111/1365-2745.12721

Roa-Fuentes, L. L., Martínez-Garza, C., Etchevers, J., and Campo, J. (2015). Recovery of soil and in a tropical pasture: passive and active restoration. *Land Degrad. Dev.* 26, 201–210. doi: 10.1002/ldr.2197

Rodríguez-Caballero, G., Caravaca, F., Fernández-González, A. J., Alguacil, M. M., Fernández-López, M., and Roldán, A. (2017). Arbuscular mycorrhizal fungi inoculation mediated changes in rhizosphere bacterial community structure while promoting revegetation in a semiarid ecosystem. *Sci. Total Environ.* 584, 838–848. doi: 10.1016/j.scitotenv.2017.01.128

Romick, T. L., and Fleming, H. P. (1998). Acetoin production as an indicator of growth and metabolic inhibition of *Listeria monocytogenes*. *J. Appl. Microbiol.* 84, 18–24.

Rout, G. R., and Sahoo, S. (2015). Role of iron in plant growth and metabolism. *Rev. Agric. Sci.* 3, 1–24. doi: 10.7831/ras.3.1

Saikia, J., Sarma, R. K., Dhandia, R., Yadav, A., Bharali, R., Gupta, V. K., et al. (2018). Alleviation of drought stress in pulse crops with ACC deaminase producing

rhizobacteria isolated from acidic soil of Northeast India. *Sci. Rep.* 8:3560. doi: 10.1038/s41598-018-21921-w

Sánchez-López, A. S., Pintelon, I., Stevens, V., Imperato, V., Timmermans, J.-P., González-Chávez, C., et al. (2018). Seed endophyte microbiome of *Crotalaria pumila* unpeeled: identification of plant-beneficial Methylobacteria. *Int. J. Mol. Sci.* 19:291. doi: 10.3390/ijms19010291

Scheublin, T. R., Ridgway, K. P., Young, J. P. W., and van der Heijden, M. G. A. (2004). Nonlegumes, legumes, and root nodules harbor different arbuscular mycorrhizal fungal communities. *Appl. Environ. Microbiol.* 70, 6240–6246.

Schlegel, H., Gottschalk, G., and Von Bartha, R. (1961). Formation and utilization of poly-β-hydroxybutyric acid by knallgas bacteria (Hydrogenomonas). *Nature* 191, 463–465.

Schwyn, B., and Neilands, J. (1987). Universal chemical assay for the detection and determination of siderophores. *Anal. Biochem.* 160, 47–56.

Seefeldt, L. C., Yang, Z. Y., Duval, S., and Dean, D. R. (2013). Nitrogenase reduction of carbon-containing compounds. *Biochim. Biophys. Acta* 1827, 1102–1111. doi: 10.1016/j.bbabio.2013.04.003

Shackira, A. M., and Puthur, J. T. (2019). "Phytostabilization of heavy metals: understanding of principles and practices," in *Plant-Metal Interactions*, eds S. Srivastava, A. Srivastava, and P. Suprasanna (Cham: Springer), 263–282. doi: 10.1007/978-3-030-20732-8_13

Sharifi, R., and Ryu, C. M. (2018a). Sniffing bacterial volatile compounds for healthier plants. *Curr. Opin. Plant Biol.* 44, 88–97. doi: 10.1016/j.pbi.2018.03.004

Sharifi, R., and Ryu, C. M. (2018b). Revisiting bacterial volatile-mediated plant growth promotion: lessons from the past and objectives for the future. *Ann. Bot.* 122, 349–358. doi: 10.1093/aob/mcy108

Shi, P., Zing, Z., Zhang, U., and Chai, T. (2017). Effect of heavy-metal on synthesis of siderophores by *Pseudomonas aeruginosa* ZGKD3. *Earth Environ. Sci.* 52:012103. doi: 10.1088/1755-1315/52/1/012103

Silver, S., and Phung, L. T. (1996). Bacterial heavy metal resistance: new surprises. *Annu. Rev. Microbiol.* 50, 753–789.

Staal, M., Lintel-Hekkert, S. T., Harren, F., and Stal, L. (2001). Nitrogenase activity in cyanobacteria measured by the acetylene reduction assay: a comparison between batch incubation and online monitoring. *Environ. Microbiol.* 3, 343–351.

Sujkowska-Rybkowska, M., Borucki, W., and Znojek, E. (2012). Structural changes in *Medicago truncatula* root nodules caused by short-term aluminum stress. *Symbiosis* 58, 161–170.

Tchounwou, P. B., Yedjou, C. G., Patlolla, A. K., and Sutton, D. J. (2012). "Heavy metal toxicity and the environment," in *Molecular, Clinical and Environmental Toxicology*, ed. A. Luch (Basel: Springer).

Thijs, S., and Vangronsveld, J. (2015). "Rhizoremediation," in *Principles of Plant-microbe Interactions*, ed. B. Lugtenberg (Cham: Springer), doi: 10.1007/978-3-319-08575-3_29

Thijs, S., Sillen, W., Rineau, F., Weyens, N., and Vangronsveld, J. (2016). Towards an enhanced understanding of plant–microbiome interactions to improve phytoremediation: engineering the metaorganism. *Front. Microbiol.* 7:341. doi: 10.3389/fmicb.2016.00341

Turnau, K. (1998). Heavy metal content and localization in mycorrhizal Euphorbia cyparissias from zinc wastes in southern Poland. *Acta Soc. Bot. Polon.* 67, 105–113.

Valledor, L., Escandon, M., Meijon, M., Nukarinen, E., Cañal, M. J., and Weckwerth, W. (2014). A universal protocol for the combined isolation of metabolites, DNA, long RNAs, small RNAs, and proteins from plants and microorganisms. *Plant J.* 79, 173–180. doi: 10.1111/tpj.12546

Viehweger, K. (2014). How plants cope with heavy metals. *Bot. Stud.* 55:35. doi: 10.1186/1999-3110-55-35

Walker, C. H., Sibly, R. M., Hopkinm, S. P., and Peakall, D. B. (2012). *Principles of Ecotoxicology*. Boca Raton, FL: CRC Press Taylor and Francis Group.

Wang, J., Xiong, Y., Zhang, J., Lu, X., and Wei, G. (2020). Naturally selected dominant weeds as heavy metal accumulators and excluders assisted by rhizosphere bacteria in a mining area. *Chemosphere* 243:125365. doi: 10.1016/j.chemosphere.2019.125365

Wang, S., Huijun, W., Junqing, Q., Lingli, M., Jun, L., Yanfei, X., et al. (2009). Molecular mechanism of plant growth promotion and induced systemic resistance to tobacco mosaic virus by *Bacillus spp*. *J. Microbiol. Biotechnol.* 19, 1250–1258.

Ważny, R., Rozpądek, P., Domka, A., Jędrzejczyk, R., Nosek, M., Hubalewska-Mazgaj, et al. (2021). The effect of endophytic fungi on growth and nickel accumulation in *Noccaea hyperaccumulators*. *Sci. Tot. Environ.* 768:144666. doi: 10.1016/j.scitotenv.2020.144666

Wellburn, A. R. (1994). The spectra determination of chlorophyll a and b, as well as total carotenoids, using various solvents with spectrophotometers of different resolution. *J. Plant Physiol.* 144, 307–313. doi: 10.1016/S0176-1617(11)81192-2

Wellburn, A. R., and Lichtenthaler, H. (1984). "Formulae and program to determine total carotenoids and chlorophylls A and B of leaf extracts in different solvents," in *Advances in Photosynthesis Research. Advances in Agricultural Biotechnology*, ed. C. Sybesma (Dordrecht: Springer), doi: 10.1007/978-94-017-6368-4_3

Weyens, N., van der Lelie, D., Taghavi, S., and Vangronsveld, J. (2009a). Phytoremediation: plant-endophyte partnerships take the challenge. *Curr. Opin. Biotechnol.* 20, 248–254. doi: 10.1016/j.copbio.2009.02.012

Weyens, N., van der Lelie, D., Taghavi, S., Newman, L., and Vangronsveld, J. (2009b). Exploiting plant–microbe partnerships to improve biomass production and remediation. *Trends Biotechnol.* 27, 591–598. doi: 10.1016/j.tibtech.2009.07.006

Wójcik, M., Gonnelli, C., Selvi, F., Dresler, S., Rostański, A., and Vangronsveld, J. (2017). Metallophytes of serpentine and calamine soils – their unique ecophysiology and potential for phytoremediation. *Adv. Bot. Res.* 83, 1–42.

Wójcik, M., Sugier, P., and Siebielec, G. (2014). Metal accumulation strategies in plants spontaneously inhabiting Zn-Pb waste deposits. *Sci. Tot. Environ.* 487, 313–322. doi: 10.1016/j.scitotenv.2014.04.024

Yan, A., Wang, Y., Tan, S. N., Mohd Yusof, M. L., Ghosh, S., and Chen, Z. (2020). Phytoremediation: a promising approach for revegetation of heavy metal-polluted land. *Front. Plant Sci.* 11:359. doi: 10.3389/fpls.2020.00359

Yang, Y., Liang, Y., Han, X., Chiu, T.-Y., Ghosh, A., Chen, H., et al. (2016). The roles of arbuscular mycorrhizal fungi (AMF) in phytoremediation and tree-herb interactions in Pb contaminated soil. *Sci. Rep.* 6:20469. doi: 10.1038/srep20469

Yu, S., Teng, C. H., Bai, X., Liang, J., Song, T., Dong, L., et al. (2017). Optimization of siderophore production by *Bacillus* sp. PZ-1 and its potential enhancement of phytoextration of Pb from soil. *J. Microbiol. Biotechnol.* 27, 1500–1512. doi: 10.4014/jmb.1705.05021

Zgorelec, Z., Bilandzija, N., Knez, K., Galic, M., and Zuzul, S. (2020). Cadmium and mercury phytostabilization from soil using Miscanthus × giganteus. *Sci. Rep.* 10:6685. doi: 10.1038/s41598-020-63488-5

Zhao, L., and Zhang, Y. (2015). Effects of phosphate solubilization and phytohormone production of *Trichoderma asperellum* Q1 on promoting cucumber growth under salt stress. *J. Integr. Agric.* 14, 1588–1597.

Złoch, M., Thiem, D., Gadzała-Kopciuch, R., and Hrynkiewicz, K. (2016). Synthesis of siderophores by plant-associated metallotolerant bacteria under exposure to $Cd2^{+}$. *Chemosphere* 156, 312–325.

Conflict of Interest: The authors declare that the research was conducted in the absence of any commercial or financial relationships that could be construed as a potential conflict of interest.

Publisher's Note: All claims expressed in this article are solely those of the authors and do not necessarily represent those of their affiliated organizations, or those of the publisher, the editors and the reviewers. Any product that may be evaluated in this article, or claim that may be made by its manufacturer, is not guaranteed or endorsed by the publisher.

frontiers | Frontiers in Microbiology

ORIGINAL RESEARCH
published: 26 April 2022
doi: 10.3389/fmicb.2022.852697

Proteomic Perspective of Cadmium Tolerance in *Providencia rettgeri* Strain KDM3 and Its *In-situ* Bioremediation Potential in Rice Ecosystem

Darshana A. Salaskar[1], Mahesh K. Padwal[2], Alka Gupta[3], Bhakti Basu[2]* and Sharad P. Kale[1]*

[1] Nuclear Agriculture and Biotechnology Division, Bhabha Atomic Research Centre, Mumbai, India, [2] Molecular Biology Division, Bhabha Atomic Research Centre, Mumbai, India, [3] Applied Genomics Section, Bhabha Atomic Research Centre, Mumbai, India

OPEN ACCESS

Edited by:
Krishnendu Pramanik, Visva-Bharati University, India

Reviewed by:
Huihui Du, Hunan Agricultural University, China
Xiaoqing Liu, Biotechnology Research Institute (CAAS), China
Yogesh Mishra, Banaras Hindu University, India

***Correspondence:**
Darshana A. Salaskar
salaskar@barc.gov.in
Bhakti Basu
bbasu@barc.gov.in

Specialty section:
This article was submitted to Terrestrial Microbiology, a section of the journal Frontiers in Microbiology

Received: *11 January 2022*
Accepted: *16 March 2022*
Published: *26 April 2022*

Citation:
Salaskar DA, Padwal MK, Gupta A, Basu B and Kale SP (2022) Proteomic Perspective of Cadmium Tolerance in Providencia rettgeri Strain KDM3 and Its In-situ Bioremediation Potential in Rice Ecosystem. Front. Microbiol. 13:852697. doi: 10.3389/fmicb.2022.852697

In this study, a multi-metal-tolerant natural bacterial isolate *Providencia rettgeri* strain KDM3 from an industrial effluent in Mumbai, India, showed high cadmium (Cd) tolerance. *Providencia rettgeri* grew in the presence of more than 100 ppm (880 μM) Cd (LD_{50} = 100 ppm) and accumulated Cd intracellularly. Following Cd exposure, a comparative proteome analysis revealed molecular mechanisms underlying Cd tolerance. Among a total of 69 differentially expressed proteins (DEPs) in Cd-exposed cells, *de novo* induction of *ahpCF* operon proteins and L-cysteine/L-cystine shuttle protein FliY was observed, while Dps and superoxide dismutase proteins were overexpressed, indicating upregulation of a robust oxidative stress defense. ENTRA1, a membrane transporter showing homology to heavy metal transporter, was also induced *de novo*. In addition, the protein disaggregation chaperone ClpB, trigger factor, and protease HslU were also overexpressed. Notably, 46 proteins from the major functional category of energy metabolism were found to be downregulated. Furthermore, the addition of *P. rettgeri* to Cd-spiked soil resulted in a significant reduction in the Cd content [roots (11%), shoot (50%), and grains (46%)] of the rice plants. Cd bioaccumulation of *P. rettgeri* improved plant growth and grain yield. We conclude that *P. rettgeri*, a highly Cd-tolerant bacterium, is an ideal candidate for *in-situ* bioremediation of Cd-contaminated agricultural soils.

Keywords: cadmium, *Providencia rettgeri*, *Oryza sativa*, bioremediation, proteomics

INTRODUCTION

Heavy metals are metallic elements with relatively high densities and are toxic at low concentrations. Historically, anthropogenic activities such as ore mining and industrialization are directly associated with environmental pollution with heavy metals worldwide (Ozaki et al., 2019; Hubeny et al., 2021). Since the heavy metals are naturally present in the earth's crust, they cannot be destroyed or degraded, but can only be transformed into a less toxic form (González Henao and Ghneim-Herrera, 2021). They enter the human body *via* polluted air, contaminated food, or drinking water. While a few are essential in trace quantities as cofactors for different enzymes,

the rest are non-essential. Nonessential heavy metals, including cadmium (Cd), are especially concerning as they pose a serious threat to human life (Rafati Rahimzadeh et al., 2017).

Cadmium is the 7th most toxic element (Fay and Mumtaz, 1996); however, it has a prolonged biological half-life of about 10–30 years (Berglund et al., 2015). At the molecular level, Cd induces reactive oxygen species (ROS) that further cause DNA damage and mutations, disrupt RedOx potential, inactivate the antioxidant enzymes, culminating in disruptions of a wide range of cellular functions such as respiration, oxidative phosphorylation, cell proliferation, etc. (Rafati Rahimzadeh et al., 2017). Some of the reported deleterious manifestations of Cd poisoning include lung damage, renal dysfunction, and bone toxicity (Kaji, 2012). A plant-based diet is the predominant route of entry of Cd into the food chain. Rice is an economically important crop in Asia and the staple food for over half of the world's population (Wang et al., 2019; Zhao and Wang, 2020). However, it is a major source of both arsenic (As) and Cd since rice plants have a higher ability to accumulate these heavy metals compared to other cereal grains (Sui et al., 2018). Since Cd(II) ionic form of Cd is highly soluble in soil, it is the most predominant toxic metal transferred from soil to food, especially in the rice grains (Zhao and Wang, 2020). Cd-contaminated rice fields reportedly caused itai-itai disease in Japan in the last century (Kaji, 2012).

In recent years, microbial remediation strategies have attracted increasing attention since they are efficient, cost-effective, sustainable, and environmentally friendly (Volesky and Holan, 1995; González Henao and Ghneim-Herrera, 2021). Microbial remediation of heavy metals consists of biosorption, bioaccumulation, biomineralization, and biotransformation (Ayangbenro and Babalola, 2017). Microbes that possess molecular mechanisms to tolerate the toxic effects of heavy metals are especially useful for heavy metal remediation. Among the 5 main resistance mechanisms reported (González Henao and Ghneim-Herrera, 2021), intracellular sequestration remains most relevant to the Cd remediation of paddy to limit the availability of Cd to the rice plants. A variety of biomass, including microbes, yeast, fungi, and plants, have been successfully used for the remediation of heavy metals from contaminated habitats (Kumar et al., 2019; Rahman, 2020; Wei et al., 2021). Conversely, such contaminated habitats are a useful resource for native flora with heavy metal resistance (Rahman, 2020; Wei et al., 2021). We have earlier reported the identification and characterization of *Providencia rettgeri* strain KDM3 isolated from metal-contaminated soil from industrial premises in Mumbai, India (Salaskar, 2015). The organism showed tolerance to high concentrations of arsenic and resistance to multiple antibiotics (Salaskar, 2015). Antibiotic and metal resistance determinants are often co-selected (Baker-Austin et al., 2006), and different *Providencia* species show tolerance to multiple heavy metals (Sharma et al., 2017; Adekanmbi et al., 2019; Shukla et al., 2021). However, the scope of heavy metal resistance in the natural isolate *P. rettgeri* KDM3 remains unexplored.

In this study, we report the resistance of the bacterial strain *P. rettgeri* KDM3 to high concentrations of Cd. Intracellular accumulation of Cd was confirmed by electron microscopy and elemental analysis. Furthermore, we investigated the determinants of Cd tolerance in *P. rettgeri* KDM3 using a proteomic approach. The first 2D proteome map of *P. rettgeri* KDM3 was generated with 147 proteins identified by mass spectrometry. Comparative proteomics revealed that the strain upregulated oxidative stress defense, membrane transport, and protein homeostasis pathways to survive Cd exposure at the expense of downregulation of various metabolic pathways. Bioaugmentation studies showed significant improvements in the growth parameters of the rice plants exposed to 100 ppm Cd and a remarkable reduction in the Cd concentration in the edible parts of the rice plant. To the best of our knowledge, this is the first study where the beneficial effect of *P. rettgeri* KDM3 is systematically assessed and till the maturation stage (135 days) of the rice plant. The organism presents great potential for *in-situ* Cd bioremediation in paddy fields.

MATERIALS AND METHODS

Bacterial Strain, Growth Conditions, and Cd Exposure

Isolation, characterization, and identification of bacterial isolate *P. rettgeri* strain KDM3 (Genbank Accession Number: KC247668.1, GI: 432140652) have been described earlier by Salaskar (2015). For various assays, *P. rettgeri* strain KDM3 cells were resuspended in fresh lysogeny broth (LB) medium at a starting cell density of $OD_{530nm} = 0.05$, and the cells were allowed to grow under standard growth conditions. When the cell density reached $OD_{530nm} = 0.5$, various Cd stress assays, such as growth experiments, microscopic investigations, and proteomic and rice ecosystem studies, were performed using $CdCl_2.2½\ H_2O$ salt. *P. rettgeri* cells in the exponential phase ($OD_{530} = 1.0–1.2$) were resuspended in the LB broth containing 0–250 μg Cd ml^{-1} (0–250 ppm) and incubated at 30°C in an orbital shaker (140 rpm). The growth of *P. rettgeri* was monitored at various time intervals till 8 h by measuring the optical density of the culture at 530 nm using UV/Vis spectrophotometer (Jasco-V-530). Plasmid isolation and plasmid curing experiments were performed as per the protocol detailed earlier (Salaskar, 2015).

Cd Concentration Measurements

The concentration of Cd accumulated by *P. rettgeri* was measured after 20 h of exposure to 0–250 ppm Cd. The bacterial cells were spun down (10,000 g, 10 min) to remove residual Cd and resuspended in 10 ml of distilled water, vortexed, and centrifuged at 10,000 g, 10 min. After centrifugation, the bacterial cell pellet was digested in a microwave digestion system (Milestone Ethos up, Italy) using 6 ml concentrated HNO_3. The cooled digested solution was further concentrated to 2 ml and diluted to 10 ml with water, and the Cd concentration was measured using a Flame Atomic Absorption Spectrometer (GBC 932 plus, Australia). The detection limit of Cd was 0.2–1.8 ppm, the sensitivity was 0.009 ppm, and the wavelength was set at 228.8 nm with D2 correction. The assay was performed in triplicates.

Microscopic Investigations and Elemental Mapping

Providencia rettgeri cells were exposed to 100 ppm Cd for 20 h. Following Cd exposure, the cells were harvested, washed, and observed under a light microscope (Carl Zeiss Axiostar plus) with a 100× oil immersion objective under hydrous conditions. *Providencia rettgeri* cells were processed similarly, except that exposure to Cd served as control. For scanning electron microscopy (SEM), the cells were washed in normal saline and fixed in 2.5% glutaraldehyde for 2 h. The cells were then dehydrated in a graded ethanol series (30–100%), spotted on aluminum studs, and dried at 37°C for 1 h. The dried samples were gold coated using the thermal evaporation technique and analyzed by SEM using a Tescan VEGA 40 Microscope. For transmission electron microscopy (TEM), cells were washed in normal saline and were fixed with 2.5% glutaraldehyde, a 0.5% paraformaldehyde mixture, dehydrated with increasing concentrations of ethanol, and embedded in epoxy resin. Then sections (50 nm) were cut and visualized under Carl Zeiss Libra 120 keV TEM without staining. Energy-filtered transmission electron microscopy (EF-TEM) was used for elemental mapping on the electron-dense area as described earlier (Saunders and Shaw, 2014; Anaganti et al., 2015), except that the slit width of the Cd-specific energy filter was set at 390 and 503 ev.

2D Gel Electrophoresis and Image Analysis

Cellular proteins were resolved by 2D gel electrophoresis as described earlier (Basu and Apte, 2012). In brief, the cellular protein samples were prepared from control or Cd-treated cells following 1 h of exposure to 100 ppm (880 μM) Cd. The cup loading method was used to resolve cellular proteins (500 μg) by isoelectric focusing (17 cm IPG strip, pI 4–7, Bio-Rad, India), followed by 12% SDS-PAGE. The gels were stained with Coomassie Brilliant Blue G250 stain and digitized using a Dyversity-6 gel imager (Syngene, UK). Three biological replicate sets were generated by repeating the experiment three times. PDQuest 2D analysis software (version 8.1.0, Bio-Rad) was used for the first level match set generated from three biological 2D gel replicates. The minimum correlation coefficient value between the replicates of group sets was 0.75. Protein spots were detected and matched between the replicates in automatic detection mode, and spuriously detected spots were removed manually. Spot densities were normalized with the local regression method. An independent Student's *t*-test was applied for statistical analysis and the protein spots with p-values ≤ 0.05 were considered as significantly differentially expressed between control and Cd-treated cells. The protein spots of interest were manually excised from the gel and further identified by mass spectrometry.

Mass Spectrometry and Protein Identification

The protein gel plugs were destained, reduced with Dithiothreitol (DTT), alkylated with iodoacetamide, in-gel digested with trypsin, and the oligopeptides were eluted as described earlier (Anaganti et al., 2015). Similarly, co-crystallization of the eluted oligopeptides and mass spectrometric (UltraFlex III MALDI-TOF/TOF mass spectrometer, Bruker Daltonics, Germany) analysis were performed as described earlier (Anaganti et al., 2015). Mascot searches were conducted using the NCBI nonredundant database (released in January 2016 or later, with a minimum of 79,354,501 entries actually searched) with the following settings: the number of missed cleavages permitted was 1; fixed modifications such as carbamidomethyl on cysteine, variable modification of oxidation on methionine residue; peptide tolerance as 100 ppm; enzyme used as trypsin; and a peptide charge setting as +1. *Providencia rettgeri* protein with significant Molecular Weight Search (MOWSE) score considered as successful identification.

Bioinformatics Analyses

The hierarchical cluster was created using the pheatmap toolbox in RStudio (Kolde, 2019). Briefly, raw protein intensity values were imported into the RStudio, row scaled, and plotted using default parameters. Gene Ontology (GO) enrichment analysis was carried out using the Bingo tool in Cytoscape (Maere et al., 2005). For this purpose, a basic ontology file in Open Biomedical Ontologies (OBO) format was downloaded from the GO website (http://geneontology.org/). *Providencia rettgeri*-specific annotations were retrieved from the Quickgo website (https://www.ebi.ac.uk/QuickGO/) using taxon ID filter (587). Protein identities were mapped to the corresponding UniProt ID for *P. rettgeri* using the UniProt ID-conversion tool. GOs were FDR corrected, and the selected ontology was plotted in RStudio using "ggplot2" for representation (Wickham, 2016).

In-situ Bioremediation Studies Using Model Rice Ecosystem

A greenhouse glass pot culture experiment was conducted using an agriculture acidic soil (pH, 5.9) in Dapoli, Maharashtra (**Table 1**). The soil was passed through a 2-mm sieve. Glass tanks (60 cm in diameter and 30 cm in height) were filled with 15 kg of sieved soil, and 60 plants were planted per pot. The experimental sets were (a) control soil with no Cd (C), (b) 100 ppm Cd in soil (T1), and (c) 100 ppm Cd with 1×10^8 cells of *P. rettgeri* strain g^{-1} soil (T2). Three replicates were maintained for each set. The pots were maintained at 60% water holding capacity for 1-week for bacterial soil colonization. The soil was treated with $CdCl_2.2½\ H_2O$ (solubility in water 135 g/100 ml at 20°C). Bacterial colonization was checked during plant growth and after crop harvest by plating the representative soil samples followed by the serial dilution technique. *Providencia rettgeri* cells were selected on agar plates containing 50 ppm kanamycin.

Seed Treatment and Rice Plant Growth

Oryza sativa BARC-KKV-13 was used in this study. Seeds were surface sterilized with 0.1% $HgCl_2$ for 1 min, washed 3–4 times with running tap water, followed by one wash with distilled water, and dried on the blotting paper. The seedlings were grown in plastic trays containing control soil for about 2 weeks, and later seedlings with similar appearance and biomass were carefully transplanted into the, respectively, developed glass ecosystem as stated above. The rice crop was grown till

TABLE 1 | Physico—chemical characteristics of the experimental soil.

Soil details	
Location	Dapoli-Maharashtra
Color	Red
Class	Inceptisol
Soil physico-chemical characteristics	**Values**
pH (soil-water 1:2.5)	5.9
Electrical conductivity (μSm^{-1})	0.11
Cation exchange capacity [c mol (p^+) kg^{-1}]	19.4
Water holding capacity (%)	55
Organic carbon (%)	1.1
Available *P* ($\mu g\ g^{-1}$)	35
Total *N* (%)	0.08
***DTPA extract ($\mu g\ g^{-1}$ soil)**	
Cd	1.6
Cu	2.72
Fe	18.58
Mn	116.8
Zn	0.32

**DTPA, DietheyleneTriamine Penta acetic acid.*

maturity (135 days). Fertilizers were applied at regular intervals as per standard agriculture practice, and flooding condition was maintained throughout the growth period by replenishing water every 2 days. After 135 days, the plants were carefully removed from the pots by separating the roots and the shoots. Shoot samples were rinsed several times with water to remove surface contamination, and the root surfaces were washed several times with tap water, followed by distilled water, and further with 0.5 mM ethylenediaminetetraacetic acid (EDTA) to remove adhering Cd on the root surface.

Determination of Plant Fresh Weight, Root Length, Shoot Length, and Cd Concentrations in Plant Parts

The various physiological parameters of plants were determined by measuring the lengths and fresh weights of plant roots, shoots, or grains. The plant shoot, root, and grain samples were dried in a hot air oven at 70°C till a constant weight was achieved, and dry matter yield was recorded. To determine the Cd content, the dried samples were finely ground and wet digested in a microwave digestion system (Milestone Ethos UP, Italy) in concentrated HNO_3 (AR grade). The cooled digested solution was further concentrated to 2 ml and diluted to 10 ml with water, and the Cd concentration was measured using a flame atomic absorption spectrometer (GBC 932 plus, Australia), as described in the Section "Cd Concentration Measurements."

Statistical Analysis

All the experiments were performed in triplicates to generate three biological replicates, and the results have been reported as means ± standard deviation (SD). The software used for statistical analyses was ANOVA in Excel 2007. Statistical analyses for various parameters in the rice ecosystem experiment included comparisons of individual groups using the *post-hoc Q*-test. The *p*-values were determined using a *post-hoc Q* table. The significant difference was determined through Tukey's mean grouping at $\alpha = 0.05$, i.e., 95% CI, and $\alpha = 0.01$, i.e., 99% CI.

RESULTS AND DISCUSSIONS

Cd Tolerance and Bioaccumulation by *P. rettgeri* Strain KDM3

Providencia species are tolerant to high concentrations of an array of heavy metals (Thacker et al., 2006; Naik et al., 2013; Salaskar, 2015). We found that arsenic-tolerant *P. rettgeri* strain KDM3 also exhibited remarkable tolerance to high concentrations of Cd. The organism could grow in the increasing concentrations of Cd, while a concentration of 100 ppm Cd (880 μM Cd) resulted in a 50% decrease in growth rate (LD_{50}), as compared to control cells (**Figure 1A**). An increase in Cd content in the media caused a proportionate increase in the Cd uptake by the growing cells (**Figure 1B**). At 200-ppm Cd exposure, *P. rettgeri* cells accumulated ≈ 1 mg/g Cd/dry weight of cells (**Figure 1B**). Exposure to Cd (100 ppm) induced morphological changes in *P. rettgeri*. Loosely packed short rods of control cells changed to characteristic chains of coccoidal lenticular shape after being exposed to 100 ppm Cd, as seen under a light microscope as well as SEM (**Figure 1C**). Transmission electron micrographs showed spread-out electron-dense depositions inside the Cd-exposed cells (**Figure 1C**), indicating the presence of Cd. The intracellular distribution of Cd was confirmed by the elemental mapping of cells through Energy-Filtered Transmission Electron Microscopy (EFTEM). A large intracellular distribution of Cd was observed in the electron-dense region of Cd-treated cells, which was absent in control cells (**Figure 1C**). From these data, we concluded that the high Cd tolerance of *P. rettgeri* KDM3 strain is due to intracellular accumulation of the toxic metal.

Reference Proteome Map of *P. rettgeri* and Functional Classification of the Identified Proteins

Even though *Providencia* is known to be able to survive high concentrations of heavy metals, its Cd stress response network has not been explored yet. Plasmid-mediated Cd resistance has been reported for *P. aeruginosa* (Chellaiah, 2018). We earlier found that the arsenic tolerance of *P. rettgeri* strain KDM3 was plasmid-borne (Salaskar, 2015); however, Cd tolerance of the organism was unaffected even after plasmid curing, indicating that the determinants of Cd tolerance were encoded on the chromosome (data not shown). To systematically investigate the response of *P. rettgeri* to Cd exposure through a proteomic approach, we first proceeded to generate the 2D proteome map of *P. rettgeri* since the reference proteome map is not available for any *Providencia* strains yet. The cellular proteins were extracted from *P.*

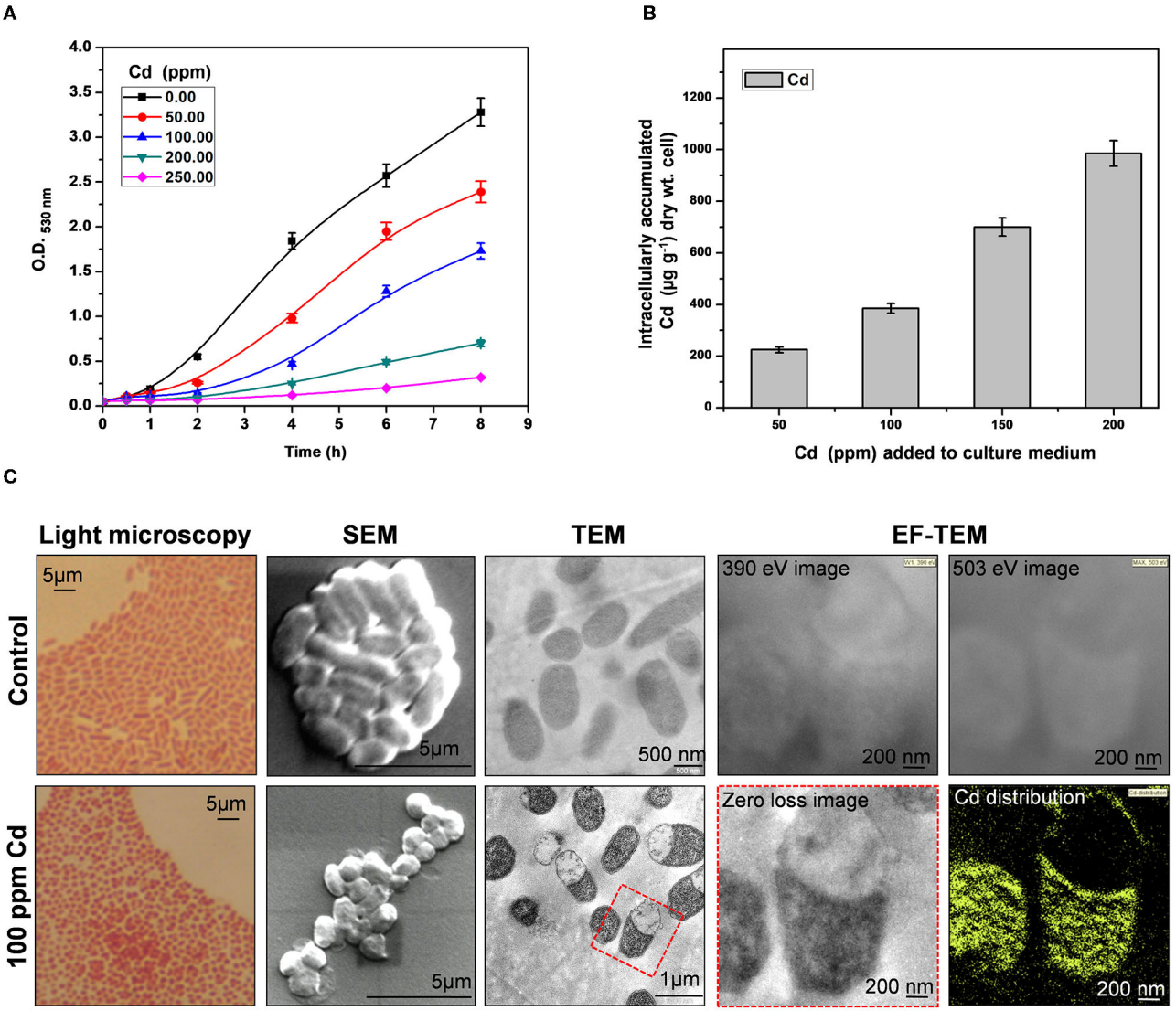

FIGURE 1 | Cadmium (Cd) tolerance and accumulation by *Providencia rettgeri*. **(A)** Growth of *P. rettgeri* in the presence of different concentrations of Cd (0–250 ppm). **(B)** Cd concentration in *P. rettgeri* cells grown in the presence of increasing concentrations of Cd for 20 h. **(C)** Morphology of *P. rettgeri* cells observed under light microscopy, scanning electron microscopy, transmission electron microscopy, and elemental mapping of cadmium using energy-filtered transmission electron microscopy. The *P. rettgeri* cells were either grown in the presence of 100 ppm Cd or not (control). The red dotted box shows the cells on which EFTEM analysis was carried out.

rettgeri cells exposed to 100 ppm Cd (test) for 1 h or not (control) and resolved by 2D gel electrophoresis. On average, PDQuest image analysis software detected about 543 high-quality spots on the 2D gel sets. Among the replicates in each group, high correlations were observed for protein spot matching in the individual group (**Supplementary Table S1**). Since a 2D proteome map is not yet available for *P. rettgeri*, we picked up a total of 144 protein spots for identification by MALDI mass spectrometry. We identified a total of 147 proteins confidently (**Figure 2A**, **Supplementary Figure S1**, **Supplementary Table S2**, **Supplementary MS Data**). The identified proteins belonged to 132 unique genes since 15 proteins (isoforms) were identified from more than one spot (**Supplementary Table S2**).

To decipher the biological processes, molecular functions, and cellular components of the identified proteins, GO enrichment analysis was carried out. Biological processes such as ribose phosphate metabolic process, TCA cycle, glycolytic process, acyl-CoA metabolic process, translation, protein folding, aerobic respiration, and response to oxidative stress were enriched among the identified proteins (**Figure 2B**, **Supplementary Table S3**). We also observed enrichment of various molecular functions such as binding of nucleotides or metal ions, translation regulation, ligase

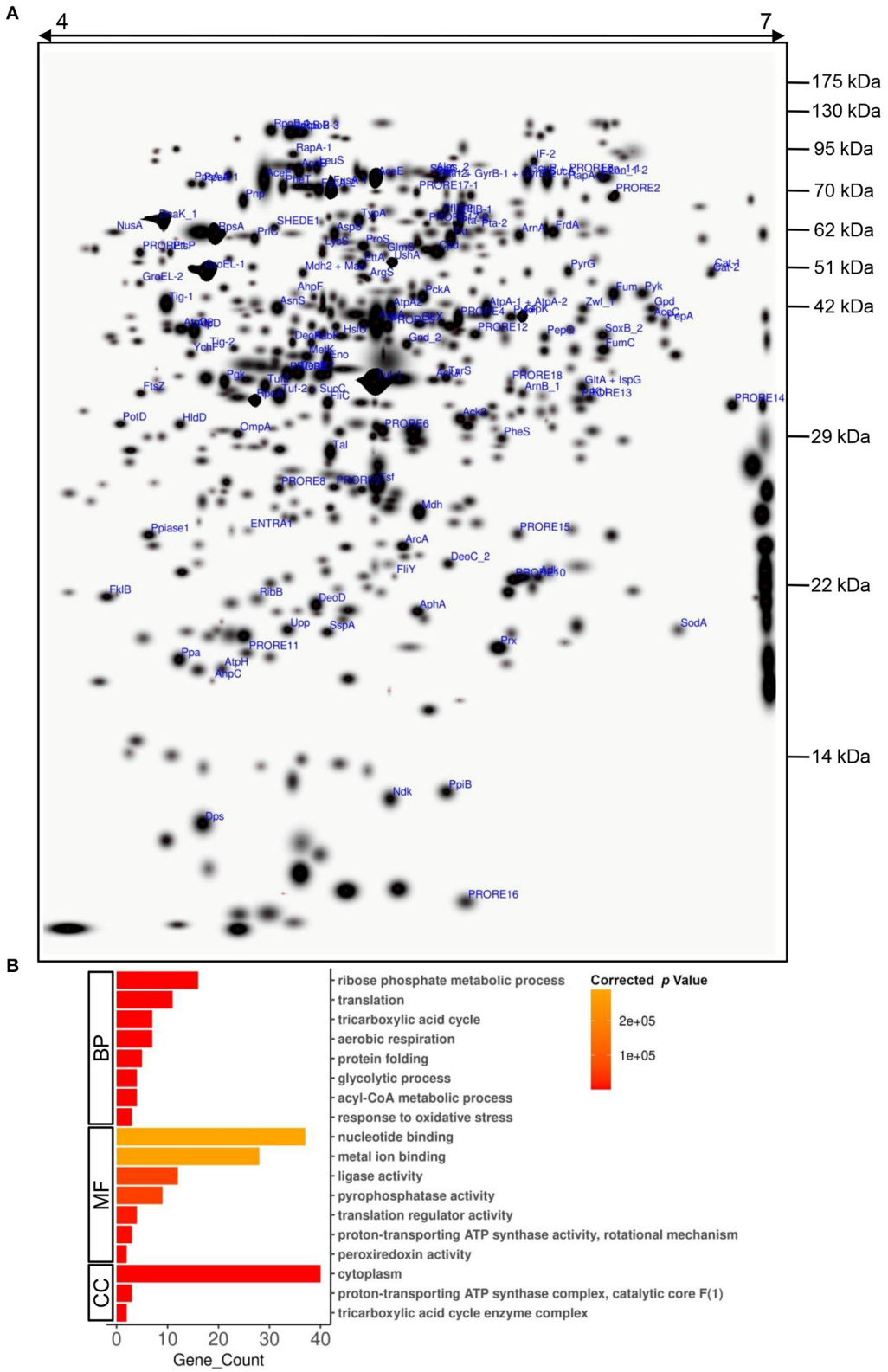

FIGURE 2 | A 2D proteome map of *P. rettgeri*. **(A)** A "master gel" representing a proteome of *P. rettgeri* control cells was created *in silico* from three biological replicate gels. The pI and molecular masses (kDa) of marker proteins are shown at the top and on the right-hand side of the gel, respectively. All the identified proteins are marked. Refer to **Supplementary Table S2** for spot ID annotations. **(B)** Gene Ontology (GO) functional classification of identified proteins using BiNGO tool. BP, biological process; MF, molecular function; CC, cellular component.

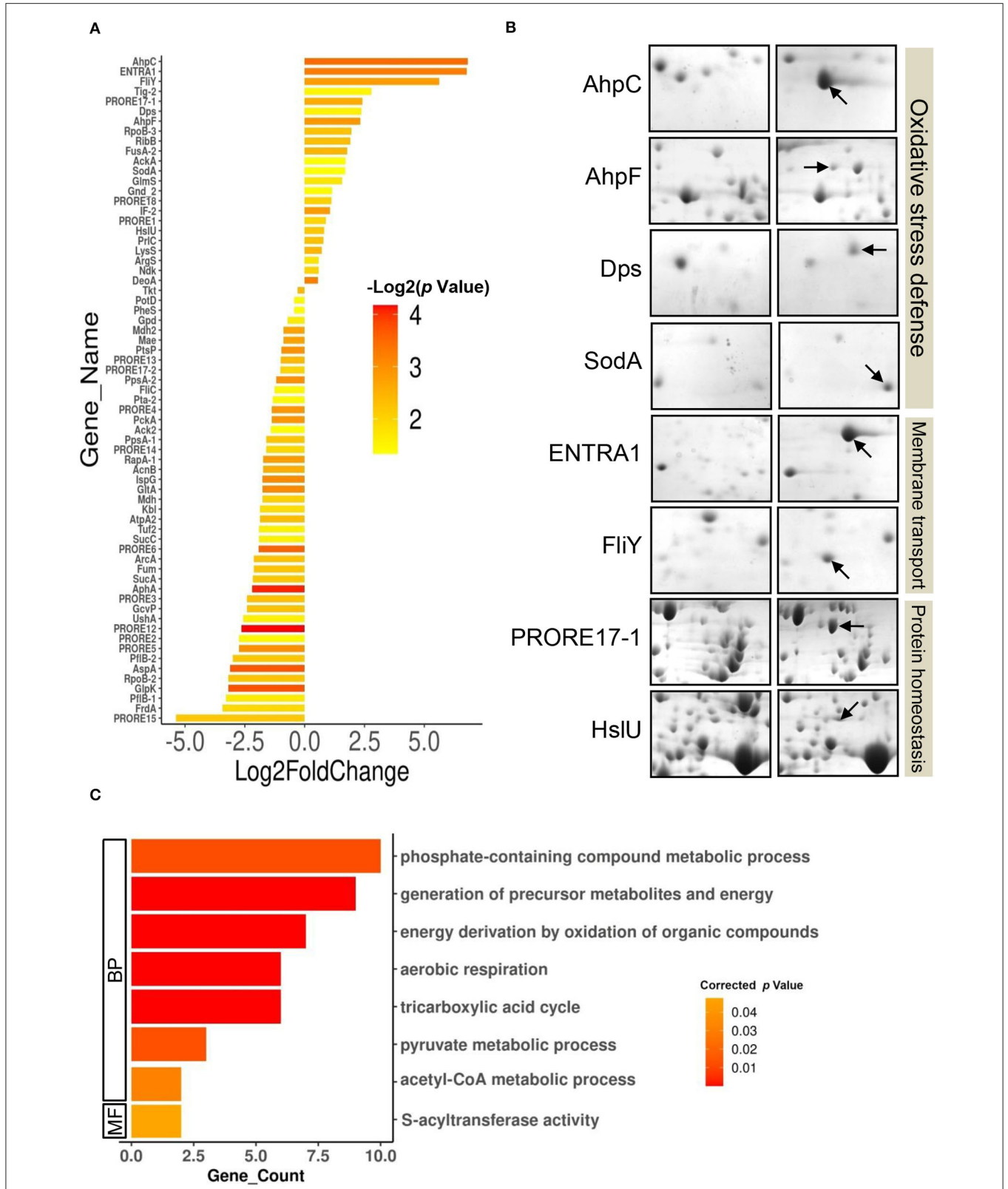

FIGURE 3 | Differentially expressed proteome of *P. rettgeri* exposed to 100 ppm Cd. **(A)** Bar plot representing the Log2 (fold change) on *X*-axis vs. *p*-value for the differentially expressed proteins (DEPs) on *Y*-axis. Log2 (fold change) is calculated by taking the ratio of the mean values of protein intensities from treated and control gels. The *p*-values plotted are calculated from the differential expression analysis using the Student's *t*-test. Bars are colored according to the *p*-values. Protein abbreviations are detailed in **Supplementary Table S2**. **(B)** *Providencia rettgeri* proteins upregulated following exposure to 100 ppm Cd. Proteins with increased abundance in Cd-treated cells, as compared to control cells, are shown by arrows. **(C)** GO functional classification of downregulated DEPs.

activity, pyrophosphatase activity, proton-transporting ATP synthase activity, and peroxiredoxin activity (**Figure 2B**, **Supplementary Table S4**). The majority of the identified proteins were cytoplasmic, while a few were part of protein complexes such as ATP synthase complex, TCA cycle enzyme complex, etc. (**Figure 2B**, **Supplementary Table S5**).

Differential Proteome of *P. rettgeri* in Response to Cd Exposure and GO-Based Functional Classification of DEPs

Furthermore, differential expression analysis on the proteome profiles of the control and test cells revealed a set of 69 proteins differentially expressed (p-value < 0.05) in response to 100 ppm Cd exposure (**Figure 3A**, **Supplementary Table S6**, **Supplementary Figure S2**). The DEPs belonged to 66 unique genes since three proteins were present in at least two spots. In all, 23 proteins were upregulated while 46 proteins were downregulated following exposure to 100 ppm Cd (**Figure 3A**, **Supplementary Table S6**). Among the upregulated proteins, *de novo* expression was observed for the typical bacterial 2-Cys peroxiredoxin AhpC (112.85-fold), while its cognate reductase AhpF showed a 5-fold increase in abundance in the cells exposed to 100 ppm Cd (**Figure 3B**, **Supplementary Table S6**). The genes encoding AhpC and AhpF proteins were found to be present in an operonic arrangement on the genome of *P. rettgeri* (**Supplementary Figure 3A**). Interestingly, the *P. rettgeri* cells retained the Cd tolerance property even when cured of the plasmid, suggesting that the *ahp* operon could be a major determinant of Cd tolerance in this organism. AhpC, belonging to a highly conserved thiol-specific antioxidant (TSA) family, possesses a peroxidase activity against H_2O_2, peroxynitrite, and organic hydroperoxides. In a homodimeric AhpC, the peroxidatic cysteine (C-47) is first oxidized to sulfenic acid intermediate and resolved by the cysteine (C-166) in the other subunit. Both the cysteine residues are completely conserved in AhpC encoded by *P. rettgeri* (**Supplementary Figure 3B**). AhpF acts as a reductase that uses electrons from NADH to reduce intermolecular disulfide bonds in an oxidized AhpC dimer (Zhang et al., 2019; Feng et al., 2020). Other noteworthy upregulated antioxidant enzymes include DNA starvation/stationary phase protection protein Dps (5.2-fold induction) and Mn-Superoxide dismutase (3.2-fold induction) (**Figure 3B**, **Supplementary Table S6**).

We also observed the *de novo* induction of 2 membrane transporters. Interestingly, ABC transporter ATP-binding protein (ENTRA1, 109-fold induction) was identified as a protein from *Enterococcus raffinosus* ATCC 49464, while amino acid ABC transporter substrate-binding protein FliY (49-fold induction) belonged to *P. rettgeri* (**Figure 3B**, **Supplementary Table S6**). Since the *P. rettgeri* strain used in this study was isolated from a natural habitat, acquisition of the transporter protein from *E. raffinosus* through horizontal transfer cannot be ruled out. The ATP-binding cassette-type vacuolar membrane transporter HMT1 from *Schizosaccharomyces pombe* (SpHMT1) was first shown to be involved in Cd ion import and Cd resistance (Ortiz et al., 1992). Later, it was demonstrated that the ATP-binding cassette transporter HMT1 constitutes a Cd detoxification mechanism that is highly conserved from bacteria to plants to humans (Preveral et al., 2009). Interestingly, ABC transporter ATP-binding protein ENTRA1 (260 amino acids), but not ABC transporter substrate-binding protein FliY, showed homology (ClustalW alignment score 211) to the C-terminal domain (254 amino acids) of SpHMT1 protein (**Supplementary Figure S4**), suggesting that ENTRA1 could be involved in Cd transport and intracellular accumulation in *P. rettgeri* cells. In *Escherichia coli*, upregulation of the periplasmic L-cystine-binding protein FliY was observed following exposure to 100 μM Cd or 0.88 mM H_2O_2 (Helbig et al., 2008; Ohtsu et al., 2010). FliY is an integral component of the L-cysteine/L-cystine shuttle system that imports L-cystine, an oxidized product of L-cysteine, from the periplasm to the cytoplasm to limit lipid peroxidation (Ohtsu et al., 2010). Cells overexpressing cystine/glutamate transporter protein acquire oxidative stress resistance independent of glutathione (GSH) (Banjac et al., 2008). ABC transporter substrate-binding protein FliY (279 amino acids) of *P. rettgeri* showed homology (ClustalW alignment score 398) to the L-cystine-binding protein TcyJ (266 amino acids) of *E. coli* (**Supplementary Figure S5**). It is, thus, tempting to speculate that the FliY protein provides an additional layer of oxidative stress resistance to Cd-exposed *P. rettgeri* cells. Additionally, an increase in abundance was seen for protein disaggregation chaperone ClpB (5.3-fold) and ATP-dependent protease, and ATPase subunit HslU (1.75-fold) (**Figure 3B**; **Supplementary Table S6**). While the organism showed a robust response to alleviate oxidative stress and revive or clear the damaged proteins, GO enrichment analysis on the 46 downregulated DEPs showed enrichment of several metabolic pathways such as the TCA cycle, aerobic respiration, and pyruvate metabolism (**Figure 3C**, **Supplementary Tables S7, S8**). Reduced metabolism could be either the direct effect of the diversion of NADH for redox reactions related to Cd bioaccumulation or a strategy adopted by the organism to limit metabolically generated ROS. Zhai et al. (2017) have also reported energy conservation and oxidative stress defense as some of the important mechanisms of Cd tolerance in *Lactobacillus plantarum*. Thus, we conclude that the Cd tolerance of *P. rettgeri* originates from the upregulation of relevant antioxidant enzymes and protein protection proteins.

Beneficial Effect of *P. rettgeri* on Cd Remediation in Model Rice Ecosystem

A rice ecosystem experiment was performed to evaluate the effect of *P. rettgeri* on different growth parameters of rice plants and the Cd accumulation in different plant parts. The rice plants grown on control soil exhibited normal growth; however, spiking of the soil with 100-ppm Cd resulted in a significant reduction in plant growth throughout the growth phase till 135 days (**Figure 4**). In contrast, the application of *P. rettgeri* cells to the 100 ppm Cd-spiked soil improved the growth of rice plants on par with control plants, demonstrating that the presence of *P. rettgeri* cells had a beneficial effect on reducing Cd toxicity (**Figure 4**). Furthermore, we found that the fresh

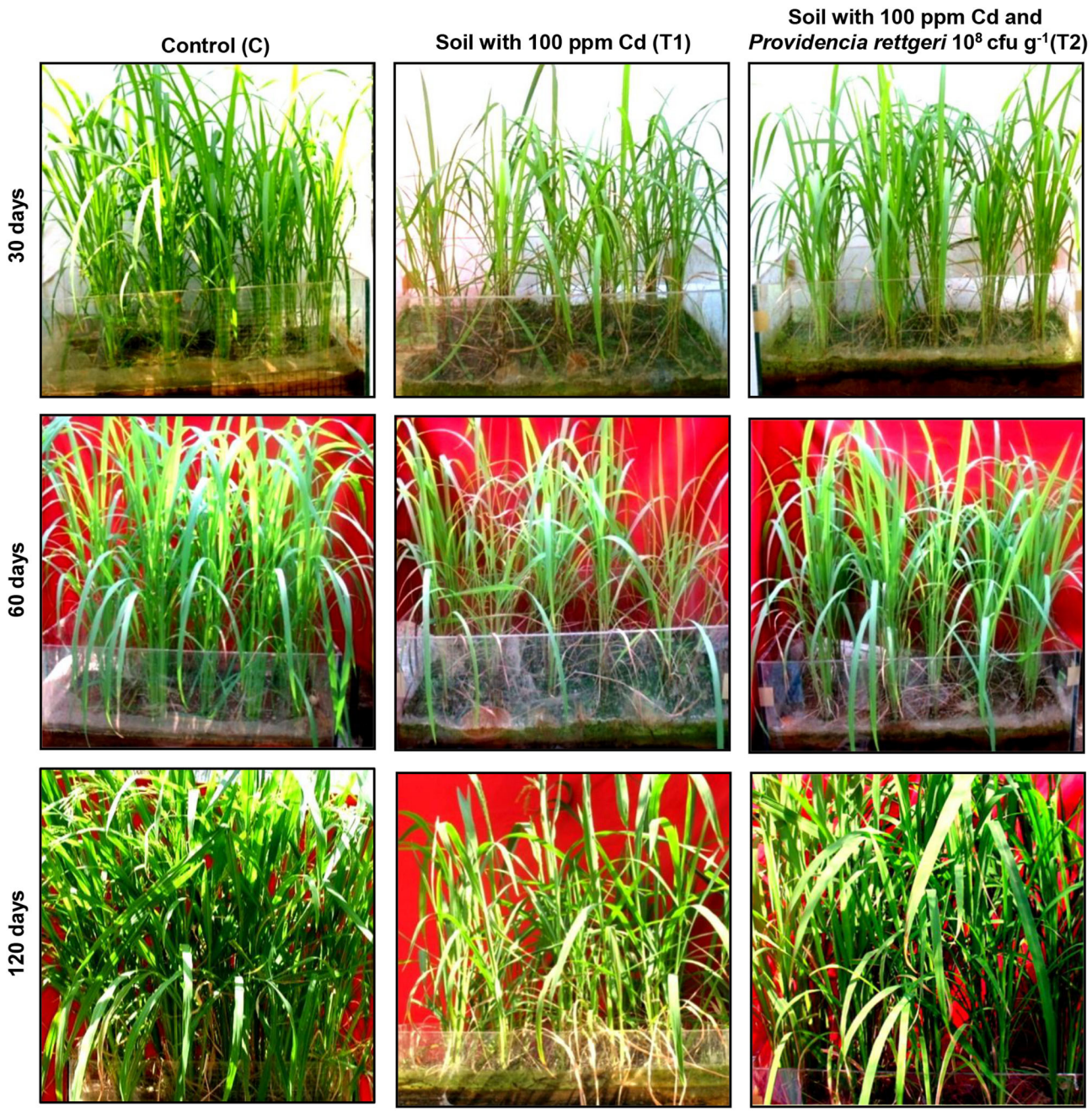

FIGURE 4 | Effect of *P. rettgeri* on Cd toxicity in rice plants. The images show the growth pattern of the rice plants grown either in the absence of Cd (C), in soil spiked with 100 ppm Cd (T1), or in soil spiked with 100 ppm Cd and 10^8 *P. rettgeri* cells per gram of soil (T2). The images were taken at the different stages of plant development. For larger images, refer to **Supplementary Figure S6**.

weights of roots, shoots, and grains of rice plants grown in the presence of 100 ppm Cd (T1) were significantly reduced as compared to control (C) plants (**Figures 5A,B**). The application of *P. rettgeri* cells to 100 ppm Cd containing soil (T2) caused a significant increase in the fresh weights of roots, shoots, and grains as compared to plants grown in the presence of 100 ppm Cd (T1). The plants exposed to 100 ppm Cd (T1) showed a significant reduction in the elongation of shoots and roots as compared to control plants (C) (**Figure 5C**). However, the application of *P. rettgeri* cells to 100 ppm Cd-containing soil (T2) nullified the toxic effects of Cd on the elongation of shoots and roots (**Figure 5C**). Cd contents in the control plant

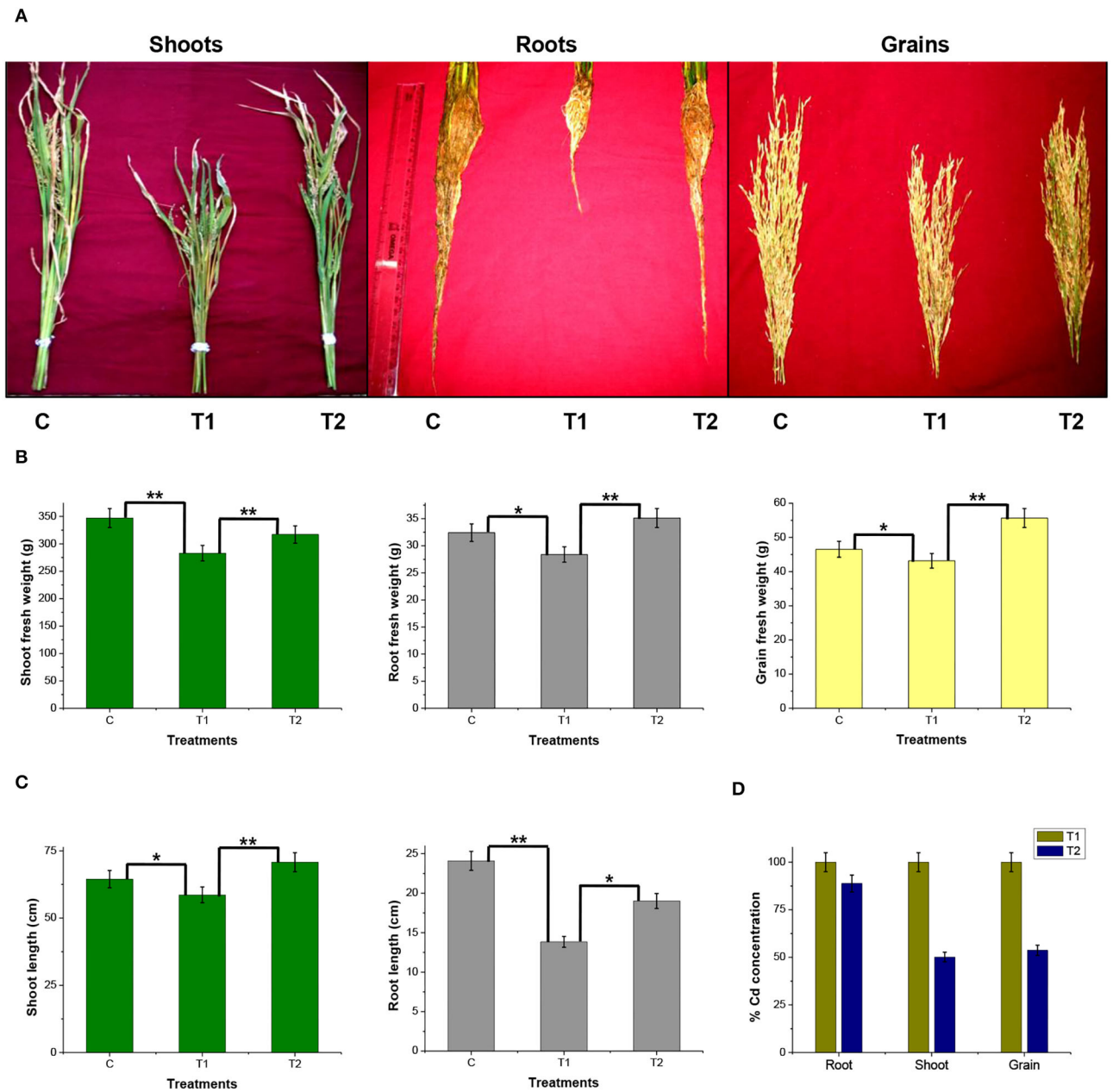

FIGURE 5 | Effect of *P. rettgeri* on different growth parameters of the rice plant. **(A)** The images show shoots, roots, and grains of rice plants harvested at the maturity stage (135 days). **(B)** Fresh weight of or **(C)** length of or **(D)** the Cd concentration in the shoots, roots, or the grains harvested from the rice plants at the maturity stage. Details of C, T1, and T2 are the same as given in **Figure 4**. The values represent means obtained from three replicates, and the bars represent the standard deviation of means. Comparisons of individual groups were carried out using the *post-hoc* Tukey's test. The *p*-values were obtained using the *post-hoc Q* table. *$\alpha \leq$ 0.05, i.e., 95% CI; **$\alpha \leq$ 0.01, i.e., 99% CI based on Tukey's mean grouping. Cd content in control plant tissues was below detectable limits.

parts were below detectable limits. In the plants exposed to 100 ppm Cd (T1), roots accumulated the highest amount of Cd (575 ppm), followed by shoots (90 ppm) and grains (36 ppm). When 100 ppm Cd soil was treated with *P. rettgeri*, Cd content in the roots and the shoots were reduced by 11.2 and 50%, respectively, while the grains showed a 46.1% reduction (**Figure 5D**). Our results demonstrate that the presence of *P. rettgeri* cells has synergistic effects on minimizing Cd toxicity in the rice ecosystem.

In-situ bioremediation of soil has gained importance in recent years. To access the feasibility of the application of any metal-tolerant bacteria at the field level, it is necessary to simulate the field conditions and study its potential for *in-situ* bioremediation. This is the first report of its kind wherein a

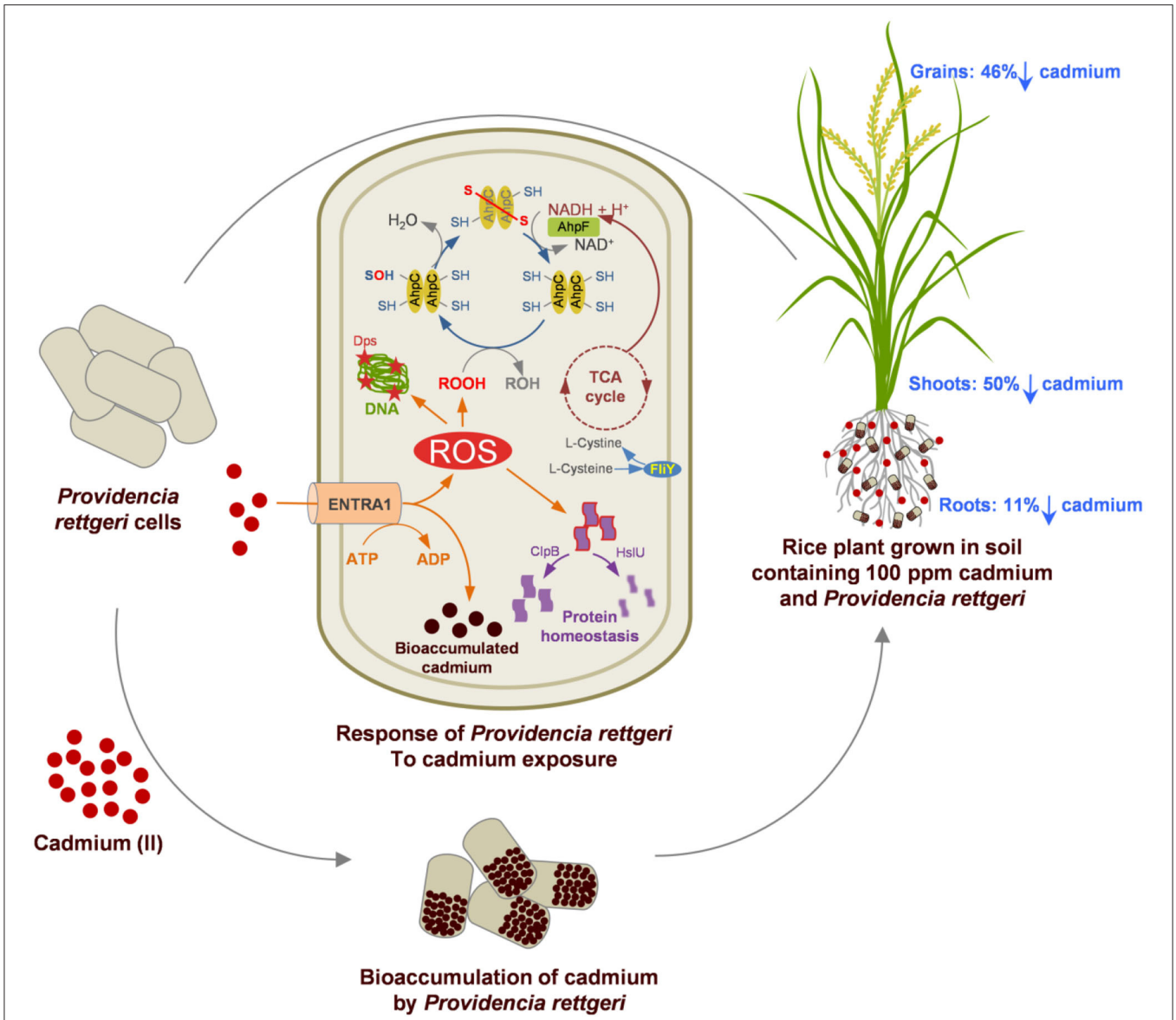

FIGURE 6 | A proteome and rice ecosystem-based model for the Cd tolerance and *in-situ* bioremediation potential of *P. rettgeri* KDM3 strain. Red dots represent Cd present in the soil, and brown dots indicate intracellularly accumulated Cd in the *P. rettgeri* cells. Percentage reduction in cadmium concentration in roots, shoots, and grains is shown by down arrows. The model at the center depicts the Cd responsive proteins involved in Cd tolerance and their possible role in Cd accumulation and cellular homeostasis. For details of Cd responsive proteins, refer to **Supplementary Table S2**.

rice field condition is simulated and developed in the form of a rice ecosystem and the potential of *P. rettgeri* bacteria for Cd *in-situ* bioremediation is studied in crops grown till full maturity (135 days). The overall outcome of the study has indicated that the Cd bioaccumulation property of *P. rettgeri* cells has favorably decreased the Cd contents (∼50%) in the edible parts of the rice plant due to reduced phytoavailability of Cd in soils. This is in agreement with *in-situ* bioremediation reported using other microbes (Chi et al., 2020; Haider et al., 2021). Various strains such as *Enterobacter aerogenes* MCC 3092, *Pseudomonas aeruginosa, Bacillus megaterium* H3, and *Neorhizobium huautlense* T1-17 were found to be potentially useful microbes in reducing phytoavailable Cd from the soil in the range of 40–60% Cd in different rice plant parts (Lin et al., 2016; Pramanik et al., 2018; Zhou et al., 2021).

CONCLUSION

The Cd tolerance of *P. rettgeri* and its potential for *in-situ* bioremediation are summarized in **Figure 6**. Cd-tolerant *P. rettgeri* bioaccumulated Cd through molecular mechanisms for Cd transport (ENTRA1), oxidative stress alleviation (AhpCF, Dps, FliY, and SodA), and proteome protection (ClpB and HslU).

This facultative aerobe was further demonstrated to be most suitable to the unique environment offered by the submerged conditions of the paddy. The presence of *P. rettgeri* significantly decreased Cd concentrations in root, shoot, and grain due to reduced Cd mobility in the soil. Bioaugmentation of Cd-contaminated soil with *P. rettgeri* offers a solution for masking Cd toxicity in the rice plants by improving overall growth till maturity and yielding low-Cd rice.

DATA AVAILABILITY STATEMENT

The datasets presented in this study can be found in online repositories. The names of the repository/repositories and accession number(s) can be found in the article/**Supplementary Material**.

AUTHOR CONTRIBUTIONS

DS: designed the experiments, carried out the experiments, analyzed the data, and written and finalized the manuscript. SK: conceptualized the project. BB: carried out proteomics experiments, analyzed the data, and written and finalized the manuscript. AG: carried out TEM experiments and analyzed data. MP: analyzed the proteomics data. All authors contributed to the article and approved the submitted version.

ACKNOWLEDGMENTS

The authors thankfully acknowledge Mr. Vikash Kumar (Nuclear Agriculture and Biotechnology Division, Bhabha Atomic Research Center) for providing seeds of *O. sativa* BARC-KKV-13 strain. They thank Mr. Anant Chavan, Mr. P. S. Tipre, and Mr. Aniket Pokle (NABTD, BARC) for the technical help provided while conducting rice ecosystem experiments. The authors also thank Dr. Anand Ballal (MBD, BARC) for providing the TEM facility and Ms. Namrata Waghmare (MBD, BARC) for TEM sample preparations.

SUPPLEMENTARY MATERIAL

The Supplementary Material for this article can be found online at: https://www.frontiersin.org/articles/10.3389/fmicb.2022.852697/full#supplementary-material

REFERENCES

Adekanmbi, A. O., Adelowo, O. O., Okoh, A. I., and Fagade, O. E. (2019). Metal-resistance encoding gene-fingerprints in some bacteria isolated from wastewaters of selected printeries in Ibadan, South-western Nigeria, Journal of Taibah University for *Science* 13, 266–273. doi: 10.1080/16583655.2018.1561968

Anaganti, N., Basu, B., Gupta, A., Joseph, D., and Apte, S. K. (2015). Depletion of reduction potential and key energy generation metabolic enzymes underlies tellurite toxicity in *Deinococcus radiodurans*. *Proteomics* 15, 89–97. doi: 10.1002/pmic.201400113

Ayangbenro, A. S., and Babalola, O. O. (2017). A new for heavy metal polluted environments: a review of microbial biosorbents. *Int. J. Environ. Res. Public Health*. 14, 94. doi: 10.3390/ijerph14010094

Baker-Austin, C., Wright, M. S., Stepanauskas, R., and McArthur, J. V. (2006). Co-selection of antibiotic and metal resistance. *Trends Microbiol.* 14, 176–182. doi: 10.1016/j.tim.2006.02.006

Banjac, A., Perisic, T., Sato, H., Seiler, A., Bannai, S., Weiss, N., et al. (2008). The cystine/cysteine cycle: a redox cycle regulating susceptibility versus resistance to cell death. *Oncogene* 27, 1618–1628. doi: 10.1038/sj.onc.1210796

Basu, B., and Apte, S. K. (2012). Gamma radiation-induced proteome of *Deinococcus radiodurans* primarily targets DNA repair and oxidative stress alleviation. *Mol. Cell. Proteomics*. 11, 011734. doi: 10.1074/mcp.M111.011734

Berglund, M., Larsson, K., Grander, M., Casteleyn, L., Kolossa-Gehring, M., and Schwedler, G. (2015). Exposure determinants of cadmium in European mothers and their children. *Environ. Res.* 141, 69–76. doi: 10.1016/j.envres.2014.09.042

Chellaiah, E. R. (2018). Cadmium (heavy metals) bioremediation by Pseudomonas aeruginosa: a minireview. *Appl. Water Sci.* 8, 154. doi: 10.1007/s13201-018-0796-5

Chi, Y., Huang, Y., Wang, J., Chen, X., Chu, S., Hayat, K., et al. (2020). Two plant growth promoting bacterial Bacillus strains possess different mechanisms in adsorption and resistance to cadmium. *Sci. Total Environ.* 741, 140422. doi: 10.1016/j.scitotenv.2020.140422

Fay, R. M., and Mumtaz, M. M. (1996). Development of a priority list of chemical mixtures occurring at 1188 hazardous waste sites, using the HazDat database. *Food Chem. Toxicol.* 34, 1163–1165. doi: 10.1016/S0278-6915(97)00090-2

Feng, X., Guo, K., and Gao, H. (2020). Plasticity of the peroxidase AhpC links multiple substrates to diverse disulfide-reducing pathways in Shewanella oneidensis. *J. Biol. Chem.* 295, 11118–11130. doi: 10.1074/jbc.RA120.014010

González Henao, S., and Ghneim-Herrera, T. (2021). Heavy metals in soils and the remediation potential of bacteria associated with the plant microbiome. *Front. Environ. Sci.* 9, 604216. doi: 10.3389/fenvs.2021.604216

Haider, F. U., Liqun, C., Coulter, J. A., Cheema, S. A., Wu, J., Zhang, R., et al. (2021). Cadmium toxicity in plants: impacts and remediation strategies. *Ecotoxicol. Environ. Safety*. 211, 111887. doi: 10.1016/j.ecoenv.2020.111887

Helbig, K., Grosse, C., and Nies, D. H. (2008). Cadmium toxicity in glutathione mutants of *Escherichia coli*. *J. Bacteriol.* 190, 5439–5454. doi: 10.1128/JB.00272-08

Hubeny, J., Harnisz, M., Korzeniewska, E., Buta, M., Zielinski, W., Rolbiecki, D., et al. (2021). Industrialization as a source of heavy metals and antibiotics which can enhance the antibiotic resistance in wastewater, sewage sludge and river water. *PLoS ONE* 16, e0252691. doi: 10.1371/journal.pone.0252691

Kaji, M. (2012). Role of experts and public participation in pollution control: the case of Itai-itai disease in Japan. *Ethics Sci. Environ. Polit.* 12, 99–111. doi: 10.3354/esep00126

Kolde, R. (2019). *Pheatmap: Pretty Heatmaps. R package version 1, 0.12.* Available online at: https://CRAN.R-project.org/package=pheatmap

Kumar, S., Prasad, S., Yadav, K. K., Shrivastava, M., Gupta, N., and Nagar, S. (2019). Hazardous heavy metals contamination of vegetables and food chain: role of sustainable remediation approaches - a review. *Environ. Res.* 179, 108792. doi: 10.1016/j.envres.2019.108792

Lin, X., Mou, R., Cao, Z., Xu, P., Wu, X., Zhu, Z., et al. (2016). Characterization of cadmium-resistant bacteria and their potential for reducing accumulation of cadmium in rice grains. *Sci. Total Environ.* 569–570, 97–104. doi: 10.1016/j.scitotenv.2016.06.121

Maere, S., Heymans, K., and Kuiper, M. (2005). BiNGO: a cytoscape plugin to assess overrepresentation of gene ontology categories in biological networks. *Bioinformatics* 21, 3448–3449. doi: 10.1093/bioinformatics/bti551

Naik, M. M., Khanolkar, D., and Dubey, S. K. (2013). Lead-resistant Providencia alcalifaciens strain 2EA bioprecipitates Pb+2 as lead phosphate. *Lett. Appl. Microbiol.* 56, 99–104. doi: 10.1111/lam.12026

Ohtsu, I., Wiriyathanawudhiwong, N., Morigasaki, S., Nakatani, T., Kadokura, H., and Takagi, H. (2010). The L-cysteine/L-cystine shuttle system provides

reducing equivalents to the periplasm in *Escherichia coli*. *J. Biol. Chem.* 285, 17479–17487. doi: 10.1074/jbc.M109.081356

Ortiz, D. F., Kreppel, L., Speiser, D. M., Scheel, G., McDonald, G., Ow, D. W. (1992). Heavy metal tolerance in the fission yeast requires an ATP-binding cassette-type vacuolar membrane transporter. EMBO *J.* 11, 3491–3499. doi: 10.1002/j.1460-2075.1992.tb05431.x

Ozaki, H., Ichise, H., Kitaura, E., Yaginuma, Y., Yoda, M., Kuno, K., et al. (2019). Immutable heavy metal pollution before and after change in industrial waste treatment procedure. *Sci. Rep.* 9, 4499. doi: 10.1038/s41598-019-40634-2

Pramanik, K., Mitra, S., Sarkar, A., and Maiti, T. K. (2018). Alleviation of phytotoxic effects of cadmium on rice seedlings by cadmium resistant PGPR strain Enterobacter aerogenes MCC 3092. *J. Hazard. Mater.* 351, 317–329. doi: 10.1016/j.jhazmat.2018.03.009

Preveral, S., Gayet, L., Moldes, C., Hoffmann, J., Mounicou, S., Gruet, A., et al. (2009). A common highly conserved cadmium detoxification mechanism from bacteria to humans: heavy metal tolerance conferred by the ATP-binding cassette (ABC) transporter SpHMT1 requires glutathione but not metal-chelating phytochelatin peptides. *J. Biol. Chem.* 284, 4936–4943. doi: 10.1074/jbc.M808130200

Rafati Rahimzadeh, M., Kazemi, S., and Moghadamnia, A. A. (2017). Cadmium toxicity and treatment: an update. *Caspian J. Intern. Med.* 8, 135–145. doi: 10.22088/cjim.8.3.135

Rahman, Z. (2020). An overview on heavy metal resistant microorganisms for simultaneous treatment of multiple chemical pollutants at co-contaminated sites, and their multipurpose application. *J. Hazard. Mater.* 396, 122682. doi: 10.1016/j.jhazmat.2020.122682

Salaskar, D. (2015). Isolation and identification of arsenic resistant *Providencia rettgeri* (KDM3) from industrial effluent contaminated soil and studies on its arsenic resistance mechanisma. *J. Microb. Biochem. Technol.* 07, 194–201. doi: 10.4172/1948-5948.1000204

Saunders, M., and Shaw, J. A. (2014). Biological applications of energy-filtered TEM. *Methods Mol. Biol.* 1117, 689–706. doi: 10.1007/978-1-62703-776-1_31

Sharma, J., Shamim, K., Dubey, S. K., and Meena, R. M. (2017). Metallothionein assisted periplasmic lead sequestration as lead sulfite by *Providencia vermicola* strain SJ2A. *Sci. Total Environ.* 579, 359–365. doi: 10.1016/j.scitotenv.2016.11.089

Shukla, A., Parmar, P., Goswami, D., Patel, B., and Saraf, M. (2021). Exemplifying an archetypal thorium-EPS complexation by novel thoriotolerant *Providencia thoriotolerans* AM3. *Sci. Rep.* 11, 3189. doi: 10.1038/s41598-021-82863-4

Sui, F.-Q., Chang, J-D., Tang, Z., Liu, W. J., Huang, X. Y., Zhao, F.-J. (2018). Nramp5 expression and functionality likely explain higher cadmium uptake in rice than in wheat and maize. *Plant Soil.* 433, 377–389. doi: 10.1007/s11104-018-3849-5

Thacker, U., Parikh, R., Shouche, Y., and Madamwar, D. (2006). Hexavalent chromium reduction by *Providencia* sp. process. *Biochemistry* 41, 1332–1337. doi: 10.1016/j.procbio.2006.01.006

Volesky, B., and Holan, Z. R. (1995). Biosorption of heavy metals. *Biotechnol. Prog.* 11, 235–250. doi: 10.1021/bp00033a001

Wang, P., Chen, H., Kopittke, P. M., and Zhao, F. J. (2019). Cadmium contamination in agricultural soils of China and the impact on food safety. *Environ. Pollut.* 249, 1038–1048. doi: 10.1016/j.envpol.2019.03.063

Wei, Z., Van Le, Q., Peng, W., Yang, Y., Yang, H., Gu, H., et al. (2021). A review on phytoremediation of contaminants in air, water and soil. *J. Hazard. Mater.* 403, 123658. doi: 10.1016/j.jhazmat.2020.123658

Wickham, H. (2016). *ggplot2: Elegant Graphics for Data Analysis*. New York, NY: Springer-Verlag. Available online at: https://ggplot2.tidyverse.org.

Zhai, Q., Xiao, Y., Zhao, J., Tian, F., Zhang, H., Narbad, A., et al. (2017). Identification of key proteins and pathways in cadmium tolerance of Lactobacillus plantarum strains by proteomic analysis. *Sci. Rep.* 7, 1182. doi: 10.1038/s41598-017-01180-x

Zhang, B., Gu, H., Yang, Y., Bai, H., Zhao, C., Su, S., et al. (2019). of AhpC in Resistance to Oxidative Stress in Burkholderia thailandensis. *Front. Microbiol.* 10, 1483. doi: 10.3389/fmicb.2019.01483

Zhao, F.-., J., and Wang, P. (2020). Arsenic and cadmium accumulation in rice and mitigation strategies. *Plant Soil* 446, 1–21. doi: 10.1007/s11104-019-04374-6

Zhou, X., Liu, X., Zhao, J., Guan, F., Yao, D., Wu, N., et al. (2021). The endophytic bacterium Bacillus koreensis 181-22 promotes rice growth and alleviates cadmium stress under cadmium exposure. *Appl. Microbiol. Biotechnol.* 105, 8517–8529. doi: 10.1007/s00253-021-11613-3

Conflict of Interest: The authors declare that the research was conducted in the absence of any commercial or financial relationships that could be construed as a potential conflict of interest.

Publisher's Note: All claims expressed in this article are solely those of the authors and do not necessarily represent those of their affiliated organizations, or those of the publisher, the editors and the reviewers. Any product that may be evaluated in this article, or claim that may be made by its manufacturer, is not guaranteed or endorsed by the publisher.

frontiers | Frontiers in Microbiology

ORIGINAL RESEARCH
published: 06 May 2022
doi: 10.3389/fmicb.2022.815704

Heavy Metal–Resistant Plant Growth–Promoting *Citrobacter werkmanii* Strain WWN1 and *Enterobacter cloacae* Strain JWM6 Enhance Wheat (*Triticum aestivum* L.) Growth by Modulating Physiological Attributes and Some Key Antioxidants Under Multi-Metal Stress

Abdul Wahab Ajmal[1], Humaira Yasmin[1]*, Muhammad Nadeem Hassan[1], Naeem Khan[2], Basit Latief Jan[3] and Saqib Mumtaz[1]*

[1] Department of Biosciences, COMSATS University Islamabad, Islamabad, Pakistan, [2] Department of Agronomy, Institute of Food and Agricultural Sciences, University of Florida, Gainesville, FL, United States, [3] Department of Clinical Pharmacy, College of Pharmacy, King Saud University, Riyadh, Saudi Arabia

OPEN ACCESS

Edited by:
Krishnendu Pramanik,
Visva-Bharati University, India

Reviewed by:
Xiuli Hao,
Huazhong Agricultural University, China
Aparna Banerjee,
Universidad Católica del Maule, Chile

***Correspondence:**
Saqib Mumtaz
saqib.mumtaz@comsats.edu.pk;
saqiosaqi@yahoo.com
Humaira Yasmin
humaira.yasmin@comsats.edu.pk

Specialty section:
This article was submitted to Terrestrial Microbiology, a section of the journal Frontiers in Microbiology

Received: 15 November 2021
Accepted: 03 February 2022
Published: 06 May 2022

Citation:
Ajmal AW, Yasmin H, Hassan MN, Khan N, Jan BL and Mumtaz S (2022) Heavy Metal–Resistant Plant Growth–Promoting Citrobacter werkmanii Strain WWN1 and Enterobacter cloacae Strain JWM6 Enhance Wheat (Triticum aestivum L.) Growth by Modulating Physiological Attributes and Some Key Antioxidants Under Multi-Metal Stress. Front. Microbiol. 13:815704. doi: 10.3389/fmicb.2022.815704

Due to wastewater irrigation, heavy metal (HM) exposure of agricultural soils is a major limiting factor for crop productivity. Plant growth–promoting bacteria (PGPB) may lower the risk of HM toxicity and increase crop yield. In this context, we evaluated two HM-resistant PGPB strains, i.e., *Citrobacter werkmanii* strain WWN1 and *Enterobacter cloacae* strain JWM6 isolated from wastewater-irrigated agricultural soils, for their efficacy to mitigate HM (Cd, Ni, and Pb) stress in a pot experiment. Increasing concentrations (0, 50, 100, and 200 ppm) of each HM were used to challenge wheat plants. Heavy metal stress negatively affected wheat growth, biomass, and physiology. The plants under elevated HM concentration accumulated significantly higher amounts of heavy metals (HMs) in shoots and roots, resulting in increased oxidative stress, which was evident from increased malondialdehyde (MDA) content in roots and shoots. Moreover, alterations in antioxidants like superoxide dismutase (SOD), peroxidase (POD), ascorbate peroxidase (APX), and catalase (CAT) were observed in plants under HM stress. The severity of damage was more pronounced with rising HM concentration. However, inoculating wheat with *Citrobacter werkmanii* strain WWN1 and *Enterobacter cloacae* strain JWM6 (10^7 CFU ml^{-1}) improved plant shoot length (11–42%), root length (19–125%), fresh weight (41–143%), dry weight (65–179%), and chlorophyll a (14%-24%) and chlorophyll b content (2–24%) under HM stress. *Citrobacter werkmanii* strain WWN1 and *Enterobacter cloacae* strain JWM6 either alone or in co-inoculation enhanced the antioxidant enzyme activity, which may lower oxidative stress in plants. However, seeds treated with the bacterial consortium showed an overall better outcome in altering oxidative stress and decreasing HM accumulation in wheat shoot and root

tissues. Fourier transform infrared spectroscopy indicated the changes induced by HMs in functional groups on the biomass surface that display effective removal of HMs from aqueous medium using PGPB. Thus, the studied bacterial strains may have adequate fertilization and remediation potential for wheat cultivated in wastewater-irrigated soils. However, molecular investigation of mechanisms adopted by these bacteria to alleviate HM stress in wheat is required to be conducted.

Keywords: heavy metals contamination, plant growth promoting bacteria, *Citrobacter* werkmanii and *Enterobacter* cloacae, wastewater irrigated agricultural soils, bioremediation and biofertilization, cadmium (Cd), lead (Pb), nickle (Ni)

INTRODUCTION

The agricultural sector is one of the most significant contributors to the world economy and serves as the basic livelihood of people in many countries, including Pakistan (Mishra et al., 2014). The importance of agriculture in providing food to an ever-increasing population can never be denied (Baldos and Hertel, 2014). However, regions around the globe practicing agriculture are facing numerous challenges, including shortage of freshwater and biotic and abiotic stresses under normal conditions (Hussain et al., 2018). Pakistan is among many other countries facing severe freshwater shortage. Due to shortage of freshwater and lack of treatment facilities, wastewater is disposed of by irrigating agricultural fields. This wastewater irrigation around industrial cities compensates for the deficiency of freshwater and supplies various nutrients necessary for plant growth (Khan and Bano, 2016). However, irrigation of agricultural fields with wastewater may alter the microbiological and physicochemical properties of soil and accumulate various biological and chemical contaminants in the land.

Among various pollutants, heavy metals (HMs) have become an alarming environmental hazard for the last few decades (Shoeva and Khlestkina, 2018). HMs enter soil via anthropogenic and geogenic sources such as industrial waste, fertilizers, sewage disposal, electroplating, and atmospheric deposition (Patel et al., 2018). HMs such as cadmium (Cd), chromium (Cr), mercury (Hg), nickel (Ni), arsenic (As), and lead (Pb) are thought to be highly toxic due to their bioaccumulative behavior and non-biodegradability (Taamalli et al., 2014). Earlier studies have highlighted that levels of Ni (30 mg/kg), Cd (6.1 mg/kg), and Pb (63.6 mg/kg) in wastewater-irrigated agricultural soils in different cities of Punjab, Pakistan, were above permissible limits (Ajmal et al., 2021; Iqbal et al., 2022). These HMs pose various environmental threats. For instance, even in small amounts, Cd in soils causes toxic effects on crops, such as reducing leaf photosynthetic efficiency, cell membrane lipid peroxidation, and inhibiting antioxidant enzymes (Rizwan et al., 2017; Ahanger et al., 2020; Kaya et al., 2020). Similarly, Pb is easily adsorbed in the soil and disturbs nutrient and plant water balance (Ashraf et al., 2015). At higher concentrations, Ni can inhibit cell division in meristematic root tissues and decrease photosynthesis and respiration (Bhalerao et al., 2015). These HMs obtained from soil enters human food chains via utilization of various cereal, legume, and vegetable crops (Kloke et al., 1984; Rizwan et al., 2016).

Among cereals, wheat (*Triticum aestivum* L.) serves as a staple food for above fifty percent of the world population. Hence, its demand is increasing with every coming day (Curtis and Halford, 2014). Meeting these increasing demands is a big question for policymakers and researchers (Shiferaw et al., 2013). Wheat can accumulate HMs in different parts like leaves, shoot, roots, and grains more than other cereal crops (Harris and Taylor, 2013). The transfer of HMs from soil to aerial parts of plants is dependent upon xylem and phloem loading (Page and Feller, 2005). So, it is crucial to minimize the uptake and translocation of HMs to edible parts of plants, which is an ultimate hazard for wheat-consuming populations (Keller et al., 2015).

In this regard, plant growth–promoting bacteria (PGPB) ameliorate plant productivity by limiting the adverse effects of biotic and abiotic stresses like pathogens, drought, salinity, and metal stress (Khanna et al., 2019a,b; Ahmad et al., 2021; Fahsi et al., 2021). The beneficial bacterial strains produce various metabolites, enzymes, and hormones that help to increase nutrient solubilization and stress alleviation. These mechanisms include siderophores, indole acetic acid (IAA), abscisic acid (ABA), ACC deaminase, and ethylene production (Mesa-Marín et al., 2018). Moreover, HM-tolerant PGPB increase plant root development and improve growth by raising the photosynthetic efficiency due to higher chlorophyll content and revamped PSII functionality (Giannakoula et al., 2021). Thus, HM-tolerant PGPB are an inexpensive, target-specific, and eco-friendly approach to cope with various biotic and abiotic stresses.

The resistance mechanisms against HMs induced by PGPB include biotransformation (change in the valence state of HMs) and bioaccumulation (HM accumulation inside the bacterial cell) (Mesa et al., 2015; Mallick et al., 2018). Therefore, PGPB can be exploited as biostimulants to increase plant growth by minimizing metal uptake by roots and restricting its transfer to aerial parts of plants (Sharaff et al., 2020). Moreover, to enhance HM resistance in plants, HM-tolerant PGPB are known to lessen the deterioration posed by reactive oxygen species (ROS) released by plants under HM stress by elevating the activity of several ROS-scavenging enzymes such as superoxide dismutase (SOD), peroxidase (POD), ascorbate reductase (APX), and catalase (CAT) (Ahmad et al., 2010, 2019; El-Meihy et al., 2019; Kohli et al., 2019).

Although HM-resistant PGPB are already reported, there are some limitations of these strains when used directly as biofertilizers (Borriss, 2011). Firstly, the soil is contaminated with several toxic HMs and chemicals; secondly, not all HM-resistant

bacteria are plant growth promoters; and thirdly, not all bacterial strains can be active in all types of environmental conditions such as pH, temperature, humidity, and other soil properties. Therefore, isolation of potent multi-metal-resistant bacteria with PGP traits is in demand to increase crop productivity under metal stress conditions.

In this context, information is scanty about the potential of Cd-, Ni-, and Pb-resistant PGP *Citrobacter werkmanii* strain WWN1 and *Enterobacter cloacae* strain JWM6 to alleviate deleterious effects on wheat growing in Cd-, Ni-, and Pb-contaminated soils by modulating osmoregulation, photosynthetic machinery, and the antioxidant defense system. Therefore, this study aimed to reveal the potential of *Citrobacter werkmanii* strain WWN1 and *Enterobacter cloacae* strain JWM6 isolated from agricultural soils irrigated with wastewater to mitigate multi-metal toxicity in wheat. Moreover, the impact of PGPB to induce HM resistance in wheat by alteration in defense metabolism was also observed. This research may offer new ways to enhance crop yield by reducing HM toxicity to plants by the application of bacteria as biofertilizers.

MATERIALS AND METHODS

Pot Experiment

A pot experiment was conducted in a greenhouse, located at COMSATS University Islamabad, Pakistan during November 2019 to March 2020. Seeds of wheat (PK-13) were obtained from the National Agricultural Research Center (NARC), Islamabad, Pakistan. *Citrobacter werkmanii* strain WWN1 (accession no.: MT941418) and *Enterobacter cloacae* strain JWM6 (accession no.: MT941425) were used to inoculate plants in this study. Both bacterial strains exhibited multi-HM (Cd, Ni, and Pb) resistance *in vitro* and were also able to remove these metals from the aqueous solution. *Citrobacter werkmanii* strain WWN1 and *Enterobacter cloacae* strain JWM6 removed 79, 87, and 43% and 78, 86, and 51% of Cd, Ni, and Pb, respectively, from 10 mg/L aqueous HMs solution. PGPB traits, i.e., phosphate, potassium, and zinc solubilization and protease and siderophore production, displayed by these strains were reported in a previous study (Ajmal et al., 2021).

The soil used in the pots contained total N = 0.05%, P = 16.2 mg/kg, Na = 4.3 meq/L, CaMg = 7.9 mq/L, Fe = 4.44 mg/kg, Zn = 0.72 mg/kg, EC = 1.3 dms^{-1}, pH = 7.79, ESP = 2.3, and organic matter = 0.82%. The soil was passed through a 2-mm sieve, dried, and thoroughly mixed with HMs cocktail containing Cd as $CdCl_2{\cdot}2H_2O$, Ni as $NiSO_4{\cdot}6H_2O$, and Pb in the form of $Pb(NO_3)_2$ to obtain final concentrations of 50, 100, and 200 ppm for each of these three HMs and control with no HM addition. Three replicates were used for each treatment. Five kilograms of soil spiked with different concentrations of HMs was put in the plastic pots (22 × 17 cm) and was left to settle for 3 months (Li et al., 2019).

Inoculum Preparation

A pure colony of each of *Citrobacter werkmanii* strain WWN1 and *Enterobacter cloacae* strain JWM6 was transferred to LB broth and incubated at 30 ± 1°C overnight to obtain respective bacterial culture. The bacterial cells were then centrifuged for 5 min at 6,000 × *g*. The resulting bacterial pellets were resuspended in sterilized distilled water (SDW). The bacterial cultures were maintained at 10^7 CFU ml^{-1} by checking the optical density using a UV–visible spectrophotometer (Sudisha et al., 2006).

Seed Sterilization and Inoculation

To surface sterilize, wheat seeds were soaked in 5% NaClO solution for 2 min and then again for 2 min in 70% ethanol. After that, seeds were rinsed with SDW thoroughly. Seeds were imbibed (12 h at room temperature) with bacterial cells (10^7 ml^{-1}) contained in 0.9% NaCl solution (Wang et al., 2016). Sterilized seeds were soaked in 0.9% NaCl solution and were sown in pots filled with HM-amended soil. Pots without added HMs and bacterial inoculation were treated as control. Pots were randomly kept in the greenhouse under natural conditions. The experiment was laid out as a completely randomized design (CRD) having three replicates for each treatment. Plants were uprooted after 120 days, and roots and shoots were parted for further analysis. A total of ten plants from each treatment were used for shoot and root length measurement and recording fresh and dry weights.

For various enzymatic analyses, the shoots and roots of sampled plants were separated and were stored at 4°C. For the estimation of bacterial colony-forming units (CFU), rhizospheric soil from each treatment was collected to check the viability of the applied bacterial inoculum. The CFU of rhizospheric soil was calculated by serial dilution and spread plate method (Humphris et al., 2005). Details of treatments used in the pot experiment are provided in **Table 1**.

Estimation of Photosynthetic Pigment Content

Chlorophyll a and chlorophyll b contents of wheat were assessed by adding 10 ml of dimethyl sulfoxide (DMSO) to fresh leaves (0.5 g) in Eppendorf tubes. The tubes were incubated at room temperature for 72 h or alternatively at 65°C in a water bath for 4 h. After incubation, the absorbance of the supernatant was checked at 665-nm and 645-nm wavelengths. Chlorophyll a and chlorophyll b were estimated by the following formula (Shoaf and Lium, 1976):

Chl a mg/g = [12.7 (OD 663) – 2.69 (OD645)] × V/1000 × W

Chl b mg/g = [22.9 (OD645) – 4.68 (OD663)] × V/1000 × W

where

V, volume of extract.

W, weight of sample.

Measurement of Malondialdehyde Content

To determine the intensity of oxidative damage on the membrane due to HM toxicity, malondialdehyde formation in roots and shoots of wheat was detected as an indication of lipid peroxidation. Briefly, 10 ml (0.1%) of trichloroacetic acid (TCA) was used to homogenize 0.5 g fresh plant tissues, and centrifugation was done at 12,000 *g*. Four milliliters of TCA containing 5% thiobarbituric acid (TBA) was added to 1 ml

TABLE 1 | Details of the treatments used in the pot experiment.

Treatments	Details
Control	Non-inoculated without HM amendment
A	Inoculated with *Citrobacter werkmanii* strain WWN1 without HM amendment
B	Inoculated with *Enterobacter cloacae* strain JWM6 without HM amendment
AB	Inoculated with bacterial consortium without HM amendment
50, 100, 200 ppm	Inoculated with HMs at respective concentrations
50 ppm + A 50 ppm + B 50 ppm + AB	Inoculated with bacteria and HMs at respective concentrations
100 ppm + A 100 ppm + B 100 ppm + AB	Inoculated with bacteria and HMs at respective concentrations
200 ppm + A 200 ppm + B 200 ppm + AB	Inoculated with bacteria and HMs at respective concentrations

HMs, Ni, Cd, and Pb.

of the supernatant. Heating of the mixture was carried out at 95°C for 25 min, and then immediate cooling was done on ice. Centrifugation of the reactant mixture was carried out at 12,000 *g* for 10 min, and the absorbance of the supernatant was recorded at 532 and 660 nm (Buege and Aust, 1978).

Measurement of Proline Content

Proline content was assessed using acidic ninhydrin (Troll and Lindsley, 1955) with slight modifications. Aqueous sulfosalicylic acid (5 ml) was used to homogenize half a gram of fresh leaves. The reaction mixture was boiled for 10 min and was then allowed to cool. Two milliliters of glacial acetic acid and 4 ml of acidic ninhydrin were added to the supernatant and were placed in a boiling water bath. The reaction mixture was then cooled to room temperature followed by addition of 4 ml of toluene. The mixture was vortexed and allowed to settle. After that, the supernatant was segregated and absorbance was recorded at 520 nm. The proline content was determined by comparing the recorded values of absorbance with a standard curve of known concentration of L-proline and was expressed as l μg/g FW of leaf tissue.

Determination of Antioxidative Enzyme Activities

Preparation of Enzyme Extracts

For the preparation of crude enzyme extract, 0.5 g fresh wheat shoots and roots were taken separately and rinsed with distilled water (DW). Homogenization of samples was carried out on ice in 5 ml sodium phosphate buffer (pH 7.8). After that, samples were centrifuged at 5000 *g* for 20 min at 4°C. The crude enzyme extract was denied light exposure by covering it with aluminum foil and was preserved at 4°C for various enzymatic assays (Azmat et al., 2020).

Superoxide Dismutase Activity

Photoreduction of nitroblue tetrazolium (NBT) was followed to check the SOD activity of the extract (Beauchamp and Fridovich, 1971). The reaction mixture included 50 mM phosphate buffer of pH 7.8, 13 mM L-methionine, 0.1 mM EDTA, 75 μM NBT, 8 μM riboflavin, and 100 μL of crude enzyme extract. Riboflavin was added lastly, and the reaction was initiated by exposing the mixture to 20-W fluorescent lamps. The reaction was then terminated by removing the mixture from the light source after 15 min. The photoreduction of NBT was noted at 560 nm using a spectrometer.

Catalase Activity

Catalase activity was measured by using the method of Kumar et al. (2010) with slight modifications. The absorbance of the reaction mixture with 100 μL of 300 mM H_2O_2, 2.8 ml of dilute 50 mM phosphate buffer (pH 7.0), and 100 μL of crude enzyme extract was measured at 240 nm.

Peroxidase Activity

4-Methylcatechol, which causes oxidation when mixed with H_2O_2, was used as a substrate to determine the POD activity of crude extract (Gorin and Heidema, 1976). The reaction mixture (3 ml) was put together by adding 100 mM sodium phosphate buffer (pH 7.0), 5 mM H_2O_2, 5 mM 4-methylcatechol, and 500 μl of crude extract, and the absorbance was recorded at 420 nm.

Ascorbate Peroxidase Activity

Ascorbate peroxidase activity was recorded by monitoring the rate of ascorbate oxidation at 290 nm (Yoshimura et al., 2000). The reaction mixture was composed of 25 mM phosphate buffer (pH 7), 1 mM H_2O_2, 0.5 mM ascorbic acid, and 100 μl of crude enzyme extract.

Determination of Heavy Metals in Plant Tissues

The total Cd, Ni, and Pb concentration in plant roots and shoots was assessed by the method described by Karstensen et al. (1998). HM accumulation in plant tissues was determined by the wet mineralization method (Lozano-Rodríguez et al., 1995). Briefly, plant tissues were washed with deionized distilled water (DDW) and dried at 80°C until a constant weight was achieved. After this, 0.25 g of each plant sample was finely ground. Three milliliters of nitric acid (65% v/v) and 2 ml of hydrogen peroxide (35% v/v) were added, and the mixture was autoclaved. After cooling, the solution volume was raised up to 50 ml using DW, and HMs were detected using atomic absorption spectroscopy.

Fourier Transform Infrared Spectroscopy Analysis of Heavy Metals Compounded to Bacterial Cells

Bacterial strains were inoculated in nutrient media spiked with 200 ppm of Pb, Ni, and Cd for 48 h and no HM-supplemented medium was treated as control. The samples were centrifuged at 4000 g for 15 min at 4°C. The resulting bacterial pellets were rinsed three times with sterilized deionized water, lyophilized, and ground in a freeze dryer. The dried bacterial biomass was used for Fourier transform infrared spectroscopy (FTIR) (Rodríguez-Sánchez et al., 2017).

Statistical Analysis

One-way (ANOVA) suited for CRD was applied to statistically analyze the samples. The mean values of the replicates were compared, and the correlation coefficient was calculated using Statistix 8.1. The significance of the difference among the treatments was measured using the least significant difference (LSD) at significance level $P < 0.05$ (Steel and Torrie, 1960). A correlation matrix heatmap was created using Origin 2020b. Principal coordinate analysis was carried out using PRIMER (Plymouth Routines in Multivariate Ecological Research), version 6.1.12, Primer-E Ltd, Plymouth, United Kingdom (Clarke and Warwick, 2001).

RESULTS

Germination Percentage

All the samples without HM (Cd, Ni, and Pb) stress whether uninoculated or inoculated with bacteria showed no significant effect on germination percentage. Similarly, no significant difference was recorded in germination percentage in the presence of 50 ppm, 100 ppm, or 200 pm of HM stress when plants were inoculated with bacteria compared to non-inoculated plants.

Colony-Forming Units of Rhizospheric Soil (CFU g^{-1})

The bacterial population of wheat rhizospheric soil was significantly reduced under HM stress. At 0 and 50 ppm of HMs, the CFU g^{-1} of rhizospheric soil was recorded as 5.4×10^6 and 4.13×10^6, respectively, after plants had been inoculated with the bacterial consortium. Under 100 ppm of HMs, *Citrobacter werkmanii* strain WWN1 showed the highest CFU g^{-1} of rhizospheric soil (3.9×10^6). In case of 200 ppm HM concentration, the bacterial consortium had the highest CFU g^{-1} of rhizospheric soil, i.e., 3.4×10^6 (**Figure 1**).

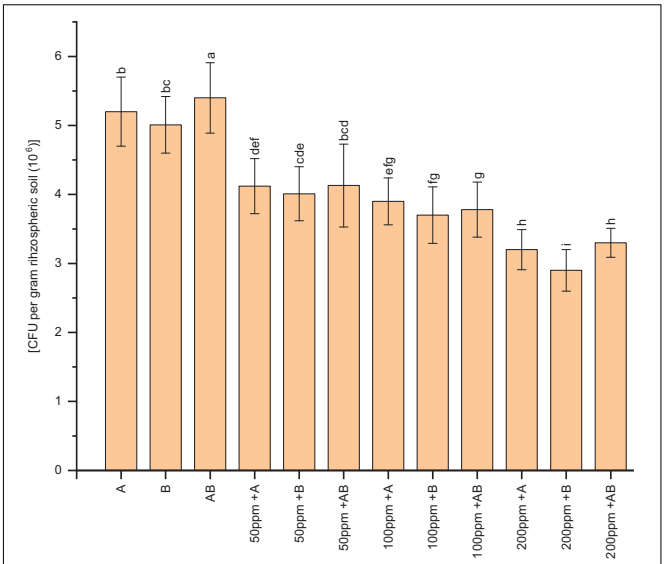

FIGURE 1 | Bacterial colonization [CFU per gram rhizospheric soil ($\times 10^6$)] in the rhizosphere of wheat under control and heavy metal (Cd, Ni, Pb) stress conditions. All the values are the mean of three replicates. Bars represent the standard error of means. Different letters above the bars indicate statistically significant difference between treatments at $P \leq 0.05$. A, *Citrobacter werkmanii* strain WWN1; B, *Enterobacter cloacae* strain JWM6; A + B, *Citrobacter* + *Enterobacter* consortium; 50 ppm, 50 ppm of Cd, Ni, and Pb; 100 ppm, 100 ppm of Cd, Ni, and Pb; 200 ppm, 200 ppm of Cd, Ni, and Pb.

Effect of Heavy Metal Concentration and the Bacterial Inoculation on Wheat Growth

Heavy metal stress had an adverse effect on the overall growth of plants. With rising HM concentration in soil, the shoot and root length decreased gradually. Under no HM stress, the shoot length ranged from 48 to 69 cm. The maximum increase in shoot length (41%) was exhibited by plants inoculated with *Citrobacter werkmanii* strain WWN1 compared to the control. At 50 ppm HM concentration, the range of shoot length was 45–59 cm. *Citrobacter werkmanii* strain WWN1 and *Enterobacter cloacae* strain JWM6 alone showed an increase of 33 and 34%, respectively, compared to uninoculated plants. When bacteria were applied in the consortium, an increase of 32% was observed for shoot length. Under 100 ppm, the shoot length ranged from 50 to 66 cm. A maximum increase of 40% (66 cm) was displayed by plants inoculated with the bacterial consortium. In case of 200 ppm, the shoot length of wheat ranged from 42 to 60 cm. A maximum increase of 42% was again observed under combined application of *Citrobacter werkmanii* strain WWN1 and *Enterobacter cloacae* strain JWM6 compared to uninoculated plants.

A similar trend was noticed in roots of plants under HM stress. At 0 ppm of HMs, the root length ranged from 19.3 to 25.1 cm. A maximum increase of 30% (25.1 cm) was observed in plants inoculated with *Enterobacter cloacae* strain JWM6. At 50 and 100 ppm, root lengths ranged from 12.8 to 29 cm and 14.4 to 31 cm, respectively. Under both of these concentrations, the bacterial consortium showed the maximum increase in root length where an increase of 125% (29 cm) and 114% (31 cm) was observed in plants inoculated with consortium as compared to uninoculated plants. Under 200 ppm of HM stress, wheat root length was measured from 12.2 to 18.5 cm. *Citrobacter werkmanii* strain WWN1 and *Enterobacter cloacae* strain JWM6 inoculated plants showed an increase of 39 and 44% in plant root length, respectively, while an increase of 51% (18.5) was observed when plants were inoculated with the bacterial consortium. Overall, under all HM concentrations, the bacterial consortium showed better improvement in shoot and root length (**Figures 2A,B**).

Effect of Heavy Metal Concentration and the Bacterial Inoculation on Wheat Biomass

The wet and dry weights of plant shoots and roots diminished with rising HM concentration. However, bacterial treatment significantly improved shoot and root biomass under HM stress. At 0 ppm of HMs, the shoot fresh weight ranged from 2.2 to 3.05 g and the dry weight ranged from 0.62 to 0.8 g. A maximum rise of 38 and 29% in shoot fresh and dry weights was detected

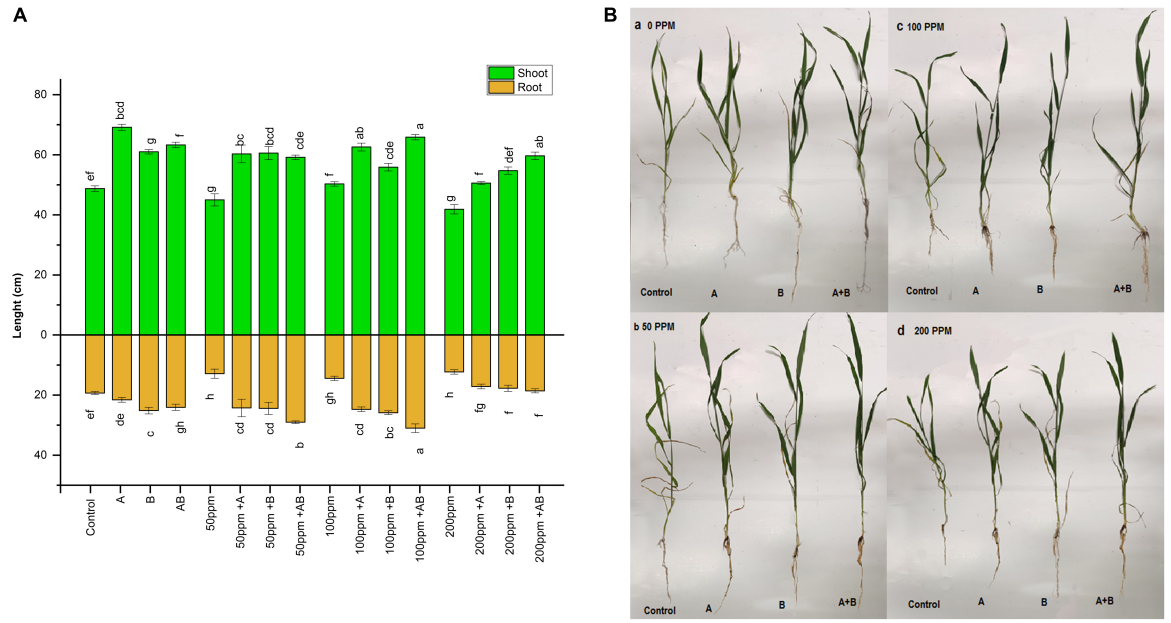

FIGURE 2 | (A) Effect of heavy metal–resistant plant growth–promoting bacteria on the length of shoots and roots of wheat (*Triticum aestivum*) under control and heavy metal (Cd, Ni, Pb) stress conditions. Values are mean of three replicates. Bars represent the standard error of means. Different letters above the bars indicate statistically significant difference between treatments at $P \leq 0.05$. Details of treatments are the same as those in **Figure 1**. **(B)** Effect of heavy metal (a) 0 ppm, (b) 50 ppm, (c) 100 ppm, and (d) 200 ppm resistant plant growth–promoting bacteria on the growth of wheat (*Triticum aestivum*) under control and heavy metal (Cd, Ni, Pb) stress conditions. Details of treatments are the same as those in **Figure 1**.

under the bacterial consortium. At 50 ppm, the fresh weight was recorded from 1.6 to 3.3 g and the dry weight ranged from 0.51 to 0.98 g. The maximum increase in shoot biomass was observed in plants after *Citrobacter werkmanii* strain WWN1 inoculation where an increase of 108% in shoot fresh weight and 90% in shoot dry weight was detected as compared to the uninoculated plants. In case of 100 ppm of HMs, the fresh weight recorded was from 1.6 to 3.38 g and the dry weight ranged from 0.46 to 0.93 g. The greatest increase of 112% in fresh weight and 100% in dry weight was observed in plants inoculated with the bacterial consortium. At 200 ppm HM stress, the fresh shoot weight ranged from 1.12 to 2.7 g and the dry weight ranged from 0.32 to 0.89 g. *Enterobacter cloacae* strain JWM6 inoculated plants showed the highest increase in fresh shoot weight (143%) and dry weight (117%) as compared to uninoculated plants (**Figure 3A**).

Heavy metals also had a negative impact on root biomass. However, inoculating plants with bacteria significantly enhanced root fresh and dry weights. Under 0 ppm of HMs, the root fresh weight ranged from 0.3 to 0.38 g and the dry weight was recorded in the range of 0.11 to 0.15 g. *Enterobacter cloacae* strain JWM6 and the bacterial consortium increased the root fresh weight by 24% and the root dry weight by 24 and 28%, respectively, when compared with the control. In case of 50 ppm of HMs, the fresh root weight ranged from 0.27 to 0.41 g and the dry weight was in the range of 0.07 to 0.16 g. A maximum rise of 51% in fresh weight and 125% in dry weight was observed when plants were applied with the bacterial consortium. At 100 ppm, root fresh and dry weights ranged from 0.2 to 0.37 g and 0.06 to 0.14 g, respectively. An increase of 84 and 110% in root fresh and dry weight was observed in plants inoculated with *Enterobacter cloacae* strain JWM6 compared to untreated plants. In case of 200 ppm, the fresh weight recorded was within 0.12–0.2 g and the dry weight was observed in the range of 0.04–0.06 g. An increase of 61% in both fresh and dry weights was observed in plants treated with *Citrobacter werkmanii* strain WWN1 (**Figure 3B**).

Effect of Heavy Metals and the Bacteria on Photosynthetic Pigments

The leaf chlorophyll content declined with an increase in HM concentration. However, bacterial inoculation significantly amplified the chlorophyll content under HM stress. Under 0 ppm of HMs, the chlorophyll a content ranged from 3.7 to 4.1 mg/g FW. Both *Citrobacter werkmanii* strain WWN1 and *Enterobacter cloacae* strain JWM6 increased the chlorophyll a content by 17 and 15%, respectively, while an increase of 21% (4.1 mg/g FW) was observed in case of plants under the inoculation of the bacterial consortium. Similarly, under HM stress, plants treated with PGPB showed a significant increase in chlorophyll a content as compared to uninoculated plants. At 50 ppm HM concentration, the chlorophyll a content ranged from 3.1 to 3.9 mg/g FW. Here *Citrobacter werkmanii* strain WWN1 increased chlorophyll a by 22%, *Enterobacter cloacae* strain JWM6 increased the chlorophyll a content by 24% (3.9 mg/g FW), and the bacterial consortium increased the chlorophyll a content by 23% in comparison to uninoculated plants. Under 100 and 200 ppm, the chlorophyll a content ranged from 2.98 to 3.68 mg/g FW and 2.76 to 3.36 mg/g FW, respectively, and a

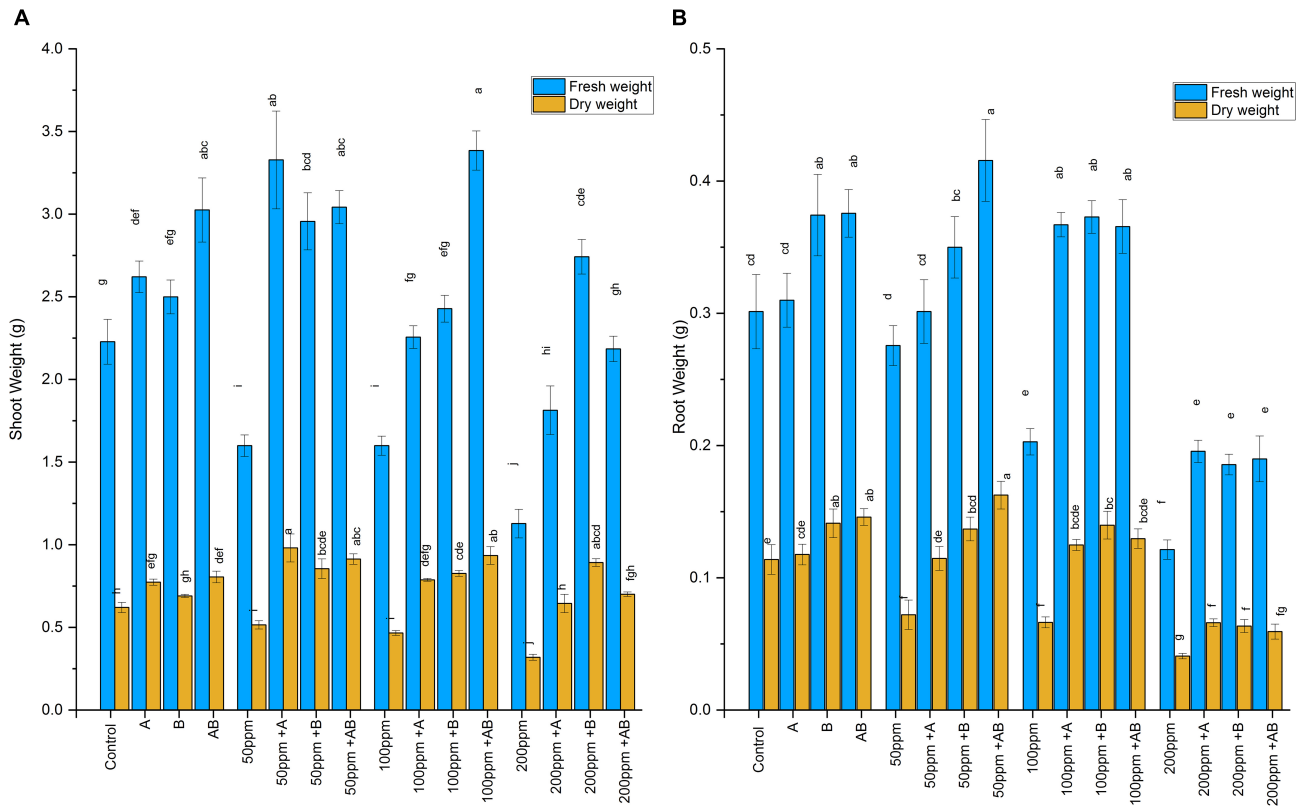

FIGURE 3 | (A) Effect of heavy metal–resistant plant growth–promoting bacteria on the fresh and dry weights of the shoots of wheat (*Triticum aestivum*) under control and heavy metal (Cd, Ni, Pb) stress conditions. Values are the mean of three replicates. Bars represent the standard error of means. Different letters above the bars indicate statistically significant difference between treatments at $P \leq 0.05$. Details of treatments are the same as those in **Figure 1**. **(B)** Effect of heavy metal–resistant plant growth–promoting bacteria on the fresh and dry weights of the roots of wheat (*Triticum aestivum*) under control and heavy metal (Cd, Ni, Pb) stress conditions. Values are the mean of three replicates. Bars represent the standard error of means. Different letters above the bars indicate statistically significant difference between treatments at $P \leq 0.05$. Details of treatments are the same as those in **Figure 1**.

maximum increase of 23% (3.68 mg/g FW) and 21% (3.36 mg/g FW) was noticed in plants treated with the bacterial consortium when compared with uninoculated plants (**Figure 4**).

Similarly, the chlorophyll b content ranged from 2.21 to 2.27 mg/g FW without HM stress and *Citrobacter werkmanii* strain WWN1 and *Enterobacter cloacae* strain JWM6 increased the chlorophyll b content by 2.1 and 2.3% respectively and their consortium increased the chlorophyll b content by 1.9% (2.26 mg/g FW) under 0 ppm of HMs. Under HM stress, plants inoculated with PGPB showed a significant rise in chlorophyll b content. For example, under 50 ppm HM stress, the chlorophyll b content ranged from 2.05 to 2.28 mg/g FW. Here *Citrobacter werkmanii* strain WWN1 and *Enterobacter cloacae* strain JWM6 alone increased the chlorophyll b content by 9.8 and 10%, respectively, and an increase of 11% (2.28 mg/g FW) was observed in plants treated with the bacterial consortium in comparison to untreated plants. In case of 100 ppm, *Citrobacter werkmanii* strain WWN1 and *Enterobacter cloacae* strain JWM6 increased the chlorophyll b content by 18 and 17%, respectively, and by 17% (2.25 mg/g FW) when these strains were applied in consortium. Under 200 ppm, the chlorophyll b content ranged from 1.81 to 2.25 mg/g FW and an increase of 22 and 23% was observed in plants inoculated with *Citrobacter werkmanii* strain WWN1 and *Enterobacter cloacae* strain JWM6, respectively. When applied in consortium, these two strains augmented the chlorophyll b content by 24% (2.25 mg/g FW) compared to uninoculated plants (**Figure 4**).

Effect of Heavy Metal Stress and the Bacterial Inoculation on Malondialdehyde Content

The MDA content of both shoots and roots of plants increased with an increase in the HM concentration. However, bacterial inoculation lowered the MDA content significantly. In pots added with 0 and 50 ppm HMs, root MDA ranged from 2.1 to 3.9 nmol g^{-1} FW and 7.7 to 2.4 nmol g^{-1} FW, respectively. A maximum decline of 44% (2.1 nmol g^{-1} FW) and 68% (2.4 nmol g^{-1} FW) was observed in plant roots treated with *Enterobacter cloacae* strain JWM6 under 0 and 50 ppm of HMs, respectively, compared to uninoculated plants. In case of 100 ppm, root MDA ranged from 9.4 to 3.5 nmol g^{-1} FW and a decline of 61 and 51% was observed in plants inoculated with *Citrobacter werkmanii* strain WWN1 and *Enterobacter cloacae* strain JWM6, respectively,

while both of these strains together reduced root MDA by 62% (3.5 nmol g^{-1} FW) in comparison to uninoculated plants. At 200 ppm, the shoot MDA content measured was between 14.63 and 6.6 nmol g^{-1} FW. A maximum decrease of 54% was noticed in plants applied with the bacterial consortium as compared to uninoculated plants.

A similar trend was observed in wheat shoots, where the MDA content increased with rising HM concentrations. However, bacterial inoculation significantly dropped the MDA content as compared to the uninoculated plants. In shoots under 0 ppm of HMs, the MDA content ranged from 1.89 to 2.66 nmol g^{-1} FW. *Citrobacter werkmanii* strain WWN1 and *Enterobacter cloacae* strain JWM6 decreased the MDA content by 12 and 6%, respectively, while a decline of 29% (1.89 nmol g^{-1} FW) was recorded in plants inoculated with the bacterial consortium. Under 50 ppm of HMs in soil, the MDA content ranged from 2.1 to 9.42 nmol g^{-1} FW. *Citrobacter werkmanii* strain WWN1 and *Enterobacter cloacae* strain JWM6 inoculated plants showed a reduction of 76% (2.1 nmol g^{-1} FW) and 66% in MDA level, respectively, when compared with uninoculated plants. In case of 100 ppm HM stress, MDA ranged from 5.29 to 15.14 nmol g^{-1} FW, whereas *Citrobacter werkmanii* strain WWN1 decreased shoot MDA content by 56% and *Enterobacter cloacae* strain JWM6 lowered MDA content by 63%. When these bacteria were applied in the form of consortium, an overall decrease of 65% (5.29 nmol g^{-1} FW) was observed compared to uninoculated plants. Under 200 ppm of HM stress, shoot MDA ranged from 17.7 to 7.01 nmol g^{-1} FW. *Citrobacter werkmanii* strain WWN1 and *Enterobacter cloacae* strain JWM6 alone decreased the shoot MDA content by 51 and 49%, respectively, while when applied in consortium, a decline of 60% (7.01 nmol g^{-1} FW) was observed compared to uninoculated plants. Overall, the bacterial consortium proved to be better in reducing the MDA content under higher HM stress than single bacterial treatment (**Figure 5A**).

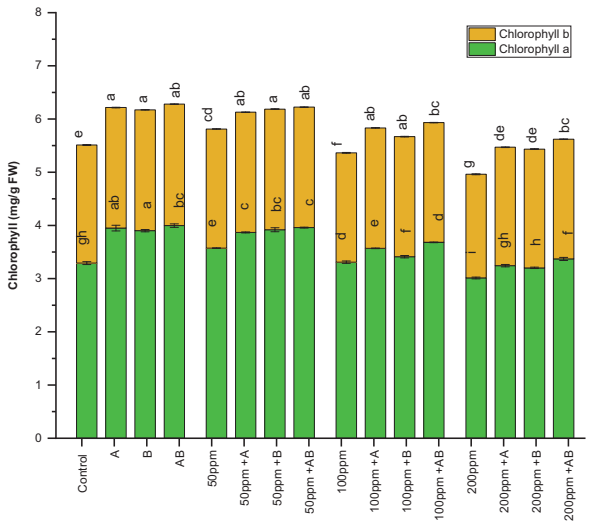

FIGURE 4 | Effect of heavy metal–resistant plant growth–promoting bacteria on chlorophyll a and chlorophyll b of wheat (*Triticum aestivum*) under control and heavy metal (Cd, Ni, Pb) stress conditions. Values are the mean of three replicates. Bars represent the standard error of means. Different letters above the bars indicate statistically significant difference between treatments at $P \leq 0.05$. Details of treatments are the same as those in **Figure 1**.

Effect of Heavy Metal Stress and the Bacteria on Proline Content

Like MDA, the proline content also escalated with rising HM stress. However, inoculation of PGPB significantly lowered the leaf proline content. Without HM stress, the proline content measured was in the range of 21–30 μg/g FW. A maximum reduction of 30% (21 μg/g FW) in proline content was measured in plants inoculated with the bacterial consortium. Under 50 ppm

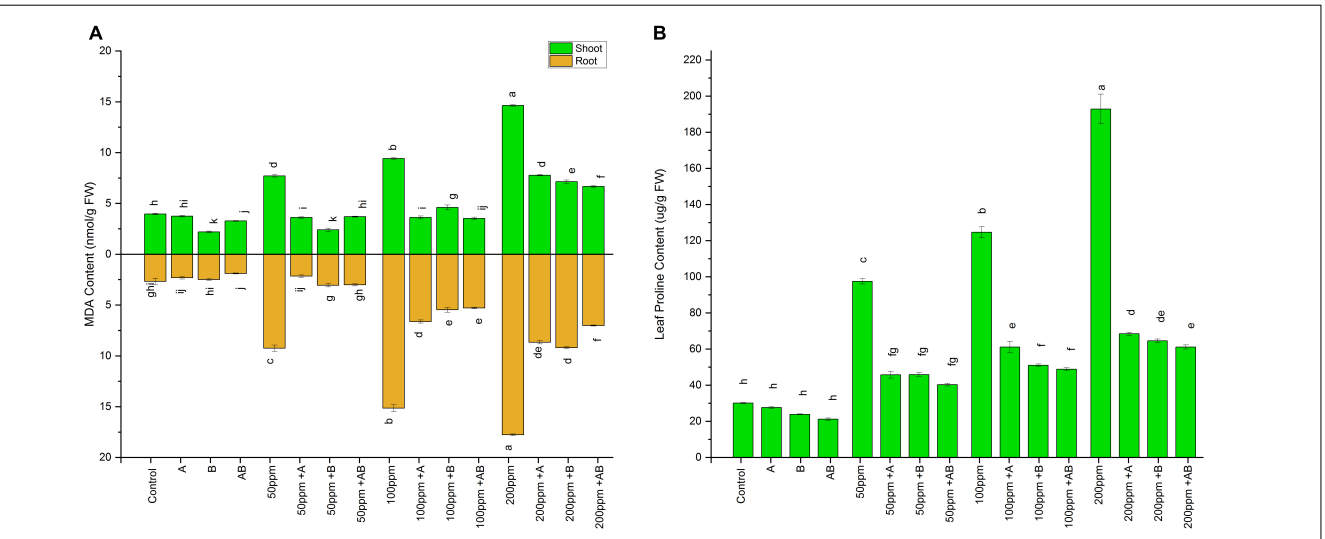

FIGURE 5 | Effect of heavy metal–resistant plant growth–promoting bacteria on **(A)** MDA and **(B)** proline activity of wheat (*Triticum aestivum* L.) in plants under control and heavy metal (Cd, Ni, Pb) stress conditions. Values are the mean of three replicates. Bars represent the standard error of means. Different letters above the bars indicate statistically significant difference between treatments at $P \leq 0.05$. Details of treatments are the same as those in **Figure 1**.

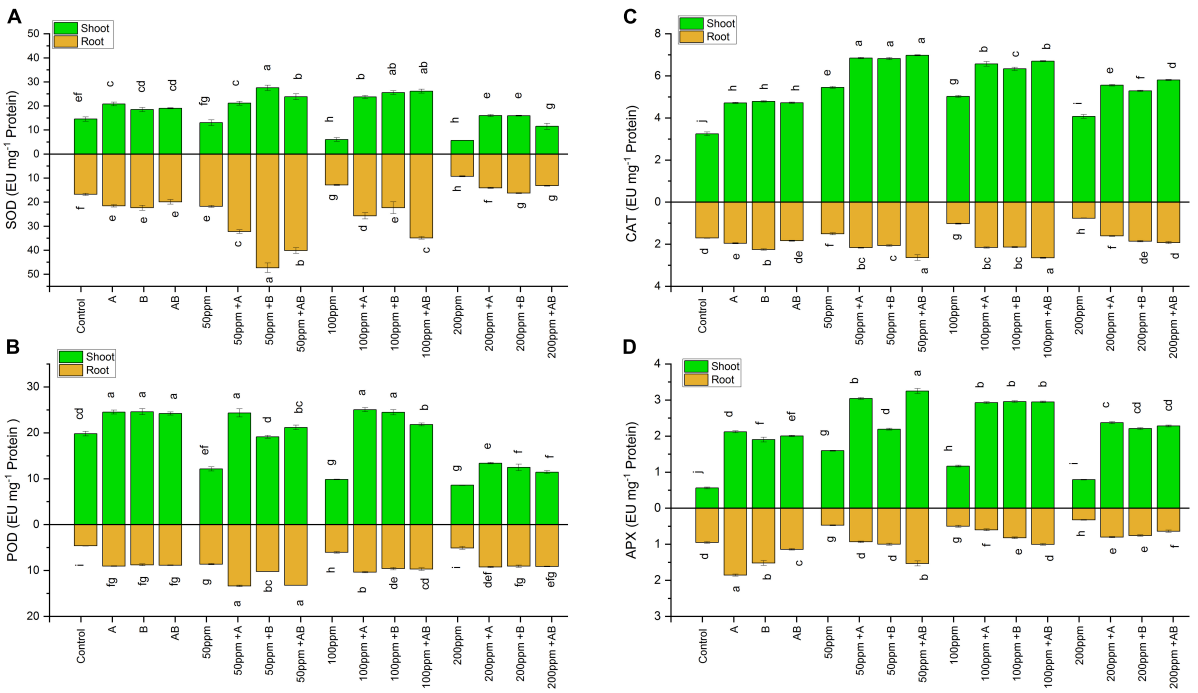

FIGURE 6 | Effect of heavy metal–resistant plant growth–promoting bacteria on **(A)** SOD, **(B)** POD, **(C)** CAT, and **(D)** APX activity of wheat (*Triticum aestivum* L.) in plants under control and heavy metal (Cd, Ni, Pb) stress conditions. Values are the mean of three replicates. Bars represent the standard error of means. Different letters above bars the indicate statistically significant difference between treatments at $P \leq 0.05$. Details of treatments are the same as those in **Figure 1**.

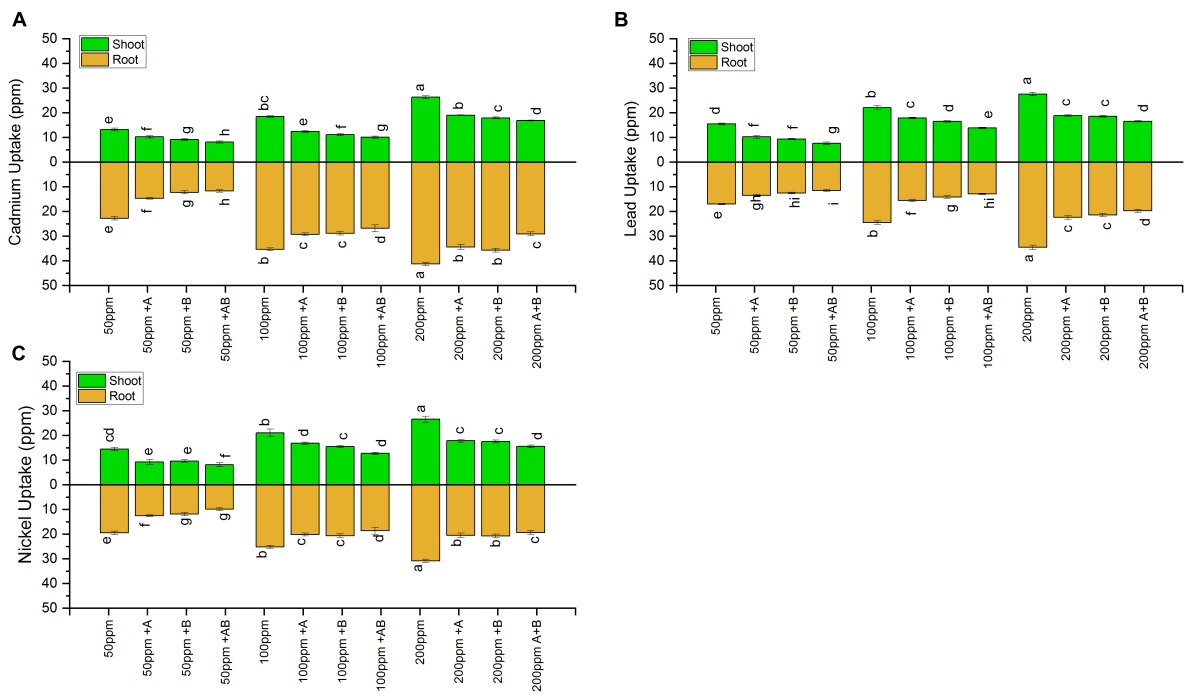

FIGURE 7 | Heavy metal **(A)** cadmium, **(B)** lead, and **(C)** nickel uptake by shoots and roots of wheat (*Triticum aestivum* L.) grown under different concentrations of multi-HMs. Values are the mean of three replicates. Bars represent the standard error of means. Different letters above the bars indicate statistically significant difference between treatments at $P \leq 0.05$. Details of treatments are the same as those in **Figure 1**.

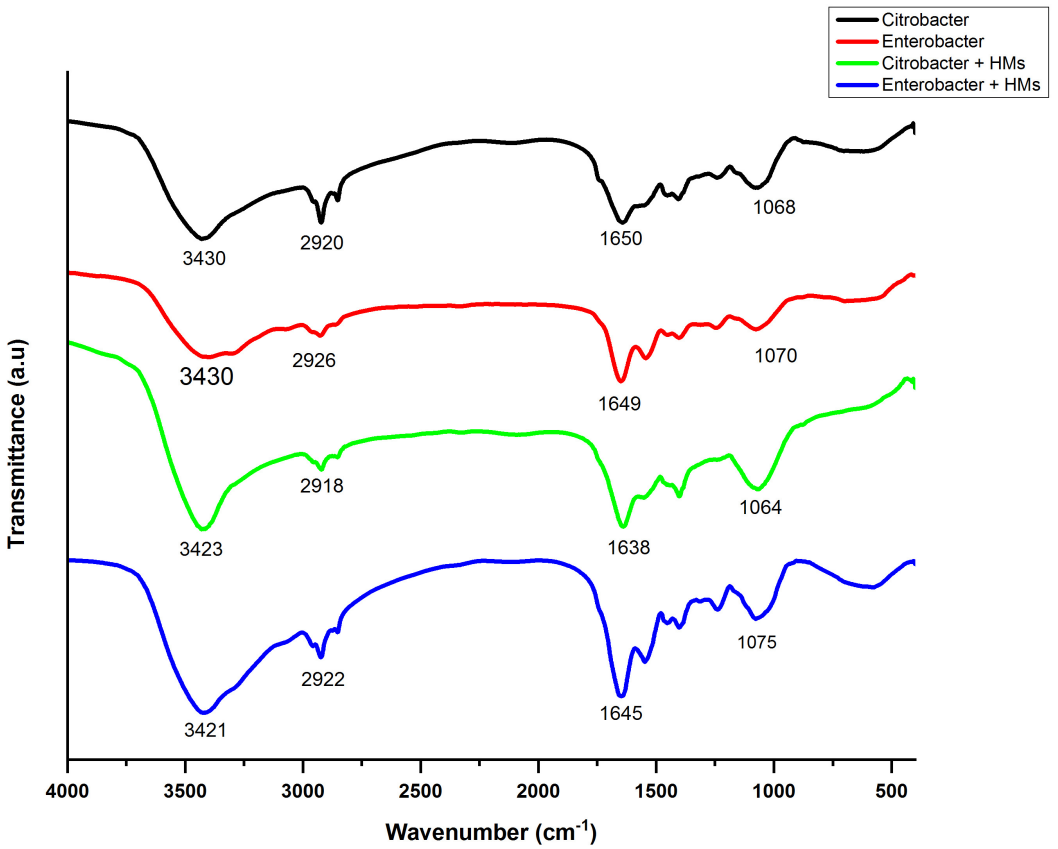

FIGURE 8 | Infrared spectra of *Citrobacter werkmanii* strain WWN1 and *Enterobacter cloacae* strain JWM6 biomass in the presence of heavy metals (HMs) (Ni, Cd, Ni).

and 200 ppm, proline ranged from 40 to 97 μg/g FW and 61 to 192 μg/g FW respectively. The bacterial consortium showed a maximum decline of 58% at 50 ppm and 68% at 200 ppm as compared to non-inoculated plants. However, in the case of 100 ppm, the proline level ranged from 49 to 124 μg/g FW. Here *Citrobacter werkmanii* strain WWN1 and *Enterobacter cloacae* strain JWM6 lowered the leaf proline content by 50 and 59%, respectively. When applied in a consortium, bacteria reduced the leaf proline content by 61% (49 μg/g FW) compared to uninoculated plants. Thus, under all three concentrations of HMs, the bacterial consortium dropped the proline content more than individual bacterial strains (**Figure 5B**).

Effect of Heavy Metal Exposure and the Bacterial Inoculation on Antioxidative Enzyme Activity of Wheat

Superoxide Dismutase Activity

The SOD activity in wheat shoots and roots declined with rising HM concentrations. However, bacterial treatment significantly boosted the shoot as well as root SOD content.

For shoots, at 0 ppm of HMs, the SOD enzyme level ranged from 14.5 to 20.7 EU mg^{-1} protein. An increase of 43% (20.7 EU mg^{-1} protein) and 23% was observed in plants treated with *Citrobacter werkmanii* strain WWN1 and *Enterobacter cloacae* strain JWM6, respectively, while bacterial consortia enhanced shoot SOD by 30% when compared with the control. In case of 50 ppm HM stress, the SOD content ranged from 13 to 29 EU mg^{-1} protein. A maximum rise of 111% (27.5 EU mg^{-1} protein) was displayed by plants applied with *Enterobacter cloacae* strain JWM6. Under 100 ppm HM concentration, the level of SOD was recorded in the range from 6 to 26 EU mg^{-1} protein. *Citrobacter werkmanii* strain WWN1 and *Enterobacter cloacae* strain JWM6 increased SOD by 293 and 322%, respectively, while plants treated with the bacterial consortium showed an increase of 332% (26 EU mg^{-1} protein) when compared to untreated plants. At 200 ppm, the shoot SOD content was in the range of 5.6–16 EU mg^{-1} protein. Both *Citrobacter werkmanii* strain WWN1 and *Enterobacter cloacae* strain JWM6 alone boosted SOD activity in shoot by 182 and 181%, respectively, and the consortium of these two strains elevated the shoot SOD content by 103% (11.5 EU mg^{-1} protein).

Similarly, in roots, in the absence of HM stress, the SOD content ranged from 16 to 22.4 EU mg^{-1} protein. An increase of 28% was recorded in plants inoculated with *Citrobacter werkmanii* strain WWN1, and a rise of 33% (22.3 EU mg^{-1} protein) was seen in plants treated with *Enterobacter cloacae* strain JWM6, while the bacterial consortium increased root

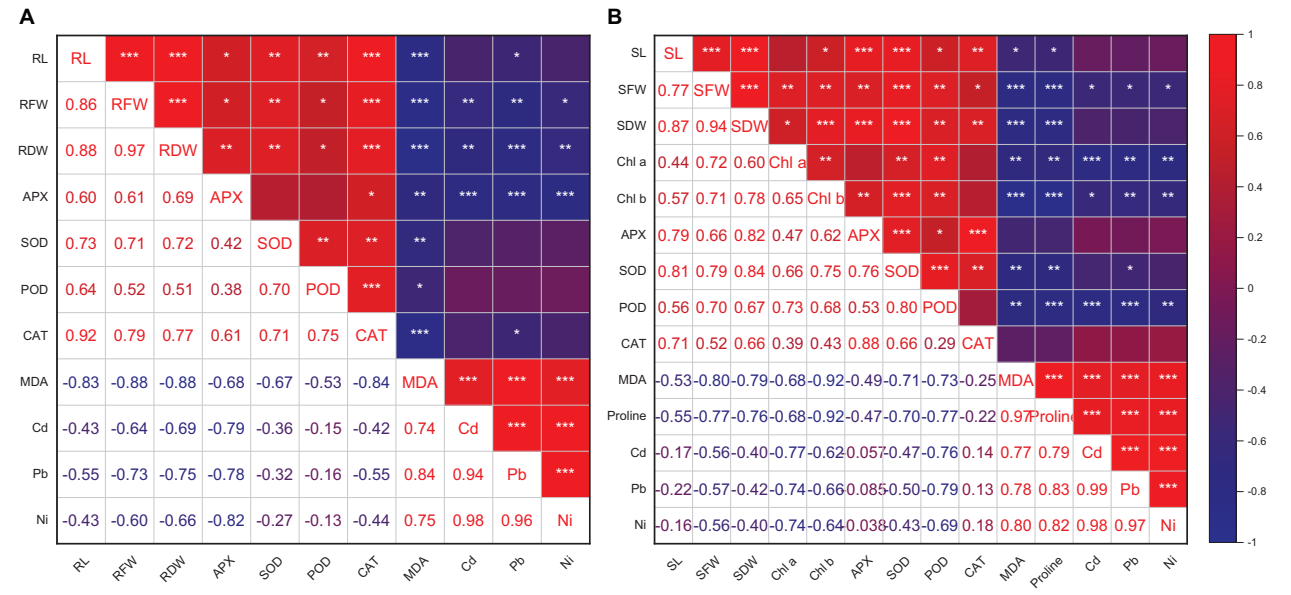

FIGURE 9 | Pearson's correlation coefficient (*r*) of growth attributes and antioxidant enzymes of wheat root **(A)** and shoot **(B)** with and without the inoculation of heavy metal–resistant plant growth–promoting bacteria under Cd, Ni, and Pb stress. RL (root length), RFW (root fresh weight), and RDW (shoot dry weight). SL, shoot length; SFW, shoot fresh weight; SDW, shoot dry weight; Chl a, chlorophyll a; Chl b, chlorophyll b. $^{*}p \leq 0.05$, $^{**}p \leq 0.01$, $^{***}p \leq 0.001$.

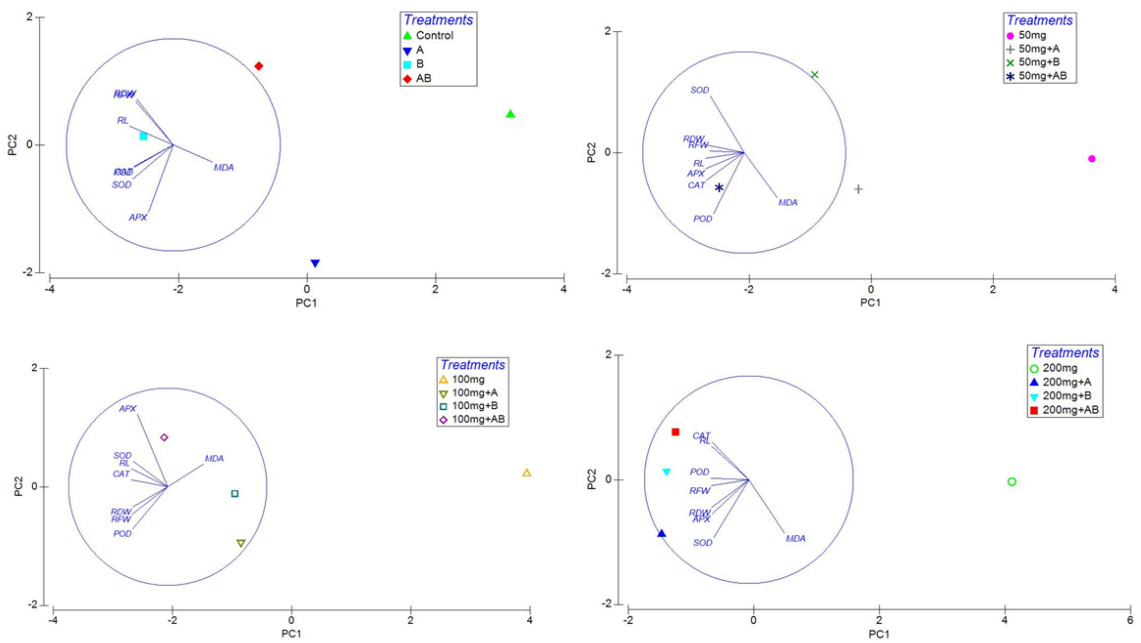

FIGURE 10 | Principal coordinate analysis (PCA) of the effect of bacterial inoculation on RL, root length; RFW, root fresh weight; and RDW, root dry weight and antioxidants in wheat roots. Details of treatments are the same as those in **Figure 1**.

SOD by 18% in comparison to untreated plants. At 50 ppm of HMs, the SOD content ranged from 21.7 to 47 EU mg^{-1} protein. A maximum increase of 117% (47 EU mg^{-1} protein) was observed in plant roots inoculated with *Enterobacter cloacae* strain JWM6. In case of 100 ppm, root SOD was in the range of 12.8–34.8 EU mg^{-1} protein. Plants treated with the bacterial consortium showed the highest increase of 170% (34.8 EU mg^{-1} protein) in root SOD when compared with non-treated plants. Under 200 ppm of HMs, root SOD ranged from 9.2 to 16.2 EU mg^{-1} protein. Plants applied with *Citrobacter werkmanii* strain WWN1 showed an increase of 75% (16.2 EU mg^{-1} protein), while *Enterobacter cloacae* strain JWM6 raised SOD

by 51%, and their consortium enhanced SOD activity by 42%. Overall, the SOD content in plant roots was greater than that in shoots (**Figure 6A**).

Peroxidase Activity

The peroxidase activity in the shoots and roots of wheat plants was amplified with an increase in HM concentration, and treatment with PGPB further enhanced POD in the shoots and roots of wheat in both the absence and presence of HMs. In case of no HMs, shoot POD ranged from 19.8 to 24.5 EU mg^{-1} protein. *Citrobacter werkmanii* strain WWN1 and *Enterobacter cloacae* strain JWM6 were able to increase shoot POD activity by 23 and 24%, respectively, while the bacterial consortium showed an increase of 22% compared to non-treated plants. In the case of 50 and 100 ppm, POD occured between 12 and 24.6 EU mg^{-1} protein and 9.8 and 21.8 EU mg^{-1} protein, respectively, and at 200 ppm, POD activity ranged from 8.5 to 13.3 EU mg^{-1} protein. Among all these three treatments, *Citrobacter werkmanii* strain WWN1 showed the maximum rise in shoot POD activity with 100% increase at 50 ppm, 154% increase at 100 ppm, and 56% rise at 200 ppm as compared to uninoculated plants.

In case of roots, a similar trend was observed where root POD increased with an increase in HM concentration and bacterial inoculation further enhanced root POD in the absence and presence of HMs. Under 0 ppm of HMs, root POD ranged from 4.6 to 9 EU mg^{-1} protein. *Citrobacter werkmanii* strain WWN1 and *Enterobacter cloacae* strain JWM6 inoculated plants showed an increase of 96% (9 EU mg^{-1} protein) and 90%, respectively, and the bacterial consortium enhanced root POD by 92% as compared to the control. In case of 50 ppm, root POD ranged from 8.6 to 13.35 EU mg^{-1} protein. An increase of 54 and 19% was observed in plants inoculated with *Citrobacter werkmanii* strain WWN1 and *Enterobacter cloacae* strain JWM6, respectively, while the bacterial consortium increased POD activity by 53% (13.32 EU mg^{-1} protein) as compared to their respective controls. At 100 ppm, the root POD content ranged from 6.1 to 10.3 EU mg^{-1} protein. A maximum increase of 71% (10.3 EU mg^{-1} protein) was observed in plants inoculated with *Citrobacter werkmanii* strain WWN1, while at 200 ppm of HMs, POD ranged from 5 to 9.2 EU mg^{-1} protein. PGPB-inoculated plants showed an increase in POD activity, i.e., 82% (9.2 EU mg^{-1} protein) increase by *Citrobacter werkmanii* strain WWN1, 78% by *Enterobacter cloacae* strain JWM6, and 80% increase in POD by the bacterial consortium compared to the respective control (**Figure 6B**).

Catalase Activity

The catalase activity in wheat shoots and roots was significantly higher under HM stress than no HM stress, and the bacterial inoculation further increased the CAT activity under HM stress. At 0 ppm of HMs, shoot CAT activity ranged from 3.2 to 4.8 EU mg^{-1} protein. An increase of 45 and 47% (4.8 EU mg^{-1} protein) was observed in plants inoculated with *Citrobacter werkmanii* strain WWN1 and *Enterobacter cloacae* strain JWM6, respectively, and their consortium increased CAT activity by 46% as compared to the control. In case of 50 ppm, shoot CAT activity was recorded as 5.4–7 EU mg^{-1} protein. Plants inoculated with *Citrobacter werkmanii* strain WWN1 and *Enterobacter cloacae* strain JWM6 showed an increase of 26% and 25%, respectively, and the bacterial consortium increased CAT activity by 28% (7 EU mg^{-1} protein) compared to the respective control. Under 100 ppm HM stress, CAT activity ranged from 5 to 6.7 EU mg^{-1} protein. *Citrobacter werkmanii* strain WWN1 and *Enterobacter cloacae* strain JWM6 increased CAT activity by 30% and 26%, respectively, while when applied in consortium, an increase of 33% (6.7 EU mg^{-1} protein) was observed compared to uninoculated plants. At 200 ppm of HMs, the catalase activity was recorded in the range of 4–5.8 EU mg^{-1} protein. The maximum CAT activity was observed in plant shoots inoculated with the bacterial consortium, where an increase of 42% (5.8 EU mg^{-1} protein) was observed as compared to uninoculated plants.

Similarly, root CAT activity was also enhanced under HM stress. Without HM stress, root CAT activity was measured as 1.7–2.3 EU mg^{-1} protein. Plants inoculated with *Enterobacter cloacae* strain JWM6 showed a maximum increase of 31% (2.25 EU mg^{-1} protein) as compared to uninoculated plants. In case of 50 and 100 ppm HMs, root CAT activity ranged from 1.5 to 2.6 EU mg^{-1} protein and 1.02–2.7 EU mg^{-1} protein, respectively. The bacterial consortium showed the maximum increase in root CAT activity at both 50 and 100 ppm as compared to their respective controls. Under 200 ppm of HMs, the root CAT was observed between 0.76 and 1.93 EU mg^{-1} protein. The bacterial inoculation increased the root CAT activity, i.e., *Citrobacter werkmanii* strain WWN1 by 109%, *Enterobacter cloacae* strain JWM6 by 142%, and the bacterial consortium by 151% as compared to uninoculated plants (**Figure 6C**).

Ascorbate Peroxidase Activity

The APX content in plants significantly increased with the application of PGPB as compared to uninoculated plants. In wheat shoots, in the absence of HM stress, the APX content ranged from 0.56 to 2.11 EU mg^{-1} protein. A maximum increase of 277% (2.11 EU mg^{-1} protein) in shoot APX activity was observed in plants inoculated with *Citrobacter werkmanii* strain WWN1 as compared to the control. At 50 ppm HM stress, shoot APX activity ranged from 1.6 to 3.2 EU mg^{-1} protein. The bacterial consortium showed a maximum increase of 103% in shoot APX as compared to uninoculated plants. In case of 100 ppm HM stress, APX activity ranged from 1.16 to 2.95 EU mg^{-1} protein and *Citrobacter werkmanii* strain WWN1, *Enterobacter cloacae* strain JWM6, and their consortium increased shoot APX by 150, 153, and 152%, respectively, as compared to the respective control. At 200 ppm of HMs, the APX content ranged from 0.79 to 2.37 EU mg^{-1} protein. *Citrobacter werkmanii* strain WWN1 and *Enterobacter cloacae* strain JWM6 showed an increase of 199% (2.37 EU mg^{-1} protein) and 180%, respectively, and the bacterial consortium increased the shoot APX by 188%.

Like shoots, the bacterial inoculation significantly improved root APX activity both without and with HM stress. In plants without HM stress, root APX ranged from 0.94 to 1.85 EU mg^{-1} protein. The highest increase of 95% (1.8 EU mg^{-1} protein) was observed in plants inoculated with *Citrobacter werkmanii* strain WWN1. At 50 and 100 ppm of HMs, the APX content

ranged from 0.47 to 1.53 EU mg^{-1} protein and 0.49 to 1 EU mg^{-1} protein, respectively. A maximum rise of 223 and 100% was observed at 50 and 100 ppm, respectively, in plant roots inoculated with the bacterial consortium. Under 200 ppm HM stress, APX was in the range of 0.32–0.80 EU mg^{-1} protein. *Enterobacter cloacae* strain JWM6 and *Citrobacter werkmanii* strain WWN1 increased root APX by 149% (0.8 EU mg^{-1} protein) and 135%, respectively, while the bacterial consortium–inoculated plants showed an increase of 98% as compared to uninoculated plants (**Figure 6D**).

Heavy Metal Accumulation in Shoots and Roots of Wheat

Inoculation with PGPB significantly reduced the HM uptake in both the shoots and roots of wheat under all HM concentrations. Under 50 ppm of added Cd, Ni, and Pb, HM accumulation in plant shoot ranged from 8.13 to 13.20 ppm for Cd, 7.6 to 15.4 ppm for Pb, and 8.2 to 14.5 ppm for Ni. The lowest HM uptake was recorded when plants were inoculated with the bacterial consortium compared to sole application of the studied bacteria. The consortium reduced the uptake of Cd by 38%, Pb by 50%, and Ni by 49% in comparison to uninoculated plants. At 100 ppm, the HM content in shoots ranged from 10.1 to 18.4 ppm (Cd), 13.8 to 22 ppm (Pb), and 12.7 to 21 ppm (Ni). The maximum decline in shoot HM uptake was observed in plants inoculated with the bacterial consortium where a decrease of 42% for Cd, 37% for Pb, and 36% for Ni was observed in plants inoculated with the bacterial consortium when compared with uninoculated plants. Under 200 ppm, Cd in the range of 16.8–26.3 ppm, Pb in the range of 16.5–27.5 ppm, and Ni in the range of 15.5–26.5 ppm were recorded in plant shoots. The maximum uptake reduction for Cd (36%), Pb (40%), and Ni (37%) was detected in plants inoculated with the bacterial consortium as compared to uninoculated plants.

Similar results were obtained for plant roots where HM accumulation increased with rising HM concentration. In roots, under 50 ppm HM concentration, HM uptake ranged from 11.6 to 22.7 ppm for Cd, from 11.5 to 16.9 ppm for Pb, and from 9.9 to 19.4 ppm for Ni. The bacterial consortium maximally reduced HM uptake, i.e., Cd by 48%, Pb by 32%, and Ni by 49%, as compared to uninoculated plants. Under 100 ppm, HMs in roots ranged from 26.8 to 35.4 ppm for Cd, 12.8 to 24.5 ppm for Pb, and 18.3 to 25.1 ppm for Ni. The maximum decrease in roots HM uptake was again observed in plants inoculated with the bacterial consortium where a decrease of 24% for Cd, 47% for Pb, and 29% for Ni was recorded compared to uninoculated plants. Under 200 ppm, the root HM concentration ranged from 29.1 to 41.2 ppm (Cd), 19.7 to 34.5 ppm (Pb), and 19.3 to 30.8 ppm (Ni). The maximum decrease for Cd (29%), Pb (42%), and Ni (29.2%) was observed in plant roots inoculated with the consortium as compared to uninoculated plants (**Figure 7**).

Fourier Transform Infrared Spectroscopy Analysis of Bacterial Biomass

Fourier transform infrared spectroscopy spectra of bacterial biomass grown in the presence as well as absence of HMs were obtained in the range of 500–4000 cm^{-1}. The FTIR spectrum of HM-loaded biomass displayed shifts in absorption peaks indicating interaction between HMs and bacterial biomass. The broad bands around 3430 cm^{-1} in control samples corresponded to alcohol/phenol O-H stretch and amine stretch. After treatment with HMs, these peaks shifted to 3423 cm^{-1} in the case of *Citrobacter werkmanii* strain WWN1 and to 3421 cm^{-1} in the case of *Enterobacter cloacae* strain JWM6 treated samples. These band peaks existed at a higher frequency in HM-loaded samples, indicating an increase in bond strength. The peaks at 2920 cm^{-1} and 2926 cm^{-1} in control samples corresponded to lipid–protein stretching. In HM-loaded samples, these peaks slightly shifted toward 2918 cm^{-1} and 2922 cm^{-1}, respectively, indicating the interaction of lipid–protein with HMs. The 1650 cm^{-1} and 1649 cm^{-1} peaks in unloaded samples represented C-N stretching. These peaks shifted to 1638 cm^{-1} and 1645 cm^{-1} in HM-loaded samples, indicating interaction of these functional groups with HMs. Similarly, in control samples, peaks at 1068 cm^{-1} and 1070 cm^{-1} indicated protein amide (C = O) stretching, which shifted to 1064 cm^{-1} and 1075 cm^{-1} in HM-loaded samples (**Figure 8**).

Pearson's Correlation Coefficient (*r*) and Principal Component Analysis

Heatmap responses of Pearson's correlation coefficient (*r*) and PCA for the antioxidant enzymes, chlorophyll contents, stress determinants, and HM (Ni, Cd, and Pb) uptake by wheat shoots and roots under various HM concentrations are given in **Figures 9**, **10**.

DISCUSSION

In the present study, we presented the beneficial role of seed inoculation with *Citrobacter werkmanii* strain WWN1 and *Enterobacter cloacae* strain JWM6 in wheat development and growth under HM stress. Siderophore production by soil bacteria such as *Citrobacter werkmanii* strain WWN1 and *Enterobacter cloacae* strain JWM6 (Ajmal et al., 2021) is a prerequisite for better nutrition and overall state of plants. Moreover, previous study revealed that both the isolates were positive for potassium, phosphate, and zinc solubilization assays *in vitro* (Ajmal et al., 2021). Resultantly, these strains might have had a positive effect on plant nutrition (Anand et al., 2016) because K, P, and Zn are very important nutrients in all metabolic processes of plants, including respiration, energy conversion, and photosynthesis. In the present study, bacterial inoculation either individually and in consortium significantly increased the growth and biomass of wheat possibly due to the production of siderophores and organic acids leading to nutrient availability to plants (Naveed et al., 2014; Shan et al., 2020; Han et al., 2021).

Contamination with HMs such as Cd, Ni, and Pb of soils results in iron deficiency in many plant species. It causes inhibition of both chloroplast and chlorophyll development, leading to leaves chlorosis (Rizwan et al., 2016). Moreover, HMs induce toxicity to thylakoid membrane integrity, which leads to inhibitions of enzymes like chlorophyll synthetase

and Rubisco, causing chlorophyll degradation (Hashem, 2014). Microbial siderophores as released by *Citrobacter werkmanii* strain WWN1 and *Enterobacter cloacae* strain JWM6 also help plants in iron uptake, making them good candidates to prevent plant chlorosis due to HM stress. In our study, under HM stress, the consortium of *Citrobacter werkmanii* strain WWN1 and *Enterobacter cloacae* strain JWM6 improved the chlorophyll content of wheat probably due to iron uptake by bacterial siderophore–Fe complexes, resulting in higher chlorophyll content and biomass production of PGPB-inoculated plants. The positive impact of *Citrobacter werkmanii* strain WWN1 and *Enterobacter cloacae* strain JWM6 under HM stress was clearly evident from morphological and biochemical improvement of plants, i.e., root and shoot length, plant biomass, and chlorophyll content, due to successful root colonization of the studied bacterial strains in wheat. Similar to our study, *Serratia* sp. and *Pseudomonas* sp. were found to colonize in roots of wheat and rice as a signature of useful plant–microbe interaction under stress conditions (Khan and Singh, 2021; Pramanik et al., 2021). Our results are also in line with other reports, where *Enterobacter* sp. and *Citrobacter* sp. enhanced growth and improved chlorophyll content in rice by alleviating HM stress (Habib et al., 2016; Li et al., 2017; Maxton et al., 2018).

In addition to the abovementioned hazards, HMs also cause severe oxidative stress due to the release of excessive ROS in plants which induces changes in antioxidant enzyme activities. Antioxidant enzymes such as SOD, POD, APX, and CAT maintain the ROS at optimum levels (Ahmad et al., 2017). Elevated levels of ROS can cause severe disruption of physiological mechanisms in wheat and other plants, resulting in reduced growth and biomass (Mittler, 2002; Rizwan et al., 2016).

Among various antioxidants, SOD is a vital enzyme that converts superoxide into hydrogen peroxide (H_2O_2) at a high rate and protects cells against the harmful effects of ROS. Various HM stresses have been related to the alteration in SOD activities in different plants (Verma and Dubey, 2003). We also observed higher production of SOD in wheat plants grown in soil supplemented with HMs when inoculated with PGPB. In our study, SOD activity was more pronounced in roots under HM stress compared to that in the roots. This might be due to early accumulation and higher concentration of HMs in root tissues, thus inducing oxidative stress, and hence, SOD content might have been increased as a protective mechanism (AbdElgawad et al., 2020).

The next step in the ROS antioxidant process includes CAT oxidation that converts hydrogen peroxide (H_2O_2) into water (Noctor and Foyer, 1998). In the current study, CAT activity was also significantly increased in plants inoculated with *Citrobacter werkmanii* strain WWN1 and *Enterobacter cloacae* strain JWM6 under HM stress, which might have resulted in improved plant growth.

Similarly, POD activity was raised in plants inoculated with PGPB under HM stress. POD eliminates H_2O_2 by breaking it up into hydrogen and oxygen (Skórzyńska-Polit et al., 2003). POD is more efficient than CAT in scavenging H_2O_2 because of higher substrate affinity (Zhang et al., 2010). Therefore, if stress is not too severe for plant defense capacity, the major response is the release of POD and SOD rather than CAT. Previous studies have also reported higher, lower, or unchanged POD levels in response to HM stress depending upon the stress severity (Li et al., 2013; Hu et al., 2015; Gu and Liang, 2020). In our study, there was a significant increase in POD activity in *Citrobacter werkmanii* strain WWN1 and *Enterobacter cloacae* strain JWM6 inoculated wheat plants as compared to uninoculated plants. Moreover, POD facilitates lignin synthesis that can form a physical barrier against toxicity of HMs (Hegedüs et al., 2001). This also indicated that bacterial inoculation efficiently helped plants under HM stress by stimulating POD.

Generally, under HM stress, the APX content was higher in shoots than in roots and the APX content in bacteria-inoculated plants was significantly higher than the uninoculated plants. This suggests that the HM-tolerant PGPB used in the study aided plants to thrive better under HM stress. Our study showed that antioxidant enzyme activities dropped with an increase in HM concentration. This may be due to inhibition of enzymes as a result of elevated HM concentration. These findings are consistent with earlier reports (Alvarez and Lamb, 1997; Schickler and Caspi, 1999; Stroiński, 1999; Fatima and Ahmad, 2005; Awan et al., 2020).

Heavy metal stress, either directly or indirectly, is also responsible for molecular damage to plants due to the release of ROS. The increase in O_2^- level might produce the hydroperoxyl radical, which converts various fatty acids to highly toxic lipid per oxides. An index of lipid peroxidation is routinely measured by the MDA content (Zhang et al., 2007). The level of MDA was significantly increased with increasing concentration of HM in soil. Moreover, the MDA content was higher in roots as compared to that in shoots, which might be because roots had stronger interaction with metals in soil. However, plants inoculated with *Citrobacter werkmanii* strain WWN1 and *Enterobacter cloacae* strain JWM6 or their consortium had a significantly lower MDA content as compared to uninoculated plants. This indicates that bacterial inoculation might have protected the plants from oxidative damage resulting from inactivation of the antioxidant enzyme system (Sgherri et al., 2007; Zhang et al., 2018).

Similarly, proline is one of the components of the non-specific defense systems toward HM toxicity and is known to play a key osmoregulatory role in plants (Saradhi, 1991). Proline is a molecular chaperone and has the ability to enhance the activity of different enzymes and protect protein integrity. In our study, *Citrobacter werkmanii* strain WWN1 and *Enterobacter cloacae* strain JWM6 treated plants showed lower proline content under HM stress in comparison to uninoculated plants. This implies that bacteria-inoculated plants may not have encountered higher HM stress and consequently lower proline accumulation was recorded (Gontia-Mishra et al., 2016). Inoculation with PGP bacteria decreased the proline content in leaves, which might have provided increased protection to plants (Sofy et al., 2020).

In addition to boosting the plant antioxidant enzyme defense system, seed inoculation with PGPB reduced the HM uptake by wheat compared with non-inoculated plants. The consortium of *Citrobacter werkmanii* strain WWN1 and *Enterobacter cloacae* strain JWM6 significantly reduced HM uptake in the shoots

and roots of wheat as compared to single bacteria. Several other studies have also revealed that PGPB reduce the uptake of HMs in wheat shoots and roots growing in the presence of various HMs (Islam et al., 2014; El-Meihy et al., 2019; Ju et al., 2019; Saeed et al., 2019).

Finally, FTIR analysis of HM-tolerant *Citrobacter werkmanii* strain WWN1 and *Enterobacter cloacae* strain JWM6 grown in HM (Cd, Pb, and Ni) spiked liquid medium confirmed the presence of various moieties in bacteria, and shifts in the peaks indicated the binding of HMs with bacteria as explained by Das et al. (2007). In FTIR data, the shift in the peaks of hydroxyl functional groups in HM-loaded samples indicated the involvement of hydroxyl groups in binding the HMs. The shift in the peak appearing in the region attributed to alkyl chains (C-H stretching vibration) of fatty acids found in the phospholipid membrane (Ueshima et al., 2008) represented the involvement of these functional groups with HMs. The peak shift in the region attributed to amide suggests that these functional groups are also a major contributor to HM removal. In case of *Citrobacter werkmanii* strain WWN1 grown in the presence of HMs, the decreased intensity in fingerprint region peaks indicated the HM ion interaction with functional groups such as phosphates and proteins on the bacterial cell surface (Murthy et al., 2014). Similarly, the shift in the fingerprint region of HM-loaded samples represents the presence of carbon and phosphorus containing oxygen atoms interacting with HMs (Parikh and Chorover, 2006). Thus, various functional groups in the studied bacteria may be responsible for HM binding, therefore reducing the solubility and bioavailability and hence mitigating the toxicity of HMs to plants.

To sum up, multiple-HM stress severely affected the growth and physiology of wheat, whereas inoculation with HM-resistant PGP *Citrobacter werkmanii* strain WWN1 and *Enterobacter cloacae* strain JWM6 either alone or in consortium reduced Cd, Pb, and Ni uptake and toxicity and enhanced wheat growth. In general, the bacterial consortium performed better than individual bacterial strains in improving plant biomass and resistivity against the studied HMs.

CONCLUSION

It is concluded that HM (Cd, Pb, and Ni) stress negatively impacted the growth, physiology, and antioxidant enzyme system of wheat. However, seed inoculation with PGP *Citrobacter werkmanii* strain WWN1 and *Enterobacter cloacae* strain JWM6 significantly improved plant growth; reduced HM accumulation in wheat shoots and roots; enhanced the production of antioxidants like SOD, POD, APX, and CAT; and lowered the MDA and proline contents in inoculated plants as compared to non-inoculated plants. Thus, seed inoculation with *Citrobacter werkmanii* strain WWN1 and *Enterobacter cloacae* strain JWM6 may be an effective method to enhance wheat production in HM-contaminated soils. However, further investigation is required to gain insight into the molecular mechanisms of HM detoxification and explore the impact of bacterial inoculation on biological activities of soil under varied environmental conditions.

DATA AVAILABILITY STATEMENT

The original contributions presented in the study are included in the article/**Supplementary Material**, further inquiries can be directed to the corresponding author/s.

AUTHOR CONTRIBUTIONS

AWA: experiment, data curation, software, methods, validation, and writing – original draft. HY: review and editing, methodolgy, resources, statistical analysis and supervision. MNH: review and editing, data curation, analysis, methododology, supervision, and resources. SM: orginal concept, funding acquisition, supervision, resources, methodolgy, software, and analysis. NK: review and editing, validation, resources. BLJ: review and editing, resources, and software.

FUNDING

We would like to extend their sincere appreciation to the Higher Education Commission of Pakistan for financial support under project number 5381/Federal/NRPU/R&D/HEC/2016.

ACKNOWLEDGMENTS

We would like to thank Researchers Supporting Project Number RSP-2021/168, King Saud University, Riyadh, Saudi Arabia.

SUPPLEMENTARY MATERIAL

The Supplementary Material for this article can be found online at: https://www.frontiersin.org/articles/10.3389/fmicb.2022.815704/full#supplementary-material

REFERENCES

AbdElgawad, H., Zinta, G., Hamed, B. A., Selim, S., Beemster, G., Hozzein, W. N., et al. (2020). Maize roots and shoots show distinct profiles of oxidative stress and antioxidant defense under heavy metal toxicity. *Environ. Pollut.* 258:113705. doi: 10.1016/j.envpol.2019.113705

Ahanger, M. A., Aziz, U., Alsahli, A. A., Alyemeni, M. N., and Ahmad, P. (2020). Combined kinetin and spermidine treatments ameliorate growth and photosynthetic inhibition in *Vigna angularis* by up-regulating antioxidant and nitrogen metabolism under cadmium stress. *Biomolecules* 10:147. doi: 10.3390/biom10010147

Ahmad, H. T., Hussain, A., Aimen, A., Jamshaid, M. U., Ditta, A., Asghar, H. N., et al. (2021). "Improving resilience against drought stress among crop plants through inoculation of plant growth-promoting rhizobacteria," in *Harsh Environment and Plant Resilience: Molecular and Functional Aspects*, 1st Edn, eds A. Husen and M. Jawaid (Berlin: Springer), 387–408. doi: 10.1007/978-3-030-65912-7_16

Ahmad, P., Jaleel, C. A., Salem, M. A., Nabi, G., and Sharma, S. (2010). Roles of enzymatic and nonenzymatic antioxidants in plants during abiotic stress. *Crit. Rev. Biotechnol.* 30, 161–175. doi: 10.3109/07388550903524243

Ahmad, P., Tripathi, D. K., Deshmukh, R., Singh, V. P., and Corpas, F. J. (2019). Revisiting the role of ROS and RNS in plants under changing environment. *Environ. Exp. Bot.* 161, 1–3. doi: 10.1016/j.envexpbot.2019.02.017

Ahmad, R., Ali, S., Hannan, F., Rizwan, M., Iqbal, M., Hassan, Z., et al. (2017). Promotive role of 5-aminolevulinic acid on chromium-induced morphological, photosynthetic, and oxidative changes in cauliflower (*Brassica oleracea botrytis* L.). *Environ. Sci. Pollut. Res.* 24, 8814–8824. doi: 10.1007/s11356-017-8603-7

Ajmal, A. W., Saroosh, S., Mulk, S., Hassan, M. N., Yasmin, H., Jabeen, Z., et al. (2021). Bacteria isolated from wastewater irrigated agricultural soils adapt to heavy metal toxicity while maintaining their plant growth promoting traits. *Sustainability* 13:7792. doi: 10.3390/su13147792

Alvarez, M., and Lamb, C. (1997). Oxidative burst-mediated defense responses in plant disease resistance. *Cold Spring Harb. Monogr. Ser.* 34, 815–840.

Anand, K., Kumari, B., and Mallick, M. (2016). Phosphate solubilizing microbes: an effective and alternative approach as biofertilizers. *J. Pharm. Pharm. Sci.* 8:37.

Ashraf, U., Kanu, A. S., Mo, Z., Hussain, S., Anjum, S. A., Khan, I., et al. (2015). Lead toxicity in rice: effects, mechanisms, and mitigation strategies—a mini review. *Environ. Sci. Pollut. Res.* 22, 18318–18332. doi: 10.1007/s11356-015-5463-x

Awan, S. A., Ilyas, N., Khan, I., Raza, M. A., Rehman, A. U., Rizwan, M., et al. (2020). *Bacillus siamensis* reduces cadmium accumulation and improves growth and antioxidant defense system in two wheat (*Triticum aestivum* L.) varieties. *Plants* 9:878. doi: 10.3390/plants9070878

Azmat, A., Yasmin, H., Hassan, M. N., Nosheen, A., Naz, R., Sajjad, M., et al. (2020). Co-application of bio-fertilizer and salicylic acid improves growth, photosynthetic pigments and stress tolerance in wheat under drought stress. *PeerJ* 8:e9960. doi: 10.7717/peerj.9960

Baldos, U. L. C., and Hertel, T. W. (2014). Global food security in 2050: the role of agricultural productivity and climate change. *Aust. J. Agric. Resour. Econ.* 58, 554–570. doi: 10.1111/1467-8489.12048

Beauchamp, C., and Fridovich, I. (1971). Superoxide dismutase: improved assays and an assay applicable to acrylamide gels. *Anal. Biochem.* 44, 276–287. doi: 10.1016/0003-2697(71)90370-8

Bhalerao, S. A., Sharma, A. S., and Poojari, A. C. (2015). Toxicity of nickel in plants. *Int. J. Pure Appl. Biosci.* 3, 345–355.

Borriss, R. (2011). "Use of plant-associated *Bacillus* strains as biofertilizers and biocontrol agents in agriculture," in *Bacteria in Agrobiology: Plant Growth Responses*, ed. D. Maheshwari (Berlin: Springer), 41–76. doi: 10.1007/978-3-642-20332-9_3

Buege, J. A., and Aust, S. D. (1978). Microsomal lipid peroxidation. *Methods Enzymol.* 52, 302–310. doi: 10.1016/S0076-6879(78)52032-6

Clarke, K., and Warwick, R. M. (2001). *Change in Marine Communities: An Approach to Statistical Analysis and Interpretation*, 2nd Edn. Plymouth: PRIMER-E.

Curtis, T., and Halford, N. (2014). Food security: the challenge of increasing wheat yield and the importance of not compromising food safety. *Ann. Appl. Biol.* 164, 354–372. doi: 10.1111/aab.12108

Das, S. K., Das, A. R., and Guha, A. K. (2007). A study on the adsorption mechanism of mercury on *Aspergillus versicolor* biomass. *Environ. Sci. Technol.* 41, 8281–8287. doi: 10.1021/es070814g

El-Meihy, R. M., Abou-Aly, H. E., Youssef, A. M., Tewfike, T. A., and El-Alkshar, E. A. (2019). Efficiency of heavy metals-tolerant plant growth promoting bacteria for alleviating heavy metals toxicity on sorghum. *Environ. Exp. Bot.* 162, 295–301. doi: 10.1016/j.envexpbot.2019.03.005

Fahsi, N., Mahdi, I., Mesfioui, A., Biskri, L., and Allaoui, A. (2021). Plant Growth-promoting rhizobacteria isolated from the Jujube (*Ziziphus lotus*) plant enhance wheat growth, Zn uptake, and heavy metal tolerance. *Agriculture* 11:316. doi: 10.3390/agriculture11040316

Fatima, R. A., and Ahmad, M. (2005). Certain antioxidant enzymes of *Allium cepa* as biomarkers for the detection of toxic heavy metals in wastewater. *Sci Total Environ.* 346, 256–273. doi: 10.1016/j.scitotenv.2004.12.004

Giannakoula, A., Therios, I., and Chatzissavvidis, C. (2021). Effect of lead and copper on photosynthetic apparatus in citrus (*Citrus aurantium* L.) plants. The role of antioxidants in oxidative damage as a response to heavy metal stress. *Plants* 10:155. doi: 10.3390/plants10010155

Gontia-Mishra, I., Sapre, S., Sharma, A., and Tiwari, S. (2016). Alleviation of mercury toxicity in wheat by the interaction of mercury-tolerant plant growth-promoting rhizobacteria. *J. Plant Growth Regul.* 35, 1000–1012. doi: 10.1007/s00344-016-9598-x

Gorin, N., and Heidema, F. T. (1976). Peroxidase activity in Golden Delicious apples as a possible parameter of ripening and senescence. *J Agric Food Chem.* 24, 200–201. doi: 10.1021/jf60203a043

Gu, Y., and Liang, C. (2020). Responses of antioxidative enzymes and gene expression in *Oryza sativa* L and *Cucumis sativus* L seedlings to microcystins stress. *Ecotoxicol. Environ. Saf.* 193:110351. doi: 10.1016/j.ecoenv.2020.110351

Habib, S., Kausar, H., Saud, H., Ismail, M., and Othman, R. (2016). Molecular characterization of stress tolerant plant growth promoting rhizobacteria (PGPR) for growth enhancement of rice. *Int. J. Agric. Biol.* 18, 184–191. doi: 10.17957/IJAB/15.0094

Han, H., Zhang, H., Qin, S., Zhang, J., Yao, L., Chen, Z., et al. (2021). Mechanisms of *Enterobacter bugandensis* TJ6 immobilization of heavy metals and inhibition of Cd and Pb uptake by wheat based on metabolomics and proteomics. *Chemosphere* 276:130157. doi: 10.1016/j.chemosphere.2021.130157

Harris, N. S., and Taylor, G. J. (2013). Cadmium uptake and partitioning in durum wheat during grain filling. *BMC Plant Biol.* 13:103. doi: 10.1186/1471-2229-13-103

Hashem, H. (2014). Cadmium toxicity induces lipid peroxidation and alters cytokinin content and antioxidant enzyme activities in soybean. *Botany* 92, 1–7. doi: 10.1139/cjb-2013-0164

Hegedüs, A., Erdei, S., and Horváth, G. (2001). Comparative studies of H2O2 detoxifying enzymes in green and greening barley seedlings under cadmium stress. *Plant Sci.* 160, 1085–1093. doi: 10.1016/S0168-9452(01)00330-2

Hu, Z., Xie, Y., Jin, G., Fu, J., and Li, H. (2015). Growth responses of two tall fescue cultivars to Pb stress and their metal accumulation characteristics. *Ecotoxicology* 24, 563–572. doi: 10.1007/s10646-014-1404-6

Humphris, S. N., Bengough, A. G., Griffiths, B. S., Kilham, K., Rodger, S., Stubbs, V., et al. (2005). Root cap influences root colonisation by *Pseudomonas fluorescens* SBW25 on maize. *FEMS Microbiol. Ecol.* 54, 123–130. doi: 10.1016/j.femsec.2005.03.005

Hussain, A., Ali, S., Rizwan, M., Ur Rehman, M. Z., Javed, M. R., Imran, M., et al. (2018). Zinc oxide nanoparticles alter the wheat physiological response and reduce the cadmium uptake by plants. *Environ. Pollut.* 242, 1518–1526. doi: 10.1016/j.envpol.2018.08.036

Iqbal, Z., Abbas, F., Ibrahim, M., Mahmood, A., Gul, M., and Qureshi, T. I. (2022). Ecological risk assessment of soils under different wastewater irrigation farming system in Punjab, Pakistan. *Int. J. Environ. Sci. Technol.* 19, 1925–1936. doi: 10.1007/s13762-021-03237-x

Islam, F., Yasmeen, T., Ali, Q., Ali, S., Arif, M. S., Hussain, S., et al. (2014). Influence of *Pseudomonas aeruginosa* as PGPR on oxidative stress tolerance in wheat under Zn stress. *Ecotoxicol. Environ. Saf.* 104, 285–293. doi: 10.1016/j.ecoenv.2014.03.008

Ju, W., Liu, L., Fang, L., Cui, Y., Duan, C., and Wu, H. (2019). Impact of co-inoculation with plant-growth-promoting rhizobacteria and rhizobium on the biochemical responses of alfalfa-soil system in copper contaminated soil. *Ecotoxicol. Environ. Saf.* 167, 218–226. doi: 10.1016/j.ecoenv.2018.10.016

Karstensen, K., Ringstad, O., Rustad, I., Kalevi, K., Jorgensen, K., Nylund, K., et al. (1998). "Methods for chemical analysis of contaminated soil samples-tests of their reproducibility between Nordic laboratories," in *Contaminated Soil 1998*, Vol. 1, (London: Thomas Telford Ltd), 261–278. *

Kaya, C., Akram, N. A., Ashraf, M., Alyemeni, M. N., and Ahmad, P. (2020). Exogenously supplied silicon (Si) improves cadmium tolerance in pepper (*Capsicum Annuum* L.) by up-regulating the synthesis of nitric oxide and hydrogen sulfide. *J Biotechnol.* 316, 35–45. doi: 10.1016/j.jbiotec.2020.04.008

Keller, C., Rizwan, M., Davidian, J.-C., Pokrovsky, O., Bovet, N., Chaurand, P., et al. (2015). Effect of silicon on wheat seedlings (*Triticum turgidum* L.) grown

in hydroponics and exposed to 0 to 30 μM Cu. *Planta* 241, 847–860. doi: 10.1007/s00425-014-2220-1

Khan, A., and Singh, A. V. (2021). Multifarious effect of ACC deaminase and EPS producing *Pseudomonas* sp. and *Serratia marcescens* to augment drought stress tolerance and nutrient status of wheat. *World J. Microbiol. Biotechnol.* 37, 1–17. doi: 10.1007/s11274-021-03166-4

Khan, N., and Bano, A. (2016). Role of plant growth promoting rhizobacteria and Ag-nano particle in the bioremediation of heavy metals and maize growth under municipal wastewater irrigation. *Int. J. Phytoremediation* 18, 211–221. doi: 10.1080/15226514.2015.1064352

Khanna, K., Jamwal, V. L., Gandhi, S. G., Ohri, P., and Bhardwaj, R. (2019a). Metal resistant PGPR lowered Cd uptake and expression of metal transporter genes with improved growth and photosynthetic pigments in *Lycopersicon esculentum* under metal toxicity. *Sci. Rep.* 9:5855. doi: 10.1038/s41598-019-41899-3

Khanna, K., Jamwal, V. L., Sharma, A., Gandhi, S. G., Ohri, P., Bhardwaj, R., et al. (2019b). Supplementation with plant growth promoting rhizobacteria (PGPR) alleviates cadmium toxicity in *Solanum lycopersicum* by modulating the expression of secondary metabolites. *Chemosphere* 230, 628–639. doi: 10.1016/j.chemosphere.2019.05.072

Kloke, A., Sauerbeck, D., and Vetter, H. (1984). "The contamination of plants and soils with heavy metals and the transport of metals in terrestrial food chains," in *Changing Metal Cycles and Human Health*, ed. J. O. Nriagu (Berlin: Springer), 113–141. doi: 10.1007/978-3-642-69314-4_7

Kohli, S. K., Khanna, K., Bhardwaj, R., Abde_Allaha, E. F., Ahmad, P., and Corpas, F. J. (2019). Assessment of subcellular ROS and NO metabolism in higher plants: multifunctional signaling molecules. *Antioxidants* 8:641. doi: 10.3390/antiox8120641

Kumar, S., Sud, N., Fonseca, F. V., Hou, Y., and Black, S. M. (2010). Shear stress stimulates nitric oxide signaling in pulmonary arterial endothelial cells via a reduction in catalase activity: role of protein kinase Cδ. *Am. J. Physiol. Lung Cell. Mol. Physiol.* 298, L105–L116. doi: 10.1152/ajplung.00290.2009

Li, H., Lei, P., Pang, X., Li, S., Xu, H., Xu, Z., et al. (2017). Enhanced tolerance to salt stress in canola (*Brassica napus* L.) seedlings inoculated with the halotolerant *Enterobacter cloacae* HSNJ4. *Appl. Soil Ecol.* 119, 26–34. doi: 10.1016/j.apsoil.2017.05.033

Li, X., Yan, Z., Gu, D., Li, D., Tao, Y., Zhang, D., et al. (2019). Characterization of cadmium-resistant rhizobacteria and their promotion effects on *Brassica napus* growth and cadmium uptake. *J. Basic Microbiol.* 59, 579–590. doi: 10.1002/jobm.201800656

Li, X., Yang, Y., Jia, L., Chen, H., and Wei, X. (2013). Zinc-induced oxidative damage, antioxidant enzyme response and proline metabolism in roots and leaves of wheat plants. *Ecotoxicol. Environ. Saf.* 89, 150–157. doi: 10.1016/j.ecoenv.2012.11.025

Lozano-Rodríguez, E., Luguera, M., Lucena, J., and Carpena-Ruiz, R. (1995). Evaluation of two different acid digestion methods in closed systems for trace element determinations in plants. *Quimica Analitica Bellaterra* 14, 27–27.

Mallick, I., Bhattacharyya, C., Mukherji, S., Dey, D., Sarkar, S. C., Mukhopadhyay, U. K., et al. (2018). Effective rhizoinoculation and biofilm formation by arsenic immobilizing halophilic plant growth promoting bacteria (PGPB) isolated from mangrove rhizosphere: a step towards arsenic rhizoremediation. *Sci. Total Environ.* 610, 1239–1250. doi: 10.1016/j.scitotenv.2017.07.234

Maxton, A., Singh, P., and Masih, S. A. (2018). ACC deaminase-producing bacteria mediated drought and salt tolerance in *Capsicum annuum*. *J. Plant Nutr.* 41, 574–583. doi: 10.1080/01904167.2017.1392574

Mesa, J., Rodríguez-Llorente, I. D., Pajuelo, E., Piedras, J. M. B., Caviedes, M. A., Redondo-Gómez, S., et al. (2015). Moving closer towards restoration of contaminated estuaries: bioaugmentation with autochthonous rhizobacteria improves metal rhizoaccumulation in native *Spartina maritima*. *J. Hazard. Mater.* 300, 263–271. doi: 10.1016/j.jhazmat.2015.07.006

Mesa-Marín, J., Del-Saz, N. F., Rodríguez-Llorente, I. D., Redondo-Gómez, S., Pajuelo, E., Ribas-Carbó, M., et al. (2018). PGPR reduce root respiration and oxidative stress enhancing spartina maritima root growth and heavy metal rhizoaccumulation. *Front. Plant Sci.* 9:1500. doi: 10.3389/fpls.2018.01500

Mishra, V., Mishra, R. K., Dikshit, A., and Pandey, A. C. (2014). "Interactions of nanoparticles with plants: an emerging prospective in the agriculture industry," in *Emerging Technologies and Management of Crop Stress Tolerance*, eds P. Ahmad and S. Rasool (Amsterdam: Elsevier), 159–180. doi: 10.1016/B978-0-12-800876-8.00008-4

Mittler, R. (2002). Oxidative stress, antioxidants and stress tolerance. *Trends Plant Sci.* 7, 405–410. doi: 10.1016/S1360-1385(02)02312-9

Murthy, S., Bali, G., and Sarangi, S. (2014). Effect of lead on growth, protein and biosorption capacity of *Bacillus cereus* isolated from industrial effluent. *J. Environ. Biol.* 35:407.

Naveed, M., Hussain, M. B., Zahir, Z. A., Mitter, B., and Sessitsch, A. (2014). Drought stress amelioration in wheat through inoculation with *Burkholderia phytofirmans* strain PsJN. *Plant Growth Regulat.* 73, 121–131. doi: 10.1007/s10725-013-9874-8

Noctor, G., and Foyer, C. H. (1998). Ascorbate and glutathione: keeping active oxygen under control. *Annu. Rev. Plant Biol.* 49, 249–279. doi: 10.1146/annurev.arplant.49.1.249

Page, V., and Feller, U. (2005). Selective transport of zinc, manganese, nickel, cobalt and cadmium in the root system and transfer to the leaves in young wheat plants. *Ann. Bot.* 96, 425–434. doi: 10.1093/aob/mci189

Parikh, S. J., and Chorover, J. (2006). ATR-FTIR spectroscopy reveals bond formation during bacterial adhesion to iron oxide. *Langmuir* 22, 8492–8500. doi: 10.1021/la061359p

Patel, P., Raju, N. J., Reddy, B. S. R., Suresh, U., Sankar, D., and Reddy, T. (2018). Heavy metal contamination in river water and sediments of the Swarnamukhi River Basin, India: risk assessment and environmental implications. *Environ. Geochem. Health* 40, 609–623. doi: 10.1007/s10653-017-0006-7

Pramanik, K., Mandal, S., Banerjee, S., Ghosh, A., Maiti, T. K., and Mandal, N. C. (2021). Unraveling the heavy metal resistance and biocontrol potential of *Pseudomonas* sp. K32 strain facilitating rice seedling growth under Cd stress. *Chemosphere* 274:129819. doi: 10.1016/j.chemosphere.2021.129819

Rizwan, M., Ali, S., Abbas, T., Zia-ur-Rehman, M., Hannan, F., Keller, C., et al. (2016). Cadmium minimization in wheat: a critical review. *Ecotoxicol. Environ. Saf.* 130, 43–53. doi: 10.1016/j.ecoenv.2016.04.001

Rizwan, M., Ali, S., Qayyum, M. F., Ok, Y. S., Adrees, M., Ibrahim, M., et al. (2017). Effect of metal and metal oxide nanoparticles on growth and physiology of globally important food crops: a critical review. *J. Hazard. Mater.* 322, 2–16. doi: 10.1016/j.jhazmat.2016.05.061

Rodríguez-Sánchez, V., Guzmán-Moreno, J., Rodríguez-González, V., Flores-de la Torre, J. A., Ramírez-Santoyo, R. M., and Vidales-Rodríguez, L. E. (2017). Biosorption of lead phosphates by lead-tolerant bacteria as a mechanism for lead immobilization. *World J. Microbiol. Biotechnol.* 33, 1–11. doi: 10.1007/s11274-017-2314-6

Saeed, Z., Naveed, M., Imran, M., Bashir, M. A., Sattar, A., Mustafa, A., et al. (2019). Combined use of *Enterobacter* sp. MN17 and zeolite reverts the adverse effects of cadmium on growth, physiology and antioxidant activity of *Brassica napus*. *PLoS One* 14:e0213016. doi: 10.1371/journal.pone.0213016

Saradhi, P. P. (1991). Proline accumulation under heavy metal stress. *J. Plant Physiol.* 138, 554–558. doi: 10.1016/S0176-1617(11)80240-3

Schickler, H., and Caspi, H. (1999). Response of antioxidative enzymes to nickel and cadmium stress in hyperaccumulator plants of the genus *Alyssum*. *Physiol. Plant.* 105, 39–44. doi: 10.1034/j.1399-3054.1999.105107.x

Sgherri, C., Quartacci, M. F., and Navari-Izzo, F. (2007). Early production of activated oxygen species in root apoplast of wheat following copper excess. *J. Plant Physiol.* 164, 1152–1160. doi: 10.1016/j.jplph.2006.05.020

Shan, S., Guo, Z., Lei, P., Li, Y., Wang, Y., Zhang, M., et al. (2020). Increased biomass and reduced tissue cadmium accumulation in rice via indigenous *Citrobacter* sp. XT1-2-2 and its mechanisms. *Sci. Total Environ.* 708:135224. doi: 10.1016/j.scitotenv.2019.135224

Sharaff, M. M., Subrahmanyam, G., Kumar, A., and Yadav, A. N. (2020). "Mechanistic understanding of the root microbiome interaction for sustainable agriculture in polluted soils," in *New and Future Developments in Microbial Biotechnology and Bioengineering*, eds A. A. Rastegari, A. N. Yadav, and N. Yadav (Amsterdam: Elsevier), 61–84. doi: 10.1016/B978-0-12-820526-6.00005-1

Shiferaw, B., Smale, M., Braun, H.-J., Duveiller, E., Reynolds, M., and Muricho, G. (2013). Crops that feed the world 10. Past successes and future challenges to the role played by wheat in global food security. *Food Secur.* 5, 291–317. doi: 10.1007/s12571-013-0263-y

Shoaf, W. T., and Lium, B. W. (1976). Improved extraction of chlorophyll a and b from algae using dimethyl sulfoxide. *Limnol. Oceanogr.* 21, 926–928. doi: 10.4319/lo.1976.21.6.0926

Shoeva, O. Y., and Khlestkina, E. (2018). Anthocyanins participate in the protection of wheat seedlings against cadmium stress. *Cereal Res. Commun.* 46, 242–252. doi: 10.1556/0806.45.2017.070

Skórzyńska-Polit, E., Dra, M., and Krupa, Z. (2003). The activity of the antioxidative system in cadmium-treated *Arabidopsis thaliana*. *Biol. Plant.* 47, 71–78. doi: 10.1023/A:1027332915500

Sofy, M. R., Seleiman, M. F., Alhammad, B. A., Alharbi, B. M., and Mohamed, H. I. (2020). Minimizing adverse effects of pb on maize plants by combined treatment with jasmonic, salicylic acids and proline. *Agronomy* 10:699. doi: 10.3390/agronomy10050699

Steel, R. G. D., and Torrie, J. H. (1960). *Principles and Procedures of Statistics : With Special Reference to the Biological Sciences*. New York, NY: McGraw-Hill.

Stroiński, A. (1999). Some physiological and biochemical aspects of plant resistance to cadmium effect. I. Antioxidative system. *Acta Physiol. Plant.* 21, 175–188. doi: 10.1007/s11738-999-0073-1

Sudisha, J., Niranjana, S., Umesha, S., Prakash, H., and Shetty, H. S. (2006). Transmission of seed-borne infection of muskmelon by *Didymella bryoniae* and effect of seed treatments on disease incidence and fruit yield. *Biol. Control* 37, 196–205. doi: 10.1016/j.biocontrol.2005.11.018

Taamalli, M., Ghabriche, R., Amari, T., Mnasri, M., Zolla, L., Lutts, S., et al. (2014). Comparative study of Cd tolerance and accumulation potential between *Cakile maritima* L.(halophyte) and *Brassica juncea* L. *Ecol. Eng.* 71, 623–627. doi: 10.1016/j.ecoleng.2014.08.013

Troll, W., and Lindsley, J. (1955). A photometric method for the determination of proline. *J. Biol. Chem.* 215, 655–660. doi: 10.1016/S0021-9258(18)65988-5

Ueshima, M., Ginn, B. R., Haack, E. A., Szymanowski, J. E., and Fein, J. B. (2008). Cd adsorption onto *Pseudomonas putida* in the presence and absence of extracellular polymeric substances. *Geochim. Cosmochim. Acta* 72, 5885–5895. doi: 10.1016/j.gca.2008.09.014

Verma, S., and Dubey, R. (2003). Lead toxicity induces lipid peroxidation and alters the activities of antioxidant enzymes in growing rice plants. *Plant Sci.* 164, 645–655. doi: 10.1016/S0168-9452(03)00022-0

Wang, Q., Chen, L., He, L.-Y., and Sheng, X.-F. (2016). Increased biomass and reduced heavy metal accumulation of edible tissues of vegetable crops in the presence of plant growth-promoting *Neorhizobium huautlense* T1-17 and biochar. *Agric. Ecosyst. Environ.* 228, 9–18. doi: 10.1016/j.agee.2016.05.006

Yoshimura, K., Yabuta, Y., Ishikawa, T., and Shigeoka, S. (2000). Expression of spinach ascorbate peroxidase isoenzymes in response to oxidative stresses. *Plant Physiol.* 123, 223–234. doi: 10.1104/pp.123.1.223

Zhang, F.-Q., Wang, Y.-S., Lou, Z.-P., and Dong, J.-D. (2007). Effect of heavy metal stress on antioxidative enzymes and lipid peroxidation in leaves and roots of two mangrove plant seedlings (*Kandelia candel* and *Bruguiera gymnorrhiza*). *Chemosphere* 67, 44–50. doi: 10.1016/j.chemosphere.2006.10.007

Zhang, H., Zhang, F., Xia, Y., Wang, G., and Shen, Z. (2010). Excess copper induces production of hydrogen peroxide in the leaf of *Elsholtzia haichowensis* through apoplastic and symplastic CuZn-superoxide dismutase. *J. Hazard. Mater.* 178, 834–843. doi: 10.1016/j.jhazmat.2010.02.014

Zhang, X., Zha, T., Guo, X., Meng, G., and Zhou, J. (2018). Spatial distribution of metal pollution of soils of Chinese provincial capital cities. *Sci. Total Environ.* 643, 1502–1513. doi: 10.1016/j.scitotenv.2018.06.177

Conflict of Interest: The authors declare that the research was conducted in the absence of any commercial or financial relationships that could be construed as a potential conflict of interest.

frontiers | Frontiers in Microbiology

ORIGINAL RESEARCH
published: 22 June 2022
doi: 10.3389/fmicb.2022.891882

Effect of Plant Growth-Promoting Bacteria on Biometrical Parameters and Antioxidant Enzymatic Activities of *Lupinus albus* var. Orden Dorado Under Mercury Stress

Marina Robas Mora, Pedro Antonio Jiménez Gómez*, Daniel González Reguero and Agustín Probanza Lobo*

Department of Pharmaceutical and Health Sciences, School of Pharmacy, CEU Universities, Universidad CEU San Pablo, Madrid, Spain

OPEN ACCESS

Edited by:
Krishnendu Pramanik, Visva-Bharati University, India

Reviewed by:
Hayssam M. Ali, King Saud University, Saudi Arabia
Himani Singh, Shri Ramswaroop Memorial University, India

***Correspondence:**
Marina Robas Mora
marina.robasmora@ceu.es
Pedro Antonio Jiménez Gómez
Pedro.jimenezgomez@ceu.es

Specialty section:
This article was submitted to Terrestrial Microbiology, a section of the journal Frontiers in Microbiology

Received: *08 March 2022*
Accepted: *02 May 2022*
Published: *22 June 2022*

Citation:
Robas Mora M, Jiménez Gómez PA, González Reguero D and Probanza Lobo A (2022) Effect of Plant Growth-Promoting Bacteria on Biometrical Parameters and Antioxidant Enzymatic Activities of Lupinus albus var. Orden Dorado Under Mercury Stress. Front. Microbiol. 13:891882. doi: 10.3389/fmicb.2022.891882

Heavy metal contamination of soils is a large-scale environmental problem. It leads to significant disqualification of the territory, in addition to being a source of the potential risk to human health. The exposure of plants to mercury (Hg) generates responses in its growth and their oxidative metabolism. The impact of increasing concentrations of Hg on the development of *Lupinus albus* var. Orden Dorado seedlings has been studied, as well as the plant's response to the maximum concentration of Hg that allows its development (16 μg ml^{-1}). The result shows that only the inoculum with plant growth promoting bacteria (PGPB) allows the biometric development of the seedling (root length, weight, and number of secondary roots) and prevents the toxic effects of the heavy metal from aborting the seedlings. Specifically, treatments with strains 11, 20 (*Bacillus toyonensis*), 48 (not determined), and 76 (*Pseudomonas syringae*) are interesting candidates for further PGPB-assisted phytoremediation trials as they promote root biomass development, through their PGPB activities. The plant antioxidant response has been analyzed by quantifying the catalase (CAT), superoxide dismutase (SOD), ascorbate peroxidase (APX), and glutathione reductase (GR) enzyme activity in the root, under 16 μg ml^{-1} of $HgCl_2$ and different PGPB treatments. Results show that, although Hg stress generally induces enzyme activity, strains 31 and 69I (*Pseudomonas corrugata*) and 18 and 43 (*Bacillus toyonensis*) can keep SOD and APX levels close to those found in control without Hg ($p < 0.01$). Strain 18 also shows a significant reduction of GR to control levels without Hg. The present work demonstrates the benefit of PGPB treatments in situations of high Hg stress. These findings may be a good starting point to justify the role of PGPB naturally isolated from bulk soil and the rhizosphere of plants subjected to high Hg pressure in plant tolerance to such abiotic stress conditions. More studies will be needed to discover the molecular mechanisms behind the phytoprotective role of the strains with the best results, to understand the complex plant-microorganism relationships and to find effective and lasting symbioses useful in bioremediation processes.

Keywords: oxidative stress, bioremediation, heavy metals – contamination, plant biometry, soil bacteria

INTRODUCTION

The World Report on Soil Resources (FAO, 2015) identified soil contamination as one of the main threats worldwide. In this same sense, the United Nations Environmental Assembly (UNEA, 2017) adopted a resolution calling for urgent decisions to address and mitigate soil pollution. According to the World Health Organization (World Health Organization [WHO], 2007), Hg is one of the ten chemicals that pose special problems for public health. Poisoning by this heavy metal can cause death (European Commission, 2011). The organic and more labile forms of Hg, mainly methylmercury, are the most toxic for human, animal, and plant health (Peralta-Videa et al., 2009). It accumulates in biological membranes due to its high lipid solubility, which facilitates its biomagnification in the food chain (Paisio et al., 2012). In the mining district of Almadén (Spain, Ciudad Real), mining activity has led to the mobilization of mercury (Hg) into more labile forms. This mobilization has promoted an increase in the concentration of Hg in certain locations (Díaz Puente, 2013).

For Hg to be incorporated into plants with storage capacity, it must be in its bioavailable form and close to the root. Given the similarity of the Hg (II) ion with essential molecules for plants, such as zinc (Zn), copper (Cu), or iron (Fe) (Patra and Sharma, 2000), it is incorporated through the pathways by which essential micronutrients are incorporated. Once incorporated, the Hg can be retained in the roots or translocated to the aerial part of the plant (Tiodar et al., 2021) and can be recovered through harvesting. Consequently, several visible symptoms start in the root cells (Tiwari and Lata, 2018). Of all of them, the inhibition of the longitudinal growth of the root is one of the first external symptoms of the toxic effect. Measurement of the relative rate of root elongation is often used as an early indicator to differentiate between sensitive and tolerant genotypes (Sabreen and Sugiyama, 2008).

Plants are also affected by Hg by altering antioxidant enzyme systems, hindering photosynthesis, interfering with nutrient uptake, unbalancing homeostasis in general, and slowing growth (Wang et al., 2012). *Lupinus* genus (lupine) is a plant with heavy metal mobilizing capacity when grown in contaminated soils (Tounsi-Hammami et al., 2020). The choice of this species is based on its ability to adapt to various ecophysiological characteristics. This adaptability allows *Lupinus* to develop in the conditions that occur in the mines, such as high salinity, excess nitrates, and low amounts of nutrients (González et al., 2021b). The ability to solubilize and absorb soil elements thanks to powerful root development makes it behave as a candidate plant for the plant growth promoting bacteria (PGPB)-assisted phytoremediation of these ecosystems. Plant tolerance to abiotic stress depends, to a large extent, on the bacteria present in its rhizosphere to mitigate the harmful effects of pollutants (Gontia-Mishra et al., 2016; Mariano et al., 2020; González et al., 2021a). Additionally, these bacteria have been used to improve plant resistance to different abiotic stress situations, such as salinity or desiccation (Ali et al., 2022), as well as the oxidative stress produced by Hg (Ajitha et al., 2021; Çavuşoğlu et al., 2022). However, no references have been found verifying the potential of PGPB in reversing lethality resulting from exposure to high Hg concentrations.

The objective of this work is the study of the effects of PGPB inoculants of *Pseudomonas* sp. and *Bacillus* sp. genera, isolated from the rhizosphere of plants naturally grown in chronic Hg polluted soils, on the germination and development of *Lupinus albus* var. Orden Dorado, under high Hg concentrations. Once the maximum concentration of Hg tolerable by the seeds in the absence of inoculum had been determined, it was sought to demonstrate whether the incorporation of PGPB reversed necrosis and cell death, allowing plant development under conditions of high Hg stress. To this end, the study of biometric parameters (weight, length of radicles, and number of secondary roots), as well as enzymes directly related to oxidative stress in plants [superoxide dismutase (SOD), catalase (CAT), ascorbate peroxidase (APX), and glutathione reductase (GR)] were quantified as measures of the plant fitness, compared with the absence of inoculum.

MATERIALS AND METHODS

Tested Strains

In total, twenty-four strains from bulk soil and rhizospheres of plants naturally grown in the mining district of Almadén, Ciudad Real (Spain) were used (**Table 1**). The experimental plot M (38°46′24.8″N, 4°51′04.7″W), is classified as an area of high contamination by Hg with concentrations of 1,710 mg kg^{-1} total Hg (Millán et al., 2011), was sampled. The plants sampled for the extraction of bacteria from the rhizosphere were *Rumex induratus* Boiss. & Reut., *Rumex bucephalophorus* L., *Avena sativa* L., *Medicago sativa* L., and *Vicia benghalensis* L., as well as bulk soil.

The strains were selected based on their biomercury remediation suitability index (BMRSI) (Robas et al., 2021). This index is calculated from the variables: (i) tolerance to abiotic pressure by Hg, quantified from the calculation of the minimum bactericidal concentration (MBC), and (ii) its PGPB activities: auxin production [indole-3-acetic acid (IAA)], the presence of the enzyme 1-aminocyclopropane-1-carboxylate decarboxylase (ACCd), production of siderophores (SID), and the phosphate solubilization capacity. The BMRSI was calculated using the following formula, where the values 1 and 0 for ACCd and PO_4^{3-} indicate presence and absence, respectively:

$$\mathrm{BMRSI} = [\mathrm{IAA}\ (\mu g.mL^{-1}) + \mathrm{ACCd}(1/0) + \mathrm{SID(cm)} + \mathrm{PO_4^{3-}}(1/0)] + [\mathrm{MBC\ Hg}(\mu g.mL^{-1})]$$

Candidates have a BMRSI > 5.5, a reference value established by the authors as a good indicator of the bioremedial capacity of the strains.

Seed Preparation

The seeds of *L. albus* var. Orden Dorado (Seed Bank of the Center for Scientific and Technological Research of Extremadura, Spain) were sterilized following the modified protocol of Abdel Latef et al. (2017). First, a 70% (v/v) ethanol bath for 30 s, followed by

TABLE 1 | Plant growth promoting bacteria (PGPB) characteristics of the tested strains.

No.	Identification 16S	Isolation origin	BMRSI (Robas et al., 2021)	MBC (μg/mL)	IAA (μg/mL)	ACCd (p/a)	Sid (cm)	PO_4^{3-} solubility (p/a)
11	*Bacillus toyonensis*	SL	7.69	87.5	5.61 ± 0.26	+	1.0	−
18	*Bacillus toyonensis*	SL	7.87	100	6.08 ± 0.02	+	0.5	−
20	*Bacillus toyonensis*	SL	7.55	100	5.96 ± 0.12	+	0.5	−
21	*Bacillus toyonensis*	SL	7.21	100	5.31 ± 0.36	+	0.8	−
22	*Bacillus toyonensis*	SL	5.75	87.5	4.57 ± 0.08	+	0.1	−
23	*Pseudomonas moraviensis*	SL	6.97	175	4.89 ± 0.03	+	0.9	−
25	*Bacillus toyonensis*	SL	7.89	150	5.85 ± 0.11	+	0.9	−
31	*Pseudomonas corrugata*	A	7.40	100	5.60 ± 0.20	+	0.7	−
43	*Bacillus toyonensis*	A	7.68	87.5	5.70 ± 0.19	+	0.9	−
48	Nd	A	6.62	100	4.92 ± 0.24	+	0.6	−
50	*Bacillus toyonensis*	A	7.08	100	5.29 ± 0.31	+	0.7	−
57	*Pseudomonas syringae*	B	7.26	175	6.38 ± 0.30	+	0.6	−
69I	*Pseudomonas corrugata*	B	7.85	75	6.08 ± 0.08	−	0.7	−
69II	*Pseudomonas corrugata*	B	8.51	350	5.71 ± 0.13	+	0.7	+
74	*Pseudomonas syringae*	B	8.07	100	6.27 ± 0.17	+	0.7	−
76	*Pseudomonas syringae*	B	7.04	350	4.99 ± 0.05	+	0.7	−
79	*Pseudomonas syringae*	B	7.55	87.5	5.27 ± 0.31	+	0.4	−
80	*Pseudomonas syringae*	B	8.42	80	6.47 ± 0.06	+	0.8	−
112	*Pseudomonas corrugata*	C	5.61	150	4.36 ± 0.09	+	0.1	−
130	*Pseudomonas corrugata*	D	8.01	160	5.85 ± 0.12	+	1.0	−
146	*Pseudomonas fluorescens*	E	7.99	80	6.09 ± 0.11	+	0.8	−
168	*Bacillus aryabhattai*	A	6.09	87.5	6.00 ± 0.08	+	0.0	+
197	*Pseudomonas* sp.	C	5.05	80	4.97 ± 0.13	−	0.0	−
211	*Bacillus drentensis*	D	7.74	80	6.16 ± 0.02	+	0.0	−

No, strain number; SL, bulk soil, (A–E) rhizospheres of (A) Rumex induratus, (B) Rumex bucephalophorus, (C) Avena sativa, (D) Medicago sativa, and (E) Vicia benghalensis. BMRSI, biomercury remediation suitability index; MBC, minimum bactericidal concentration; IAA, indole-3-acetic acid production; ACCd, ACC deaminase production; SID, siderophore production; Solub PO_4^{3-}, phosphate solubilization; +, positive result; –, negative result; Nd, strain not determined.

two consecutive washes with sterile distilled water for 1 min each. They were imbibed in sterile water and kept refrigerated (4°C) for 24 h. Pre-germination was carried out in trays with autoclaved vermiculite and irrigated with sterile water up to field capacity. The incubation of the trays was carried out in the dark, at room temperature (20 ± 2°C), and with aluminum foil wrapping the tray superficially to avoid environmental contamination and fungal growth. The pre-germinated seeds with a visible 1 ± 0.2 cm emerged radicle, were transferred in blocks of nine seeds, to Ø140 mm Petri dishes prepared with sterile vermiculite (121°C, 1 atm, and 20 min steam heat sterilization).

Determination of the Maximum Tolerance of Hg by the Seeds

Dilutions of Hg (using $HgCl_2$) were prepared in sterile distilled water at 0.0625, 0.25, 0.5, 1.0, 2.0, 4.0, 8.0, and 16 $\mu g.mL^{-1}$. Each plate, containing nine *L. albus* var. Orden Dorado seedlings, was irrigated with 50 ml of each $HgCl_2$ dilution (experimental volume up to previously assayed water holding capacity, the WHO). The plates were incubated in darkness, humidity (daily hydration status check and maintenance at the WHO with distilled water), and room temperature (20 ± 2°C) for 120 h.

Inoculation of the Seeds With the Plant Growth Promoting Bacteria Strains and Growth Conditions

A bacterial suspension was made in a sterile 0.45% saline solution (to ensure osmolarity) with a final microbial density of 0.5 McFarland. This process was repeated for each of the 24 bacterial strains tested. For each PGPB treatment, five pre-germinated *L. albus* var. Order Dorado seeds were inoculated with 1 ml of the corresponding bacterial suspension. Sterile vermiculite was brought to field capacity with 16 $\mu g\ ml^{-1}$ $HgCl_2$ dilution. The Hg-free control consisted of nine pregerminated seeds of *L. albus* var. Golden Orden watered with 50 ml of distilled water. Control with Hg was treated with 50 ml of a 16 $\mu g\ ml^{-1}$ $HgCl_2$ dilution. Both controls were without PGPB inoculum. The plates were incubated in darkness, humidity (daily hydration status check and maintenance at field capacity with distilled water), and room temperature (20 ± 2°C) for 120 h.

Harvest

Seedlings were subjected to different PGPB treatments after 5 days of sowing (120 h), and their controls were harvested. All plants were completely removed from the substrate and washed in a 0.45% saline solution to maintain osmolarity. The root part was then excised to proceed with measurements. For each biometric and enzymatic measurement, five treatment replicates were used ($n = 5$).

Biometry

For each treatment and control, biometric measurements of root length (cm), root weight (g), and number of secondary roots (No) were made. For root length measurement, a caliper (precision ± 0.5 mm) was used. For root weight, a precision balance (Gram RYI, FinTech, Cardiff, United Kingdom) was

used (linearity and reproducibility ± 0.0002). All samples were handled minimally and under aseptic conditions. Groups of treatments with a minimum mass of 1 g were kept at −80°C for enzymatic measurements.

Enzymatic Measurements

Catalase, SOD, APX, and GR enzyme activities were assayed.

Enzymes were extracted at 4°C from 1 g of fresh radicle sample, with a mortar and using 50 mg of polyvinylpolypyrrolidone (PVPP) and 10 ml of the following medium: 50 mM K-phosphate buffer (pH 7.8) with 0.1 mM EDTA (for SOD, CAT, and APX). The same medium, supplemented with 10 Mm of β-mercaptoethanol, was used for the GR extraction.

Superoxide Dismutase Activity

This activity was measured based on the ability of SOD to inhibit the reduction of nitro blue tetrazolium (NBT) by photochemically generated superoxide radicals. One unit of SOD is defined as the amount of enzyme needed to inhibit the reduction rate of NBT by 50% at 25°C (Burd et al., 2000).

Catalase Activity

This activity was measured following the Aebi (1984) method. H_2O_2 consumption was monitored for 1 min at 240 nm (Spectrophotometer visible GENESYS^{TM} 30, Thermo Fisher Scientific^{TM}, Hampton, NH, United States). This was done by mixing 50 mM potassium phosphate buffer with 10 mM H_2O_2 and 100 μl of the extract.

Ascorbate Peroxidase Activity

This activity was measured in a 1 ml reaction containing 80 nM potassium phosphate buffer, 2.5 mM H_2O_2, and 1 M sodium ascorbate. H_2O_2 was added to start the reaction and the decrease in absorbance was measured for 1 min at 290 nm, (Spectrophotometer visible GENESYS^{TM} 30, Thermo Fisher Scientific^{TM}, Hampton, NH, United States) to determine the oxidation rate of ascorbate (Amako et al., 1994).

Glutathione Reductase Activity

This activity was estimated spectrophotometrically at 25°C, according to the Carlberg and Mannervik (1985) method. The method is based on the measurement at 340 nm of the reduction of NADPH oxidation (Spectrophotometer visible GENESYS^{TM} 30, Thermo Fisher Scientific^{TM}, Hampton, NH, United States). The reaction mixture contained 50 mM Tris-$MgCl_2$ buffer, 3 mM, 1 mM GSSG, 50 μl enzyme, and 0.3 mM NADPH, added to start the reaction. The activity was calculated with the initial rate of the reaction and the molar extinction coefficient of NADPH (ε_{340} = 6.22 mM^{-1} cm^{-1}).

Statistical Analysis

The Kruskal–Wallis statistical analysis was carried out based on non-parametric tests ($N < 30$). The variables analyzed were root length and weight, number of secondary roots, and enzymatic activities (SOD, CAT, APX, and GR). For those cases in which the value of $p < 0.01$, a *post hoc* pairwise comparison test was carried out for all treatments against controls, using the non-parametric Mann–Whitney *U*-test, applied to two independent samples. Statistically different results were those for which the value of p was <0.01. Duncan's test was used to group the treatments, based on the difference in their means. A principal component analysis (PCA) was carried out for the reduction of the model. The projection of the two variables that best explain the model on the two-dimensional plane was carried out to study possible groupings between treatments. All analyses were carried out using SPSS Statistics AMOS^{TM} v. 27.0 software (IBM® Company, Armonk, NY, United States).

RESULTS

The results on seed germination and biometry under increasing concentrations of $HgCl_2$ are shown in **Figure 1**.

Results show the ability of *L. albus* var. Orden Dorado seeds to tolerate high concentrations of Hg, to the detriment of root elongation and weight. The highest concentration at which the seeds were able to germinate was selected (16 μg mL^{-1}).

The biometry results in the presence of the PGPB strains and 16 μg mL^{-1} of $HgCl_2$ are shown in **Table 2**.

Seeds treated with strains 18, 31, 43, 69I, 69II, and 130 develop secondary roots in at least three of their replicates. Specifically, the treatment with strain 20, makes the five replicates develop secondary roots in values that range between 1 and 6 secondary roots per seedling.

All biometric parameters in control without PGPB inoculum, both in the presence of Hg and in its absence, were significantly lower. The observation of the seeds in control with Hg shows that the root elongation was minimal and did not undergo variations concerning the moment of sowing (emerged radicle in pre-germination). The accumulation of Hg in embryonic tissue was evident to the naked eye.

The results of the antioxidant response in the presence of the PGPB strains and 16 μg ml^{-1} of $HgCl_2$ are shown in **Table 3**. Treatments with strains 18, 31, 43, and 69I maintain the levels of antioxidant enzymatic activity of control without Hg ($p < 0.01$), for the enzymes SOD and APX. Strain 18, on the other hand, maintains GR levels statistically analogous to those of control without Hg ($p < 0.01$).

Principal component analysis allows ordering the variables according to their variance. The variable that most contributes to the explanation of the model is the root length (63.95% of the variance), followed by the root weight (28.17% of the variance), explaining between them 92.12% of the model. The correlation matrix (**Table 4**), furthermore, establishes a strong positive correlation between them ($R = 0.750$).

In **Figure 2**, the two main components (PC1 and PC2) have been projected. The analysis allows the segregation of the strains into two large groups: (i) those that promote biometric improvements in the plant under Hg stress conditions (strains 11, 18, 20, 23, 31, 43, 48, 69I, 74, 76, 79, and 112). Of these, strains 11, 20, 48, and 76 are especially noteworthy. (ii) Those that buffer the antioxidant enzymatic response under Hg stress conditions to

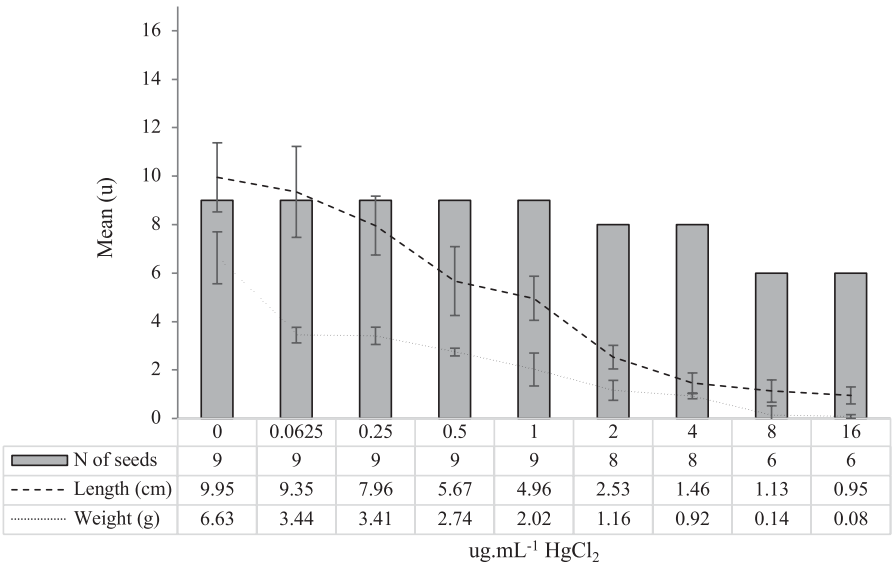

FIGURE 1 | The mean (n = 5 of experimental units with 9 seeds) germination number of seeds (No), root length (cm), and root weight (g) for each concentration of $HgCl_2$ tested ($\mu g\ ml^{-1}$), after 120 h of development.

TABLE 2 | The mean values of replicates (n = 5) ± SD for root length (cm), root weight (g) of the different treatments, and controls (absence of Hg and presence of Hg).

No.	Length (cm)	Weight (g)	Sec. roots (No)	No.	Length (cm)	Weight (g)	Sec. roots (No)
11	15.5 ± 3.87	0.78 ± 0.16	0.00	69II	9.73 ± 0.88	0.5 ± 0.06[b]	1.20
18	13.3 ± 1.10	0.61 ± 0.07	6.50	74	13.05 ± 0.91	0.70 ± 0.09	0.50
20	17.1 ± 0.61	0.81 ± 0.15	0.50	76	17.18 ± 1.05	0.79 ± 0.11	0.25
21	6.50 ± 0.76[a]	0.31 ± 0.05[b]	0.00	79	13.70 ± 0.81	0.79 ± 0.03	0.00
22	8.10 ± 0.29[a]	0.36 ± 0.05[b]	0.00	80	7.23 ± 2.75[a]	0.40 ± 0.05[b]	0.00
23	12.93 ± 0.57	0.75 ± 0.11	0.75	112	13.68 ± 1.48	0.72 ± 0.12	0.00
25	8.60 ± 0.86[a]	0.5 ± 0.08[b]	0.00	130	12.83 ± 0.99	0.68 ± 0.05	2.00
31	11.95 ± 0.47	0.70 ± 0.07	1.00	146	13.50 ± 1.41	0.74 ± 0.05	0.00
43	16.40 ± 2.15	0.65 ± 0.10	1.20	168	7.83 ± 0.30[a]	0.37 ± 0.05[b]	1.25
48	15.77 ± 1.50	0.85 ± 0.13	0.00	197	14.53 ± 0.87	0.85 ± 0.15	0.75
50	10.82 ± 1.68	0.50 ± 0.02[b]	0.00	211	13.10 ± 0.87	0.89 ± 0.06	0.75
57	7.57 ± 0.48[a]	0.27 ± 0.03	0.00	Cont. −Hg	7.63 ± 0.06[a]	0.42 ± 0.01[b]	0.15
69I	14.82 ± 1.72	0.52 ± 0.13[b]	2.00	Cont. +Hg	1.48 ± 0.02	0.05 ± 0.00	0.00

Data with superscripts indicate that there are no significant differences with control without Hg (Duncan's test; "a" for length and "b" for weight). The absence of superscripts means that the means are statistically different from control without Hg. The shaded cells indicate that the differences with control without Hg are statistically significant ($p < 0.05$). The number of secondary roots is not accompanied by ± SD since it is a discrete variable.

levels not significantly different from control in the absence of Hg (strains 18, 31, 43, and 69I).

DISCUSSION

Exposure of *L. albus* seedlings to increasing concentrations of Hg in the absence of PGPB inocula caused physically detectable phytotoxic effects from 24 h after exposure. Since Hg is a non-essential element in biological systems, there are no specific pathways for its metabolism and/or excretion (Kumari et al., 2020). As Hg accumulates and as observed in our results, the toxic effects become more evident as its concentration increases (**Figure 1**). In the present study, the phytotoxic effects were evaluated at 120 h of growth. The biometric damages (weight and root length) became significantly notable ($p < 0.05$) from a concentration of 0.5 $\mu g\ ml^{-1}$ of $HgCl_2$, compared with control without Hg. From this concentration, the radicles appeared thickened and necrotic, something that coincides with what was observed by other authors, working with several herbaceous species, such as *Medicago sativa* (Ortega-Villasante et al., 2007; Zhou et al., 2007) or *Allium sativum* (Zhao et al., 2013). At the highest concentrations (8 and 16 $\mu g\ ml^{-1}$), the inhibition of root elongation was total, resulting in weights and lengths close to zero (**Figure 1**). Given that the objective of the present study was to verify whether PGPB inocula allowed to mitigate, or even reverse, the phytotoxic effects of high Hg pressure exposure, the maximum concentration at which the

TABLE 3 | The mean values of replicates (n = 5) ± SD for the antioxidant enzymatic activity (enzyme mg Prot^{-1} min^{-1}) in the presence of PGPB treatments and controls (absence of Hg and presence of Hg).

No.	CAT	SOD	APX	GR	No	CAT	SOD	APX	GR
11	3.60 ± 0.18	8.63 ± 0.34	9.18 ± 0.45	3.78 ± 0.16	69II	7.05 ± 0.64	13.07 ± 0.42	11.02 ± 0.35	3.78 ± 0.16
18	2.23 ± 0.20	3.30 ± 0.40[a]	3.48 ± 0.66[a]	1.40 ± 0.78[a]	74	3.60 ± 0.18	8.23 ± 0.51	9.18 ± 0.71	3.56 ± 0.16
20	4.20 ± 0.16	9.36 ± 0.48	10.90 ± 0.67	3.17 ± 0.18	76	4.20 ± 0.16	9.36 ± 0.48	5.02 ± 0.42	3.37 ± 0.67
21	6.14 ± 0.39	11.58 ± 0.41	11.82 ± 0.37	4.86 ± 0.46	79	2.64 ± 0.17	6.40 ± 0.63	6.73 ± 0.68	2.56 ± 0.12
22	7.42 ± 0.40	8.42 ± 0.65	9.42 ± 0.28	10.42 ± 0.26	80	4.62 ± 0.09	11.05 ± 0.41	11.38 ± 0.39	4.41 ± 0.59
23	3.68 ± 0.51	10.70 ± 0.32	5.77 ± 0.33	3.41 ± 0.67	112	4.70 ± 0.09	6.58 ± 0.53	6.73 ± 0.70	4.66 ± 0.12
25	5.47 ± 0.33	12.79 ± 0.31	12.09 ± 0.28	5.49 ± 0.33	130	5.83 ± 0.08	13.83 ± 0.66	15.18 ± 0.21	5.95 ± 0.44
31	2.81 ± 0.41	4.99 ± 0.16[a]	3.69 ± 0.13[a]	3.27 ± 0.31	146	7.78 ± 0.08	18.27 ± 0.96	19.79 ± 0.65	7.8 ± 0.50
43	3.89 ± 0.19	3.21 ± 0.91[a]	3.27 ± 0.40[a]	3.18 ± 0.33	168	3.34 ± 0.19	7.99 ± 0.49	8.90 ± 0.56	3.23 ± 0.37
48	7.42 ± 0.26	12.09 ± 0.53	12.39 ± 0.60	5.00 ± 0.27	197	8.39 ± 0.52	20.76 ± 0.90	22.72 ± 0.59	8.60 ± 0.65
50	5.78 ± 0.32	11.73 ± 0.21	11.00 ± 0.52	4.92 ± 0.49	211	11.02 ± 0.89	26.84 ± 0.52	28.82 ± 0.15	11.05 ± 0.38
57	6.83 ± 0.25	10.91 ± 0.63	12.04 ± 0.28	5.60 ± 0.51	Cont −Hg	1.25 ± 0.02	3.25 ± 0.03[a]	3.19 ± 0.00[a]	1.20 ± 0.01[a]
69I	3.04 ± 0.16	3.41 ± 1.05[a]	4.02 ± 0.21[a]	3.03 ± 0.40	Cont. +Hg	0.04 ± 0.01	0.19 ± 0.00	0.04 ± 0.00	0.00 ± 0.01

Data with superscripts indicate that there are no significant differences with control without Hg (Duncan's test). The absence of superscripts means that the means are statistically different from the control without Hg. The shaded cells indicate that the differences with the control without Hg are not statistically significant ($p > 0.05$).

seeds survived (16 μg ml^{-1}) was selected for all further trials. At this concentration, growth inhibition of 33.34% was recorded, results analogous to those observed by Pokorska-Niewiada et al. (2018) in *Secale cereale* (34.6%) at a concentration somewhat higher than that tested in the present work (20 μg ml^{-1}).

Recent research focuses on the role that microorganisms that inhabit the rhizosphere can play to help the plant in its development in soils contaminated with Hg (Tiodar et al., 2021). Specifically, there is consensus on the importance of understanding the complex plant-microorganism interactions under stress conditions. In the present study, we proceeded with PGPB inocula isolated from the rhizosphere of plants that naturally grow in the mining district of Almadén (Spain) (**Table 1**). We agree with other authors that, in a situation of Hg stress, plants are more dependent on microbial activity, and are capable of reducing the harmful effect of metals (Amari et al., 2017). This is what we observed after inoculation with the selected PGPB strains. In the presence of Hg, they reversed the process and produced improvements in root length and weight parameters, as well as in the number of secondary roots, in some cases, even significantly compared with control in the absence of Hg. Such is the case of seeds treated with PGPB 18, 31, 43, 69I, 130, and 168, to a greater extent, and strains 20, 23, 74, 76, 197, and 211, to a lesser degree. Although we agree with the observations of Zafar et al. (2015) and Mukhraiya and Bhat (2017), according to which exposure to Hg produces a significant reduction in seed weight, compared with control in the absence of Hg, it is considered that this parameter is not a good indicator of biometric enhancement. The generalized increase in weight in the presence of Hg and PGPB treatment may be due to abnormal thickening due to Hg pressure rather than adequate root development or an increase in the number of secondary roots (Sabreen and Sugiyama, 2008).

One of the mechanisms by which bacteria can facilitate seed development under abiotic stress conditions is through the synthesis of phytohormones. In the present study, those auxin-producing PGPB (5.5–6.0 μg ml^{-1}), such as IAA, have been used as a selection criterion. These hormones are produced in the plant stems and transported to the root tips (Tiodar et al., 2021) where, at moderate concentrations, they favor elongation and promote the development of secondary roots, as occurs in plants inoculated with strains 18, 31, 43, 69I, 130, and 168. On the contrary, IAA concentrations ≥6.0 μg ml^{-}has an inhibitory effect on root growth and development. In part, this could be related to ethylene synthesis (Glick, 2003), which translates into an almost null secondary roots development when seeds are inoculated with strains 57, 74, 80, and 211. The regulation of ACC concentrations in response to stress conditions is another mechanism by which bacteria exert a beneficial effect on plants subjected to abiotic stress (Saleem et al., 2007). The hydrolysis of ACC by the bacterial enzyme ACC deaminase (ACCd) produces a decrease in ethylene levels, which increases root development (Glick, 2003; Belimov et al., 2009). Strains 11, 20, 48, and 76 produce significantly higher root elongation than the rest of the traits and controls, possibly due to the combined action of blocking the effect of ethylene produced by the plant under Hg stress conditions *via* ACCd and the

TABLE 4 | A correlation matrix exists between variables.

	Length (cm)	Weight (g)	CAT	SOD	APX	GR
Length (cm)	1.00					
Weight (g)	0.75	1.00				
CAT	−0.06	0.31	1.00			
SOD	−0.03	0.42	0.90	1.00		
APX	0.06	0.37	0.89	0.97	1.00	
GR	−0.11	0.26	0.93	0.82	0.84	1.00

Determinant 8.31 × 10^{-5}. Enzymatic activity (enzyme mg Prot^{-1} min^{-1}). CAT, catalase; SOD, superoxide dismutase; APX, ascorbate peroxidase; and GR, glutathione reductase.

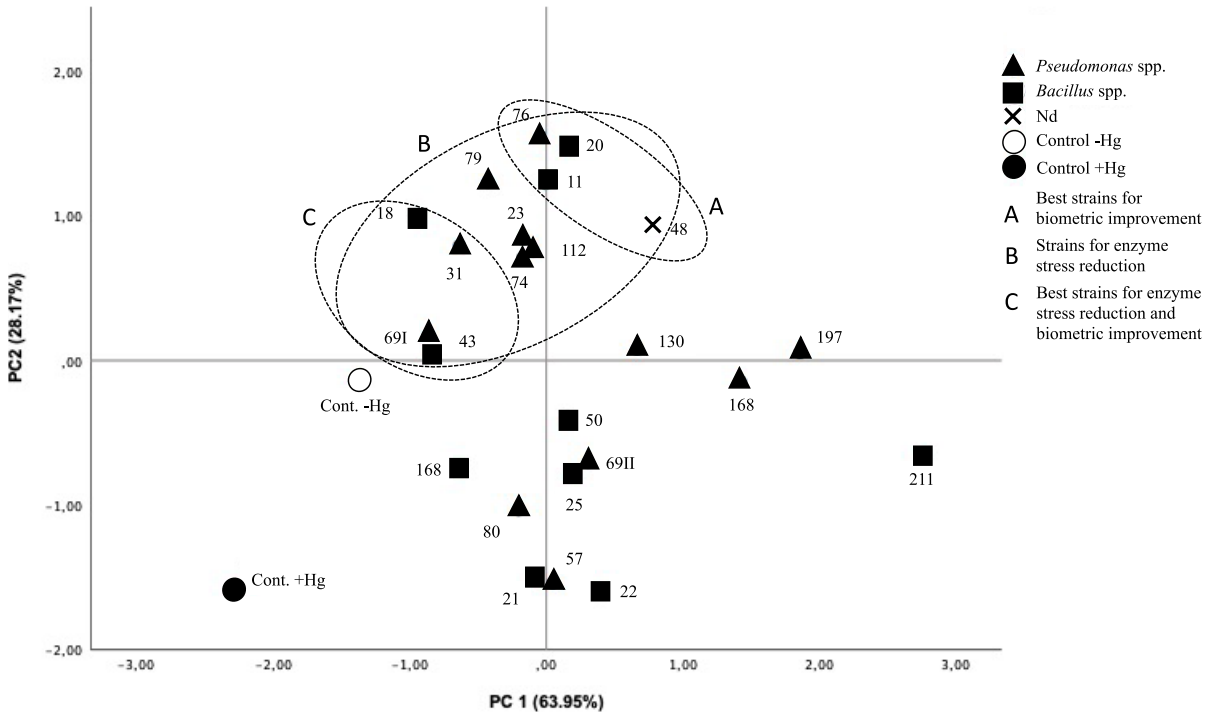

FIGURE 2 | Projection of the two main components (PC1 63.95% and PC2 28.17%). Treatments with higher elongations and root weights segregate toward the quadrant (*x*, *y*). Treatments with a high antioxidant response, which distances them from control in the absence of Hg, segregate toward the (*x*, –*y*) quadrant. Treatments close to control without Hg are grouped in the (–*x*, –*y*) quadrant.

activation of cell elongation by the moderate production of IAA. In addition, bacterial siderophores counteract the plant's inability to accumulate enough Fe from the soil, favoring its bioavailability and avoiding a stressful situation that can promote an increase in ethylene concentration. Unlike what happens with other heavy metals, the role of siderophores in relation to Hg chelation is not known, although it is believed that they could improve Hg absorption in the root (Tiodar et al., 2021). Strains 11, 21, 23, 25, 43, 80, 130, and 146 are good producers of siderophores and could be interesting for further field use in bioremediation processes, where Fe is a limiting element. Strains 11 and 20 (*Bacillus toyonensis*), 48 (not described), and 76 (*Pseudomonas corrugata*), capable of favoring plant development by promoting their growth in the presence of high heavy metals pressure, are interesting candidates for further biotechnological uses, in which an increase in root biomass or plant cover is sought.

Another consequence of Hg exposure is the appearance of oxidative stress with the accumulation of reactive oxygen species (ROS) (Çavuşoğlu et al., 2022) and an increase in the antioxidant enzymatic response (Kim et al., 2017). When plants exceed the threshold of tolerance to heavy metals, their metabolism can be altered, cellular homeostasis is compromised, electron transport chains and the functioning of lipids and proteins are altered, DNA damage is produced and activates the antioxidant defense system (Yang et al., 2018). In the present work, we observe how the exposure of *L. albus* to Hg in the absence of PGPB causes the necrosis of the seeds at 24 h of exposure, which translates into an antioxidant activity tending to zero for the four quantified enzymes. This should not be interpreted as a lack of activity *per se*, but rather the death of the seeds in the absence of PGPB treatment that neutralizes Hg toxicity, as occurs in treatments with PGPB 18, 23, 41, and 69I. The molecular mechanisms by which heavy metals induce ROS formation are not well described, although they have been shown to induce oxidative stress (Cargnelutti et al., 2006; Ajitha et al., 2021; Çavuşoğlu et al., 2022). Traditionally, the accumulation of ROS has been considered a negative effect on plants, the prelude to the cell degradation process. However, there is evidence that it can be a nuclear part of the cellular response system (Flores-Cáceres, 2013), being able to act as secondary messengers that regulate growth and development functions (Foyer and Noctor, 2005). Consequently, it is important for the plant to control the concentration of ROS, but not to eliminate them completely (Çavuşoğlu et al., 2022). In this sense, Kim et al. (2017) studied the role of GR in mitigating the toxicity of Hg (and other heavy metals) on the development of *Arabidopsis thaliana*. They concluded that GR has a much stronger binding affinity for Hg than for Cd, Cu, or Zn, suggesting that tight binding of GR to Hg prevents its uptake, leading to a low accumulation of Hg in plant cells, additionally improving their physiology. This fact is observed in the treatment with strain 18.

In accordance with other authors (Sapre et al., 2019), in the present study, it has been shown that seeds are viable at high Hg concentrations only when treated with PGPB. In the assays

carried out in this work, the seeds were developed under the same conditions (environmental, model plant species, and Hg concentration), so the unequal enzymatic responses could be explained by the PGPB effect. For further biotechnological uses of PGPB strains in biotechnological processes, those treatments that manage to mitigate the accumulation of ROS in the plant will be interesting. This effect has been observed by other authors after the use of PGPB from the *Bacillus* sp. (Vardharajula et al., 2011; Moreno-Galván et al., 2020) and *Pseudomonas* sp. genera (Dos Santos et al., 2021). In the present work, strains 31 and 69I (*P. corrugata*) and 18 and 43 (*Bacillus toyonensis*) can maintain the SOD and APX enzymatic responses at low-stress levels, without significant differences compared with control in the absence of Hg ($p < 0.01$). Additionally, strain 18 shows a significant reduction to control levels in the absence of Hg in the GR enzyme. This minimizing effect of enzymatic activity in the presence of abiotic stress has been documented by other authors when working with PGPB inocula and other heavy metals, such as Pb (Abdelkrim et al., 2018), Cu (Fatnassi et al., 2015), Zn (Islam et al., 2014) and Cd (Azimychetabi et al., 2021). According to Kasim et al. (2013), a decrease in antioxidant activity in plants subjected to PGPB treatment can be interpreted as a better adaptation to stress conditions, as it plays a phytoprotective role, which protects plants from abiotic stress. Treatment with strains 18, 31, 43, and 69I could be indicated to improve plant physiology in biotechnological processes involved in the recovery of environments contaminated with heavy metals.

CONCLUSION

The recovery of Hg-contaminated sites is a topic of current interest. Phytoremediation of Hg-contaminated soils is an emerging strategy. Species, such as *L. albus* have improved tolerance to inhibitory concentrations of Hg when inoculated with PGPB. The symbiotic relationship of some of these PGPB with plants exerts a phytoprotective role that improves their fitness, from biometrics to oxidative stress alleviation. In particular, we find that treating *L. albus* var. Orden Dorado seeds with strains 31 and 69I (*P. corrugata*), 18 and 43 (*Bacillus toyonensis*) in the presence of high Hg concentrations, minimize the antioxidant response of the seed at these levels of treatment in the absence of Hg. This reflects the phytoprotective nature of these PGPB traits, and as a result, they are postulated as good candidates for further bioremediation processes, in which plant physiology improvement is sought. Similarly, treatment of *L. albus* var. Orden Dorado seedlings with PGPB strains 11 and 20 (*B. toyonensis*), 48 (Not described), and 76 (*P. corrugata*) improves plant biometry (root length and weight) due to the unique combination of their PGPB activities. This makes them good candidates for further bioremediation trials where there is a special interest in achieving notable increases in biomass and plant cover. A detailed investigation is needed to understand the molecular mechanisms underlying Hg uptake, accumulation, and sequestration in plants, and the interactions between plants and their associated microorganisms. In this sense, it is also necessary to unravel the molecular mechanisms by which certain PGPB indirectly prevent Hg from exerting a phytoprotective role as described in this work.

DATA AVAILABILITY STATEMENT

The original contributions presented in this study are included in the article/supplementary material, further inquiries can be directed to the corresponding author/s.

AUTHOR CONTRIBUTIONS

MR and PJ: conceptualization. MR, DG, AP, and PJ: methodology. MR: software, writing—original draft preparation, and visualization. PJ: validation and data curation. MR, AP, and PJ: formal analysis and writing—review and editing. MR and DG: investigation. AP and PJ: resources, supervision, and funding acquisition. AP: project administration. All authors read and agreed to the published version of the manuscript.

FUNDING

This research has been funded by the Fundacióìn Universitaria San Pablo CEU and Banco Santander, grant number FUSP-BS-PPC01/2014. Grants to recognized research groups 2021/22 (Vice President for Research and Teaching Staff, CEU San Pablo University).

ACKNOWLEDGMENTS

We are grateful to the Seed Bank of the Center for Scientific and Technological Research of Extremadura, for its permanent availability in the supply of seeds for trials.

REFERENCES

Abdel Latef, A. A. H., Abu Alhmad, M. F., and Abdelfattah, K. E. (2017). The possible roles of priming with ZnO nanoparticles in mitigation of salinity stress in Lupine (*Lupinus termis*) Plants. *J. Plant Growth Regul.* 36, 60–70.

Abdelkrim, S., Jebara, S. H., and Jebara, M. (2018). Antioxidant systems responses and the compatible solutes as contributing factors to lead accumulation and tolerance in *Lathyrus sativus* inoculated by plant growth promoting rhizobacteria. *Ecotoxicol. Environ. Saf.* 166, 427–436. doi: 10.1016/j.ecoenv.2018.09.115

Aebi, H. (1984). Catalase *in vitro*. *Methods Enzymol.* 105, 121–126.

Ajitha, V., Sreevidya, C. P., Sarasan, M., Park, J. C., Mohandas, A., Singh, I. S. B., et al. (2021). Effects of zinc and mercury on ROS-mediated oxidative stress-induced physiological impairments and antioxidant responses in the microalga Chlorella vulgaris. *Environ. Sci. Pollut. Res.* 28, 32475–32492. doi: 10.1007/s11356-021-12950-6

Ali, B., Wang, X., Saleem, M. H., Hafeez, A., Afridi, M. S., Khan, S., et al. (2022). PGPR-Mediated salt tolerance in maize by modulating plant physiology, antioxidant defense, compatible solutes accumulation and bio-surfactant producing genes. *Plants* 11:345. doi: 10.3390/plants11030345

Amako, K., Chen, G.-X., and Asada, K. (1994). Separate assays specific for ascorbate peroxidase and guaiacol peroxidase and for the chloroplastic and cytosolic isozymes of ascorbate peroxidase in plants. *Plant Cell Physiol*. 35, 497–504. doi: 10.1093/oxfordjournals.pcp.a078621

Amari, T., Ghnaya, T., and Abdelly, C. (2017). Nickel, cadmium, and lead phytotoxicity and potential of halophytic plants in heavy metal extraction. *S. Afr. J. Bot*. 111, 99–110. doi: 10.1016/j.sajb.2017.03.011

Azimychetabi, Z., Sabokdast Nodehi, M., Karami Moghadam, T., and Motesharezadeh, B. (2021). Cadmium stress alters the essential oil composition and the expression of genes involved in their synthesis in peppermint (*Mentha piperita* L.). *Ind. Crops Prod*. 168:113602. doi: 10.1016/j.indcrop.2021.113602

Belimov, A. A., Dodd, I. C., Hontzeas, N., Theobald, J. C., Safronova, V. I., and Davies, W. J. (2009). Rhizosphere bacteria containing 1-aminocyclopropane-1-carboxylate deaminase increase yield of plants grown in drying soil via both local and systemic hormone signalling. *New Phytol.* 181, 413–423. doi: 10.1111/j.1469-8137.2008.02657.x

Burd, G. I., Dixon, D. G., and Glick, B. R. (2000). Plant growth-promoting bacteria that decrease heavy metal toxicity in plants. *Can. J. Microbiol.* 46, 237–245. doi: 10.1139/w99-143

Cargnelutti, D., Tabaldi, L. A., Spanevello, R. M., de Oliveira Jucoski, G., Battisti, V., Redin, M., et al. (2006). Mercury toxicity induces oxidative stress in growing cucumber seedlings. *Chemosphere* 65, 999–1006. doi: 10.1016/j.chemosphere.2006.03.037

Carlberg, I., and Mannervik, B. (1985). Glutatione Reductase. *Methods Enzymol*. 113, 484–490.

Çavuşoğlu, D., Macar, O., Kalefetoğlu Macar, T., Çavuşoğlu, K., and Yalçın, E. (2022). Mitigative effect of green tea extract against mercury (II) chloride toxicity in *Allium cepa* L. model. *Environ. Sci. Pollut. Res. Int*. 4, 27862–27874. doi: 10.1007/s11356-021-17781-z

Díaz Puente, F. J. (2013). *Variación de la Actividad Fisiológica de la Microflora del Suelo en Terrenos Afectados por Actividades Mineras.* Ph.D. tesis. Madrid: Universidad Complutense.

Dos Santos, M., Dias-Filho, M. B., and Cajueiro, E. S. (2021). Successful plant growth-promoting microbes: inoculation methods and abiotic factors. *Front. Sustain. Food Syst*. 5:606454. doi: 10.3389/fsufs.2021.606454

European Commission (2011). *Council Conclusions, 2011. Review of the Community Strategy Concerning Mercury*. Available online at: http://ec.europa.eu/environment/chemicals/mercury/ (accessed March 14, 2011).

FAO (2015). *Estado Mundial del Recurso Suelo. Resumen Técnico*. Rome: FAO.

Fatnassi, I. C., Chiboub, M., Saadani, O., Jebara, M., and Jebara, S. H. (2015). Impact of dual inoculation with Rhizobium and PGPR on growth and antioxidant status of *Vicia faba* L. under copper stress. *C. R. Biol*. 338, 241–254. doi: 10.1016/j.crvi.2015.02.001

Flores-Cáceres, M. L. (2013). *Caracterización de los Mecanismos de Respuesta Antioxidantede Medicago sativa a Metales Pesados*. Ph.D. tesis. Madrid: Universidad Autónoma de Madrid.

Foyer, C. H., and Noctor, G. (2005). Oxidant and antioxidant signalling in plants: a re-evaluation of the concept of oxidative stress in a physiological context. *Plant Cell Environ*. 28, 1056–1071. doi: 10.1111/j.1365-3040.2005.01327.x

Glick, B. R. (2003). Phytoremediation: synergistic use of plants and bacteria to clean up the environment. *Biotechnol. Adv*. 21, 383–393. doi: 10.1016/s0734-9750(03)00055-7

Gontia-Mishra, I., Sapre, S., Sharma, A., and Tiwari, S. (2016). Alleviation of mercury toxicity in wheat by the interaction of mercury-tolerant plant growth-promoting rhizobacteria. *J. Plant Growth Regul*. 35, 1000–1012.

González, D., Robas, M., Probanza, A., and Jiménez, P. A. (2021b). Selection of mercury-resistant PGPR strains using the BMRSI for bioremediation purposes. *Int. J. Environ. Res. Public Health* 18:9867. doi: 10.3390/ijerph18189867

González, D., Blanco, C., Probanza, A., Jiménez, P. A., and Robas, M. (2021a). Evaluation of the PGPR capacity of four bacterial strains and their mixtures, tested on *Lupinus albus* var. dorado seedlings, for the bioremediation of mercury-polluted soils. *Processes* 9:1293.

Islam, F., Yasmeen, T., Ali, Q., Ali, S., Arif, M. S., Hussain, S., et al. (2014). Influence of *Pseudomonas aeruginosa* as PGPR on oxidative stress tolerance in wheat under Zn stress. *Ecotoxicol. Environ. Saf.* 104, 285–293. doi: 10.1016/j.ecoenv.2014.03.008

Kasim, W. A., Osman, M. E., Omar, M. N., and Abd El-Daim, I. A. (2013). Control of drought stress in wheat using plant-growth-promoting bacteria. *J. Plant Growth Regul*. 32, 122–130. doi: 10.1007/s00344-012-9283-7

Kim, Y. O., Bae, H. J., Cho, E., and Kang, H. (2017). Exogenous glutathione enhances mercury tolerance by inhibiting mercury entry into plant cells. *Front. Plant Sci.* 8:683. doi: 10.3389/fpls.2017.00683

Kumari, S., Jamwal, R., Mishra, N., and Singh, D. K. (2020). Recent developments in environmental mercury bioremediation and its toxicity: a review. *Environ. Nanotechnol. Monit. Manage.* 13:100283.

Mariano, C., Mello, I. S., Barros, B. M., da Silva, G. F., Terezo, A. J., and Soares, M. A. (2020). Mercury alters the rhizobacterial community in Brazilian wetlands and it can be bioremediated by the plant-bacteria association. *Environ. Sci. Pollut. Res*. 27, 13550–13564.

Millán, R., Schmid, M. J., Carrasco-Gil, S., Villadóniga, M., Rico, C., Sánchez Ledesma, D. M., et al. (2011). Spatial variation of biological and pedological properties in an area affected by a metallurgical Mercury plant: Almadenejos (Spain). *Appl. Geochem*. 26, 174–181. doi: 10.1016/j.apgeochem.2010.11.016

Moreno-Galván, A., Romero-Perdomo, F. A., Estrada-Bonilla, G., Meneses, C. H., and Bonilla, R. R. (2020). Dry-Caribbean *Bacillus* spp. strains ameliorate drought stress in maize by a strain-specific antioxidant response modulation. *Microorganisms* 8:823. doi: 10.3390/microorganisms8060823

Mukhraiya, D., and Bhat, J. L. (2017). Assessment of mercury toxicity on seed germination, growth and antioxidant enzyme expression of *Sorghum vulgare* var. SG- 1000 seedlings. *IJTAS* 9, 45–50.

Ortega-Villasante, C., Hernández, L. E., Rellán-Alvarez, R., Del Campo, F. F., and Carpena-Ruiz, R. O. (2007). Rapid alteration of cellular redox homeostasis upon exposure to cadmium and mercury in alfalfa seedlings. *New phytol*. 176, 96–107. doi: 10.1111/j.1469-8137.2007.02162.x

Paisio, C. E., González, P. S., Talano, M. A., and Agostini, E. (2012). Remediación biológica de Mercurio: Recientes avances. *Rev. Latinoam. Biotecnol. Amb. Algal.* 3, 119–146.

Patra, M., and Sharma, A. (2000). Mercury toxicity in plants. *Bot. Rev*. 66, 379–422.

Peralta-Videa, J. R., Lopez, M. L., Narayan, M., Saupe, G., and Gardea-Torresdey, J. (2009). The biochemistry of environmental heavy metal uptake by plants: Implications for the food chain. *Int. J. Biochem. Cell Biol.* 41, 1665–1677. doi: 10.1016/j.biocel.2009.03.005

Pokorska-Niewiada, K., Rajkowska-Myśliwiec, M., and Protasowicki, M. (2018). Acute lethal toxicity of heavy metals to the seeds of plants of high importance to humans. *Bull. Environ. Contam. Toxicol.* 101, 222–228. doi: 10.1007/s00128-018-2382-9

Robas, M., Jiménez, P. A., González, D., and Probanza, A. (2021). Bio-mercury remediation suitability index: a novel proposal that compiles the PGPR features of bacterial strains and its potential use in phytoremediation. *Int. J. Environ. Res. Public Health* 18:4213. doi: 10.3390/ijerph18084213

Sabreen, S., and Sugiyama, S. (2008). Trade-off between cadmium tolerance and relative growth rate in 10 grass species. *Environ. Exp. Bot*. 63, 327–332. doi: 10.1016/j.envexpbot.2007.10.019

Saleem, M., Arshad, M., Hussain, S., and Bhatti, A. S. (2007). Perspective of plant growth promoting rhizobacteria (PGPR) containing ACC deaminase in stress agriculture. *J. Ind. Microbiol. Biotechnol.* 34, 635–648. doi: 10.1007/s10295-007-0240-6

Sapre, S., Deshmukh, R., Gontia-Mishra, I., and Tiwari, S. (2019). "Problem of Mercury Toxicity in Crop Plants: Can Plant Growth Promoting Microbes (PGPM) Be an Effective Solution?," in *Field Crops: Sustainable Management by PGPR. Sustainable Development and Biodiversity*, eds D. Maheshwari and S. Dheeman (Cham: Springer).

Tiodar, E. D., Văcar, C. L., and Podar, D. (2021). Phytoremediation and Microorganisms-Assisted Phytoremediation of Mercury-Contaminated Soils: Challenges and Perspectives. *Int. J. Environ. Res. Public Health* 18:2435. doi: 10.3390/ijerph18052435

Tiwari, S., and Lata, C. (2018). Heavy metal stress, signaling, and tolerance due to plant-associated microbes: an overview. *Front. Plant Sci*. 9:452. doi: 10.3389/fpls.2018.00452

Tounsi-Hammami, S., Dhane-Fitouri, S., Le Roux, C., Hammami, Z., and Ben Jeddi, F. (2020). Potential of native inoculum to improve the nodulation and growth of white lupin in Tunisia. *Ann. Inst. Nat. Rech. Agron. Tunis.* 93, 102–114.

UNEA (2017). *3rd meeting of the UN Environment Assembly (UNEA 3).* Nairobi: UNEA.

Vardharajula, S., Zulfikar Ali, S., Grover, M., Reddy, G., and Bandi, V. (2011). Drought-tolerant plant growth promoting *Bacillus* spp.: effect on growth, osmolytes, and antioxidant status of maize under drought stress. *J. Plant Interact.* 6, 1–14. doi: 10.1080/17429145.2010.535178

Wang, J., Feng, X., Anderson, C. W., Xing, Y., and Shang, L. (2012). Remediation of mercury contaminated sites - A review. *J. Hazard Mater.* 22, 1–18. doi: 10.1016/j.jhazmat.2012.04.035

World Health Organization [WHO] (2007). *Exposure to Mercury: a Major Public Health Concern*. Geneva: World Health Organization.

Yang, J., Li, G., Bishopp, A., Heenatigala, P. P. M., Hu, S., Chen, Y., et al. (2018). Comparison of growth on mercuric chloride for three lemnaceae species reveals differences in growth dynamics that effect their suitability for use in either monitoring or remediating ecosystems contaminated with mercury. *Front. Chem.* 16:112. doi: 10.3389/fchem.2018.00112

Zafar, M., Khan, M., Athar, M., Shafiq, M., Farooqi, Z. U., and Kabir, M. (2015). Effect of Mercury on Seed Germination and Seedling Growth of Mungbean (*Vigna radiata* (L.) Wilczek). *J. Appl. Sci. Environ. Manage.* 19, 191–199. doi: 10.4314/jasem.v19i2.4

Zhao, J., Gao, Y., Li, Y. F., Hu, Y., Peng, X., Dong, Y., et al. (2013). Selenium inhibits the phytotoxicity of mercury in garlic (*Allium sativum*). *Environ. Res.* 125, 75–81. doi: 10.1016/j.envres.2013.01.010

Zhou, Z. S., Huang, S. Q., Guo, K., Mehta, S. K., Zhang, P. C., and Yang, Z. M. (2007). Metabolic adaptations to mercury-induced oxidative stress in roots of *Medicago sativa* L. *J. Inorg. Biochem.* 101, 1–9. doi: 10.1016/j.jinorgbio.2006.05.011

Conflict of Interest: The authors declare that the research was conducted in the absence of any commercial or financial relationships that could be construed as a potential conflict of interest.

Publisher's Note: All claims expressed in this article are solely those of the authors and do not necessarily represent those of their affiliated organizations, or those of the publisher, the editors and the reviewers. Any product that may be evaluated in this article, or claim that may be made by its manufacturer, is not guaranteed or endorsed by the publisher.

frontiers | Frontiers in Microbiology

ORIGINAL RESEARCH
published: 07 July 2022
doi: 10.3389/fmicb.2022.926748

Cloning of Nitrate Reductase and Nitrite Reductase Genes and Their Functional Analysis in Regulating Cr(VI) Reduction in Ectomycorrhizal Fungus *Pisolithus* sp.1

*Liang Shi[1], Binhao Liu[1], Xinzhe Zhang[1], Yuan Bu[1], Zhenguo Shen[1], Jianwen Zou[2] and Yahua Chen[1,2,3,4,5]**

[1] College of Life Sciences, Nanjing Agricultural University, Nanjing, China, [2] College of Resources and Environmental Sciences, Nanjing Agricultural University, Nanjing, China, [3] Jiangsu Collaborative Innovation Center for Solid Organic Waste Resource, Nanjing Agricultural University, Nanjing, China, [4] National Joint Local Engineering Research Center for Rural Land Resources Use and Consolidation, Nanjing Agricultural University, Nanjing, China, [5] The Collaborated Laboratory of Plant Molecular Ecology (between College of Life Sciences of Nanjing Agricultural University and Asian Natural Environmental Science Center of the University of Tokyo), Nanjing Agricultural University, Nanjing, China

OPEN ACCESS

Edited by:
Krishnendu Pramanik,
Visva-Bharati University, India

Reviewed by:
Kostyantyn Dmytruk,
National Academy of Sciences of Ukraine (NAN Ukraine), Ukraine
Richard Villemur,
Université du Québec, Canada
Rosa María Martínez-Espinosa,
University of Alicante, Spain

***Correspondence:**
Yahua Chen
yahuachen@njau.edu.cn

Specialty section:
This article was submitted to Terrestrial Microbiology, a section of the journal Frontiers in Microbiology

Received: 23 April 2022
Accepted: 24 May 2022
Published: 07 July 2022

Citation:
Shi L, Liu B, Zhang X, Bu Y, Shen Z, Zou J and Chen Y (2022) Cloning of Nitrate Reductase and Nitrite Reductase Genes and Their Functional Analysis in Regulating Cr(VI) Reduction in Ectomycorrhizal Fungus Pisolithus sp.1. Front. Microbiol. 13:926748. doi: 10.3389/fmicb.2022.926748

Assimilatory-type nitrate reductase (NR) and nitrite reductase (NiR) are the key enzymes that involve in nitrate assimilation and nitrogen cycling in microorganisms. NR and NiR with NADH or NADPH and FMN or FAD domains could be coupled to the reduction process of hexavalent chromium [Cr(VI)] in microorganisms. A new assimilatory-type NR gene (named *niaD*) and a new assimilatory-type NiR gene (named *niiA*) are cloned, identified, and functionally characterized by 5′ and 3′ RACE, alignment, annotation, phylogenetic tree, and yeast mutant complementation analyses from *Pisolithus* sp.1, a dominant symbiotic ectomycorrhizal fungi (EMF) that can assist in phytoremediation. Assimilatory-type *niaD* and *niiA* were 2,754 bp and 3,468 bp and encode a polypeptide with 917 and 1,155 amino acid residues, respectively. The isoelectric points of NR (*Pisolithus* sp.1 NR) and NiR (*Pisolithus* sp.1 NiR) of *Pisolithus* sp.1 are 6.07 and 6.38, respectively. The calculated molecular mass of *Pisolithus* sp.1 NR and *Pisolithus* sp.1 NiR is 102.065 and 126.914 kDa, respectively. Yeast mutant complementation analysis, protein purification, and activities of NR and NiR under Cr treatment suggest that *Pisolithus* sp.1 NR is a functional NR that mediates Cr(VI) tolerance and reduction. The multiple alignment demonstrates that *Pisolithus* sp.1 NR is potentially a nicotinamide adenine dinucleotide phosphate-dependent flavin mononucleotide reductase and also Class II chromate reductase. Our results suggest that *Pisolithus* sp.1 NR plays a key role in Cr(VI) reduction in the EMF *Pisolithus* sp.1.

Keywords: Cr(VI) reduction, ectomycorrhizal fungi, nitrate reductase, phytoremediation, tolerance, yeast

INTRODUCTION

Chromium (Cr) is one of the top 20 pollutants in the list of super hazardous substances all over the world (Johnston and Chrysochoou, 2012; Dhal et al., 2013). The toxicity of hexavalent chromium [Cr(VI)] is 100 times that of trivalent chromium [Cr(III)], and the toxicity can be related to the solubility. Cr(VI) is highly soluble and toxic to microorganisms, plants, and animals, entailing mutagenic and carcinogenic effects whereas the latter is considered to be less soluble and less toxic (Nancharaiah et al., 2010). Excessive Cr(VI) and Cr(III) can cause lung cancer, kidney disease, dermatitis, etc. (Das et al., 2014; Viti et al., 2014). Therefore, the reduction of Cr(VI) to Cr(III) constitutes a potential detoxification process that might be achieved chemically or biologically.

Ectomycorrhizal fungi (EMF) can help host plants absorb water and mineral elements, improve the survival and growth rate of the host plants, and beneficial for their surviving in a variety of harsh and barren environments such as pests and diseases, salt stress, heavy metal (HM) stress, and drought stress (Pena and Polle, 2013; Chen Y.H. et al., 2015; Wen et al., 2017; Shi et al., 2018, 2019). *Pisolithus* sp. as one kind of EMF is widely distributed all over the world and can tolerate HMs such as manganese (Mn), copper (Cu), and lead. In addition, *Pisolithus* sp. can enhance the Cu tolerance of host plants such as *Acacia*, *Eucalyptus urophylla*, and black pine (Aggangan and Aggangan, 2012; Silva et al., 2013; Wen et al., 2017) while can also significantly reduce the stress of Mn on *Eucalyptus grandis* (Canton et al., 2016). In the previous study, we collected, isolated, and screened a strain of *Pisolithus* sp.1 (accession number: KY075875.1) with the ability of Cr(VI) reduction. In liquid medium, 75% of Cr(VI) can be reduced to Cr(III), and extracellular reduction of Cr(VI) can be accelerated by hydrogen ions (H^+) generated by *Pisolithus* sp.1 by reducing the pH in the medium within 12 days (Shi et al., 2018). In addition, through the transcriptome sequencing of *Pisolithus* sp.1 [Cr(VI)-tolerant strain] and *Pisolithus* sp.2 [Cr(VI)-sensitive strain] before and after Cr(VI) treatment, the results of comparative transcriptome analysis found that compared with the control group [without Cr(VI)], the differentially expressed genes in *Pisolithus* sp.1 were only significantly enriched in the nitrogen metabolism pathway but did not significantly enrich in *Pisolithus* sp.2, and the relative expression levels of the genes encoding nitrate reductase (NR) (*niaD*) and nitrite reductase (NiR) (*niiA*) in *Pisolithus* sp.1 were higher in the presence of 10 mg/L Cr(VI) treatment (Shi et al., 2020).

Cr(VI) can interfere with nitrogen metabolism in plants, and NR plays an important role in the response of plants to Cr (Singh et al., 2013). For example, selenium nanoparticles can induce and increase the activity of NR in wheat, which can regulate Cr(VI) reduction (Yu et al., 2016). The expression fold of genes encoding the dissimilatory NR (narIJHG) and napAB, and the assimilation NR nasA, can be upregulated 3–20 times after been treated by 10 mg/L Cr(VI). In addition, the denitrification genes encoding the NiR NirK, the NO reductase NorB and the N_2O reductase NosZ were upregulated 67, 152 and 207.5 times, respectively, under Cr(VI) treatment (Viamajala et al., 2002; Han et al., 2010). The above results showed that Cr(VI) has a positive effect on the expression of assimilative or dissimilatory genes encoding NR and NiR. Studies have also found that Cr(VI) can interact with various oxidoreductase in bacteria, including iron reductase, NR, NiR, glutathione reductase, lipid-based reductase, ferrioxy acid-$NADP^+$ reductase, and other metal reductase while to be reduced by themselves (Ahemad, 2014). Therefore, the oxidation state of Cr [such as Cr(VI)] may induce some oxidoreductases to participate in the redox process, and this process will be coupled with the reduction of Cr(VI) to Cr(III) (Chovanec et al., 2012).

Actually, NR and NiR genes involved in nitrate assimilation are completely distinct from reductases involved in denitrification (dissimilation), which is a respiratory system. Assimilative nitrate reduction is a process in which nitrate is reduced to nitrite and ammonia, and ammonia is assimilated into amino acids. The reduced nitrogen here becomes the nitrogen source for the microorganisms. The dissimilatory nitrate reduction is nitrate respiration by microorganisms under anaerobic or micro-oxygen conditions, that is, NO_3^- or NO_2^- is used instead of O_2 as an electron acceptor for respiratory metabolism. Dissimilatory nitrate reduction is further divided into fermentative nitrate reduction and respiratory nitrate reduction. In fermentative nitrate reduction, nitrate is an "incidental" electron acceptor in the fermentation process, rather than a terminal acceptor, which is an incomplete reduction, and the fermentation products are mainly nitrite and NH_4^+. The products of respiratory nitrate reduction are gaseous N_2O, N_2, and this process is called denitrification (Il'ina and Khodakova, 1973; Jin et al., 2019). At present, there is no information about the type of genes encoding NR and NiR in *Pisolithus* sp., and NR or NiR has not been reported to be involved in Cr(VI) reduction in EMF. To solve the above questions, in this study, assimilatory NR and NiR genes were cloned, identified, analyzed, and functionally characterized from *Pisolithus* sp.1 by 5′ and 3′ RACE, alignment, yeast mutant complementation analysis, protein purification, and its reducing ability to Cr(VI).

MATERIALS AND METHODS

Strains, Plasmids, and Culture Conditions

Pisolithus sp.1 (KY075875) was isolated from a sporophore in Sanqing Mountain, Jiangxi Province, China (28.54°N, 118.03°E), and the detailed information was referred to Shi et al. (2018). The mycelia of *Pisolithus* sp.1 were incubated in solid Kottke medium at 25°C for 18 days, and then, mycelia were collected, quickly frozen in liquid nitrogen, and saved at −80°C for RNA extraction and gene cloning. *Escherichia coli* DH5α was used for the transformation and propagation of plasmids and was cultured in Luriae–Bertani (LB) medium at 37°C. Cr(VI) tolerance assays were performed using the wild-type (WT) *Saccharomyces cerevisiae* strain BY4741 (MATa *his3Δ1 leu2Δ0 met15Δ0 ura3Δ0*) and Cr-sensitive Δ*ycf1* mutant (MATa *his3Δ1 leu2Δ0 met15Δ0 ura3Δ0 YCF1:kanMXX4*), which were grown in both yeast extract peptone dextrose medium and a synthetic defined medium at 30°C. The pYES2-NTB vector was used

for heterogenous expression of the *niaD* and *niiA* gene in *S. cerevisiae*.

RNA Extraction and cDNA Synthesis

For total RNA extraction, approximately 0.5 g of fresh mycelia from the *Pisolithus* sp.1 strain was frozen, grounded into a fine powder in liquid nitrogen and homogenized in RNAiso Plus solution. Total RNAs were extracted using the RNAiso Plus Kit (TaKaRa, Dalian, China) according to the manufacturer's protocol. Then, the quantity and the purity of the RNA were determined by UV measurement using the NanoDrop 2000c spectrophotometer (Thermo Scientific, Shanghai, China). First-strand cDNA was synthesized from the total RNA using the PrimeScriptII Frist-Strand cDNA Synthesis Kit (TaKaRa, Dalian, China). The synthesized first-strand cDNA was used as the PCR template and saved at −20°C.

Cloning of *niaD* and *niiA*

Based on the results of transcriptome sequencing (Shi et al., 2020; accession number: SRR8837356-SRR8837367), compared with the control group [without Cr(VI)], the differentially expressed genes in *Pisolithus* sp.1 were only significantly enriched in the nitrogen metabolism pathway but did not significantly enrich in *Pisolithus* sp.2, and the relative expression levels of the NR gene *niaD* and NiR gene *niiA* in *Pisolithus* sp.1 were higher in the presence of 10 mg/L Cr(VI) treatment. The 5′ race and 3′ race primers of *niaD and niiA* genes were designed based on the sequencing results of *niaD* and *niiA* (**Table 1** and **Supplementary Table 1**). For 5′ race PCR amplification, using cDNA of *Pisolithus* sp.1 as a template, PCR system (25 μl): template cDNA 0.5 μl, 5 GeneRacer outer primer (10 μm) 1.0 μl, *niaD*-R1 or *niiA*-R1 (10 μm) 1.0 μl, and Platinum PCR SuperMix High Fidelity (Invitrogen) 22.5 μl. The first round of PCR condition is pre-denaturation at 94°C for 2 min; denaturation at 94°C for 30 s, annealing and extension at 72°C for 30 s, 5 cycles; then denaturation at 94°C for 30 s, annealing and extension at 70°C for 30 s, 5 cycles; and denaturation at 94°C for 30 s, annealing and extension at 66°C for 30 s, 25 cycles. For the second round of PCR, using the production of the first-round PCR as a template, PCR system (25 μl): template cDNA 0.5 μl, 5 GeneRacer Inner primer (10 μm) 1.0 μl, *niaD*-R2 or *niiA*-R2 (10 μm) 1.0 μl, 10 Platinum PCR SuperMix High Fidelity (Invitrogen) 22.5 μl. The second round of reaction conditions is pre-denaturation at 94°C for 2 min; denaturation at 94°C for 30 s, annealing and extension at 66°C for 30 s, 30 cycles. For 3′ race PCR amplification, the first and the second reaction condition and system are the same with 5′race, just use 3GeneRacer Inner/Outer primer, *niaD*-F1, *niaD*-F2, *niiA*-F1, *niiA*-F2 instead of 5GeneRacer inner/outer primer, *niaD*-R1, *niaD*-R2, *niiA*-R1, and *niiA*-R2, respectively. After 5′ and 3′ RACE, the PCR products were purified using the BioTeke Gel Extraction Kit (BioTeke, Beijing, China). The fragment was cloned into the pMD18-T Simple Cloning Vector (TaKaRa, Dalian, China) and transformed into competent *Escherichia coli* DH5a for DNA sequencing. To obtain the complete *niaD* and *niiA*, full-length PCR was performed with high fidelity KOD FX (Toyobo, Shanghai, China) using the primers *niaD* full length and *niiA* full length (**Table 1**).

TABLE 1 | Primers used in this study.

Gene name	Primer name	Sequence (5′-3′)
niaD-5′race	*niaD-R1*	CAATTGTCAGGAGTCTCGCGATCCA
	niaD-R2	CGTCGTGGAGAGATGCTGGTAAGAATG
	Outer primer	CGACTGGAGCACGAGGACACTGA
	Inner primer	GGACACTGACATGGACTGAAGGAGTA
niiA-5′race	*niiA-R1*	GCCGAGCGTACCATTCCACTTGAT
	niiA-R2	GCGATTGTAAGCCAGGTGCGTTT
	Outer primer	CGACTGGAGCACGAGGACACTGA
	Inner primer	GGACACTGACATGGACTGAAGGAGTA
niaD-3′race	*niaD–F1*	GACACCAGCGATACAGAGACGAGAGT
	niaD–F2	GGAGGACATTCTCTGTCGTGCTGAACT
	Outer primer	GCTGTCAACGATACGCTACGTAACG
	Inner primer	CGCTACGTAACGGCATGACAGTG
niiA-3′race	*niiA–F1*	CGGTACCTGCCTGAACGACATGCA
	niiA–F2	GGGACGACCTGCAGCTCCTGCTT
	Outer primer	GCTGTCAACGATACGCTACGTAACG
	Inner primer	CGCTACGTAACGGCATGACAGTG
niaD-full length	Forward primer	AAGATATCTTAAGAATGTTTGACG
	Reverse primer	CCTATACAGCAAACACAGGCAGAT
niiA-full length	Forward primer	GACTCGGTTGGAGCCTTATC
	Reverse primer	CAATCTGACTGCTCAATGCATACGA
niaD-Yeast complementation	Forward primer	[a]ACCGAGCTCGGATCCATGT TTGACGAATATGTCGAC
	Reverse primer	[b]ATGCGGCCCTCTAGAT CAGAATACTACGAGGTGGT
niiA-Yeast complementation	Forward primer	[a]ACCGAGCTCGGATCCA TGATGAACAGTACACTAGGC
	Reverse primer	[b]ATGCGGCCCTCTAG ATCAGGCAGGTACCGTCGCTA

Underlined sequences are a, BamH1 and b, Xba1 sites.

Bioinformatic Analysis

The open reading frame (ORF) was predicted using the ORF Finder[1]. The cloned *niaD* and *niiA* were analyzed to predict the amino acid sequences using the DNAMAN software package (version 7.0.2.176, Lynnon BioSoft, Canada). The amino acid sequences of *niaD* and *niiA* were analyzed and performed using protein Basic Local Alignment Search Tool (BLAST) algorithms[2]. The predicted amino acid sequences were used to search for conserved domains with NCBI Conserved Domain Search database[3]. The theoretical pIs and molecular masses were predicted using the Compute pI/Mw tool from the Expert Protein Analysis System (ExPASy) database[4]). The potential transmembrane domains in the protein sequences were predicted using the TMHMM Server v.2.0[5], HMMTOP program[6] (Tusnády and Simon, 2001), TMpred[7], and the network protein sequence

[1]http://www.ncbi.nlm.nih.gov/gorf/orfig.cgi
[2]http://www.ncbi.nlm.nih.gov/BLAST
[3]http://www.ncbi.nlm.nih.gov/Structure/cdd/wrpsb.cgi
[4]http://www.expasy.ch/tools/pi_tool.html
[5]http://www.cbs.dtu.dk/services/TMHMM/
[6]http://www.enzim.hu/hmmtop/
[7]http://www.ch.embnet.org/software/TMPRED_form.html

analysis (NPSA)[8]. The putative amino acid sequences of *niaD* and *niiA* and the other NRs and NiRs from different organisms were aligned using the DNAMAN software package and the Clustal X program, version 1.83. A phylogenetic analysis was performed using the maximum likelihood method in the MEGA5 program.

Gene Function Analysis

To insert the *niaD* or *niiA* gene into the expression vector pYES2, the cloned genes were amplified by PCR using primers with *BamH1* and *Xba1* restriction sites (**Table 1**). The amplified product was cloned into the corresponding restriction site of pYES2 vector, and the yeast cells were transformed by electro-transformation after sequencing verification (Rono et al., 2021). The transformed yeast cells were selectively cultured on SD-Ura solid medium which containing 2% glucose (mass/volume ratio) but the lack of uracil, and clones were picked after 2–3 days. The plasmids were extracted for PCR verification, and the recombinant strain was stored at −70°C. The mutant strain (Δ*ycf1*), which was transformed using the empty pYES2 vector, was used as controls. To determine the Cr(VI) tolerance of recombinant yeast cells, receptively, the recombinant yeast strains (Δ*ycf1*-pYES2, Δ*ycf1*-pYES2-*niaD,* and Δ*ycf1*-pYES2-*niiA*) were cultured on SD-Ura liquid medium which containing 2% glucose to optical density (OD_{600}) = 1.0. All the cultures were serially diluted (10^0, 10^{-1}, 10^{-2}, 10^{-3}, 10^{-4}, and 10^{-5}) and 5 μl of each dilution was spotted on SD-Ura solid medium with and without Cr (0, 10, 20, and 40 mg L^{-1}). The spotted plates were then incubated at 30°C for 3 days and photographed.

Further, the tolerance and reduction abilities of transformants to Cr(VI) were also measured in a liquid SD broth. The transformants Δ*ycf1*-pYES2, Δ*ycf1*-pYES2-*niaD* and Δ*ycf1*-pYES2-*niiA* were inoculated separately in 50 ml SD-Ura liquid medium with the starting OD_{600} of 0.05 and allowed to grow at 30°C for 5 h at 220 rpm. After 5 h, the cultures were subjected to different concentrations of Cr(VI) (0, 5, and 10 mg/L) and incubated at 30°C for 24 h. The effect of Cr(VI) on each culture was recorded as OD_{600} after 24 h, and compared with control [without Cr(VI)], we calculate the inhibition rate of each strain in 5 and 10 mg/L of Cr(VI) treatments. In addition, we determine Cr(VI) concentration in supernatant of all treatments and calculate the Cr(VI) reduction rates of each strain. For Cr determination, after samples were treated by Cr(VI) for 24 h, the supernatant of samples was obtained by the centrifugation at 4,000 rpm for 10 min and was passed through a 0.22-μm filter. Cr was analyzed by atomic absorption spectrometry (ZEEnit700® P, Analytik Jena AG, Germany). About 1 ml aliquots of medium were passed through 0.22-μm filters, and 1,000 μl of 1,5-diphenylcarbazide (0.5 g in 100 ml absolute ethanol and 400 ml 3.6 N H_2SO_4) was added. The violet complex formed was analyzed at 540 nm using a UV–vis spectrophotometer (UV2450, Shimadzu Business Systems Corporation, Japan). The percentage of Cr (VI) reduction was calculated using the following formulas:

$$C_{PR} = (A_{oCr(VI)} - A_{sCr(VI)})/A_{oCr(VI)} \times 100$$

where C_{PR} is the percentage of Cr(VI) reduction, $A_{oCr(VI)}$ is the original absorbance of the samples which are treated by Cr for 0 h after inoculation with yeast, and $A_{sCr(VI)}$ is the absorbance of the samples which are treated by Cr for 24 h after inoculation with yeast.

Protein Purification and Activities

The *niaD* and *niiA* genes were inserted into vector pET28b, creating plasmid pET28b-*niaD* and pET28b-*niiA*. Plasmids pET28b-*niaD* and pET28b-*niiA* were transformed into *Escherichia coli* (*E. coli*) BL21 and grown aerobically in 100 ml LB medium supplemented with 50 μg ml^{-1} kanamycin at 37°C to OD_{600} = 0.5, at which time 0.3 mm isopropyl β-D-1-thiogalactopyranosid (IPTG) was added, and growth was continued at 37°C for an additional 4 h. The cells were harvested by centrifugation (15 min at 5,000 × *g*), and NR was purified as described previously (Chen J. et al., 2015). Protein purity was confirmed by sodium dodecyl sulfate polyacrylamide gel electrophoresis (SDS-PAGE), and protein concentrations were determined using the Bradford method (Bradford, 1976).

NR and NiR activities were determined at 37°C in an assay mixture containing 5 μm Cr(VI) in 1 ml of 25 mm of Bis-Tris Propane buffer (pH 7.0). Purified NR/NiR (1 μm), 0.2 mM NADPH or NADH, and 25 μm FMN or FAD were added. At 0–160 min, 0.1 ml portions were filtered through 3-kDa cutoff Amicon Ultrafilters (Millipore). Cr(VI), Cr(III), and total Cr in the filtrate were determined referred to Shi et al. (2018).

Statistical Analysis

The data were analyzed using analysis of variance (ANOVA) (SPSS 16.0; SPSS, Inc., Chicago, IL, United States), followed by Tukey's honestly significant difference (HSD) test ($p < 0.05$) to determine the differences between the yeast strains according to each treatment. The data represent the mean ± standard deviation (SD) for four independent replicates.

RESULTS

Cloning of *niaD* and *niiA*

Using the 5′ RACE (**Supplementary Figure 1**) and 3′ RACE (**Supplementary Figure 2**) techniques, we cloned the full-length cDNA sequences of the gene encoding the assimilatory nitrate reductase (NR) (*Pisolithus* sp.1 NR) named *niaD* with 2,932 bp (GenBank accession number: OM220115) and the gene encoding the assimilatory nitrite reductase (NiR) (*Pisolithus* sp.1 NiR) named *niiA* with 3,982 bp (GenBank accession number: OM220116) length (**Figure 1**). The open reading frame (ORF) of *niaD* consisted of 2,754 bp predicted to code 917 amino acids (GenBank accession number: OM339169), and the ORF of *niiA* with 3,468 bp length corresponded to 1,155 amino acids (GenBank accession number: OM339170). The isoelectric point (pI) of *Pisolithus* sp.1 NR and the calculated molecular mass were 6.07 and 102.065 kDa, respectively; the pI of *Pisolithus* sp.1 NiR and the calculated molecular mass were 6.38 and 126.914 kDa, respectively. Based on the amino acid sequences of two proteins, we found 51.4% of hydrophobic

[8]http://npsa-pbil.ibcp.fr/cgi-bin/npsa_automat.pl?page?/NPSA/npsa_htm.html

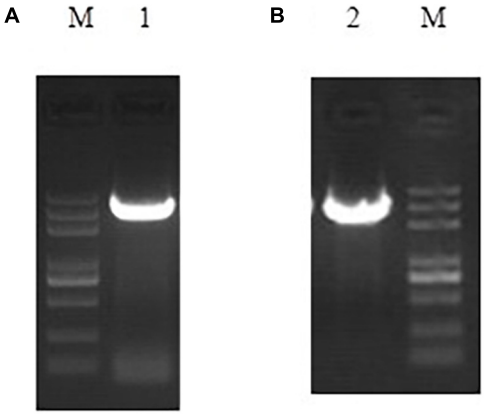

FIGURE 1 | Full-length PCR amplification results of *niiA* **(A)** and *niaD* **(B)**.

and 48.4% of hydrophilic amino acids in the *Pisolithus* sp.1 NR whereas 48.2% of hydrophobic and 51.9% of hydrophilic amino acids in the *Pisolithus* sp.1 NiR. The ExPASy online hydrophobic predications of these two proteins are also shown in **Supplementary Figure 3**. The results from the NCBI Conserved Domain Search further confirmed that *Pisolithus* sp.1 NR and *Pisolithus* sp.1 NiR belong to the PLN02252 and Rieske superfamily, respectively. However, there were no any transmembrane-spanning (TMs) domains found in *Pisolithus* sp.1 NR and *Pisolithus* sp.1 NiR using TMHMM software (**Supplementary Figure 4**). The signal peptide prediction analysis indicated that no signal peptide sequence was observed in *Pisolithus* sp.1 NR or *Pisolithus* sp.1 NiR.

Phylogenetic Analysis of Protein

The deduced *Pisolithus* sp.1 NR proteins were compared with other 18 EMF NRs, and *Pisolithus* sp.1 NiR proteins were compared with other 40 NiRs of EMF (the species name, gene IDs, and accession number are shown in **Supplementary Tables 2**, **3**. A total of two main clades were distinguished (**Supplementary Figure 5A**), one branch for the *Pisolithus* sp.1 NR, *Pisolithus tinctorius* NR and another 16 EMF NRs, and the second branch for the *Coprinopsis cinerea okayama* NR. *Pisolithus* sp.1 NR was closely related to *Pisolithus tinctorius* NR (AGO04408, 100% similarity). For NiR, two main clades were distinguished (**Supplementary Figure 5B**), one branch for the *Pisolithus* sp.1 NiR, *Paxillus ammoniavirescens* NiR and another 15 EMF NiRs, and the second branch for the *Polyporus arcularius* NiR, *Polyporus brumalis* NiR and another 22 EMF NiRs. *Pisolithus* sp.1 NiR was closely related to *Paxillus ammonia virescens* NiR (KAF8843892, 99% similarity).

Multiple Sequence Alignment

The homology comparison results of *Pisolithus* sp.1 NR ORF BlastP showed that the top 18 EMF with the highest homology to the amino acid sequence encoded by *Pisolithus* sp.1 NR are *Pisolithus tinctorius* (AGO04408.1), *Paxillus involutus* (KIJ15906.1), *Suillus tomentosus* (KAG1876842.1), and so on (**Supplementary Figure 6**). After multiple comparisons of the amino acid sequence encoded by *Pisolithus* sp.1 NR with the above-mentioned 18 fungal sequences, it is found that there is high homology between these 19 amino acid sequences, especially in the conserved binding domains that constitute NR, such as molyopterin binding domains, which the homology is the highest (**Supplementary Figure 6**). The above results indicate that the full-length sequence of *niaD* cloned by RACE is the complete sequence of the NR gene.

The homology comparison results of *Pisolithus* sp.1 NiR ORF BlastP showed that the top 36 EMF with the highest homology to the amino acid sequence encoded by *Pisolithus* sp.1 NiR are *Xerocomus badius* (KAF8552377.1), *Gyrodon lividus* (KAF9219484.1), *Paxillus ammoniavirescens* (KAF8843892.1), *Heliocybe sulcata* (TFK51421.1), and so on (**Figure 2**). After multiple comparisons of the amino acid sequence encoded by *Pisolithus* sp.1 NiR with the above-mentioned 36 fungal sequences, it is found that there is high homology between these 37 amino acid sequences. The putative iron-sulfur center [4Fe-4S] and siroheme domains were localized in the predicted *Pisolithus* sp.1 NiR sequence by comparison with known NiRs. CX5CXnGCX3C as the consensus sequence, where the cysteine residues have been proposed to be involved in the binding of the tetranuclear iron-sulfur center and siroheme to the NiR. The 5 amino acids VGTTW separating the very N-terminus cysteines are identical in *P. ammoniavirescens*, *H. sulcata*, *Rhizopogon vinicolor,* and so on. The region around the cysteine consensus sequence is highly conserved among NiRs but poorly conserved between NiRs and sulfite reductase (**Figure 2B**). Regarding the FAD and NAD(P)H-binding domains, the amino acid sequence analyses revealed a common motif sequence GXGXXG compatible with a β sheet-α helix-β sheet folding. This motif has been found two times in the N-termini of NiRs although in *Suillus weaverae*, *Suillus hirtellus*, *Serpula lacrymans* var. *Lacrymans*, *Neolentinus lepideus*, *Gloeophyllum trabeum*, and *Sistotremastrum suecicum*, the Wrst is less conserved (**Figure 2A**).

Functional Complementation Verification

niaD and *niiA* were transformed into the yeast mutant (Δ*ycf1*) using the pYES2 vector to examine their functions of Cr(VI) tolerance and reduction. With the gradually dilution of the yeast cells, the growth of Δ*ycf1*-pYES2, Δ*ycf1*-pYES2-*niaD,* and Δ*ycf1*-pYES2-*niiA* strain decreased in SD-Ura solid medium with different Cr(VI) concentrations (0, 10, 20, and 40 mg/L) (**Figure 3**). Compared with the strongly inhibited growth of *ycf1* yeast cells transformed with the empty pYES2 vector, *niaD* expression recovered the yeast growth in 20 and 40 mg/L Cr(VI) treatments (**Figure 3**).

It was also observed that the mutant strain (Δ*ycf1*) transformed with *niaD* and *niiA* grew well in Cr(VI)-supplemented SD-Ura liquid medium compared to the Δ*ycf1*-pYES2 strain, and 10 mg/L Cr(VI) did not inhibit the growth of Δ*ycf1*-pYES2-*niaD* strain compared with Δ*ycf1*-pYES2 and Δ*ycf1*-pYES2-*niiA* strains (**Figure 4A**). In addition, compared with Δ*ycf1*-pYES2 and Δ*ycf1*-pYES2-*niiA* strain,

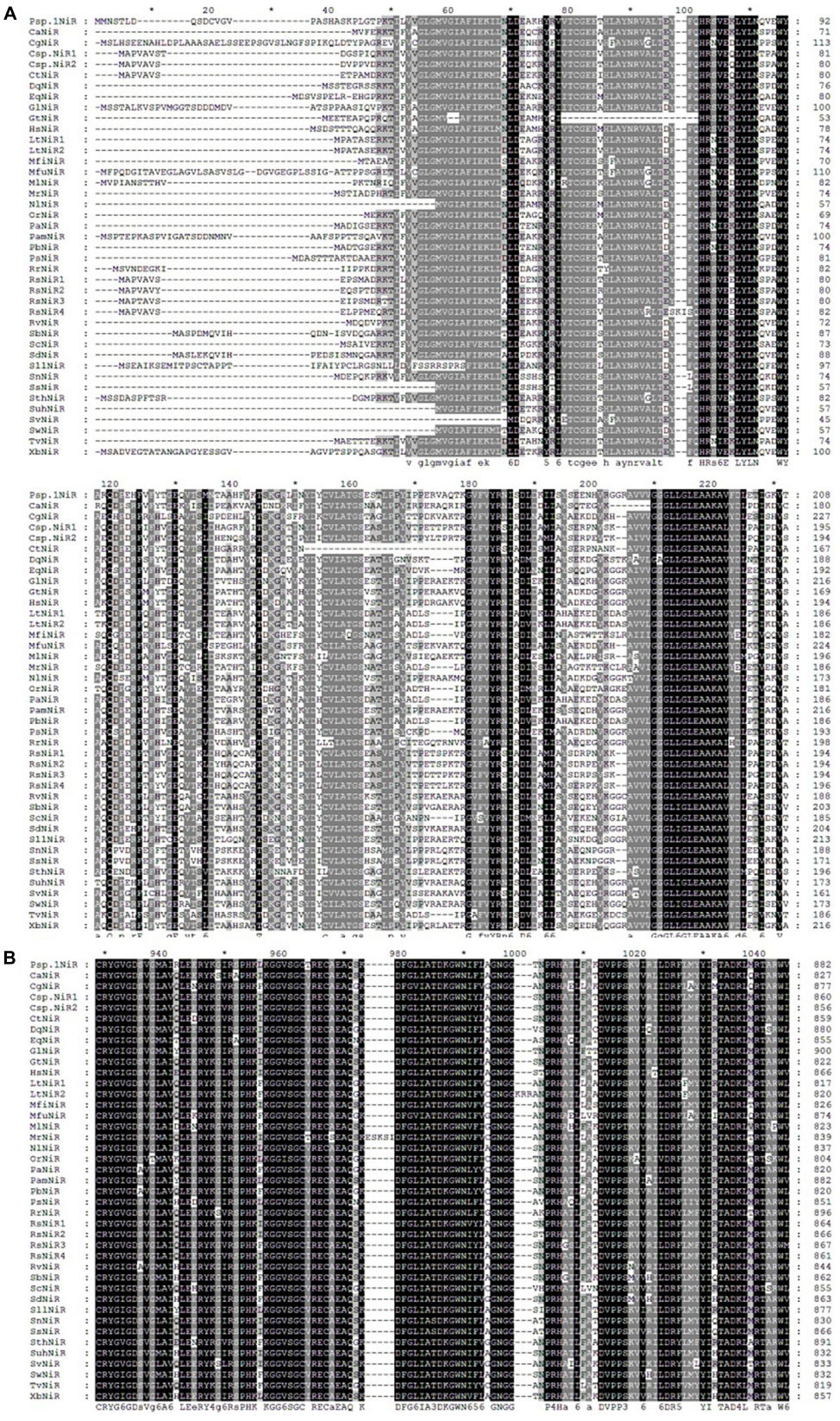

FIGURE 2 | (Continued)

FIGURE 2 | Multiple sequence alignment of the N-terminal part **(A)** and the region corresponding to Fe/S and siroheme domain **(B)** in *niiA* encoded amino acid from *Pisolithus* sp.1 and other EMF. The two signatures, CXXXXXC and CXXXC, that characterize the (Fe/S)-siroheme-binding site are indicated (I, II). The GXGXXG motifs probably involved in nucleotide binding. The two signatures, CXXXXXC and CXXXC, that characterize the (Fe/S)-siroheme-binding site are indicated (I, II). Accession numbers are as follows: *Pisolithus* sp.1 (Pisolithus sp.1NiR); *Cantharellus anzutake* (CaNiR), XP_038913312; *Cortinarius glaucopus* (CgNiR), KAF8804920; *Ceratobasidium* sp. (Csp.NiR1), KAF8599087; *Ceratobasidium* sp. (Csp.NiR2), QRW14243; *Ceratobasidium theobromae* (CtNiR), KAB5593146; *Daedalea quercina* (DqNiR), KZT68487; *Exidia qlandulosa* (EqNiR), KZV93274; *Gyrodon lividus* (GlNiR), KAF9219484; *Gloeophyllum trabeum* (GtNiR), XP_007868164; *Heliocybe sulcata* (HsNiR), TFK51421; *Lentinus tigrinus (*LtNiR1), RPD71067; *Lentinus tigrinus* (LtNiR2), RPD56290; *Marasmius fiardii* (MfiNiR), KAF9267857; *Macrolepiota fuliginosa* (MfuNiR), KAF9446723; *Microbotryum lychnidis-dioicae* (MlNiR), KDE09322; *Moniliophthora roreri* (MrNiR), ESK92732; *Neolentinus lepideus* (NlNiR), KZT30290; *Obba rivulosa* (OrNiR), OCH89826; *Polyporus arcularius* (PaNiR), TFK84168; *Paxillus ammoniavirescens* (PamNiR), KAF8843892; *Polyporus brumalis* (PbNiR), RDX45056; *Punctularia strigosozonata* (PsNiR), XP_007380627; *Ramaria rubella* (RrNiR), KAF8587207; *Rhizoctonia solani* (RsNiR1), QRW27772; *Rhizoctonia solani* (RsNiR2), CEL51481; *Rhizoctonia solani* (RsNR3), CUA70758; *Rhizoctonia solani* (RsNR4), EUC59403; *Rhizopogon vinicolor* (RvNiR), OAX35873; *Suillus brevipes* (SbNiR), KAG3229875; *Sparassis crispa* (ScNiR), XP_027609679; *Suillus decipiens* (SdNiR), KAG2067852; *Suillus hirtellus* (SuhNiR), KAG2059534; *Stereum hirsutum* (SthNiR), XP_007309002; *Serpula lacrymans* var. *lacrymans* (SllNiR), XP_007318270; *Sistotremastrum niveocremeum* (SnNiR), KZS88669; *Sistotremastrum suecicum* (SsNiR), KZT38055; *Serendipita vermifera* (SvNiR), PVF95350; *Suillus weaverae* (SwNiR), KAG2343131; *Trametes versicolor* (TvNiR), XP_008033405; *Xerocomus badius* (XbNiR), KAF8552377.

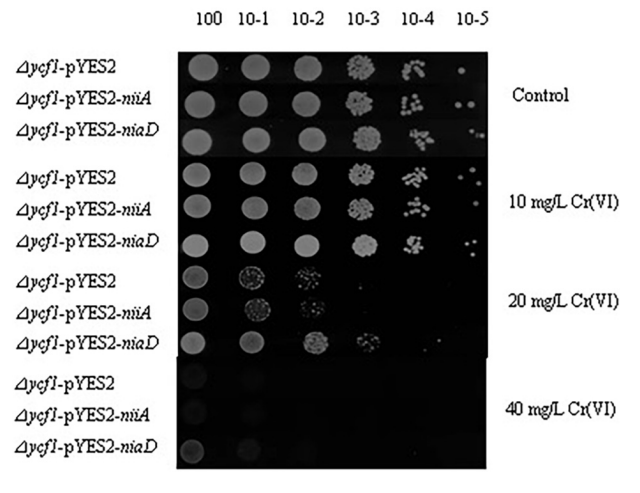

FIGURE 3 | Functional complementation of Cr(VI)-sensitive yeast mutants on selective media. Mutant strains (Δ*ycf1*) were transformed with empty vector pYES2, pYES2-*niiA* or pYES2-*niaD*. Diluted transformant cultures were spotted on SD-Ura medium with or without metal supplement as indicated.

Δ*ycf1*-pYES2-*niaD* strain also has the highest Cr(VI) reduction ability (**Figure 4B**).

Cr(VI) Reduction by Purified Protein

The purification of *NR* and *NiR* was finished by SDS-PAGE (**Supplementary Figure 7**), **Figure 5** shows that Cr(VI) was fully reduced by NR within 160 min, and Cr(VI) was 25% reduced by NiR at the same time.

DISCUSSION

The NR that exists in EMF is an enzyme composed of Mo element, flavin, and heme subunits. It participates in the assimilation of nitrate and provides N nutrition for mycorrhizal symbionts (Okiobe et al., 2019). The NR genes has been found in some EMF fungi, such as *Hebeloma* sp., *Tuber borchii*, *Laccaria bicolor,* and *Wilcoxina mikolae* var. m*ikolae,* which prove that NR plays an indispensable role in the establishment of EMF-plant symbiosis (Guescini et al., 2003).

In our study, the full-length cDNA of the NR and the NiR gene was cloned from the *Pisolithus* sp.1 using the 5′ and 3′ RACE approach, named *Pisolithus* sp.1 NR and *Pisolithus* sp.1 NiR, respectively. By comparing the amino acid sequence of NR with other 18 species of fungi, it is found that the homology between *Pisolithus* sp.1 NR and *Pisolithus tinctorius* NR reached up to 100%; the homology between *Pisolithus* sp.1 NiR and *Paxillus ammonia* virescens NiR up to 99%. *Pisolithus* sp.1 like some fungi, especially EMF fungi, has a conserved NR gene. Previous studies have proved that *Pisolithus* sp.1 can increase the N absorption of *Pinus thunbergii* (Shi et al., 2019). However, we did not find any transmembrane-spanning (TMs) domains and signal peptides in *Pisolithus* sp.1 NR and *Pisolithus* sp.1 NiR (**Supplementary Figure 4**), and they should belong to assimilatory enzymes.

The formation process of ectomycorrhiza involves the expression of genes related to symbiosis between plants and EMF. The expression of these genes at a specific time and space will cause the morphological and physiological changes, and this process plays an important role in the formation and coordinated development of mutually beneficial symbiosis (Quéré et al., 2005; Willmann et al., 2014).

On the other hand, *niaD* is the first NR gene to be identified and found in EMF with Cr(VI) tolerance and reduction function in our study. Some previous studies have shown that some NR or NiR have Cr(VI) reduction function in bacteria (Bencheikh-Latmani et al., 2005; Chai et al., 2018). For example, such NR of *Vibrio harveyi* KCTC 2720 and NfsA of *E. coli* have a facultative function to reduce Cr(VI) (Pradhan et al., 2016). It suggests that *niaD* is potentially a novel Cr(VI) reductase in EMF. In our previous study, the relative transcription of *niaD* significantly increased after *Pisolithus* sp.1 was treated by Cr(VI), which indicated that *niaD* was an Cr(VI)-inducible reducing enzyme (Shi et al., 2020).

Chromate reductase includes Class I and Class II chromate reductase, and Class I chromate reductases are efficient chromate and quinone reducers, but have no activity with nitro compounds, whereas the Class II chromate reductase enzymes all reduce quinones and nitro compounds effectively, but vary in their ability to transform chromate (Pradhan et al., 2016). The Class I enzymes reduce chromate at a greater rate than the Class II enzymes (Park et al., 2002). As shown in **Figure 6**,

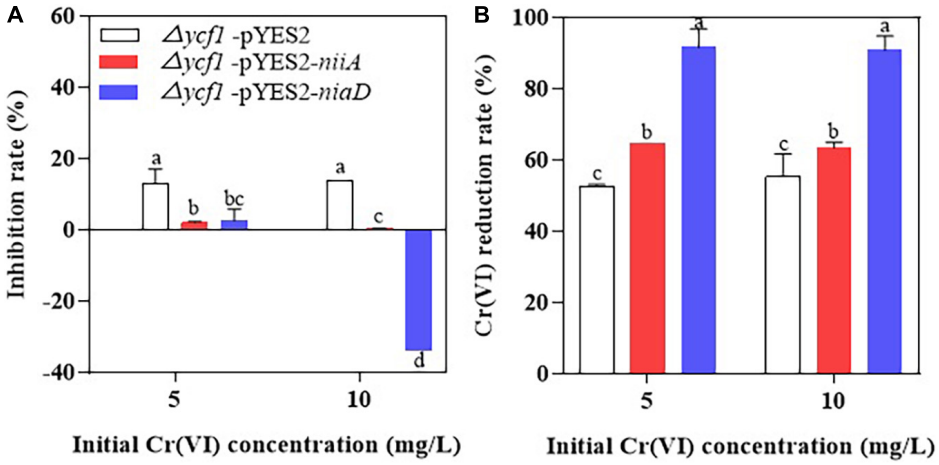

FIGURE 4 | The inhibition rate of Cr(VI) on yeast growth **(A)** and Cr(VI) reduction rates of yeasts **(B)**. Mutant strains (Δ*ycf1*) were transformed with empty vector pYES2, pYES2-*niiA* or pYES2-*niaD* in SD-Ura liquid medium with or without metal supplementation.

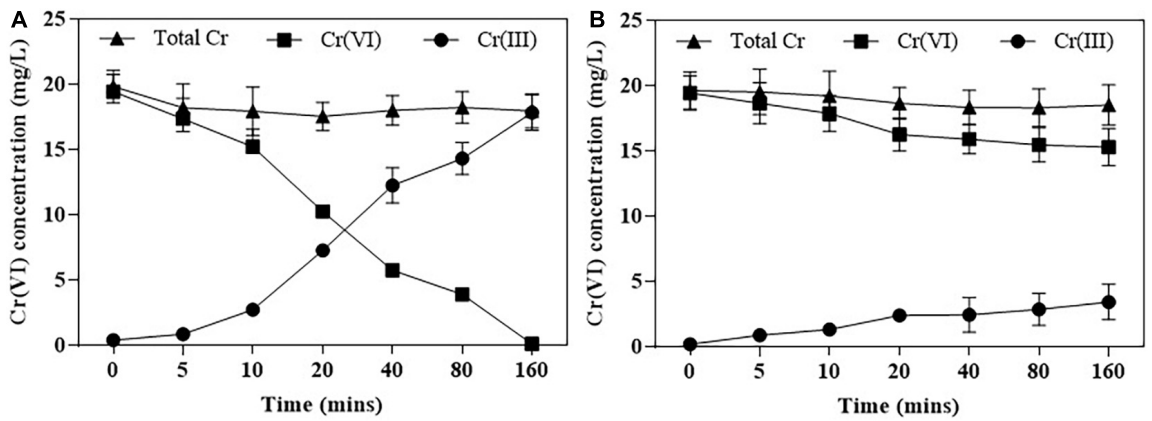

FIGURE 5 | Cr(VI) reduction by purified NR **(A)** and NiR **(B)**. Cr(VI) reduction was assayed in Bis-Tris Propane buffer (pH 7.0). Error bars represent standard deviation (SD) from three independent assays.

Pisolithus sp.1 NR is highly conserved compared with pgr1 which was identified as a Class II chromate reductases (Koósz et al., 2008). The chromate reductases are also classified based on their homology and specificity for reducing Cr(VI). For example, the Class I chromate reductases transfer two electrons from themselves either simultaneously ("tight"; such as YieF) or non-simultaneously ("semi-tight"; such as ChrR) (Ackerley et al., 2004; Thatoi et al., 2014). NitR belongs to Class I chromate reductase and it bears poor homology with NfsA, one of the Class II chromate reductases. Therefore, *Pisolithus* sp.1 NR may share poor homology with Class I chromate reductase due to it belongs to Class II chromate reductase (Chai et al., 2018).

Various groups of oxidoreductase enzymes such as chromate reductase, NR, iron reductase, quinone reductase, hydrogenase, flavin reductase, and NAD(P)H-dependent reductase showing potential toward reduction of chromate have been identified in different microorganisms. In addition, comparative structural analyses of seven well-studied enzymes involved in chromate reduction from Protein Data Bank (PDB) database were categorized either NADPH-dependent FMN reductase or FMN-dependent NR (Pradhan et al., 2016). The FMN- and NADPH-binding sites are critical to the function of the chromate reductases. FMN is firmly anchored to the reductases by several hydrogen bonds and transfer the electron from NADH to the substrate scilicet Cr(VI) (Eswaramoorthy et al., 2012). Hence, FMN-binding site represents the enzyme active site (Matin et al., 2005) and hydrogen bonds between FMN molecules and different monomers possibly play a central role in chromate reductase activity. The NADPH-binding site is also important for enzyme activity, and NAD(P)H provides electrons for Cr(VI) reduction. The FMN- and NADPH-binding

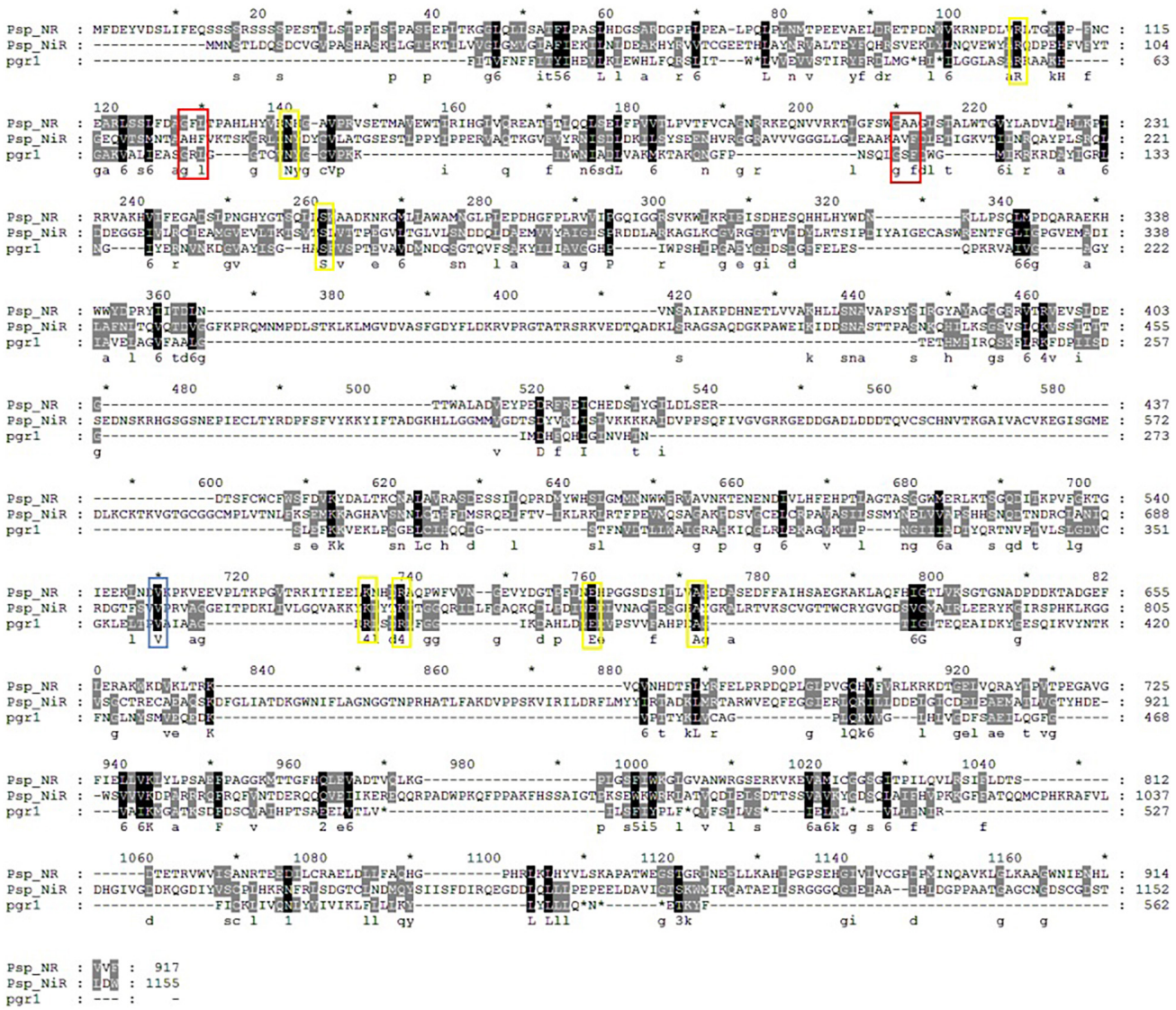

FIGURE 6 | Multiple alignment of *Pisolithus* sp.1 NR, *Pisolithus* sp.1 NiR and the pgr1. The FMN-binding and NADPH-binding sites are labeled with yellow and blue rectangles, respectively, and the sites marked with red rectangles are both FMN- and NADPH-binding sites.

sites of *Pisolithus* sp.1 NR are more conserved with that of pgr1, all of which are identical or conserved substitutions (**Figure 6**). Combined with the results in **Figure 5**, 0.2 mm NADPH and 25 μm FMN were the best cofactor for the reduction of Cr(VI) by *Pisolithus* sp.1. Therefore, *Pisolithus* sp.1 NR is possibly a NADPH-dependent FMN-reductase, which reduces Cr(VI) with the identical electron transport pathway of pgr1.

In conclusion, *niaD* and *niiA* are novel NR and NiR genes in *Pisolithus* sp.1, were cloned, identified, and functionally characterized by 5′ and 3′ RACE, alignment, annotation, phylogenetic tree, yeast mutant complementation analysis, protein purification, and function on Cr(VI) reduction. The open reading frame (ORF) of *niaD* consisted of 2,754 bp predicted to code 917 amino acids, and the ORF of *niiA* with 3,468 bp length corresponded to 1,155 amino acids. *Pisolithus* sp.1 NR and *Pisolithus* sp.1 NiR had no transmembrane-spanning (TMs) domains. *Pisolithus* sp.1 NR is highly conserved compared with pgr1 (chromate reductase in *Schizosaccharomyces pombe*), which was identified as a Class II and NADPH-dependent FMN chromate reductase.

DATA AVAILABILITY STATEMENT

The datasets presented in this study can be found in online repositories. The names of the repository/repositories and accession number(s) can be found in the article/**Supplementary Material**.

AUTHOR CONTRIBUTIONS

LS contributed to the experimental design, conceptualization, data curation, and original draft. BL carried out the experiments and data analysis. XZ performed the data analysis. YB interpreted the data. ZS and JZ contributed to the review, supervision, and conceptualization. YC contributed to the supervision, conceptualization, writing, reviewing, and editing. All authors contributed to the article and approved the submitted version.

FUNDING

This work was supported by the National Natural Science Foundation of China (31901180), the China Agriculture Research System of MOF and MARA, the China Postdoctoral Science Foundation (2019M651845), the Fundamental Research Funds for central Universities of Nanjing Agricultural University (KYQN202061), and the International Postdoctoral Exchange Fellowship Program (2020105).

ACKNOWLEDGMENTS

Thanks for the support of postdoctoral flow station of biology and agricultural resources and environment in Nanjing Agricultural University.

SUPPLEMENTARY MATERIAL

The Supplementary Material for this article can be found online at: https://www.frontiersin.org/articles/10.3389/fmicb.2022.926748/full#supplementary-material

REFERENCES

Ackerley, F. D., Gonzalez, F. C., Park, H. C., and Blake, K. M. (2004). Chromate-reducing properties of soluble flavoproteins from *Pseudomonas putida* and *Escherichia coli*. *Appl. Environ. Microbiol.* 70, 873–882. doi: 10.1128/AEM.70.2.873-882.2004

Aggangan, N. S., and Aggangan, B. J. S. (2012). Selection of ectomycorrhizal fungi and tree species for rehabilitation of Cu mine tailings in the philippines. *J. Environ. Manage.* 15, 59–71.

Ahemad, M. (2014). Bacterial mechanisms for Cr(VI) resistance and reduction: an overview and recent advances. *Folia Microbiol. (Praha)* 59, 321–332. doi: 10.1007/s12223-014-0304-8

Bencheikh-Latmani, R., Williams, S. M., Haucke, L., Criddle, C. S., and Tebo, B. M. (2005). Global transcriptional profiling of *Shewanella oneidensis* MR-1 during Cr(VI) and U(VI) reduction. *Appl. Environ. Microbiol.* 71, 7453–7460. doi: 10.1128/AEM.71.11.7453-7460.2005

Bradford, M. M. (1976). A rapid and sensitive method for the quantitation of microgram quantities of protein utilizing the principle of protein-dye binding. *Anal. Biochem.* 72, 248–254. doi: 10.1006/abio.1976.9999

Canton, G. C., Bertolazi, A. A., Cogo, A. J. D., Eutropio, F. J., Melo, J., de Souza, S. B., et al. (2016). Biochemical andecophysiological responses to manganese stress by ectomycorrhizal fungus *Pisolithus tinctorius* and in association with *Eucalyptus grandis*. *Mycorrhiza* 26, 475–487. doi: 10.1007/s00572-016-0686-3

Chai, L. Y., Ding, C. L., Tang, C. J., Yang, W. C., Yang, Z. H., Wang, Y. Y., et al. (2018). Discerning three novel chromate reduce and transport genes of highly efficient *Pannonibacter phragmitetus* BB: from genome to gene and protein. *Ecotoxicol. Environ. Safe.* 162, 139–146. doi: 10.1016/j.ecoenv.2018.06.090

Chen, J., Bhattacharjee, H., and Rosen, B. P. (2015). ArsH is an organoarsenical oxidase that confers resistance to trivalent forms of the herbicide monosodium methylarsenate and the poultry growth promoter roxarsone. *Mol. Microbiol.* 96, 1042–1052. doi: 10.1111/mmi.12988

Chen, Y. H., Nara, K., Wen, Z. G., Shi, L., Xia, Y., Shen, Z. G., et al. (2015). Growth and photosynthetic responses of ectomycorrhizal pine seedlings exposedto elevated Cu in soils. *Mycorrhiza* 25, 561–571. doi: 10.1007/s00572-015-0629-4

Chovanec, P., Sparacino-Watkins, C., Zhang, N., Basu, P., and Stolz, J. F. (2012). Microbial reduction of chromate in the presence of nitrate by three nitrate respiring organisms. *Front. Microbiol.* 3:416. doi: 10.3389/fmicb.2012.00416

Das, S., Mishra, J., Das, S. K., Pandey, S., Rao, D. S., Chakraborty, A., et al. (2014). Investigation on mechanism of Cr(VI) reduction and removal by *Bacillus amyloliquefaciens*, a novel chromate tolerant bacterium isolated from chromite mine soil. *Chemosphere* 96, 112–121. doi: 10.1016/j.chemosphere.2013.08.080

Dhal, B., Thatoi, H. N., Das, N. N., and Pandey, B. D. (2013). Chemical and microbialremediation of hexavalent chromium from contaminated soil and mining/ metallurgical solid waste: a review. *J. Hazard. Mater.* 25, 272–291. doi: 10.1016/j.jhazmat.2013.01.048

Eswaramoorthy, S., Poulain, S., Hienerwadel, R., Bremond, N., Sylvester, M. D., Zhang, Y. B., et al. (2012). Crystal structure of ChrR—a quinone reductase with the capacity to reduce chromate. *PLoS One* 7:e36017. doi: 10.1371/journal.pone.0036017

Guescini, M., Pierleroni, R., Palma, F., Zeppa, S., Vallorani, L., Potenza, L., et al. (2003). Characterization of the *Tuber borchii* nitrate reductase gene and its role in ectomycorrhizae. *Mol. Genet. Genomics* 269, 807–816. doi: 10.1007/s00438-003-0894-3

Han, R., Geller, J. T., Yang, L., Brodie, E. L., Chakraborty, R., Larsen, J. T., et al. (2010). Physiological and transcriptional studies of Cr(VI) reduction under aerobic and denitrifying conditions by an aquifer-derived pseudomonad. *Environ. Sci. Technol.* 44, 7491–7494. doi: 10.1021/es101152r

Il'ina, T. K., and Khodakova, R. N. (1973). Processes of nitrate reduction by soil microorganisms. *Mikrobiologiia* 42, 475–480.

Jin, P., Chen, Y. Y., Yao, R., Zheng, Z. W., and Du, Q. Z. (2019). New insight into the nitrogen metabolism of simultaneous heterotrophic nitrification-aerobic denitrification bacterium in mRNA expression. *J. Hazard. Mater.* 371, 295–303. doi: 10.1016/j.jhazmat.2019.03.023

Johnston, C. P., and Chrysochoou, M. (2012). Investigation of chromate coordination on ferrihydrite by in situ ATR-FTIR spectroscopy and theoretical frequency calculations. *Environ. Sci. Technol.* 46, 5851–5858. doi: 10.1021/es300660r

Koósz, Z., Gazdag, Z., Miklós, I., Benko, Z., Belágyi, J., Antal, J., et al. (2008). Effects of decreased specific glutathione reductase activity in a chromate-tolerant mutant of *Schizosaccharomyces pombe*. *Folia Microbiol.* 53, 308–314. doi: 10.1007/s12223-008-0048-4

Matin, A., Ackerley, D. F., Lynch, S. V., and Gonzalez, C. F. (2005). ChrR, a soluble quinone reductase of *Pseudomonas putida* that defends against H_2O_2. *J. Biol. Chem.* 280, 22590–22595. doi: 10.1074/jbc.M501654200

Nancharaiah, Y. V., Dodge, C., Venugopalan, V. P., Narasimhan, S. V., and Francis, A. J. (2010). Immobilization of Cr(VI) and its reduction to Cr(III) phosphate by granular biofilms comprising a mixture of microbes. *Appl. Environ. Microb.* 76, 2433–2438. doi: 10.1128/AEM.02792-09

Okiobe, S. T., Augustin, J., Mansour, I., and Veresoglou, S. D. (2019). Disentangling direct and indirect effects of mycorrhiza on nitrous oxide activity and denitrification. *Soil. Biol. Biochem.* 134, 142–151.

Park, C. H., Gonzalez, D., Ackerley, D., Keyhan, M., and Matin, A. (2002). "Molecular engineering of soluble bacterial proteins with chromate reductase activity," in *Remediation and Beneficial Reuse of Contaminated Sediments*, eds M. Pellei, A. Porta, and R. E. Hinchee (Columbus, OH: Batelle Press).

Pena, R., and Polle, A. (2013). Attributing functions to ectomycorrhizal fungal identities in assemblages for nitrogen acquisition under stress. *ISME J.* 8:321. doi: 10.1038/ismej.2013.158

Pradhan, S. K., Singh, N. R., Rath, B. P., and Thatoi, H. (2016). Bacterial chromate reduction: a review of important genomic, proteomic, and bioinformatic analysis. *Crit. Rev. Environ. Sci. Technol.* 46, 1659–1703.

Quéré, A. L., Wright, D. P., Söderström, B. S., Tunlid, A., and Johansson, T. (2005). Global patterns of gene regulation associated with the development of ectomycorrhiza between birch (*Betula pendula* Roth.) and *Paxillus involutus* (Batsch) Fr. *Mol. Plant. Microbe Interact.* 18, 659–673. doi: 10.1094/MPMI-18-0659

Rono, J. K., Wang, L. L., Wu, X. C., Cao, H. W., Zhao, Y. N., Khan, I. U., et al. (2021). Identification of a new function of metallothionein-like gene *OsMT1e* for cadmium detoxification and potential phytoremediation. *Chemosphere* 265:129136. doi: 10.1016/j.chemosphere.2020.129136

Shi, L., Deng, X. P., Yang, Y., Jia, Q. Y., Wang, C. C., Shen, Z. G., et al. (2019). A Cr(VI)-tolerant strain, *Pisolithus* sp.1, with a high accumulation capacity of Cr inmycelium and highly efficient assisting *Pinus thunbergii* for phytoremediation. *Chemosphere* 224, 862–872. doi: 10.1016/j.chemosphere.2019.03.015

Shi, L., Dong, P. C., Song, W. Y., Li, C. X., Lu, H. N., Wen, Z. G., et al. (2020). Comparative transcriptomic analysis reveals novel insights into the response to Cr(VI) exposure in Cr(VI) tolerant ectomycorrhizal fungi *Pisolithus* sp. 1 LS-2017. *Ecotoxicol. Environ. Safe.* 188:109935. doi: 10.1016/j.ecoenv.2019.109935

Shi, L., Xue, J. W., Liu, B. H., Dong, P. C., Wen, Z. G., Shen, Z. G., et al. (2018). Hydrogen ions and organic acids secreted by ectomycorrhizal fungi, *Pisolithus* sp.1, are involved in the efficient removal of hexavalent chromium from waste water. *Ecotoxicol. Environ. Safe.* 161, 430–436. doi: 10.1016/j.ecoenv.2018.06.004

Silva, R. F., Lupatini, M., and Trindade, L. (2013). Copper resistance of different ectomycorrhizal fungi such as *Pisolithus microcarpus*, *Pisolithus* sp., *Scleroderma* sp and *Suillus* sp. *Braz. J. Microbiol.* 44, 613–627. doi: 10.1590/S1517-83822013005000039

Singh, H. P., Mahajan, P., Kaur, S., Batish, D. R., and Kohli, R. K. (2013). Chromium toxicity and tolerance in plants. *Environ. Chem. Lett.* 11, 229–254.

Thatoi, H., Das, S., Mishra, J., Rath, B. P., and Das, N. (2014). Bacterial chromate reductase, a potential enzyme for bioremediation of hexavalent chromium: a review. *J. Environ. Manag.* 146, 383–399. doi: 10.1016/j.jenvman.2014.07.014

Tusnády, G. E., and Simon, I. (2001). The HMMTOP transmembrane topology prediction server. *Bioinformatics* 9, 849–850. doi: 10.1093/bioinformatics/17.9.849

Viamajala, S., Peyton, B. M., Apel, W. A., and Petersen, J. N. (2002). Chromate/nitrite interactions in *Shewanella oneidensis* MR-1: evidence for multiple hexavalent chromium [Cr(VI)] reduction mechanisms dependent on physiological growth conditions. *Biotechnol. Bioeng.* 78, 770–778.

Viti, C., Marchi, E., Decorosi, F., and Giovannetti, L. (2014). Molecular mechanisms of Cr(VI) resistance in bacteria and fungi. *Fems. Microbiol. Rev.* 38, 633–659. doi: 10.1111/1574-6976.12051

Wen, Z. G., Shi, L., Tang, Y. Z., Shen, Z. G., Xia, Y., and Chen, Y. H. (2017). Effects of *Pisolithus tinctorius* and *Cenococcum geophilum* inoculation on pine in copper-contaminated soil to enhance phytoremediation. *Int. J. Phytoremediat.* 19, 387–394. doi: 10.1080/15226514.2016.1244155

Willmann, A., Thomfohrde, S., Haensch, R., and Nehls, U. (2014). The poplar *NRT2* gene family of high affinity nitrate importers: impact of nitrogen nutrition and ectomycorrhiza formation. *Environ. Exper. Bot.* 108, 79–88.

Yu, X. A., Jiang, Y. M., Huang, H. Y., Shi, J. J., Wu, K. J., Zhang, P. Y., et al. (2016). Simultaneous aerobic denitrification and Cr(VI) reduction by *Pseudomonas brassicacearum* LZ-4 in wastewater. *Bioresour. Technol.* 21, 121–129. doi: 10.1016/j.biortech.2016.09.037

Conflict of Interest: The authors declare that the research was conducted in the absence of any commercial or financial relationships that could be construed as a potential conflict of interest.

Publisher's Note: All claims expressed in this article are solely those of the authors and do not necessarily represent those of their affiliated organizations, or those of the publisher, the editors and the reviewers. Any product that may be evaluated in this article, or claim that may be made by its manufacturer, is not guaranteed or endorsed by the publisher.

frontiers | Frontiers in Microbiology

TYPE Original Research
PUBLISHED 29 September 2022
DOI 10.3389/fmicb.2022.907557

OPEN ACCESS

EDITED BY
Pablo Cornejo,
University of La Frontera, Chile

REVIEWED BY
Estéfani García Ríos,
Instituto de Salud Carlos III (ISCIII), Spain
Josef Trögl,
Jan Evangelista Purkyně University in Ústí nad Labem, Czechia
Yunus Effendi,
Leibniz University Hannover, Germany

*CORRESPONDENCE
Daniel González-Reguero
daniel.gonzalezreguero@ceu.es
Pedro A. Jiménez
pedro.jimenezgomez@ceu.es

†These authors have contributed equally to this work

SPECIALTY SECTION
This article was submitted to Terrestrial Microbiology, a section of the journal Frontiers in Microbiology

RECEIVED 29 March 2022
ACCEPTED 12 September 2022
PUBLISHED 29 September 2022

CITATION
González-Reguero D, Robas-Mora M, Probanza A and Jiménez PA (2022) Evaluation of the oxidative stress alleviation in *Lupinus albus* var. orden Dorado by the inoculation of four plant growth-promoting bacteria and their mixtures in mercury-polluted soils. *Front. Microbiol.* 13:907557. doi: 10.3389/fmicb.2022.907557

Evaluation of the oxidative stress alleviation in *Lupinus albus* var. orden Dorado by the inoculation of four plant growth-promoting bacteria and their mixtures in mercury-polluted soils

Daniel González-Reguero*†, Marina Robas-Mora†, Agustín Probanza and Pedro A. Jiménez*†

Department of Pharmaceutical Science and Health, San Pablo University, CEU Universities, Boadilla del Monte, Spain

Mercury (Hg) pollution is a serious environmental and public health problem. Hg has the ability to biomagnify through the trophic chain and generate various pathologies in humans. The exposure of plants to Hg affects normal plant growth and its stress levels, producing oxidative cell damage. Root inoculation with plant growth-promoting bacteria (PGPB) can help reduce the absorption of Hg, minimizing the harmful effects of this metal in the plant. This study evaluates the phytoprotective capacity of four bacterial strains selected for their PGPB capabilities, quantified by the calculation of the biomercuroremediator suitability index (IIBMR), and their consortia, in the *Lupinus albus* var. orden Dorado. The oxidative stress modulating capacity in the inoculated plant was analyzed by measuring the activity of the enzymes catalase (CAT), superoxide dismutase (SOD), ascorbate peroxidase (APX), and glutathione reductase (GR). In turn, the phytoprotective capacity of these PGPBs against the bioaccumulation of Hg was studied in plants grown in soils highly contaminated by Hg vs. soils in the absence of Hg contamination. The results of the oxidative stress alleviation and Hg bioaccumulation were compared with the biometric data of *Lupinus albus* var. orden Dorado previously obtained under the same soil conditions of Hg concentration. The results show that the biological behavior of plants (biometrics, bioaccumulation of Hg, and activity of regulatory enzymes of reactive oxygen species [ROS]) is significantly improved by the inoculation of strains B1 (*Pseudomonas moraviensis*) and B2 (*Pseudomonas baetica*), as well as their corresponding consortium (CS5).

In light of the conclusions of this work, the use of these strains, as well as their consortium, is postulated as good candidates for their subsequent use in phytostimulation and phytoprotection processes in areas contaminated with Hg.

KEYWORDS

heavy metal, reactive oxygen species (ROS), catalase (CAT), superoxide dismutase (SOD), ascorbate peroxidase (APX), glutathione reductase (GR), phytoprotection

Introduction

Heavy metal pollution is an environmental threat that affects all types of living organisms, including plants, animals, and humans. Particularly, mercury (Hg) is one of the most polluting heavy metals. Even at relatively low concentrations, it has the ability to bioaccumulate and transmit through the food chain (Bjørklund et al., 2019). The accumulation of Hg can lead to pathologies that affect the central nervous system, one of the most important being Minamata syndrome (Gil-Hernández et al., 2020; Marumoto et al., 2020).

The presence of Hg at low concentrations is widely described in numerous ecosystems. Exceptionally, environments with extremely high concentrations of this heavy metal have also been described, such as those detected in the mining region of Almadén (>8889 μg/g de Hg) (US Environmental Protection Agency, 2011). The presence of this heavy metal and other polluting substances can affect plant development (Kim et al., 2017; Loix et al., 2017; Sachdev et al., 2021).

One way to evaluate the effects of Hg pollution on plant development is by studying its response to this abiotic stress. To do this, plants synthesize antioxidant enzymes that fight reactive forms of oxygen (ROS). ROS accumulation alters the metabolic balance and physiology of the plant. The main types of ROS are hydrogen peroxide (H_2O_2), hydroxyl radicals (−HO), oxygen singlet ($^1O_2$), and superoxide anion (O^-_2). Its cytoplasmic accumulation induces high oxidative stress and can produce harmful effects on the cell. To mitigate these effects, detoxifying mechanisms are expressed. However, when antioxidant processes and detoxification mechanisms are not able to eliminate excess ROS, oxidative stress harms the plant (Loix et al., 2017). It is proven that Hg induces oxidative stress causing lipid peroxidation, enzymatic inactivation, DNA and membrane damage (Cargnelutti et al., 2006; Tamizselvi and Napoleon, 2022), inhibits photosynthesis, transpiration, and nutrient transport in plants (Cargnelutti et al., 2006; Zhou et al., 2007; Ajitha et al., 2021). Its effects can even lead to the premature death of the plant (Ercal et al., 2001). The accumulation of these reactive species in cells can be reduced by activating different enzyme systems, including catalase activities (CAT), superoxide dismutase (SOD), ascorbate peroxidase (APX), and glutathione reductase (GR) (Loix et al., 2017; Sachdev et al., 2021).

The use of plant growth-promoting bacteria (PGPB) in soils contaminated with Hg has traditionally focused on the phytoextraction of this metal, as well as on the direct promotion of plant growth (Gontia-Mishra et al., 2016; Mariano et al., 2020; González et al., 2021a). These bacteria have also been used to improve the resistance of plants against different situations of abiotic stress such as salinity or desiccation (Ansari et al., 2021; Ha-Tran et al., 2021; Khalilpour et al., 2021; Ali et al., 2022), as well as the oxidative stress produced by Hg (Cho and Park, 2000; Cargnelutti et al., 2006; Ajitha et al., 2021; Quiñones et al., 2021; Çavuşoğlu et al., 2022). To alleviate the harmful effect of pollutants, plants rely heavily on bacteria present in their rhizospheres.

The present work studies the effect of the inoculation of four PGPB strains and their combination in consortia formed by pairs, on the oxidative stress of *Lupinus albus* var. orden Dorado grown in different growing matrixes with the presence of Hg. Likewise, the phytoprotective effect of PGPBs that manifest the best results in the reduction of oxidative stress is studied. As an indicator, we use the concentration of Hg accumulated in plants. Additionally, we relate these variables to biometrics and the activity of ROS-regulating enzymes.

Materials and methods

Bacterial strains and mixtures

The isolates used in this study come from the free soil and rhizosphere of plants that grow naturally on plot 6 of the mining district of Almadén in Ciudad Real, Spain (Millán et al., 2007). The strains were selected based on their Biomercuroremediator Suitability Index values (BRMSI) (Robas et al., 2021), which evaluates PGPB activities and their tolerance to Hg. The tolerance to Hg is assessed using the minimum bactericidal concentration (MBC) and the PGP activities are as follows: production of auxin (3-indoleacetic acid: IAA), presence of the enzyme 1-animociclopropane-1-carboxylate decarboxylase

(ACCd), production of siderophores (SIDs), and the solubilizing capacity of phosphates. The BMRSI is calculated using the following formula, where 1 and 0 for the ACCd and PO_4^{-3} indicate presence or absence:

$$\text{BRMSI} = [\text{IAA } (\mu g\ mL^{-1}) + \text{ACCd } (1/0) + \text{SID (cm)} + PO_4^{-3}\ (1/0)] + [\text{MBC Hg } (\mu g\ mL^{-1})]$$

The PGPB capacity in the presence of Hg of the four bacterial isolates (**Table 1**) was analyzed by González et al. (2021b) (BRMSI **Supplementary Table 1**). The activity of the four strains was tested, as well as the combination consortium in pairs (**Table 2**).

The results of the biometrics of *Lupinus albus* var. orden Dorado inoculated with these PGPB and their respective consortia are shown in **Supplementary Table 2**. In all the experiments carried out, "control" means without inoculum.

The four bacteria isolates were subjected to the mutual compatibility test by cross streak method (**Supplementary Figure 1**) in standard method agar plates (SMA, Pronadisa®, Madrid, Spain). No inhibition was observed on the cross point in any of the combinations, which indicate the compatibility among the isolates.

Tested plants

Lupinus albus var. orden Dorado seeds were used from the seed bank of the Technological and Scientific Research Centre of Extremadura.

Growing matrixes

Four types of growing matrixes were used: to free soil from the mining district of Almadén and sterile vermiculite. The characteristics of the different growing matrixes are as follows:

- Contaminated soil, high concentration of Hg ("Soil +Hg"), from "Plot 6" of the mining district of Almadén (**Table 3**).
- Control soil with low Hg concentration ("Soil −Hg"), obtained from "Plot 2" of the mining district of Almadén. The concentration of soluble and interchangeable Hg in this plot is low enough to be considered negligible (**Table 3**).
- Vermiculite without Hg ("Vermiculite −Hg"): vermiculite is an inert substrate with neutral pH commonly used in hydroponic crops.
- Vermiculite was added with a solution of 8 mg/kg of $HgCl_2$ (concentration of Hg analogous to that found in the soluble fraction of the plot "Plot 6") ("Vermiculite +Hg").

Seed pre-germination

As a preliminary step, the seeds were soaked in water at 4°C for 24 h. The surface was sterilized with three washes of 70% ethanol for 30 s (Abdel Latef et al., 2017). Trays were used with sterile vermiculite and watered with sterile water to field capacity. The seeds were then sown and kept in darkness for 72 h at 25°C. Seeds with an emerged radicle of 3 ± 0.2 cm were selected for the study.

Sowing conditions and inoculation with the strains and mixtures

Sterile forest trays were used (Plásticos Solanas S.L., Zaragoza, España), each of them composed of 12 alveoli of 18 cm in height, with a capacity of 300 cm^3, and a light of 5.3 cm × 5.3 cm. Eleven trays were used for each type of growing matrix. To avoid cross-contamination, four pre-germinated seeds were sown in each alveolus. In each tray, a single bacterial strain (or consortium) and/or control was inoculated, in such a way that 48 seeds were tested for each condition.

A bacterial suspension in 0.45% saline was performed and the inoculum density was adjusted to 0.5 McFarland. Each seed was inoculated with 1 ml of the suspension. To the control, seeds were added to 1 ml of 0.45% saline per seed without bacterial suspension.

Plant growth conditions

A plant growth chamber (phytotron) equipped with white and yellow light with a photoperiod of 11 h of light was used (light intensity: 505 $\mu mol\ m^{-2}\ s^{-1}$, temperature stable at 25 ± 3°C). Irrigation was carried out every 48 h by capillarity with sterile water, with an experimental volume of 350 mL/tray (12 alveoli).

TABLE 1 Bacterial isolates according to their BMRSI in the presence of Hg (González et al., 2021b).

Strain	$HgCl_2$ tolerance(μg/mL)	BMRSI	Strain origin	16S rRNA identification
A1	140	6.54	*Avena sativa*	*Brevibacterium frigoritolerans*
A2	140	7.30	*BS*	*Bacillus toyonensis*
B1	140	7.20	*BS*	*Pseudomonas moraviensis*
B2	140	6.92	*Avena sativa*	*Pseudomonas baetica*

TABLE 2 Consortia formed to screen the strains in Table 1.

	CS1	CS2	CS3	CS4	CS5	CS6
Strains	A1 + B1	A1 + A2	A1 + B2	B1 + A2	B1 + B2	A2 + B2

TABLE 3 Hg speciation on study soils (Millán et al., 2007).

Soil	Total Hg (mg/Kg)	Soluble Hg (mg/Kg)	Exchangeable Hg (mg/Kg)
Plot 6 (Soil +Hg)	1710	0.609	7.3
Plot 2 (Soil −Hg)	5.03	0.0417	0.285

Harvest

Twenty-one days after seeding, the plants were harvested. To carry out the enzymatic measurements, six replicas were used for each treatment. Each replica was formed by a *mixture* of two plants (one plant per alveolus) until reaching 3 g. Four enzymatic measures related to protection against oxidative stress in plants were performed. The enzymatic activities tested were superoxide dismutase (SOD), catalase (CAT), ascorbate peroxidase (APX), and glutathione reductase (GR).

To study the concentration of accumulated Hg, three replicates were taken per treatment of each growing matrix. Each sample consists of 12 plants (three plants per alveolus) up to 25 g per sample. The analysis was only carried out in those treatments with greater statistical significance.

Antioxidative defense enzymes

The enzymes were extracted at 4°C starting from 1 g of fresh sample per replica, with a mortar and using 50 mg polyvinylpolypyrrolidone (PVPP) and 10 ml of the following medium: 50 mM of K-phosphate buffer (pH 7.8) with 0.1 mM EDTA (for SOD, CAT, and APX). The same medium, supplemented with 10 Mm of β-mercaptoethanol was used for GR.

Superoxide dismutase activity

The SOD activity was measured based on the ability of SOD to inhibit the reduction of tetrazoyl nitro-blue (NBT) by photochemically generated superoxide radicals. A SOD unit is defined as the amount of enzyme needed to inhibit the NBT reduction rate by 50% at 25°C (Burd et al., 2000).

Catalase activity

The method of Aebi (1984) was carried out. H_2O_2 consumption was monitored for 1 min at 240 nm. This was carried out by mixing 50 mM potassium phosphate buffer with 10 mM of H_2O_2 and 100 μL of the extract.

Ascorbate peroxidase activity

The reaction was measured in a total volume of 1 mL that contains 80 nM of potassium phosphate buffer, 2.5 mM H_2O_2, and 1M sodium ascorbate. To determine the oxidation ratio of ascorbate, H_2O_2 was added to begin the reaction and the reduction of absorbances was measured for 1min at 290 nm (Amako et al., 1994).

Glutathione reductase activity

Glutathione reductase activity was estimated spectrophotometrically, according to the method of Carlberg and Mannervik (1985) at 25°C and 340 nm. The reaction mixture contained 50 mM of buffer Tris–$MgCl_2$, 3 mM, 1 mM of GSSG, 50 μl of enzyme, and 0.3 mM NADPH, which were added to initiate the reaction. The activity was calculated with the initial rate of the reaction and the molar extinction coefficient of NADPH (ε_{340} = 6.22 mM−1 cm^{-1}).

Analysis of Hg content in plant

The root and aerial fraction of each replica was dried in dry heat furnaces at 60°C for 24 h. It was sprayed and each fraction was digested separately in the acidic medium (HNO_3/HCl 2/0.5% weight/volume) under pressure for the determination of trace elements according to the regulations UNE-EN 13805. The digest was analyzed by mass spectrometry with inductively coupled plasma (ICP-MS).

By using a calibration curve, a relationship between the concentration of the pattern (μg L^{-1} or mg L^{-1}) and signal (ICP-MS) was established for each of the elements. The value of the element signal in the 12 samples is interpolated on the calibration line resulting in the total concentration of the element in the sample.

The values of the Hg pattern to establish the calibration line were as follows, expressed in μg/L: 0.00; 0.05; 0.10; 0.50; 1.00; 5.00; 10.00. Expression in mg kg^{-1} from μg L^{-1}:

$$Cf\left(\frac{\mu g}{Kg}\right) = X\left(\frac{\mu g}{L}\right) \cdot D \cdot \frac{V\,(mL)}{W\,(g)} \cdot 10^{-3}$$

where Cf (mg kg^{-1}) is the sample metal content, X (μg L^{-1}) corresponds to the interpolated experimental value or the experimental value extrapolated from the standard addition, D is the dilution performed for determination, dilution factor, V (mL) corresponds to the flask volume, and W(g) to the sample weight.

Statistical analysis

For statistical analysis, SPSS v.27.0 software was used (Version 27.0 IBM Corp, Armonk, NY, USA). The Kolmogorov–Smirnov test was performed to check the normality of all

variables. Subsequently, an ANOVA of a Kruskal–Wallis factor was performed. For the statistical analysis of the total Hg concentration accumulated in the plant, the normality of the sample data was verified using the Shapiro–Wilk test. An ANOVA was performed to determine the existence of significant differences (p-value $\leq$ 0.05). Next, a *post hoc* analysis of less significance differences (LSDs) was performed with the aim of evaluating whether the differences in Hg concentration in the plant are significant. "Substrate with Hg" is considered to be the joint analysis of the data of vermiculite supplemented with Hg and soil with a high concentration of Hg. The joint analysis of the data for vermiculite without Hg and soil without Hg is considered "substrate without Hg."

A principal component analysis (PCA) was performed starting with the 3D projection of the load factors. Next, an analysis was elaborated with the biometric data (**Supplementary Table 2**; González et al., 2021a), the concentration of Hg in the plant, and the results of the ROS enzymatic activity. All the statistical differences refer to the comparison of the variables that the plants manifest according to their inocula against their respective non-inoculated controls.

Results

Antioxidative defense enzymes analysis

Kruskal–Wallis ANOVA revealed that plants grown with the different inocula in the substrates without Hg showed no significant differences in the enzyme activity produced in response to oxidative stress. In contrast, in plants inoculated with strains B1 (*Pseudomonas moraviensis*) and B2 (*Pseudomonas baetica*), as well as their respective CS5 consortium, the differences in the activity of the four enzymes were significantly lower (p-value $\leq$ 0.001) when they were grown in soils with high levels of Hg.

Figure 1 shows the Kruskal–Wallis analysis and the comparison of means of the enzymes CAT (**Figure 1A**), SOD (**Figure 1B**), APX (**Figure 1C**), and GR (**Figure 1D**). **Figures 1A–D** shows the behavior of the activity of ROS-regulating enzymes of strains B1, B2, and their respective consortium (CS5). The CS6 consortium (formed by strains A2 and B2) is able to induce a significant reduction in the activity of the SOD enzyme by jointly analyzing substrates with high Hg concentration (**Figure 1B**).

Figure 2 shows the results of the enzymatic activities of plants subjected to different bacterial inoculums, comparing the behavior in the presence of Hg vs. the absence of Hg. We can observe that the reduction of the activity of the four enzymes in plants inoculated with strains B1 and B2 in soils with Hg reduces their activity to levels similar to those observed in plants grown in substrates in the absence of Hg.

Analysis of Hg content in plant

In order to understand the bioaccumulation of Hg, we proceeded to analyze the samples of plants grown in soils with Hg whose inoculation induced a significantly lower enzymatic activity. Likewise, the data of plants inoculated with the same PGPB and grown in soils in the absence of Hg are collected comparatively (**Table 4**). The ability of *Lupinus albus to* bioaccumulate Hg is observed mainly at the root. In plants inoculated with B1 and the CS5 consortium (B1 + B2), a significant difference in the concentration of Hg in the whole plant (total, aerial, and root) is detected with respect to the control. In the aerial part of the plants subjected to the three treatments, a significant difference in the concentration of Hg with respect to the control in soils with a high concentration of Hg is also observed.

Principal component analysis

In order to discriminate the overall behavior of the plants tested on different growing matrixes with their respective inoculum, a PCA was carried out. **Figure 3** shows the 2D graphs of the load factors on a rotated space of PCA1 vs. PCA2 (**Figure 3A**), and PCA1 vs. PCA3 (**Figure 3B**). The variables are segregated into three groups according to their biological behavior, namely, enzymatic activity, biometrics, and bioaccumulation of Hg. **Table 5** shows that the accumulation of three factors explains the model with accumulative variance greater than 87%.

Figure 4 shows the 2D projected PCA model. It can be observed how the inoculum of bacteria B1 and B2 individually is segregated from the rest of the treatments. This separation corresponds to a greater effect on the decrease in enzymatic activity (ROS), as well as an increase in biometric factors. The main factor in the abscissa axis that determines the behavior of the plant turns out to be the concentration of Hg in the soil. Likewise, the main segregation factor in the ordinate axis is the treatment with an individual inoculum of PGPB B1 and B2. The phytoprotective and plant growth-promoting effects are significantly favorable in plants grown in soils with Hg when inoculated with strains B1 and B2 independently.

Discussion

In the present study, four strains have been used whose PGP activities were tested in media with the presence of Hg vs. the absence of Hg. In the same way, their respective consortia were tested in pairs (González et al., 2021b).

The plant model of (*Lupinus albus*), as well as other legumes (Harzalli Jebara et al., 2017), has phytoextractor capacity (Zornoza et al., 2010; Rocio et al., 2013; Quiñones et al., 2021).

10.3389/fmicb.2022.907557

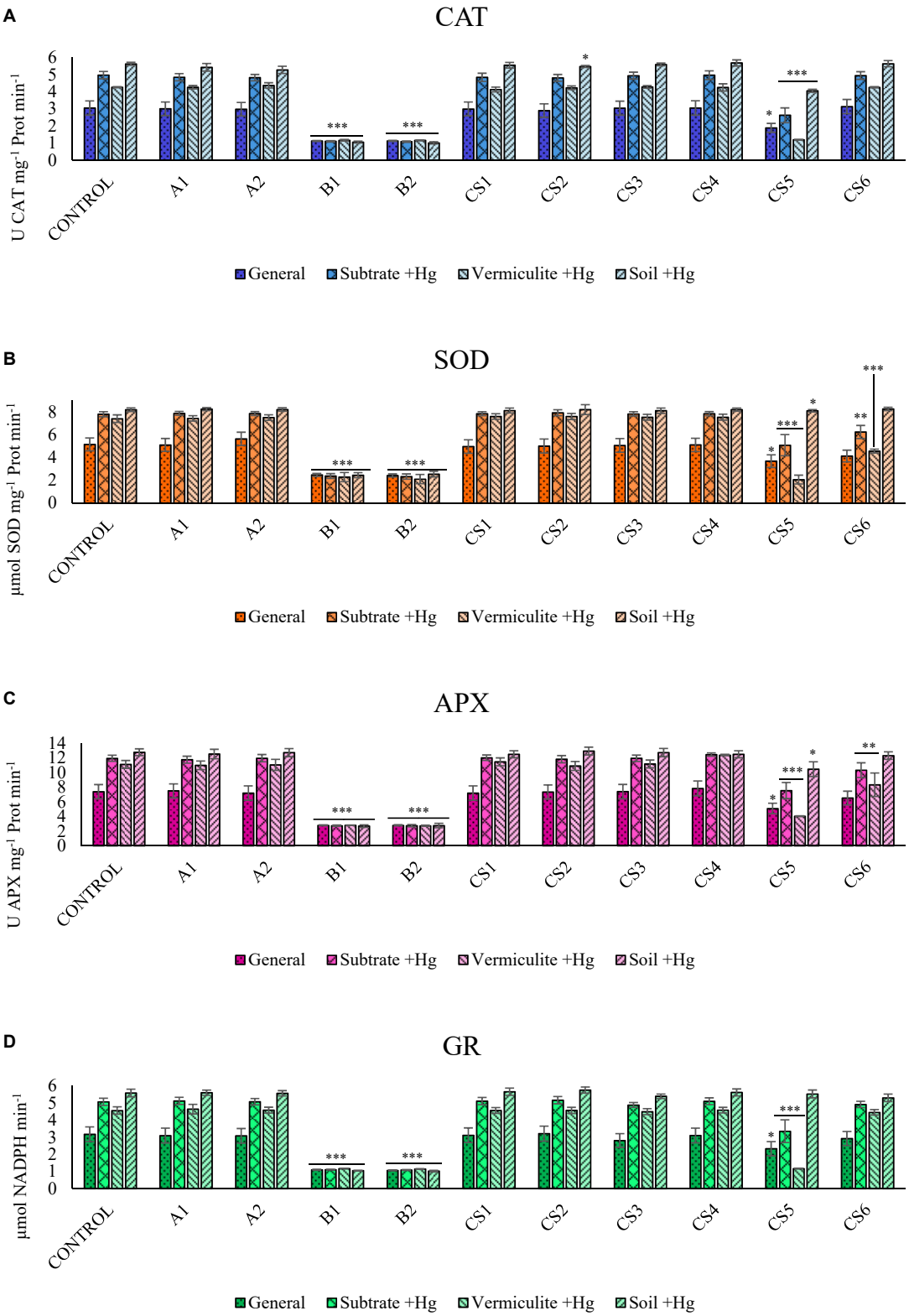

FIGURE 1
Kruskal–Wallis ANOVA results for enzyme activity: CAT **(A)**, SOD **(B)**, APX **(C)**, and GR **(D)**. Data clusters for statistical treatment: "General": dataset for plants grown in all growing matrixes; "Substrates +Hg": dataset for plants in Hg supplemented vermiculite ("Vermiculite +Hg") and soil with high Hg concentration ("Soil +Hg"); "Vermiculite +Hg": dataset for plants in supplemented vermiculite; "Soil +Hg": dataset of plants in soil with Hg high concentration. The bars indicate the standard error. Asterisks indicate the level of significance compared to control; *p-value $\leq$ 0.05, **p-value $\leq$ 0.003, and ***p-value $\leq$ 0.001.

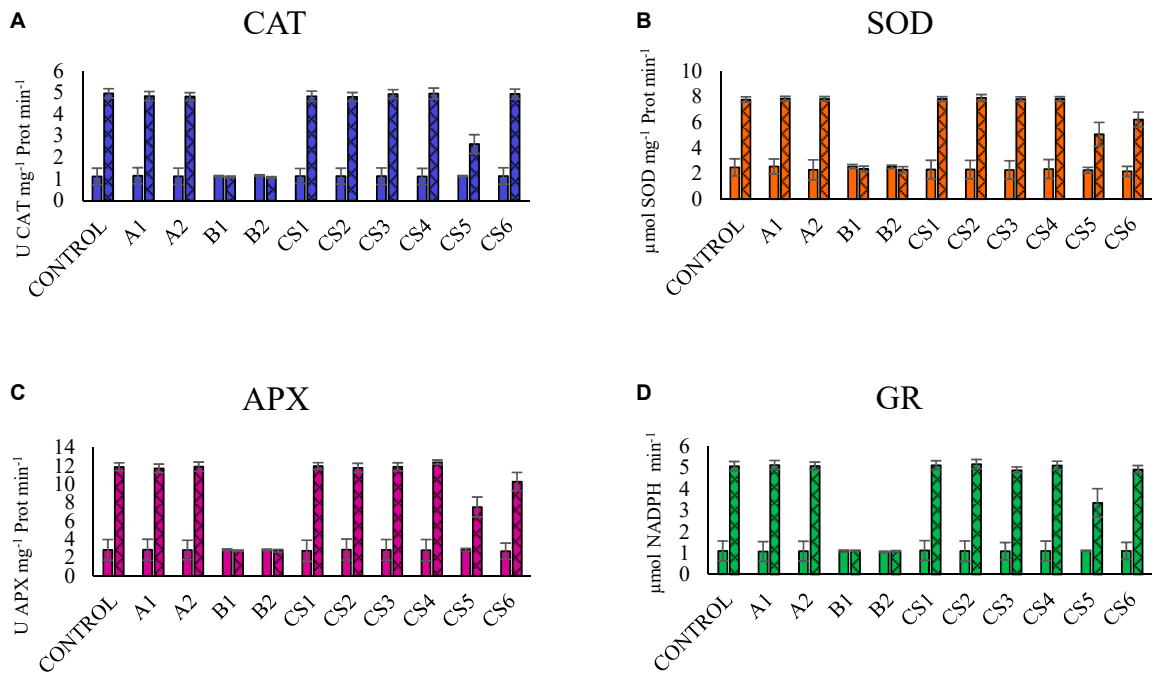

FIGURE 2
Comparison of the results of the enzymatic activity of CAT **(A)**, SOD **(B)**, APX **(C)**, and GR **(D)** in plants grown in the substrate without Hg (smooth) vs. with a high concentration of Hg (double scratching). The bars indicate the standard deviation.

In addition, its ability to absorb and resist the presence of heavy metals, such as Hg, is known. As well as its tolerance to high soil salinity (Rodriguez et al., 2007).

To evaluate the phytoprotective capacity of the strains against Hg, the plants were grown in two different substrates (free soil and vermiculite). Similarly, two types of soil were used to establish the comparison of the presence of Hg vs. the absence of Hg, both from the mining district of Almadén: soil with a high concentration of Hg (soil +Hg), and a control soil with a minimum concentration of Hg (soil −Hg). Vermiculite is a suitable substrate for the study of bacterial inocula in plants

TABLE 4 Comparison of the concentration of Hg in the plants tested in soils with high concentration of Hg.

Treatment	Total (µg/g)	Aerial (µg/g)	Root (µg/g)
CONTROL−	0.00 ± 0.01	0.00 ± 0.01	0.00 ± 0.01
B1−	0.00 ± 0.01	0.00 ± 0.01	0.00 ± 0.01
B2−	0.00 ± 0.01	0.00 ± 0.01	0.00 ± 0.01
CS5−	0.00 ± 0.01	0.00 ± 0.01	0.00 ± 0.01
CONTROL+	10.23 ± 0.03	0.22 ± 0.02	10.01 ± 0.14
B1+	9.52 ± 0.08*	0.16 ± 0.02*	9.36 ± 0.14*
B2+	10.23 ± 0.03	0.15 ± 0.01*	10.07 ± 0.12
CS5+	7.88 ± 0.06*	0.13 ± 0.03*	7.75 ± 0.13*

*Indicates significant differences with respect to their respective controls (p-value ≤ 0.001).

(Rodríguez et al., 2006; González et al., 2021a; Yuan et al., 2022) and avoids the shielding effect that a complex matrix, such as soil, can produce.

Hg induces physiological and metabolic alterations in plants, such as ROS and decreased plant growth (Çavuşoğlu et al., 2022). This article analyzes the negative influence of Hg on these variables (**Figure 2**). Likewise, it is known that the use of PGPB minimizes these effects (Pirzadah et al., 2018), stimulating different defense mechanisms (Loix et al., 2017).

Antioxidative defense enzymes

Oxidative stress caused by Hg has been studied in different plant models (Cho and Park, 2000; Cargnelutti et al., 2006; Çavuşoğlu et al., 2022), observing how this heavy metal increases stress and ROS accumulation. The production of CAT, SOD, APX, and GR enzymes catalyze the degradation of H_20_2, HO^-, $^1O_2$, and O^-_2. Therefore, enzymatic activity is interpreted as a protective response against ROS, whose function is induced by the effect of Hg. The increase in CAT and SOD has been studied as a marker of oxidative stress against heavy metals in plants without a bacterial inoculum (Macar et al., 2020; Çavuşoğlu et al., 2022). In the present study, it was observed that the activity of these enzymes is significantly higher in plants grown with Hg vs. without Hg (**Figure 2**). This effect has also been observed by other authors when confronting plants with other metals, such

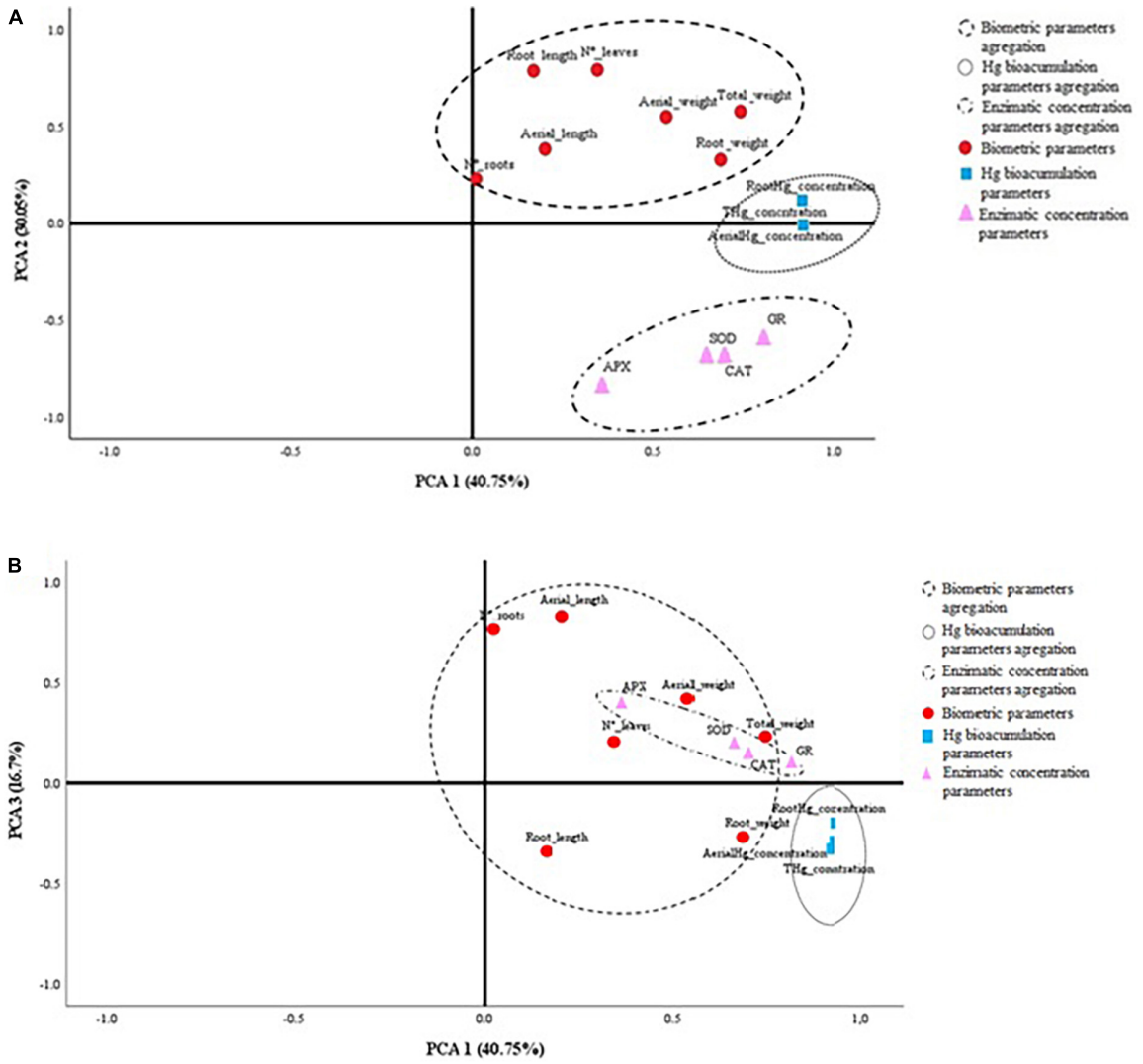

FIGURE 3
2D representation of the physiological and biometric variables of the plants according to the load factors of the PCA. **(A)** PCA1 vs. PCA2; **(B)** PCA1 vs. PCA3.

as cadmium (Cd) or lead (Pb) (Aras, 2012; Azimychetabi et al., 2021). Likewise, this effect has been observed in the enzymes APX and GR when facing different plant species with heavy metals (Hashem et al., 2016; Liu et al., 2018; Azimychetabi et al., 2021). Similarly, Pirzadah et al. (2018) investigate the effect of Hg on oxidative stress in plants not inoculated with PGPB, finding similar results to those described in the present work.

TABLE 5 Three main components that describe the model.

Component	Total	% variance	% acumulated
1	5.666	40.471	40.471
2	4.206	30.045	70.516
3	2.337	16.696	87.212

The effect that PGPB inoculation induces the decrease of ROS is known (Heidari and Golpayegani, 2012; Morcillo and Manzanera, 2021) in substrates contaminated by different heavy metals: Hg (Pirzadah et al., 2018), Pb (Abdelkrim et al., 2018), Cu (Fatnassi et al., 2015), Zn (Islam et al., 2014), and Cd (Azimychetabi et al., 2021; Renu et al., 2022). The PGPB species commonly used are those belonging to the genus *Bacillus* (Vardharajula et al., 2011; Moreno-Galván et al., 2020) and *Pseudomonas* (Sandhya et al., 2010). In the present study, the strains that produce a greater reduction in enzymatic activity in plants grown in the presence of Hg are B1 (*Pseudomonas baetica*) and B2 (*Pseudomonas moraviensis*) (**Figures 1A–D**) used both individually and in the consortium.

In the results obtained, a significant reduction in the levels of CAT (**Figure 1A**) and APX (**Figure 1C**) enzyme

10.3389/fmicb.2022.907557

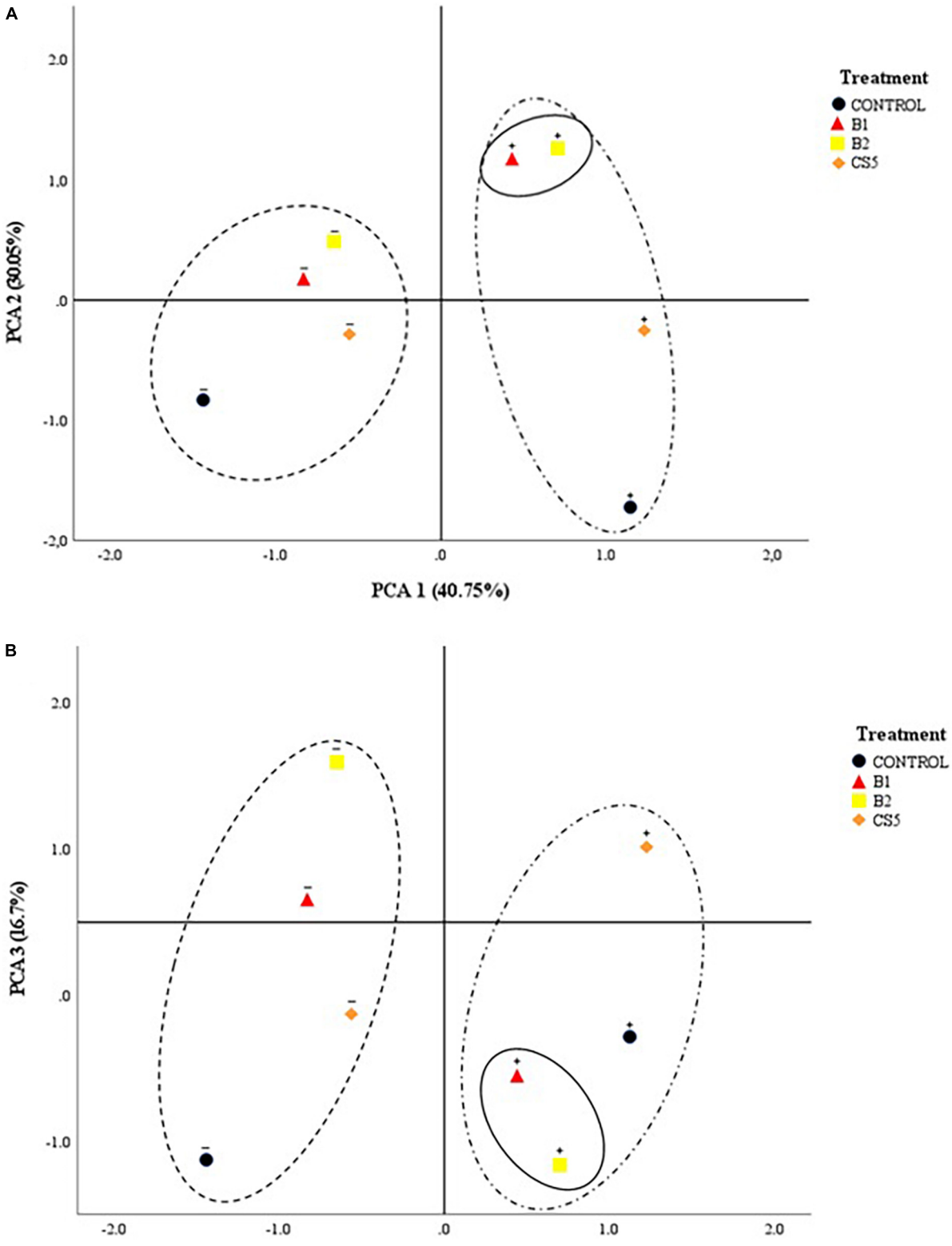

FIGURE 4
2D projection of the main components: **(A)** PCA1 vs. PCA2 and **(B)** PCA1 vs. PCA3 of the biological treatment (B1, B2, and CS5). The "+" sign on the treatment refers to "soil with a high concentration of Hg"; the "−" sign above the treatment refers to "soil without Hg."

activities was observed. This reduction is strongly correlated with the enzymatic activity of SOD (**Supplementary Table 3**). The SOD enzyme catalyzes singlet oxygen into a less reactive form of oxygen (H_2O_2). However, H_2O_2 is also toxic at high concentrations and must be eliminated by conversion to H_2O. CAT catalyzes the decomposition of H_2O_2 to H_2O and O_2. Similarly, the enzyme APX breaks down the H_2O_2 in H_2O by the reducing power of ascorbic acid. Plants possess enzymes such as CAT and APX that help maintain intracellular levels of H_2O_2 (Gill and Tuteja, 2010). For this reason, the correlation observed between the activity of SOD enzymes against CAT and APX in plants grown in the presence of Hg acquires biological meaning and is interpreted as metabolically related phytoprotection mechanisms. The inoculum of the B1 and B2 strains induce a better response of the plant subjected to oxidative stress.

Glutathione reductase is involved in the reduction of glutathione disulfide (GSSG) to glutathione (GSH) with NADPH expenditure. GSH plays a very important role in the redox regulation of the cell cycle and in the defense mechanisms against oxidative stress (Sánchez-Fernández et al., 1997). The increase in GR in substrates with Hg (**Figure 1D**) corroborates what we have found and is consistent with what has been described by other authors, indicating that how Hg increases oxidative stress in the plant (Pirzadah et al., 2018). We also observed how strains B1, B2, and their CS5 consortium (**Figure 1D**) show significantly lower enzymatic activity of this enzyme in plants grown in soil with Hg.

Analysis of Hg content in plant and principal component analysis

Plants of different species have been shown to accumulate Hg in different tissues, but the mechanism of absorption is unknown. To date, no membrane transporters involved in Hg root absorption have been identified. Due to the similarities between Cd and Hg, transmembrane Cd conveyors may be used (Lombi et al., 2001) for Hg input (Tiodar et al., 2021). The bioaccumulation of Hg in *Elodea nuttallii* has been analyzed, and it has been concluded that Cu transporters could be involved in the process (Regier et al., 2013). *Lupinus albus* is a known plant species accumulating Hg (Zornoza et al., 2010; Rocio et al., 2013; González et al., 2021a; Quiñones et al., 2021). Numerous metal carrier homologues have been identified in *Lupinus* roots (Tian et al., 2009). Whether these transporters could play a similar role in Hg absorption remains to be demonstrated. Quiñones et al. (2013, 2021) have used this plant species to demonstrate its ability to accumulate significant amounts of Hg in roots and nodules. This fact can induce a reduction in biomass production. This fact coincides with what has been observed in the present work. Nevertheless, plants inoculated with B1 and B2 are able to increase plant growth, even in substrates with high concentration of Hg. Likewise, there is evidence that inoculation with B1 and CS5 protects the plant against the contaminant, observing tissue concentrations of Hg significantly lower than the control (**Table 4**). These variables of root bioaccumulation of Hg and biometrics (total weight of the plant and root weight) present a positive correlation (**Figure 3**). In this same sense, the PCA segregates the behavior of plants treated with B1 and B2 in the presence of Hg. This fact leads us to think that the biological treatment with these strains in soils with a high concentration of Hg determines both the improvement of biometric variables, the reduction of the concentration of Hg in the plant, as well as the reduction of the activity of the enzymes that regulate the concentration of ROS.

The results of the present study show the capacity of phytoprotection against the accumulation of Hg and reduction of oxidative stress in *L. albus* var. orden Dorado of the strains B1 (*Pseudomonas moraviensis*) and B2 (*Pseudomonas baetica*), as well as of their respective CS5 consortium. For this reason, the convenience of using these strains for further use in phytostimulation and phytoprotection in soils contaminated with Hg is postulated.

Conclusion

It can be extracted as a conclusion that the biological behavior of plants [biometrics, bioaccumulation of Hg and activity of catalase enzymes (CAT), superoxide dismutase (SOD), ascorbate peroxidase (APX), glutathione reductase (GR)] is significantly improved by inoculation with strains B1 (*Pseudomonas moraviensis*) and B2 (*Pseudomonas baetica*), as well as their corresponding consortium (CS5). In a particular way we can conclude as follows:

First, the bacteria B1 and CS5 exert a phytoprotective effect showing significantly lower systemic Hg concentration values and, especially, at the root. The B2 strain significantly reduces the bioabsorption of Hg in the aerial part of the plant.

Second, B1 and B2 significantly promote the plant growth of *Lupinus albus* growth. Its consortium (CS5) reduces oxidative stress, especially when the plant grows in highly contaminated soils with Hg.

In the light of the conclusions of this work, the use of strains B1 (*Pseudomonas moraviensis*) and B2 (*Pseudomonas baetica*) is postulated, as well as their consortium (CS5) as good candidates for their subsequent use phytostimulation and phytoprotection in areas contaminated with Hg.

Data availability statement

The original contributions presented in this study are included in the article/**Supplementary material**, further inquiries can be directed to the corresponding authors.

Author contributions

AP and PJ supervised the project and acquired funding for this research. All authors contributed on design the experiments, making intellectual contributions, conduct the experiments, analyze the data, writing and editing of this manuscript, and approved the submitted version.

Funding

Grant GIR: Grants to recognized research groups of the vice-rectorate of professors and researchers of the University San Pablo CEU.

Acknowledgments

We thank the Centre for Scientific and Technological Research of Extremadura for the facilities offered for access to seeds of *Lupinus albus* var. orden Dorado.

Conflict of interest

The authors declare that the research was conducted in the absence of any commercial or financial relationships that could be construed as a potential conflict of interest.

Publisher's note

All claims expressed in this article are solely those of the authors and do not necessarily represent those of their affiliated organizations, or those of the publisher, the editors and the reviewers. Any product that may be evaluated in this article, or claim that may be made by its manufacturer, is not guaranteed or endorsed by the publisher.

Supplementary material

The Supplementary Material for this article can be found online at: https://www.frontiersin.org/articles/10.3389/fmicb.2022.907557/full#supplementary-material

References

Abdel Latef, A. A. H., Abu Alhmad, M. F., and Abdelfattah, K. E. (2017). The possible roles of priming with ZnO nanoparticles in mitigation of salinity stress in lupine (*Lupinus termis*) Plants. *J. Plant Growth Regul.* 36, 60–70. doi: 10.1007/s00344-016-9618-x

Abdelkrim, S., Jebara, S. H., and Jebara, M. (2018). Antioxidant systems responses and the compatible solutes as contributing factors to lead accumulation and tolerance in *Lathyrus sativus* inoculated by plant growth promoting rhizobacteria. *Ecotoxicol. Environ. Saf.* 166, 427–436. doi: 10.1016/j.ecoenv.2018.09.115

Aebi, H. (1984). "[13] Catalase in vitro," in *Methods in enzymology*, ed. Elsevier (Amsterdam: Elsevier), 121–126.

Ajitha, V., Sreevidya, C. P., Sarasan, M., Park, J. C., Mohandas, A., Singh, I. S. B., et al. (2021). Effects of zinc and mercury on ROS-mediated oxidative stress-induced physiological impairments and antioxidant responses in the microalga *Chlorella vulgaris*. *Environ. Sci. Pollut. Res.* 28, 32475–32492. doi: 10.1007/s11356-021-12950-6

Ali, B., Wang, X., Saleem, M. H., Hafeez, A., Afridi, M. S., Khan, S., et al. (2022). PGPR-Mediated salt tolerance in maize by modulating plant physiology. Antioxidant defense, compatible solutes accumulation and biosurfactant producing genes. *Plants* 11:345. doi: 10.3390/plants11030345

Amako, K., Chen, G.-X., and Asada, K. (1994). Separate assays specific for ascorbate peroxidase and guaiacol peroxidase and for the chloroplastic and cytosolic isozymes of ascorbate peroxidase in plants. *Plant Cell Physiol.* 35, 497–504.

Ansari, F., Jabeen, M., and Ahmad, I. (2021). *Pseudomonas* azotoformans FAP5, a novel biofilm-forming PGPR strain, alleviates drought stress in wheat plant. *Int. J. Environ. Sci. Technol.* 18, 3855–3870.

Aras, S. (2012). "Comparative genotoxicity analysis of heavy metal contamination in higher plants," in *Ecotoxicology*, Chap. 6, ed. S. S. Aydin (Rijeka: IntechOpen), doi: 10.5772/30073

Azimychetabi, Z., Sabokdast Nodehi, M., Karami Moghadam, T., and Motesharezadeh, B. (2021). Cadmium stress alters the essential oil composition and the expression of genes involved in their synthesis in peppermint (*Mentha piperita* L.). *Ind. Crops Prod.* 168:113602. doi: 10.1016/j.indcrop.2021.113602

Bjørklund, G., Tinkov, A. A., Dadar, M., Rahman, M. M., Chirumbolo, S., Skalny, A. V., et al. (2019). Insights into the potential role of mercury in Alzheimer's disease. *J. Mol. Neurosci.* 67, 511–533.

Burd, G. I., Dixon, D. G., and Glick, B. R. (2000). Plant growth-promoting bacteria that decrease heavy metal toxicity in plants. *Can. J. Microbiol.* 46, 237–245.

Cargnelutti, D., Tabaldi, L. A., Spanevello, R. M., de Oliveira Jucoski, G., Battisti, V., Redin, M., et al. (2006). Mercury toxicity induces oxidative stress in growing cucumber seedlings. *Chemosphere* 65, 999–1006. doi: 10.1016/j.chemosphere.2006.03.037

Carlberg, I., and Mannervik, B. (1985). "[59] Glutathione reductase," in *Methods in enzymology*, ed. Elsevier (Amsterdam: Elsevier), 484–490.

Çavuşoğlu, D., Macar, O., Kalefetoğlu Macar, T., Çavuşoğlu, K., and Yalçın, E. (2022). Mitigative effect of green tea extract against mercury(II) chloride toxicity in *Allium cepa* L. model. *Environ. Sci. Pollut. Res.* 29, 27862–27874. doi: 10.1007/s11356-021-17781-z

Cho, U.-H., and Park, J.-O. (2000). Mercury-induced oxidative stress in tomato seedlings. *Plant Sci.* 156, 1–9. doi: 10.1016/s0168-9452(00)00227-2

Ercal, N., Gurer-Orhan, H., and Aykin-Burns, N. (2001). Toxic metals and oxidative stress part I: Mechanisms involved in metal-induced oxidative damage. *Curr. Top. Med. Chem.* 1, 529–539.

Fatnassi, I. C., Chiboub, M., Saadani, O., Jebara, M., and Jebara, S. H. (2015). Impact of dual inoculation with rhizobium and PGPR on growth and antioxidant status of *Vicia faba* L. under copper stress. *C. R. Biol.* 338, 241–254. doi: 10.1016/j.crvi.2015.02.001

Gil-Hernández, F., Gómez-Fernández, A. R., la Torre-Aguilar, M. J., Pérez-Navero, J. L., Flores-Rojas, K., Martín-Borreguero, P., et al. (2020). Neurotoxicity by mercury is not associated with autism spectrum disorders in Spanish children. *Ital. J. Pediatr.* 46:19.

Gill, S. S., and Tuteja, N. (2010). Reactive oxygen species and antioxidant machinery in abiotic stress tolerance in crop plants. *Plant Physiol. Biochem.* 48, 909–930.

Gontia-Mishra, I., Sapre, S., Sharma, A., and Tiwari, S. (2016). Alleviation of mercury toxicity in wheat by the interaction of mercury-tolerant plant growth-promoting rhizobacteria. *J. Plant Growth Regul.* 35, 1000–1012.

González, D., Blanco, C., Probanza, A., Jiménez, P. A., and Robas, M. (2021a). Evaluation of the PGPR capacity of four bacterial strains and their mixtures, tested on *Lupinus albus* var. Dorado seedlings, for the bioremediation of mercury-polluted soils. *Processes* 9:1293.

González, D., Robas, M., Probanza, A., and Jiménez, P. A. (2021b). Selection of mercury-resistant PGPR strains using the BMRSI for bioremediation purposes. *Int. J. Environ. Res. Public. Health* 18:9867. doi: 10.3390/ijerph18189867

Harzalli Jebara, S., Fatnassi, I. C., Abdelkrim Ayed, S., Chiboub, M., and Jebara, M. (2017). Potentialities and limit of legume-plant growth promoting bacteria symbioses use in phytoremediation of heavy metal contaminated soils. *Int. J. Plant Biol. Res* 5:8.

Hashem, A., Abd Allah, E. F., Alqarawi, A. A., and Egamberdieva, D. (2016). Bioremediation of adverse impact of cadmium toxicity on cassia italica mill by arbuscular mycorrhizal fungi. *Saudi J. Biol. Sci.* 23, 39–47. doi: 10.1016/j.sjbs.2015.11.007

Ha-Tran, D. M., Nguyen, T. T. M., Hung, S.-H., Huang, E., and Huang, C.-C. (2021). Roles of plant growth-promoting rhizobacteria (PGPR) in stimulating salinity stress defense in plants: A review. *Int. J. Mol. Sci.* 22:3154. doi: 10.3390/ijms22063154

Heidari, M., and Golpayegani, A. (2012). Effects of water stress and inoculation with plant growth promoting rhizobacteria (PGPR) on antioxidant status and photosynthetic pigments in basil (*Ocimum basilicum* L.). *J. Saudi Soc. Agric. Sci.* 11, 57–61. doi: 10.1016/j.jssas.2011.09.001

Islam, F., Yasmeen, T., Ali, Q., Ali, S., Arif, M. S., Hussain, S., et al. (2014). Influence of *Pseudomonas aeruginosa* as PGPR on oxidative stress tolerance in wheat under Zn stress. *Ecotoxicol. Environ. Saf.* 104, 285–293. doi: 10.1016/j.ecoenv.2014.03.008

Khalilpour, M., Mozafari, V., and Abbaszadeh-Dahaji, P. (2021). Tolerance to salinity and drought stresses in pistachio (*Pistacia vera* L.) seedlings inoculated with indigenous stress-tolerant PGPR isolates. *Sci. Hortic.* 289:110440.

Kim, Y. O., Bae, H. J., Cho, E., and Kang, H. (2017). Exogenous glutathione enhances mercury tolerance by inhibiting mercury entry into plant cells. *Front. Plant Sci.* 8:683. doi: 10.3389/fpls.2017.00683

Liu, Y.-R., Delgado-Baquerizo, M., Bi, L., Zhu, J., and He, J.-Z. (2018). Consistent responses of soil microbial taxonomic and functional attributes to mercury pollution across China. *Microbiome* 6, 1–12. doi: 10.1186/s40168-018-0572-7

Loix, C., Huybrechts, M., Vangronsveld, J., Gielen, M., Keunen, E., and Cuypers, A. (2017). Reciprocal interactions between cadmium-induced cell wall responses and oxidative stress in plants. *Front. Plant Sci* 8:1867. doi: 10.3389/fpls.2017.01867

Lombi, E., Zhao, F., McGrath, S., Young, S., and Sacchi, G. (2001). Physiological evidence for a high-affinity cadmium transporter highly expressed in a *Thlaspi caerulescens* ecotype. *New Phytol.* 149, 53–60. doi: 10.1046/j.1469-8137.2001.00003.x

Macar, O., Kalefetoğlu Macar, T., Çavuşoğlu, K., and Yalçın, E. (2020). Determination of protective effect of carob (*Ceratonia siliqua* L.) extract against cobalt(II) nitrate-induced toxicity. *Environ. Sci. Pollut. Res.* 27, 40253–40261. doi: 10.1007/s11356-020-10009-6

Mariano, C., Mello, I. S., Barros, B. M., da Silva, G. F., Terezo, A. J., and Soares, M. A. (2020). Mercury alters the rhizobacterial community in Brazilian wetlands and it can be bioremediated by the plant-bacteria association. *Environ. Sci. Pollut. Res.* 27, 13550–13564. doi: 10.1007/s11356-020-07913-2

Marumoto, M., Sakamoto, M., Marumoto, K., Tsuruta, S., and Komohara, Y. (2020). Mercury and selenium localization in the cerebrum, cerebellum, liver, and kidney of a minamata disease case. *Acta Histochem. Cytochem.* 53, 147–155. doi: 10.1267/ahc.20-00009

Millán, R., Carpena, R., Schmid, T., Sierra, M., Moreno, E., Peñalosa, J., et al. (2007). Rehabilitación de suelos contaminados con mercurio: Estrategias aplicables en el área de Almadén. *Rev. Ecosistemas* 16.

Morcillo, R. J. L., and Manzanera, M. (2021). The effects of plant-associated bacterial exopolysaccharides on plant abiotic stress tolerance. *Metabolites* 11:337. doi: 10.3390/metabo11060337

Moreno-Galván, A., Romero-Perdomo, F. A., Estrada-Bonilla, G., Meneses, C. H., and Bonilla, R. R. (2020). Dry-Caribbean *Bacillus* spp. Strains ameliorate drought stress in maize by a strain-specific antioxidant response modulation. *Microorganisms* 8:823. doi: 10.3390/microorganisms8060823

Pirzadah, T. B., Malik, B., Tahir, I., Irfan, Q. M., and Rehman, R. U. (2018). Characterization of mercury-induced stress biomarkers in *Fagopyrum tataricum* plants. *Int. J. Phytoremediation* 20, 225–236. doi: 10.1080/15226514.2017.1374332

Quiñones, M. A., Fajardo, S., Fernández-Pascual, M., Lucas, M. M., and Pueyo, J. J. (2021). Nodulated white lupin plants growing in contaminated soils accumulate unusually high mercury concentrations in their nodules, roots and especially cluster roots. *Horticulturae* 7:302.

Quiñones, M. A., Ruiz-Díez, B., Fajardo, S., López-Berdonces, M. A., Higueras, P. L., and Fernández-Pascual, M. (2013). *Lupinus albus* plants acquire mercury tolerance when inoculated with an Hg-resistant bradyrhizobium strain. *Plant Physiol. Biochem.* 73, 168–175. doi: 10.1016/j.plaphy.2013.09.015

Regier, N., Larras, F., Bravo, A. G., Ungureanu, V.-G., Amouroux, D., and Cosio, C. (2013). Mercury bioaccumulation in the aquatic plant *Elodea nuttallii* in the field and in microcosm: Accumulation in shoots from the water might involve copper transporters. *Chemosphere* 90, 595–602. doi: 10.1016/j.chemosphere.2012.08.043

Renu, S., Sarim, K. Mohd, Singh, D. P., Sahu, U., Bhoyar, M. S., Sahu, A., et al. (2022). Deciphering cadmium (Cd) tolerance in newly isolated bacterial strain, ochrobactrum intermedium BB12, and its role in alleviation of Cd stress in spinach plant (*Spinacia oleracea* L.). *Front. Microbiol.* 12:758144. doi: 10.3389/fmicb.2021.758144

Robas, M., Jiménez, P. A., González, D., and Probanza, A. (2021). Bio-mercury remediation suitability index: A novel proposal that compiles the PGPR features of bacterial strains and its potential use in phytoremediation. *Int. J. Environ. Res. Public. Health* 18:4213. doi: 10.3390/ijerph18084213

Rocio, M., Elvira, E., Pilar, Z., and María-José, S. (2013). Could an abandoned mercury mine area be cropped? *Environ. Res.* 125, 150–159.

Rodríguez, H., Fraga, R., Gonzalez, T., and Bashan, Y. (2006). Genetics of phosphate solubilization and its potential applications for improving plant growth-promoting bacteria. *Plant Soil* 287, 15–21.

Rodriguez, L., Rincón, J., Asencio, I., and Rodríguez-Castellanos, L. (2007). Capability of selected crop plants for shoot mercury accumulation from polluted soils: Phytoremediation perspectives. *Int. J. Phytoremediation* 9, 1–13. doi: 10.1080/15226510601139359

Sachdev, S., Ansari, S. A., Ansari, M. I., Fujita, M., and Hasanuzzaman, M. (2021). Abiotic stress and reactive oxygen species: Generation, signaling, and defense mechanisms. *Antioxidants* 10:277.

Sánchez-Fernández, R., Fricker, M., Corben, L. B., White, N. S., Sheard, N., Leaver, C. J., et al. (1997). Cell proliferation and hair tip growth in the Arabidopsis root are under mechanistically different forms of redox control. *Proc. Natl. Acad. Sci. U.S.A.* 94, 2745–2750. doi: 10.1073/pnas.94.6.2745

Sandhya, V., Ali, S. Z., Grover, M., Reddy, G., and Venkateswarlu, B. (2010). Effect of plant growth promoting *Pseudomonas* spp. on compatible solutes, antioxidant status and plant growth of maize under drought stress. *Plant Growth Regul.* 62, 21–30. doi: 10.1007/s10725-010-9479-4

Tamizselvi, R., and Napoleon, A. A. (2022). Fluorescent and colorimetric chemosensor for the detection of toxic metal ions of mercury and lead–A mini review. *ECS Trans.* 107:16489.

Tian, L., Peel, G. J., Lei, Z., Aziz, N., Dai, X., He, J., et al. (2009). Transcript and proteomic analysis of developing white lupin (*Lupinus albus* L.) roots. *BMC Plant Biol.* 9:9892. doi: 10.1186/1471-2229-9-1

Tiodar, E. D., Văcar, C. L., and Podar, D. (2021). Phytoremediation and microorganisms-assisted phytoremediation of mercury-contaminated soils: Challenges and perspectives. *Int. J. Environ. Res. Public. Health* 18:2435. doi: 10.3390/ijerph18052435

US Environmental Protection Agency (2011). *2010 Biennial national listing of fish advisories*. Washington, DC: US Environmental Protection Agency.

Vardharajula, S., Zulfikar Ali, S., Grover, M., Reddy, G., and Bandi, V. (2011). Drought-tolerant plant growth promoting *Bacillus* spp.: Effect on growth, osmolytes, and antioxidant status of maize under drought stress. *J. Plant Interact.* 6, 1–14. doi: 10.1080/17429145.2010.535178

Yuan, Y., Zu, M., Sun, L., Zuo, J., and Tao, J. (2022). Isolation and Screening of 1-aminocyclopropane-1-carboxylic acid (ACC) deaminase producing PGPR from Paeonia lactiflora rhizosphere and enhancement of plant growth. *Sci. Hortic.* 297:110956.

Zhou, Z. S., Huang, S. Q., Guo, K., Mehta, S. K., Zhang, P. C., and Yang, Z. M. (2007). Metabolic adaptations to mercury-induced oxidative stress in roots of *Medicago sativa* L. *J. Inorg. Biochem.* 101, 1–9. doi: 10.1016/j.jinorgbio.2006.05.011

Zornoza, P., Millán, R., Sierra, M. J., Seco, A., and Esteban, E. (2010). Efficiency of white lupin in the removal of mercury from contaminated soils: Soil and hydroponic experiments. *J. Environ. Sci.* 22, 421–427. doi: 10.1016/s1001-0742(09)60124-8

Frontiers in Microbiology

Explores the habitable world and the potential of microbial life

The largest and most cited microbiology journal which advances our understanding of the role microbes play in addressing global challenges such as healthcare, food security, and climate change.

Discover the latest Research Topics

See more →

Frontiers

Avenue du Tribunal-Fédéral 34
1005 Lausanne, Switzerland
frontiersin.org

Contact us

+41 (0)21 510 17 00
frontiersin.org/about/contact